# MEMBRANE SEPARATION PRINCIPLES AND APPLICATIONS

# Handbooks in Separation Science

The goal of the series and volume editors is to develop a new vehicle for collating, interpreting, and disseminating the essential fundamental and practical information of separation science for future generations of separation scientists and to do this by creating the seminal work in the field. Each volume is designed to cover a specific topic and contains relatively succinct chapters with a sharp focus and clear presentation contributed by leading scientists in the field. The target audience for these volumes is professional scientists with responsibility for managing or participating in research projects in either academia or industry. Included in this group are graduate students and professionals in disciplines other than separation science seeking insight into a topic at a level associated with current capabilities. The current volume follows on from the success of earlier volumes with additional volumes in production or planned for the future.

Handbooks in Separation Science

# MEMBRANE SEPARATION PRINCIPLES AND APPLICATIONS

## FROM MATERIAL SELECTION TO MECHANISMS AND INDUSTRIAL USES

*Edited by*

AHMAD FAUZI ISMAIL
MUKHLIS A. RAHMAN
MOHD HAFIZ DZARFAN OTHMAN
TAKESHI MATSUURA

*Series Editor*

COLIN F. POOLE

ELSEVIER

# Contributors

**Khairul Hamimah Abas**   Faculty of Electrical Engineering, Universiti Teknologi Malaysia, Skudai, Malaysia

**Muhammad Nidzhom Zainol Abidin**   Advanced Membrane Technology Research Centre (AMTEC), Faculty of Chemical and Energy Engineering, Universiti Teknologi Malaysia, Skudai, Malaysia

**Mohd Ridhwan Adam**   Advanced Membrane Technology Research Centre (AMTEC), Faculty of Chemical and Energy Engineering, Universiti Teknologi Malaysia, Skudai, Malaysia

**Mohd Haiqal Abd Aziz**   Advanced Membrane Technology Research Centre (AMTEC), Faculty of Chemical and Energy Engineering, Universiti Teknologi Malaysia, Skudai, Malaysia

**Fakhir U. Baig**   Petro Sep Corporation, Mississauga, ON, Canada

**J.J. Beh**   School of Chemical Engineering, Universiti Sains Malaysia, Nibong Tebal, Malaysia

**Woon Chan Chong**   Centre for Sustainable Process Technology (CESPRO), Faculty of Engineering and Built Environment, Universiti Kebangsaan Malaysia, Selangor, Malaysia

**Tai Shung Chung**   Department of Chemical and Biomolecular Engineering, National University of Singapore, Singapore, Singapore

**Mohamad Izrin Mohamad Esham**   Advanced Membrane Technology Research Centre (AMTEC), Faculty of Chemical and Energy Engineering, Universiti Teknologi Malaysia, Skudai, Malaysia

**Pei Sean Goh**   Advanced Membrane Technology Research Centre (AMTEC), Faculty of Chemical and Energy Engineering, Universiti Teknologi Malaysia, Skudai, Malaysia

**Hasrinah Hasbullah**   Advanced Membrane Technology Research Centre (AMTEC), Faculty of Chemical and Energy Engineering, Universiti Teknologi Malaysia, Skudai, Malaysia

**Kah Chun Ho**   Centre for Sustainable Process Technology (CESPRO), Faculty of Engineering and Built Environment, Universiti Kebangsaan Malaysia, Selangor, Malaysia

**Dan Hua**   Department of Chemical and Biomolecular Engineering, National University of Singapore, Singapore, Singapore

**Siti Khadijah Hubadillah**   Advanced Membrane Technology Research Centre (AMTEC), Faculty of Chemical and Energy Engineering, Universiti Teknologi Malaysia, Skudai, Malaysia

**Ahmad Fauzi Ismail**  Advanced Membrane Technology Research Centre (AMTEC), Faculty of Chemical and Energy Engineering, Universiti Teknologi Malaysia, Skudai, Malaysia

**Juhana Jaafar**  Advanced Membrane Technology Research Centre (AMTEC), Faculty of Chemical and Energy Engineering, Universiti Teknologi Malaysia, Skudai, Malaysia

**Woei Jye Lau**  Advanced Membrane Technology Research Centre (AMTEC), Faculty of Chemical and Energy Engineering, Universiti Teknologi Malaysia, Skudai, Malaysia

**S.O. Lai**  Universiti Tunku Abdul Rahman (UTAR), Kajang, Malaysia

**Sumarni Mansur**  Advanced Membrane Technology Research Centre (AMTEC), Faculty of Chemical and Energy Engineering, Universiti Teknologi Malaysia, Skudai, Malaysia

**Takeshi Matsuura**  Department of Chemical and Biological Engineering, University of Ottawa, Ottawa, ON, Canada

**Abdul Wahab Mohammad**  Centre for Sustainable Process Technology (CESPRO), Faculty of Engineering and Built Environment, Universiti Kebangsaan Malaysia, Selangor, Malaysia

**Ali Moslehyani**  Department of Chemical and Biological Engineering, University of Ottawa, Ottawa, ON, Canada; Advanced Membrane Technology Research Centre (AMTEC), Faculty of Chemical and Energy Engineering, Universiti Teknologi Malaysia, Skudai, Malaysia; Department of Chemical Engineering and Applied Chemistry, University of Toronto, Toronto, ON, Canada

**Nizar Mu'ammar Mahpoz**  Advanced Membrane Technology Research Centre (AMTEC), Faculty of Chemical and Energy Engineering, Universiti Teknologi Malaysia, Skudai, Malaysia

**Be Cheer Ng**  Advanced Membrane Technology Research Centre (AMTEC), Faculty of Chemical and Energy Engineering, Universiti Teknologi Malaysia, Skudai, Malaysia

**B.S. Ooi**  School of Chemical Engineering, Universiti Sains Malaysia, Nibong Tebal, Malaysia

**Mohd Hafiz Dzarfan Othman**  Advanced Membrane Technology Research Centre (AMTEC), Faculty of Chemical and Energy Engineering, Universiti Teknologi Malaysia, Skudai, Malaysia

**Mohamad Zahir Mohd Pauzi**  Advanced Membrane Technology Research Centre (AMTEC), Faculty of Chemical and Energy Engineering, Universiti Teknologi Malaysia, Skudai, Malaysia

**Mihir Kumar Purkait**  Department of Chemical Engineering, Indian Institute of Technology Guwahati, Guwahati, India

**Yanuardi Raharjo**  Advanced Membrane Technology Research Centre (AMTEC), Faculty of Chemical and Energy Engineering, Universiti Teknologi Malaysia, Skudai, Malaysia

**Mukhlis A. Rahman** Advanced Membrane Technology Research Centre (AMTEC), Faculty of Chemical and Energy Engineering, Universiti Teknologi Malaysia, Skudai, Malaysia

**Norzeti Hanani Mohd Ripin** Advanced Membrane Technology Research Centre (AMTEC), Faculty of Chemical and Energy Engineering, Universiti Teknologi Malaysia, Skudai, Malaysia

**Sarina Mat Rosid** Advanced Membrane Technology Research Centre (AMTEC), Faculty of Chemical and Energy Engineering, Universiti Teknologi Malaysia, Skudai, Malaysia

**Noresah Said** Advanced Membrane Technology Research Centre (AMTEC), Faculty of Chemical and Energy Engineering, Universiti Teknologi Malaysia, Skudai, Malaysia

**Gui Min Shi** Department of Chemical and Biomolecular Engineering, National University of Singapore, Singapore, Singapore

**Randeep Singh** Department of Chemical Engineering, Indian Institute of Technology Guwahati, Guwahati, India

**J.Y. Sum** School of Chemical Engineering, Universiti Sains Malaysia, Nibong Tebal, Malaysia

**Zhong Sheng Tai** Advanced Membrane Technology Research Centre (AMTEC), Faculty of Chemical and Energy Engineering, Universiti Teknologi Malaysia, Skudai, Malaysia

**Yeit Haan Teow** Centre for Sustainable Process Technology (CESPRO), Faculty of Engineering and Built Environment, Universiti Kebangsaan Malaysia, Selangor, Malaysia

**Yi-Ning Wang** Singapore Membrane Technology Centre, Nanyang Environmental and Water Research Institute, Singapore, Singapore

**Rong Wang** Singapore Membrane Technology Centre, Nanyang Environmental and Water Research Institute; School of Civil and Environmental Engineering, Nanyang Technological University, Singapore, Singapore

**Zhentao Wu** Aston Institute of Materials Research, School of Engineering and Applied Science, Aston University, Birmingham, United Kingdom

**Nur Zhatul Shima Yahaya** Advanced Membrane Technology Research Centre (AMTEC), Faculty of Chemical and Energy Engineering, Universiti Teknologi Malaysia, Skudai, Malaysia

**Muhamad Zulhilmi Zailani** Advanced Membrane Technology Research Centre (AMTEC), Faculty of Chemical and Energy Engineering, Universiti Teknologi Malaysia, Skudai, Malaysia

**Notices**
Knowledge and best practice in this field are constantly changing. As new research and
experience broaden our understanding, changes in research methods, professional practices,
or medical treatment may become necessary.

Practitioners and researchers must always rely on their own experience and knowledge in
evaluating and using any information, methods, compounds, or experiments described
herein. In using such information or methods they should be mindful of their own safety and
the safety of others, including parties for whom they have a professional responsibility.

To the fullest extent of the law, neither the Publisher nor the authors, contributors, or editors,
assume any liability for any injury and/or damage to persons or property as a matter of
products liability, negligence or otherwise, or from any use or operation of any methods,
products, instructions, or ideas contained in the material herein.

For information on all Elsevier publications
visit our website at https://www.elsevier.com/books-and-journals

Working together
to grow libraries in
developing countries

www.elsevier.com • www.bookaid.org

# Index

Note: Page numbers followed by *f* indicate figures and *t* indicate tables.

C H A P T E R

# 1

# Reverse Osmosis Membrane Separation Technology

*Yi-Ning Wang\*, Rong Wang\*,†*

**\*Singapore Membrane Technology Centre, Nanyang Environmental and Water Research Institute, Singapore, Singapore**
**†School of Civil and Environmental Engineering, Nanyang Technological University, Singapore, Singapore**

O U T L I N E

1

## List of Symbols

| | |
|---|---|
| $A$ | water permeability coefficient |
| $B$ | solute permeability coefficient |
| $c$ | solute concentration |
| $c_b$ | bulk concentration |
| $c_f$ | feed concentration |
| $c_m$ | solute concentration near membrane surface |
| $c_p$ | solute concentration in the permeate |
| $C_{wm}$ | the concentration of water inside the selective layer |
| $d_h$ | hydraulic diameter |
| $D$ | diffusion coefficient of solute |
| $D_{sm}$ | diffusion coefficient of solute inside RO rejection layer |
| $D_{wm}$ | diffusion coefficient of water inside RO rejection layer |
| $J$ | water flux |
| $J_s$ | solute flux |
| $k$ | mass transfer coefficient |
| $K_{sm}$ | solute partitioning coefficient in the selective layer |
| $L$ | channel length |
| $l_m$ | thickness of a selective layer |
| $P$ | hydraulic pressure |
| $R$ | rejection |
| $Re$ | Reynolds number |
| $R_g$ | universal gas constant ($8.31 \text{ J mol}^{-1} \text{ K}^{-1}$) |
| $R_{int}$ | intrinsic rejection of a membrane |
| $R_m$ | membrane hydraulic resistance |
| $Sc$ | Schemidt number |
| $Sh$ | Sherwood number |
| $T$ | absolute temperature (K) |
| $u$ | cross-flow velocity |
| $V_w$ | molar volume of water |
| $v$ | kinematic viscosity |
| $\eta$ | dynamic viscosity of water |
| $\delta$ | boundary layer thickness |
| $\pi$ | osmotic pressure |

## 1.1  INTRODUCTION OF REVERSE OSMOSIS

Osmosis, also called forward osmosis (FO), a natural phenomenon discovered as early as 1748, is a diffusion of fluid (usually water) through a semi-permeable membrane from a solution with a low solute concentration
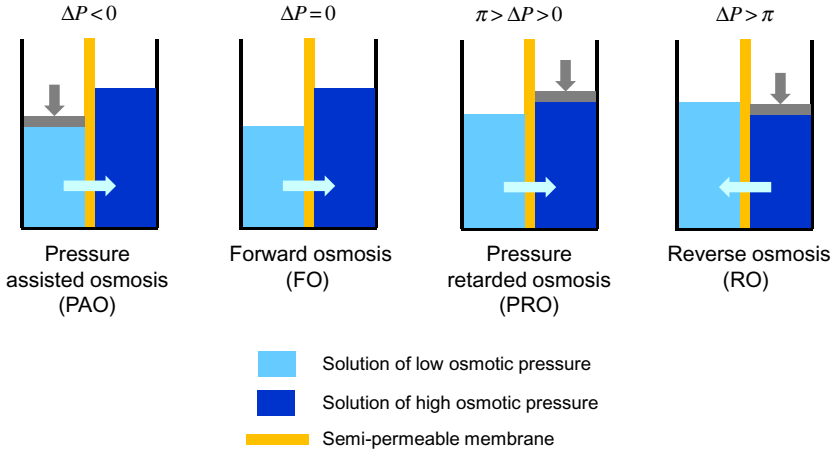
FIG. 1.1    Osmotic membrane processes including pressure assisted osmosis (PAO), forward osmosis (FO), pressure retarded osmosis (PRO) and reverse osmosis (RO).

to a solution with a higher solute concentration until an equilibrium of fluid concentration on both sides of the membrane is reached [1]. The driving force for water transport is the chemical potential difference (i.e., osmotic pressure difference) across the membrane. Reverse osmosis (RO) is achieved by applying a pressure in excess of the osmotic pressure gradient to drive the water to flow from the high solute concentration side to the low solute concentration side, i.e., in an oppose direction to the automatic water flow in the FO process. Fig. 1.1 illustrates four osmotic membrane processes including pressure assisted osmosis (PAO), FO, pressure retarded osmosis (PRO) and RO. The four processes are similar in a way that a semi-permeable membrane is placed in between a solution of low osmotic pressure and a solution of high osmotic pressure. The first three (PAO, FO, and PRO) are the processes (partially) driven by osmotic pressure difference, where water flows from the low osmotic pressure side to the high osmotic pressure side. They are not able to achieve desalination by themselves. Only when the water flow direction is reversed in the RO process, can clean and desalted water be directly obtained by this pressure driven membrane process.

## 1.1.1  Historic Development of RO

The use of RO as a feasible separation process was first demonstrated in the early 1960s. The milestones of RO membrane development are shown in Fig. 1.2. The first practical RO membrane made of cellulose acetate (CA) was reported by Loeb and Sourirajan in 1962 [2]. This membrane exhibited high flux and salt rejection owing to the asymmetric structure (a thin skin
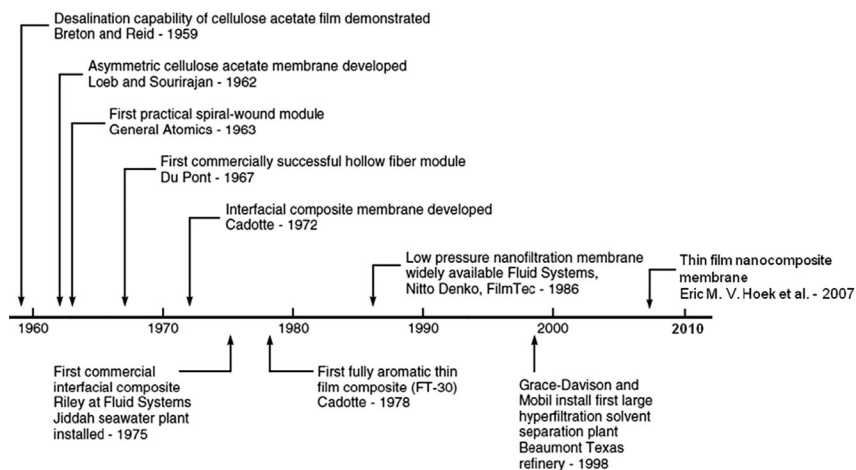
**FIG. 1.2**    Milestones of RO membrane development. *Adapted from Baker RW. Reverse osmosis. Membrane technology and applications. John Wiley & Sons, Ltd; 2004. p. 191–235.*

layer on a porous substrate). Cadotte and Petersen later made the first efficient thin-film composite (TFC) membrane based on the reaction of phenylene diamine and trimesoyl chloride, which was a key breakthrough to make the large-scale application of RO membranes economically feasible [3]. Today, the state-of-art desalination RO membranes are still TFC polyamide (PA) RO membranes [4]. Although they are produced based on the original chemistry discovered during the 1980s, the performance of RO membranes have been improved significantly over the 30 years [5], by closer monitoring of the recipes for the substrates and selective layer and/or applying coating, etc. [6]. More than sevenfold decrease in salt passage has expanded the range of saline feeds, while the increased lifespan (2.3 times) and increased water permeability (2.5 times) have greatly reduced the real cost (one twelfth) [5, 7]. Currently, TFC RO membranes are produced in flat sheet configuration and mostly supplied in spiral wound module (SWM). With the aim of further reducing energy cost in desalination (theoretical minimal energy required to desalinate 35 g/L seawater at 50% recovery is $\sim$1.06 kWh/m$^3$, while the real energy consumption is $\sim$2–5 kWh/m$^3$ [8, 9]), extensive researches are focused on developing more superior performing, fouling resistant and chlorine resistant RO membranes, in addition to the optimizations of the process and membrane module design.

Since 2007, the emerging thin-film nanocomposite (TFN) membranes/mixed matrix membranes (MMMs), i.e., TFC membranes with incorporated nanoparticles/inorganic particles in the selective layer and/or the support layer, have attracted great interests in fabricating high performance RO membranes [10, 11], due to their enhanced performance as compared with pristine TFC membranes [12].

## 1.1.2 Basic Properties of RO Membrane

The basic properties of RO membrane are summarized in Table 1.1 along with other types of pressure driven membranes such as nanofiltration (NF), ultrafiltration (UF), and microfiltration (MF), which are categorized based on the pore size or operating pressure range. MF and UF membranes are the low-pressure membranes with relatively larger pores. They are usually adopted in the pretreatment of RO/NF processes to protect the RO/NF membranes. They are also used as the support for fabricating TFC RO and NF membranes. RO membranes have the tightest surface "pores" (<2 nm (diameter), generally considered as non-porous membrane) and are able to retain dissolved ions (including monovalent ions $Na^+$ and $Cl^-$) and small organic molecules. RO membranes can be further divided into seawater RO (SWRO) and brackish water RO (BWRO) membranes. SWRO membranes have high NaCl rejection (>99%) and are used for seawater desalination. The trade-off for this high

**TABLE 1.1**  Typical Properties of Pressure-Driven Membranes

| | Microfiltration | Ultrafiltration | Nanofiltration | Reverse osmosis |
|---|---|---|---|---|
| Surface pore size (nm) | 50–10,000 | 1–100 | ~2 | <2 |
| Operating pressure (bar) | 0.1–2.0 | 1.0–5.0 | 2.0–10 | 10–100 |
| Water permeability ($L/m^2h/bar$) | >500 | 20–500 | 5–50 | 0.5–10 |
| MWCO (Da) | Not applicable | 1000–300,000 | >100 | >10 |
| Targeted contaminants | Bacteria, algae, suspended solids, turbidity | Bacteria, virus, colloids, macromolecules | Di- and multi-valent ions, natural organic matter, small organic molecules | Dissolved ions, small molecules |
| Membrane materials | Polymeric, inorganic | Polymeric, inorganic | Thin-film composite polyamide, cellulose acetate, etc. [13] | Thin-film composite polyamide, cellulose acetate |

*Note*: MWCO, molecular weight cut-off.
*Adapted from Fane AG, Wang R, Tang C. Membrane technology for water: microfiltration, ultrafiltration, nanofiltration, and reverse osmosis. Treatise on water science, vol. 4. Amsterdam; Hackensack, NJ: Elsevier Science; 2011. p. 301; Mulder M. Basic principles of membrane technology. The Netherlands: Kluwer Academic Publishers; 1996.*
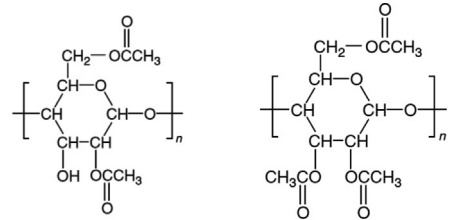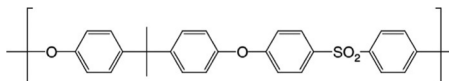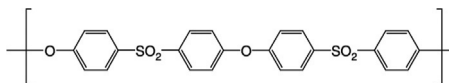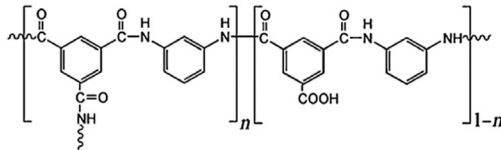
rejection is the low water permeability ($<1$ L/m$^2$ h/bar). High pressure of above 60 bar is generally required in real operation to overcome the seawater osmotic pressure to produce reasonably high-water flux. BWRO membranes have relatively low NaCl rejection ($>95\%$) and higher water permeability ($1$–$10$ L/m$^2$ h/bar), and are used for water/wastewater treatment where feed salt content is much lower compared to that of seawater. NF membranes are similar to RO membranes, but the bigger "pore" size of NF membranes as compared with RO membranes leads to the higher water permeability and much lower rejection to the monovalent ions (e.g., $10\%$–$90\%$ rejection to Na$^+$ depending strongly on the surface charges of the membrane). NF membranes can effectively remove di- and multi-valent ions, which makes them useful for water softening.

During a pressure driven membrane process, a feed stream is divided into two streams, i.e., retentate stream (or concentrate stream) that is retained by the membrane and permeate stream that passes through the membrane. It is widely accepted that the transport of molecules through the selective skin layer of a RO membrane is best described by the solution-diffusion model [14, 15]. It assumes that both the solvent and the solute are absorbed to the skin layer, and then diffuse through the non-porous layer independent of each other under their respective chemical potential gradient. A separation is achieved between the solvent and the solute (or among different permeants) because of the differences in the amount of the molecules that dissolve in the membrane (solubility) and the rate at which the molecules diffuse through the membrane (diffusivity) [14]. RO membranes generally allow high absorption of water molecules and fast diffusion of them through the selective layer, as compared with sodium chloride [15].

## 1.2  RO MEMBRANE FABRICATION

RO membranes are generally categorized into integrally skinned asymmetric membranes and TFC membranes based on the structure and materials. The common materials used for RO membrane fabrication are summarized in Table 1.2. An integrally skinned asymmetric membrane is made of one polymeric material, and CA membranes (made of cellulose esters) are the most widely used examples [15]. The TFC RO membrane is the state-of-the-art RO membrane, which comprises two or more polymer materials. The porous membrane support is typically made of polysulfone (PSf) or polyethersulfone (PES). The ultrathin selective layer is generally made of polyamide (PA), which has relatively high water flux and high solute rejection, as well as good chemical, mechanical, and thermal stability (Table 1.2) [9].

**TABLE 1.2  Typical Materials for RO Membrane Preparation**

| Polymer | Structure | Properties |
|---|---|---|
| Cellulose esters |  Cellulose diacetate    Cellulose triacetate | − Hydrophilic<br>− Cellulose diacetate and triacetate and their blends are widely used for making RO membranes<br>− Cellulose acetate membranes are subject to hydrolysis and microbial attack<br>− Stable over narrow pH range |
| Polysufone (PSf) |  | − High performance polymer with excellent chemical and thermal stability<br>− Form porous support layer of RO and NF membranes |
| Polyethersulfone (PES) |  | − Similar to PSf, high chemical and thermal stability<br>− Less hydrophobic than PSf<br>− Form porous support layer of RO and NF membranes |
| Polyamide (PA) |  Crosslinked polyamide | − Good thermal stability, chemical resistance and mechanical strength<br>− Used as ultrathin dense layer for RO membranes<br>− Low resistance to chlorine |

## 1.2.1 Cellulose Acetate Membrane

Cellulose esters, including cellulose diacetate and cellulose triacetate, are used to prepare the integrally skinned asymmetric RO membranes via phase inversion. Phase inversion refers to a process whereby a polymer solution (liquid form; in which the solvent system is the continuous phase) inverts into a swollen three-dimensional macromolecular network or gel (solid form; where the polymer is the continuous phase) [9]. In other words, a liquid polymer solution is precipitated into two phases: a polymer-rich phase that forms the matrix of the membrane, and a polymer-lean phase that forms the membrane pores in an unstable nascent membrane structure. For RO membrane/RO substrate preparation, the precipitation is generally achieved by the immersion of a polymer solution into a non-solvent coagulant bath, such as water (solvent containing water coagulant bath is usually adopted for hollow fiber membrane preparation [16]). Both flat-sheet membranes and hollow fiber membranes can be fabricated using this method.

Despite the ease of preparation (i.e., one step casting), it is generally difficult for the integrally skinned asymmetric RO membranes to achieve both high water permeability and high solute rejection. Formation of a dense skin layer requires a relatively high polymer concentration, which results in a less porous/less permeable support and therefore an increased overall hydraulic resistance of the membrane. It has been reported that the polymer concentration for making integrally skinned asymmetric CA membrane is higher than that of TFC membrane with CA support [17, 18]. A common practice for increasing the solute rejection of CA membrane is to adopt an annealing post-treatment, such as heating in a bath of hot water for a few minutes [19]. This process modifies the selective layer by eliminating the micropores and producing a denser skin, resulting in a decrease in water flux and an increase in salt rejection [19]. The annealing temperature determines the final properties of the membrane and a higher temperature generally leads to a denser skin layer. To compensate the low permeability, the commercial CA RO membrane is preferentially made into hollow fiber modules (e.g., Toyobo hollow fiber membrane with a very small outer diameter of ~165 μm [20]), which can provide sufficiently high water productivity owing to the high packing density (high specific membrane area) [21]. Considerable research efforts have been made to optimize CA membranes via changing the compositions of polymer solution (e.g., type and concentration of polymer/additives) and casting/spinning conditions (e.g., composition and temperature of coagulant bath), and modifying the surface properties, etc. [22–24]. However, their drawbacks of poor stability against chemicals, bacteria, and temperature and lower water permeability make it less competitive than the TFC polyamide membranes (see Tables 1.2 and 1.3).

TABLE 1.3   Comparison of CA RO Membrane and TFC RO Membrane

|  | Cellulose acetate (CA) RO membrane | Thin-film composite (TFC) polyamide (PA) RO membrane |
|---|---|---|
| Water permeability (L/m$^2$h/bar) | Low ($\sim$1 L/m$^2$ h/bar or less) | High |
| NaCl rejection (%) | 85–98 | 95–99.9 |
| Surface hydrophilicity | Very hydrophilic | Less hydrophilic |
| Surface roughness | Smooth | Rough surface with ridge-and-valley structure |
| Operating pH range | 5–7 | 3–10 (2–11 for certain membranes) |
| Maximum operating temperature (°C) | 30 | 45 |
| Resistance to biodegradation | Low | Relatively good |
| Resistance to chlorine | Stable at low levels (<1 ppm) | Low tolerance to free chlorine (<0.1 ppm) |

*Adapted from Fane AG, Wang R, Tang C. Membrane technology for water: microfiltration, ultrafiltration, nanofiltration, and reverse osmosis. Treatise on water science, vol. 4. Amsterdam; Hackensack, NJ: Elsevier Science; 2011. p. 301.*

## 1.2.2 TFC Polyamide Membrane

A TFC polyamide (PA) RO membrane generally comprises three layers, including an aromatic PA selective layer (typically <200 nm thick), a microporous support (usually a UF membrane, 20–50 μm), and a non-woven fabric (backing layer, 100–200 μm) [9]. A schematic of a typical TFC RO membrane is shown in Fig. 1.3. The selective layer and the support are produced separately, enabling the optimization of each individual layer for the respective specific function, i.e., the top selective layer is thin but dense enough to attain high solvent flux and high solute rejection;



Polyamide 0.05–0.3 μm

Polysulfone ~20–50 μm

Backing layer ~100–200 μm
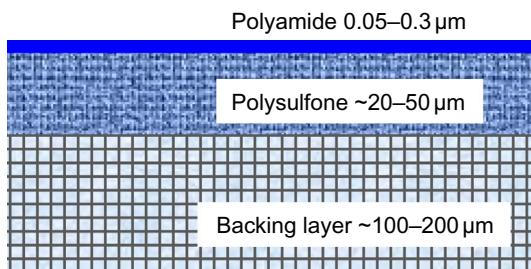
FIG. 1.3   Schematic of a thin-film composite PA membrane.

and the support is porous enough to provide low resistance to permeate while maintaining high mechanical strength [25]. This approach provides great flexibility for utilizing different materials to tailor the membrane structure and properties.

The PA layer of a TFC RO membrane is formed on a porous membrane support via interfacial polymerization between amines (e.g., m-phenylenediamine, MPD) and aromatic acyl chlorides (e.g., trimesoyl chloride, TMC). In the process of preparation (Fig. 1.4), a membrane support (UF or MF membrane) is immersed in an aqueous solution containing MPD. After removing the excess MPD, the membrane surface is immersed in/contacted with a water-immiscible solvent containing dissolved TMC. Due to the rapid hydrolysis of acyl chloride in the aqueous phase and the asymmetric solubility, the reaction is diffusion-controlled and comprises three stages [26]: At the incipient stage, a loose polymer film begins to emerge in the interface between two immiscible solvents; then amines in the aqueous phase diffuse to the organic phase and the film becomes dense and grows perpendicularly towards the organic phase; finally the increase in thickness and density of the film inhibits the diffusion of the monomers and the reaction. The advantage of interfacial reaction is the fast reaction kinetics and self-inhibiting, resulting in an extremely thin film. Heat treatment is often applied to complete the interfacial reaction and further cross-linking [19]. The type and concentration of monomers/solvents/additives, polymerization condition, and curing process
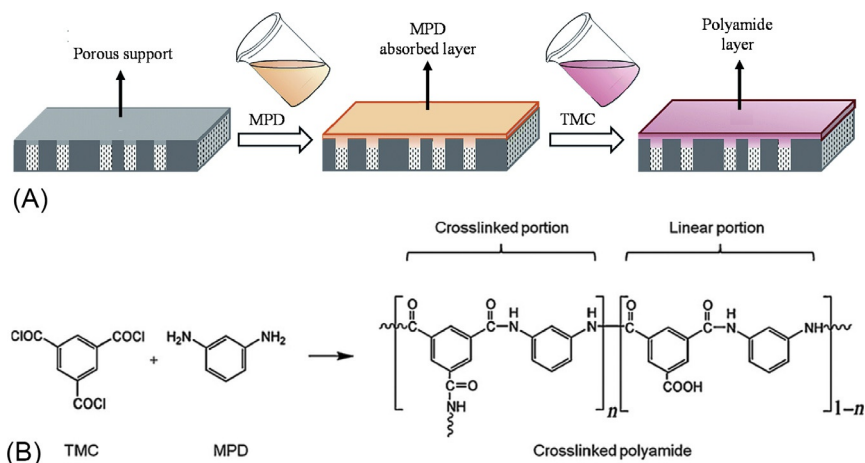


FIG. 1.4    (A) Schematic of the formation of a thin-film composite membrane via interfacial polymerization; (B) reaction between MPD and TMC. *Adapted from Weng X, Ji Y, Zhao F, An Q, Gao C. Tailoring the structure of polyamide thin film composite membrane with zwitterions to achieve high water permeability and antifouling property. RSC Adv 2015;5(120):98730-9*

can affect the performance of the PA layer and these conditions need to be optimized for fabricating high-performance TFC membranes [27, 28].

In addition to the control of the reaction parameters of interfacial polymerization, the surface properties of the support such as pore structure, surface morphology and chemistry are also important for the PA layer formation [27, 29]. For example, a relatively porous and hydrophobic support could result in the formation of a more permeable and rougher skin layer; whereas a smoother PA layer with lower permeability is formed on a support of hydrophilic surface [30]. The increasing surface pore size was also found to increase the RO membrane water permeability [31]. Although it has been found that the support surface properties play an important role in forming PA layer, the mechanisms are yet to be systematically investigated. Besides the surface properties, an ideal support of a RO membrane shall possess good mechanical, chemical, thermal, and biological stabilities and relatively low hydraulic resistance.

In the aspect of RO support preparation, phase inversion is the most extensively used method, with which an asymmetric UF membrane is generally formed from polymers PSf or PES (Table 1.2). Similar to the CA RO membrane fabrication and other UF membrane preparation, factors such as the composition of polymer solution (e.g., the type and concentration of polymer/additive), and coagulant bath, etc. have been shown to influence the properties of resultant supports [15, 27]. For the commercially available TFC membranes, the TFC RO supports are produced in flat sheets; hollow fiber TFC RO membranes are only prepared in lab scale currently due to the challenges of large-scale production. Nevertheless, the high performance hollow fiber TFC RO membranes have been recently developed in a few research labs with promising applications in brackish water desalination and surface water treatment [32].

On the other hand, the recently emerged nanofibrous membranes produced by electrospinning have attracted many interests in preparing membranes or membrane supports [29, 33]. Electrospinning involves a process during which polymer is stretched into nanofibers from its solution under an applied electrostatic force. This technique is so versatile that the produced nanofibrous membranes can be tailored with desired pore size, porosity, and thickness by varying the polymer solution and electrospinning conditions [29, 34]. A typical nanofibrous membrane has interconnected pores and relatively high porosity, which is favorable for making RO/NF membranes with high water permeability [33]. Nevertheless, the surface pore size of the nanofibrous membrane support needs to be carefully controlled within a certain range for the successful formation of PA selective layer. The nanofibrous support with high porosity may also require other treatment to enhance its stability against high pressure, such as heat pressing [33].

## 1.2.3 Membrane With a Polyelectrolyte Multilayer Film

RO/NF membranes can be prepared by the layer-by-layer assembly of polyelectrolytes onto a charged support (UF or NF supports), where a polycation (e.g., polyallylamine hydrochloride, PAH) and a polyanion (e.g., poly(sodium 4-styrene-sulfonate), PSS) are deposited alternately [35–37]. Fig. 1.5 presents a schematic of layer-by-layer assembly cycle. The rejection property of the membrane usually depends on several factors, such as the type and concentration of polyelectrolytes, ionic condition of the polyelectrolyte solution, contact time, and the number of bilayers (one positively charged layer and one negatively charged layer) [37, 38]. These conditions may influence both the tightness of the "pores" in the membrane skin layer as well as the surface charge, thereby affecting the passage of solutes, especially charged solutes. This method is more widely used for NF membrane preparation, as the monovalent rejection of the polyelectrolyte film is not very high while the divalent ions are much better retained. To enhance the solute rejection and the film stability, cross-linking via heat treatment and/or the use of cross-linking agents are generally adopted [37–40].

## 1.2.4 Recent Advances in Membranes

### 1.2.4.1 Mixed Matrix Membranes

Mixed matrix membranes (MMMs) for RO applications are fabricated by incorporating inorganic nanoparticles into membrane matrix via blending the materials into the polymer solution for the support or the monomer solution for the PA layer [27, 41]. The membrane with nanoparticles embedded PA layer is also named thin-film nanocomposite (TFN) membrane. The pioneering study by Hoek's group [12] reported the fabrication of a TFN RO membrane via immobilizing zeolite NaA nanoparticles in the PA layer at loadings of 0.004%–0.4% (w/v). The results
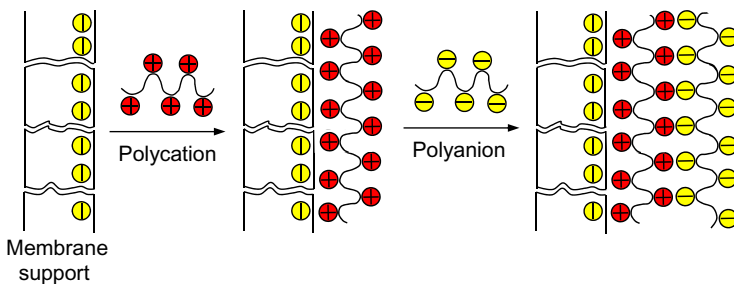


**FIG. 1.5** Schematic of layer-by-layer assembly for preparing polyelectrolyte multilayer film.
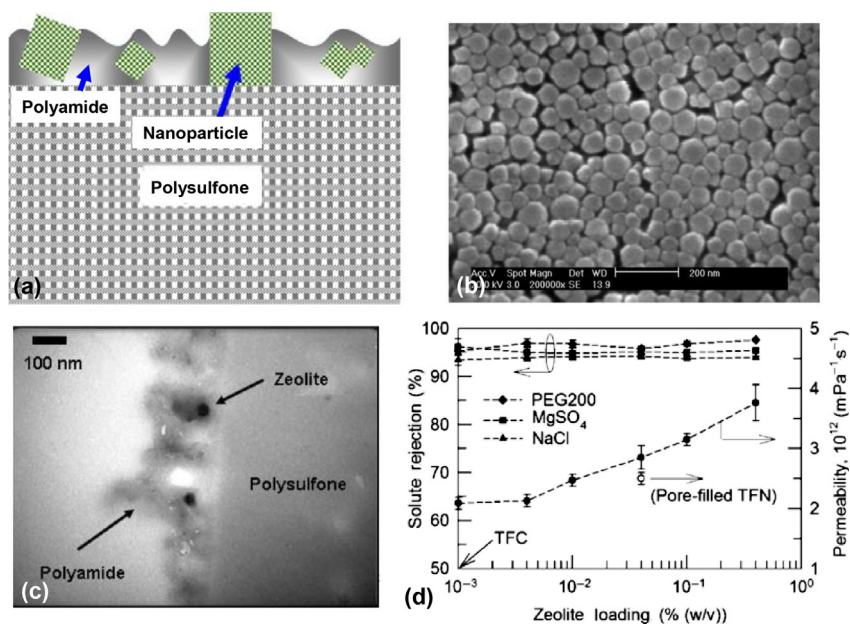
FIG. 1.6   Zeolite nanoparticle-embedded TFN membranes. (A) Schematic of TFN membranes; (B) SEM image of zeolite nanoparticles; (C) TEM image of PA layer with embedded zeolite nanopartilces; and (D) water permeability and solute rejection performance upon zeolite loading. *Reproduced from Jeong BH, Hoek EMV, Yan Y, Subramani A, Huang X, Hurwitz G, et al. Interfacial polymerization of thin film nanocomposites: a new concept for reverse osmosis membranes. J Membr Sci 2007;294(1-2):1-7.*

demonstrated dramatic increase in water permeability upon zeolite incorporation, while solute rejection remained comparable to the pure TFC membrane (Fig. 1.6). The improved intrinsic properties of the TFN membranes could be attributed to the unique pore structure of zeolite molecular sieve particles, which provide a preferential flow path for water molecules through its internal pore structure. In addition, the hydrophilicity and negative charges of zeolite nanoparticles could result in greater affinity for water molecules and thus increase the repulsion of anions [10]. Similar to zeolites that provide size and shape selectivities, silica ($SiO_2$) are also available in various forms and sizes, such as nonporous silica and mesoporous silica. The latter has pore size range of $\sim$2–50 nm, which could make even shorter water flow path in TFN membranes [42]. However, increasing mesopore size of silica may cause sacrificed salt retention [43]. Besides the selection of nanoparticles, the loading of nanoparticles shall also be carefully controlled to minimally affect the crosslinking degree of PA layer [27]. Other promising nanoparticles for MMM preparation include titanium nanotube, silver (Ag), carbon nanotube (CNT), and grapheme oxide (GO), etc. In addition to the enhanced separation

properties, TFN membranes may exhibit improved chemical and thermal stability, improved reaction and sorption capacity [27]. For example, the TFN membrane with Ag incorporated in the selective layer exhibited better anti-biofouling property [44], and CNT embedded TFN membranes showed improved resistance to chlorine and fouling [45].

On the other hand, MMMs with fillers in the supports have also been extensively investigated [27]. Although TFN approach seems to be more effective to improve RO membrane separation property, the nanoparticle incorporation in the supports may benefit in a different way. Similar to the effect of changing polymer solution composition (see Section 1.3.2), a small amount of fillers in the support can significantly change the support's properties, which may subsequently affect the selective layer formation [27]. The hydrophilic inorganic particles such as silica, zeolites, $TiO_2$, and CNTs could increase the hydrophilicity of the support layer. Meanwhile, the changed pore structure (especially the surface characteristics of the support) may contribute to the enhanced water permeability [46]. This approach is very helpful in decreasing the structural parameter of the support layer of FO membranes to reduce the internal concentration polarization effect, thereby increasing FO water flux [46]. Moreover, the fillers with superior mechanical property such as CNT can significantly increase the tensile strength of the MMM membranes [47]. However, there are still some challenges encountered during TFN membrane/MMM fabrication, such as poor dispersion of nanoparticles in the casting solution, agglomeration of nanoparticles in the PA layer, lack of interaction between nanoparticles and membrane matrix (leach out easily), and unknown water and ion transport mechanisms especially for nonporous nanoparticles [10].

### 1.2.4.2 Biomimetic Membranes

Different from the MMMs, the fillers used in biomimetic membranes are aquaporin (AQP) laden vesicles. AQPs are known as water channels, which selectively conduct water molecules while preventing the passage of ions and other solutes (Fig. 1.7A). These characteristics make them perfect for desalination. The single channel permeability of AQP is $\sim2$–$14 \times 10^{-14}$ cm$^3$ water molecules/s (CNT is on the orders of $10^{-14}$–$10^{-12}$ cm$^3$/s but without perfect solute rejection) [48–50]. AQP laden vesicles have been demonstrated to possess high water productivity as compared to that of commercial RO membranes [51]. Among different methods of making biomimetic membranes, TFC membrane is still the most practical and promising approach [48]. Conceptually, the way of immobilizing biomolecules into a PA layer is similar to the TFN membrane fabrication. The fabrication of biomimetic TFC RO membrane has been firstly successfully demonstrated by Zhao et al. [52], and the resultant membrane showed 25% increase in water flux without compromising

(A)

(B)
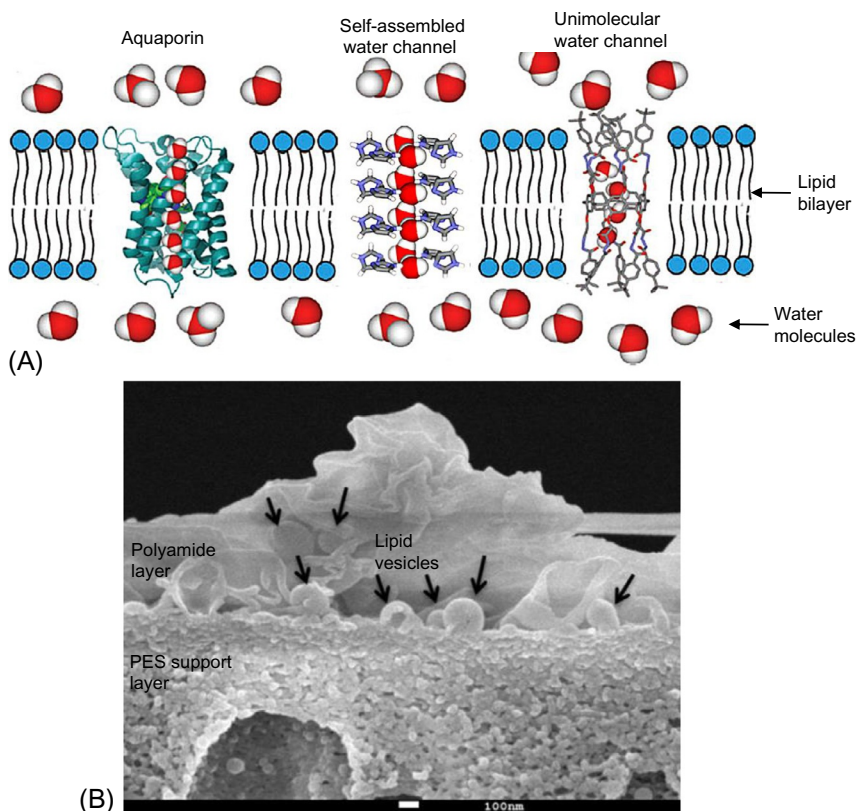
**FIG. 1.7** Water channels and biomimetic membranes. (A) Aquaporin and synthetic water channels (self-assembled artificial water channel and unimolecular artificial water channel); (B) biomimetic TFC RO membranes with incorporated aquaporins (spanned in lipid vesicles) in the PA layer. *Adapted from Li X, Chou S, Wang R, Shi L, Fang W, Chaitra G, et al. Nature gives the best solution for desalination: aquaporin-based hollow fiber composite membrane with superior performance. J Membr Sci 2015;494:68–77; Barboiu M. Artificial water channels—incipient innovative developments. Chem Commun 2016;52(33):5657–65.*

the NaCl rejection. Later Li et al. showed that the water permeability of AQP incorporated TFC hollow fiber membrane reached ∼8 L/m$^2$ h/bar, which was twice as high as those of pristine TFC membrane and commercial BWRO membranes [32]. A cross-sectional SEM image of biomimetic RO membrane is shown in Fig. 1.7B, where the AQP laden vesicles can be observed within the PA layer. Despite the superior separation performances, other issues shall be taken into consideration, such as membrane stability (very few studies looked into the long term stability [53]), scalability, and production cost. A comprehensive review on biomimetic membranes can be found elsewhere [48]. On the other

hand, the high performance of natural water channel has inspired researchers to synthesize artificial water channels with nanotubular structures (Fig. 1.7A), which have potential to overcome the challenges faced by AQP based biomimetic membranes [54].

## 1.3 MEMBRANE PROPERTIES AND CHARACTERIZATIONS

Membrane separation properties generally consist of water permeability and solute rejection, which directly determines membrane productivity. In addition, other important characteristics include hydrophilicity, surface roughness and charge, and membrane stability, which are not only related to the separation properties, but also influence membrane fouling significantly. Correspondingly, membrane characterization (Table 1.4) provides the information about the important membrane properties. It can guide the optimization of membrane fabrication to achieve excellent separation efficiency and fouling resistance.

TABLE 1.4  Membrane Characterization Methods

| | Instrument | Membrane characteristics |
|---|---|---|
| Performance test | Membrane filtration setup | Water permeability, solute rejection, pore size distribution |
| Microscopic methods | SEM | Surface/cross-section features |
| | TEM | Cross-section of membrane/cake layer |
| | CLSM | Membrane structure/foulant composition |
| | AFM | Roughness, surface morphology |
| Spectroscopic methods | FTIR | Membrane/foulant functional groups |
| | XPS | Elements/chemical bonding |
| | EDX | Elemental mapping of membrane/foulants |
| | EIS | Structural information of sublayers |
| Other methods | Goniometer/tensiometer | Hydrophilicity/hydrophobicity |
| | Streaming potential analyzer | Surface charge |
| | AFM force measurement | Interaction force (membrane-foulant) |

*Adapted from Fane AG, Wang R, Tang C. Membrane technology for water: microfiltration, ultrafiltration, nanofiltration, and reverse osmosis. Treatise on water science, vol. 4. Amsterdam; Hackensack, NJ: Elsevier Science; 2011. p. 301.*

### 1.3.1 Membrane Properties

#### 1.3.1.1 Water Permeability and Solute Permeability

The solution-diffusion model assumes that the solute and solvent are absorbed into and diffuse through the membrane selective layer, independent of each other, under the respective chemical potential gradient. According to the model, the water flux $J$ and the solute flux $J_s$ are proportional to the net pressure difference and the concentration difference, respectively, across the membrane [9]:

$$J = A(\Delta P - \Delta \pi) \tag{1.1}$$

$$J_s = B\Delta c \tag{1.2}$$

where $A$ is defined as water permeability coefficient and $B$ is the solute permeability coefficient. $\Delta P$ and $\Delta \pi$ are hydraulic pressure difference and osmotic pressure difference across the membrane, respectively. $\Delta c$ is the concentration difference across the membrane. The transport coefficients in this model can be related to membrane properties as shown below:

$$A = \frac{D_{wm} C_{wm} V_w}{R_g T l_m} \tag{1.3}$$

$$B = \frac{D_{sm} K_{sm}}{l_m} \tag{1.4}$$

where $D_{wm}$ and $D_{sm}$ are water diffusion coefficient and solute diffusion coefficient inside the selective layer, respectively. $C_{sm}$ is the concentration of water inside the selective layer, $V_w$ is the molar volume of water, $K_{sm}$ is the solute partitioning coefficient in the selective layer, $lm$ is the thickness of the selective layer, $R_g$ is universal gas constant, and $T$ is absolute temperature.

The intrinsic rejection of a RO membrane $R_{int}$ is defined as [55]:

$$R_{int} = 1 - \frac{c_p}{c_m} \tag{1.5}$$

where $c_p$ and $c_m$ are the solute concentration in permeate and at the feed solution/membrane interface, respectively, and $R_{int}$ can be determined using the following equation:

$$R_{int} = \left(1 + \frac{B}{A(\Delta P - \Delta \pi)}\right)^{-1} \tag{1.6}$$

According to the above Eqs. (1.3), (1.4), and (1.6), the intrinsic rejection can be improved by increasing the preferential absorption of water molecules to the solutes, enhancing the diffusion coefficient of water molecules inside the selective layer compared with that of solutes, and increasing the applied pressure. This intrinsic rejection is different from

apparent rejection $R$, which is directly measured from experiments and can be greatly affected by the concentration polarization (CP) (as discussed in Section 1.5):

$$R = 1 - \frac{c_p}{c_f} \tag{1.7}$$

where $c_f$ is the solute concentration in the feed. In general, apparent rejection $R$ has smaller value than intrinsic rejection $R_{int}$ due to the CP effect.

In addition to the solution diffusion model, permeate water flux $J$ can be also correlated to the driving force by following Darcy's law and is commonly presented in terms of membrane hydraulic resistance $R_m$ and dynamic viscosity of the permeating water $\eta$ [9]:

$$J = \frac{\Delta P - \Delta \pi}{\eta R_m} \tag{1.8}$$

Although $A$ and $B$ value are the intrinsic properties of a membrane, the measured water flux and rejection are affected by different operating conditions, which generally include the applied pressure, cross-flow velocity of the feed stream, feed concentration (or recovery), and temperature (Fig. 1.8). At a relatively low applied pressure (low water flux level), the water flux increases linearly with applied pressure (Eq. 1.2 or
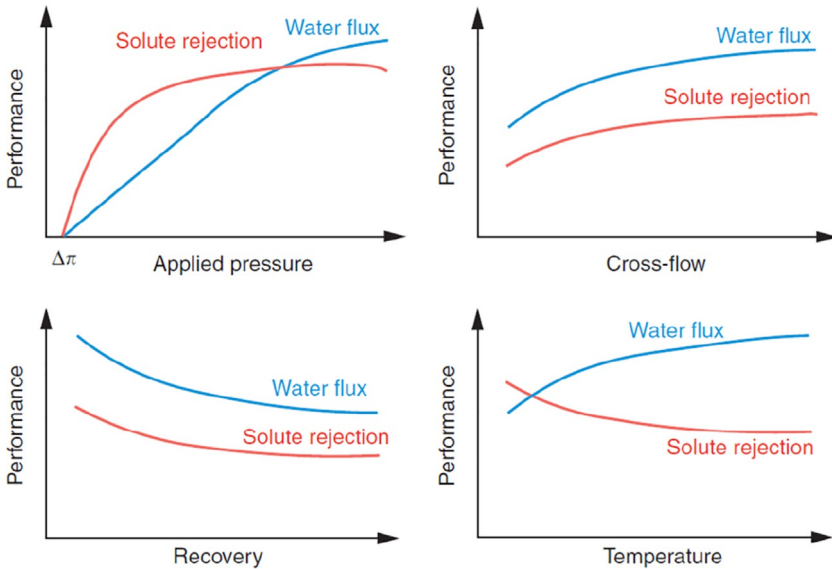


**FIG. 1.8**   Effect of operating conditions on RO membrane performance. *Adapted from Fane AG, Wang R, Tang C. Membrane technology for water: microfiltration, ultrafiltration, nanofiltration, and reverse osmosis. Treatise on water science, vol. 4. Amsterdam; Hackensack, NJ: Elsevier Science; 2011. p. 301.*

Eq. 1.8), the solute rejection also increases with increasing pressure based on the solution diffusion model (Eq. 1.6). However, at a higher applied pressure, the water flux increase deviates from the linear line, due to the increased concentration polarization (i.e., increased concentration/osmotic pressure at membrane surface, see Section 1.5). The increased concentration at membrane surface also results in a lower apparent rejection. Increasing the cross-flow velocity tends to increase both water flux and solute rejection, as a result of reduced concentration polarization. Increasing the recovery or increasing the feed concentration has an effect of reducing both water flux and solute rejection, due to the increased osmotic pressure of the bulk solution. Hence, the recovery for a typical SWRO desalination plant is limited to 50%, while that for a water reclamation plant is controlled below 80% [9]. Increasing the system temperature can lead to an increase in both water flux and solute flux, due to the enhanced diffusion coefficient ($D_{wm}$ and $D_{sm}$) in the membrane selective layer. The solute flux generally increases more drastically than the water flux, so the solute rejection tends to decrease at a higher temperature. It is noted that the change in temperature affects the intrinsic properties of membrane selective layer, while the other operating conditions discussed here are related to the solute concentration at membrane surface.

### 1.3.1.2 Hydrophilicity

Hydrophilicity is a characteristic of materials exhibiting an affinity to water. The surface of a hydrophilic membrane can readily absorb water. In contrast, a hydrophobic membrane has little or no tendency to absorb water. The relative hydrophilicity/hydrophobicity can be determined using contact angle measurement (see Table 1.4). In general, a hydrophilic membrane surface is preferred in RO applications for enhancing water permeability and reducing membrane fouling propensity [56–58]. In this regard, CA membrane surface is preferred compared to a typical TFC membrane surface (a comparison of the two membranes is shown in Table 1.3).

### 1.3.1.3 Surface Roughness

Membrane surface roughness is an important parameter affecting RO membrane fouling. A rougher surface is subject to more membrane fouling due to the decreased shear force over the rougher surface and the increased membrane non-homogeneity (i.e., varied flux distribution over the membrane surface and the local high flux would promote fouling (see Section 1.6)) [9]. TFC RO membranes consisting of PA skin layer have ridge and valley surface morphology that contributes to the roughness. In contrast, CA membrane as well as semi-aromatic NF membranes

possess smoother surface, which is less prone to initial foulant deposition/growth [58–60]. Nevertheless, surface modification can be applied to decrease the roughness, such as the polyvinyl alcohol (PVA) coating on BW30 membrane (Dow Filmtec) [61].

### 1.3.1.4 Surface Charge

The surface charge of a membrane is generally dependent on its charged functional groups or the preferential adsorption of some specific ionic species [9]. Most TFC RO membranes have negatively charged active surfaces at neutral pH, due to the presence of –COOH functional groups on the PA layer. The surface charge can influence solute rejection. For example, the rejection of sodium chloride by a typical RO membrane can be partially contributed by Donnan exclusion effect [13], i.e., $Cl^-$ is retained by the negatively charged surface due to electrostatic repulsion, and $Na^+$ is also retained to maintain charge neutrality [13]. The rejection of charged trace organic solutes is also affected by the charge of membrane [62]. Moreover, the membrane water permeability may be affected by surface charge, as evidenced by the lowest water flux at pH 5 (i.e., the isoelectric point of the membrane) where membrane surface is least charged [63]. On the other hand, the membrane surface charge plays an important role in fouling. The attractive force between oppositely charged foulants and membrane surface has a strong tendency to induce foulant deposition [64]. Membrane-foulant interaction can greatly affect flux performance at initial fouling stage [65].

### 1.3.1.5 Stability

The mechanical, chemical and thermal stabilities of a membrane are important for it to be successfully applied in a membrane process. The requirement of the mechanical strength of a RO membrane depends on its application. For example, SWRO membrane shall withstand higher pressure than the BWRO membrane. The chemical and thermal stabilities are closely related to the type of materials used for membrane fabrication. The RO membranes made of CA have relatively poor stability against chemicals, bacteria, and temperature. The typical operating conditions for such membranes are in range of pH 5–7 to avoid the hydrolysis of the polymer, at temperature below 30°C to avoid the annealing effect (see Section 1.2.1). In contrast, the most widely used TFC RO membranes with PA selective layer are generally more stable, except that it has low chlorine resistance. To prevent unacceptable membrane damage, the chlorine level shall be carefully controlled at a level below 0.1 ppm (Table 1.3) [66, 67].

## 1.3.2 Membrane Characterizations

### 1.3.2.1 Performance Tests

Membrane filtration setup is used to test water permeability and the rejection of the solutes of interests. NaCl rejection is the most commonly used separation efficiency indicator for RO membranes. Molecular weight cut-off (MWCO), defined as the molecular weight of a solute that is rejected by membrane at 90%, is also used to represent the "pore size" or the selectivity of RO membrane (see Table 1.1), although this concept is more commonly used for UF/MF membranes or the support of RO/NF membranes.

### 1.3.2.2 Microscopic Methods

Microscopic characterization is used for the visualization of the morphology and the structure of membrane surface and cross-section. It can be also used for the characterization of fouled membranes to provide the details about the morphology, structure and properties of the foulant cake layer. Scanning electron microscopy (SEM) is the most widely used tool to visualize the surface and cross section of clean and fouled membranes, attributing to its high resolution (as good as 5 nm for polymeric samples) and relatively easy sample preparation [68]. Transmission electron microscopy (TEM) generally provides higher resolution (atomic scale for crystalline samples), especially in detailing the structural information of membranes and foulants [61, 69], but the sample preparation demands more skilled hands and complicated procedures. Compared to SEM and TEM, confocal laser scanning microscopy (CLSM) has lower resolution (microscale), but it is a powerful tool for characterizing membrane biofouling [70] and macroporous structure [68, 71]. Atomic force microscopy (AFM) provides the information about membrane surface topography and is used as a standard method to measure membrane surface roughness [58].

### 1.3.2.3 Spectroscopic Methods

Most spectroscopic methods are used to provide the chemistry information of membranes, such as Fourier transform infrared spectroscopy (FTIR), X-ray photoelectron spectroscopy (XPS), and energy dispersive spectroscopy (EDX). FTIR identifies various chemical bonds of membrane materials based on its adsorption of infrared irradiation [61]. XPS and EDX are able to identify elements. The former is a highly surface-sensitive technique that measures the elemental composition and chemical bonding for top 1–5 nm surface region [9]. It can detect all the elements with an atomic number of 3 and above, with detection limit of parts per thousand for most of the elements. Moreover, the depth profile with XPS can be obtained using ion beam to etch the layers of membrane surface [72]. EDX is a less

sensitive technique, but it can be coupled with SEM or TEM to analyze specific locations with constructed elemental mapping. Different from these chemistry analyzing techniques, electrical impedance spectroscopy (EIS) provides the structural information of membrane supports [73].

### 1.3.2.4 Other Characterization Techniques

The contact angle of a flat-sheet membrane surface is measured using a goniometer to provide the hydrophilicity/hydrophobicity information, while the dynamic contact angle of a hollow fiber membrane is measured using a tensiometer according to Wilhelmy method [74]. The zeta potential is measured using streaming potential analyzer for understanding surface charge characteristics. The measurement can be performed at a series of pHs/ionic strength to obtain the isoelectric point or comprehensive information of surface charge. AFM force measurement (different from imaging mode for obtaining topography) can be used to characterize the interaction between the membrane surfaces (or fouled membrane surfaces) and foulants. Such interaction forces correlate well with membrane fouling behavior [75, 76]. All the characterization methods are summarized in Table 1.4.

## 1.4 MEMBRANE MODULES AND PROCESS OPERATION

### 1.4.1 Membrane Modules

RO membrane modules are generally classified into four groups, including spiral wound module (SWM), hollow fiber module, plate-and-frame module and tubular module. Although the SWM design is dominant in the market, other types of modules can still find their niche applications.

### 1.4.1.1 Spiral Wound Module (SWM)

SWM is the most widely used design for RO/NF membranes applied in water industry. The schematic of SWM is shown in Fig. 1.9A. Flat sheet membranes are sealed on three sides to form leaves attached to a permeate tube along the unsealed edge. A permeate spacer is placed inside each leaf to support the membranes and to allow permeate to flow to the permeate tube. A net-like feed spacer fits between the leaves to define the feed channel height ($\sim$1 mm). It also plays an important role in promoting mass transfer in boundary layer to control the concentration polarization (Section 1.5). Several leaves and feed spacers are wound around the permeate tube to form a SWM with outer rigid casing. There is a trade-off between feed spacer thickness (fouling reduction) and membrane area (productivity). Due to the presence of spacer, the packing density of SWM is lower than that of hollow fiber module.
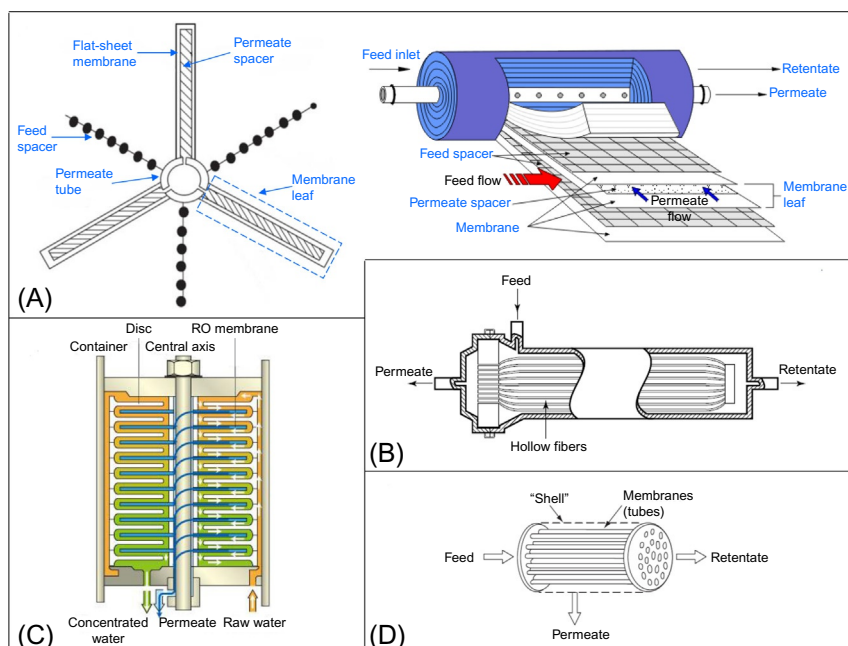
**FIG. 1.9** RO membrane modules. (A) Spiral wound module; (B) hollow fiber module; (C) plate-and-frame module; and (D) tubular module. *Adapted from Baker RW. Reverse osmosis. Membrane technology and applications. John Wiley & Sons, Ltd; 2004. p. 191–235; Fane AG, Wang R, Tang C. Membrane technology for water: microfiltration, ultrafiltration, nanofiltration, and reverse osmosis. Treatise on water science, vol. 4. Amsterdam; Hackensack, NJ: Elsevier Science; 2011. p. 301; kobelco-eco.co. Available from: http://www.kobelco-eco.co.jp/english/product/dt_module/genri.html.*

A typical pressure vessel consists of 6–8 SWMs in series. In a real application, the membrane modules at back are exposed to higher feed salinity and concentration, resulting in lower water flux. The lower flux may lead to less accumulation of particulates, organic foulants and biofilms, despite the increased feed concentration. However, the possibility of mineral scale formation increases, as scaling is much more sensitive to the increased concentration of scale precursors. Therefore, in RO systems the fouling caused by the particulates, organic matters, and biofilm formation is usually more pronounced in the first two membrane elements of the pressure vessels, and the last two elements suffer more from mineral scaling [77].

### 1.4.1.2 Hollow Fiber Module

A large number of membrane fibers are potted in a "shell and tube" arrangement to form a hollow fiber RO membrane module (Fig. 1.9B). It is generally a shell-side feed module, where high pressure up to 1000 psi is applied externally on the shell side of the membranes. Hence, hollow fiber membranes are self-support and have small diameters [78].

Currently, the only large company that makes hollow-fiber RO membrane elements is Toyobo, Japan. The membranes are made of cellulose triacetate, which has high chlorine resistance, but relatively low water permeability (compared to TFC RO membranes). A high productivity per module can be still attained due to the major advantage of high packing density of hollow fiber module. The feed water flow regime in a hollow fiber module is laminar, resulting in little or no "scrubbing effect" and thus promoting membrane fouling. Therefore, it requires more enhanced water pretreatment to remove particulate foulants from the feed.

### 1.4.1.3 Plate-and-Frame Module

Plate-and-frame module uses flat sheet TFC membranes. The membranes and discs are installed to a pressure tight case using the central axis only, allowing easy assembly and disassembly (Fig. 1.9C). The flat sheets can be easily removed from the module and hand-cleaned individually (i.e., easier maintenance and better cleaning). However, it has lower packing density, which is about half of that of SWM. As a result, the plate-and-frame module is not ideal for municipal water RO desalination, but for high solids applications such as food processing [77].

### 1.4.1.4 Tubular Module

As shown in Fig. 1.9D, tubular module employs membranes of tube shape (similar to hollow fiber membrane, but with larger diameter of 5–15 mm), the material of which is generally cellulosic based for RO applications. Similar to the plate-and-frame module, the tubular module has relatively low packing density and allows for robust cleaning methods, therefore it is generally used to process difficult feed streams such as those with high solids content and/or greases and fats. For the control of concentration polarization, a high flow rate is required to achieve turbulent flow regime.

## 1.4.2 Process Operation

Membrane filtration can be operated in cross-flow and dead-end modes. The cross-flow filtration is dominant in most RO and NF processes to provide a steady production rate with a continuous cross-flow to control the concentration polarization and fouling. The dead-end mode is used in some low pressure membrane (i.e., UF/MF) processes for energy saving, such as the pre-treatment of RO where feed streams have relatively low levels of suspended solids or turbidity [9].

Membrane modules can be connected in parallel or in series or the combination of both. In a typical SWRO plant, the modules are arranged in both parallel and series. As shown in Fig. 1.10A, the feed to each pressure
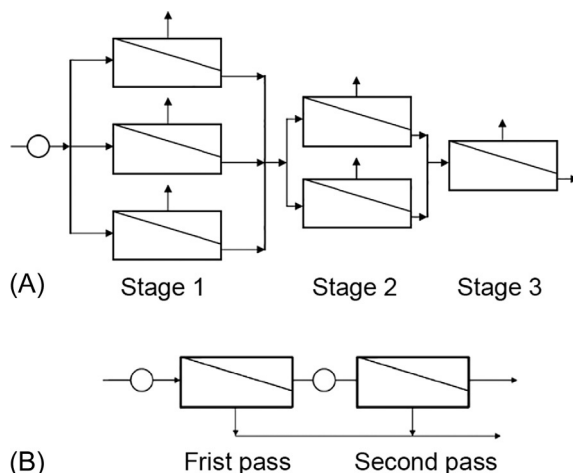
FIG. 1.10  Membrane module/pressure vessel connection in (A) tapered cascade 3:2:1 array; (B) two-pass connection. *Adapted from Fane AG, Wang R, Tang C. Membrane technology for water: microfiltration, ultrafiltration, nanofiltration, and reverse osmosis. Treatise on water science, vol. 4. Amsterdam; Hackensack, NJ: Elsevier Science; 2011. p. 301.*

vessel in Stage 1 is similar because they are connected in parallel. The concentrate from Stage 1 enters as the feed to Stage 2 and possibly followed by Stage 3 to increase the total recovery. As the volume of the feed to Stage 2 and 3 decreases, there are fewer numbers of pressure vessels in parallel, which is known as tapered cascade. Two-pass connection (Fig. 1.10B) is adopted to attain higher removal efficiency of contaminants, such as boron [79, 80]. In this arrangement, the permeate from the first pass enters the second pass as the feed for further treatment. The product water from the second pass will be improved in quality.

## 1.5  CONCENTRATION POLARIZATION

RO membrane process and other pressure driven membrane processes accomplish a separation with their ability to transport one component more readily than another. For a feed containing a solute and a solvent, the solvent permeates through the membrane whereas the solute is (partly) retained by the membrane under applied pressure. Hence, the concentration of the solute in the permeate is lower than that in the bulk of the feed solution. The retained solutes accumulate at the membrane surface, leading to a higher solute concentration near the surface compared to the bulk concentration. This phenomenon is known as concentration polarization (CP) [15]. This concentration build-up leads to a
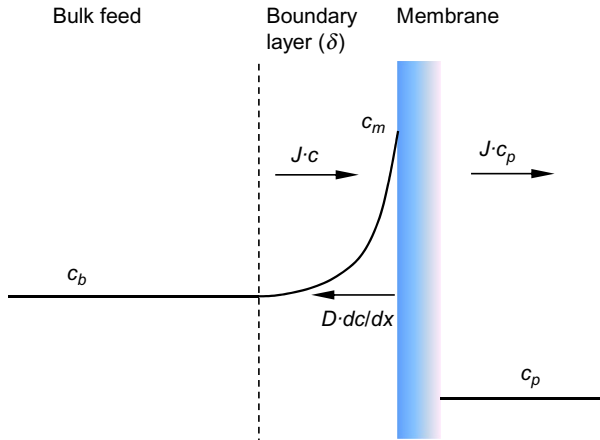
FIG. 1.11    Concentration polarization profile.

diffusive flow of the solute back to the bulk of the feed, which will reach a steady-state condition after certain period of time. The convective transport of the solute will be balanced by the permeate flow through the membrane and the diffusive back transport to the bulk, as shown in Fig. 1.11 and Eq. (1.9):

$$Jc + D\frac{dc}{dx} = Jc_p \tag{1.9}$$

The boundary conditions are:

$$x = 0, c = c_m,$$

$$x = \delta, c = c_b.$$

Integration of Eq. (1.9) results in

$$\ln\frac{c_m - c_p}{c_b - c_p} = \frac{J\delta}{D} \tag{1.10}$$

or

$$\frac{c_m - c_p}{c_b - c_p} = \exp\left(\frac{J\delta}{D}\right) \tag{1.11}$$

The ratio of the diffusion coefficient $D$ and the thickness of boundary layer $\delta$ is called mass transfer coefficient, $k$:

$$k = \frac{D}{\delta} \tag{1.12}$$

The definition of intrinsic rejection $R_{int}$ of a RO membrane can be found in Eq. (1.5). By substituting Eqs. (1.5) and (1.12) into Eq. (1.11), we have:

$$\frac{c_m}{c_b} = \frac{\exp(J/k)}{R_{int} + (1 - R_{int})\exp(J/k)} \tag{1.13}$$

The ratio $c_m/c_b$ is the concentration polarization modulus. It increases with the increasing flux $J$, with increasing $R_{int}$ and with decreasing $k$, when $R_{int} \ll 1$. When the solutes are completely retained by the membrane, i.e., $R_{int} = 1$ and $c_p = 0$, Eq. (1.13) becomes:

$$\frac{c_m}{c_b} = \exp(J/k) \tag{1.14}$$

The mass transfer coefficient $k$ can be determined from Sherwood number $Sh$:

$$Sh = \frac{kd_h}{D} \tag{1.15}$$

Sherwood number is related to Reynolds number $Re$ and Schmidt number $Sc$:

$$Sh = a \cdot Re^b Sc^c (d_h/L)^d \tag{1.16}$$

$$Sc = \frac{v}{D} \tag{1.17}$$

$$Re = \frac{ud_h}{\nu} \tag{1.18}$$

where $d_h$ is the hydraulic diameter, $L$ is the channel length, $u$ is the cross-flow velocity, and $v$ is the kinematic viscosity. In Eq. 1.16, $a$, $b$, $c$, and $d$ are the constant and their magnitudes depend on the flow regime and the geometry of flow channel [9].

CP gives rise to an increased solute concentration at the membrane surface, which decreases the water flux and apparent solute rejection (see Fig. 1.8 and Section 1.3.1.1). The CP of foulants can accelerate membrane fouling [81]. The presence of foulant cake layer on the other hand may also enhance the CP, which is called cake-enhanced CP [82]. This phenomenon is caused by the decreased mass transfer of solutes (e.g., ions) in the cake layer, as a result of decreased shear flow rate within the layer. Because the CP modulus ($c_m/c_b$) increases with increasing water flux and decreasing mass transfer coefficient, the CP can be controlled by operating at a lower water flux, and enhancing the mass transfer at membrane surface via increasing the cross-flow velocity and/or the use of a well-designed spacer, etc.

## 1.6 MEMBRANE FOULING AND CONTROL

Membrane fouling is defined as the deposition of contaminants on a membrane surface and/or inside membrane pores. Non-porous RO membranes generally suffer from the foulant cake deposition on the membrane
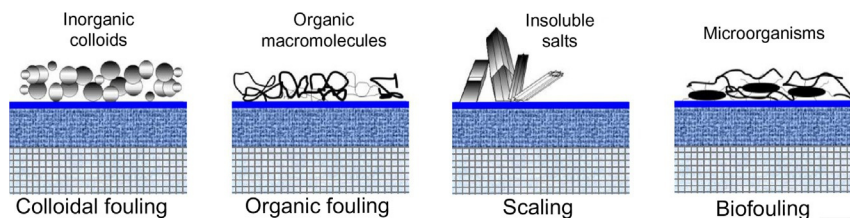
FIG. 1.12    Types of membrane foulants.

surface. According to the nature of foulants, membrane fouling can be categorized into colloidal fouling, organic fouling, inorganic scaling, and biofouling (Fig. 1.12).

Similar to the CP, membrane fouling can directly lead to water flux drop during constant pressure operation. However, the foulant layer remains on the membrane surface when the permeate flux is reduced to zero, while CP disappears in absence of permeate flux. The timescale for CP to reach a stable condition or disappear is short, while the fouling typically occurs over longer timescale (rapid fouling can occur under unfavorable conditions). Although CP and fouling are two different phenomena, CP can accelerate membrane fouling as CP causes increased foulant concentration at membrane surface, while foulant deposition can result in enhanced CP.

## 1.6.1 Factors Affecting Membrane Fouling

A great number of factors can affect RO membrane fouling. In general, these factors are classified into three groups as shown in Fig. 1.13, including membrane properties, feed water composition, and hydrodynamic conditions.

### 1.6.1.1 Membrane Properties

The membrane properties such as hydrophilicity, roughness, and surface charge can affect membrane fouling. Generally, a membrane with hydrophilic and smooth surface and low surface charge is preferred to resist fouling at initial stage [57, 58, 83, 84]. For example, a NF membrane with a smooth and hydrophilic surface exhibited more sustainable flux performance at the initial stage of bovine serum albumin (BSA) fouling, as compared with other RO/NF membranes of rougher and less hydrophilic surfaces [65]. In addition, the surface functional groups are also important to membrane fouling. The $-COO^-$ on the TFC PA membrane surface may interact with specific ions such as $Ca^{2+}$, which accelerates membrane fouling [85]. However, these effects could hardly be observed under severe fouling conditions such as at longer fouling duration, as

**Feedwater composition**

Foulant type, concentration
pH, ionic strength,
specific ions such as $Ca^{2+}$

**Hydrodynamic conditions**

Flux
Cross-flow velocity
Recovery
Temperature
Module and spacer design

**Membrane properties**

Roughness
Charge
Hydrophobicity
Surface functional groups
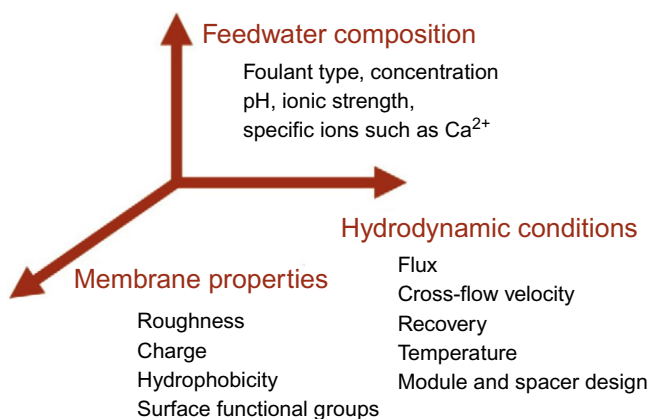
**FIG. 1.13** Factors affecting membrane fouling. *Reprinted from Tang CY, Chong TH, Fane AG. Colloidal interactions and fouling of NF and RO membranes: a review. Adv Colloid Interface Sci 2011;164(1–2):126–43.*

fouling is dominated by foulant-deposited-foulant interaction instead of foulant-membrane interaction [76, 86].

### 1.6.1.2 Feed Water Composition

The type and concentration of foulants can significantly affect membrane fouling. For instance, the feed water containing a high concentration of sparingly soluble salts is susceptible to scale formation [87], while the presence of microorganisms and nutrients may promote biofouling. On the other hand, the solution chemistry such as pH, ionic strength, and specific ions can drastically change the physiochemical properties of foulants (i.e., functional groups, size, charge, conformation, etc.) [88], or affect the interaction between foulants or between foulants and membranes [89]. Unfavorable solution conditions can lead to less repulsion between foulants and/or foulants and membrane, resulting in severe organic and colloidal fouling [65, 86, 90–92].

### 1.6.1.3 Hydrodynamic Conditions

Hydrodynamic conditions, including the level of water flux/pressure, cross-flow velocity, recovery, temperature and module/spacer design, are important to membrane fouling. The influence of some factors on membrane performance (in the absence of foulants) has been discussed in Section 1.3.1.1. Those factors affecting CP can also influence the membrane fouling. For example, a high-water flux level leads to more severe CP of foulants, which may promote gel formation on the membrane surface. In addition, the greater drag force towards membrane surface may facilitate foulant deposition [65]. Increasing cross-flow velocity enhances mass

transfer at membrane surface, resulting in less CP as well as less foulant deposition [65]. The use of spacer helps to increase turbulence of flow and thus enhance the mass transfer, but it is noted that the poor design of spacer (e.g., presence of hydraulic dead zones) may promote foulant deposition [85, 93].

## 1.6.2 Fouling Mitigation

In addition to the control of the parameters that affect fouling (discussed in Sections 1.6.1.1–1.6.1.3), other measures are also commonly applied to mitigate fouling, including pretreatment of feed water, enhancing membrane antifouling property, using chemicals/agents during RO operation and frequent cleaning [94]. These methods are summarized as follows:

- Properly designed RO system and operating conditions. For example, selection of suitable membrane modules and operating conditions (i.e., recovery, cross-flow velocity, pressure or flux level, etc.) according to the feed water composition.
- Enhancing antifouling property of the membrane. To make membrane surface smoother and more hydrophilic is a common strategy to reduce fouling, which can be achieved by surface modification through coating and grafting, etc. [94]. Recently, use of novel materials such as silver nanoparticles and graphene oxide (GO) to impart anti-biofouling properties has become an attractive direction [27, 94].
- Pretreatment of feed solution. A good pretreatment system is essential to achieve a long RO membrane life. Different pretreatment processes can be chosen depending on the feed composition and the RO membrane materials/modules. The following methods are commonly used in pretreatment: coagulation and granular media filtration, UF/MF, adsorption by activated carbon, chlorination [15, 95]. It is noted that CA RO membrane demands bacteria-free feed water and the chlorination in pretreatment is an essential step [19].
- Use of chemicals during RO process. For example, adding a complexing agent such as ethylenediaminetetraacetic acid (EDTA) to reduce free calcium ions is helpful in fouling control; pH adjustment is important to alter the charge of proteins and thereby affecting the foulant-foulant or foulant-membrane interactions.
- Cleaning. Although the above-mentioned methods are able to reduce fouling to certain extent, various cleaning methods are always employed in practical applications. Physical cleaning and chemical cleaning are the common methods used for RO membranes [15, 94]. A typical cleaning regime consists of flushing membrane modules by circulating cleaning solutions at a high flow rate, followed by soaking

and then second time flush, and so on. The commonly used chemical cleaning agents include acids, alkalis, chelatants, detergents and sterilizers [15, 19].

## 1.7 RO APPLICATIONS

RO has received various applications mainly comprising water production and solute concentration. The former produces clean water/desalted water (solvent) from feed water while the latter focuses on the production of concentrated solutes.

### 1.7.1 Desalination and Water Reclamation

#### 1.7.1.1 Desalination

More than one-half of the RO systems currently installed are for the desalination of seawater and brackish water [96]. Table 1.5 presents a comparison of the components in seawater and brackish water. The data show

**TABLE 1.5**   Comparison of the Components in Seawater and Brackish Water

| Components | Seawater (mg/L) | Brackish water 1 (mg/L) | Brackish water 2 (mg/L) |
| --- | --- | --- | --- |
| $Ca^{2+}$ | 440–670 | 175 | 179 |
| $Mg^{2+}$ | 1400–1550 | 58 | 132 |
| $Ba^{2+}$ | 0.010 | <0.10 | 0.06 |
| $Sr^{2+}$ | 5–7.5 | – | 26.4 |
| Boron | 4.9–5.3 | – | – |
| $Na^+$ | 12,000 | 170 | 905 |
| $Cl^-$ | 21,000–23,000 | 72 | 1867 |
| $SO_4^{2-}$ | 2400–2670 | 670 | 384 |
| $HCO_3^-$ | 120–142 | 260 | 146 |
| TDS | 38,000–40,000 | 1320 | 3664 |
| DOC | <2 | – | 1.4 |

*Note*: the seawater source is surface water from the Mediterranean Sea (Toulon, France), and both of the brackish water sources are groundwaters (the first is from Port Hueneme, CA, USA; the second is from Martin county, FL, USA).
*Adapted from Greenlee LF, Lawler DF, Freeman BD, Marrot B, Moulin P. Reverse osmosis desalination: water sources, technology, and today's challenges. Water Res 2009 43(9):2317–48.*

obvious differences between the two types of water. The seawater has a much higher total dissolved solids (TDS) concentration, mainly due to the large amounts of $Na^+$ and $Cl^-$ (the ratios of Na/TDS and Cl/TDS in seawater are significantly higher than that in brackish water). The boron content in seawater is generally higher than that in brackish water [97].

A typical RO system for water production consists of pretreatment, membrane separation, and post treatment [9, 98]. The examples of different RO systems are shown in Table 1.6. For seawater desalination, SWRO membranes are used to attain high salt rejection during the membrane process. The high osmotic pressure (high salinity) requires an operating pressure of ~60–70 bar, making SWRO more energy intensive than other RO/water source options. Media filtration or low-pressure membrane process (MF or UF) is adopted for the pretreatment of seawater to reduce membrane fouling. The product water is usually conditioned by the addition of calcium ions to meet the requirement of World Health Organization (WHO) [99]. The concentrate brine will pass through an energy recovery device prior to the discharge to ocean or further treatment. Since the end of the 1970s, the energy consumption of SWRO has been reduced significantly from more than 15 kWh/m$^3$ to ~2 kWh/m$^3$ due to continual technological improvements (Fig. 1.14) [8]. The current energy consumption is close to the thermal minimum energy of desalination (1.06 kWh/m$^3$ for seawater of 35 g/L at 50% recovery) [8]. The actual consumption is higher than this minimum value, as desalination plants are finite in size and do not operate as a reversible thermodynamic process [8]. BWRO is usually operated at modest-size plants (not a limitless source) with higher recovery (75%–90%). The lower salinity of brackish water requires much lower pressure (6–30 bar) [97] and thus lower energy consumption.

SWRO generally faces the fouling problem caused by particulate matter, organic compounds, and biological growth, while the high recovery in BWRO causes severe scaling problems mainly due to the calcium sulfate and carbonate precipitation. In addition, boron removal of RO system is also a concern for achieving drinking water standard, due to the low rejection of boron compared to other ions at neutral pH [97]. The high boron concentration in seawater often requires a second RO pass to further reduce the boron content to meet the drinking water quality (<2.4 mg/L [100]). Although boron concentration in brackish water is low, the relatively low rejection of BWRO membrane and higher recovery still demands another boron removal strategy, such as boron-specific ion exchange [97].

### 1.7.1.2 Water Reclamation/Wastewater Treatment

Wastewater sources that use RO treatment include municipal wastewater, industrial wastewater, and other contaminated water sources (e.g., leachate water). When the feed water is wastewater or treated wastewater,

**TABLE 1.6** Examples of RO Systems for Desalination and Water Reclamation

| Application | Source water | Membranes | Pressure (bar) | Pretreatment | Posttreatment | Target removals |
|---|---|---|---|---|---|---|
| Desalination | Seawater | SWRO | 60–70 | Media filtration or MF/UF | Calcium addition, alkalinity adjustment, disinfection | Salinity |
| | Brackish groundwater | BWRO | 6–30 | Filtration | | Salinity |
| Reclamation | Treated wastewater | BWRO | <20 bar | MF/UF | Advanced oxidation treatment | Pathogens, trace organics |
| | Wastewater | BWRO | | Membrane bioreactor (MBR) | Advanced oxidation treatment | Pathogens, trace organics |

Adapted from Fane AG, Wang R, Tang C. Membrane technology for water: microfiltration, ultrafiltration, nanofiltration, and reverse osmosis. Treatise on water science, vol. 4. Amsterdam; Hackensack, NJ: Elsevier Science; 2011. p. 301; Greenlee LF, Lawler DF, Freeman BD, Marrot B, Moulin P. Reverse osmosis desalination: water sources, technology, and today's challenges. Water Res 2009 43(9):2317–48.
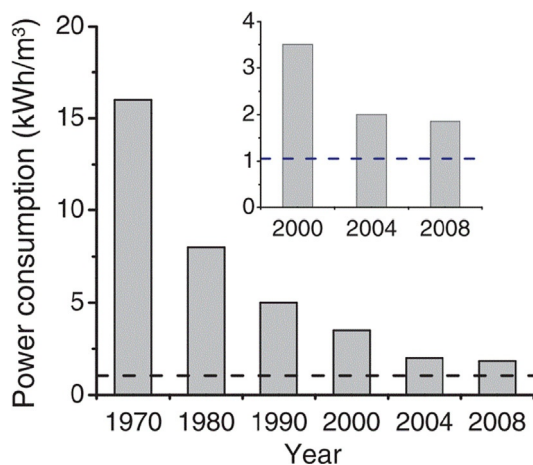
FIG. 1.14  The change in energy consumption for the reverse osmosis stage in SWRO plants from the 1970s to 2008. The *horizontal dashed line* corresponds to the theoretical minimum energy (1.06 kWh/m$^3$) required for desalination of 35 g/L seawater at 50% recovery. The energy data presented here exclude the energy required for intake, pretreatment, post-treatment, and brine discharge. *Reprinted from Elimelech M, Phillip WA. The future of seawater desalination: energy, technology, and the environment. Science 2011;333(6043):712–7.*

the target removals are pathogens and trace organics, instead of salinity (Table 1.6). In the case of municipal wastewater, the treated wastewater (i.e., secondary effluent) as RO feed is more common, as it builds on the existing municipal wastewater infrastructure. MF/UF pretreatment is generally operated in the dead-end cycles to provide the feed with low solid content to the RO unit. The low salinity content allows the RO to operate at much lower pressure with higher recovery (75% vs. 50%) as compared to a SWRO unit. Advanced oxidation (e.g., UV) as post treatment can provide an added barrier to virus and oxidize the trace organics present in the RO permeates. The high quality permeate water produced by the dual membrane reclamation processes (MF/UF + RO) is generally suitable for the demanding industrial applications (e.g., ultrapure water for the electronics, pharmaceutical, and power generation industries) and indirect potable reuse (IPR). A comprehensive review of membrane reclamation plant and comparison with SWRO was given by Côté et al. [99]. The detailed reviews on pretreatment and retentate treatment technology can be also found elsewhere [95, 101, 102].

The target for water treatment varies for different industrial wastewaters and contaminated water sources. For example, the targets of RO treatment for landfill leachate and electroplating wastewater are for purification and discharge [103, 104], while the wastewaters from dairy industry, textile industry, and olive mill are often reused after RO

treatment [105–107], and some RO process is targeted for zero liquid discharge [108]. The pretreatment and post-treatment processes depend on both the wastewater sources and the final target. For high recovery or zero liquid discharge, controlled crystallization can be used as a post treatment [103, 108]. When treated water is recycled as process water (without the demand of ultrapure water quality), the wastewater is generally pretreated by UF and no post treatment is needed after RO unit [106]. One of the most attractive applications is to separate valuable products from wastewater, such as the reclamation of plating wastewater and recovery of heavy metals [19]. An example is the recovery of nickel from nickel plate rinsing tanks. The use of RO unit produces a permeate water with low concentration of nickel for reuse and a retentate stream with concentrated nickel that can be sent back to plating tank [19].

## 1.7.2  Ultrapure Water Production

Ultrapure water production for the electronics industry is an established application of RO. The usual feed is the municipal drinking water, typically containing less than 200 mg/L dissolved solids. To meet the requirement of extraordinarily high purity (almost only water molecules present in the ultrapure water, refer to Table 1.7 for the specifications of drinking water and ultrapure water), the municipal drinking water undergoes extensive treatment with a complex array of operations [19]. As the key part of the process, RO unit removes more than 98% of dissolved salts and particulates under high recovery (>90%). In addition to RO, carbon absorption removes dissolved organics, ion exchange step removes trace ionic impurities, and UV sterilizers and cartridge microfilters are used to maintain sterility [19].

## 1.7.3  Solute Concentration

### 1.7.3.1  Concentration of Juices and Dairy Products

The start of the interests in RO concentration of fruit juices dates back to 40 years ago, due to its advantages over conventional thermal based processes: (1) low damage to the thermal sensitive components, (2) low energy consumption, and (3) ability to produce high quality products (retain the flavor of products) [96]. Prior studies have reported RO applications for various juice concentrations, including apple, pear, grape, orange, blackcurrent, etc. [109–113] (Table 1.8). The high solid content in the feed preferentially uses the plate-and-frame module or tubular module which is suitable for tougher cleaning methods [96] (the description of different RO membrane modules can be found in Section 1.4). In an example of the concentration of apple juice, the RO-evaporation system

**TABLE 1.7**    Specifications for Typical Municipal Drinking Water and Ultrapure Water

| | Ultrapure water | Drinking water |
|---|---|---|
| Resistivity (MΩ cm) | 18.2 | – |
| TOC (ppb) | <5 | 5000 |
| Particles/L by laser >0.1 μm | <100 | – |
| Bacteria/100 mL by culture | <0.1 | <30 |
| Silica, dissolved (ppb) | <3 | 3000 |
| Boron (ppb) | <1 | 40 |
| Ions (ppb) | | |
| $Na^+$ | <0.01 | 3000 |
| $K^+$ | <0.02 | 2000 |
| $Cl^-$ | <0.02 | 10,000 |
| $Br^-$ | <0.02 | – |
| $NO_3^-$ | <0.02 | – |
| $SO_4^{2-}$ | <0.02 | 15,000 |
| Total ions | <0.1 | <100,000 |

*Adapted from Baker RW. Reverse osmosis. Membrane technology and applications. John Wiley & Sons, Ltd; 2004. p. 191–235.*

shows excellent performance [117]. RO as pre-concentration step can remove more than 50% of the water prior to evaporation, while maintaining 98%–99% of sugar and acid as well as 80%–90% of volatile flavors in the concentrate. It achieves a sugar concentration level of 20–25°Brix, while the subsequent evaporation can boost the level to above 75°Brix. This combined system can save energy of 60%–75% as compared to direct evaporation. Meanwhile, the permeate water from the RO unit can be recycled as process water (i.e., water reuse) [117].

Similar to fruit juices, milk and whey can be also concentrated by RO, with the advantage of low temperature operation. Pre-concentration of milk and whey prior to transportation can reduce transportation costs [96, 117]. The main application of RO seems to be the treatment of dairy process waters and effluents, in order to recover milk proteins and lactose, while obtaining a permeate that can be recycled for rinsing or cooling [105, 117]. Most of earlier work used spiral wound modules (SWM) because of their availability and low cost [105, 117]. On the other hand, concentration of milk by RO has great potential for ice-cream manufacturing, as ~70% of water can be removed while the solids can be well retained [117].

TABLE 1.8    Performance of RO Membrane in Juice Concentration and Dealcoholization

| | Feed | Membrane | Initial concentration | Final concentration | Operating conditions | Ref. |
|---|---|---|---|---|---|---|
| Juices | Apple juice | Tubular PA membrane | 11°Brix | 26°Brix | $P = 55$ bar, $T = 35$°C | [109] |
| | Blackcurrent juice | Tubular PA membrane | 16.5°Brix | 28.6°Brix | $P = 60$ bar, $T = 25$°C | [110] |
| | Orange juice | Plate-and-frame PA membrane | 8°Brix | 36°Brix | $P = 60$ bar, $T = 25$°C | [111] |
| | Grape juice | Plate-and-frame PA membrane | 14.7°Brix | 28.2°Brix | $P = 60$ bar, $T = 40$°C | [112] |
| | Pear juice | PA membrane (pilot plant) | 11.9°Brix | 28.9°Brix | $P = 40$ bar, $T = 25$–27°C | [113] |
| Fermented beverage | Home-made alcoholic beverage[a] | Spiral wound membrane | 5.5%v/v | 0.5%v/v | $P = 35$ bar, $T = 0$°C | [114] |
| | Beer[b] | CA membrane | 5.28%v/v | – | $P = 35$ bar, $T = 0$°C, $R_E = 3.6\%$ | [115] |
| | Red wine[c] | CA membrane | 12%v/v | 8.4%v/v | $P = 16$ bar, $T = 30$°C, $R_E = 2.5\%$ | [116] |

Note: $P$, feed pressure (bar); $T$, temperature (°C); $R_E$, ethanol rejection (%); initial and final concentrations for juices are in the unit of °Brix (sugar content) and those for fermented beverages are in the unit of %v/v (alcohol concentration).
[a] Operated in continuous mode.
[b] Operated in diafiltration mode.
[c] Operated in semi-continuous mode.

### 1.7.3.2 *Dealcoholization of Fermented Beverage*

The demand for low-alcohol and alcohol-free drinks has been constantly growing. RO can be used to reduce the alcohol from wine, beer and cider without altering their flavor and quality [96, 117, 118]. Because this process is carried out at low temperature compared to traditional distillation, it does not involve phase change for alcohol removal [115]. Examples of RO dealcoholization are listed in Table 1.8. The dealcoholization by RO often comprises the following steps [117]:

- Pre-concentration—the fermented beverage is separated into a permeate stream containing water and alcohol, and a retentate stream consisting of concentrated drinks and flavors.
- Diafiltration—addition of desalted and deoxygenized water by keeping the feed volume constant to achieve higher removal of alcohol and higher retention of desired aroma.
- Alcohol adjustment—fine tuning of taste and alcohol content by addition of desalted and deoxygenized water.

## 1.7.4 Organic Solvent Separation

Although the RO membranes are designed for the applications related to aqueous solution, the membrane materials are considered chemically resistant to some organic solvent, driving the applications of RO for the treatment of solvent-contaminated wastewater [96]. Earlier work has shown the feasibility of separation of small solvent molecules from larger hydrocarbons using cellulose acetate (CA) and TFC polyamide (PA) RO membranes [96]. However, the membrane materials CA and polysulfone are not resistant to certain solvents or hydrocarbons [96, 119]. Hence, it was later found that some other polymers such as polyimide show good resistance to solvent [119]. One commercial project by Mobil Oil developed a RO process to separate up to 50% solvent from the dewaxed oil using polyimide SWMs to save the energy of conventional solvent dewaxing process [19, 119]. Recently, solvent resistant nanofiltration (NF) has gained more and more interests in the field of organic solvent separation; as the solvent resistant NF membranes show significantly better stability during long term run and much higher solvent flux, as compared to the conventional RO membranes [120].

## 1.8 CONCLUSIONS

Reverse osmosis (RO) has a significant role in water industry. It is widely used for desalination, water reclamation and ultrapure water production. In addition, it also has niche applications such as solute

concentration and selective separation. Since the introduction of first thin-film composite membranes in 1980s, TFC PA membranes have continuously advanced and are still the state-of-the-art RO membranes with more than 100 times better performance than their first generation membranes [19]. The further improvement of membrane performance may rely on the novel materials (e.g., emerging mixed matrix membranes and biomimetic membranes) [4]. Besides high-performance membranes, the successful operation of RO plants also depends on smart membrane element design/process design, and appropriate process operating conditions, to minimize the negative effects from concentration polarization and membrane fouling, to meet the requirement of product water as well as to reduce capital cost and energy consumption. For example, the optimization of membrane module design with improved hydrodynamics, improved cleaning methods and energy recovery devices can contribute significantly to energy and cost saving.

# References

[1] Wang LK, Chen JP, Hung YT, Shammas NK, editors. Handbook of environmental engineering. Membrane and desalination technologies, vol. 13. Totowa, NJ: Humana Press; 2011.

[2] Loeb S, Sourirajan S. Sea water demineralization by means of an osmotic membrane. University of California, Department of Engineering; 1960.

[3] Cadotte JE, Peterson RJ. Thin-film composite reverse-osmosis membranes: origin, development, and recent advances. In: Turbak AF, editor. Synthetic membranes, vol. 1 desalination. p. 350, ACS Symposium Series, 53. Washington, DC: Am. Chemical Soc.; 1981.

[4] Park HB, Kamcev J, Robeson LM, Elimelech M, Freeman BD. Maximizing the right stuff: the trade-off between membrane permeability and selectivity. Science 2017;356 (6343):1138–48.

[5] Lee KP, Arnot TC, Mattia D. A review of reverse osmosis membrane materials for desalination—development to date and future potential. J Membr Sci 2011;370(1):1–22.

[6] Rodríguez-Calvo A, Silva-Castro GA, Osorio F, González-López J, Calvo C. Reverse osmosis seawater desalination: current status of membrane systems. Desalin Water Treat 2015;56(4):849–61.

[7] Birkett J, Truby R. A figure of merit for appreciating improvements in RO membrane performance. International Desalination Association News; 2007.

[8] Elimelech M, Phillip WA. The future of seawater desalination: Energy, technology, and the environment. Science 2011;333(6043):712–7.

[9] Fane AG, Wang R, Tang C. Membrane technology for water: microfiltration, ultrafiltration, nanofiltration, and reverse osmosis. Treatise on water science, vol. 4. Amsterdam; Hackensack, NJ: Elsevier Science; 2011;301.

[10] Lau WJ, Gray S, Matsuura T, Emadzadeh D, Paul Chen J, Ismail AF. A review on polyamide thin film nanocomposite (TFN) membranes: history, applications, challenges and approaches. Water Res 2015;80:306–24.

[11] Giwa A, Akther N, Dufour V, Hasan SW. A critical review on recent polymeric and nano-enhanced membranes for reverse osmosis. RSC Adv 2016;6(10):8134–63.

[12] Jeong BH, Hoek EMV, Yan Y, Subramani A, Huang X, Hurwitz G, et al. Interfacial polymerization of thin film nanocomposites: a new concept for reverse osmosis membranes. J Membr Sci 2007;294(1–2):1–7.

[13] Schäfer AI, Fane AG, Waite TD. In: Schäfer AI, Fane AG, Waite TD, editors. Nanofiltration—principles and applications. UK: Elsevier Advanced Technology; 2005.

[14] Wijmans JG, Baker RW. The solution-diffusion model: a review. J Membr Sci 1995;107(1):1–21.

[15] Mulder M. Basic Principles of Membrane Technology. The Netherlands: Kluwer Academic Publishers; 1996.

[16] Yan J, Lau WWY. Effect of internal coagulant on morphology of polysulfone hollow hiber membranes. I. Sep Sci Technol 1998;33(1):33–5.

[17] Nguyen TPN, Yun ET, Kim IC, Kwon YN. Preparation of cellulose triacetate/cellulose acetate (CTA/CA)-based membranes for forward osmosis. J Membr Sci 2013;433:49–59.

[18] Ong RC, Chung TS, de Wit J, Helmer BJ. Novel cellulose ester substrates for high performance flat-sheet thin-film composite (TFC) forward osmosis (FO) membranes. J Membr Sci 2014;473:63–71.

[19] Baker RW. Reverse osmosis. Membrane technology and applications. John Wiley & Sons, Ltd; 2004. p. 191–235.

[20] Kumano A, Fujiwara N. Cellulose triacetate membranes for reverse osmosis. In: Advanced membrane technology and applications. Wiley; 2008. p. 21–46.

[21] AlBatniji MS. Performance optimization of brackish water reverse osmosis desalination plants in Gaza strip. The Islamic University of Gaza; 2016.

[22] Pageau L, Sourirajan S. Improvement of porous cellulose acetate reverse osmosis membranes by change of casting conditions. J Appl Polym Sci 1972;16(12):3185–206.

[23] Idris A, Ismail AF, Noordin MY, Shilton SJ. Optimization of cellulose acetate hollow fiber reverse osmosis membrane production using Taguchi method. J Membr Sci 2002;205(1–2):223–37.

[24] Saljoughi E, Mohammadi T. Cellulose acetate (CA)/polyvinylpyrrolidone (PVP) blend asymmetric membranes: preparation, morphology and performance. Desalination 2009;249(2):850–4.

[25] Petersen RJ. Composite reverse osmosis and nanofiltration membranes. J Membr Sci 1993;83(1):81–150.

[26] Freger V. Kinetics of film formation by interfacial polycondensation. Langmuir 2005;21(5):1884–94.

[27] Li D, Yan Y, Wang H. Recent advances in polymer and polymer composite membranes for reverse and forward osmosis processes. Prog Polym Sci 2016;61:104–55.

[28] Wei J, Liu X, Qiu C, Wang R, Tang CY. Influence of monomer concentrations on the performance of polyamide-based thin film composite forward osmosis membranes. J Membr Sci 2011;381(1–2):110–7.

[29] Xu G-R, Xu J-M, Feng H-J, Zhao H-L, Wu S-B. Tailoring structures and performance of polyamide thin film composite (PA-TFC) desalination membranes via sublayers adjustment-a review. Desalination 2017;417:19–35.

[30] Ghosh AK, Hoek EMV. Impacts of support membrane structure and chemistry on polyamide–polysulfone interfacial composite membranes. J Membr Sci 2009;336 (1–2):140–8.

[31] Lee J, Jang JH, Chae HR, Lee SH, Lee CH, Park PK, et al. A facile route to enhance the water flux of a thin-film composite reverse osmosis membrane: incorporating thickness-controlled graphene oxide into a highly porous support layer. J Mater Chem A 2015;3(44):22053–60.

[32] Li X, Chou S, Wang R, Shi L, Fang W, Chaitra G, et al. Nature gives the best solution for desalination: aquaporin-based hollow fiber composite membrane with superior performance. J Membr Sci 2015;494:68–77.

[33] Ahmed FE, Lalia BS, Hashaikeh R. A review on electrospinning for membrane fabrication: challenges and applications. Desalination 2015;356:15–30.

[34] Bui NN, McCutcheon JR. Nanofiber supported thin-film composite membrane for pressure-retarded osmosis. Environ Sci Technol 2014;48(7):4129–36.

[35] Malaisamy R, Talla-Nwafo A, Jones KL. Polyelectrolyte modification of nanofiltration membrane for selective removal of monovalent anions. Sep Purif Technol 2011;77(3):367–74.

[36] Liu C, Shi L, Wang R. Crosslinked layer-by-layer polyelectrolyte nanofiltration hollow fiber membrane for low-pressure water softening with the presence of $SO_4^{2-}$ in feed water. J Membr Sci 2015;486:169–76.

[37] Xu GR, Wang SH, Zhao HL, Wu SB, Xu JM, Li L, et al. Layer-by-layer (LBL) assembly technology as promising strategy for tailoring pressure-driven desalination membranes. J Membr Sci 2015;493:428–43.

[38] Duong PHH, Zuo J, Chung T-S. Highly crosslinked layer-by-layer polyelectrolyte FO membranes: understanding effects of salt concentration and deposition time on FO performance. J Membr Sci 2013;427:411–21.

[39] Qiu C, Qi S, Tang CY. Synthesis of high flux forward osmosis membranes by chemically crosslinked layer-by-layer polyelectrolytes. J Membr Sci 2011;381(1–2):74–80.

[40] Sullivan DM, Bruening ML. Ultrathin, cross-linked polyimide pervaporation membranes prepared from polyelectrolyte multilayers. J Membr Sci 2005;248(1–2):161–70.

[41] Hoek EMV, Ghosh AK. Nanotechnology-based membranes for water purification. In: Nanotechnology applications for clean water. William Andrew Publishing; 2009. p. 47–58.

[42] Yin J, Kim ES, Yang J, Deng B. Fabrication of a novel thin-film nanocomposite (TFN) membrane containing MCM-41 silica nanoparticles (NPs) for water purification. J Membr Sci 2012;423-424:238–46.

[43] Wu H, Tang B, Wu P. Optimizing polyamide thin film composite membrane covalently bonded with modified mesoporous silica nanoparticles. J Membr Sci 2013;428:341–8.

[44] Liu Y, Rosenfield E, Hu M, Mi B. Direct observation of bacterial deposition on and detachment from nanocomposite membranes embedded with silver nanoparticles. Water Res 2013;47(9):2949–58.

[45] Zhao H, Qiu S, Wu L, Zhang L, Chen H, Gao C. Improving the performance of polyamide reverse osmosis membrane by incorporation of modified multi-walled carbon nanotubes. J Membr Sci 2014;450:249–56.

[46] Ma N, Wei J, Qi S, Zhao Y, Gao Y, Tang CY. Nanocomposite substrates for controlling internal concentration polarization in forward osmosis membranes. J Membr Sci 2013;441:54–62.

[47] Tian M, Wang Y-N, Wang R. Synthesis and characterization of novel high-performance thin film nanocomposite (TFN) FO membranes with nanofibrous substrate reinforced by functionalized carbon nanotubes. Desalination 2015;370:79–86.

[48] Tang C, Wang Z, Petrinić I, Fane AG, Hélix-Nielsen C. Biomimetic aquaporin membranes coming of age. Desalination 2015;368:89–105.

[49] Hovijitra NT, Wuu JJ, Peaker B, Swartz JR. Cell-free synthesis of functional aquaporin Z in synthetic liposomes. Biotechnol Bioeng 2009;104(1):40–9.

[50] Holt JK, Park HG, Wang Y, Stadermann M, Artyukhin AB, Grigoropoulos CP, et al. Fast mass transport through sub-2-nanometer carbon nanotubes. Science 2006;312(5776): 1034–7.

[51] Kumar M, Grzelakowski M, Zilles J, Clark M, Meier W. Highly permeable polymeric membranes based on the incorporation of the functional water channel protein Aquaporin Z. Proc Natl Acad Sci U S A 2007;104(52):20719–24.

[52] Zhao Y, Vararattanavech A, Li X, Hélixnielsen C, Vissing T, Torres J, et al. Effects of proteoliposome composition and draw solution types on separation performance of

aquaporin-based proteoliposomes: implications for seawater desalination using aquaporin-based biomimetic membranes. Environ Sci Technol 2013;47(3):1496–503.

[53] Qi S, Wang R, Chaitra GKM, Torres J, Hu X, Fane AG. Aquaporin-based biomimetic reverse osmosis membranes: stability and long term performance. J Membr Sci 2016;508:94–103.

[54] Barboiu M. Artificial water channels—incipient innovative developments. Chem Commun 2016;52(33):5657–65.

[55] Ho W, Sirkar K. Membrane handbook. Springer US; 2012.

[56] Tang CY, Chong TH, Fane AG. Colloidal interactions and fouling of NF and RO membranes: a review. Adv Colloid Interf Sci 2011;164(1–2):126–43.

[57] Zhu X, Elimelech M. Fouling of reverse osmosis membranes by aluminum oxide colloids. J Environ Eng 1995;121(12):884–92.

[58] Elimelech M, Zhu X, Childress AE, Hong S. Role of membrane surface morphology in colloidal fouling of cellulose acetate and composite aromatic polyamide reverse osmosis membranes. J Membr Sci 1997;127(1):101–9.

[59] Wei J, Qiu C, Wang YN, Wang R, Tang CY. Comparison of NF-like and RO-like thin film composite osmotically-driven membranes-Implications for membrane selection and process optimization. J Membr Sci 2013;427:460–71.

[60] Gu Y, Wang YN, Wei J, Tang CY. Organic fouling of thin-film composite polyamide and cellulose triacetate forward osmosis membranes by oppositely charged macromolecules. Water Res 2013;47(5):1867–74.

[61] Tang CY, Kwon YN, Leckie JO. Probing the nano- and micro-scales of reverse osmosis membranes—a comprehensive characterization of physiochemical properties of uncoated and coated membranes by XPS, TEM, ATR-FTIR, and streaming potential measurements. J Membr Sci 2007;287(1):146–56.

[62] Tang CY, Fu QS, Robertson AP, Criddle CS, Leckie JO. Use of reverse osmosis membranes to remove perfluorooctane sulfonate (PFOS) from semiconductor wastewater. Environ Sci Technol 2006;40(23):7343–9.

[63] Childress AE, Elimelech M. Relating nanofiltration membrane performance to membrane charge (electrokinetic) characteristics. Environ Sci Technol 2000;34(17):3710–16.

[64] Jones KL, O'Melia CR. Protein and humic acid adsorption onto hydrophilic membrane surfaces: effects of pH and ionic strength. J Membr Sci 2000;165(1):31–46.

[65] Wang YN, Tang CY. Protein fouling of nanofiltration, reverse osmosis, and ultrafiltration membranes—the role of hydrodynamic conditions, solution chemistry, and membrane properties. J Membr Sci 2011;376(1–2):275–82.

[66] Kwon YN, Tang CY, Leckie JO. Change of membrane performance due to chlorination of crosslinked polyamide membranes. J Appl Polym Sci 2006;102(6):5895–902.

[67] Do VT, Tang CY, Reinhard M, Leckie JO. Effects of chlorine exposure conditions on physiochemical properties and performance of a polyamide membrane-mechanisms and implications. Environ Sci Technol 2012;46(24):13184–92.

[68] Wang YN, Wei J, She Q, Pacheco F, Tang CY. Microscopic characterization of FO/PRO membranes—a comparative study of CLSM, TEM and SEM. Environ Sci Technol 2012;46(18):9995–10003.

[69] Tang CY, Kwon YN, Leckie JO. Characterization of humic acid fouled reverse osmosis and nanofiltration membranes by transmission electron microscopy and streaming potential measurements. Environ Sci Technol 2007;41(3):942–9.

[70] Yun MA, Yeon KM, Park JS, Lee CH, Chun J, Lim DJ. Characterization of biofilm structure and its effect on membrane permeability in MBR for dye wastewater treatment. Water Res 2006;40(1):45–52.

[71] Conchello J-A, Lichtman JW. Optical sectioning microscopy. Nat Meth 2005;2(12):920–31.

[72] Chen Y, Liu C, Setiawan L, Wang Y-N, Hu X, Wang R. Enhancing pressure retarded osmosis performance with low-pressure nanofiltration pretreatment: membrane fouling analysis and mitigation. J Membr Sci 2017;543:114–22.

[73] Coster HGL, Chilcott TC, Coster ACF. Impedance spectroscopy of interfaces, membranes and ultrastructures. Bioelectrochem Bioenerg 1996;40(2):79–98.

[74] Loh CH, Wang R. Effects of additives and coagulant temperature on fabrication of high performance PVDF/Pluronic F127 blend hollow fiber membranes via nonsolvent induced phase separation. Chin J Chem Eng 2012;20(1):71–9.

[75] Lee S, Elimelech M. Relating organic fouling of reverse osmosis membranes to intermolecular adhesion forces. Environ Sci Technol 2006;40(3):980–7.

[76] Tang CY, Kwon YN, Leckie JO. The role of foulant-foulant electrostatic interaction on limiting flux for RO and NF membranes during humic acid fouling—theoretical basis, experimental evidence, and AFM interaction force measurement. J Membr Sci 2009; 326(2):526–32.

[77] Nikolay V. Desalination engineering: planning and design. McGraw-Hill Professional; 2012. 1 p.

[78] Fane AG, Wang R, Hu MX. Synthetic membranes for water purification: status and future. Angew Chem Int Ed 2015;54(11):3368–86.

[79] Wang Y-N, Li W, Wang R, Tang CY. Enhancing boron rejection in FO using alkaline draw solutions. Water Res 2017;118:20–5.

[80] Güler E, Kaya C, Kabay N, Arda M. Boron removal from seawater: state-of-the-art review. Desalination 2015;356:85–93.

[81] Wang Y-N, Wang R, Li W, Tang CY. Whey recovery using forward osmosis—evaluating the factors limiting the flux performance. J Membr Sci 2017;533:179–89.

[82] Hoek EMV, Elimelech M. Cake-enhanced concentration polarization: a new fouling mechanism for salt-rejecting membranes. Environ Sci Technol 2003;37(24):5581–8.

[83] Vrijenhoek EM, Elimelech M, Hong S, editors. Influence of membrane properties, solution chemistry, and hydrodynamics on colloidal fouling of reverse osmosis and nanofiltration membranes. ACS Division of Environmental Chemistry; 2000. Preprints.

[84] Tang CY, Fu QS, Criddle CS, Leckie JO. Effect of flux (transmembrane pressure) and membrane properties on fouling and rejection of reverse osmosis and nanofiltration membranes treating perfluorooctane sulfonate containing wastewater. Environ Sci Technol 2007;41(6):2008–14.

[85] Wang YN, Järvelä E, Wei J, Zhang M, Kyllönen H, Wang R, et al. Gypsum scaling and membrane integrity of osmotically driven membranes: the effect of membrane materials and operating conditions. Desalination 2016;377:1–10.

[86] Wang YN, Tang CY. Fouling of nanofiltration, reverse osmosis and ultrafiltration membranes by protein mixtures: the role of inter-foulant-species interaction. Environ Sci Technol 2011;45(15):6373–9. [Epub 2011 Jul 5].

[87] Antony A, Low JH, Gray S, Childress AE, Le-Clech P, Leslie G. Scale formation and control in high pressure membrane water treatment systems: a review. J Membr Sci 2011;383(1–2):1–16.

[88] Stumm W, Morgan J. Aquatic chemistry: chemical equilibria and rates in natural waters. 3rd ed. New York: Wiley-Interscience; 1996. 1040 p.

[89] Wang YN, Li X, Wang R. Silica scaling and scaling control in pressure retarded osmosis processes. J Membr Sci 2017;541:73–84.

[90] Ang WS, Elimelech M. Protein (BSA) fouling of reverse osmosis membranes: implications for wastewater reclamation. J Membr Sci 2007;296(1–2):83–92.

[91] Tang CY, Kwon YN, Leckie JO. Fouling of reverse osmosis and nanofiltration membranes by humic acid—effects of solution composition and hydrodynamic conditions. J Membr Sci 2007;290(1–2):86–94.

[92] Zhu X, Elimelech M. Colloidal fouling of reverse osmosis membranes: measurements and fouling mechanisms. Environ Sci Technol 1997;31(12):3654–62.

[93] Gao Y, Haavisto S, Li W, Tang CY, Salmela J, Fane AG. Novel approach to characterizing the growth of a fouling layer during membrane filtration via optical coherence tomography. Environ Sci Technol 2014;48(24):14273–81.

[94] Jiang S, Li Y, Ladewig BP. A review of reverse osmosis membrane fouling and control strategies. Sci Total Environ 2017;595:567–83.

[95] Sohn J, Valavala R, Han J, Her N, Yoon Y. Pretreatment in reverse osmosis seawater desalination: a short review. Environ Eng Res 2011;16(4):205–12.

[96] Wenten IG, Khoiruddin. Reverse osmosis applications: prospect and challenges. Desalination 2016;391:112–25.

[97] Greenlee LF, Lawler DF, Freeman BD, Marrot B, Moulin P. Reverse osmosis desalination: water sources, technology, and today's challenges. Water Res 2009;43(9):2317–48.

[98] Shenvi SS, Isloor AM, Ismail AF. A review on RO membrane technology: developments and challenges. Desalination 2015;368:10–26.

[99] Côté P, Liu M, Siverns S. Water reclamation and desalination by membranes. In: Advanced membrane technology and applications. Wiley; 2008. p. 171–87.

[100] Wang B, Guo X, Bai P. Removal technology of boron dissolved in aqueous solutions—a review. Colloids Surf A Physicochem Eng Asp 2014;444:338–44.

[101] Jamaly S, Darwish NN, Ahmed I, Hasan SW. A short review on reverse osmosis pretreatment technologies. Desalination 2014;354:30–8.

[102] Pérez-González A, Urtiaga AM, Ibáñez R, Ortiz I. State of the art and review on the treatment technologies of water reverse osmosis concentrates. Water Res 2012; 46(2):267–83.

[103] Peters TA. Purification of landfill leachate with reverse osmosis and nanofiltration. Desalination 1998;119(1):289–93.

[104] Chai X, Chen G, Yue PL, Mi Y. Pilot scale membrane separation of electroplating waste water by reverse osmosis. J Membr Sci 1997;123(2):235–42.

[105] Vourch M, Balannec B, Chaufer B, Dorange G. Treatment of dairy industry wastewater by reverse osmosis for water reuse. Desalination 2008;219(1):190–202.

[106] Coskun T, Debik E, Demir NM. Treatment of olive mill wastewaters by nanofiltration and reverse osmosis membranes. Desalination 2010;259(1):65–70.

[107] De Jager D, Sheldon MS, Edwards W. Colour removal from textile wastewater using a pilot-scale dual-stage MBR and subsequent RO system. Sep Purif Technol 2014;135:135–44.

[108] Rautenbach R, Vossenkaul K, Linn T, Katz T. Waste water treatment by membrane processes—new development in ultrafiltration, nanofiltration and reverse osmosis. Desalination 1997;108(1):247–53.

[109] Alvarez V, Alvarez S, Riera FA, Alvarez R. Permeate flux prediction in apple juice concentration by reverse osmosis. J Membr Sci 1997;127(1):25–34.

[110] Pap N, Kertész S, Pongrácz E, Myllykoski L, Keiski RL, Vatai G, et al. Concentration of blackcurrant juice by reverse osmosis. Desalination 2009;241(1):256–64.

[111] Jesus DF, Leite MF, Silva LFM, Modesta RD, Matta VM, Cabral LMC. Orange (Citrus sinensis) juice concentration by reverse osmosis. J Food Eng 2007;81(2):287–91.

[112] Gurak PD, Cabral LMC, Rocha-Leão MHM, Matta VM, Freitas SP. Quality evaluation of grape juice concentrated by reverse osmosis. J Food Eng 2010;96(3):421–6.

[113] Echavarría AP, Falguera V, Torras C, Berdún C, Pagán J, Ibarz A. Ultrafiltration and reverse osmosis for clarification and concentration of fruit juices at pilot plant scale. LWT-Food Sci Technol 2012;46(1):189–95.

[114] Pilipovik MV, Riverol C. Assessing dealcoholization systems based on reverse osmosis. J Food Eng 2005;69(4):437–41.

[115] Catarino M, Mendes A, Madeira LM, Ferreira A. Alcohol removal from beer by reverse osmosis. Sep Sci Technol 2007;42(13):3011–27.

[116] Catarino M, Mendes A. Dealcoholizing wine by membrane separation processes. Innovative Food Sci Emerg Technol 2011;12(3):330–7.

[117] Peinemann KV, Nunes SP, Giorno L. Membrane technology, volume 3: membranes for food applications. Wiley; 2010.

[118] López M, Alvarez S, Riera FA, Alvarez R. Production of low alcohol content apple cider by reverse osmosis. Ind Eng Chem Res 2002;41(25):6600–6.

[119] White LS, Nitsch AR. Solvent recovery from lube oil filtrates with a polyimide membrane. J Membr Sci 2000;179(1):267–74.

[120] Vandezande P, Gevers LEM, Vankelecom IFJ. Solvent resistant nanofiltration: separating on a molecular level. Chem Soc Rev 2008;37(2):365–405.

## Further Reading

[121] Weng X, Ji Y, Zhao F, An Q, Gao C. Tailoring the structure of polyamide thin film composite membrane with zwitterions to achieve high water permeability and antifouling property. RSC Adv 2015;5(120):98730–9.

[122] kobelco-eco.co. Available from: http://www.kobelco-eco.co.jp/english/product/dt_module/genri.html.

# Materials and Engineering Design of Interfacial Polymerized Thin Film Composite Nanofiltration Membrane for Industrial Applications

*B.S. Ooi\*, J.Y. Sum\*, J.J. Beh\*, Woei Jye Lau[†],
S.O. Lai[‡]*

**\*School of Chemical Engineering, Universiti Sains Malaysia,
Nibong Tebal, Malaysia**
**[†]Advanced Membrane Technology Research Centre (AMTEC), Faculty of
Chemical and Energy Engineering, Universiti Teknologi Malaysia,
Skudai, Malaysia**
**[‡]Universiti Tunku Abdul Rahman (UTAR), Kajang, Malaysia**

O U T L I N E

# 2.1 INTRODUCTION

The term nanofiltration (NF) was first coined after low-pressure reverse osmosis was produced. As the name implied, NF has a pore dimension in nanoscale ranging from 1 nm to 10 nm with the capability to retain solute with the size of 1 nm or more. Compared to an RO membrane, an NF membrane has different separation mechanism whereby charge exclusion can be a dominating factor compare to the sieving mechanism. This allows NF to have specific applications in water treatment [1], wastewater treatment [2–4], hardness removal [5, 6] and bio-separation [7, 8].

There are many ways to produce polymeric nanofiltration, including phase inversion technique for asymmetric membrane, interfacial polymerization, coating [9–12], and layer-by-layer assembly methods [13, 14]. Among these methods, interfacial polymerization (IP) is known to be a simple method due to its flexibility in optimizing the support layer and the thin film layer, separately. Interfacial polymerization was initially proposed by Wittbecker and Morgan in 1959 whereby polymerization occurs in the interface of two immiscible phases whereby one phase is common water, and the other phase consists of a low dielectric constant solvent such as n-hexane. The thin film composite membrane could be optimized by tailoring the properties of both support and selective layer separately. The semipermeable skin layer is designed for higher water flux and better solute rejection whereas the desired qualities such as high porosity and excellent mechanical strength were optimized for the support layer [15].

In selecting a nanofiltration membrane for a specific application, rejection and water permeability are two critical parameters to evaluate their performance. Its performance relies on the membrane materials, operating conditions, and solution chemistry. Membrane rejection is typically evaluated using mono and divalent ions such as NaCl, $Na_2SO_4$, $MgSO_4$, and $MgCl_2$. It is commonly accepted that NF can reject at least 95% $MgSO_4$. Interfacial polymerized TFC NF membrane has been successfully commercialized and used in the water treatment industry partly to replace the energy-intensive reverse osmosis system. Before the year 2020, NF will dominate the membrane market with an expected growth of $445.1 million or annual growth rate of 15.6% [16]. The market is shared by the top-ranked nanofiltration manufacturers such as Koch Membrane, Microdyn-Nadir, Hydranautics, GE Osmonics, Toray, and Dow-Film. Table 2.1 summarizes the performance of some commercially available NF membranes. In average, the flux of an NF membrane is within 2–14 L/h m$^2$ bar with >95% rejection of the multivalent ions.

## 2.2 MEMBRANE CHARACTERISTICS AND ITS PERFORMANCE

A membrane prepared via IP process has different morphology depends on the process conditions namely the reactant concentrations, the ratio of reactants, the solubility of the reactants in the organic phase, diffusion rate and the kinetics of hydrolysis and crosslinking [17].

The ideal thickness of the ultra-thin skin layer that governs the membrane flux is preferably under 0.10 μm. It is necessary to produce membranes with higher productivities without severely affecting the membrane selectivity. Various studies revealed that the membrane performance is related to the molecular arrangement or chemical structure of the skin layer. The desired properties of the thin film included defined pore size (<1 nm), narrow pore size distribution, defect-free, smooth morphology, and thin and robust pores. Research works to enhance the membrane performance could be categorized into two areas namely (i) preparation condition, e.g., reaction time, concentration, pH, temperature, and humidity (ii) material selection such as functionality of the reactants and its solubility or partitioning coefficient.

Significant improvement has been achieved in fabricating the polymeric and the nanocomposite membrane via interfacial polymerization. The IP process can be further based on the type of monomer and reaction (polycondensation or polyaddition). Polycondensation is commonly used to produce the commercially available polyamide NF membrane whereas polyaddition involves radical polymerization of alkene and initiators that being immobilized on the solid substrate. The success of IP in producing

TABLE 2.1    Commercial Thin Film Composite NF Membrane and Their Performance

| Membrane | Material | Manufacturer | Contact angle | Retention | Water permeability (L/m$^2$ h bar) | References |
|---|---|---|---|---|---|---|
| NF40 | Polypiperazinamide | Dow-Film Tec | | 20 bar, 2000 ppm NaCl = 45% 20 bar, 2000 ppm Na$_2$SO$_4$ = 95% 20 bar, 2000 ppm MgCl$_2$ = 70% | 2.15 | [18, 19] |
| NF90 | Polyamide | Dow-Film Tec | 54.6 | 5 bar, 5000 ppm KCl = 75% 5 bar, 5000 ppm Na$_2$SO$_4$ = 95% 5 bar, 5000 ppm MgSO$_4$ = 95% | 10.2 (PWP) | [18, 20] |
| NF270 | Polypiperazinamide | Dow-Film Tec | 42.7 | 5 bar, 5000 ppm KCl = 35% 5 bar, 5000 ppm Na$_2$SO$_4$ = 95% 5 bar, 5000 ppm MgSO$_4$ = 95% | 13.5 (PWP) $3.7 \times 10^{-11}$ m$^3$/(m$^2$ s Pa) | [18, 20, 21] |
| [a]N30F | Polyethersulfone | MICRODYN-NADIR GmBH | 88 | 5 bar, 5000 ppm KCl = 2%; 5 bar, 5000 ppm Na$_2$SO$_4$ = 30% 5 bar, 5000 ppm MgSO$_4$ = 30% | 4.45 (PWP) | [20, 22] |
| SU600 | Polyamide | Toray | | 3.5 bars, 1000 ppm NaCl = 55% | 8 | [18] |

| | | | | | | |
|---|---|---|---|---|---|---|
| UTC20 | Polypiperazinamide (MWCO = 180) | Toray | 36 | 10 bar, 1500 ppm NaCl = 55% <br> 10 bar, 1500 ppm $Na_2SO_4$ = 93% <br> 10 bar, 1500 ppm $MgCl_2$ = 98% | 9.7 | [18] |
| DL | Crosslinked aromatic polyamide (MWCO = 150–300) | GE Osmonics | 44 | 4 bar, 2482 ppm NaCl = 40% <br> 4 bar, 2464 ppm, $MgSO_4$ = 97.6% | 7 | [22, 23] |
| [a]NTR7450 | Sulfonated polyethersulfone (MWCO = 600–800) | Nitto-Denko | 70 | 10 bar, 5000 ppm NaCl = 51% <br> 10 bar, 5000 ppm $Na_2SO_4$ = 92% <br> 10 bar, 5000 ppm $MgCl_2$ = 13% | 5.7 (PWP) | [18, 22] |

[a] *The membranes are not produced via interfacial polymerization.*
*PWP*, pure water permeability.

defect-free ultrathin films lies on the "self-sealing" and "self-termination" mechanism as a result of the slow solute diffusion [24].

The other parameters involved in IP process include the porosity of support layer, wettability, monomer concentration, type of monomer, type of organic solvent, reaction time, solution pH, and the presence of additives. In general, during polymerization two competing phenomena are occurring namely nucleation and crystallization as well as polymer growth (crosslinking, hydrolysis, and film growth). Fast nucleation will induce smaller nodule structure or tighter skin layer whereas excess film growth reduces the membrane permeability. A membrane with thinner skin layer has higher permeability but may compensate its structure robustness. Depending on the applications of the NF membrane, the operation that required low transmembrane pressure has the luxury of having thinner film layer.

## 2.3 MATERIAL SELECTION

Compared to an RO membrane, nanofiltration has higher flexibility in choosing the type of monomer involved in the IP process. Nonplanar molecules with a functional group provide a broader choice for an NF membrane compared to an RO membrane, which is mainly limited by m-phenylenediamine. To date, many monomers are being employed to synthesize the TFC NF membrane. The standard material used for the polymerization process of reverse osmosis and NF include polyamide and polyester but are not limited to other polymers such as polyurea, polyurethanes, polyesters, and polycarbonate.

### 2.3.1 Polyamide

TFC membranes are typically made from a thin polyamide layer deposited onto the porous layer. A thin polyamide layer with the thickness < 200 nm are formed by reacting the diacyl/triacyl chloride with diamine monomers such as semiaromatic polyamide (piperazine-isophthaloyl chloride) [17, 25], aliphatic or aromatic diamine [26–28], aromatic-cycloaliphatic (cyclohexane-1,3,5-tricarbonyl chloride and m-phenylenediamine-4-methyl) [29, 30], polysulfonamide [31], polyvinylamine [32], cyclen [33], and dopamine [34]. The wholly aromatic MPD-membranes normally give higher water and salt transport compared to the nonplanar piperazine membranes. Different monomer combination produces membrane ranging from RO to NF with specific applications in low-pressure desalination or selective organic solute separations. As the flux is increased, the selectivity of the membrane may increase to allow

the permeation of monovalent ions while rejecting the hardness solution (divalent ions) and bigger organic compounds.

The thinner skin layer of the NF compared to the RO membrane enables it to operate at higher flux but much lower pressure (<7 bar). Although the PA membrane is relatively hydrophilic with good chemical stability, the PA membrane is considered to have poor chlorine tolerance (<0.1 ppm) compared to other polymers. The membrane is not biodegradable as compared to a cellulose acetate membrane and can operate within a pH of 3–9 [35]. The membrane with amide group exhibits a positive charge at a pH lower their isoelectric point (around pH 5), which means that polyamide membrane is mildly negative charge in most of the water stream.

It is commonly known that a polyamide membrane with its hydrophilic nature has enhanced antifouling properties. A TFC polyamide membrane utilizing natural polymer, such as the Sericin-TMC membrane, possessed a better antifouling property compared to the conventional polyamide based nanofiltration (NF270) [36]. Besides antifouling properties, polyamide with antibacterial properties also could be tailored made via interfacial polymerization. A new nanofiltration membrane prepared by interfacial polymerization of polyhexamethylene guanidine hydrochloride (PHGH) and trimesoyl chloride (TMC) demonstrated the improvement in term of antibiofouling performance [37]. Similar to the nanofiltration containing zwitterionic moieties, polyamide with N-aminoethyl piperazine propane sulfonate also showed excellent bacterial adsorption resistance [38]. Fig. 2.1 shows that a polyamide TFC membrane can be tailor-made using different bi-amine monomers or oligomers.

## 2.3.2 Polyester

Polyester membrane exhibits better chlorine resistance compared to the polyamide membrane. The incorporation of the ester linkage can significantly increase chlorine resistance and oxidation of the membrane. The polyester TFC membrane can be synthesized by incorporating monomers such as triethanolamine [39], bisphenol A [40], tannic acid [41], resorcinol [42], pentaerythritol [43] and hyperbranched polyester [44, 45]. In general, the polyester membrane exhibits negatively charged surface with higher rejection toward divalent anions like the common NF membrane. It was expected that by having higher negative charge, the membrane could be more resistant toward organic fouling such as humic acid.

Because amines react with acyl chloride groups much more readily than alcohols, the synthesis of a TFC polyester membrane is not as easy as that of a TFC polyamide membrane. In view of this, polyesteramide thin-film-composite (TFC) membranes that combine the benefits of polyamide and polyester can be produced by tailoring the ester/amide ratio.
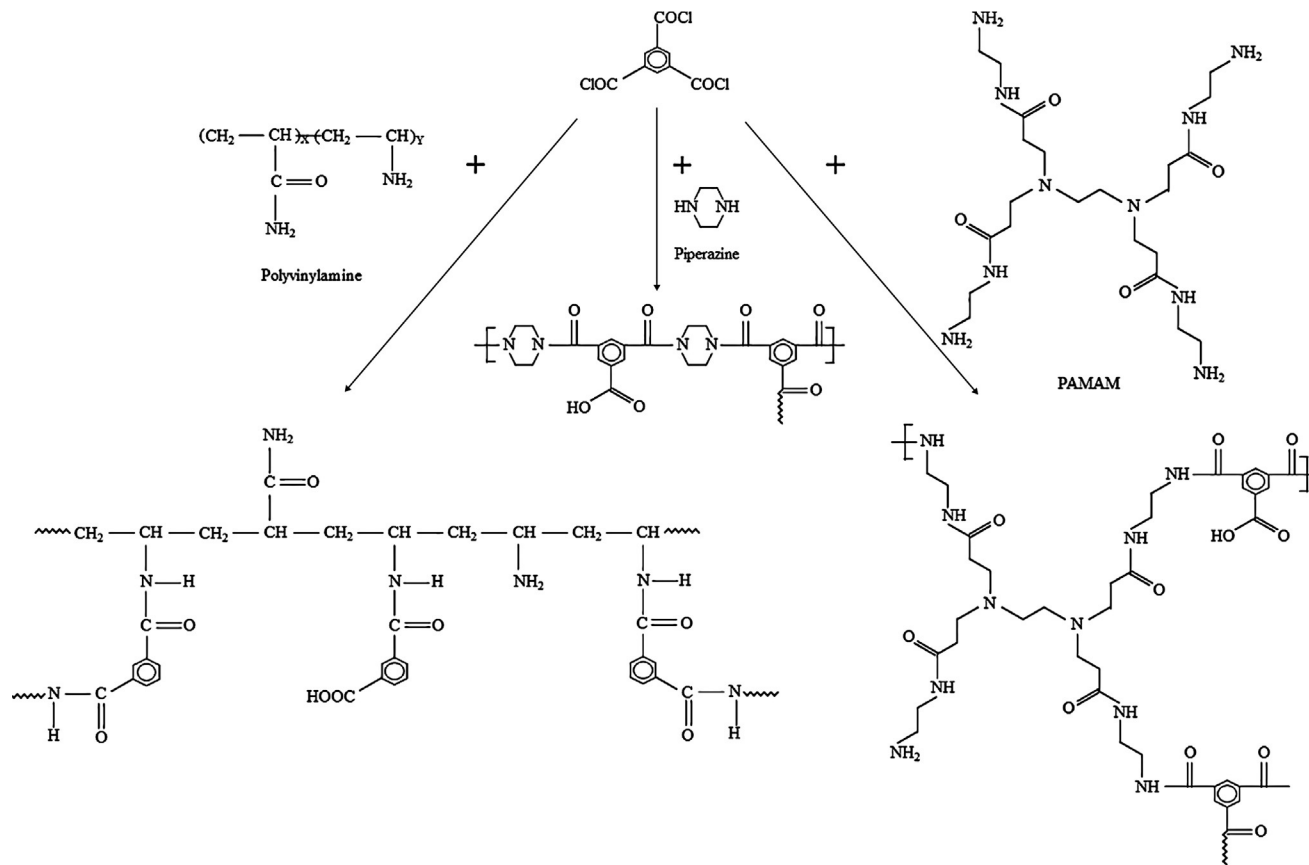
FIG. 2.1   Interfacial polymerized thin film composite polyamide membrane using different monomers.
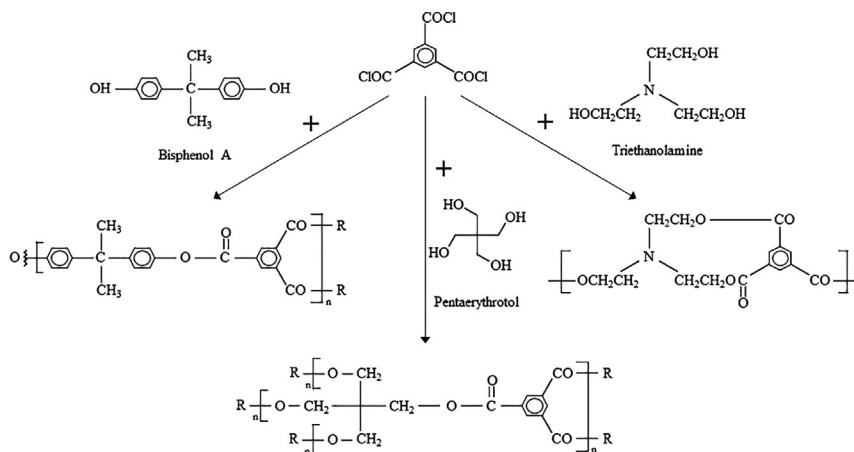
FIG. 2.2    Polyester produced via interfacial polymerization using various alcohol groups.

The polyesteramide membrane has a relatively good oxidative resistance compared to the polyamide membrane [46]. The fluxes of the polyester membranes are lower (0.7–2.5 L atm$^{-1}$ m$^{-2}$ h$^{-1}$) compared to the polyamide membrane [42], and their rejection is not comparable to polyamide membrane. For example, the polyester TFC membrane synthesized from triethanolamine (TEOA) and trimesoyl chloride (TMC) were tested on salts separation at 0.6 MPa. The rejection of the mono and divalent salts decreased following the order of $Na_2SO_4 > MgSO_4 > NaCl > MgCl_2$ [39]. The obtained results showed that the polyester NF membrane is relatively loose compared to polyamide TFC membrane. Fig. 2.2 shows that polyester membrane can be produced via interfacial polymerization based on different alcohol groups.

## 2.3.3 Polyamine

Compared to polyamide NF membrane, which usually contains piperazine in the aqueous phase, polyamine NF membrane uses oxidant reacting compound, which protects the membrane from damage by chlorine. Theoretically, it is deduced that membranes, which are derived from polyethyleneimine and trimesoyl chloride, have better pH stability and resistance toward a nucleophilic attack as compared to polyamide membranes [47]. Lee et al. proposed the synthesis of a TFC polyamine membrane with low pH stability by reacting cyanuric chloride and diethylene triamine monomeric amines. The membranes were found to have higher salt rejection and water permeability [48]. A fluorinated polyamine monomer [$CF_3(CF_2)_6CONH(CH_2CH_2NH)_2CH_2CH_2NH_2$] was also synthesized and utilized to perform interfacial polymerization with trimesoyl chloride.

The surface free energy of the NF membrane is as low as 23.0 mJ/m$^2$, which could resist the adhesion of foulants such as bovine serum albumin (BSA) and humic acid [49].

### 2.3.4 Polyurethane

A new type and uncommon TFC-NF membranes can be prepared via interfacial polymerization of poly(bis-MPA) and methylene diphenyl diisocyanate [50]. The membrane rejection toward MgSO$_4$ is lower than 40%, indicating that it is a loose NF membrane. However, the membrane claimed to have more organic fouling resistance even though not much information could be obtained for the PU membrane synthesized via interfacial polymerization.

## 2.4 CONTROL OF INTERFACIAL POLYMERIZATION

Over the years, research has been carried out to enhance the membrane performance by varying the reaction conditions such as types of monomer, monomer concentrations, curing conditions, types of solvent, and presence of additives in the solvent [15, 51–55]. These parameters show high impact toward the membrane properties such as surface morphology, chemical and bonding property, mechanical property, permeability, and selectivity.

### 2.4.1 Monomer

The properties of a thin film can be manipulated by changing the chemical structure, size, solubility, shape, and reactivity of the monomer [28]. Besides, Chen et al. found that monomer concentrations, as well as wetting/swelling agents, could play an essential role in the membrane properties too [56]. For example, a thin-film-composite (TFC) nanofiltration (NF) membrane composed of aliphatic piperazine and aromatic *m*-phenylene diamine mixture was employed to separate oleic acid. It was found that the monomer concentrations and drying times have great impacts toward the membrane's properties [53]. Roh and co-workers demonstrated that increasing the diamine concentration during MPD/TMC reaction caused a drop in surface hydrophilicity and thus led to the declination of flux [52]. The authors pointed out that membrane permeability is determined by counterbalancing both the film thickness and surface hydrophilicity.

One of the methods to increase the flux is by hydrophilizing the membrane material. In membrane technology, concern was given to producing a membrane with superior permeability and selectivity, which can be achieved via chemical approach. For instance, the hydrophilic

hydroxyl-ended hyperbranched polyester (HPE) was employed as a mono-mer in synthesizing NF membrane by in-situ IP process with trimesoyl chloride (TMC) [57]. The membrane showed enhanced permeability with-out scarifying its rejection capability. Another TFC membrane synthesized from hyperbranched polyethyleneimine (PEI) renders similar result by incorporating the free rotating amines group that could enhance the water permeation [53, 58].

## 2.4.2 Reaction Conditions

Many studies have been carried out to relate the membrane synthesis conditions toward their performance. Past study suggested that temp-erature and relative humidity were dominant factors in tuning the final thickness, structure, and performance of the skin layer. Mickols found that the controlling parameters for the membrane flux are the reaction time as well as the amine solution temperature [59]. The skin thickness could alter the membrane flux, but the membrane selectivity was found to be independent of film thickness [15]. The results obtained from the attenu-ated total reflectance infrared (ATR-IR) spectroscopy show that reaction time, relative humidity, and reaction temperature are determining factors. An exciting study showed that the immerse time in an organic solution, as well as the ratio of m-phenylene diamine and m-Aminophenol, could affect the water permeability [60].

## 2.4.3 Support Layer

A TFC membrane consists of a skin layer residing on a support mem-brane. The support aims to provide mechanical strength for moderate to high-pressure operations. The support layer itself must have optimum pore size to diminish the additional resistance for water transport. A TFC membrane is considered to be more advantageous than its prede-cessor asymmetric membrane as it allows separate optimization of the skin layer and support layer [17, 61–63]. However, recent studies revealed that these two layers are in fact closely interrelated as the polyamide film grows directly on top of the support surface. The surface features of support are essential in defining the structural integrity and uniformity of the skin layer [63–66].

Singh and co-workers reported on the effect of different pore size dis-tribution of polysulfone to the resulting polyamide thin layer properties [67]. The substrate with a smaller pore size (0.07 μm) shows higher salt rejection efficiency in comparison with the substrate of higher pore size (0.15 μm). The hydrophilicity of the membrane substrate will determine the penetration of water into the pores, and thus the thickness of skin layer formed [63]. Fig. 2.3 illustrates the impact of pore opening and its surface
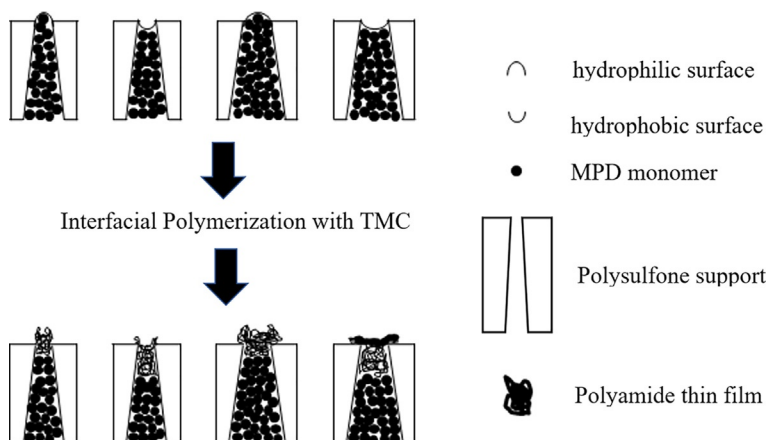
**FIG. 2.3**    Conceptual model illustrating the impact of support pore structure and hydrophilicity toward polyamide thin film formation during interfacial polymerization [63].

chemical property to the film formation. Support with more significant, hydrophobic characteristics will produce a more permeable TFC membrane with a rougher and thinner skin layer because less polymer is formed within the pores.

Besides asymmetric support, fibrous materials are also employed as a TFC support layer. A study was carried out to synthesize thin film nanofibrous composite (TFNC) membranes using the self-support nanofibrous polyethylene terephthalate. Results showed that the TFNC-NF membrane had improved salt rejection and 4-fold water flux than the TFC NF membrane. The improved flux in TFNC membranes is due to the low water permeation resistance of the nanofibrous support and the more prominent pore structure [68]. In another study, the polyethersulfone (PES) nanofibrous supporting layer was modified with dopamine which offers an innovative way for the synthesis of composite NF membranes with high salt rejection (~99.4%) and high flux (~63.0 L/m² h) [69]. Other scaffolds such as ultra-fine cellulose [70] and polyacrylonitrile nanofibers [71] were also reported with good performance.

## 2.5  CONVENTIONAL APPLICATIONS OF TFC NANOFILTRATION

### 2.5.1  Water Softening

Water softening is a process that removes calcium, magnesium, and other metal ions from the resources such as groundwater and seawater. A hardness of 300–500 mg/L as $CaCO_3$ caused scaling in heating vessels

and pipes. The conventional methods for removing water hardness rely on ion-exchange, precipitation, and sequestration by chelating agents. Reverse osmosis and nanofiltration are alternatives for water softening with NF have a typical TDS reduction of 70%–80%. From the economical aspect, the NF process is approximately 25% more costly that an anion exchange on a 20-year present worth basis [72] mainly due to the higher capital cost of NF alternatives. However, as plant capacities increase, the costs difference between the two processes decrease [72]. Compared to the conventional softening method, operation costs of NF are considerably low as expensive regenerations using large amounts of salt can be avoided. Another report showed that for a small-scale plant, NF is a more cost-effective method for color removal. For such a system, the NF systems could treat the water at a much lower price compared to lime soda, ozonation, and adsorption using granulated activated carbon [73]. It is expected that following the recent improvement in NF performance and lower operating pressure requirements, both CAPEX and OPEX of NF can be further reduced.

The ultimate aim of membrane development is to develop membranes with increasing flux and enhanced rejections which are practical for desalination [28]. Desalination is one of the central sectors that contribute to a 15% market growth forecast of nanofiltration (NF) [16]. Nanofiltration (NF) is a suitable seawater softening method that provides excellent permeates for oilfield-water injection whereby the concentration of multivalent ions such as $Ca^{2+}$ and $Mg^{2+}$ in permeate were kept at very low level [74]. The pilot-scale testing revealed that with the presence of antiscalant, total hardness with a 87.7%–93.5% removal rate can be achieved using NF system [75]. This enables NF to be effectively used in seawater softening and provide excellent feed for seawater reverse osmosis [76].

## 2.5.2 Wastewater and Water Treatment

Nanofiltration has been applied as a hybrid technology to treat the wastewater from leachate [77], textile effluent [3], tannery industries [78], pharmaceutical industries [79, 80], and agriculture industries [81, 82]. The common solute to be retained includes the divalent ions as well as medium to high molecular weight organic molecule (>200 Da). NF is synergetically combined with other technologies such as coagulation-flocculation [83], adsorption [84], ozonation [4, 85], and photocatalysis [86] to polish the quality of the permeate further.

Membrane fouling is a significant problem for the applications of NF membrane in wastewater treatment. A rapid decline in rejection efficiency and permeate flux was commonly attributed to the fast concentration polarization buildup and deposition of hydrophilic small-molecular-weight

carbohydrates such as fulvic-like substances [87]. Pretreatment prior to NF is the most practical way to reduce fouling, prolong the membrane lifespan and improve its performance [88]. In a technical and economic feasibility study of an olive oil mill effluent treatment, nanofiltration was coupled with dissolved air flotation pretreatment. The system demonstrated itself to be able to achieve high volume reduction factors and the rejection for total suspended solids (>80%), total organic carbon (>60%), chemical oxygen demand (50%–70%), and oil and grease (60%–80%) [89].

Effluents from the textile industries consist of various pollutants such as an organic material with high chemical oxygen demand, high suspended solids, color, and other soluble substances [90]. Nanofiltration is widely applied to treat the textile wastewater by removing the color and reuse the water. Textile wastewater was recovered and reused using a membrane pilot plant. It was found that NF90 membrane could yield a COD reduction of 99% and the salt retention of 75%–95%. Later, it was scaled up for long duration experiments using a spiral-wound module. It was found that the fouling phenomena were not significant and the foulants can be easily cleaned [91].

### 2.5.3 Food Processing

One of the promising applications of NF in the food industry is related to beverage industries. Fruit juices have been traditionally concentrated by the thermal operation; however, the high operating temperature resulted in color changes as well as loss of juice aroma. NF membrane which is an isothermal process that offers a better way to preserve the original taste of the clarified juice by simple sieving mechanism. The NF system was used to concentrate fruit juice from 10° Brix to 45° Brix at much lower energy requirement compared to evaporation [92].

Other common applications of NF in food industries include waste stream whey processing. Acid whey contains 0.55%–0.75% ($w/v$) of protein, 4.2%–4.9% (w/v) of lactose and up to 93.5% (w/v) of water [93]. The presence of high concentrations of lactate exerts operational problems in the dryer due to its stickiness [94]. Whey demineralization by nanofiltration allows concentration and demineralization of the whey to be carried out in a one-step process before spray drying [95]. Under uncharged conditions, lactose can be retained preferentially over lactic acid due to its bigger molecular weight. On the contrary, under acidic condition, NF can be used to retain lactose while allowing the permeation of lactic acid. The high selectivity of NF demineralization process results in a 30% reduction in lactic acid content and a reduction of 46%–60% in monovalent ions salt content [95].

# 2.6 FUNCTIONALIZED TFC NANOFILTRATION AND ITS APPLICATIONS

## 2.6.1 Positively Charged Thin Film Composite Membrane

Hardness removal from the wastewater using positively charged nanofiltration can be achieved using a membrane with bigger pore size due to its additional electrostatic repulsion in addition to the steric hindrance. Bivalent cations such as calcium and magnesium can be easily retained by the positively charged membrane. The solute rejection behaviors of positively charged membranes are following a common trend of $MgCl_2 > MgSO_4 > Na_2SO_4 > NaCl$.

Many attempts to produce a positively charged membrane using a different route has been reported. Most of the methods are through grafting, coating, or the bulk polymerization with limited literature being reported via IP method. The membrane bears the dissociable primary and secondary amine, and its charge depends on the dissociation constant of the amine as well as the number of amine groups. Commonly, macromolecule carrying the polyamine groups could be employed to produce positively charged membrane. A monomer with high amine groups has a lower partition coefficient and suffers from diffusional resistance during interfacial polymerization, which explains why IP is not a favorable process to produce NF membrane. Monomers or polymers such as poly(ethylene imine), poly(vinylamine), poly(amidoamine) and poly(dopamine) are commonly used to prepare positively charged nanofiltration.

### 2.6.1.1 Poly (Ethylene Imine)

Despite its technical difficulties in preparing positively charged NF membranes via an IP route, it was reported that quaternized branched polyethyleneimine (BPEI) had been successfully introduced into the TFC NF membrane via an IP process. The membrane showed a typical NF rejection trend of $MgCl_2 > MgSO_4 > Na_2SO_4 > NaCl$ [96]. Another successful case was demonstrated by the membrane that bears fixed quaternary ammonium moieties that had been synthesized by functionalizing the branched polyethyleneimine via reaction with glycidyl trimethyl ammonium chloride (GTACl). The membrane showed a significant increase of selectivity toward chloride- and sulfate-bearing solutes [97]. In one of the studies, the skin layer of the composite hollow fiber (HF) was formed through an IP of branched polyethyleneimine (BPEI) and trimesoyl chloride (TMC). The resulting membrane acquired a positively charged surface with pure water permeability (PWP) of about 17 $l/m^2$ h bar and a molecular weight cut-off (MWCO) of around 500 Da, or equivalent to a pore diameter of about 1.29 nm [18, 98].

A positively charged NF membrane had been employed for hardness removal and waste recovery. For example, composite nanofiltration membrane with the positively charged surface was synthesized by reacting BPEI and trimesoyl chloride (TMC). The membrane was used for efficient recovery of lithium from mixed $LiCl/MgCl_2$ solution. The mass ratio of $Mg^{2+}$ to $Li^+$ in the permeate decreased after the filtration [99]. Such a membrane was also employed for phosphorus recovery in which the membrane effectively rejected the heavy metal ions such as Pb, Cu, Zn, and Ni while allowing the passage of phosphate to achieve phosphorus recovery [100]. Other laboratory demonstrations found that the rejection rates of cationic dyes at neutral pH were >96% using positively charged NF membrane [101].

### 2.6.1.2 Poly(vinylamine)

Thin film composite membranes that carry poly(vinylamine) (PVAm) within the skin layer were also reported in producing positively charged NF membranes at a lower solution pH [32]. The membrane showed the typical rejection trend of a positively charged membrane (NaCl < $Na_2SO_4$ < $MgSO_4$ < $MgCl_2$) at pH 6.0 with recorded water permeability of $8.5 \, l/m^2$ h bar [102]. Besides the IP process, the positively charged membrane was also successfully developed via a layer-by-layer assembly method. Under this method, PVA and polyvinyl sulfate (PVS) were adsorbed layer-by-layer on the porous supports to form the polyelectrolyte membrane. The strong rejection of $Mg^{2+}$ of this membrane proved the presence of the positively charged ammonium groups of PVA in the membrane that repel the divalent magnesium ions [103].

### 2.6.1.3 Poly (amidoamine)

Another easy way to introduce the positively charged moieties is by grafting poly (amidoamine) dendrimer (PAMAM) on the interfacially polymerized layer. The resultant membrane recorded >99% rejection over the heavy metal ions such as $Pb^{2+}$, $Cu^{2+}$, $Ni^{2+}$, $Cd^{2+}$, $Zn^{2+}$, and $As^{5+}$, with a moderate pure water permeability (PWP) of $3.6 \, L \, m^{-2} \, h^{-1} \, bar^{-1}$ at 10 bar [104]. An easy method was also reported by reacting the carboxylic acids on the surface of a polyamide thin film composite with poly(amidoamine) in the presence of 2-chloro-1-methylpyridinium iodide as an activating agent. The membrane showed an elevated isoelectric point to pH 9.9 because of the high density of free protonated amino groups. The membrane showed excellent rejections toward metal ions including $Cu^{2+}$, $Ni^{2+}$, and $Pb^{2+}$ [105].

The research was carried out by embedding poly(dopamine) modified multiwall carbon nanotubes (PDA-MWCNTs) in polyamide thin-film composite membranes. The membranes showed improved flux with salt

rejection decreased in the sequence of $ZnCl_2$ (93.0%) > $MgCl_2$ (91.5%) > $CuCl_2$ (90.5%) $\approx$ $CaCl_2$, indicated that it is suitable for water softening [106]. A new nanofiltration membrane was synthesized by reacting poly(amidoamine) and trimesoyl chloride. During acidic solution filtration, the pH in the feed increased from 2 to 9, which showed that the membrane could enhance the proton permeation [107]. The membrane was found to be more positively charged due to the profound amine groups; however, its $MgSO_4$ rejection is poor due to the pore opening phenomenon. This problem was solved by one of the recent work that incorporated PAMAM and piperazine as co-monomer to form the skin layer with better divalent rejection [108]. The membrane has a lower isoelectric point and at the same time allow better rejection of $MgSO_4$.

Higher generation PAMAM (G4 and G5) were also incorporated into the TFC membrane. It was found that the pure water flux was improved for 106% at similar separation performance [109]. Researchers found that the surface charge of the thin layers was changed by incorporating PAMAM with different generations and concentrations. The membrane showed negatively charge behavior with higher $Na_2SO_4$ rejection compared to $MgCl_2$ [110]. This phenomenon might be due to the competitive hydrolysis rate of the carboxyl group to form a negative carboxylate group due to the poor partitioning of PAMAM into the organic phase. By increasing the concentrations and generations of the PAMAM, the cationic surface charge of the thin layers was increased [111]. Based on this observation, it can be concluded that the charge of the membrane does not only depend on the material itself but to a great extent depends on the processing conditions. It is especially true for the membrane prepared via the IP route.

### 2.6.1.4 Poly (dopamine)

Positively charged composite NF membranes were synthesized by depositing the poly (dopamine) (PDA) followed by grafting the poly (ethylene imine) (PEI) on the polyethersulfone support. The salts rejection followed the sequence of $MgCl_2$ > $CaCl_2$ > $MgSO_4$ > $Na_2SO_4$, showing that the membranes surface carried positive charge [112]. Compared to poly (ethylene imine), poly (vinylamine), and poly (amidoamine), polydopamine membranes are seldom synthesized via interfacial polymerization due to its complex nature of the monomer. The membrane was commonly prepared via self-polymerization [34], coating [113], and deposition [114] methods. Nonetheless, TFC-NF membranes with good structural stability were prepared via IP process under the mediation of polydopamine (PD). Under optimal conditions, the membrane exhibited flux as high as 22.8 L/(m$^2$ h) while the rejection of $Na_2SO_4$ reached 93.5% under 0.2 MPa [115] without showing the evidence of positively charged surface.

## 2.6.2 Chemical Resistance Nanofiltration

Since the first commercial applications of organic solvent nanofiltration (OSN) or solvent resistance nanofiltration (SRNF) around 1990, the NF membrane with more robust materials has been continuously developed to work in harsh conditions such as extreme pH conditions and the processes with organic solvents [116–118]. It was reported that energy requirement for solvents recovery could be reduced by >70% using NF assisted evaporation process [119].

SRNF membrane provides an effective chemicals recovery method for oleochemical industry [119, 120] and pharmaceutical industry [121]. For example, SelRO@ NF membranes commercialized by Koch Membrane claimed to have excellent stability in organic solvents. Their membranes are found suitable for extreme conditions in the separation of heavy metals under both acids and alkaline conditions. Although the composition of the membrane is not entirely open, it is unlikely that the membrane is produced via interfacial polymerization. SRNF membranes are commonly produced by coating or crosslinking the chemically stable polymer such as poly (vinylidene fluoride) (PVDF), polyetherketons (PEEK), polyetherimide (PEI), poly(phenelene sulfide)(PPS) and polybenzimidazole (PBI).

High flux solvent-stable TFC-OSN membranes are crucial. In one article, diaminopiperazine (DAP) and trimesoyl chloride (TMC) reacted with the polythiosemicarbazide support to give the high fluxes filtration toward solvents like dimethylsulfoxide, tetrahydrofuran, and dimethylformamide [122]. Another example includes a TFC membrane with cross-linked polyimide substrate with the skin being subjected to the posttreatment of glycerol/sodium dodecyl sulphate and dimethyl sulfoxide (DMSO). The membrane was very permeable to methanol ($5.12 \, \mathrm{lm^{-2} \, h^{-1} \, bar^{-1}}$), dimethylformamide ($3.92 \, \mathrm{lm^{-2} \, h^{-1} \, bar^{-1}}$) and DMSO ($3.34 \, \mathrm{lm^{-2} \, h^{-1} \, bar^{-1}}$) but could retain tetracycline well [123]. Jimenez Solomon et al. [124] reported that solvent activation of the TFC membranes after IP could improve the organic solvent permeation without compromising their selectivity.

An OSN membrane is also applied to filter the solvent containing dye solution. Mixed matrix membranes (MMMs) consist of carboxyl-functionalized multiwalled carbon nanotubes (MWCNTs-COOH) in P84 polyimide with the aid of 1,6-hexanediamine (HDA) as chemical crosslinker were employed for organic solvent nanofiltration (OSN). The cross-linked MMM has a rejection of 85% to rose bengal (1017.65 Da) while ethanol permeance is 9.6 LMH·bar$^{-1}$ at 5 bar [125]. Tris(hydroxymethyl) aminomethane (Tris), a hydrophilic monoamine, was added to the dope to modify polyimide OSN membranes during phase inversion [126]. The isopropanol (IPA) permeability of the crosslinked membranes was increased as much as 270% with slightly drop of dyes rejections.

## 2.6.3 Thin Film Nanocomposite Membrane (TFN)

A thin film nanocomposite membrane is an ideal membrane structure whereby the functional nanomaterials will be embedded within the active layer, which is usually around 100 nm thickness. There is a growing number of research in fabricating thin film nanocomposite nanofiltration membranes whereby inorganic materials such as silica [127–129], Graphene oxide [130–133], CNT [134–136], ZnO [137, 138], TiO$_2$ [139, 140], zeolite [141], MOF [142, 143], and other functional materials were embedded within the selective layer. The advantage of adding such nanomaterials is to combine the hydrophilicity or channeling effect of nanomaterials and the flexibility of the polymeric materials.

Nanomaterials could enhance the water permeability due to its channeling effect and micro-porosity with the former is more relevant to RO membrane, and the latter applies to the UF membrane. The permeability of an NF membrane, which has pore size lies between RO and UF, could be enhanced via both effects. It is expected that a nanostructured material with a hydrophilic outer layer and a hydrophobic inner layer is more beneficial concerning water permeability. The outer hydrophilic layer helps to reduce the surface tension or capillary force while the inner hydrophobic layer is helping the transport of water molecules through the frictionless channel. For separation involves bigger solute, micro-porosity increment due to the incorporation of NPs could enhance the membrane permeability while retaining its rejection capacity. Besides flux enhancement, it is widely reported that TFN membrane shows improved antifouling properties due to the changes of skin layer microstructures and surface features.

TFN membrane with antifouling properties finds its great potential in wastewater treatment and bio-separation. TFN membrane with antifouling properties can be enhanced by incorporating the functionalized carbon nanotube (CNT). There are many ways to functionalize the CNT to enhance the surface hydrophilicity and therefore enhance their antifouling properties of the membrane such as via sulfonation [144], carboxylation [134], coating [135], amination [145], and zwitterionic modification [146].

Two-dimensional (2D) graphenes are becoming the popular materials for preparing membranes with superior performance. For example, a polypiperazinamide membrane mediated with partially reduced graphene oxide increases the membrane hydrophilicity [147]. It was found that water flux of the TFN membrane with graphene oxide was doubled and the salt rejection of Na$_2$SO$_4$ increased from 95.0% to 97.1%, compared to the neat PA membrane [148].

Metal organic framework (MOF) is a class of porous crystalline compound that offers the advantage of a large surface area with defined

porosity. Recently, MOF incorporated polymeric membranes have gained importance in membrane separation due to its organic solvent resistance [143, 149]. Furthermore, a hybrid membrane with MOF decorated on the GO sheets was synthesized and utilized as an effective bactericidal agent [150]. Zeolite nanoparticles were also incorporated into the TFN membrane via interfacial polymerization. The membrane showed similar rejection of $MgSO_4$ with a reduced rejection of positively charged small molecular weight pharmaceuticals compounds [141]. The membrane dosed with zeolite is more hydrophilic and render the membrane with better antifouling properties. This property makes the polyamide membrane mediated with UZM-5 was developed to improve both rejection and permeate flux in oil separation [151].

## 2.7 SEPARATION PRINCIPLES AND SOLUTE TRANSPORTATION

It is commonly known that IP is limited by diffusional control. Increasing the concentrations of diamine increased the driving force of the diamine to transfer into the organic phase. As a result, it is expected that thicker and highly crosslinked layer can be produced at high concentrations of diamine. For NF membrane with lower operating pressure, skin layer with thickness around 30 nm is expected to give superior water permeability. On the other hand, assuming that the polymer undergoes binodal demixing in the organic phase whereby nucleation and crystallization will be taken place, higher diamine concentration is beneficial in producing a membrane with a smaller nucleus. A skin layer with a smaller nucleus gives a membrane with smaller pore size.
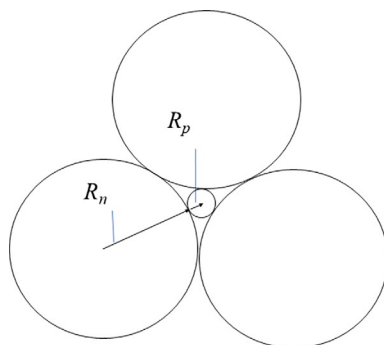


FIG. 2.4    Nodules and pore size of the nanofiltration.

Based on Fig. 2.4, by assuming the nucleus (nodule) to be spherical, three adjacent nuclei surround a space to form the pore. The pore radius ($R_p$) can be related to nucleus radius ($R_n$) as $R_p = 0.1547R_n$. Based on the analysis of the polyamide NF membrane, the nodule sizes (diameter) observed by the AFM were in the range of 360–480 Å [152]. This nodule size can be translated into pore radius of 2.8 nm to 3.7 nm.

Taking NF270 as an example, by assuming that the membrane consists of cylindrical pores ($\tau = 1$) with nodule radius of 2.7 nm (which gives pore radius of 0.42 nm) [21] and adopting the thickness of $104 \pm 23$ nm (measured using TEM) [153], the theoretical water permeability predicted using Kozeny-Carman equaion [154] (Eq. 2.1) is approximately $6.84 \times 10^{-10}$ m$^3$/m$^2$ s Pa. This prediction is an order of magnitude higher compared to the flux of commercial NF270 ($3.7 \times 10^{-11}$ m$^3$/m$^2$ s Pa) (Table 2.1), which shows that the actual permeability is much lower than the ideal permeability. For nanofiltration, the pore size should be lesser or equal to 0.379 nm for separation of hydrated SO$_4^{2-}$ [18]. Given this, improving the water permeability by increasing the pore size is in fact not practical. Furthermore, for a dense membrane, nodule size has minimal effect on the porosity. Based on these arguments, the only way to increase the permeability of the membrane (without compensating its rejection capability) could be achieved by reducing the tortuosity and thickness of the skin layer. Therefore, an effort to increase the micro-porosity and introducing the channeling effect by incorporating nanomaterials as discussed earlier is crucial to increase the membrane permeability.

$$J = -\frac{d_p^2}{180(1-\varepsilon)^2\mu}\frac{\varepsilon^3}{\tau}\frac{\Delta P}{\Delta x} \tag{2.1}$$

where $\varepsilon$ is the porosity, $\mu$ is the viscosity, $\Delta P$ is the pressure difference, $\Delta x$ is membrane thickness, $\tau$ is tortuosity factor, $J$ is solvent flux, and $d_p$ is nodule diameter.

## 2.7.1 Driving Force of NF Process

The transport equation of solute and water across the membrane depends on all forms of energy acting on the solute. The separation principles of the nanofiltration are no different with other pressure driven processes (e.g., microfiltration, ultrafiltration, and reverse osmosis) except the additional electrical potential. A potential difference arises because of changes in pressure, concentration, temperature, or electrical potential in both feed and permeate solutions. The first five terms on the right of Eq. (2.2) constitute the chemical potential of the system with the last term contributes to the mechanical potential. For an NF membrane,

the solute or solvent permeability is solely dependent on the chemical potential.

$$\mu_i = \mu_i^o + \overline{S}_i T + \overline{V}_i P + RT \ln a_i + ZF\psi + V(\rho_s - \rho)gz \tag{2.2}$$

- Gravitational potential
- Electrical potential
- Free energy of mixing
- Pressure energy
- Thermal energy
- Reference energy

where $\mu$ is the available potential; $R$ is the gas constant; $a_i$ is the activity of component; $T$ is the temperature; $i$; $V$ is the molar volume of component $i$; $p$ is the pressure; $F$ is the Faraday constant; and $\psi$ is the electrical potential; $S$ is the entropy.

To fully realize the potential of NF and to predict the performance of membrane, the modeling of solute and solvent transport through the membrane is necessary. Membrane separations are based on the differences in the transport rates of the components through the porous/dense membrane phase. The transport rate is controlled by the driving force and their mobility within the membrane phase. Their mobility is primarily determined by the solute's molecular size, and the concentration of the solute in the interphase and the membrane structure.

## 2.7.2 Membrane Transport Model

For an RO and an NF membrane, it is erroneous to assume that the membrane consists of virtual (visible) pores as what could be observed in loose ultrafiltration and microfiltration. Instead, the pore size is contributed by the membrane free volume due to the polymer packing density. The membranes are generally characterized by free volume, d-spacing, and chain mobility. These properties can be obtained with good confidence using PALS and simulated using molecular dynamics and Monte Carlo simulations. Nonetheless, still a great deal of literature reporting on the equivalence pore size assuming the validity of the cylindrical pores and adopting the Hagen-Poiseuille equation.

All the models that describe the transport of a solute through the membrane can be categorized as a mechanism-independent (phenomenological) model or a mechanistic model. The former model ignores the structure of the membrane while the latter take into account the physical and chemical properties of both the membrane and solution [155]. Examples

of the mechanism-independent model and mechanistic model are the Spiegler-Kedem model and the solution-diffusion model, respectively.

### 2.7.2.1 Spiegler-Kedem Model

In this model, the solvent flux is proportional to the pressure gradient across the membrane obeying the irreversible thermodynamic principles. The solute moves across the membrane by convection through the pores and diffuses within the nonporous matrix. The reflection coefficient ($\sigma$) indicates the degree of selectivity of the membrane. For $\sigma = 1$, the solute is wholly rejected, whereas, if $\sigma = 0$, no separation takes place, solute transport simultaneously with the solvent. This model is less suitable for an NF membrane especially with a loose structure whereby electrical potential cannot be neglected. The solvent and ion flux could be expressed as below [156, 157]:

$$\text{Solvent flux}: \quad J_v = -L_p \left( \frac{dp}{dx} - \sigma \frac{d\pi}{dx} \right) \tag{2.3}$$

$$\text{Ion flux}: \quad J_i = -P_s \frac{dC_i}{dx} + (1 - \sigma) C_i J_v \tag{2.4}$$

where $L_p$ is specific hydraulic permeability, m$^4$/N s, $p$ is operating pressure at the feed side of the membrane, N/m$^2$, $x$ is axial direction, $m$, $\sigma$ is reflection coefficient, $\pi$ is osmotic pressure, N/m$^2$, $P_s$ is local solute permeability, m$^2$/s, $C_i$ is the concentration in solution, mol/m$^3$.

### 2.7.2.2 Solution-Diffusion Model

In the solution diffusion model, permeants first dissolve in the membrane matrix and then diffuse through the membrane across the potential (concentration) gradient. Ions and solvent diffuse independently (uncoupled) of each other through the membrane. The convective term disappears due to the solute and is unlikely transported via convection. As this model ruled out the possibility of convective and electrical mobility, this model is seldom used for NF, and it is more suitable for an RO membrane. The solvent and ion flux could be expressed as below [158]:

$$\text{Solvent flux}: \quad J_v = \frac{D_i K_i c_{i0}}{l} \left[ 1 - \exp \left( \frac{-v_i (\Delta p - \Delta \pi)}{RT} \right) \right] \tag{2.5}$$

$$\text{Ion flux}: \quad J_j = \frac{D_j K_j}{l} \left[ c_{j0} - c_{ji} \exp \left( \frac{-v_j (p_0 - p_l)}{RT} \right) \right] \tag{2.6}$$

where $D_i$, $D_j$ are Fick's law diffusion coefficient, m$^2$/s, $K_i$, $K_j$ are liquid phase/membrane phase sorption coefficient, $c_{io}$, $c_{jo}$ are mole concentration of component $i$ and $j$ at membrane wall side, mol/m$^3$, $\Delta p$ is the difference in hydrostatic pressure across the membrane, atm, $\Delta \pi$ is osmotic pressure

difference across a membrane, atm, $v_i$, $v_j$ are molar volume of component $i$ and $j$, m$^3$/mol.

### 2.7.2.3 Kimura-Sourirajan Model

It is a generalized capillary-diffusion model in which solvent transport through the membrane by preferentially sorbs at the membrane-solution interface. Solvent/water transport through the capillary of the membrane via viscous flow; therefore, it is proportional to the effective pressure. On the other hand, solute pass through the pores by diffusion and hence its permeability is proportional to its concentration gradient across the membrane. A higher rejection is expected at elevated pressure due to the diluted permeate. However, this model is lacking the appropriate charged species separation as the contribution of electrostatic charge is not exclusively expressed. The solvent and ion flux could be expressed as below [159]:

$$\text{Solvent flux}: \quad N_B = A[P - \pi(X_{A2}) - \pi(X_{A3})] \tag{2.7}$$

$$\text{Ion flux}: \quad N_A = \frac{D_{AM}}{K.\delta}(c_2 X_{A2} - c_3 X_{A3}) \tag{2.8}$$

where $A$ is pure water permeability constant, mol/(m$^2$ s atm), $\pi(X_{A2})$ is osmotic pressure corresponding to mole fractions of solute at concentrated boundary solution on the high-pressure side, $\pi(X_{A3})$ is osmotic pressure corresponding to mole fractions of solute at the side of permeates, $c_2$, $c_3$ are molar density of solution (mole/cm$^3$), $D_{AM}/K\delta$ is solute transport parameter, m/s.

### 2.7.2.4 Maxwell-Stefan Model

These equations describe the diffusion of species under the driving forces, which is equal to the friction of that species with all the other components in the system [160]. The friction coefficient is specific for each pair of species and depends on the ionic strength. The common form of the Maxwell-Stefan equation of a species $i$ in one-dimensional transport is:

$$-\frac{d\mu_i}{dy} - V_{m,i}\frac{dP}{dy} - z_i F\frac{d\varnothing}{dy} = \sum_{j=1}^{n}\left[x_j \zeta_{i,j}(u_i - u_j)\right] \tag{2.9}$$

where $\mu$ is chemical potential (J), $Vm$ is molar volume (m$^3$/mol), $u$ is diffusive velocity (m/s), $x$ is mole fraction, $\zeta$ is diffusive friction coefficient (kg/s mol), $\varPhi$ is electrical potential (J/C).

### 2.7.2.5 Extended Nernst-Planck (ENP) Model

This is an alternative membrane transport model accounted for the porous structure that was simplified from the generalized Maxwell-Stefan equations. The extended Nernst-Planck model takes into account the convection, diffusion and electrical potential gradient for ions transport

through the membrane pores [161]. Compared to the nonporous model such as solution-diffusion model and kimura-Sourirajan Model, this mechanistic model could better explain the transport mechanism of nanofiltration that has looser skin layer. The detail of the transport equation is given below:

$$\text{Solvent flux}: \ J_v = \frac{-D_i.A_k}{\Delta x}\left\{\frac{1}{2}. \ \ln\frac{Z(C_{ip})^2 - 2C_{ip}Z(C_{ip}) - A}{Z(C_i^m)^2 - 2C_{ip}Z(C_i^m) - A}\right.$$

$$\left. + \frac{C_{ip}}{2B}. \ \ln\left(\frac{Z(C_{ip}) - C_{ip} - B}{Z(C_{ip}) - C_{ip} + B}.\frac{Z(C_i^m) - C_{ip} + B}{Z(C_i^m) - C_{ip} - B}\right)\right\}$$

$$(2.10)$$

$$\text{Ion flux}: \ j_i = j_v c_i^m - D_i\frac{dc_i^m}{dx} - \frac{Fz_i c_i^m D_i}{RT}\frac{d\psi}{dx} \qquad (2.11)$$

where $D_i$ is an effective diffusivity of solute in the membrane, m$^2$/s, $A_k$ is surface porosity, $\Delta x$ is membrane thickness, m, $C_{ip}$ is permeate concentration, mol/m$^3$, $C_i^m$ is concentration in membrane, mol/m$^3$, $c_i$ is mole concentration of component $i$ in membrane, mol/m$^3$, $j_v$ is volume flux based on membrane pore area, mol m$^2$ s$^{-1}$, $F$ is Faraday constant, C mol$^{-1}$, $z_i$ is valence of $i$th ion, $\psi$ is electric potential, $V$, $R$ is gas constant, J K$^{-1}$ mol$^{-1}$, $T$ is temperature, $K$.

Under this model, few structural models were derived based on the steric and partitioning condition between the membrane pores and the external solution, for example, Teorell-Meyer-Siever Model, space charge model, Donnan Steric Pore Model (DSPM), DSPM & dielectric exclusion model.

### 2.7.2.5.1 Teorell-Meyer-Siever Model (TMS)

In this model, it was assumed that uniform distribution of fixed charges and mobile species can be achieved based on Donnan equilibrium between the external solution and the membrane pore [162]. This equation provides a relation between the concentration of charged components within the membrane and in the bulk solution.

$$\left(\frac{\gamma_i c_i^m}{\gamma_i^0 C_i}\right)^{1/z_i} = \exp\left(-\frac{F}{RT}\Delta\psi_D\right) \qquad (2.12)$$

where $z_i$ is valence of $i$th ion, $\gamma_i^o$ is activity coefficient in the external solution, $\gamma_i$ is activity coefficient in the membrane, $R$ is gas constant, J K$^{-1}$ mol$^{-1}$, $T$ is temperature, $K$, $F$ is Faraday constant, C mol$^{-1}$, $\Delta\psi_D$ is Donnan potential at interface, $V$.

#### 2.7.2.5.2 Donnan Steric Pore Model (DSPM)

For DSPM, a porous membrane type was assumed. The solute velocity was assumed fully developed and followed the Hagen-Poiseuille type. At the solution-membrane interface, the Donnan equilibrium, as well as the steric effect, was taken into account [163]. The steric effect is a function of solute to pore radius.

$$\left(\frac{\gamma_i c_i^m}{\gamma_i^0 C_i}\right)^{1/z_i} = \Phi_i \exp\left(-\frac{F}{RT}\Delta\psi_D\right) \tag{2.13}$$

where $z_i$ is valence of $i$th ion, $\gamma_i^o$ is activity coefficient in the external solution, $\gamma_i$ is activity coefficient in the membrane, $R$ is gas constant, $J\,K^{-1}\,mol^{-1}$, $T$ is temperature, $K$, $F$ is Faraday constant, $C\,mol^{-1}$, $\Delta\psi_D$ is Donnan potential at interface, $V$, $\Phi_i$ is steric partition effect.

#### 2.7.2.5.3 Donnan Steric Pore Model & Dielectric Exclusion (DSPM&DE)

This model includes three separation mechanisms namely steric hindrance, Donnan equilibrium and dielectric exclusion for ionic partitioning at the interfaces. The solvation energy at feed/membrane interfaces is important in determining the rejection [164]:

$$\frac{c_i(0^+)}{c_i(0^-)} = \varphi_i \exp\left(-z_i \Delta\psi_{D0}\right) \exp\left(-z_i^2 \Delta W_0\right) \tag{2.14}$$

where $c_i(0^+)$ is mole concentration at feed/membrane interface, feed side, $mol/m^3$, $c_i(0^-)$ is mole concentration at feed/membrane interface, membrane side, $mol/m^3$, $\varphi_i$ is steric partitioning coefficient, $z_i$ is valence of $i$th ion, $\Delta\psi_{D0}$ is Donnan potential at interface at feed/membrane interface, $V$, $\Delta W_0$ is the dimensionless excess solvation energy at feed/membrane interface.

### 2.7.2.6 Space Charge Model (SC)

The space-charge model was first proposed by Osterle and co-workers [163, 165]. The basic equations include electric potential in the axial/radial direction, the Poisson-Boltzmann equation for ion concentration, the Nernst-Planck equations for ionic transport, and the Navier-Stokes equation for the force balance.

*In flux in x-direction:*

$$j_i = u_x c_i + D_i \frac{\partial c_i}{\partial x} - \frac{D_i}{RT} z_i c_i F \frac{\partial\varphi}{\partial x} \tag{2.15}$$

*Ion flux in r-direction:*

$$j_{r,i} = u_r c_i + D_i \frac{\partial c_i}{\partial r} - \frac{D_i}{RT} z_i c_i F \frac{\partial \varphi}{\partial r} \tag{2.16}$$

where $j_i$ is ion flux in the axial direction, mol/(m$^2$ s$^{-1}$), $j_{r,i}$ is ion flux in the radial direction, mol/(m$^2$ s$^{-1}$), $u_x$ is mass flux in axial direction, ms$^{-1}$, $u_r$ is mass flux in radial direction, ms$^{-1}$, $c_i$ is concentration in the membrane, mol m$^{-3}$, $r$ is radial variable of capillary, $m$, $D_i$ is diffusivity of ion i, m$^2$/s, $R$ is gas constant, J K$^{-1}$ mol$^{-1}$, $T$ is temperature, $K$, $F$ is Faraday constant, C mol$^{-1}$, $\varphi_T$ is total electrostatic potential in capillary, $V$.

## 2.8 CONCLUSION

Nanofiltration, which evolved from the energy intensive reverse osmosis, has gained tremendous interest from the industries. NF could find its applications in water, wastewater, and pharmaceutical industries under isothermal conditions. It has added advantages compared to other conventional technologies, which include lower footprint, ease of scale up, and economical viability due to its chemical-free process. Membrane fouling remains a challenging issue to handle although burgeoning research on the new material and system has been carried out over the past 30 years. A wide choice of membrane material for an NF membrane prepared using interfacial polymerization methods make it a viable technique to produce high flux and TFC membrane with better antifouling properties. However, an NF membrane is still far from performing at a level that would spur the rapid acceptance for a harsh process, such as corrosive effluent. Although the TFC membrane prepared via interfacial polymerization gave the highest membrane permeability, this technique still has limitations in preparing the SRNF membrane. Recent advances in membrane synthesis using other methods has enabled a more extensive choice of materials suited for SRNF membrane.

Continuous effort to enhance the functionality of the NF membrane via nanocomposite membrane is necessary. With the advances of 2D and 3D nanomaterials, the thin film nanocomposite membrane, which possesses the desired properties of the inorganic membrane, could be synthesized via the facile and economic IP route. Despite significant achievement in membrane flux increment, membrane permeability still has room for improvement by order of magnitude via thickness and tortuosity reduction. It can be achieved by incorporating the porous nanomaterial within the skin layer and optimizing the support layer using nanofibrous materials. An inorganic membrane, which is mechanically and chemically more robust than the polymeric membrane, will inevitably dominate the market once the production cost can be lower down. Until then, the polymeric membrane is still high in demand for the conventional

process. For the water and wastewater treatment, the primary concern remains on how the permeability could be enhanced at a lower expense of energy. This can be achieved by incorporating the nanomaterial with a channeling effect that reduces the membrane tortuosity and the effective thickness.

The membrane transport modeling using both phenomenological and mechanistic approach has been well studied by taking into account the physical and chemical properties of both membrane and solution properties. The proposed model is beneficial in predicting the overall plant performance as its calculation is not time consuming and reliable. Complex molecular scale modeling of the water and solute transport that dynamically simulate the real systems were performed. The simulation would improve the understanding of intermolecular interaction at membrane surface (fouling) and within the matrix (permeability).

In overall, there is still room for improvement of the TFC NF membrane regarding flux enhancement as well as antifouling properties. Besides the conventional applications, functionalized NF membranes make it applicable for more specific applications. It can be achieved by reengineering the material and method to produce the membrane aided with the traditional understanding of membrane transportation.

## Acknowledgment

## References

[1] Tinghir A, Bonnelye V, Masereel P. Degrémont's largest nanofiltration plant: NOM removal at the Vegi 2000. Desalin Water Treat 2009;5(1–3):178–82.

[2] Hosseini SS, Nazif A, Alaei Shahmirzadi MA, Ortiz I. Fabrication, tuning and optimization of poly (acrilontryle) nanofiltration membranes for effective nickel and chromium removal from electroplating wastewater. Sep Purif Technol 2017;187:46–59.

[3] Babu J, Murthy ZVP. Treatment of textile dyes containing wastewaters with PES/PVA thin film composite nanofiltration membranes. Sep Purif Technol 2017;183:66–72.

[4] Miralles-Cuevas S, Oller I, Agüera A, Llorca M, Sánchez Pérez JA, Malato S. Combination of nanofiltration and ozonation for the remediation of real municipal wastewater effluents: acute and chronic toxicity assessment. J Hazard Mater 2017;323:442–51.

[5] Tonko CM, Kiraly A, Mizsey P, Patzay G, Csefalvay E. Limitation of hardness from thermal water by means of nanofiltration. Water Sci Technol 2013;67(9):2025–32.

[6] Gorenflo A, Velázquez-Padrón D, Frimmel FH. Nanofiltration of a German groundwater of high hardness and NOM content: performance and costs. Desalination 2003;151(3):253–65.

[7] Cao J, Wang G, Wu S, Zhang W, Liu C, Li H, et al. Comparison of nanofiltration and evaporation technologies on the storage stability of milk protein concentrates. Dairy Sci Technol 2016;96(1):107–21.

[8] Li H, Shi W, Wang W, Zhu H. The extraction of sericin protein from silk reeling waste-water by hollow fiber nanofiltration membrane integrated process. Sep Purif Technol 2015;146:342–50.

[9] Zhao F-Y, An Q-F, Ji Y-L, Gao C-J. A novel type of polyelectrolyte complex/MWCNT hybrid nanofiltration membranes for water softening. J Membr Sci 2015;492:412–21.

[10] Zhao S, Yao Y, Ba C, Zheng W, Economy J, Wang P. Enhancing the performance of poly-ethylenimine modified nanofiltration membrane by coating a layer of sulfonated poly(ether ether ketone) for removing sulfamerazine. J Membr Sci 2015;492:620–9.

[11] Akbari A, Solymani H, Rostami SMM. Preparation and characterization of a novel pos-itively charged nanofiltration membrane based on polysulfone. J Appl Polym Sci 2015;132(22). https://doi.org/10.1002/app.41988.

[12] Zheng Y, Yao G, Cheng Q, Yu S, Liu M, Gao C. Positively charged thin-film composite hollow fiber nanofiltration membrane for the removal of cationic dyes through sub-merged filtration. Desalination 2013;328:42–50.

[13] Chen Q, Yu P, Huang W, Yu S, Liu M, Gao C. High-flux composite hollow fiber nanofiltration membranes fabricated through layer-by-layer deposition of oppo-sitely charged crosslinked polyelectrolytes for dye removal. J Membr Sci 2015;492:312–21.

[14] Guo H, Chen M, Liu Q, Wang Z, Cui S, Zhang G. LbL assembly of sulfonated cyclohexanone–formaldehyde condensation polymer and poly(ethyleneimine) toward rejection of both cationic ions and dyes. Desalination 2015;365:108–16.

[15] Rao AP, Joshi S, Trivedi J, Devmurari C, Shah V. Structure–performance correlation of polyamide thin film composite membranes: effect of coating conditions on film forma-tion. J Membr Sci 2003;211(1):13–24.

[16] Gagliardi M. Global markets and technologies for nanofiltration. BCC Res 2014;132.

[17] Petersen RJ. Composite reverse osmosis and nanofiltration membranes. J Membr Sci 1993;83(1):81–150.

[18] Fang W, Shi L, Wang R. Interfacially polymerized composite nanofiltration hollow fiber membranes for low-pressure water softening. J Membr Sci 2013;430:129–39.

[19] Schaep J, Vandecasteele C, Wahab Mohammad A, Richard Bowen W. Modelling the retention of ionic components for different nanofiltration membranes. Sep Purif Technol 2001;22:169–79.

[20] Hilal N, Al-Zoubi H, Darwish NA, Mohammad AW. Nanofiltration of magnesium chlo-ride, sodium carbonate, and calcium sulphate in salt solutions. Sep Sci Technol 2005;40(16):3299–321.

[21] Nghiem LD, Hawkes S. Effects of membrane fouling on the nanofiltration of pharmaceu-tically active compounds (PhACs): mechanisms and role of membrane pore size. Sep Purif Technol 2007;57(1):176–84.

[22] Boussu K, Van der Bruggen B, Volodin A, Van Haesendonck C, Delcour J, Van Der Meeren P, et al. Characterization of commercial nanofiltration membranes and compar-ison with self-made polyethersulfone membranes. Desalination 2006;191(1–3):245–53.

[23] Al-Amoudi A, Williams P, Al-Hobaib AS, Lovitt RW. Cleaning results of new and fouled nanofiltration membrane characterized by contact angle, updated DSPM, flux and salts rejection. Appl Surf Sci 2008;254(13):3983–92.

[24] Freger V. Kinetics of film formation by interfacial polycondensation. Langmuir 2005;21(5):1884–94.

[25] Mehta R, Brahmbhatt H, Mukherjee M, Bhattacharya A. Tuning separation behavior of tailor-made thin film poly(piperazine-amide) composite membranes for pesticides and salts from water. Desalination 2017;404:280–90.

[26] Cadotte JE. Evolution of composite reverse osmosis membranes. Washington, DC: ACS Publications; 1985.

[27] Sundet SA. Production of composite membranes. Google Patents; 1985.

[28] Tomaschke JE. amine monomers and their use in preparing interfacially synthesized membranes for reverse osmosis and nanofiltration. Google Patents; 1999.

[29] Yu S, Liu M, Lü Z, Zhou Y, Gao C. Aromatic-cycloaliphatic polyamide thin-film composite membrane with improved chlorine resistance prepared from m-phenylenediamine-4-methyl and cyclohexane-1,3,5-tricarbonyl chloride. J Membr Sci 2009;344(1–2):155–64.

[30] Chen G-E, Liu Y-J, Xu Z-L, Tang Y-J, Huang H-H, Sun L. Fabrication and characterization of a novel nanofiltration membrane by the interfacial polymerization of 1,4-diaminocyclohexane (DCH) and trimesoyl chloride (TMC). RSC Adv 2015; 5(51):40742–52.

[31] Trushinski B, Dickson J, Smyth T, Childs R, McCarry B. Polysulfonamide thin-film composite reverse osmosis membranes. J Membr Sci 1998;143(1):181–8.

[32] Yu S, Ma M, Liu J, Tao J, Liu M, Gao C. Study on polyamide thin-film composite nanofiltration membrane by interfacial polymerization of polyvinylamine (PVAm) and isophthaloyl chloride (IPC). J Membr Sci 2011;379(1–2):164–73.

[33] Chen G-E, Liu Y-J, Xu Z-L, Hu D, Huang H-H, Sun L. Preparation and characterization of a composite nanofiltration membrane from cyclen and trimesoyl chloride prepared by interfacial polymerization. J Appl Polym Sci 2015;132(33). https://doi.org/10.1002/app.42345.

[34] Zhao J, Su Y, He X, Zhao X, Li Y, Zhang R, et al. Dopamine composite nanofiltration membranes prepared by self-polymerization and interfacial polymerization. J Membr Sci 2014;465:41–8.

[35] Nunes SP, Peinemann K-V. Membrane technology. New York: Wiley Online Library; 2001.

[36] Zhou C, Shi Y, Sun C, Yu S, Liu M, Gao C. Thin-film composite membranes formed by interfacial polymerization with natural material sericin and trimesoyl chloride for nanofiltration. J Membr Sci 2014;471:381–91.

[37] Li X, Cao Y, Yu H, Kang G, Jie X, Liu Z, et al. A novel composite nanofiltration membrane prepared with PHGH and TMC by interfacial polymerization. J Membr Sci 2014;466:82–91.

[38] An Q-F, Sun W-D, Zhao Q, Ji Y-L, Gao C-J. Study on a novel nanofiltration membrane prepared by interfacial polymerization with zwitterionic amine monomers. J Membr Sci 2013;431:171–9.

[39] Tang B, Huo Z, Wu P. Study on a novel polyester composite nanofiltration membrane by interfacial polymerization of triethanolamine (TEOA) and trimesoyl chloride (TMC): I. Preparation, characterization and nanofiltration properties test of membrane. J Membr Sci 2008;320(1–2):198–205.

[40] Seman MNA, Khayet M, Hilal N. Nanofiltration thin-film composite polyester polyethersulfone-based membranes prepared by interfacial polymerization. J Membr Sci 2010;348(1):109–16.

[41] Zhang Y, Su Y, Peng J, Zhao X, Liu J, Zhao J, et al. Composite nanofiltration membranes prepared by interfacial polymerization with natural material tannic acid and trimesoyl chloride. J Membr Sci 2013;429:235–42.

[42] Bera A, Bhalani DV, Jewrajka SK, Ghosh PK. The effect of phenol functionality on the characteristic features and performance of fully aromatic polyester thin film composite nanofiltration membranes. RSC Adv 2016;6(102):99867–77.

[43] Cheng J, Shi W, Zhang L, Zhang R. A novel polyester composite nanofiltration membrane formed by interfacial polymerization of pentaerythritol (PE) and trimesoyl chloride (TMC). Appl Surf Sci 2017;416:152–9.

[44] Wei X, Kong X, Yang J, Zhang G, Chen J, Wang J. Structure influence of hyperbranched polyester on structure and properties of synthesized nanofiltration membranes. J Membr Sci 2013;440:67–76.

[45] Kong X, Zhang Y, Zeng S-Y, Zhu B-K, Zhu L-P, Fang L-F, et al. Incorporating hyperbranched polyester into cross-linked polyamide layer to enhance both permeability and selectivity of nanofiltration membrane. J Membr Sci 2016;518:141–9.

[46] Razdan U, Kulkarni S. Nanofiltration thin-film-composite polyesteramide membranes based on bulky diols. Desalination 2004;161(1):25–32.

[47] Lee KP, Zheng J, Bargeman G, Kemperman AJB, Benes NE. pH stable thin film composite polyamine nanofiltration membranes by interfacial polymerisation. J Membr Sci 2015;478:75–84.

[48] Lee KP, Bargeman G, de Rooij R, Kemperman AJB, Benes NE. Interfacial polymerization of cyanuric chloride and monomeric amines: pH resistant thin film composite polyamine nanofiltration membranes. J Membr Sci 2017;523:487–96.

[49] Li Y, Su Y, Zhao X, Zhang R, Liu Y, Fan X, et al. Preparation of antifouling nanofiltration membrane via interfacial polymerization of fluorinated polyamine and trimesoyl chloride. Ind Eng Chem Res 2015;54(33):8302–10.

[50] Mahdavi H, Razmi F, Shahalizade T. Polyurethane TFC nanofiltration membranes based on interfacial polymerization of poly(bis-MPA) and MDI on the polyethersulfone support. Sep Purif Technol 2016;162:37–44.

[51] Ghosh AK, Jeong B-H, Huang X, Hoek EM. Impacts of reaction and curing conditions on polyamide composite reverse osmosis membrane properties. J Membr Sci 2008;311 (1):34–45.

[52] Roh IJ, Greenberg AR, Khare VP. Synthesis and characterization of interfacially polymerized polyamide thin films. Desalination 2006;191(1–3):279–90.

[53] Kim IC, Jegal J, Lee KH. Effect of aqueous and organic solutions on the performance of polyamide thin-film-composite nanofiltration membranes. J Polym Sci B Polym Phys 2002;40(19):2151–63.

[54] Saha N, Joshi S. Performance evaluation of thin film composite polyamide nanofiltration membrane with variation in monomer type. J Membr Sci 2009;342(1):60–9.

[55] Soroush A, Barzin J, Barikani M, Fathizadeh M. Interfacially polymerized polyamide thin film composite membranes: preparation, characterization and performance evaluation. Desalination 2012;287:310–6.

[56] Chen SH, Chang DJ, Liou RM, Hsu CS, Lin SS. Preparation and separation properties of polyamide nanofiltration membrane. J Appl Polym Sci 2002;83(5):1112–8.

[57] Wei X-Z, Zhu L-P, Deng H-Y, Xu Y-Y, Zhu B-K, Huang Z-M. New type of nanofiltration membrane based on crosslinked hyperbranched polymers. J Membr Sci 2008;323(2): 278–287.

[58] Wei X-Z, Yang J, Xu Y-Y, Zhu B-K, Zhang G-L. Preparation and characterization of low-pressure nanofiltration membranes and the application in the separation process of dye molecules. J Porous Mater 2012;19(5):721–31.

[59] Mickols WE. Composite membrane and method for making the same. Google Patents; 2002.

[60] Jayarani M, Kulkarni S. Thin-film composite poly (esteramide)-based membranes. Desalination 2000;130(1):17–30.

[61] Cadotte JE, inventor; FilmTec Corporation, assignee. Interfacially synthesized reverse osmosis membrane;1981.

[62] Han G, Chung TS, Toriida M, Tamai S. Thin-film composite forward osmosis membranes with novel hydrophilic supports for desalination. J Membr Sci 2012;423: 543–55.

[63] Ghosh AK, Hoek EM. Impacts of support membrane structure and chemistry on polyamide–polysulfone interfacial composite membranes. J Membr Sci 2009;336 (1):140–8.

[64] Sukitpaneenit P, Chung TS. High performance thin-film composite forward osmosis hollow fiber membranes with macrovoid-free and highly porous structure for sustainable water production. Environ Sci Technol 2012;46(13):7358–65.

[65] Chen J, Ahmad A, Ooi B. Poly (N-isopropylacrylamide-co-acrylic acid) hydrogels for copper ion adsorption: equilibrium isotherms, kinetic and thermodynamic studies. J Environ Chem Eng 2013;1(3):339–48.

[66] Dumée L, Lee J, Sears K, Tardy B, Duke M, Gray S. Fabrication of thin film composite poly (amide)-carbon-nanotube supported membranes for enhanced performance in osmotically driven desalination systems. J Membr Sci 2013;427:422–30.

[67] Singh PS, Joshi S, Trivedi J, Devmurari C, Rao AP, Ghosh P. Probing the structural variations of thin film composite RO membranes obtained by coating polyamide over polysulfone membranes of different pore dimensions. J Membr Sci 2006;278(1): 19–25.

[68] Mahdavi H, Moslehi M. A new thin film composite nanofiltration membrane based on PET nanofiber support and polyamide top layer: preparation and characterization. J Polym Res 2016;23(12):257.

[69] Shen L, Yang Y, Zhao J, Wang X. High-performance nanofiltration membrane prepared by dopamine-assisted interfacial polymerization on PES nanofibrous scaffolds. Desalin Water Treat 2016;57(21):9549–57.

[70] Wang X, Yeh T-M, Wang Z, Yang R, Wang R, Ma H, et al. Nanofiltration membranes prepared by interfacial polymerization on thin-film nanofibrous composite scaffold. Polymer 2014;55(6):1358–66.

[71] Yoon K, Hsiao BS, Chu B. High flux nanofiltration membranes based on interfacially polymerized polyamide barrier layer on polyacrylonitrile nanofibrous scaffolds. J Membr Sci 2009;326(2):484–92.

[72] Bergman RA. Membrane softening versus lime softening in Florida: a cost comparison update. Desalination 1995;102(1):11–24.

[73] Shahmansouri A, Bellona C. Nanofiltration technology in water treatment and reuse: applications and costs. Water Sci Technol 2015;71(3):309–19.

[74] Su B, Dou M, Wang Y, Gao X, Gao C. Study on seawater nanofiltration softening technology for offshore oilfield polymer solution preparation. Desalin Water Treat 2013; 51(25–27):5064–73.

[75] Song Y, Li T, Zhou J, Pan F, Su B, Gao C. Comprehensive pilot-scale investigation of seawater nanofiltration softening by increasing permeate recovery with recirculation. Desalin Water Treat 2016;57(37):17271–82.

[76] Su BW, Wang YH, Gao XL, editors. Pilot study on nanofiltration seawater softening for SWRO desalination. Adv Mater Res 2012;550-553:2178–81. editors.

[77] Amaral MCS, Pereira HV, Nani E, Lange LC. Treatment of landfill leachate by hybrid precipitation/microfiltration/nanofiltration process. Water Sci Technol 2015;72 (2):269–76.

[78] Religaa P, Kazmierczak B. Desalination of chromium tannery wastewater by nanofiltration with different diafiltration mode. Desalin Water Treat 2017;64:409–13.

[79] Lan Y, Coetsier C, Causserand C, Serrano KG. Feasibility of micropollutants treatment by coupling nanofiltration and electrochemical oxidation: case of hospital wastewater. Int J Chem React Eng 2015;13(2):153–9.

[80] Vergili I, Gencdal S. Applicability of combined Fenton oxidation and nanofiltration to pharmaceutical wastewater. Desalin Water Treat 2015;56(13):3501–9.

[81] Pulido JMO. A review on the use of membrane technology and fouling control for olive mill wastewater treatment. Sci Total Environ 2016;563:664–75.

[82] Zacharof M-P, Mandale SJ, Williams PM, Lovitt RW. Nanofiltration of treated digested agricultural wastewater for recovery of carboxylic acids. J Clean Prod 2016;112:4749–61.

[83] Liang C-Z, Sun S-P, Zhao B-W, Chung T-S. Integration of nanofiltration hollow fiber membranes with coagulation–flocculation to treat colored wastewater from a dyestuff manufacturer: a pilot-scale study. Ind Eng Chem Res 2015;54(44):11159–66.

[84] Woo YC, Lee JJ, Shim W-G, Shon HK, Tijing LD, Yao M, et al. Effect of powdered activated carbon on integrated submerged membrane bioreactor–nanofiltration process for wastewater reclamation. Bioresour Technol 2016;210:18–25.

[85] Azaïs A, Mendret J, Petit E, Brosillon S. Influence of volumetric reduction factor during ozonation of nanofiltration concentrates for wastewater reuse. Chemosphere 2016;165:497–506.

[86] Esmaili Z, Cheshmberah F, Solaimany Nazar AR, Farhadian M. Treatment of florfenicol of synthetic trout fish farm wastewater through nanofiltration and photocatalyst oxidation. Environ Technol 2017;38(16):2040–7.

[87] Shang W, Sun F, Chen L. Nanofiltration fouling propensity caused by wastewater effluent organic matters and surface-water dissolved organic matters. Environ Technol 2017;1–12. https://doi.org/10.1080/09593330.2017.1344324.

[88] Lee JJ, Woo YC, Kang J-S, Kang CY, Kim H-S. Effect of various pretreatments on the performance of nanofiltration for wastewater reuse. Desalin Water Treat 2016;57(16):7522–30.

[89] Sanches S, Fraga MC, Silva NA, Nunes P, Crespo JG, Pereira VJ. Pilot scale nanofiltration treatment of olive mill wastewater: a technical and economical evaluation. Environ Sci Pollut Res 2017;24(4):3506–18.

[90] Savin I-I, Butnaru R. Wastewater characteristics in textile finishing mills. Environ Eng Manag J 2008;7(6):859–64.

[91] Gozálvez-Zafrilla JM, Sanz-Escribano D, Lora-García J, León Hidalgo MC. Nanofiltration of secondary effluent for wastewater reuse in the textile industry. Desalination 2008;222(1):272–9.

[92] Salehi F. Current and future applications for nanofiltration technology in the food processing. Food Bioprod Process 2014;92(2):161–77.

[93] Lievore P, Simões DR, Silva KM, Drunkler NL, Barana AC, Nogueira A, et al. Chemical characterisation and application of acid whey in fermented milk. J Food Sci Technol 2015;52(4):2083–92.

[94] Chandrapala J, Chen GQ, Kezia K, Bowman EG, Vasiljevic T, Kentish SE. Removal of lactate from acid whey using nanofiltration. J Food Eng 2016;177:59–64.

[95] Bédas M, Tanguy G, Dolivet A, Méjean S, Gaucheron F, Garric G, et al. Nanofiltration of lactic acid whey prior to spray drying: scaling up to a semi-industrial scale. LWT Food Sci Technol 2017;79:355–60.

[96] Pal A, Dey TK, Bindal RC. Intrinsic dependence of hydrophilic and electrokinetic features of positively charged thin film composite nanofiltration membranes on molecular weights of poly(ethyleneimine)s. Polymer 2016;93:99–114.

[97] Dey TK, Bindal RC, Prabhakar S, Tewari PK. Development, characterization and performance evaluation of positively-charged thin film-composite nanofiltration membrane containing fixed quaternary ammonium moieties. Sep Sci Technol 2011;46(6):933–43.

[98] Sun SP, Hatton TA, Chan SY, Chung T-S. Novel thin-film composite nanofiltration hollow fiber membranes with double repulsion for effective removal of emerging organic matters from water. J Membr Sci 2012;401:152–62.

[99] Li X, Zhang C, Zhang S, Li J, He B, Cui Z. Preparation and characterization of positively charged polyamide composite nanofiltration hollow fiber membrane for lithium and magnesium separation. Desalination 2015;369:26–36.

[100] Thong Z, Cui Y, Ong YK, Chung T-S. Molecular design of nanofiltration membranes for the recovery of phosphorus from sewage sludge. ACS Sustain Chem Eng 2016;4(10):5570–7.

[101] Wei X, Wang S, Shi Y, Xiang H, Chen J. Application of positively charged composite hollow-fiber nanofiltration membranes for dye purification. Ind Eng Chem Res 2014;53(36):14036–45.

[102] Liu M, Zheng Y, Shuai S, Zhou Q, Yu S, Gao C. Thin-film composite membrane formed by interfacial polymerization of polyvinylamine (PVAm) and trimesoyl chloride (TMC) for nanofiltration. Desalination 2012;288:98–107.

[103] Jin W, Toutianoush A, Tieke B. Use of polyelectrolyte layer-by-layer assemblies as nanofiltration and reverse osmosis membranes. Langmuir 2003;19(7):2550–3.

[104] Zhu W-P, Gao J, Sun S-P, Zhang S, Chung T-S. Poly(amidoamine) dendrimer (PAMAM) grafted on thin film composite (TFC) nanofiltration (NF) hollow fiber membranes for heavy metal removal. J Membr Sci 2015;487:117–26.

[105] Li M, Lv Z, Zheng J, Hu J, Jiang C, Ueda M, et al. Positively charged nanofiltration membrane with dendritic surface for toxic element removal. ACS Sustain Chem Eng 2017;5(1):784–92.

[106] Zhao F-Y, Ji Y-L, Weng X-D, Mi Y-F, Ye C-C, An Q-F, et al. High-flux positively charged nanocomposite nanofiltration membranes filled with poly (dopamine) modified multiwall carbon nanotubes. ACS Appl Mater Interfaces 2016;8(10):6693–700.

[107] Lianchao L, Baoguo W, Huimin T, Tianlu C, Jiping X. A novel nanofiltration membrane prepared with PAMAM and TMC by in situ interfacial polymerization on PEK-C ultrafiltration membrane. J Membr Sci 2006;269(1):84–93.

[108] Sum JY, Ahmad AL, Ooi BS. Synthesis of thin film composite membrane using mixed dendritic poly(amidoamine) and void filling piperazine monomers. J Membr Sci 2014;466:183–91.

[109] Tang Y-J, Xu Z-L, Huang B-Q, Wei Y-M, Yang H. Novel polyamide thin-film composite nanofiltration membrane modified with poly (amidoamine) and $SiO_2$ gel. RSC Adv 2016;6(51):45585–94.

[110] Xu X-X, Zhou C-L, Zeng B-R, Xia H-P, Lan W-G, He X-M. Structure and properties of polyamidoamine/polyacrylonitrile composite nanofiltration membrane prepared by interfacial polymerization. Sep Purif Technol 2012;96:229–36.

[111] Mansourpanah Y, Jafari Z. Efficacy of different generations and concentrations of PAMAM–NH 2 on the performance and structure of TFC membranes. React Funct Polym 2015;93:178–89.

[112] Zhang R, Su Y, Zhao X, Li Y, Zhao J, Jiang Z. A novel positively charged composite nanofiltration membrane prepared by bio-inspired adhesion of polydopamine and surface grafting of poly(ethylene imine). J Membr Sci 2014;470:9–17.

[113] Guo H, Deng Y, Yao Z, Yang Z, Wang J, Lin C, et al. A highly selective surface coating for enhanced membrane rejection of endocrine disrupting compounds: mechanistic insights and implications. Water Res 2017;121:197–203.

[114] Wang J, Zhu J, Tsehaye MT, Li J, Dong G, Yuan S, et al. High flux electroneutral loose nanofiltration membranes based on rapid deposition of polydopamine/polyethyleneimine. J Mater Chem A 2017;5(28):14847–57.

[115] Li Y, Su Y, Li J, Zhao X, Zhang R, Fan X, et al. Preparation of thin film composite nanofiltration membrane with improved structural stability through the mediation of polydopamine. J Membr Sci 2015;476:10–9.

[116] Volkov AV, Stamatialis DF, Khotimsky VS, Volkov VV, Wessling M, Platé NA. Poly[1-(trimethylsilyl)-1-propyne] as a solvent resistance nanofiltration membrane material. J Membr Sci 2006;281(1):351–7.

[117] Xu Y, You F, Sun H, Shao L. Realizing mussel-inspired polydopamine selective layer with strong solvent resistance in nanofiltration toward sustainable reclamation. ACS Sustain Chem Eng 2017;5(6):5520–8.

[118] Wang Z, Wei Y-M, Xu Z-L, Cao Y, Dong Z-Q, Shi X-L. Preparation, characterization and solvent resistance of γ-$Al_2O_3$/α-$Al_2O_3$ inorganic hollow fiber nanofiltration membrane. J Membr Sci 2016;503:69–80.

[119] Werth K, Kaupenjohann P, Skiborowski M. The potential of organic solvent nanofiltration processes for oleochemical industry. Sep Purif Technol 2017;182:185–96.

[120] Li X, Chen B, Cai W, Wang T, Wu Z, Li J. Highly stable PDMS-PTFPMS/PVDF OSN membranes for hexane recovery during vegetable oil production. RSC Adv 2017;7(19): 11381–11388.

[121] Buonomenna MG, Bae J. Organic solvent nanofiltration in pharmaceutical industry. Sep Purif Rev 2015;44(2):157–82.

[122] Aburabie J, Neelakanda P, Karunakaran M, Peinemann K-V. Thin-film composite crosslinked polythiosemicarbazide membranes for organic solvent nanofiltration (OSN). React Funct Polym 2015;86:225–32.

[123] Sun S-P, Chung T-S, Lu K-J, Chan S-Y. Enhancement of flux and solvent stability of Matrimid® thin-film composite membranes for organic solvent nanofiltration. AICHE J 2014;60(10):3623–33.

[124] Solomon MFJ, Bhole Y, Livingston AG. High flux membranes for organic solvent nano-filtration (OSN)—interfacial polymerization with solvent activation. J Membr Sci 2012;423:371–82.

[125] Davood Abadi Farahani MH, Hua D, Chung T-S. Cross-linked mixed matrix mem-branes consisting of carboxyl-functionalized multi-walled carbon nanotubes and P84 polyimide for organic solvent nanofiltration (OSN). Sep Purif Technol 2017;186:243–54.

[126] Xu YC, Cheng XQ, Long J, Shao L. A novel monoamine modification strategy toward high-performance organic solvent nanofiltration (OSN) membrane for sustainable molecular separations. J Membr Sci 2016;497:77–89.

[127] Lv Y, Du Y, Qiu W-Z, Xu Z-K. Nanocomposite membranes via the codeposition of poly-dopamine/polyethylenimine with silica nanoparticles for enhanced mechanical strength and high water permeability. ACS Appl Mater Interfaces 2017;9(3):2966–72.

[128] Rakhshan N, Pakizeh M. The effect of chemical modification of $SiO_2$ nanoparticles on the nanofiltration characteristics of polyamide membrane. Korean J Chem Eng 2015; 32(12):2524–33.

[129] Li Q, Wang Y, Song J, Guan Y, Yu H, Pan X, et al. Influence of silica nanospheres on the separation performance of thin film composite poly(piperazine-amide) nanofiltration membranes. Appl Surf Sci 2015;324:757–64.

[130] Wang J, Wang Y, Zhu J, Zhang Y, Liu J, Van der Bruggen B. Construction of $TiO_2$@gra-phene oxide incorporated antifouling nanofiltration membrane with elevated filtration performance. J Membr Sci 2017;533:279–88.

[131] Li H, Shi W, Du Q, Zhou R, Zhang H, Qin X. Improved separation and antifouling prop-erties of thin-film composite nanofiltration membrane by the incorporation of cGO. Appl Surf Sci 2017;407:260–75.

[132] Zhang C, Wei K, Zhang W, Bai Y, Sun Y, Gu J. Graphene oxide quantum dots incorpo-rated into a thin film nanocomposite membrane with high flux and antifouling prop-erties for low-pressure nanofiltration. ACS Appl Mater Interfaces 2017;9(12):11082–94.

[133] Lai GS, Lau WJ, Goh PS, Ismail AF, Yusof N, Tan YH. Graphene oxide incorporated thin film nanocomposite nanofiltration membrane for enhanced salt removal perfor-mance. Desalination 2016;387:14–24.

[134] Li H, Shi W, Su Y, Zhang H, Qin X. Preparation and characterization of carboxylated multiwalled carbon nanotube/polyamide composite nanofiltration membranes with improved performance. J Appl Polym Sci 2017;134(36):45268.

[135] Mahdavi MR, Delnavaz M, Vatanpour V, Farahbakhsh J. Effect of blending polypyrrole coated multiwalled carbon nanotube on desalination performance and antifouling property of thin film nanocomposite nanofiltration membranes. Sep Purif Technol 2017;184:119–27.

[136] Song X, Wang L, Mao L, Wang Z. Nanocomposite membrane with different carbon nanotubes location for nanofiltration and forward osmosis applications. ACS Sustain Chem Eng 2016;4(6):2990–7.

[137] Al-Hobaib A, El Ghoul J, El Mir L. Synthesis and characterization of polyamide thin-film nanocomposite membrane containing ZnO nanoparticles. Membr Water Treat 2015;6(4):309–21.

[138] Pal A, Dey TK, Singhal A, Bindal RC, Tewari PK. Nano-ZnO impregnated inorganic-polymer hybrid thinfilm nanocomposite nanofiltration membranes: an investigation of variation in structure, morphology and transport properties. RSC Adv 2015;5(43): 34134–34151.

[139] Peyravi M, Jahanshahi M, Rahimpour A, Javadi A, Hajavi S. Novel thin film nanocomposite membranes incorporated with functionalized $TiO_2$ nanoparticles for organic solvent nanofiltration. Chem Eng J 2014;241:155–66.

[140] Lee HS, Im SJ, Kim JH, Kim HJ, Kim JP, Min BR. Polyamide thin-film nanofiltration membranes containing $TiO_2$ nanoparticles. Desalination 2008;219(1):48–56.

[141] L-x D, X-c H, Wang Z, Yang Z, X-m W, Tang CY. A thin-film nanocomposite nanofiltration membrane prepared on a support with in situ embedded zeolite nanoparticles. Sep Purif Technol 2016;166:230–9.

[142] Basu S, Balakrishnan M. Polyamide thin film composite membranes containing ZIF-8 for the separation of pharmaceutical compounds from aqueous streams. Sep Purif Technol 2017;179:118–25.

[143] Guo X, Liu D, Han T, Huang H, Yang Q, Zhong C. Preparation of thin film nanocomposite membranes with surface modified MOF for high flux organic solvent nanofiltration. AICHE J 2017;63(4):1303–12.

[144] Zheng J, Li M, Yu K, Hu J, Zhang X, Wang L. Sulfonated multiwall carbon nanotubes assisted thin-film nanocomposite membrane with enhanced water flux and antifouling property. J Membr Sci 2017;524:344–53.

[145] Zarrabi H, Yekavalangi ME, Vatanpour V, Shockravi A, Safarpour M. Improvement in desalination performance of thin film nanocomposite nanofiltration membrane using amine-functionalized multiwalled carbon nanotube. Desalination 2016;394:83–90.

[146] Zheng J, Li M, Yao Y, Zhang X, Wang L. Zwitterionic carbon nanotube assisted thin-film nanocomposite membranes with excellent efficiency for separation of mono/divalent ions from brackish water. J Mater Chem A 2017;5(26):13730–9.

[147] Safarpour M, Vatanpour V, Khataee A, Esmaeili M. Development of a novel high flux and fouling-resistant thin film composite nanofiltration membrane by embedding reduced graphene oxide/$TiO_2$. Sep Purif Technol 2015;154:96–107.

[148] Wen P, Chen Y, Hu X, Cheng B, Liu D, Zhang Y, et al. Polyamide thin film composite nanofiltration membrane modified with acyl chlorided graphene oxide. J Membr Sci 2017;535:208–20.

[149] Echaide-Gorriz C, Navarro M, Tellez C, Coronas J. Simultaneous use of MOFs MIL-101 (Cr) and ZIF-11 in thin film nanocomposite membranes for organic solvent nanofiltration. Dalton Trans 2017;46(19):6244–52.

[150] Wang J, Wang Y, Zhang Y, Uliana A, Zhu J, Liu J, et al. Zeolitic imidazolate framework/graphene oxide hybrid nanosheets functionalized thin film nanocomposite membrane for enhanced antimicrobial performance. ACS Appl Mater Interfaces 2016;8(38): 25508–25519.

[151] Namvar-Mahboub M, Pakizeh M, Davari S. Preparation and characterization of UZM-5/polyamide thin film nanocomposite membrane for dewaxing solvent recovery. J Membr Sci 2014;459:22–32.

[152] Singh PS, Ray P, Xie Z, Hoang M. Synchrotron SAXS to probe cross-linked network of polyamide 'reverse osmosis' and 'nanofiltration' membranes. J Membr Sci 2012;421:51–9.

[153] Lin L, Feng C, Lopez R, Coronell O. Identifying facile and accurate methods to measure the thickness of the active layers of thin-film composite membranes–a comparison of seven characterization techniques. J Membr Sci 2016;498:167–79.

[154] Nagy E. Basic equations of the mass transport through a membrane layer. Amsterdam: Elsevier; 2012.

[155] Garcia-Aleman J, Dickson JM. Mathematical modeling of nanofiltration membranes with mixed electrolyte solutions. J Membr Sci 2004;235(1):1–13.

[156] Spiegler K, Kedem O. Thermodynamics of hyperfiltration (reverse osmosis): criteria for efficient membranes. Desalination 1966;1(4):311–26.

[157] Urama RI, Mariñas BJ. Mechanistic interpretation of solute permeation through a fully aromatic polyamide reverse osmosis membrane. J Membr Sci 1997;123(2):267–80.

[158] Wijmans J, Baker R. The solution-diffusion model: a review. J Membr Sci 1995; 107(1–2):1–21.

[159] Kimura S, Sourirajan S. Analysis of data in reverse osmosis with porous cellulose acetate membranes used. AICHE J 1967;13(3):497–503.

[160] Straatsma J, Bargeman G, van der Horst HC, Wesselingh JA. Can nanofiltration be fully predicted by a model? J Membr Sci 2002;198(2):273–84.

[161] Déon S, Escoda A, Fievet P, Salut R. Prediction of single salt rejection by NF membranes: an experimental methodology to assess physical parameters from membrane and streaming potentials. Desalination 2013;315:37–45.

[162] Tsuru T, Nakao S-i, Kimura S. Calculation of ion rejection by extended Nernst–Planck equation with charged reverse osmosis membranes for single and mixed electrolyte solutions. J Chem Eng Jpn 1991;24(4):511–7.

[163] Bowen WR, Mohammad AW, Hilal N. Characterisation of nanofiltration membranes for predictive purposes—use of salts, uncharged solutes and atomic force microscopy. J Membr Sci 1997;126(1):91–105.

[164] Bandini S, Vezzani D. Nanofiltration modeling: the role of dielectric exclusion in membrane characterization. Chem Eng Sci 2003;58(15):3303–26.

[165] Hijnen H, Smit J. The effect of the pH on electrolyte transport through microporous membranes bearing either weakly or strongly dissociating acid groups. A theoretical analysis using the space-charge model for a cylindrical capillary. J Membr Sci 1995;99(3):285–302.

# Recent Progresses of Ultrafiltration (UF) Membranes and Processes in Water Treatment

*Ali Moslehyani*[*,†,‡], *Ahmad Fauzi Ismail*[†], *Takeshi Matsuura*[*], *Mukhlis A. Rahman*[†], *Pei Sean Goh*[†]

**\*Department of Chemical and Biological Engineering, University of Ottawa, Ottawa, ON, Canada**
**†Advanced Membrane Technology Research Centre (AMTEC), Faculty of Chemical and Energy Engineering, Universiti Teknologi Malaysia, Skudai, Malaysia**
**‡Department of Chemical Engineering and Applied Chemistry, University of Toronto, Toronto, ON, Canada**

## 3.1  INTRODUCTION

Ultrafiltration (UF) refers to the filtrated separation of particles in the colloid-size range [1–5]. In the UF process, the transfer of the dispersed phase ("solute" in its most general sense) through the membrane pores is much less than the "solvent" for one of several reasons [6–9]:

**A.** Due to adsorption (primary adsorption).
**B.** Due to size exclusion (sieving).
**C.** Due to deposition on the surface (cake formation).

By using a membrane surface, UF can separate dissolved macromolecules and tiny suspended particles from a fluid feed with the range of pore size between 1 and 100 nm, which means that UF is between microfiltration (MF) and nanofiltration (NF) [10–12].

The UF membranes can concentrate the large components of the feed fluid on one side of the membrane, as the microsolutes and the solvent are depleted as they can move through the membrane [8, 12, 13]. The UF membrane acts as a selective barrier retaining molecules with molecular weights higher than a few thousand of Dalton (macrosolute), while molecules with the small sizes (solvent and microsolutes) move freely through the membrane pores. The UF membrane is often rated, somewhat randomly, by the molecular weight cut off (MWCO), that is, UF membranes have a molecular weight cut off (MWCO) between 1000 and 1,000,000 [9, 12, 14, 15].

Compared to a reverse osmosis (RO) membrane, a UF membrane is used with lower operating pressure to retain larger solutes. The range of 1–10 bars is the typical operating pressure for UF. Generally, UF membranes are classified as an asymmetric membrane with a porous sublayer and a thin top layer, which governs the UF separation performance. A UF membrane is often operated in a tangential flow mode where the feed stream sweeps tangentially across the upstream surface of membranes

as filtration occurs, thereby maximizing flux rates and membrane life [16, 17]. Some of the UF membrane properties are pore size, pore size distribution, surface pore size, rejection, flux, percentage of porosity, solvent resistance, temperature stability, flux decline and pressure resistance. Retentivity is critical, and the skin plays a principal role in the UF membrane performance. The internal pore blockage should be prevented to maintain and provide a high flux rate [18–21].

UF is a pressure-driven membrane transport process that has been applied in a small laboratory scale as well as in a large industrial scale. The interest has grown in recent years to use UF for the separation of dissolved molecules of different sizes and properties. Depending on their pore size, UF technology is applied for essential separation processes such as filtration of colloidal suspensions, treatment of product streams in the food and beverage industry, recovery of useful material from coating or dyeing baths in the automobile and textile industries and treatment of industrial wastewaters, also in medical, biotechnological industries, paper industry, and the dairy industry [22–25].

## 3.2  RECENT PROGRESSES IN UF MEMBRANE DEVELOPMENT

The membrane separation process is known to be useful for the desalination of seawater and brackish water, wastewater treatment, removal of toxic substances from drinking water, and production of ultra-pure water for the semiconductor industry. UF, NF, and RO filtration have been successfully applied for the removal of colloidal particles, turbidity, dissolved organic matter (DOM), and microorganisms. This advanced technology can produce water quality better than the current regulatory requirements and therefore can replace conventional clarification and filtration methods [26–28].

Asymmetric polymeric UF membranes have to satisfy strict operating parameters requirements such as solvent resistance, pH resistance, chemical resistance, thermal and mechanical stability; also high selectivity, flux, high durability (most extended possible life) and low cost of material on the market today [29–31]. Recently, five different polymeric membranes, including two MF and three polyacrylonitrile UF membranes, were compared for the treatment of industrial wastewater. MF membranes showed higher permeability and less rejection while UF membranes optimal results [28, 32].

### 3.2.1  Material Selection for Polymeric UF Membrane

In the fabrication of mixed matrix UF membranes, particles/nanoparticles should be compatible with membrane polymer. When the casting solution is prepared, loading of particles or nanoparticles in the polymeric

solution should be set at an optimum value for avoiding particle agglomeration at the skin layer and sublayer of the UF membrane. Therefore, the selection of particles and nanoparticles is a great deal of interest for all researchers who produce mixed matrix UF membranes [9, 33–37].

In fact, the degree of entrapment of particles/nanoparticles in the polymer matrix depends mainly on the compatibility between polymer and particles/nanoparticles. The loading of particles/nanoparticles usually enhances the membrane performance, but the membrane performance gradually deteriorates if the particles/nanoparticles are not strongly entrapped in the membrane. Therefore, the material selection of particles/nanoparticles and polymers available in the market is one of the most important aspects to be considered in UF membrane fabrication [33, 37–39].

### 3.2.1.1 Polymer

Polymer plays an essential and ubiquitous role in many technologies, including UF, and is separated into numerous classes according to their physical and chemical properties. Polymer morphology plays a significant role to determine bulk physical properties by which the behavior of the polymer as a continuous macroscopic material is determined. In fact, chemical properties of polymer determine the bulk physical properties as well through the interactions between polymer chains working via various physical forces. In a much larger scale, their chemical properties determine how the bulk polymer interacts with other chemicals and solvents [13, 40, 41].

At present, some synthetic polymers such as polyether sulfone (PES), polysulfone (PSf) and polyvinylidene fluoride (PVDF) are used for UF membrane. On the other hand, before the evolution of polymer synthesis, natural polymers were used. Due to the serious concerns over the environmental effects and awareness that petroleum resources are limited, the use of biodegradable polymers produced from extensive sources such as cellulose, chitin, and starch has significantly increased. Accordingly, this type of polymers has been widely commercialized in membrane filtration technology [39, 42, 43].

### 3.2.1.2 Nanoparticles

Particles and nanoparticles, when incorporated in the polymeric phase of UF membranes can significantly increase the UF performance. Currently, carbon nanotubes (CNTs), graphene, clays, carbon molecular sieve, metallic oxide, zeolites are known to be effective for removing organic compounds when incorporated in the polymeric membrane. Nanostructured materials are highly capable of decreasing the toxicity of organic pollutants to an allowable level owing to their large surface area and uniformity in size. As discussed earlier, the compatibility of particles and nanoparticles with the polymer matrix is essential. Therefore, finding novel and potentially powerful particles and nanoparticles is always a challenging task for membrane R & D [32, 44–48].

## 3.3  POLYMERIC UF MEMBRANE CONFIGURATIONS

Polymeric membranes of different shapes such as flat sheet, hollow fibers, and nanofiber sheet (see Fig. 3.1) have been used for submerged UF membrane. Hollow fiber membranes have always shown higher efficiency and longer lifetime; however, flat sheet membranes are easier to use in UF [49, 50].
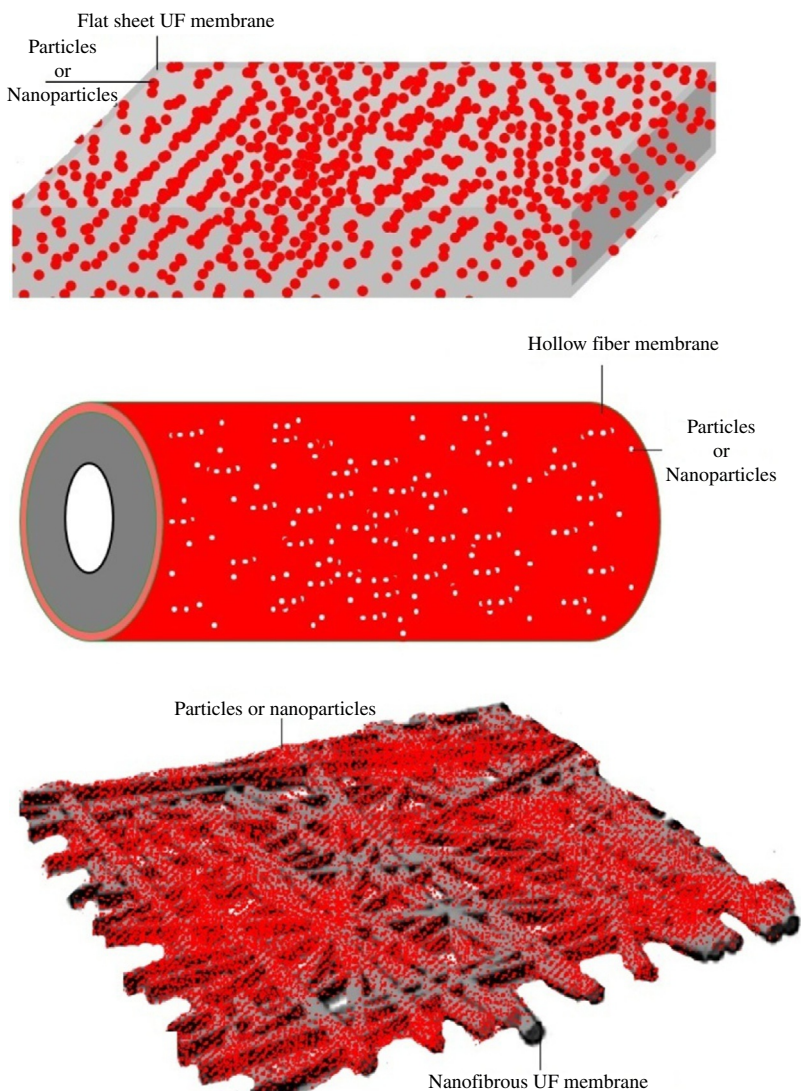


FIG. 3.1   Various UF membrane shapes.

Recently, nanofiber mat has been used for UF membrane, but not many data are available for this kind of membrane [51].

### 3.3.1 Flat Sheet UF Membrane

The membrane can be produced as flat sheets or hollow fibers. To fabricate a flat sheet, a polymer solution is spread on a support glass plate using a casting knife. On the other hand, hollow fibers provide a higher surface area per unit volume of membrane modules [52–55]. The flat sheet membrane and hollow fibers can be prepared by using a casting technique and a spinning technique, respectively [56, 57].

The casting of flat sheet membranes is a well-established phase inversion technique. First, a polymer is dissolved in a suitable solvent or a mixture of solvents and nonsolvent (in phase inversion) to form a homogeneous dope solution. The dope solution is then cast on a suitable support such as glass plate or nonwoven polyester sheet using a casting knife. As depicted in Fig. 3.2, the casting knife is made of a metal blade moving on two runners that can provide a gap between the blade and support accurately [58, 59]. This gap determines the thickness of the membrane produced. A pneumatically controlled flat sheet membrane casting system has been developed by combining semi-technical hand-casting knife and pneumatic system.

This system offers an easier casting operation by controlling several casting variables such as shear rate and forced convection residence time. Then, the cast film is instantly dried, or the solvent is partially evaporated before the cast film is immersed into a coagulation bath. The resultant membranes were used in commercial plate-and-frame and spiral wound systems [10, 60].



1. Air compressor
2. Pneumatic system
3. Casting knife
4. Trolley push button
5. Trolley and glass plate
6. Evaporation chamber
7. Coagulation bath
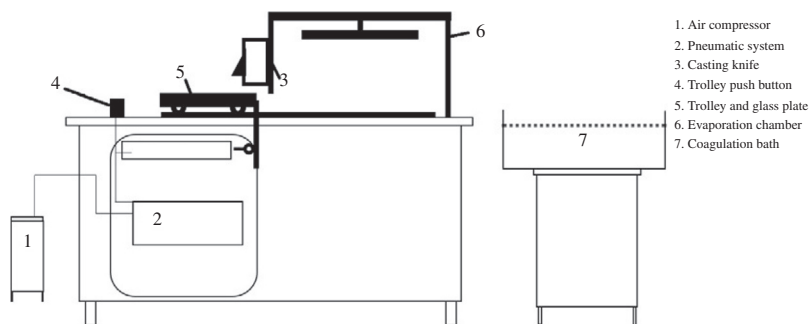
FIG. 3.2    Flat sheet membrane casting equipment.

### 3.3.2 Hollow Fibers UF Membrane

Hollow fibers were fabricated by the spinning process, which involves the extrusion of a polymer solution through an annular spinneret. Hollow fiber membranes can have either dense or asymmetric structures depending on the way the gel filaments are solidified [61–63]. Melt spinning usually obtains a dense structure while solution spinning (phase inversion) is used to obtain an asymmetric structure. A hollow fiber spinning system is shown schematically in Fig. 3.3. The fibers are almost instantaneously formed as the polymer solution leaves through the spinneret. The spinneret consists of two concentric capillaries; outer capillary and central capillary. The outer capillary has an outer diameter of around 400 μm and an inner diameter of approximately 200 μm while the central capillary has a diameter of about 100 μm. The polymer solution is forced to come out of the outer capillary and air, or a secondary solution is simultaneously delivered through the inner capillary. Typically water is delivered through the inner capillary when asymmetric hollow fibers are spun [9, 64–66].

### 3.3.3 Nanofibrous UF Membrane

A UF electrospun nanofibrous membrane is a novel technology for removing organic contaminants in the wastewater by membrane adsorption, offering an alternative option to the effluent treatment. In particular, electrospun nanofibrous membrane looks promising due to high permeation and rejection rate, when they can be used many times via appropriate desorption after each test [67]. For this reason, electrospun nanofibrous membranes have come to the forefront of R & D recently as one of the most



1. Solution tank
2. Gear pump
3. Syringe pump
4. Spinneret
5. Conceptive chamber
6. Coagulant bath
7. Treatment bath
8. Wind-up drum
9. Controller
10. Internal coagulant
11. Polymer dope
12. Hollow fiber
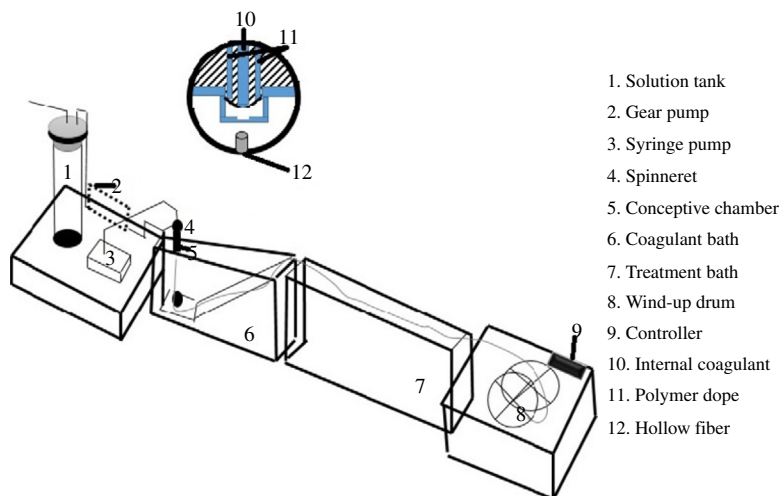
FIG. 3.3    Hollow fiber spinning system.

efficient techniques to remove the organic pollutants from wastewater at lower operating costs. However, the incorporation of suitable and compatible particles and nanoparticles, as adsorbents, is the most challenging parameter to use electrospun nanofibrous membrane for membrane adsorption. In several studies, a hot pressing technique has been used for enhancing the compactness of the membrane or nonwoven supports and via pressure and heat of hot press system [68, 69] (Figs. 3.4 and 3.5).

### 3.3.4 Mixed Matrix Membranes

Mixed matrix materials (MMMs) are structured with functional particles embedded within a polymer matrix. These materials are also known as heterogeneous or hybrid materials. Selection of particles and polymer
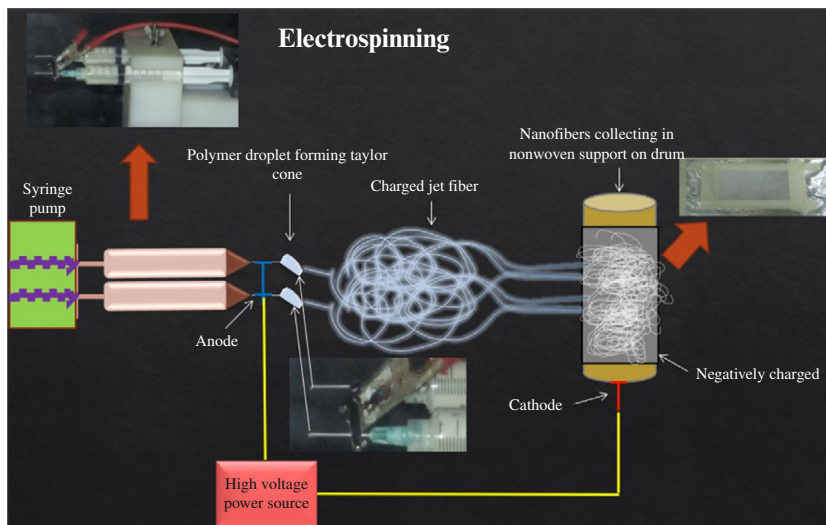


**FIG. 3.4**    Electro-spinning procedure.
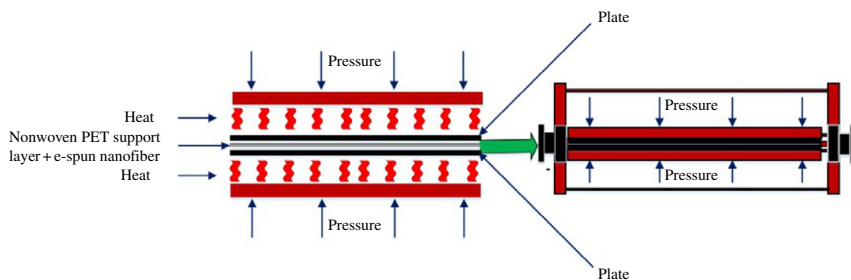


**FIG. 3.5**    Illustration of the hot-pressing method.
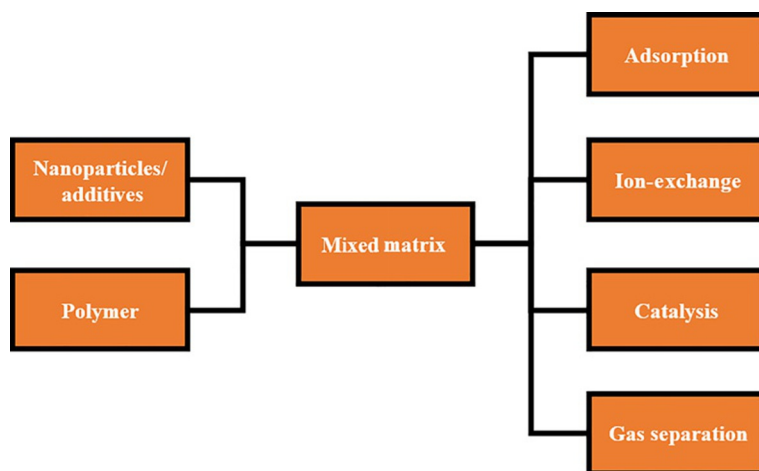
FIG. 3.6 Schematic representation of the mixed matrix membrane.

binder or polymer matrix will determine its function such as adsorption, catalysis, ion-exchange or separation membrane [9, 70–74]. The concept of mixed matrix membrane is schematically presented in Fig. 3.6. MMMs are formed by dispersing molecular sieve entities into a polymer matrix [75–79]. Fig. 3.7 illustrates the structure of a mixed matrix film. In Fig. 3.7, the molecular sieves are uniformly distributed within the polymer matrix. It is believed that this emerging approach synergistically combines the best features of both phases and simultaneously to compensate the weakness in each medium [80, 81]. In a molecular sieves-polymer mixed matrix system, the high selectivity benefits of the molecular sieve are
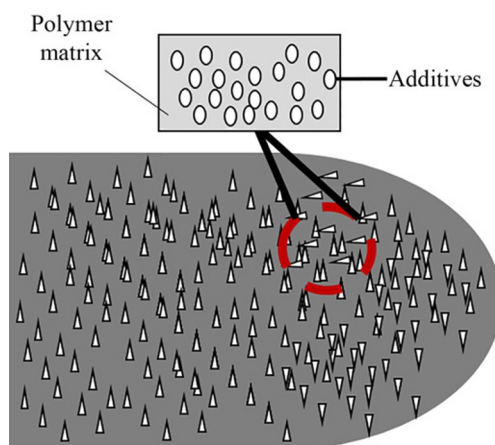


FIG. 3.7 A schematic diagram of an MMM film.

combined with desirable mechanical properties and economical process-abilities of polymers. In turn, the costly processing and severe mechanical problems in purely molecular sieving membranes can be overcome, and the limit in the trade-off between productively and selection of polymer materials can be surpassed [82–84].

## 3.4  FOULING MITIGATION

### 3.4.1  Fouling Type and Methods to Control Fouling

The decrease in the permeation rate during membrane process, called fouling, is recognized as the main problem in the application of membrane technologies. Several types of fouling can occur in membrane systems including inorganic fouling, particulate and colloidal fouling, organic fouling, and biofouling [31, 85, 86]. Pore blocking and cake formation are considered as the two primary mechanisms of membrane fouling while other factors such as adsorption, particle deposition within the pores, and formation of the cake layer affect membrane fouling through the modification of either or both mechanisms. Pore blockage increases the membrane resistance, while cake formation creates an additional layer of resistance to permeate flow. The severity of these phenomena depends on the nature of the particle, the operating conditions such as pH, ionic strength, pressure, and particle concentration and the nature of the membrane. Development of effective methods to control fouling is based on an understanding of the fouling mechanism and the influence of the process parameters on the membrane fouling. To discuss approaches to mitigate membrane fouling we will first outline the main particularities of this process [87–91].

Generally, for MF and UF, two types of fouling phenomena are distinguished. The first is macrosolute or particle adsorption, which refers to the specific intermolecular interactions between the particles and the membrane that occur even in the absence of filtration. It is usually irreversible, adhesive fouling. In water treatment applications, the foulants are usually adhesive due to hydrophobic interactions, hydrogen bonding, van der Waals attractions, and extracellular macromolecular interactions among others. The second type is known as filtration-induced macrosolute or particle deposition, which is often reversible, nonadhesive fouling, where the accumulation of cells, cell debris, and other rejected particles on the top surface of the membrane is prominent. It occurs as external fouling or cake formation. Reversible fouling resulting from cake formation was found to be only weakly dependent on membrane surface chemistry; in contrast, irreversible fouling exhibited a marked dependence on surface chemistry [92, 93].

Membrane fouling is an incredibly complex physicochemical phenomenon. Usually, several mechanisms are involved simultaneously. Thus, in case of protein-containing solutions, it was suggested that it began with protein aggregates depositing on the membrane surface, thereby blocking its pores. Disulphide linkages, van der Waals forces, electrostatic interactions, hydrophobic interactions, and hydrogen bonding all contributed to membrane fouling by a proteinous substance, mostly through adhesive fouling [94–96]. On the contrary, for filtration of river water, cake formation on the surface of the membrane resulted in more pronounced UF membrane fouling than the adsorption of small substances inside the pores of the membrane. UF membrane fouling was dominated by the cake layer formation attributed to the accumulation of dissolved organic materials and suspended colloids in the raw water. The particles are driven to the membrane surface by the flow of permeate to form a cake layer on the membrane unless the shear rate is very high to prevent cake formation. The undetachable cake layer accumulates on the membrane and results in fouling in the long term [97–99].

Biofouling is another major problem, which destroys the structural integrity of the membrane, and this leads to subsequent irreversible membrane damage, shortens membrane life, increases operational and maintenance costs, and reduces efficiency. It is initiated by irreversible adhesion of one or more bacteria to the membrane surface, followed by growth and multiplication of the sessile cells at the expense of feed water nutrients. It can eventually form a confluent lawn of bacteria, otherwise known as a biofilm on the membrane surface. Chemical properties of membrane surface, its roughness, pore shape, and size distribution are found to be the main factors controlling the biofouling potentials [100, 101]. The complexity of membrane fouling predetermines the exploiting of a variety of approaches to control this adverse process. Here these approaches are categorized under four main topics: (i) Pretreatment of feed; (ii) Membrane materials/surface modification; (iii) Operating parameters; and (iv) Cleaning procedures. Approaches discussed in the first three topics are focused on preventing or mitigation of the membrane fouling, whereas methods of the fourth topic are assigned to cope with consequences of the membrane fouling [102–104].

## 3.4.2 Cleaning Method

This is a standard method of reduction of membrane fouling employed in cross-flow filtration processes. Cross-flow filtration techniques in membrane technologies have been employed on a global scale for the removal of particles, colloidal species, and microorganisms but the principal limitation lies in the flux decline associated with particle formation on the

membrane, thus hindering mass transfer. Backflush was used to eliminate particle deposition, which allowed efficient flux recovery [31, 45, 105].

In MF, high feed/retentate velocities are used to reduce cake formation and concentration polarization. As well, it is a common practice to pump filtrate back through the membrane into the feed channel to give a periodic backwash. This lifts the deposited material off the surface of the membrane. The backwash pressures need to be greater than the operating filtration pressure. The efficiency and effectiveness of this technique are limited to surface deposits removal from the membrane. It becomes ineffective with strong adhesion of deposits and if there is any pore fouling. Periodic backwashing improves membrane permeability and reduces fouling, thus leading to optimal, stable hydraulic operating conditions. Air backwashing in submerged membrane reactors can increase the flux up to fivefold. When the technique is carried out at a faster rate, it is known as backpulsing or backshocking. Backpulsing is a cyclic process of forward filtration followed by reverse filtration [87, 106–108].

Reversal filtration involves a reversal of the flow through the membrane by changing the orientation of the trans-membrane pressure (TMP). More rapid backwashing has been claimed to be more effective, and backpulses are of short duration and may be operated continuously or periodically [109–112]. They are particularly useful with colloidal suspensions and with streams requiring protein transmissions through the membrane. The backpressure is applied in an extremely rapid pulse every few seconds throughout the process. The reverse flow removes the particles that are reversibly deposited on or within the pores of the membrane, while the foulants are swept off the membrane via the cross-flow. These actions subsequently reduce fouling and improve permeate flux over time. Cross-flow filtration with rapid backpulsing has been studied in-depth by many groups in different membrane/foulant system, who documented the method as an effective means of controlling fouling and increasing permeate flux for nonadhesive foulants that exhibit reversible fouling. The use of rapid backpulsing was also studied extensively [29, 113–115].

## 3.5 SURFACE MODIFICATION

Surface modification has been potentially used to minimize the fouling on the membrane surface and maximize the membrane performance regarding permeability and solute rejection. The primary parameter which plays an essential role in membrane surface modification is the use of materials with a favorable effect on the structure of membranes such nanoparticles and nanotubes or some adsorptive materials [116].

Alternatively, modifying membranes and membrane surfaces aim at fabrication of antifouling membranes by inhibiting microbial growth on the membrane. The proper membrane material selection can also improve the membrane and membrane surfaces concerning antifouling behavior, which consequently reduces cake layer formation and concentration polarization and overall fouling reduction. Many marketable and commercial membranes are made of PES, polyvinylidenefluoride (PVDF) and other hydrophobic polymers due to their high chemical, thermal and mechanical properties [116, 117]. On the other hand, hydrophilic nanoparticles are often used to be blended with the hydrophobic polymer. Hence, the combination of hydrophobic polymer and hydrophilic nanoparticles can enhance the membrane performance significantly, as reported by many researchers [32, 107, 116, 118–120].

Other methods can be used to change the hydrophobic surface to hydrophilic. They are (i) coating and (ii) grafting. In the first method, the membrane is immersed in the coating solution. The second grafting method is a kind of immobilization, where hydrophilic species are grafted on the membrane surface from grafting solutions [121, 122]. Another type of membrane grafting is done by photo-induced grafting, which is mainly used for functionalization of membrane surface due to their numerous features. Its advantages are the low cost of the process operation, selective absorption of UV light without affecting the bulk polymer, mild reaction conditions and permanent alteration of the membrane surface with facile control of the chemistry [107, 120, 123–126]. In fact, many researchers have recommended a combination of surface modification and cleaning procedure to increase the permeability and separation performance of the membranes which reduces the fouling on the membrane surface due to bacterial suspensions, clay suspensions, and oil emulsions [31, 127].

## 3.6 RECENT PROGRESSES IN UF MEMBRANE AND UF MEMBRANE PROCESSES

UF is increasingly used in water treatment due to a decrease in membrane prices, improving module design, operability, and economics of membrane separation processes. Furthermore, as the regulation for chemical and biological contaminants in water have become more stringent, membrane processes including NF, UF, and MF have been utilized as treatment alternatives to replace conventional processes which employ chemical coagulation for removing dissolved species and filtration for removing suspended species. MF has been used in water treatment for removing suspended solids (larger than 0.1 µm). MF has also been used by water utilities in place of conventional processes where treatment objectives are suspended solids control and microbial removal. However,

MF cannot achieve a reliable degree of dissolved organic control while UF does. Denitrification can be done by physicochemical treatment techniques such as RO, ion exchange and electrodialysis. Pesticides on the other hand usually require activated carbon treatment or oxidation by strong chemical agents. Lyonnaise des Eaux, a company in the water treatment business, developed an industrial scale MBR system to remove pesticide by combining biological denitrification and powdered activated carbon adsorption. UF has been used to remove many contaminants [128–130].

UF can be a very promising liquid-solid separation process as it can remove particulates and macromolecules in the range of 0.02 μm to 1 nm. Although UF has a broad molecular weight cut off (MWCO) range, it is less effective in removing low molecular weight organic matters. A combination of UF and coagulant or absorbent has been proven to remove organic matters in water significantly. However, MWCO is not the only factor that will determine the membrane rejection. Factors such as membrane characteristics, feed properties, operational conditions, pretreatment procedure, module configurations, solution chemistry and the presence of other solutes have been reported to influence the membrane performance. UF membranes are made from various types of polymer, but two most common membrane materials are PS and cellulose acetate (CA). There were 34 UF plants in operation or under construction worldwide having a total capacity of 34 million gallons per day [130–132].

### 3.6.1 Antibacterial Membrane

Since the 1990s, MF was evaluated by water supply agencies as a cost-effective alternative to the conventional pretreatment for desalination by RO. However, because an MF membrane can remove substances larger than 50 nm and bacteria while bacteria and virus pass through, many researchers have turned to UF, which allows removal of 3 nm or larger substances, and subsequently reduces the biofouling problem of RO membrane. Furthermore, the disinfection process (via UV, ozonation, or chlorination) after the membrane filtration process is also recommended as a secondary bacteria control barrier and distribution system protection [133]. The other promising way is to incorporate an antibacterial agent into polymeric membrane so that removal and disinfection can be carried out simultaneously in a membrane.

Recently, Moslehyani et al. reported that the key advantage of an antibacterial membrane is the enhancement of antibacterial action by the incorporated antibacterial agent. When the feed solution comes to contact with the membrane surface, the antibacterial agent is released to disrupt the bacterial cell wall membrane. Therefore, membrane filtration and

disinfection occur simultaneously. As a result, a biofilm covers the membrane surface creating a newer, smoother and more antiadherence surface, further enhancing the antibacterial capacity of the membrane. It is known that the smoother surface is less prone to fouling due to the decreased interaction between the colloidal particle and the surface [6].

Antibacterial compounds are defined as a synthetic or natural compound that destroys bacteria or suppresses their growth or their ability to reproduce. There are many antibacterial products commercially available for cleaning and hygienic purposes. In addition, the invention of loading/incorporating antibacterial agents into our daily needs such as clothing, soap, containers for food-packaging, and water filtration system is frequently undertaken. Water treatment and effluent disinfection using membrane technologies have been in growing interest due to the environmental factor as compared to the common disinfectant, chlorine. Therefore, the combination of membrane technologies and the relevancy of the incorporation of an antibacterial agent such as silver is an area of interest [8, 11, 134]. Factors affecting bacterial attachment and transport are summarized in Table 3.1.

**TABLE 3.1**  Factors Affecting Bacterial Attachment and Transport

| Factor | Effect on transport and attachment |
| --- | --- |
| Ionic strength | Attachment increases with higher ionic strength due to electrical double-layer size reduction |
| Clay-content | Attachment increases with high clay content due to the larger specific area of adsorption |
| Oxygen limitations | Oxygen-limited biofilms exhibit lower shear removal rates but higher sloughing |
| Charge on media | Attachment of negatively charged bacteria will be high in positively charged media |
| Flow rate | Higher flow rates reduce bacterial attachment |
| Nutrient concentration | Bacterial size is reduced in higher nutrient concentrations |
| Bacterial size | Smaller bacteria may interact with media less and may not be removed by filtration as easily as bigger bacteria. On the other hand, larger bacteria have been shown to move faster than small bacteria |
| Cell concentration | At low cell density, attachment is favored. Bacteria tend to move from high concentration areas by a tumbling diffusive flux |
| Bacterial motility | Motile bacteria may migrate faster than nonmotile bacteria through chemotaxis |
| Water content | Bacteria move faster through the unsaturated soil of higher water content |

## 3.6.2 Adsorptive Membrane

Contamination of drinking water with heavy metals is a significant public health concern worldwide. For example, the presence of lead in drinking water has been reported in more than 70 countries. Millions of people, mainly in developing countries such as India and Bangladesh, are at high risk due to contamination of ground and surface water. In the aqueous solution, heavy metals are colorless and odorless, and it is not easy to detect them visibly. Because of this, its contamination is a serious concern for the environment and living creatures. It is known that long-term exposure to drinking water contaminated with heavy metal can cause various kinds of cancers. Conventional technologies to remove heavy metal ions are chemical precipitation, coagulation and flocculation, ion exchange and membrane filtration. Membrane filtration processes such as NF and RO are also known to be effective to eliminate arsenics (As). However, they consume high-energy due to the requirement of high pumping pressure. The pore sizes of MF and UF are too large to remove the dissolved metallic minerals. Thus, the inconsistent and/or incomplete removal of heavy metal by conventional technologies has urged to search for efficient, environmentally friendly, and low-cost treatment technology for hazardous decontamination [68].

Recently, Moslehyani et al. reported that electrospun adsorptive nanofiber membrane (EANM) is a novel technology with a high potential to remove heavy metals from drinking water due to EANM's high permeation rate and adsorption capacity, particularly when they can be used multiple times via appropriate desorption. For this reason, EANMs have come to the forefront of R & D recently as one of the most efficient techniques to remove arsenic at low operation cost. However, the use of suitable and compatible adsorbent particles is the most challenging parameter in the preparation of highly efficient EANMs [135].

## 3.6.3 UF Photocatalytic Membranes

Photolysis as a critical component of photodegradation technology has been studied for the last few decades. The reaction scheme implies that an interface is formed between the (solid) photocatalyst and a liquid or a gas phase containing the reactants. Particularly, understanding the mechanisms and kinetics of photocatalytic membrane process is the most significant part of the whole process [136–138]. A photocatalyst is a semiconductor that converts the light energy to the chemical energy of the electron-hole pairs. Therefore, a suitable energy bandgap together with chemical and physical stability, nontoxic nature, availability, and low cost should be considered when a solid photocatalyst is chosen [138–140]. In general, the photodegradation has three main products including nonreacted (similar to the initial feed), intermediate product,

and final product [45, 141]. To understand the mechanism of photodegradation is necessary to understand the role of the ultraviolet radiation in the photocatalytic reaction. In the photocatalyst, there is a conduction band and a valence band separated by a bandgap of energy. When the photocatalyst is exposed to ultraviolet photons, whose energy ($h\nu$) is higher than or equal to the bandgap, the transfer of an electron occurs from the valence band to the conduction band to create electron-hole pair [138, 142–144]. The lowest energy level of the conduction band corresponds to the reduction potential of the photoelectrons while the highest one corresponds to the oxidizing power of the electron holes as is illustrated in Fig. 3.8.

When no electron and hole scavengers are available, the input energy is dissipated as heat within a few nanoseconds by recombination.

Several steps involved in the photocatalytic reaction are given below with an example of typical photocatalyst $TiO_2$.

I. Photocatalyst excitation

$$TiO_2 + UV(h\nu) \Rightarrow TiO_2(e_{CB-} + h_{VB+})$$
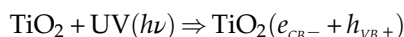
II. Photocatalyst adsorption

$$TiO_2(h_{VB+}) + H_2O \Rightarrow TiO_2 + H^+ + OH^\bullet$$

$$TiO_2(h_{VB+}) + OH^- \Rightarrow TiO_2 + OH^\bullet$$
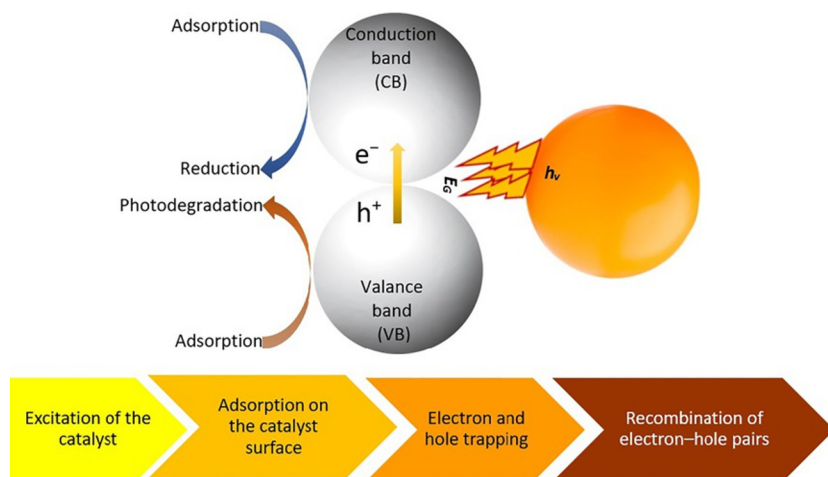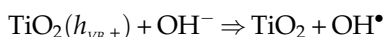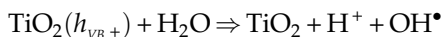


FIG. 3.8   Photocatalyst mechanism during photodegradation.

III. Photocatalyst electron-hole trapping

$$\text{TiO}_2(e_{CB-}) + \text{O}_2 \Rightarrow \text{TiO}_2 + \text{O}_2{}^{\bullet-}$$

$$\text{O}_2{}^{\bullet-} + \text{H}^+ \Rightarrow \text{H} + \text{O}_2{}^{\bullet}$$
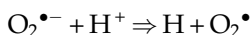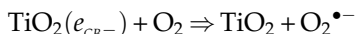
IV. Photocatalyst electron-hole pairs recombination

$$e^- + h^+ \Rightarrow \text{heat}$$
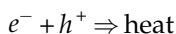
Many organic reactants accept hydroxyl radicals generated in the photocatalytic adsorption process in water, which act as electron donors when they are oxidized. Thus, the organic reactants are degraded to the intermediate substrate and further decomposed into carbon dioxide and water [136, 145–147].

As well, photocatalytic reaction process is described by the following three steps [148, 149]:

  I. External mass transfer of reactant to the solid photocatalyst surface.
 II. Internal mass transfer via intra diffusion of a photocatalyst.
III. Organic compounds decomposition by diffused photocatalyst.

Moslehyani et al. [98] constructed photocatalytic membrane reactor (PMR) to study oil-water treatment. In the photocatalytic reactor, UF membrane was used to retain the unreacted oil while TiO$_2$ photocatalyst was suspended in the feed. PMR is a novel method for oily wastewater treatment, and its performance in the degradation of toxic hydrocarbon compounds and purification of oily wastewater looks very promising.

## 3.7  SUMMARY

The water and wastewater industry has been faced with many challenges over the last three decades and is currently looking for economical methods of treatment. The removal of particulate matters by chemical and physical methods is commonly used for the treatment of drinking water as well as the surface water sources. More focus is nowadays placed on membrane technology for water treatment, where the choice of membrane, module configuration, process and operating parameters, and pretreatment among others are essential to make the process most effective. Membrane processes are very promising due to their potential to remove particles, including microorganisms, organic pollutants, inorganic salts, and to achieve biologically stable water by reducing microbial regrowth in the distribution system. Among others, UF is considered as the most

efficient and economical process among all types of membrane technology that is used for water and wastewater treatment.

## Acknowledgments

## References

[1] Gao W, Liang H, Ma J, Han M, Chen Z-l, Han Z-s, et al. Membrane fouling control in ultrafiltration technology for drinking water production: a review. Desalination 2011;272(1):1–8.

[2] Fu F, Wang Q. Removal of heavy metal ions from wastewaters: a review. J Environ Manage 2011;92(3):407–18.

[3] Goosen M, Sablani S, Al-Hinai H, Al-Obeidani S, Al-Belushi R, Jackson D. Fouling of reverse osmosis and ultrafiltration membranes: a critical review. Sep Sci Technol 2005;39(10):2261–97.

[4] Blatt WF, Dravid A, Michaels AS, Nelsen L. Solute polarization and cake formation in membrane ultrafiltration: causes, consequences and control techniques. In: Flinn JE, editor. Membrane science technology. NY: Plenum Press; 1970. p. 47–97.

[5] Borneman Z, Gökmen V, Nijhuis HH. Selective removal of polyphenols and brown colour in apple juices using PES/PVP membranes in a single ultrafiltration process. Sep Purif Technol 2001;22:53–61.

[6] Moslehyani A, Mobaraki M, Ismail A, Matsuura T, Hashemifard S, Othman M, et al. Effect of HNTs modification in nanocomposite membrane enhancement for bacterial removal by cross-flow ultrafiltration system. React Funct Polym 2015;95:80–7.

[7] Moslehyani A. Photocatalytic membrane reactor for degradation and separation of hydrocarbon components from oily wastewater. Universiti Teknologi Malaysia; 2015.

[8] Basri H, Ismail A, Aziz M. Polyethersulfone (PES)-silver composite UF membrane: effect of silver loading and PVP molecular weight on membrane morphology and antibacterial activity. Desalination 2011;273(1):72–80.

[9] Nunes SP, Peinemann K-V. Membrane technology: Wiley online. Library; 2001.

[10] Moslehyani A. Silver ion exchange fillers incorporated with mixed matrix membrane for antibacterial application. Universiti Teknologi Malaysia; 2012.

[11] Basri H, Ismail A, Aziz M, Nagai K, Matsuura T, Abdullah M, et al. Silver-filled polyethersulfone membranes for antibacterial applications—effect of PVP and TAP addition on silver dispersion. Desalination 2010;261(3):264–71.

[12] Cheryan M. Ultrafiltration handbook. Technomic Publishing Co. Inc; 1986.

[13] Belfort G. Synthetic membrane process: fundamentals and water applications. Elsevier; 2012.

[14] Zularisam A, Ismail A, Salim R. Behaviours of natural organic matter in membrane filtration for surface water treatment—a review. Desalination 2006;194(1–3):211–31.

[15] Zularisam A, Ismail AF, Salim M, Sakinah M, Hiroaki O. Fabrication, fouling and foulant analyses of asymmetric polysulfone (PSF) ultrafiltration membrane fouled with natural organic matter (NOM) source waters. J Membr Sci 2007;299(1):97–113.

[16] Porter MC. Handbook of industrial membrane technology. Elsevier; 1989.

[17] Ho W, Sirkar K, editors. Membrane handbook. Springer Science & Business Media; 1992.

[18] Wahid ZA, Munaim MSA. Membrane: for surface water treatment. Penerbit Universiti Malaysia Pahang; 2009.

[19] Sakinah AMM, Ismail A, Hassan O, Zularisam A, Illias RM. Influence of starch pretreatment on yield of cyclodextrins and performance of ultrafiltration membranes. Universiti Teknologi Malaysia; 2009.

[20] Pabby AK, Rizvi SS, Requena AMS, editors. Handbook of membrane separations: chemical, pharmaceutical, food, and biotechnological applications. CRC Press; 2015.

[21] Paul DR, Yampol'skii YP. Polymeric gas separation membranes. CRC Press; 1993.

[22] Ab Wahid ZA. Natural organic matter removal from surface water using submerged ultrafiltration membrane unit. Universiti Teknologi Malaysia; 2008.

[23] Bowen WR, Hilal N, Lovitt RW, Williams PM. Visualisation of an ultrafiltration membrane by non-contact atomic force microscopy at single pore resolution. J Membr Sci 1996;110(2):229–32.

[24] Fane A, Fell C. A review of fouling and fouling control in ultrafiltration. Desalination 1987;62:117–36.

[25] Marshall A, Munro P, Trägårdh G. The effect of protein fouling in microfiltration and ultrafiltration on permeate flux, protein retention and selectivity: a literature review. Desalination 1993;91(1):65–108.

[26] Morales MA. Innovative water and energy demand management practices in the public water supply sectors. University of Florida; 2014.

[27] Al Fartoosi FM. The impact of maritime oil pollution in the marine environment: case study of maritime oil pollution in the navigational channel of Shatt Al-Arab. Dissertation, World Marine University; 2013.

[28] Gonite T. Simulation of water transport through nano-foam filter. Institute of Technology, School of Graduate Studies, Addis Ababa University; 2015.

[29] Moslehyani A, Mobaraki M, Matsuura T, Ismail A, Othman M, Chowdhury M. Novel green hybrid processes for oily water photooxidation and purification from merchant ship. Desalination 2016;391:98–104.

[30] Bellona C, Drewes JE, Xu P, Amy G. Factors affecting the rejection of organic solutes during NF/RO treatment—a literature review. Water Res 2004;38(12):2795–809.

[31] Shi X, Tal G, Hankins NP, Gitis V. Fouling and cleaning of ultrafiltration membranes: a review. J Water Proc Eng 2014;1:121–38.

[32] Padaki M, Murali RS, Abdullah M, Misdan N, Moslehyani A, Kassim M, et al. Membrane technology enhancement in oil-water separation. A review. Desalination 2015;357:197–207.

[33] Howe KJ, Clark MM. Fouling of microfiltration and ultrafiltration membranes by natural waters. Environ Sci Technol 2002;36(16):3571–6.

[34] Chun Y, Mulcahy D, Zou L, Kim IS. A short review of membrane fouling in forward osmosis processes. Membranes 2017;7(2):30.

[35] Ramesh A, Lee D, Wang M, Hsu J, Juang R, Hwang K, et al. Biofouling in membrane bioreactor. Sep Sci Technol 2006;41(7):1345–70.

[36] Afonso MD, Bórquez R. Review of the treatment of seafood processing wastewaters and recovery of proteins therein by membrane separation processes—prospects of the ultrafiltration of wastewaters from the fish meal industry. Desalination 2002;142(1):29–45.

[37] Lee KP, Arnot TC, Mattia D. A review of reverse osmosis membrane materials for desalination—development to date and future potential. J Membr Sci 2011;370(1):1–22.

[38] Pal P, Sikder J, Roy S, Giorno L. Process intensification in lactic acid production: a review of membrane based processes. Chem Eng Proc: Proc Intensific 2009;48(11):1549–59.

[39] Lloyd DR, editor. Materials science of synthetic membranes. ACS Publications; 1985.

[40] Mulder J. Basic principles of membrane technology. Springer Science & Business Media; 2012.

[41] Pendergast MM, Hoek EM. A review of water treatment membrane nanotechnologies. Energy Environ Sci 2011;4(6):1946–71.

[42] Porcelli N, Judd S. Chemical cleaning of potable water membranes: a review. Sep Purif Technol 2010;71(2):137–43.

[43] Moslehyani A, Junin R, Ismail AF. Polyethersulfone ultrafiltration membrane for oil-in-water emulsion separation (Presented).

[44] Haberkamp J, Ruhl AS, Ernst M, Jekel M. Impact of coagulation and adsorption on DOC fractions of secondary effluent and resulting fouling behaviour in ultrafiltration. Water Res 2007;41(17):3794–802.

[45] Moslehyani A, Ismail A, Othman M, Isloor AM. Novel hybrid photocatalytic reactor-UF nanocomposite membrane system for bilge water degradation and separation. RSC Adv 2015;5(56):45331–40.

[46] Mobaraki M, Ismail AF, Yusof N, Moslehyani A, editors. Taguchi optimization for nanocomposite PVDF ultrafiltration membrane for oily water treatment. National Congress on membrane technology 2016 (NATCOM 2016); 2016.

[47] Lee N, Amy G, Croué J-P, Buisson H. Identification and understanding of fouling in low-pressure membrane (MF/UF) filtration by natural organic matter (NOM). Water Res 2004;38(20):4511–23.

[48] Cho J, Amy G, Pellegrino J. Membrane filtration of natural organic matter: factors and mechanisms affecting rejection and flux decline with charged ultrafiltration (UF) membrane. J Membr Sci 2000;164(1):89–110.

[49] Mercier-Bonin M, Lagane C, Fonade C. Influence of a gas/liquid two-phase flow on the ultrafiltration and microfiltration performances: case of a ceramic flat sheet membrane. J Membr Sci 2000;180(1):93–102.

[50] Pezeshk N, Rana D, Narbaitz R, Matsuura T. Novel modified PVDF ultrafiltration flat-sheet membranes. J Membr Sci 2012;389:280–6.

[51] Yan L, Li YS, Xiang CB, Xianda S. Effect of nano-sized $Al_2O_3$-particle addition on PVDF ultrafiltration membrane performance. J Membr Sci 2006;276(1):162–7.

[52] Nayak MC, Isloor AM, Moslehyani A, Ismail N, Ismail A. Fabrication of novel PPSU/ZSM-5 ultrafiltration hollow fiber membranes for separation of proteins and hazardous reactive dyes. J Taiwan Inst Chem Eng 2018;82:342–50.

[53] Ibrahim GS, Isloor AM, Moslehyani A, Ismail A. Bio-inspired, fouling resistant, tannic acid functionalized halloysite nanotube reinforced polysulfone loose nanofiltration hollow fiber membranes for efficient dye and salt separation. J Water Proc Eng 2017;20:138–48.

[54] Chandra SW, Isloor AM, Moslehyani A, Ismail A, editors. Preparation and characterization of PPSU membranes with BiOCl nanowafers loaded on activated charcoal for oil in water separation. International symposium for research scholars on metallurgy, Materials Science Engineering; 2016.

[55] Nayak MC, Isloor AM, Moslehyani A, Ismail A. Preparation and characterization of PPSU membranes with BiOCl nanowafers loaded on activated charcoal for oil in water separation. J Taiwan Inst Chem Eng 2017;77:293–301.

[56] Luo M-L, Zhao J-Q, Tang W, Pu C-S. Hydrophilic modification of poly(ether sulfone) ultrafiltration membrane surface by self-assembly of $TiO_2$ nanoparticles. Appl Surf Sci 2005;249(1):76–84.

[57] Ndinisa N, Fane A, Wiley D. Fouling control in a submerged flat sheet membrane system. Part I. Bubbling and hydrodynamic effects. Sep Sci Technol 2006;41(7):1383–409.

[58] Cho J, Amy G, Pellegrino J. Membrane filtration of natural organic matter: initial comparison of rejection and flux decline characteristics with ultrafiltration and nanofiltration membranes. Water Res 1999;33(11):2517–26.

[59] Katsoufidou K, Yiantsios S, Karabelas A. Experimental study of ultrafiltration membrane fouling by sodium alginate and flux recovery by backwashing. J Membr Sci 2007;300(1):137–46.

[60] Idris A, Zain NM, Noordin M. Synthesis, characterization and performance of asymmetric polyethersulfone (PES) ultrafiltration membranes with polyethylene glycol of different molecular weights as additives. Desalination 2007;207(1–3):324–39.

[61] Skouteris G, Hermosilla D, López P, Negro C, Blanco Á. Anaerobic membrane bioreactors for wastewater treatment: a review. Chem Eng J 2012;198:138–48.

[62] Zhao C, Zhou X, Yue Y. Determination of pore size and pore size distribution on the surface of hollow-fiber filtration membranes: a review of methods. Desalination 2000;129(2):107–23.

[63] Qin J-J, Li Y, Lee L-S, Lee H. Cellulose acetate hollow fiber ultrafiltration membranes made from CA/PVP 360 K/NMP/water. J Membr Sci 2003;218(1):173–83.

[64] Bonyadi S, Mackley M. The development of novel micro-capillary film membranes. J Membr Sci 2012;389:137–47.

[65] Baker RW. Membrane technology and applications. Chichester, Wiley; 2004.

[66] Baker RW. Membrane Technology. Wiley Online Library; 2000.

[67] Tang Z, Wei J, Yung L, Ji B, Ma H, Qiu C, et al. UV-cured poly(vinyl alcohol) ultrafiltration nanofibrous membrane based on electrospun nanofiber scaffolds. J Membr Sci 2009;328:1):1–5.

[68] Moslehyani A, Matsuura T, Ismail AF, Othman MHD, editors. A review on application of electrospun polymeric nanofibers. National Congress on membrane technology 2016 (NATCOM 2016); 2016.

[69] Fan Z, Wang Z, Sun N, Wang J, Wang S. Performance improvement of polysulfone ultrafiltration membrane by blending with polyaniline nanofibers. J Membr Sci 2008; 320(1):363–71.

[70] Moslehyani A, Ismail A, Malek R, Hashemifard S. Effect of Ag ion exchanged halloysite nanotubes on the performance of polyethersulfone mixed matrix membrane for bacterial removal. International conference on membrane science and technology, Bangkok; 2012.

[71] Adams R, Carson C, Ward J, Tannenbaum R, Koros W. Metal organic framework mixed matrix membranes for gas separations. Microporous Mesoporous Mater 2010;131 (1):13–20.

[72] Adoor SG, Sairam M, Manjeshwar LS, Raju K, Aminabhavi TM. Sodium montmorillonite clay loaded novel mixed matrix membranes of poly(vinyl alcohol) for pervaporation dehydration of aqueous mixtures of isopropanol and 1,4-dioxane. J Membr Sci 2006; 285(1):182–95.

[73] Moslehyani A, Ismail AF, Malek RA, Hashemifard SA, editors. Effect of Ag+ ion exchanged halloysite nanotubes on the performance of polyethersulfone mixed matrix membrane for bacterial removal. Accepted in Euro Membrane London 2012; 2012: Euro Membrane; 2012.

[74] Moslehyani A, Ismail AF, editors. Effect of silver ion exchange halloysite nanotubes on the performance of polyethersulfone mixed matrix membrane for bacterial removal. Accepted in 2nd international conference on Water Research (Singapore Expo); 2013.

[75] Moslehyani A, Ismail AF, Malek RA, Hashemifard SA, editors. Polyethersulfone silver halloysite nanotubes mixed matrix membrane for bacterial removal. Presented in 4th international conference on biotechnology for the Wellness Industry 2012. Institute of Bioproduct Development Universiti Teknologi Malaysia; 2012.

[76] Guan H-M, Chung T-S, Huang Z, Chng ML, Kulprathipanja S. Poly(vinyl alcohol) multilayer mixed matrix membranes for the dehydration of ethanol-water mixture. J Membr Sci 2006;268(2):113–22.

[77] Seoane B, Coronas J, Gascon I, Benavides ME, Karvan O, Caro J, et al. Metal-organic framework based mixed matrix membranes: a solution for highly efficient $CO_2$ capture? Chem Soc Rev 2015;44(8):2421–54.

[78] Sairam M, Patil MB, Veerapur RS, Patil SA, Aminabhavi TM. Novel dense poly(vinyl alcohol)—$TiO_2$ mixed matrix membranes for pervaporation separation of water-isopropanol mixtures at 30°C. J Membr Sci 2006;281(1):95–102.

[79] Yin J, Deng B. Polymer-matrix nanocomposite membranes for water treatment. J Membr Sci 2015;479:256–75.

[80] Harun Z, Shohur MF, Jamalludin MR, Yunos MZ, Basri H. Hydrophilicity effect of rice husk silica on mixed matrix PSF membrane properties. Jurnal Teknol 2014;70(2):15–8.

[81] Galjaard G, Kruithof J, Kamp PC. Influence of NOM and membrane surface charge on UF-membrane fouling. Int Water Assoc 2005;1.

[82] Moslehyani A, Ismail AF, editors. PVDF/MWCNT MMMs for petroleum post treatment using cross-flow ultrafiltration system. Invited Speaker in Asian Nano Forum Conference (ANFC); 2015.

[83] Sorribas S, Kudasheva A, Almendro E, Zornoza B, de la Iglesia Ó, Téllez C, et al. Pervaporation and membrane reactor performance of polyimide based mixed matrix membranes containing MOF HKUST-1. Chem Eng Sci 2015;124:37–44.

[84] Hsieh H. Inorganic membranes for separation and reaction. Elsevier; 1996.

[85] She Q, Wang R, Fane AG, Tang CY. Membrane fouling in osmotically driven membrane processes: a review. J Membr Sci 2016;499:201–33.

[86] Warsinger DM, Swaminathan J, Guillen-Burrieza E, Arafat HA. Scaling and fouling in membrane distillation for desalination applications: a review. Desalination 2015;356:294–313.

[87] Regula C, Carretier E, Wyart Y, Gésan-Guiziou G, Vincent A, Boudot D, et al. Chemical cleaning/disinfection and ageing of organic UF membranes: a review. Water Res 2014;56:325–65.

[88] Chang H, Liang H, Qu F, Ma J, Ren N, Li G. Towards a better hydraulic cleaning strategy for ultrafiltration membrane fouling by humic acid: effect of backwash water composition. J Environ Sci 2016;43:177–86.

[89] Woo YC, Lee JJ, Tijing LD, Shon HK, Yao M, Kim H-S. Characteristics of membrane fouling by consecutive chemical cleaning in pressurized ultrafiltration as pre-treatment of seawater desalination. Desalination 2015;369:51–61.

[90] Qu F, Du X, Liu B, He J, Ren N, Li G, et al. Control of ultrafiltration membrane fouling caused by Microcystis cells with permanganate preoxidation: significance of in situ formed manganese dioxide. Chem Eng J 2015;279:56–65.

[91] Arhin SG, Banadda N, Komakech AJ, Kabenge I, Wanyama J. Membrane fouling control in low pressure membranes: a review on pretreatment techniques for fouling abatement. Environ Eng Res 2016;21(2):109–20.

[92] Liu G, Yu S, Yang H, Hu J, Zhang Y, He B, et al. Molecular mechanisms of ultrafiltration membrane fouling in polymer-flooding wastewater treatment: role of ions in polymeric fouling. Environ Sci Technol 2016;50(3):1393–402.

[93] Naidu G, Jeong S, Vigneswaran S, Hwang T-M, Choi Y-J, Kim S-H. A review on fouling of membrane distillation. Desalin Water Treat 2016;57(22):10052–76.

[94] Chellam S, Sari MA. Aluminum electrocoagulation as pretreatment during microfiltration of surface water containing NOM: a review of fouling, NOM, DBP, and virus control. J Hazard Mater 2016;304:490–501.

[95] Saqib J, Aljundi IH. Membrane fouling and modification using surface treatment and layer-by-layer assembly of polyelectrolytes: state-of-the-art review. J Water Proc Eng 2016;11:68–87.

[96] Dong H, Gao B, Yue Q, Sun S, Wang Y, Li Q. Floc properties and membrane fouling of different monomer and polymer Fe coagulants in coagulation-ultrafiltration process: the role of Fe(III) species. Chem Eng J 2014;258:442–9.

[97] Chang X, Wang Z, Quan S, Xu Y, Jiang Z, Shao L. Exploring the synergetic effects of graphene oxide (GO) and polyvinylpyrrodione (PVP) on poly(vinylylidenefluoride) (PVDF) ultrafiltration membrane performance. Appl Surf Sci 2014;316:537–48.

[98] Moslehyani A, Ismail A, Othman M, Matsuura T. Design and performance study of hybrid photocatalytic reactor-PVDF/MWCNT nanocomposite membrane system for treatment of petroleum refinery wastewater. Desalination 2015;363:99–111.

[99] X-Flow B. The XIGA-concept: a new module system for ultrafiltration. Filtr Sep 1997;34 (6):562–3.

[100] Lee YK, Won Y-J, Yoo JH, Ahn KH, Lee C-H. Flow analysis and fouling on the patterned membrane surface. J Membr Sci 2013;427:320–5.

[101] Yu W, Graham NJ. Application of Fe(II)/$K_2MnO_4$ as a pre-treatment for controlling UF membrane fouling in drinking water treatment. J Membr Sci 2015;473:283–91.

[102] Wang L, Miao R, Wang X, Lv Y, Meng X, Yang Y, et al. Fouling behavior of typical organic foulants in polyvinylidene fluoride ultrafiltration membranes: characterization from microforces. Environ Sci Technol 2013;47(8):3708–14.

[103] Reid AL, BCEE P. Increasing the ratio of membrane surface area to volume for micro and ultrafiltration membrane filter tubes. J NEWWA 2014;317.

[104] Darowna D, Wróbel R, Morawski AW, Mozia S. The influence of feed composition on fouling and stability of a polyethersulfone ultrafiltration membrane in a photocatalytic membrane reactor. Chem Eng J 2017;310:360–7.

[105] Su W, Chen C, Xu H, Yang W, Dai H. Filtering whitewater with an ultrafiltration membrane: effects of the interaction between dissolved organics and metal ions on membrane fouling. Bioresources 2015;11(1):1108–24.

[106] Wang Z, Ma J, Tang CY, Kimura K, Wang Q, Han X. Membrane cleaning in membrane bioreactors: a review. J Membr Sci 2014;468:276–307.

[107] Kang G-d, Cao Y-m. Application and modification of poly(vinylidene fluoride) (PVDF) membranes—a review. J Membr Sci 2014;463:145–65.

[108] Kanchanatip E, Su B-R, Tulaphol S, Den W, Grisdanurak N, Kuo C-C. Fouling characterization and control for harvesting microalgae Arthrospira (spirulina) maxima using a submerged, disc-type ultrafiltration membrane. Bioresour Technol 2016;209:23–30.

[109] Ismail AF, Lau W, Emadzadeh D, Moslehyani A. The effect of SPEEK additive on polyethersulfone nanofiltration membrane for dye removal; 2013.

[110] Chang H, Liang H, Qu F, Liu B, Yu H, Du X, et al. Hydraulic backwashing for low-pressure membranes in drinking water treatment: a review. J Membr Sci 2017; 540:362–80.

[111] Liu Y, Huang H, Huo P, Gu J. Exploration of zwitterionic cellulose acetate antifouling ultrafiltration membrane for bovine serum albumin (BSA) separation. Carbohydr Polym 2017;165:266–75.

[112] Lalia BS, Kochkodan V, Hashaikeh R, Hilal N. A review on membrane fabrication: structure, properties and performance relationship. Desalination 2013;326:77–95.

[113] Kaner P, Rubakh E, Asatekin A. Zwitterion-containing polymer additives for fouling resistant ultrafiltration membranes. J Membr Sci 2017;533:141–59.

[114] Moslehyani A, Ismail AF, Othman MHD, Ng BC, Abdullah S, Rahman M, et al., editors. Photocatalytic membrane reactor for oil in water emulsion degradation and separation. International conference on membrane science and technology (MST), Kuala Lumpur, Malaysia; 2013.

[115] Moslehyani A, Mobaraki M, Ismail A, Othman M, Mayahi A, Shamsaei E, et al. PVDF membrane for oil-in-water separation via cross-flow ultrafiltration process. J Teknol 2015;78.

[116] Moghimifar V, Raisi A, Aroujalian A. Surface modification of polyethersulfone ultrafiltration membranes by corona plasma-assisted coating $TiO_2$ nanoparticles. J Membr Sci 2014;461:69–80.

[117] Moslehyani A, Ismail AF, Othman MHD, editors. Novel green process via nanocomposite photocatalytic membrane reactor (NPMR) for oily ballast water photooxidation and separation from merchant ship. Presented in 2nd international conference on desalination using membrane technology 2015; 2015.

[118] Luo H, Wang Q, Zhang TC, Tao T, Zhou A, Chen L, et al. A review on the recovery methods of draw solutes in forward osmosis. J Water Proc Eng 2014;4:212–23.

[119] Kochkodan V, Hilal N. A comprehensive review on surface modified polymer membranes for biofouling mitigation. Desalination 2015;356:187–207.

[120] Gao Y, Hu M, Mi B. Membrane surface modification with $TiO_2$-graphene oxide for enhanced photocatalytic performance. J Membr Sci 2014;455:349–56.

[121] Cassano A, Conidi C, Drioli E. Membrane processing. Conventional and advanced food processing technologies; 2015. 537–66.

[122] Hilal N, Ismail AF, Matsuura T, Oatley-Radcliffe D. Membrane characterization. Elsevier; 2017.

[123] Lee H, Yanilmaz M, Toprakci O, Fu K, Zhang X. A review of recent developments in membrane separators for rechargeable lithium-ion batteries. Energy Environ Sci 2014; 7(12):3857–86.

[124] Rana D, Matsuura T. Surface modifications for antifouling membranes. Chem Rev 2010;110(4):2448–71.

[125] Smitha B, Sridhar S, Khan A. Solid polymer electrolyte membranes for fuel cell applications—a review. J Membr Sci 2005;259(1):10–26.

[126] Hilal N, Ogunbiyi OO, Miles NJ, Nigmatullin R. Methods employed for control of fouling in MF and UF membranes: a comprehensive review. Sep Sci Technol 2005; 40(10):1957–2005.

[127] Meares P. Membrane separation processes. Elsevier Science & Technology; 1976.

[128] Lee C, Bae S, Han S, Kang L. Application of ultrafiltration hybrid membrane processes for reuse of secondary effluent. Desalination 2007;202(1):239–46.

[129] Judd S. The MBR book: principles and applications of membrane bioreactors for water and wastewater treatment. Elsevier; 2010.

[130] Basile A, Charcosset C. Integrated membrane systems and processes. John Wiley & Sons; 2015.

[131] Squillace M, McLeod A. Marketing conserved water. Environ Law 2016;46:1.

[132] Lau W, Ismail A, Matsuura T, Nazri N, Yuliwati E. Advanced materials in ultrafiltration and nanofiltration membranes. Handbook of Membrane Separations; 2015. p. 7–34.

[133] Zhao C, Lv J, Xu X, Zhang G, Yang Y, Yang F. Highly antifouling and antibacterial performance of poly(vinylidene fluoride) ultrafiltration membranes blending with copper oxide and graphene oxide nanofillers for effective wastewater treatment. J Colloid Interface Sci 2017;505:341–51.

[134] Basri H, Ismail A, Aziz M. Microstructure and anti-adhesion properties of PES/TAP/Ag hybrid ultrafiltration membrane. Desalination 2012;287:71–7.

[135] Moslehyani A, Matsuura T, Ismail AF, Othman MHD, editors. Preparation and characterization of electro-spun nanofiber membranes (ENMs) for membrane adsorption. National Congress on membrane technology 2016 (NATCOM 2016); 2016.

[136] Moslehyani A, Ismail A, Othman MHD, Ng B, Abdullah S, Rahman MA. Photocatalytic Membrane Reac; 2013.

[137] Wang R, Ren D, Xia S, Zhang Y, Zhao J. Photocatalytic degradation of bisphenol A (BPA) using immobilized $TiO_2$ and UV illumination in a horizontal circulating bed photocatalytic reactor (HCBPR). J Hazard Mater 2009;169(1):926–32.

[138] De Lasa HI, Serrano B, Salaices M. Photocatalytic reaction engineering. Springer; 2005.

[139] Mozia S, Tomaszewska M, Morawski AW. A new photocatalytic membrane reactor (PMR) for removal of azo-dye Acid Red 18 from water. Appl Catal B Environ 2005;59(1):131–7.

[140] Basile A, Gallucci F. Membranes for membrane reactors: preparation, optimization and selection. John Wiley & Sons; 2010.

[141] Moslehyani A, Ismail A, Othman M, Matsuura T. Hydrocarbon degradation and separation of bilge water via a novel $TiO_2$-HNTs/PVDF-based photocatalytic membrane reactor (PMR). RSC Adv 2015;5(19):14147–55.

[142] Leong S, Razmjou A, Wang K, Hapgood K, Zhang X, Wang H. TiO$_2$ based photocatalytic membranes: a review. J Membr Sci 2014;472:167–84.

[143] Dalrymple OK, Stefanakos E, Trotz MA, Goswami DY. A review of the mechanisms and modeling of photocatalytic disinfection. Appl Catal B Environ 2010;98(1):27–38.

[144] Augugliaro V, García-López E, Loddo V, Malato-Rodríguez S, Maldonado I, Marcì G, et al. Degradation of lincomycin in aqueous medium: coupling of solar photocatalysis and membrane separation. Sol Energy 2005;79(4):402–8.

[145] Nor N, Jaafar J, Ismail A, Mohamed MA, Rahman M, Othman M, et al. Preparation and performance of PVDF-based nanocomposite membrane consisting of TiO$_2$ nanofibers for organic pollutant decomposition in wastewater under UV irradiation. Desalination 2016;391:89–97.

[146] Zangeneh H, Zinatizadeh A, Habibi M, Akia M, Isa MH. Photocatalytic oxidation of organic dyes and pollutants in wastewater using different modified titanium dioxides: a comparative review. J Ind Eng Chem 2015;26:1–36.

[147] Zhang H, Quan X, Chen S, Zhao H. Fabrication and characterization of silica/titania nanotubes composite membrane with photocatalytic capability. Environ Sci Technol 2006;40(19):6104–9.

[148] Sabate J, Anderson M, Kikkawa H, Xu Q, Cervera-March S, Hill C. Nature and properties of pure and doped TiO$_2$ ceramic membranes affecting the photocatalytic degradation of 3-chlorosalicylic acid as a model of halogenated organic compounds. J Catal 1992;134(1):36–46.

[149] Mozia S. Photocatalytic membrane reactors (PMRs) in water and wastewater treatment. A review. Sep Purif Technol 2010;73(2):71–91.

## Further Reading

[150] Moslehyani A, Mobaraki M, Ismail AF, Othman MHD. In: Oily bilge water treatment of oil tanker via a novel, efficient hybrid system. International conference on membrane science and technology (MST 2015); 2015.

[151] Lin T, Shen B, Chen W, Zhang X. Interaction mechanisms associated with organic colloid fouling of ultrafiltration membrane in a drinking water treatment system. Desalination 2014;332(1):100–8.

# C H A P T E R

# 4

# Microfiltration Membranes

*Randeep Singh, Mihir Kumar Purkait*

**Department of Chemical Engineering, Indian Institute of Technology
Guwahati, Guwahati, India**

## O U T L I N E

## 4.1 INTRODUCTION

In recent times, membrane technology has seen significant development. Numerous applications are proposed for membrane processes of which microfiltration and ultrafiltration are considered as the most critical membrane technologies. These membrane processes are regarded as necessary for chemical and biochemical processing because of their economic and availability of membranes with higher overall membrane flux, lower process cost, and low fouling [1]. The advancement in the membrane research has provided with membranes with better chemical, thermal, and mechanical stabilities. Therefore, these membranes can be employed for previously not possible industrial applications. These membranes are capable of high temperature, high pressure, and corrosive applications with good resilience [2–7].

Microfiltration membranes are generally pressure driven processes with pores in the range of 0.1–10 μm. The overall membrane flux of a microfiltration membrane can be given by using the following relation:

$$F = \alpha \cdot \Delta P \tag{4.1}$$

where, $F$ represents the overall membrane flux, $\alpha$ the permeability constant, and $\Delta P$ the transmembrane pressure. For the calculation of various membrane parameters, it is assumed that the pores of these membranes are uniform and cylindrical so that the Hagen-Poiseuille and Kozeny-Carman equations can be applied [8–10]. The Hagen-Poiseuille relation can be used as given in the following relation:

$$F = \frac{\eta r^2}{8 \eta \tau} \frac{\Delta P}{\Delta l} \tag{4.2}$$

where, $\mu$ represents the membrane porosity, $r$ the membrane pore radius, $\eta$ the dynamic viscosity, $\Delta l$ the membrane thickness, and $\tau$ the tortuosity factor.

In case, where feed particles are assumed as spherical and agglomerate then the Kozeny-Carman equation can be applied to the microfiltration membrane system as given in the following relation:

$$F = \frac{\mu^3}{\chi \eta A^2} \frac{\Delta P}{\Delta x} \tag{4.3}$$

where, $\chi$ represents the pore geometry dependent dimensionless constant and $A$ the spherical particles per unit volume surface area.

Eqs. (4.2), (4.3) confirm that the membrane flux relates to the membrane structural features, pore size ($r$) and porosity ($\mu$). Therefore, to have an overall effective membrane flux it is essential to have a microfiltration membrane with narrow pore size distribution and high porosity.

Microfiltration membranes prepared from inorganic materials are more suitable for different industrial applications because of their excellent

chemical, thermal, and mechanical stabilities. There are various preparation techniques available for the preparation of these membranes, which allows the use of different types of materials. For example, for hydrophobic membranes: polyvinylidenefluoride, polytetrafluoroethylene, polyethylene, and polypropylene; hydrophilic membranes: cellulose, polysulfone, polycarbonate, polyamide, and polyetheretherketone; and ceramic membranes: alumina, zirconia, kaolin, and titania. In addition to these other materials are also used for the preparation of glass ($SiO_2$) and metal membranes (stainless steel, silver, tungsten). The successfully prepared membranes are characterized by using various characterization techniques for their morphological as well as permeation properties, such as thermogravimetric analysis, X-ray diffraction, Fourier transforms infrared spectroscopy, (field) scanning electron microscopy, liquid-liquid displacement porosimetry, hydraulic permeability, and pure water permeation.

Initially, polymeric membranes were used prominently for various membrane-based applications due to their advantages, such as easy to cast, scale-up, and low cost. Despite having so many advantages the polymeric membranes were not able to make membrane processes acceptable on an industrial level because of their severe disadvantages, such as fouling and thus short lifespan, incapability to withstand harsh chemical, thermal, or mechanical conditions, and limited strength. Therefore, ceramic membranes are always preferred over polymeric membranes for industrial applications, but their high cost is one factor which always halts their progress in the field. The main reasons for the high cost of ceramic membranes are the sintering temperature, membrane materials, and the preparation procedure. This shows that if these three factors can be controlled, then the cost of a ceramic membrane can be brought down. The problem here is that all the three factors are equally important for a successful membrane. The sintering temperature cannot be replaced. Similarly, the preparation procedures would also remain the same. Therefore, the only possible thing which can be changed is the membrane materials. Thus, cost-effective raw materials have to be searched and developed for the preparation of low-cost ceramic membranes. This chapter along with the basics of the microfiltration membrane processes explains about the various low-cost ceramic membrane materials used by various researchers worldwide.

In this chapter, the preparation as well as characterization methods and techniques are discussed in detail along with the various modes and modules used for the microfiltration membrane processes. The problem of fouling is the most concerning object of membrane processes and is discussed in this chapter along with the various methods and techniques to decrease the phenomenon of fouling effectively and efficiently. This chapter discusses in detail the various low-cost ceramic membrane applications in various fields. The chapter at its end discusses about the cost estimation of the prepared membranes.

## 4.2  MODES AND MODULES

### 4.2.1  Modes

The two important modes of membrane process operations are dead-end filtration and cross-flow. Both are equally important and are used worldwide. Generally, the dead-end filtration is used in batch configuration and cross flow in continuous mode. Also, dead-end filtration is commonly used on a laboratory scale and cross-flow is favored to be used on industrial scale. These selections are based on the advantages and disadvantages of these modes of membrane operations, such as low fouling, scale of operation, etc. For example, the dead-end filtration provides high recovery as well as fouling. Therefore, the high recovery favor it for better recovery results and the fouling problem associated with it causes flux decline which make it unfavorable for large scale operations. Whereas, cross flow provides less recovery and low fouling. This makes it a better choice for large-scale operations. Also, both the modes can be used in single or multiple pass configurations, which allow the feed or permeate to be circulated across the membrane single or multiple times to improve the efficiency of the overall membrane process.

#### 4.2.1.1  Batch

Batch mode is the most widely used mode of membrane processes. In this mode, a predefined amount of feed is provided to the membrane. The process runs until the feed is not over or refilled. It is advised as a virtuous mode of membrane process because it allows the cleaning of the membranes as well as the overall membrane setup in between two runs. This makes this mode of operation beneficial for the membrane process in terms of enhanced membrane process efficiency, membrane life, reduced cost, and low fouling. Therefore, it is best to be used in industries, such as food, pharmaceutical, and biotechnology.

#### 4.2.1.2  Semi-Batch

Semi-batch mode of membrane processes is similar to batch mode of membrane operation with the only difference that it allows recirculation/addition/removal of feed/retentate/permeate. This arrangement helps in the improvement of selectivity and better control of the overall membrane process. Also, it helps in the reduction of total load on the downstream processing of permeate and retentate. This mode of membrane operations is widely used in process industries due to its low fouling and effective efficiency characteristics.

### 4.2.1.3 *Continuous*

Continuous mode of membrane processes consists of continuous addition of feed and removal of permeate from a membrane system. The main attribute of this system is that it is capable of handling large volumes of feed. This makes it an industry favorite, because it reduces the overall membrane operation time. The only drawback of this system is fouling, which occurs due to the nature of its continuous operation and results in gradual decline in overall efficiency of the process. It would be suitable and has potential for the acceptance of membrane separation processes on a larger scale if membranes with better antifouling properties could be developed in the near future.

## 4.2.2 Modules

The industrial applications require a process to have capabilities to work efficiently and effectively on a large scale. In case of membrane processes too it is required for the membranes to handle large sums of feed to be acceptable on an industrial scale. Also, it is better for the membrane setups to be compact so that they acquire less space. Therefore, membranes are assembled in units which are compact and also fulfill the area requirements of membranes to carry out the membrane process operations successfully. These units are known as modules, which are further characterized based on their geometry and configurations. For example, plate and frame for flat membranes and tubular for tubular (hollow) membranes.

Typically, all the membrane modules consist of an inlet for feed and outlets for permeate and retentate. The feed enters the membrane module via inlet and later separates into two different streams (permeate and retentate) inside the membrane module and come out via respective outlets. The permeate stream consists of components allowed by the membrane to pass through and the components rejected by the membrane forms the retentate stream.

The membrane modules enhanced the applicability of membranes on industrial scale for various applications. The different types of membrane modules available are used by industries as per the requirements of different applications. The different types of membrane modules commonly available and used in membrane processes are discussed in detail in the following sections.

### 4.2.2.1 *Plate and Frame*

Plate and frame membrane modules accommodate membranes of flat sheet configurations in a casket form. A plate and frame module is shown in Fig. 4.1. This arrangement makes it possible for the module to house more
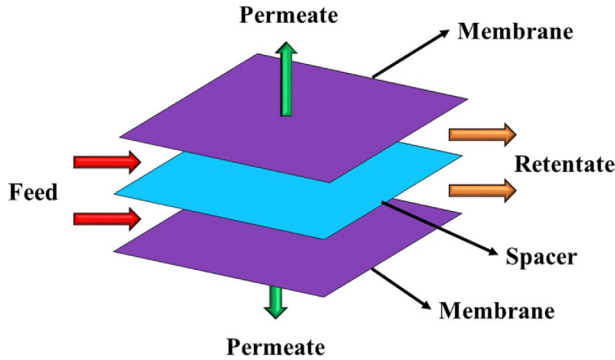
FIG. 4.1    Schematic representation of a plate and frame membrane module.

than one membrane in a stacked fashion that is one over other. The membranes are arranged in a fashion that the feed and permeate sides face each other and the module seems to be a compartment buildup of set of membranes. These individual compartments formed are separated by using spacers and the module is sealed. Furthermore, the module is housed between plates to form the final plate and frame module assembly. Plate and frame modules have packing density in the range of 100–400 $m^2/m^3$.

### 4.2.2.2 Spiral Wound

Spiral wound membrane modules are similar to plate and frame modules as they also accommodate flat sheet membranes but at the same time different as in this module the membranes are wrapped around a permeant collection tube as shown in Fig. 4.2. This arrangement enhances the efficiency and effectiveness of the membrane module. Thus, spiral wound membrane module is among the most extensively used membrane modules. In this membrane module, the feed runs parallel to the central porous tube and this central porous tube also functions as the permeant collector. The average packing density provided by this membrane module is around 300–1000 $m^2/m^3$. Generally, more than one membrane
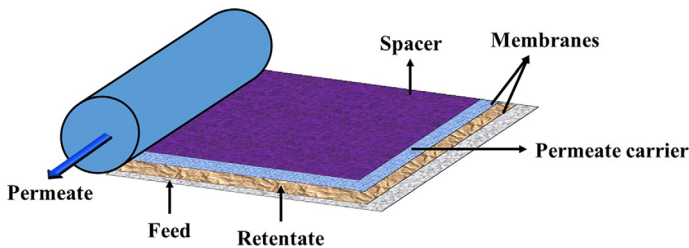


FIG. 4.2    Schematic representation of spiral wound membrane module.

modules are used together so as to make the overall membrane process economical and efficient.

### 4.2.2.3 Tubular

Tubular membrane modules are used for housing tubular membranes as shown in Fig. 4.3. In this membrane module, the tubular membranes are assembled inside a metallic, ceramic, or polymeric porous tube. This porous tube works as support for the tubular membranes. The number of tubular membranes that can be packed inside the supporting tube is not limited and can be set as per the requirement. This membrane module gets the feed through the tubular membranes and permeant is collected through the supporting porous tube. Tubular membrane module is commonly used for ceramic membranes with an average packing density of 300 m$^2$/m$^3$.

### 4.2.2.4 Perforated Block

The tubular membrane modules are widely used for their better efficiencies and effective membrane operations. Therefore, they are further modified for enhanced overall membrane flux and selectivity. Perforated block membrane module is a good example of such a modified tubular membrane module. In this membrane module, a coarsely porous ceramic monolithic block is assembled into a supporting tube. This perforated block contains a number of cylindrical channels parallel to its length. The inner surface of these channels is used to have a layer of ceramic membrane. The permeant has to pass this layer of the ceramic membrane and thin walls of the membrane module so as to exit from the module. This arrangement provides possibilities for having number of channels with different shape variations. Tami industries provide 14 different shapes
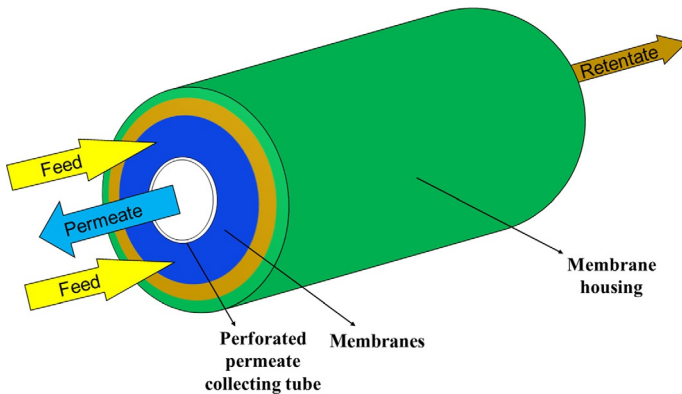


**FIG. 4.3**    Schematic representation of tubular membrane module.

with up to 39 individual channels, which offers hydraulic diameters in the long range of 2–14 mm [11].

### 4.2.2.5 Rotating Disk

Rotating disk membrane module is widely used membrane module in food, pharmaceutical, and biotechnology applications. This system provides a large area with minimal membrane fouling and enhanced membrane flux. In this membrane module, multiple disks are mounted on a single shaft and this system rotates between fixed circular membranes. Also, multishaft systems are successfully developed and are in use in different parts of the world. This system is capable of using circular membranes with an average area of 2 m$^2$.

## 4.3 FOULING AND ITS CORRECTIVE MEASURES

The biggest disadvantage of membrane processes is the phenomenon of concentration polarization and fouling. This is the consequence of the selective behavior of the membranes as they allow specific feed components to pass through them and retain the remaining. This results in the accumulation of the retained feed components on the membrane surface in a mass transfer boundary layer. This accumulation of the feed components over the membrane surface gradually declines the membrane flux. The accumulated material give rise to a concentration gradient between the solution at the membrane surface and bulk, this results in the back transport by diffusion of the feed components accumulated over the membrane surface. This phenomenon is known as concentration polarization [1] and is shown in Fig. 4.4. On the other hand, fouling is the membrane phenomenon occurs due to the deposition of the retained feed components over the membrane surface or in the membrane pores. This results in the long-term membrane flux decline and it depends upon the physicochemical nature of the membrane, feed, and system design.

In case of reverse osmosis and nanofiltration, the membrane usually separates low molecular weight feed components from a feed. This leads to the increase in the osmotic pressure which is directly proportional to the feed component concentration over the membrane surface and results in overall membrane flux decline. Then again, in the case of microfiltration and ultrafiltration, because high molecular weight feed components are retained, the osmotic pressure remains low. The retained feed components usually precipitate and form a solid layer over the membrane surface. This solid layer itself acts as a membrane, thereby affecting the membrane performance by a decline in membrane flux and rejection or selectivity profile of the membrane.
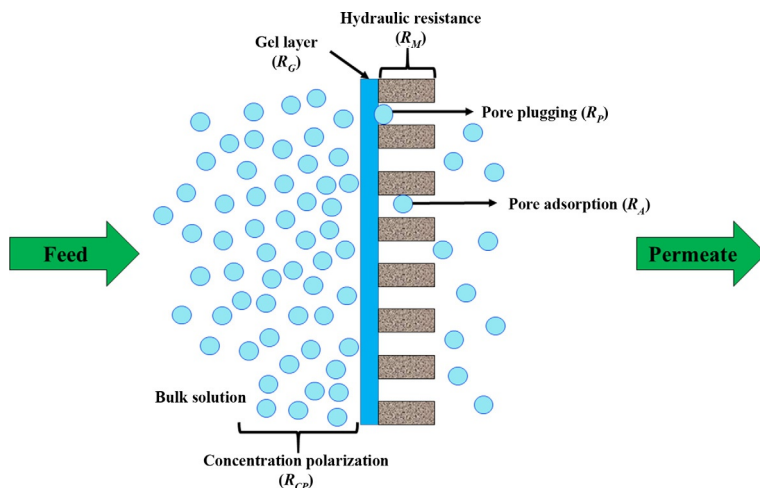
**FIG. 4.4** Schematic representation of concentration polarization and fouling in a membrane process.

There are four plausible ways for the accumulation of the feed components over the membrane surface. First, is using adsorption, wherein attractive interactions between the membrane and feed components exist. Second, the accumulation of the feed components in the membrane pores, thereby, blocking the pores and is known as pore blockage. This phenomenon generally takes place in micro- and ultra-filtration membranes. Third, layer by layer accumulation of the feed components over the membrane surface. This results in gradual decrease of the membrane flux due to the additional hydraulic resistance. Lastly, the gel layer formation because of the concentration polarization of the feed components over the membrane surface.

Film theory model is the basic model used for the understanding of concentration polarization. This model explains the transport phenomena across a membrane when flux becomes independent of pressure on polarized layer formation. According to the film theory model the feed component accumulates over the membrane surface by convective transport at a rate $F_s$, which is defined as:

$$F_s = FC_B \tag{4.4}$$

where, $F$ represents the permeate flux and $C_B$ the retained feed components bulk concentration. The developed gradient results into backward transport of the feed component into the bulk solution using diffusional effect, which is given as:

$$F_s = D\frac{dC}{dx} \tag{4.5}$$

where $D$ represents the diffusion coefficient and $dC/dx$ the concentration gradient over a differential element in the boundary layer.

On attainment of steady state, the Eqs. (4.4), (4.5) can be equated and integrated over the boundary layer giving:

$$F = \frac{D}{\delta} \ln \frac{C_G}{C_B} = k \ln \frac{C_G}{C_B} \qquad (4.6)$$

where, $C_G$ represents the gel layer concentration and $k$ the mass transfer coefficient given by:

$$k = \frac{D}{\delta} \qquad (4.7)$$

where, $\delta$ represents the thickness of the boundary layer.

There are several correlations for the correlating mass transfer coefficient and physical properties of the system [12–14]. However, these correlations are not universal. Therefore, in case of microfiltration membrane process estimation of the mass transfer coefficient can be done by dimensional analysis. Thus, by using the $\pi$ theorem, the following relation can be obtained:

$$S_h = A\,(R_e)^{\alpha}\,(S_c)^{\beta} \qquad (4.8)$$

where $S_h$, $R_e$, $S_c$ represent the Sherwood, Reynolds, and Schmidt numbers, respectively. Furthermore, the dimensionless numbers can be obtained by using Eqs. (4.9), (4.11), and (4.12).

$$S_h = \frac{kd_h}{D} \qquad (4.9)$$

where, $d_h$ represents the hydraulic diameter, given by:

$$d_h = 4\frac{\text{Cross section for flow}}{\text{Wetted perimeter}} \qquad (4.10)$$

The state of turbulence in the system can be given as:

$$R_e = \frac{V \rho d_h}{\mu} \qquad (4.11)$$

On the other hand, Schmidt number is used to measure the ratio between momentum and mass transfer as:

$$S_c = \frac{\mu}{\rho D} \qquad (4.12)$$

Also, the constants $\alpha$ and $\beta$ in Eq. (4.8) are determined according to the state of the velocity and concentration profiles development along the channel.

The concentration polarization because of its reversible nature can be reduced by using simple hydrodynamic means, such as feed flow velocity, module design, and use of other physical means, such as the use of an

agitator over the membrane surface. On the other hand, membrane fouling is challenging to control. However, methods such as feed pretreatment, membrane modification, change in operating conditions, flow manipulations, and membrane cleaning are some of the commonly used methods for preventing fouling in a membrane process.

## 4.3.1 Evaluation of Membrane Fouling

The total fouling resistance ($R_T$) in a microfiltration membrane process is given by the sum of hydraulic resistance ($R_M$), reversible fouling resistance ($R_R$) and irreversible fouling resistance ($R_{IR}$) as:

$$R_T = R_M + R_R + R_{IR} \tag{4.13}$$

where, $R_R$ represents the permeation resistance caused by reversible adsorption, concentration polarization, and cake or gel layer resistance. Similarly, $R_{IR}$ represents the permeation resistance caused by irreversible adsorption and internal pore blocking of the membrane. The hydraulic permeation resistance ($R_M$) can be evaluated by using the pure water flux obtained for the fresh membrane after compaction and is given by the following relation:

$$R_M = \frac{\Delta P}{\eta_w F_w} \tag{4.14}$$

where, $\Delta P$ represents the transmembrane pressure, $\eta_w$ water viscosity, and $F_w$ the membrane pure water flux.

The irreversible fouling resistance of the membrane is evaluated using cleaned membrane after the microfiltration membrane operation and is given by the following relation:

$$R_{IR} = \frac{\Delta P}{\eta_w F_w^{\text{clean}}} - R_M \tag{4.15}$$

The total permeation resistance is evaluated by using the following relation:

$$R_T = \frac{\Delta P}{\eta_{\text{permeate}} F} \tag{4.16}$$

where, $F$ represents the overall membrane permeate flux and $\eta_{\text{permeate}}$ the permeant viscosity.

The reversible fouling resistance can be calculated by using the following relation:

$$R_R = R_T - R_{IR} - R_M \tag{4.17}$$

In cases of low fouling, the $R_{IR}/R_R$ values will be insignificant. Therefore, it will be interesting to evaluate the contributions of $R_M$, $R_{IR}$, and $R_R$ to $R_T$ for various cases.

## 4.3.2 Methods to Abstain Fouling

The problem of fouling makes it difficult for the membranes to be used for critical industrial applications. Therefore, it is essential to tackle this problem of membrane fouling. Generally, membranes are modified in such a way that the feed components repel themselves from the membrane surface. There are two ways to do so. First, the membrane is made hydrophilic in case of hydrophobic feed components by using hydrophilic components as membrane materials. These materials are either grafted/coated or directly blended within the membranes to impart hydrophilicity to the membranes. This leads to increase in the antifouling nature of the membranes. Second, a charge can be imparted on membranes so that the feed components will not attract toward the membrane surface and thus fouling of the membrane could be reduced. The two methods are shown in Fig. 4.5. These methods are described in the following sections.

### 4.3.2.1 Increase in the Hydrophilicity of the Membranes by Blending Method

In this method, the hydrophilic membrane materials are directly blended with membranes during the membrane preparation process. Hydrophilic polymers, charged polymers, organic acids, and surfactants are some of the examples of commonly used hydrophilic components for the modification of membranes to reduce overall membrane fouling. Nowadays, materials such as co-polymers and stimuli-responsive materials are also commonly used. In addition to the hydrophilic organic components, there are some inorganic components which are used for the enhancement of the antifouling nature of the membranes, such as metallic nanoparticles, carbon nanotubes. Therefore, this method is prominent, easy to use, and result oriented.
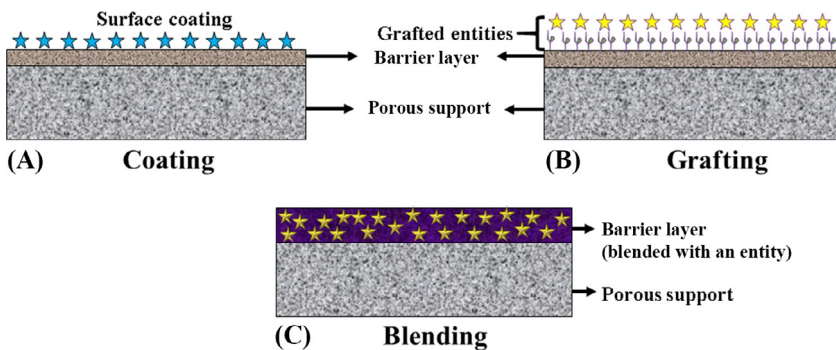


FIG. 4.5   Schematic representation of (A) coating, (B) grafting, and (C) blending of (hydrophilic or responsive) components.

### 4.3.2.2 *Antifouling Membranes by Surface Modification*

The prepared membranes are also modified by modifying their surface. Generally, a hydrophilic component is either coated or grafted over the membrane surface to achieve the goal of antifouling. There are two methods to do the surface modification of the membranes viz. physical method and chemical method.

#### 4.3.2.2.1 Physical Modification

In this method, the hydrophilic components are coated on the membrane surface with physical interactions and without any covalent bonding. In simple words, the chemical composition of the membrane remains unchanged even after the surface modification. However, a chemical reaction might be needed during the process of membrane modification. The membranes are either directly coated with the hydrophilic component or first dipped in a solution containing chemically active monomers. Later, the monomers are immobilized on the membrane surface by cross-linking or polymerization without the chemical participation of the base membrane. Commonly used hydrophilic materials for this purpose are polyvinyl alcohol, chitosan, and polyethylene glycol.

#### 4.3.2.2.2 Chemical Modification

In this method, the membranes are modified by covalent bonding interaction. Firstly, the membrane base polymer chains are activated chemically or by irradiation. Then the hydrophilic components are coated or grafted over the active membrane surface. In this method too, the basic membrane properties are not changed. The advantage of this method is that due to the presence of covalent bonding between the hydrophilic component and membrane surface the membrane modifying agent will remain intact over the membrane surface for a longer period of time.

## 4.4 PREPARATION

Broadly, membranes can be divided into two categories on the basis of the materials used for their preparation viz. polymeric and ceramic. Therefore, various methods and techniques are discussed in the following sections for the successful preparation of these two types of membranes along with the techniques used to synthesize the membranes having structural and functional attributes of both type of membranes (solution coating technique for the preparation of composite membranes).

## 4.4.1 Polymeric Membranes

Polymeric microfiltration membranes are prepared by using various methods and techniques available, such as stretching, track-etching, solution coating, sintering, and phase inversion. These methods and techniques are systematically discussed in this section while giving importance to the type of membrane pores and membrane structure obtained.

### 4.4.1.1 Stretching

Stretching is a commonly used technique for polymeric microfiltration membrane preparation. In this technique, an extruded thin film or foil prepared from crystalline or semi-crystalline polymers is stretched perpendicular to the direction of extrusion [1]. This process results in the formation of membrane pores due to the mechanical stress induced by the stretching process on the membrane. Generally, the membrane pore size of the membranes prepared by using stretching technique lies in the range of 0.1–3.0 μm. Stretching technique is suitable for the preparation of highly porous membranes. "Celgard" and "Gore-Tex" are two trade names for the poly(propylene) and poly(tetrafluoroethylene) microfiltration membranes prepared by using stretching technique.

### 4.4.1.2 Track-Etching

Track-etching method is a popular method for the preparation of microfiltration membranes with uniform cylindrical pores [1, 15]. In this method, pores are formed by perpendicularly irradiating the polymer film with particles. This results in the formation of tracks on the polymer film due to the damage of the material at point of particle radiation impact. Further, the irradiated polymer film with developed tracks is immersed in acidic or basic medium depending upon the type of materials used. This finally results into the formation of uniform and symmetrical cylindrical pores from the tracks present on the polymer film. Membranes with pore size in the range of 0.02–10 μm are obtained with this method. Generally, the membranes developed with this method carries low porosity, which directly depends upon the time of irradiation of the polymer film and the membrane pore diameter depends upon the total etching time. Therefore, regulating these two parameters of the process membranes with optimum porosity and pore size can be obtained.

### 4.4.1.3 Sintering

Sintering is a special technique in case of preparation of polymeric microfiltration membranes. In this technique, polymers in powder form of defined particle size are compressed and sintered at elevated temperatures. The sintering at high temperatures results in the fusion of the particles and disappearance of the interfaces present in between the polymer

particles resulting in the formation of a porous microfiltration membrane. The most suitable polymer for the preparation of polymeric microfiltration membranes by this method is poly(tetrafluoroethylene).

### 4.4.1.4 *Phase Inversion*

The most commonly used method for the preparation of polymeric membranes is phase inversion. Basically, phase inversion technique works on the principle of phase change in which a polymer solution separates into two separate phases, namely, a polymer-rich solid phase and a polymer-lean liquid phase [1, 15]. The solid and liquid phases form the membrane matrix and pores, respectively. The phase transition is an important factor in this method which controls this overall membrane preparation process. The membrane morphology can be regulated by optimally regulating this phase transition involved in the process and both a porous as well as nonporous membrane can be obtained. Also, there is no restriction for the selection of a polymer for membrane preparation by this method but the only requirement of the method is that the polymer should be soluble in a solvent or solvent mixture so that successful phase inversion could take place. Commonly used solvents for this method are N-methyl-2-pyrrolidone (NMP), dimethylacetamide (DMAc), and dimethyl sulfoxide (DMSO).

### 4.4.1.5 *Solution Coating*

Composite membranes are required in case of replacement of dense polymeric membranes with low flux profiles [1]. The composite membranes are made up of two different materials, suppose polymeric and ceramic in case of polymer-ceramic composite membranes, where one material forms a very selective thin top layer deposited over a porous sublayer made up of a second material. The top layer determines the selectivity of the membrane and the sublayer works as a support. This arrangement provides membranes with strength and high flux profiles. There are various methods available to carry out this procedure for the preparation of composite materials, such as dip coating, plasma polymerization, interfacial polymerization, and in-situ polymerization.

## 4.4.2 Ceramic Membranes

In general, there are two ways to prepare symmetric ceramic membranes viz. paste and uni-axial method [1, 15–17]. These two methods involve the preparation of a proper inorganic mixture constituting the various membrane materials, such as organic and inorganic pore formers, binders, and membrane base materials. Therefore, the membrane preparation process starts with proper mixing of dry inorganic raw materials.

TABLE 4.1    Raw Material Composition of a Low-Cost Ceramic Membrane

| Raw material | Composition (wt %) |
|---|---|
| Kaolin | 30.0 |
| Quartz | 11.0 |
| Calcium carbonate, etc. | 19.0 |
| Sodium carbonate | 7.0 |
| Boric acid | 3.5 |
| Sodium metasilicate | 3.5 |
| Water | 26.0 |
| Feldspar | 0.0 |

The composition of a typical low-cost ceramic membrane is shown in Table 4.1. This section describes about these two ceramic membrane preparation methods in detail.

### 4.4.2.1 Paste Method

Paste method is a convenient method for the preparation of ceramic membranes. In this method, the raw materials were mixed together by using distilled water to form a paste [16, 18]. This paste is then casted in the form of circular disks or tubular shapes by using a respective casing. The casing is removed prior to the introduction of the cast to a distributed pressure for 24–48 h. This prevents occurrence of deformation and helps in making the inorganic matrix homogeneous. Later, the cast is introduced to sequential steps of heat treatment so as to make the membrane ready for its implementation in a membrane process. The first step includes drying of the prepared cast at room temperature for 12–24 h. Then in the second step of the heat treatment the cast is dried for 12 h at 100°C in a hot air oven. The next step involves the drying of the cast for 24 h at 250°C. In this step, the heating rate is maintained low in 100–250°C range to prevent initiation of thermal stresses generated due to loss of moisture. Finally, the cast is heated to the desired sintering temperature with a heating rate of 2–3°C per min. The cast is kept at the sintering temperature for about 3–5 h depending upon the type of raw materials used. Also, the sintering temperature and time is different for the preparation of membranes with different morphological properties. The characterization techniques, such as Thermogravimetric analysis (TGA) and X-ray diffraction (XRD) helps in the selection of the minimum sintering temperature for a membrane. Lastly, the membranes are cooled either by using atmospheric or

controlled cooling to avoid the generation of any thermal stresses. This procedure results in the formation of a hard, rigid, and porous membrane, which is further polished with silicon carbide abrasive paper (C-220) to give the membrane required smoothness and finish.

### 4.4.2.2 *Uni-Axial Method*

Uni-axial method is the most commonly used ceramic membrane preparation method [18, 19]. In this method, the mixture of raw materials is casted in the required shape and compressed under very high pressure (30–50 MPa). Later, the cast is dried and sintered in a similar fashion to the paste method. The type of raw materials, sintering temperature, and time, and procedure of the processes, such as drying, sintering, and cooling determine the properties of the prepared ceramic membranes in both paste as well as uni-axial method.

### 4.4.2.3 *Other Methods*

Ceramic membranes are also prepared by using methods, such as slip casting, tape casting, dip coating, sol-gel, and extrusion. These methods are also commonly used for the preparation of ceramic membranes in disk or tubular forms. The subsequent sections give a brief introduction about these methods.

#### 4.4.2.3.1 Slip Casting

Slip casting method uses a porous mold for the preparation of a ceramic membrane from a powder suspension. The diffusion of the solvent from the suspension through the pores of the mold forms a gel layer on the mold surface due to the precipitation of the particles. The suspension particles concentrate at the substrate and suspension boundary due to the capillary suction effect of the porous substrate. The casted membranes are then dried and sintered for finally giving defect free permeable ceramic membranes.

#### 4.4.2.3.2 Tape Casting

Tape casting method is used to prepare ceramic membranes with less thickness. Slurry preparation and shaping are two important steps of this method. The slurry is prepared from the raw materials, which mainly consists of inorganic materials, binders, and plasticizers. The solvent for the slurry could be water or any organic liquid. Deflocculants are also commonly used in this method for the stability of the suspension. The prepared slurry is homogenized by using milling and sonication. Subsequently, shaping of the prepared slurry is done by using a doctor blade. Later, the casted ceramic membrane is dried to obtain the final membrane.

### 4.4.2.3.3 Dip Coating

Dip coating method of ceramic membrane preparation coats a material layer over a support by dipping the support in the suspension of the coating material. The membrane pore size can be controlled by controlling the viscosity of the material suspension as well as dipping time or speed. Accordingly, the process of dipping and drying can be fixed as per the requirements.

### 4.4.2.3.4 Extrusion

Extrusion method involves flow of the paste through a nozzle under the influence of compaction for the preparation of ceramic membranes. Porous tubular ceramic membranes can be prepared on a large scale by using this method. The die or cast used for the preparation of the membrane defines the shape, size, and porosity of the prepared membranes. The rheological properties of the paste play an important role in this method, therefore, great care should be taken regarding ceramic grain size, type, and ratios of the organic additives for the successful preparation of ceramic membranes by this method.

## 4.5 CHARACTERIZATION

Membrane characterization is important in terms of their physical and chemical analysis for their respective morphological and behavioral individualities. The characterization techniques for membranes are well categorized based on their morphological, permeation, and functional characteristics. Notably, the two important features of membranes are their pores and functional (or physicochemical) attributes and the whole characterization of a membrane is based on these two membrane aspects. Because it is important to know that whether the prepared membrane contains the theoretically defined physical and functional features (or not), different characterization techniques are employed. These characterization techniques help in analyzing the prepared membranes in different ways, such as relating two membranes from same batch for any difference (or similarity); the results or changes occurred by virtue of the preparation process regarding the membranes morphological and functional characteristics; and analysis of membranes morphology and performance.

Membranes with good flux and separation profiles are desired, and both of these properties depends upon the physical as well as chemical attributes of the membranes. Therefore, it is essential to critically asses the prepared membranes for these particular traits before their inception in any process. Various techniques are available for this purpose, which can be categorized by considering membranes physical and chemical attributes. The characterization techniques regarding the analysis of

membranes physical traits cover the membrane properties, such as membrane pore configuration, charge, and mechanical, chemical, temperature as well as pressure dependent stability. Therefore, these techniques characterize everything from feed to permeate regarding a membrane process. On the other hand, techniques based on the chemical traits covers the properties of the membrane, such as membrane composition and surface interactions with different feed components, which predicts the membrane function and performance under different feed types and process conditions. Altogether, these chemical traits based membrane characterization techniques are essential as they analyze a membrane surface to provide details of the complexities present there and up to a depth of some micrometers into the membrane surface. Therefore, these two types of membrane characterizations are essential for the in-depth assessment of the membranes for their effective and efficient performance.

In this section, some of the critical membrane characterization techniques based upon the membranes physical as well as chemical traits are explained in detail.

## 4.5.1  Membrane Morphological Analysis

The first line of membrane characterization is the analysis of the morphology of a membrane. This confirms the presence of desired features, such as porosity, pore size, pore size distribution, and membrane structure. Therefore, before going for any other analysis, it is better to analyze the prepared membrane by using morphological characterization techniques, such as scanning electron microscope.

### 4.5.1.1  Scanning Electron Microscopy

The scanning electron microscope (SEM), invented in 1937 by Manfred von Ardenne [20], is currently a commonly used instrument for the morphological analysis of different materials including membranes. Membranes are analyzed for their top surfaces as well as cross-sections. The SEM micrographs infer the effect of different preparation techniques, conditions, and materials on the membrane morphology. Therefore, by using SEM micrographs the best of preparation techniques, conditions, and materials can be chosen very easily.

Fig. 4.6 shows top surface FESEM micrograph for Kaolin based low-cost microfiltration ceramic membrane prepared using uniaxial dry compaction method [19]. It can be seen that the prepared membrane is without pinholes and cracks. Also, the maximum observable pore size of the membrane surface is about 5–10 μm. This confirms the suitability of membranes for microfiltration applications.
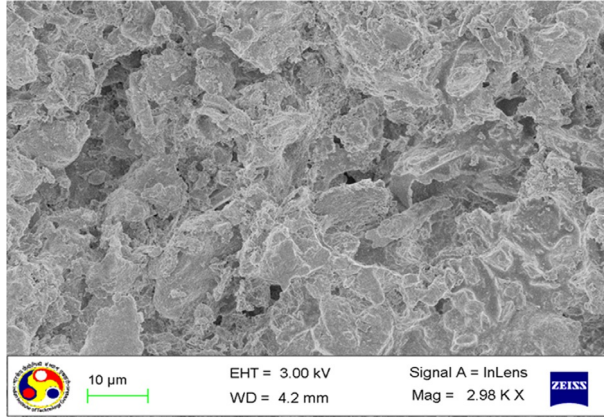
**FIG. 4.6**    Top surface FESEM micrograph of a low-cost ceramic membrane.

### 4.5.1.2 Membrane Pore Size and Pore Size Distribution

There are various methods available for the estimation of membrane pore size and pore size distribution. These are SEM, gas permeation, and liquid permeation and are explained in this section. The membrane pore sizes calculated from these methods vary from each other and thus a comparative study is presented at the end of this section to observe the difference.

- *SEM technique*: The obtained SEM micrograph (Fig. 4.6) can be used for the estimation of membranes average pore size ($d_s$) and pore size distribution by using ImageJ software [16, 21]. Approximately pore diameters of 500 pores (visible in SEM micrographs) are measured using the software. Because pore size and average pore size distribution values are critically dependent on the sampling procedure, generally, more than one SEM micrographs are evaluated. Also, these micrographs are chosen randomly from the selected sections of the membranes to obtain pore size distributions representing the existing porous texture of the membrane. It is assumed that the membrane pores are cylindrical to calculate the average membrane pore diameter from SEM micrographs as:

$$d_s = \left[ \frac{\sum_{i=1}^{n} n_i d_i^2}{\sum_{i=1}^{n} n_i} \right]^{0.5} \tag{4.18}$$

where, $n$ represents the number of pores and $d_i$ the pore diameter (µm) of $i$th pore.
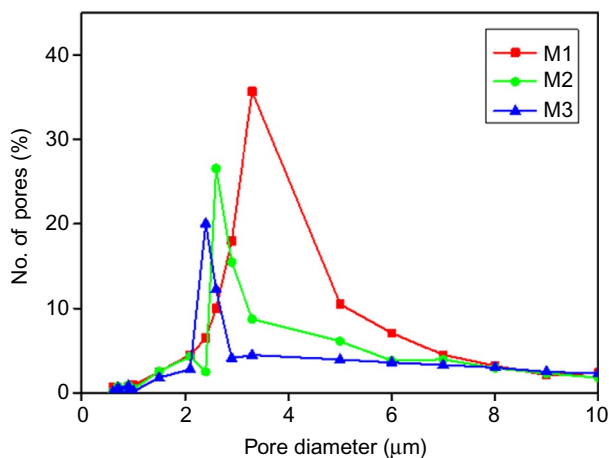
FIG. 4.7 FESEM based pore size distributions of M1, M2, and M3 membranes.

The results regarding membrane pore size distributions are shown in Fig. 4.7. It can be observed from the figure that the membranes had a distinct porous structure with pores ranging from 2–10 μm. Also, the pore size distributions involve single peak profile with broader pore size distributions for the membranes fabricated at lower pressures. The membrane average pore size of the membranes comes out to be as 3.23 μm, 2.45 μm and 2.33 μm for M1, M2 and M3 membranes, respectively, from the SEM micrographs analysis. Further, it can also be observed that the maximum number of pores (%) varied significantly with fabrication pressure and are 35%, 26% and 20% for M1, M2 and M3 membranes, respectively. In this regard, it can be analyzed from the data trends presented by Nandi et al. [16] that the pore size distributions of the membranes fabricated by paste method varied from 0.1–3 μm with 25% pores possessing a pore diameter of about 0.5 μm. The average pore size of the membrane is 0.55 μm. Thus, it is apparent that uniaxial dry compaction method provides the membrane with significantly wider pore size distribution than the membrane obtained with the paste method. This is a critical observation given the fact that the presence or absence of water strongly influences plasticity of the green mold and hence membrane morphology after sintering.

The above discussion shows that how SEM micrographs can be used to infer effects of different preparation conditions, techniques, and materials on the prepared membranes.

- *Gas permeation technique*: In this technique, a gas is permeated across the membrane wetted by a liquid; therefore, this technique is also known as gas-liquid displacement technique. In case of hydrophilic membranes

water is used as the wetting liquid, whereas, in case of hydrophobic membranes, a mixture of alcohol and water is used [22]. The technique is based on the phenomenon that the wetting liquid is trapped in the membrane pores by capillary forces and is not able to leak out of the membrane. Therefore, on the application of external pressure, the liquid permeates out of the membrane pores. The external pressure is applied in the form of a gas, and the gas will force the liquid to permeate across the membrane. The first pore going to be empty is the largest pore available in the membrane. The pore size is inferred from this process by using Laplace equation as:

$$P_p = \frac{4\,\sigma\,cos\theta}{d_g} \tag{4.19}$$

where, $P_p$ represents the differential gas pressure on the wetting liquid present in the membrane pore (kPa), $\sigma$ the surface tension at the gas-liquid interface (dyne/cm), $\theta$ the contact angle between the wetting liquid and membrane surface (°), and $d_g$ the pore size (μm). Depending upon the conditions and process variables the Eq. (4.19) can be further simplified.

This method is also used for the estimation of membrane pore size distribution by gradually increasing the applied gas pressure, which further displaces the wetting liquid from the next small pore and so on. This generated data concerning the gas flow is plotted as a function of applied pressure and can be used for the calculation of membrane pore size distribution by using Laplace equation at each data point.

The ceramic microfiltration membrane pore size ($d_g$) and pore size distribution along with effective membrane porosity ($\varepsilon/q^2$) can also be calculated by gas permeation across a membrane. The results from this technique decipher the distribution of pore percentage present in the membrane matrix in the range of macroporous (pore dia >50 nm) and mesoporous (pore dia <50 nm) [1]. The following expressions can be used to calculate the average membrane pore size and effective membrane porosity for gas phase [23]:

$$K = 2.133 \times \frac{r \times \nu_g}{l_m} \times \frac{\varepsilon}{q^2} + 1.6 \times \frac{r^2}{l_m \times \eta} \times \frac{\varepsilon}{q^2} \times P \tag{4.20}$$

$$d_g = 2 \times r = 2.666 \times \frac{B}{A} \times \nu_g \times \eta \tag{4.21}$$

where,

$$A = 2.133 \times \frac{r \times \nu_g}{l_m} \times \frac{\varepsilon}{q^2} \tag{4.22}$$

$$B = 1.6 \times \frac{r^2}{l_m \times \eta} \times \frac{\varepsilon}{q^2} \tag{4.23}$$

$$K = \frac{Q \times P_2}{S \times \Delta P} \tag{4.24}$$

and

$K$ represents the effective permeability factor of the membrane and $P$ the average pressure on the membrane.

Eq. (4.21) can be used to calculate the average membrane pore size ($d_g$) by using known values of $\eta$ (permeant viscosity), $\nu_g$ (molecular speed of the permeant), $A$, and $B$. The values of $A$ and $B$ can be obtained from the slope ($B$) and intercept ($A$) of the linear plot of $K$ vs $P$. On the other hand, Eq. (4.20) can be used for the calculation of effective membrane porosity ($\varepsilon/q^2$) by using known values of $A$ and $d_g$. The first term (intercept) in Eq. (4.20) corresponds to Knudsen permeance and the second term (slope) to the viscous permeance. Therefore, the percentage contribution of pores (and pore sizes) toward viscous and Knudsen flow transport mechanisms can be obtained from the values of slope and intercept obtained from the graph.

- *Liquid permeation technique*: The flux and separation factors of a membrane are its success parameters. Therefore, a membrane with high flux and separation efficiency traits is the demand of any membrane process. Liquid permeation across the membrane is the crucial technique which confirms the membrane flux and separation efficiency. Also, it is used for the determination of membrane hydraulic permeability ($P_m$) and hydraulic pore size ($d_l$). This technique involves measurement of pure water permeation, at specific trans-membrane pressures ($\Delta P$) and regular intervals, across the membrane for the evaluation of $P_m$ and $d_l$ as a function of time. Membranes are compacted at pressures higher than the operating pressure to get a membrane with uniform and stable pores, which results in stable flux profile of membrane. Therefore, eliminating chances of error in the desired calculations of membrane parameters, such as pure water flux, hydraulic permeability, pore size, and pore size distribution. The membrane flux profile during compaction is shown in Fig. 4.8. Further, the $P_m$ and $d_l$ are calculated by assuming membrane pores of cylindrical symmetry by using following expressions [24]:

$$J_w = \frac{Q}{S \cdot \Delta t} = \frac{\Delta P \, \varepsilon_m d_l^2}{\mu_w \, 32 l_m} = P_m \times \Delta P \tag{4.25}$$

$$P_m = \frac{\varepsilon_m d_l^2}{32 \, l_m \mu_w} \tag{4.26}$$

$$d_l = \left[ \frac{32 \, l_m \, \mu_w \, P_m}{\varepsilon_m} \right]^{0.5} \tag{4.27}$$
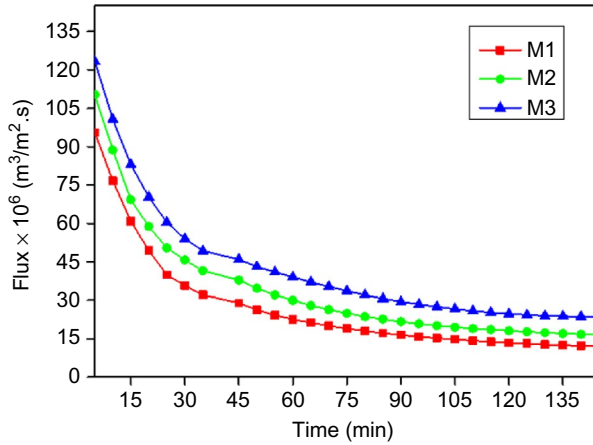
**FIG. 4.8** Membrane flux profile during compaction.

The term $\varepsilon_m \, d_l^2$ in Eq. (4.25) corresponds to the effective permeable area factor that defines the actual permeable area accessible during filtration. Therefore, the higher the value of $\varepsilon_m \, d_l^2$ higher will be the permeation and henceforth a higher membrane permeability. Besides, in the given expressions the terms $\Delta P$, $\mu_w$, and $l_m$ represents the transmembrane pressure differential, feed viscosity, and membrane thickness, respectively.

• *Comparative analysis of membrane pore sizes obtained from different techniques*: In this section, the pore sizes calculated from different techniques, such as SEM, gas permeation, and liquid permeation are compared with each other to have a better understanding of significant differences among the calculated pore sizes. In general, it is observed that the average membrane pore size calculated from gas permeation technique is the smallest amongst the other techniques, whereas, the one calculated by using liquid permeation comes out to be the largest. On the other hand, the membrane average pore size calculated by using SEM technique lies in between the pore sizes calculated by using other two techniques. The reason behind this variation is that the gas molecules can permeate across the membrane via small voids and interstices as compared to liquid molecules, which results in the estimation of smallest pore sizes and further results into overall small average membrane pore size ($d_g$). Conversely, the liquid permeation technique detects actual pores as well as voids without interconnection present in the membranes. Henceforth, pore size ($d_l$) greater than $d_g$. On the other hand, average membrane pore size ($d_s$) calculated by using SEM technique contains a possibility of overestimation because in this technique pores only with size $\geq$50 nm are selected. This results in $d_s$ higher than $d_g$ and higher or lower than $d_l$.

The average membrane pore size calculated by using liquid permeation technique is considered best because the hydraulic permeability involves permeation of liquid through pores accountable for microfiltration as compared to gas permeation or SEM technique. However, gas permeation technique is good for the evaluation of pores of varying sizes and their percentage distribution. SEM technique, on the other hand, is better for the evaluation of possible available pore sizes and their distributions.

## 4.5.2 Membrane Structural and Functional Analysis

Membranes are prepared with different modified structural and functional attributes for their successful implementation in different membrane processes. For example, membranes with better strength, chemical, and mechanical stability (in harsh environmental conditions), and stimuli-responsive functional mechanisms. Therefore, there are different techniques available which are used for the analysis of these particular attributes of the prepared membranes, such as thermogravimetric analysis, X-ray diffraction, and Fourier transform infrared spectroscopy. These techniques are highly efficient in the analysis of membranes and provide an accurate and detailed report about the materials used and membranes prepared. In this section, the techniques commonly used for the analysis of membrane and their materials are discussed appropriately.

### 4.5.2.1 Thermogravimetric Analysis

The temperature-based stability of membranes is analyzed by using thermogravimetric analysis (TGA). This technique gives insight into the effect of temperature on the membrane pore structure, size, and membrane strength. The membrane raw material or membrane is heated in a α-alumina crucible starting from room temperature to 1000°C with a heating rate equivalent to 10°C/min.

Nandi et al. [16] observed a total weight loss of 28.5% in the membrane sample. Out of the total weight loss the 2.5% weight loss is observed at 105°C for the removal of water molecules from the membrane. Approximately, 4% weight loss is observed in the range of 105–450°C representing predehydration process of kaolin and dehydration of crystal water of boric acid. A second endothermic peak commences after 513°C, representing loss of structural hydroxyl groups because of the transformation of kaolinite to metakaolinite [17]. Carbon dioxide formation (and hence, formation of membrane porous structure) starts at 730°C. There is a weight loss of approx. 10% in the range of 663–745°C corresponding to the calcinations of $CaCO_3$. On the other hand, $Na_2CO_3$ calcinations starts at

800–843°C, and in this temperature range, very little weight loss in the membrane sample is seen. Therefore, it can be concluded that the minimum sintering temperature for the given membrane is 843°C. This is how TGA analysis of a membrane sample is carried out and information is gained. A model TGA profile of a ceramic microfiltration membrane is shown in Fig. 4.9.

### 4.5.2.2 X-Ray Diffraction Analysis

X-ray diffraction (XRD) technique is used to analyze membranes and membrane raw materials for the estimation of different phase transformations that occurred during their preparation. Therefore, XRD analysis can also be used to further confirm the sintering temperature, based on the structural stability of a membrane, estimated from TGA analysis. This approach is reported by Nandi et al. [25] in their work, where they discussed about the preparation and characterization of ceramic membranes for microfiltration applications. In this method, membrane samples calcined at different temperatures are analyzed with XRD technique as shown in Fig. 4.10. It can be seen from the figure that peaks corresponding to raw materials (XRD analysis at 25°C) disappeared for the sample calcined at 850°C. Furthermore, new peaks arrived at 850°C are stable up to 1000°C. It can be concluded from the XRD analysis of this particular
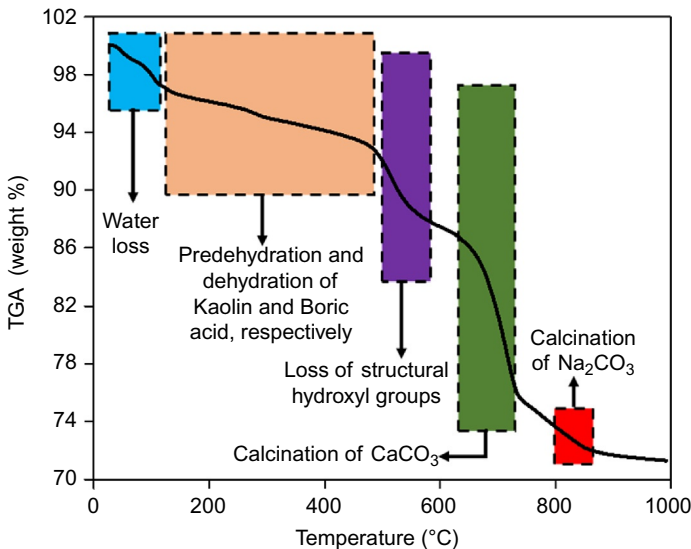


**FIG. 4.9** TGA profile of a ceramic microfiltration membrane (model composition given in Table 4.1).
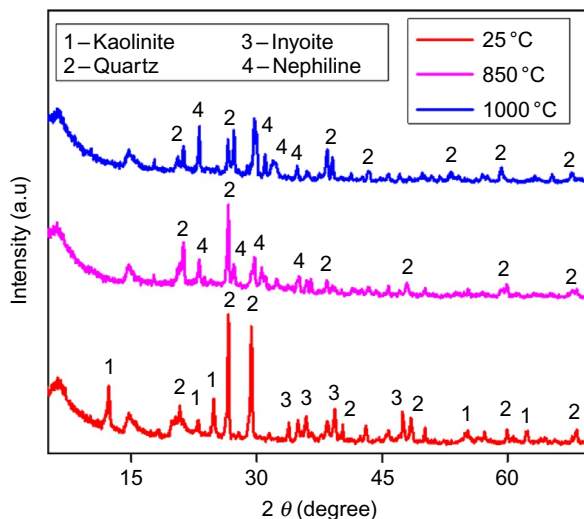
**FIG. 4.10** XRD graph of a ceramic membrane raw materials (model composition given in Table 4.1).

sample that a sintering temperature of 850°C is sufficient for membrane preparation.

### 4.5.2.3 Fourier Transform Infrared Analysis

Generally, the membrane preparation process requires number of ingredients, such as pore formers, binders, viscosity enhancers, and functional or nonfunctional additives. Usually, these ingredients used are organic in nature. Therefore, to assess the successful assimilation of these compounds in the membranes or the successful synthesis of novel membrane materials Fourier transform infrared (FTIR) spectroscopic analysis is commonly used.

Basically, this technique measures the intensity of absorption or transmittance of infrared rays by a sample in a range of infrared region wavelengths. The absorption or transmittance bands for different molecular components, present in the sample, is different and thus FTIR helps to confirm the presence or absence of a particular component in the sample. The FTIR technique achieve this differentiation on the basis of interatomic bond strength measurement, such as $C{=}C$, $C{-}C$, and $C{-}H$. Therefore, FTIR analysis is a convenient technique to assess the purity or successful synthesis of a membrane material and also the successful preparation of a membrane with specific materials. Another important feature of FTIR analysis is that the plausible molecular structure of an organic compound produced in the polymeric membrane can also be interpreted.

## 4.6 CERAMIC MEMBRANE APPLICATIONS

Nowadays, ceramic membranes are used for various industrial applications worldwide. Efforts are made on large scale to replace the polymeric membranes with ceramic membranes. The reason being the various advantages of ceramic membranes, such as long life, long-term stability, and chemical, thermal, and mechanical resistance. The only disadvantage not allowing their widespread use is their high cost. Also, there is need to develop methods for the large-scale production and increase in the high-density packing of ceramic membranes. Because these disadvantages are barrier in the advancement of ceramic membranes and their use. Therefore, in this section various ceramic membrane applications are discussed, where researchers have used low-cost ceramic membranes successfully. These applications further provide strength to the advancement and widespread use of ceramic membrane on industrial level.

### 4.6.1 Oily Wastewater Treatment

Microfiltration membrane processes provides numerous advantages for various industrial applications, such as they are economical, effective, and efficient. Among different industrial applications an important membrane process application is oily-wastewater treatment. Microfiltration membrane process due to its ability to process low feed concentrations is promising for this application, because the typical oily-wastewater composition varies from 50 mg/L to 1000 mg/L of oil. The highly efficient microfiltration membrane process helps in achieving separation efficiency of almost 90%–99% even with low oil concentrations.

Much research has been done in the field of oily-wastewater treatment by various researchers throughout the world. Nowadays, low-cost ceramic membranes are getting much attention due to their low cost and other separation-related attributes, which play an essential role in this field. Researchers have used various types of clays and zeolites to bring the overall membrane cost down [26–28]. For instance, Nandi et al. [16] used paste method for the preparation of low-cost ceramic membranes by using a mixture of kaolin, quartz, calcium carbonate, sodium carbonate, boric acid, and sodium metasilicate. Membranes with 0.77 µm average pore size and 42% porosity are obtained. These membranes, when tested at a transmembrane pressure of 206.80 kPa and 150 mg/L oil feed, has given results for the overall membrane permeate flux and oil rejection as $15.05 \times 10^{-6} \text{ m}^3/\text{m}^2$ s and 98.5%, respectively. Monash et al. [6] used uni-axial method for the preparation of low-cost ceramic membranes by using kaolin, feldspar, quartz, pyrophyllite, ball clay, calcium carbonate titanium dioxide, and polyvinyl alcohol as a binder. This resulted in membranes with 0.83 µm average pore

size and 36% porosity. Also, an overall membrane permeate flux of value $2.50 \times 10^{-5}$ m$^3$/m$^2$ s and 99% oil rejection is obtained when the membrane is tested with a feed with an oil concentration of 200 mg/L. Vasanth et al. [29] also prepared low-cost ceramic membranes by using the same inorganic precursor formulations as Nandi et al. [16] by using a uni-axial method. The membranes resulted in an average pore size of 1.06 μm and a porosity of 26%. The prepared membrane tested with a feed of 200 mg/L oil concentration and given an overall membrane permeate flux of $0.65 \times 10^{-4}$ m$^3$/m$^2$ s and oil rejection equivalent to 96% at a transmembrane pressure of 69 kPa. Similarly, Abbasi et al. [9] reported a membrane prepared from mullite, which is further produced from a mixture of kaolin, clay, and α-alumina with an average pore size of 0.578 μm and porosity of 38%. This membrane has provided an overall membrane permeate flux of 244 L/m$^2$ h and 93.8% oil rejection. On the other hand, Emani et al. [19] reported a comparative study of low-cost ceramic membranes regarding membrane pore size distribution and the outcome of the study reveals that the membranes prepared with uni-axial dry compaction method results in membranes with broader membrane pore size distributions as compared to paste method. The effect of fabrication pressures on the prepared membranes is also reported. The membrane prepared at a fabrication pressure of 25 MPa provide better results regarding overall membrane flux and oil rejection, that is, $24 \times 10^{-6}$ m$^3$/m$^2$ s of 95.20%, respectively, along with a fouling index of 29.47% at a transmembrane pressure of 206.70 kPa. The membrane prepared at a fabrication pressure of 73 MPa shown better fouling index of 15.54% as compared to the other membrane prepared at 25 MPa fabrication pressure with low overall membrane permeate flux ($8 \times 10^{-6}$ m$^3$/m$^2$ s) and high oil rejection (97.9%).

The above-stated studies confirm the potential of low-cost ceramic membranes for successful oily wastewater treatment. Membranes prepared by different methods viz. paste or uni-axial show different results in terms of membrane average pore size and pore size distribution, which affects the overall membrane performance. Furthermore, the preparation conditions and membrane materials also play an essential role in the performance of the membranes. Therefore, the optimization and selection of the preparation conditions and membrane materials are very important. Thus, there is a broad scope for the development of novel membrane materials, fabrication processes, and operations for their utilization in oily wastewater treatment.

## 4.6.2 Juice Clarification

Juice clarification is a prominent sector where membrane processes are widely used for their advantages like no requirement of additive (chemicals or salts) for processing of the feed, cost, effective yield, and ability to

handle large feeds. The juice clarification is required because the most popular fruits used in the food industry are citrus fruits, such as lemon, orange, mosambi, and pineapple. These fruits contain both low molecular compounds, such as sucrose, salt, acids, flavor, and aroma compounds as well as high molecular weight compounds, such as pectin, cellulose, and hemicellulose along with haze producing proteins and microorganisms [30]. The presence of protein and pectic material in addition to their fermentation causes a bitter taste, cloudiness, and postbottling haze formation on storage of the juices for extended periods. Therefore, it is essential to eliminate these undesired materials from the produced juice while retaining the essential low molecular weight solutes, such as sugar, salt, acid, aroma, and flavor [24].

In recent times membrane processes, such as microfiltration, ultrafiltration, and reverse osmosis are widely used for the juice clarification application of food industry. Both polymeric, as well as ceramic membranes, are used for this application. It is well known that the membrane processes are affected by the problem of fouling, especially the polymeric membranes. Therefore, it is important to identify novel membrane materials and optimal membrane morphological parameters, such as average membrane pore size, pore size distribution, and porosity. Because membranes with high membrane permeate flux and low fouling are preferred, these parameters play a vital role in achieving the membranes with desired properties. Also, it is essential that the juice quality should not be compromised. Rai et al. [31] reported the effect of increasing average membrane pore size on the overall membrane permeate flux and shown that flux increases too many folds on the increase in the average membrane pore size without compromising the juice quality. Similarly, Youn et al. [32] observed while comparing ultrafiltration and microfiltration membranes, for mosambi juice quality and overall membrane flux, that microfiltration membranes provide membrane flux 2–3 folds higher than the ultrafiltration membranes without compromising on the juice quality. The optimum average membrane pore size for better flux and juice quality is inferred as 0.05 μm by various studies done using various fruit juices [16, 33–35].

Research is also done for examination of pretreatment methods for juice clarification regarding lower fouling with higher overall membrane flux and enhanced juice quality. The pretreatment of juice with enzymes (pectinases) for the removal of higher molecular weight unwanted compounds is very famous and widely adopted. Nandi et al. [35] successfully reported the use of enzyme pretreatment for the mosambi juice clarification before clarifying the juice with a low-cost ceramic membrane. Pectinase enzyme with enzyme activity 3.5 units/mg is used in this study for enzymatic pretreatment of the mosambi juice. The permeate membrane flux ($21.45 \times 10^{-6}$ m$^3$/m$^2$ s) obtained for the membrane is also high in case of enzyme treated juice. Furthermore, the mosambi juice was perfectly

consumable even after 30 days of storage period. Therefore, this study confirms that the enzyme pretreatment of juice is beneficial for the juice clarification and overall membrane process.

The assessment of the literature available for juice clarification using membrane processes infers that initially polymeric membranes were used for the juice clarification application. This is because of their low cost as compared to ceramic membranes. Ceramic membranes are more advantageous as compared to polymeric membranes on an industrial scale. The ceramic membranes have a longer lifespan and low fouling qualities, which are very important for any membrane process to be successful. Therefore, it is anticipated to lower the overall cost of ceramic membranes by using low-cost inorganic precursors and membrane materials. Higher membrane flux is always suitable for a membrane process, and it is confirmed that the average membrane pore size plays a little role in the overall juice quality. Therefore, it is essential to optimize the morphological parameters, such as average membrane pore size, pore size distribution, and membrane porosity regarding the maximum membrane permeate flux while ensuring the juice quality and low membrane fouling. This can be done by studying and implementing the conceptual phenomenological models to quantify the dependence of membrane permeate flux on membrane morphological parameters, likewise done by Nandi et al. [35]. Thus, ceramic membranes can be placed as the ideal option for the juice clarification application of food industry.

## 4.6.3 Heavy Metal Removal

The metallic elements having a relatively high density and are toxic even at low concentrations are termed as heavy metals. Heavy metals, such as iron, fluorine, cadmium, mercury, chromium, lead, nickel, copper, and zinc occurs as natural constituents of the earth crust. They are tenacious pollutants of the environment and cannot be degraded. They tend to enter the human body through food, water, air, and accumulates in the body. The bio-toxic effects of heavy metals include gastrointestinal disorders, stomatitis, diarrhea, hemoglobinuria, tremor, ataxia, paralysis, depression, vomiting, and pneumonia. The effect of heavy metals depending upon their concentration and period of exposure may be toxic on acute, subchronic or chronic levels. The heavy metals effect may also be neurotoxic, mutagenic, carcinogenic, or teratogenic. Therefore, it is essential to get rid of these heavy metals from the food chain and drinking water, in particular, because drinking water is the primary source of these heavy metals.

Low-cost ceramic membranes are suitable for the removal of heavy metals from water and have the potential to make the water safe for

drinking. Because the better thermal and chemical properties make them a better choice for the heavy metal removal application, researchers all over the world have studied heavy metal removal by using ceramic membranes. Basumatary et al. [36] used MCM-41 composite ceramic membrane for the removal of chromium (VI) from aqueous solutions. The composite membrane is prepared by using hydrothermal synthesis method, and the ceramic support is prepared by employing facile uniaxial compaction method. Rejection equivalent to 80% is obtained at pH 2 with feed concentration of 1000 ppm at an applied pressure of 207 kPa. Vasanth et al. [37] reported 94% Cr (VI) removal by using low-cost ceramic microfiltration membrane assisted with baker's yeast. Similarly, Kumar et al. [38] reported 78% Cr (VI) removal by using a low-cost ceramic tubular membrane with initial feed concentration of 1000 ppm at 345 kPa applied pressure. Also, literature is available for the removal of arsenic and fluoride from aqueous solutions by using low-cost ceramic membranes [18, 39–41]. In addition to the use of low-cost ceramic membranes, other techniques are also used synergistically with the membrane process, such as electrocoagulation and micellar enhanced microfiltration [18, 42].

The literature reported confirms that the low-cost ceramic membranes are probably the best for heavy metal removal from aqueous solutions. There is a need for the search and development of novel low-cost inorganic precursors and membrane materials. The new materials will further cut the cost down for the membranes and make them accessible for the industrial applications of heavy metal removal.

### 4.6.4 Protein Separation

Proteins make a prominent source of nutrition and health products. In many processes, they are just wasted as in case of whey proteins, but membrane processes made it possible to separate, concentrate and use these otherwise wasted proteins successfully. Similarly, membrane processes are used widely for protein separation, concentration, and fractionation applications of various food-based industries. Bovine milk is the primary source of human proteins, which mainly consists of proteins (3.2 w/w%), fat (3.4 w/w%), lactose (4.9 w/w%), and ash (0.7 w/w%). The milk proteins are mainly divided into two categories, (i) casein and (ii) whey proteins. The amount of casein proteins is higher (2.6 w/w% of total 3.2 w/w% of milk proteins) as compared to whey proteins (0.6 w/w% of the total 3.2 w/w% milk proteins). Therefore, it is essential to separate the two proteins for their use in the preparation of different milk products. Furthermore, the separation of these two proteins provides fractions rich in a specific protein or protein component, such as

α-lactalbumin, β-casein, and immunoglobulin-Ig. These fractionated components are used for the preparation of different edible products for different age groups, such as infants, elders, or people with special needs.

The advantages of ceramic membranes to withstand pH values ranging from 0.5 to 13.5 and temperatures over 100°C provides them chemical, thermal, and mechanical stability. Thus, making the ceramic membranes better than the polymeric membranes. Also, the availability of cross-flow microfiltration mode further makes the ceramic membrane processes economic and efficient for the separation of proteins and thus enhanced the use of microfiltration on an industrial scale for various applications. In case of the food industry, the microfiltration is primarily used for the removal of bacteria, whey defatting, micellar casein enrichment of milk for cheese making, and other applications. It is essential for the membrane separation processes to optimize the membranes for their molecular weight cut off or average membrane pore size, pore size distribution, porosity, transmembrane pressures, and temperatures of the feed, because these factors play an essential role and bring out the best of the overall process. These factors are optimized regarding high membrane flux and low fouling.

## 4.7  COST ESTIMATION

The industrial applications demand cost-effective processes due to their sheer size. Therefore, for the successful implementation of membrane processes, especially ceramic membranes, it is essential for them to be cost-effective. The cost of a membrane mainly depends upon its raw material, preparation procedure, and sintering temperature (in case of ceramic membranes) along with the shipment cost of the membranes. All the said parameters are essential for a membrane, and it is difficult to compromise on anyone. However, the only viable thing to cut the cost of membranes is the raw materials, where cheap raw materials can be used for the preparation of membranes. This leads to a noticeable decrease in the cost of the membranes. Thence, cheap raw materials are required for the preparation of low-cost ceramic membranes taking care that there should not be any compromise on the membrane properties and performance.

The membrane cost on a large scale as said mainly depends upon the fabrication, shipment, and raw materials. Therefore, to estimate the accurate cost of a membrane; these costs along with the bare module costs should be considered. Also, care should be taken in procuring the exact market rates for a region since the prices for raw materials or other commodities vary from region to region. The other factors which influence the membrane cost are its fouling characteristics, on-time performance, durability, long-term stability, and life cycle in the process application.

Therefore, in the cost estimation of the membranes, these factors should also be considered in addition to the government set labor charges. Thus, by precisely considering all these charges the accurate cost of a membrane can be estimated.

Nandi et al. [35] and Emani et al. [43] used low-cost raw materials for the successful preparation of low-cost ceramic membranes with a total cost of membranes as $ 130/m$^2$ and $ 78/m$^2$, respectively. The characterization and analysis studies performed on the membranes shown consistency in their properties and performance. Both these studies confirm that it is possible to reduce the cost of ceramic membranes while maintaining their properties and performance. Still, there is scope for reducing the membrane costs by a significant margin by research and development of novel raw materials or by using the waste materials generated by various process industries.

# References

[1] Mulder M. Basic principles of membrane technology. Dordrecht: Kluwer Academic Publishers; 1991.
[2] Sourirajan S. Reverse osmosis. London: Logos Press; 1970.
[3] Meares P. Membrane separation processes. Amsterdam: Elsevier; 1976.
[4] Cuperus FP, Nijhuis HH. Applications of membrane technology to food processing. Trends Food Sci Technol 1993;4:277–86.
[5] DeFriend KA, Wiesner MR, Barron AR. Alumina and aluminate ultra-filtration membranes derived from alumina nanoparticles. J Membr Sci 2003;224:11–28.
[6] Yoshino Y, Suzuki T, Nair BN, Taguchi H, Itoh N. Development of tubular substrates, silica based membranes and membrane modules for hydrogen separation at high temperature. J Membr Sci 2005;267:8–17.
[7] Wang YH, Tian TF, Liu XQ, Meng GY. Titania membrane preparation with chemical stability for very harsh environments applications. J Membr Sci 2006;280:261–9.
[8] Sutera SP, Skalak R. The history of Poiseuille's Law. Annu Rev Fluid Mech 1993;25(1):19.
[9] Carman PC. Trans I C E London 1937;15:150.
[10] Kedem O, Katchalsky A. Thermodynamic analysis of the permeability of biological membranes to non-electrolytes. Biochim Biophys Acta 1958;.
[11] Purchas DB, Sutherland K, editors. Handbook of filter media. United Kingdom: Elsevier Science & Technology Books; 2002.
[12] Gekas V, Hallstrom B. Mass transfer in the membrane concentration polarization layer under turbulent dross flow: I. Critical literature review and adaptation of existing Sherwood correlation to membrane operations. J Membr Sci 1987;30:153–70.
[13] Sherwood RK, Pigford RL, Wilke CR. Mass transfer. New York: McGraw-Hill; 1975.
[14] Treybal RE. Mass transfer operations. New York: McGraw-Hill; 1981.
[15] Baker RW. Membrane technology and applications. 2nd ed. Chichester, UK: John Wiley & Sons; 2004.
[16] Nandi BK, Uppaluri R, Purkait MK. Treatment of oily wastewater using low-cost ceramic membrane: flux decline mechanism and economic feasibility. Sep Sci Technol 2009;44:2840–69.
[17] Chena YF, Wang MC, Hon MH. Phase transformation, and growth of mullite in kaolin ceramics. J Afr Earth Sci 2006;46:245–52.

[18] Ghosh D, Sinha MK, Purkait MK. A comparative analysis of low-cost ceramic membrane preparation for effective fluoride removal using hybrid technique. Desalination 2013;327:2–13.

[19] Emani S, Uppalur R, Purkait MK. Microfiltration of oil–water emulsions using low cost ceramic membranes prepared with the uniaxial dry compaction method. Ceram Int 2014;40:1155–64.

[20] Ardenne MV. Das elektronen-rastermikroskop. Z Phy 1938;109(9–10):553–72.

[21] Singh R, Purkait MK. Role of poly(2-acrylamido-2-methyl-1-propanesulfonic acid) in the modification of polysulfone membranes for ultrafiltration. J Appl Polym Sci 2017;134:45290.

[22] Chisti Y. Principles of membrane separation processes. In: Subramanian G, editor. Bio-separation and bioprocessing: a handbook. Weinheim: Wiley-VCH Verlag GmbH; 2007.

[23] Marchese J, Pagliero CL. Characterization of asymmetric polysulphone membranes for gas separation. Gas Sep Purif 1991;5:215–21.

[24] Cheryan M. Ultrafiltration and microfiltration handbook. Lancaster, PA, USA: Technomic Publishing Co Inc; 1998.

[25] Nandi BK, Uppaluri R, Purkait MK. Preparation and characterization of low-cost ceramic membranes for micro-filtration applications. Appl Clay Sci 2008;42:102–10.

[26] Saffaj N, Persin M, Younsi SA, Albizane A, Cretin M, Larbot A. Removal of salts and dyes by low $ZnAl_2O_4$–$TiO_2$ ultrafiltration membrane deposited on support made from clay. Sep Purif Technol 2005;47:36–42.

[27] Weir MR, Rutindeka E, Detellier C, Feng CY, Wang Q, Matsuura T, Van Mao RL. Fabrication, characterization and preliminary testing of all inorganic ultrafiltration membranes composed entirely of a naturally occurring sepiolite clay mineral. J Membr Sci 2001;182:41–50.

[28] Dong Y, Chen S, Zhang X, Yang J, Liu X, Meng G. Fabrication and characterization of low-cost tubular mineral-based ceramic membranes for microfiltration from natural zeolite. J Membr Sci 2006;281:592–9.

[29] Vasanth D, Uppaluri R, Pugazhenthi G. Performance of low-cost ceramic microfiltration membranes for the treatment of oil in water emulsions. Sep Sci Technol 2013;48:1–10.

[30] Nandi BK, Das B, Uppaluri R, Purkait MK. Microfiltration of mosambi juice using low-cost ceramic membrane. J Food Eng 2009;95:597–605.

[31] Rai P, Majumdar GC, Sharma G, DassGupta S, De S. Effect of various cutoff membranes on permeate flux and quality during filtration of mosambi (*Citrus sinensis* (L.) Osbeck) juice. Food Bioprod Process 2006;84:213–9.

[32] Youn KS, Hong JH, Bae DH, Kim SJ, Kim SD. Effective clarifying process of reconstituted apple juice using membrane filtration with filter-aid pretreatment. J Membr Sci 2004;228:179–86.

[33] Jegatheesan V, Phong DD, Shu L, Aim RB. Performance of ceramic micro- and ultrafiltration membranes treating limed and partially clarified sugar cane juice. J Membr Sci 2009;327:69–77.

[34] Barros STD, Andrade CMG, Mendes ES, Peres L. Study of fouling mechanism in pineapple juice clarification by ultrafiltration. J Membr Sci 2003;215:213–24.

[35] Nandi BK, Uppaluri R, Purkait MK. Identification of optimal membrane morphological parameters during microfiltration of mosambi juice using low-cost ceramic membranes. LWT Food Sci Technol 2011;44:214–23.

[36] Basumatary AK, Kumar RV, Ghoshal AK, Pugazhenthi G. Synthesis and characterization of MCM-41-ceramic composite membrane for the separation of chromic acid from aqueous solution. J Membr Sci 2015;475:521–32.

[37] Vasanth D, Pugazhenthi G, Uppaluri R. Biomass assisted microfiltration of chromium(VI) using Baker's yeast by ceramic membrane prepared from low-cost raw materials. 2012;285:239–44.

[38] Kumar RV, Pugazhenthi G. Removal of chromium from synthetic wastewater using MFI zeolite membrane supported on inexpensive tubular ceramic substrate. J Water Reuse Desalin 2017;365–77.

[39] Zaspalis V, Pagana A, Sklari S. Arsenic removal from contaminated water by iron oxide sorbents and porous ceramic membranes. Desalination 2007;217:167–80.

[40] Pagana AE, Sklari SD, Kikkinides ES, Zaspalis VT. Microporous ceramic membrane technology for the removal of arsenic and chromium ions from contaminated water. Microporous Mesoporous Mater 2008;110(1):150–6.

[41] Sklari S, Pagana A, Nalbandian L, Zaspalis V. Ceramic membrane materials and process for the removal of As(III)/As(V) ions from water. J Water Process Eng 2015;5:42–7.

[42] Jana S, Purkait MK, Mohanty K. Preparation and characterization of low-cost ceramic microfiltration membranes for the removal of chromate from aqueous solutions. Appl Clay Sci 2010;47:317–24.

[43] Emani S, Uppaluri R, Purkait MK. Preparation and characterization of low cost ceramic membranes for mosambi juice clarification. Desalination 2013;317:32–40.

# Inorganic Membranes for Gas Separations

*Zhentao Wu*

**Aston Institute of Materials Research, School of Engineering and Applied Science, Aston University, Birmingham, United Kingdom**

## 5.1  INTRODUCTION

Membrane technology has been adopted for a broad spectrum of applications of great importance, which include, but not limited to, Water & Waste Water Treatment, Food & Beverage, Medical & Pharmaceutical, Industry Processing and Gas Separation [1–4]. Among these applications, gas separation using membrane technology is a fast-growing sector in the last several decades [5, 6], and has so far become a fundamental technique for gas separation in industry, apart from conventional technologies such as cryogenic distillation, absorption, and adsorption. Moreover, the robust growth is predicted to continue to the next decade. In a more recent market report published by Credence Research [7], "the global gas separation membranes market was valued at US$ 1,720.4 Mn in 2015, and is expected to reach US$ 3,325.2 Mn by 2024, expanding at a CAGR of 8.2% from 2016 to 2024."

From membrane material point of view, gas separation membranes can be classified mainly as polymeric membrane and inorganic membrane. Polymeric membranes have been widely used in various membrane processes, particularly large-scale applications, for many years, mainly due to the relatively low costs. Compared to inorganic membranes, polymeric membranes keep leading a very high global share of gas separation membrane market, of 77.46% in 2015 [7]. Generally, most of the polymeric membranes are made of synthetic polymers, considering the chemical, thermal and mechanical properties and membrane microstructures required by specific applications. Consequently, handling and disposing of used polymeric membranes, which have a limited product lifetime, will gradually raise more environmental concerns soon. From this perspective, inorganic membranes that are significantly more durable and with less environmental impacts will play an increasingly important role in different membrane separation processes, including gas separation, in the coming decades. As a result, this chapter will focus on critical fundamental aspects of inorganic membranes for gas separation, which is expected to help potential readers who are seeking for appropriate knowledge in this area before further exploring more professional expertise that can be obtained from other monographs.

# 5.2  COMMON CONSIDERATIONS AND GENERAL PRINCIPLES

The first large-scale gas separation using inorganic membranes can be traced back to 1940s, in the Manhattan Project to enrich uranium by separating uranium isotopes as $UF_6$ [8]. From today's view, it is not a very good case for gas separation. For instance, the membrane functioned actually as a porous media in which diffusivity difference between isotopes enabled the separation/enrichment to occur. This resulted in very low separating efficiencies, for example, over 1000 stages were required to enrich the product by only 3%–4%. However, this application led to following isotope enrichment projects in the 1950s and 1960s [8] and formed the basis of research, development, and application of some present commercial inorganic membranes.

To date, different types of inorganic membranes, which are made of a wide range of materials and through various fabrication processes, have been developed for many gas separation applications [6, 8, 9]. To avoid unnecessary repetitions across these topics, this section aims at outlining some common considerations and general principles related to research and development of inorganic membranes for gas separation. More detailed information on each type of inorganic membranes will be further detailed in Sections 5.3–5.5.

## 5.2.1  Membrane Material and Microstructure

Membrane material and microstructure directly affect the function and performance of a membrane, and subsequently determining the related applications. Inorganic membranes for gas separation can be made with different materials and of various microstructures. From a material point of view, inorganic membranes can be ceramic-, metal- and carbon-based, and in some cases, a mixture of these materials, the so-called dual-phase material, is employed for multiple functions or promoted membrane performance in separation. While from a microstructure point of view, inorganic membranes can be dense or porous, following different separating or transport mechanisms when gas species permeate through membranes. When the membrane is very thin, which is typically preferred due to the higher permeation flux, a highly porous substrate is needed to provide mechanical strength of the membrane. This further categorizes membranes into self-supported and supported membranes. For the latter one, the dense or porous membrane, which is sometimes quoted as the separating layer, is formed on the surface of a porous substrate with transport resistance much smaller than the membrane itself. Because

membrane material and microstructure are much correlated to each other, and affect the following membrane formation process, as well as the membrane performance and application, they are used to categorize the contents of Sections 5.3–5.5 in this chapter, which hopefully will contribute to a better reading experience for readers interested in this chapter.

## 5.2.2 Membrane Formation

Membrane material and microstructure both affect the selection of membrane formation processes. For instance, the preparation of ceramic membranes, either dense or porous, typically involved the following steps [10]: (1) formation of suspensions/solutions containing ceramic particles, (2) rearrangement of particle packing into a membrane precursor that is shaped into specific membrane configurations (exampled shaping technology include casting or spin-coating for flat membranes, and ram extrusion or dip-coating for tubular membranes), and (3) consolidation of such membrane precursor via a high temperature heat treatment, when membrane microstructures (dense or porous for instance) can be finalized. In contrast, hydrothermal method and electroless plating are more suitable for microporous membranes such as zeolite and dense Pd-based membrane, respectively.

Apart from membrane material, permeation (permeation flux, permeance and permeability) and selectivity, the two membrane performance indicators, also "steer" the membrane formation process. Generally, a thinner membrane would lead to a higher permeation flux, mainly due to a lower membrane resistance. While at the same time, there is a higher chance of forming defects that can impair membrane selectivity, especially for gas separations. From this perspective, the quality of membrane substrates, such as surface smoothness, pore size distribution and porosity, etc., also determines the final membrane performance, in addition to the membrane formation process itself. For gas separations, there are mainly three groups of inorganic membranes mainly investigated, which are dense ceramic membranes (Section 5.3), dense metallic membranes (Section 5.4) and microporous membranes (Section 5.5).

### 5.2.2.1 Dense Ceramic Membranes

Dense ceramic membranes typically have no open pores nor interconnected pore network throughout the membrane, following a solution-diffusion type mechanism when gas species permeate through the membrane [10, 11]. Membranes of this type can be formed directly from ceramic particles, sometimes with a small amount of additives, via shaping technologies such as pressing and extrusion to obtain self-supported membranes. The formation of thin membranes on the surface of a porous substrate normally involve the use of a slurry consisting of ceramic

particles and a liquid phase with additives dissolved inside. The application of such a slurry onto substrates, i.e., the shaping technology, includes slip casting, tape casting and spin coating, etc. [10]. The key step of forming a high quality dense ceramic membrane is the final high temperature heat treatment, in which porosity of the precursor membrane is reduced to nearly zero, with the membrane density approaching the theoretic density of the membrane material. In most cases, the membrane density needs to be over 90% of theoretic values. Most of dense ceramic membranes are for high temperature applications [12], which imposes an extra challenge for supported membranes, mainly due to the potential mismatch of thermal expansion coefficients between the dense separating layer and the porous substrates that are made of different materials.

### 5.2.2.2 *Dense Metallic Membranes*

Similar to dense ceramic membranes, the dense metallic membranes, which are normally Pd-based, relies on a solution-diffusion type mechanism to selectively separate high purity hydrogen from a gas mixture [12]. Considering the high costs of precious metals, supported membranes [13], which normally consist of a defect-free Pd-based separating layer of several to several tens of microns in thickness formed on the surface of a highly porous substrate, is preferred for reduced material costs and enhanced hydrogen permeation. Sometimes less expensive metallic additives (binary, ternary, and multicomponent) are used for similar purposes [13], and the most successful one is Pd-Ag alloy. The porous substrate can be metal or ceramic based [12] , with physical vapor deposition (PVD), chemical vapor deposition (CVD), electroless plating (ELP), electroplating and diffusion welding [12–14] widely used to prepare the supported dense metallic membranes. Among these fabrication processes, ELP is one of the methods widely studied and used, mainly due to its advantages such as uniformity of membrane composition and microstructure on substrates of complicated shapes, good adhesion to substrates, low costs due to simplicity in equipment and operation, etc. [14].

### 5.2.2.3 *Microporous Membranes*

Microporous membranes, which have pore sizes smaller than 2 nm, can be used for gas separation [4]. Microporous inorganic membranes normally need a porous support due to the considerations of mechanical properties, that is, a supported membrane structure. The membrane (or separating layer) materials can be amorphous, such as silica and carbon, or polycrystalline, such as zeolite.

The sol-gel method is the most popular and successful process forming microporous silica membranes, typically on the smooth surface of a second mesoporous (pore size between 2 and 50 nm) ceramic-based intermediate layer (such as gamma-alumina, zirconia and titania), which is further supported by a third macroporous (pore size larger than 50 nm) layer on
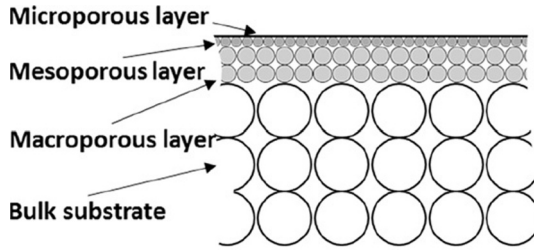
**FIG. 5.1** Schematic presentation of the laminated structure of ceramic membranes. *Redrawn based on Fig. 2.6 of Burggraaf AJ, Cot L. Fundamentals of inorganic membrane science and technology. Membrane science and technology series, 4; 1996.*

top of a bulk substrate providing significant mechanical strength, the so-called laminated structure very common to commercialized ceramic membranes (Fig. 5.1). The sol-gel method can be further classified into a polymeric route, particulate-sol and template method, which will be introduced in Section 5.5.

Preparation of microporous carbon membranes typically involves pyrolysis (carbonation) of a polymeric membrane at elevated temperatures and under vacuum or a nonoxidative atmosphere (helium or nitrogen for instance) [4]. The use of a polymeric membrane as the precursor means that, in addition to a supported membrane structure, a self-supporting membrane such as microporous carbon hollow fiber membranes can be prepared directly from polymeric hollow fiber membranes [6].

Polycrystalline zeolite membranes are usually prepared under hydrothermal conditions, including in situ synthesis, secondary growth, and vapor phase transport method [4]. For in situ synthesis, membrane support is in direct contact with a precursor solution or gel, in order to form a continuous zeolite separating layer. To speed up the nucleation, microwave heating has been found efficiently in reducing the synthesis time needed, as well as improving the membrane integrity. In contrast, for the secondary growth method, zeolite seeds are deposited on support surface before hydrothermal synthesis. While for the vapor phase transport method, hydrogel is first deposited onto a membrane support, prior to being in contact with a vaporized solvent inside an autoclave to allow the crystallization of the dry hydrogel.

## 5.2.3 Gas Separation Mechanism

### 5.2.3.1 Dense Ceramic Membranes

Dense ceramic membranes are mainly made of materials with perovskite or fluorite type structures [11] for the separation of oxygen or hydrogen at elevated temperatures [10, 12, 15]. Because this type of membranes

has no open pores, they rely on well-balanced mixed conductivity, that is, mixed ionic-electronic conductivity for oxygen transport, and mixed protonic-electric conductivity for hydrogen transport, to achieve high permeation fluxes at as low as possible temperatures, via strategies such as lattice doping, dual-phase material, and thinner separating layer, etc. It is also due to the unique transport mechanism, for instance, vacancy mechanism and interstitial mechanism that forming the pathway only for oxygen ions to migrate through, membranes of this type normally have theoretically 100% selectivity to oxygen or hydrogen.

### 5.2.3.2 Dense Metallic Membranes

Similar to dense ceramic membranes, dense metallic membranes rely on a solution-diffusion type mechanism for separating highly pure hydrogen from gas mixtures. Hydrogen transports through the membrane in the form of atomic hydrogen, which is why the theoretical selectivity to hydrogen can be infinite if there are no defects inside the membrane. However, this is normally quite difficult, especially when the metallic membrane is very thin.

### 5.2.3.3 Microporous Membranes

Gaseous molecules can transport through a porous membrane via different mechanisms, such as Knudsen diffusion, slip flow, surface diffusion, viscous flow, and molecular sieving, etc. [8, 10, 16, 17], depending on the factors such as pore diameter, molecule size (kinetic diameter), mean free path of molecules, and interactions between gaseous molecules and porous membrane materials, etc. While for an inorganic microporous membrane, Knudsen diffusion, surface diffusion, and molecular sieving have been commonly accepted as the main transport mechanisms [16]. Because kinetic diameters of gaseous molecules are quite small, normally of several hundred pm, only microporous membranes (pore size less than 2 nm) with very small pore size can provide reasonable perm-selectivity. In addition to membrane material and membrane microstructures, factors such as operating temperatures and pressures, as well as interactions between gaseous molecules and pore surface, also affect the membrane transport process. For instance, hydrophobicity and hydrophilicity of zeolite membrane materials can affect the separating selectivity in pervaporation, in addition to membrane pore size [4].

## 5.2.4 Performance Indicators

For both dense and microporous membranes, two major performance indicators, that is, permeation and selectivity, are widely used for evaluating the membrane separation performance [18].

### 5.2.4.1 Permeation

Permeation flux, permeance, and permeability are the three permeation related concepts widely used for gas separation.

*Permeation flux* is the flow rate of a permeated gas component normalized by membrane area (mol m$^{-2}$ s$^{-1}$). Permeation flux is typically used together with specified operating parameters, especially transmembrane pressure or partial pressure and temperature.

*Permeance* is permeation flux normalized by pressure (mol m$^{-2}$ s$^{-1}$ Pa$^{-1}$), and can be used to characterize the gas transport through the membrane. A practical unit of permeance is GPU (gas permeation unit, 1 GPU $= 10^{-6}$ cm$^3$ (STP) cm$^{-2}$ s$^{-1}$ cmHg$^{-1}$).

*Permeability* characterizes the intrinsic permeation property of a gas transporting through a membrane and is permeance multiplied by membrane thickness (mol m m$^{-2}$ s$^{-1}$ Pa$^{-1}$). Barrer is a unit for permeability still widely used today, named after Richard Maling Barrer FRS$^L$ (1910–1996) who is credited with breakthrough research in polymer membranes and molecular transport in microporous media and establishing the field of zeolite research and its applications in industry (1 Barrer $= 10^{-10}$ cm$^3$ (STP) cm cm$^{-2}$ s$^{-1}$ cmHg$^{-1}$).

### 5.2.4.2 Selectivity

Selectivity, or separating factor, indicates the extent of separating the target gaseous component from a gas mixture ($\alpha_{i,j} = \frac{y_i/y_j}{x_i/x_j}$, where $i$ and $j$ represent different gas components, $y$ and $x$ represent molar fractions at permeate and retentate side, respectively). When the partial pressure at the permeate side is minimal and negligible in comparison to the feed side, selectivity is equal to the ideal selectivity, which is the ratio of the permeability of the gas components [10, 19].

## 5.3  DENSE CERAMIC MEMBRANES

Dense ceramic membranes are mainly developed for separating oxygen or hydrogen from gas mixtures, depending on the type of mixed conducting behavior of the membrane materials, that is, mixed ionic-electronic conductivity for selective oxygen permeation, or mixed protonic-electronic conductivity for hydrogen permeation [10, 11, 20, 21]. It should be noted here that, although mixed conductivity can be achieved by mixing ceramic and metallic materials, that is, dual-phase materials, this section will focus on single phase ceramic membrane only.

## 5.3.1 Mixed Ionic-Electronic Conducting (MIEC) Ceramics

Most of MIEC ceramics are of perovskite or perovskite-related structures, named after a mineral oxide of $CaTiO_3$ with a typical formula of $ABO_3$ [10, 11]. The ideal structure of this oxide was first thought to be cubic and was later found to be orthorhombic. However, the name of perovskite has been retained and kept using until today.

### 5.3.1.1 Material Structure and Basic Concepts

A ceramic material of an ideal perovskite structure and $ABO_3$ formula has the A site cation coordinated to 12 oxygen ions forming a cuboctahedral coordination, and the B site cation coordinated to 6 oxygen ions forming an octahedral geometry [10, 11], as shown in Fig. 5.2. A-site cations, which are typically larger than the B-site cations, are commonly from the lanthanides or alkaline earth metals, and B site cations are of transition metals or nontransition metals. Common formulas that can be derived from $ABO_3$ include $A^{2+}B^{4+}O_3$, $A^{1+}B^{5+}O_3$, and $A^{3+}B^{3+}O_3$. Some structural parameters, such as tolerance factor and specific free volume, were used to guide the design of this structure, due to a considerable number of potential combinations of cations from the periodic table of elements.

However, the ideal perovskite structure in Fig. 5.2 is too "perfect" to exhibit any mixed ionic-electronic conductivity, because oxygen ions or electrons cannot move across the lattices without "mobile carriers." This means that some imperfections or defects have to be "created," according to the nonstoichiometry, for the conduction or diffusion to take place [11, 22]. As a result, the actual formula of most perovskite ceramics is $ABO_{3-\delta}$, with $\delta$ representing the nonstoichiometry regarding oxygen ions "missing" from the crystal lattice, for example, oxygen vacancies. Among various ways of creating such mobile carriers, doping A and/or B sites
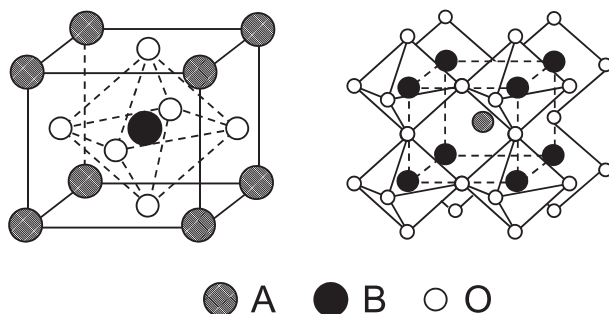


**FIG. 5.2** Ideal structure and the packing arrangement of perovskite $ABO_3$ compounds. *Redrawn based on Fig. 10.10 of Burggraaf AJ, Cot L. Fundamentals of inorganic membrane science and technology. Membrane science and technology series, 4; 1996.*

with different cations has been widely acknowledged as an efficient and accessible method, which leads to a more common formula of $A_xA'_{1-x}B_yB'_{1-y}O_{3-\delta}$.

The most important defects for MIEC materials include ion defects and electron defects, for the transport of oxygen ions and electrons, respectively, in the opposite directions across a membrane. Ion defects may take the form of vacancies, interstitial ions, impurities or dopants with charges different from those expected from the overall stoichiometry. Electron defects may be in the form of ions with charges deviating from the standard lattice ions, as a consequence of the transition of electrons from customarily filled energy levels to ordinarily empty levels. Defect theory has been used to explain conductive properties of MIEC materials, which has been systematically reviewed in the literature [11].

The quantity of such vacancies for transporting ions and electrons is directly correlated to the mixed conductivity of the material, and subsequently the capability of oxygen permeating through the membrane, when the electroneutrality of the membrane needs to be maintained without external circuit. As a result, ionic and electronic conductivities should be balanced from material design point of view, or in another expression the transfer number of oxygen ions and electrons should be "equal," in order for the highest possible oxygen permeation that can be achieved by a particular material composition [10, 11, 20], because the excessive conductivity is not able to benefit oxygen transport through such membranes.

### 5.3.1.2 Membrane Transport

Generally, the selective transport of oxygen through a dense ceramic MIEC membrane is driven by the pressure difference and consists of five sequential steps, as shown schematically in Fig. 5.3.
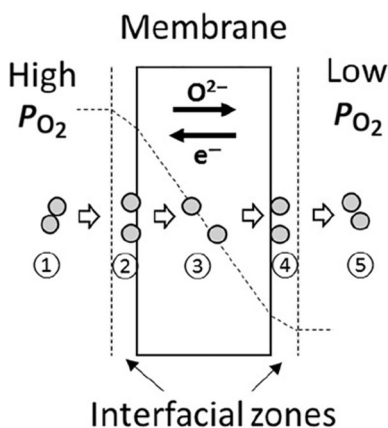


FIG. 5.3   Schematic presentation of oxygen permeation through a dense MIEC membrane.

**(1)** At the side with high oxygen partial pressure, for example, the feed side, oxygen molecules from gas bulk phase transport through an interfacial zone, before migrating to the membrane surface

**(2)** At the feed side surface, oxygen molecules dissociate into oxygen ions and reach oxygen defects on the surface

**(3)** Oxygen ions transport across the membrane, with electrons transport in the opposite direction to maintain electroneutrality of the membrane

**(4)** Oxygen ions reach the permeate side surface and recombine into oxygen molecules

**(5)** Oxygen molecules diffuse through the interfacial zone and transport to the permeate side bulk phase of low oxygen partial pressure.

If a mass transfer in the two gas bulk phases, which is more related to separator design at a unit level, is not considered, oxygen permeation mainly consists of two processes, for example, surface exchange (step 2 and step 4) and bulk diffusion (step 3) (Fig. 5.3).

Reducing membrane thickness can be helpful for increasing permeation fluxes, due to the lower resistance of bulk diffusion (step 3). However, when the membrane thickness is reduced to a certain level that the slowest transport step is not bulk diffusion, further reducing membrane thickness is not beneficial anymore. The corresponding membrane thickness is named as characteristic thickness, $L_c$ [11]. Characteristic thickness offers a way of evaluating how thin a specific MIEC membrane need to be and what is the controlling step of oxygen permeation and is thus useful for guiding engineering design of related membrane microstructures and operating conditions. While it should be noted that, the value of characteristic thickness can be affected by a variety of factors in addition to the membrane material. For instance, increasing temperatures will kinetically speed up both bulk diffusion (step 3) and surface exchanges (step 2 and step 4), while at different rates, which allows the controlling step to change with the operating temperatures. Moreover, porous coatings on membrane surface can promote surface exchanges, which, as a result, can lead to further reduced characteristic thickness. It will become more complicated if there are catalytic reactions at the permeate side of the membrane, such as a catalytic membrane reactor, together with a much lower oxygen partial pressure due to the quick consumption of permeated oxygen.

Because oxygen transport through a dense MIEC membrane can be considered a pressure driven process, different ways can be used for such operations, which include pressurizing the feed side, vacuuming the permeate side and using steam as the sweep gas to collect the permeated oxygen [21]. Each operation has certain advantages and disadvantages regarding economics and requirements on materials, and thus requiring systematic evaluation from engineering design point of view.

### 5.3.1.3 *Membrane Configuration, Microstructure, and Fabrication*

MIEC membranes have three significant configurations, like disc/flat sheet, tube, and capillary, for different scales of applications, depending on the surface area/volume ratio of the separator required. Capillary membranes usually have the highest membrane area per unit volume of the separator, mainly due to the small diameter. However, its mechanical robustness is always of concerns for engineering applications.

For each of these membrane configurations, the membrane can be self-supported or form a thin separating layer on a porous substrate, which has been introduced in Section 5.2. Conventional methods such as pressing and ram extrusion have been used to prepare self-supported disc and tubular MIEC membranes, with a typical symmetric membrane microstructure. For self-supported capillary/hollow fiber membranes, a phase inversion assisted process was developed, which allows the formation of adjustable asymmetric membrane microstructures with a thinner separating layer, and as thus higher oxygen permeation fluxes [10], as shown in Fig. 5.4.

Dense MIEC hollow fiber membranes can be asymmetric or symmetric, depending on the fabricating parameters used, such as types of bore liquids and suspension formulations [10]. Asymmetric membranes normally consist of two sub-microstructures, such as oriented microvoids/channels and a densified ceramic phase. When the microvoids are initiated from both the inner and outer surfaces, which is governed by a phase-inversion assisted process, the membrane has dense surfaces (inner and outer) and a third dense intermediate layer (Fig. 5.4A), all serving as oxygen separating layers. The microvoids contribute to a lower transport resistance, and as thus increasing oxygen permeation flux when compared to counterparts with a symmetric microstructure (Fig. 5.4D). Other variations in asymmetric microstructures, shown in Fig. 5.4B and C, has only one dense layer, either the inner or outer surface, and as a result further promote oxygen
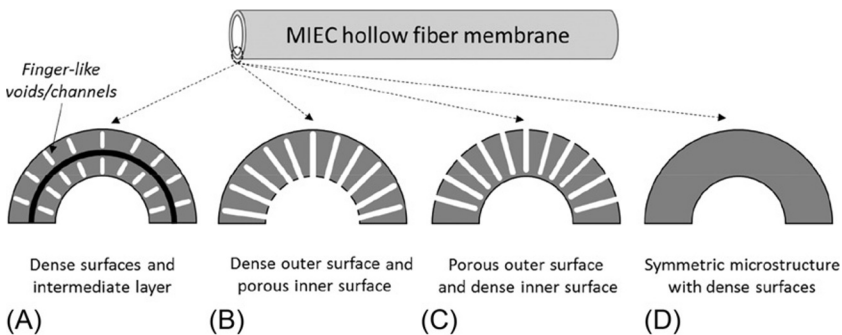


FIG. 5.4 Schematic presentation of asymmetric (A–C) and symmetric (D) MIEC hollow fiber membranes.
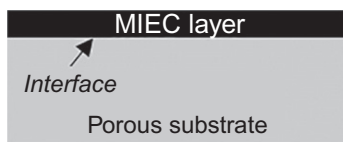
FIG. 5.5 A schematic presentation of supported MIEC membrane.

permeation. However, mechanical robustness of such structures can be a challenge for engineering applications.

For supported membranes, a thin and fully integrated MIEC separating layer need to form on top of a porous substrate (Fig. 5.5), which can be achieved via the methods briefly introduced in Section 5.2. However, when the substrate is made of a material different from the top separating layer, some specific challenges during the fabrication of such membranes need to be addressed.

Typical challenges include, but not limited to,

- possible solid-state reactions at the interface, because the MIEC layer needs to be densified at a temperature higher than 1000°C and consists of relatively active elements such as Co that can react with support materials at high temperatures
- Mismatch in shrinkage or shrinking rate during the high-temperature sintering, which will lead to the formation of macrocracks in the MIEC separating layer
- Insufficient adhesion at the interface leading to membrane peeling off
- Different thermal expansion coefficients, leading to the formation of microcracks during thermal cycles and damaging the membrane selectivity
- Different chemical expansion coefficients, due to the loss of lattice oxygen under low oxygen partial pressures. This will also lead to microcracks and poor membrane selectivity during temperature and pressure cycles.

### 5.3.1.4 MICE Membranes Based on Material Families

As previously introduced, doping different cations at the A and/or B sites of perovskite lattices allows the improvement of oxygen transport, which also help to increase the membrane chemical robustness against low oxygen partial pressures, $CO_2$ and reducing atmospheres [10, 11, 21, 22]. This leads to a considerable number of investigations on MIEC membranes with diverse compositions. Three essential families, Sr(Co, Fe)$O_3$, La(Co,Fe)$O_3$ and LaGaO$_3$, will be briefly introduced in this section.

*Sr(Co,Fe)$O_{3-\delta}$ (SCFO)*: membranes of this group typically have high oxygen permeation, mainly due to the high concentration of Co. Famous examples included $SrCo_{0.8}Fe_{0.2}O_{3-\delta}$ and $Ba_{0.5}Sr_{0.5}Co_{0.8}Fe_{0.2}O_{3-\delta}$.

However, insufficient chemical stabilities under reducing atmospheres, which is also due to the presence of concentrated Co, limit the applications of such membranes to oxygen separation only.

*La(Co,Fe)O$_{3-\delta}$ (LCFO)*: despite oxygen permeation lower than SCFO, the improved stability and more balanced mixed conductivity made membranes of this group attracting for oxygen separation. Typical examples included La$_x$Sr$_{1-x}$Co$_y$Fe$_{1-y}$O$_{3-\delta}$, which is also widely used as a cathode material of solid oxide fuel cell (SOFC) and commercially available.

*LaGaO$_{3-\delta}$ (LGO)*: LGO normally exhibits excellent ionic conductivity and low electronic conductivity, mainly due to the substitution of Co by Ga at B-sites of perovskite lattice. This also helps to improve the chemical stability under reducing atmospheres and reduce thermal expansion coefficients.

Apart from the three families above introduced, there are quite some membrane materials not summarized here. New MIEC materials have been kept reported for several decades, with both oxygen permeation flux and materials stabilities improved continuously, together with signs of progress in membrane fabrication methods. To date, there are still technical barriers hindering engineering adoptions of such membranes, which include relatively high operating temperatures, insufficient oxygen permeation and stability, mechanical robustness [23], uniformity of material compositions and membrane lifetime, as well as economic feasibilities, which are all related to the nature of perovskite materials. From this point of view, break-through in material design and development would be more likely to bring fundamental changes to the current scenario.

## 5.3.2 Mixed Protonic-Electronic Conducting Ceramics

Mixed protonic-electronic conducting ceramics have been investigated for hydrogen separation at high temperatures for many years [10, 20, 24]. Materials of this type usually have a perovskite type structure. Although dual-phase materials can have similarly mixed conductivity, they will not be discussed in this section, similar to MIEC materials above introduced.

Mixed protonic-electronic conducting ceramics have many similarities to MIEC, such as the perovskite type structure, mixed conductivity for selective permeation but only significant at high temperatures (>700°C), and gas transport through a dense membrane via a solution-diffusion type mechanism without external circuits (Fig. 5.6), etc. However, it receives much less attention when compared with MIEC materials, despite the increasing demand for highly pure hydrogen, which is an important chemical and clean energy carrier, and its operating temperatures matching well with the various processes of converting methane or coal into syngas (CO + H$_2$).

Hydrogen-rich stream    Hydrogen-lean stream

Mixed protonic-electronic conducting membrane

↓ H⁺    ↓ e⁻
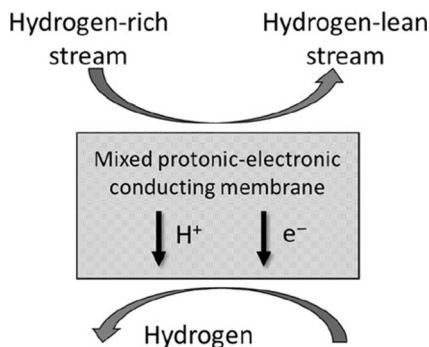
Hydrogen

**FIG. 5.6** Schematic presentation of hydrogen transport through a dense mixed protonic-electronic conducting membrane. *Redrawn based on Fig. 2.1 of Gupta VK, Lin JYS. Ceramic proton conductors. In: Nonporous inorganic membranes. Wiley-VCH Verlag GmbH & Co. KGaA; 2006. p. 49–76.*

### 5.3.2.1 Hydrogen Transport Mechanisms

Different from MIEC membranes for oxygen transport, protons are not an intrinsic part of the stoichiometry of perovskite structure [24] and behave as a foreign species/defects generally in equilibrium with ambient hydrogen and water vapor, which complicates the transport of hydrogen at a protonic state through a dense membrane of this type.

A proton is an elementary positively charged particle and needs to attach to an adjacent electron cloud [20]. In a perovskite structure, protons are attracted to oxygen ions to form the hydroxide ion. As a result, the proton attached to a standard oxygen ion can be treated as an interstitial proton, when the interstitial site is actively displaced toward a particular oxygen ion, or the oxygen ion with the attached proton is considered as a substitutional hydroxide ion [10, 20, 24]. This leads to two widely acknowledged mechanisms for hydrogen transport, such as hoping mechanism and hydroxyl ion migration. For the hoping mechanism, protons jump between stationary oxygen ions, from the feed side toward the permeate side, with each jump followed by a rotation around the oxygen ion to get in position for the next jump [10]. The proton jump is usually the rate-limiting step, as the rotation is relatively more straightforward. The hydroxyl ion migration is suitable for dominant long-range transport processes in oxides when proceeding on interstitial lattice sites, thus cannot provide a dominant conductivity, but accomplishes minority oxygen transport in a proton conductor [10]. It should be noted that migration of oxygen ions plays a vital role in proton conduction, which requires oxygen vacancies that can be created by doping, and will be outlined in the next section.

### 5.3.2.2 Mixed Protonic-Electronic Conducting Materials

In 1981, Iwahara et al. [25] discovered that some ceramics with a perovskite-type structure showed reasonable mixed protonic-electronic conductivity when exposed to a hydrogen atmosphere at high

temperatures. These materials were based on $SrCeO_3$, using trivalent cations to replace partially (doping) tetravalent $Ce^{4+}$, such as $SrCe_{0.95}Yb_{0.05}O_{3-\delta}$, with $\delta$ representing oxygen vacancies. Following this investigation, mixed protonic-electronic conducting ceramics based on $SrZrO_3$, $BaZrO_3$, $BaCeO_3$, and $SrTiO_3$ were developed [10, 24]. A general formula of $AB_{1-x}M_xO_{3-\delta}$ can be used to describe the materials of this type, with the A site element commonly from the group with calcium, strontium or barium, the B site element from the group consisting of cerium, terbium, zirconium, or thallium, and various doping elements M lower than the limit to form solid solution ($x < 0.2$) [10]. In contrast to the diverse formulas of MIEC materials, the quantity of mixed protonic-electronic ceramics is still so far insufficient.

Compared to MIEC, mixed protonic-electronic conducting ceramics have more types of charged carriers, such as protons, hydroxyl ions, oxygen ions/vacancies, electrons and electronic holes [24]. This means that the correlation between electrical conductivity and hydrogen permeation can be more complicated than the one for MIEC. For example, materials based on $BaCeO_3$ have relatively high electrical conductivity. While the contribution from oxygen ions to the total conduction increases with the temperatures, with the transfer number of protons decreasing at the same time [26]. In contrast, $SrCeO_3$ based materials have a lower conductivity, but a higher transport number of protons. Materials with Zr at the B site are less conducting than those with Ce at the B site, but more chemically and mechanically robust and more stable when exposed to carbon dioxide [10]. In addition to conductivity, material stabilities under reducing, moisture-containing, and $CO_2$-containing atmospheres can also be adjusted, considering the environment of using such membranes for hydrogen separation [24].

### 5.3.2.3 Preparation of Mixed Protonic-Electronic Conducting Membranes

In addition to the same material structure as MIEC materials, mixed protonic-electronic conducting materials and membranes can be prepared by the methods that have been used for MIEC materials and membranes. Fabricating such membranes typically consists of three steps, synthesizing ceramic powder, shaping into a membrane configuration, and thermal treatment to fully density the membrane.

Popular methods for preparing ceramic powders include solid state reaction and wet-chemistry approaches such as EDTA and citrate methods. Solid state reaction is suitable for preparing a relatively higher quantity of samples. Oxides or carbonates containing the required A and B site elements are usually ball-milled and ground in a liquid media. The mixture is then dried and sintered (typically around 950°C) to form a single-phase material. Critical issues related to this method include material compositions deviating slightly from the designed stoichiometry,

which can affect the membrane permeation performance and consequently lead to conflicting results, and relatively big particle sizes that can affect the following membrane shaping processes, as well as membrane performance, because bigger particles will result in larger grains and fewer grain boundaries inside a dense membrane, and as thus affecting the diffusion efficiencies. Wet-chemistry routes involve the use of chemicals such as nitrates to form chelates, to achieve element mixing at an atomic level, and as thus better in controlling the material composition. Pyrolysis of EDTA and citrate provides energy to form precursor powders much smaller in sizes, leading to a reduced particle size after secondary sintering. The grain sizes of the resultant membrane can be smaller in this case, and with more grain boundaries.

The synthesized powder can be directly shaped into self-supported membranes, using methods such as pressing, ram extrusion and phase-inversion assisted process (Section 5.2), or be used to form a slurry coated onto a porous substrate to form a supported membrane, which is very similar to MIEC membranes. Precursor membranes need a high-temperature sintering process to form a dense and integrated membrane before selective hydrogen permeation can proceed. In contrast to MIEC membranes, the characteristic thickness of mixed protonic-electronic conducting membrane has not been adequately investigated [24].

## 5.4 DENSE METALLIC MEMBRANES

Dense metallic membranes, mainly Pd-based membranes, have been widely studied for hydrogen separation and used commercially [12]. In contrast to the ceramic counterparts (Section 5.3.2), Pd-based membranes are more permeable to hydrogen in a lower temperature range (300–600°C), and are thus suitable for hydrogen purification/recovery [27], and very commonly membrane reactors coupling hydrogenation or dehydrogenation reactions [28].

Hydrogen diffusion through palladium has been known since the 1860s when it was found that palladium can absorb hydrogen of several hundred times of its volume at room temperature. This enables the use of Pd as a membrane to selectively separate hydrogen, when a pressure difference is formed across the membrane to allow hydrogen to continuously dissolve into the Pd membrane from the feed side, before being released at the permeate side.

### 5.4.1 Separation Mechanism

Hydrogen transport through a dense metallic membrane is based on a solution-diffusion mechanism and consists of the following five steps, as shown in Fig. 5.7:
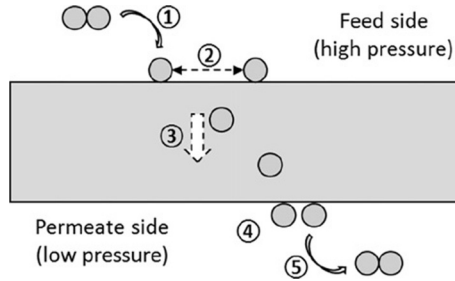
**FIG. 5.7** Schematic presentation of hydrogen transport through a dense Pd-based membrane. *Redrawn based on Fig. 6 of Yun S, Ted Oyama S. Correlations in palladium membranes for hydrogen separation: a review. J Membr Sci 2011;375(1):28–45.*

1. Hydrogen molecules in the gas phase are chemically adsorbed on the membrane surface (feed side)
2. Adsorbed hydrogen molecules dissociated into atomic hydrogen and dissolved into the membrane
3. Atomic hydrogen diffuses through the membrane toward the permeate side
4. At the permeate side surface, atomic hydrogen is recombined into molecules
5. Hydrogen molecules desorb from the surface and migrate into the gas phase

Similar to the dense ceramic membranes (Section 5.3), the transport consists of two processes, such as surface exchange (steps 2 and 4) and bulk diffusion (step 3), when the gas phase resistance can be neglected. How the surface exchange and bulk diffusion affect the transport process is reflected in the permeation flux equation expressed below [27]:

$$J = \frac{P}{\delta}\left(p_h^n - p_l^n\right) \tag{5.1}$$

where $J$ is the hydrogen permeation flux (cm$^3$/cm$^2$ min); $P$ is the permeability constant of hydrogen through the membrane (cm$^3$ cm/cm$^2$ min - bar$^n$); $\delta$ is the membrane thickness (cm); $p_h$ and $p_l$ are the hydrogen partial pressures on the high pressure and low-pressure side, respectively, and $n$ is a constant indicating pressure dependency. If the bulk diffusion of atomic hydrogen is the rate-controlling step, the value of $n$ should be 0.5 according to Sieverts' law [29]. However, when the surface processes also affect the hydrogen permeation, $n$ should be between 0.5 and 1 [13], particularly when the membrane is very thin. It should be noted that, if the gas phase resistance is not negligible, $n$ values can be higher than 0.5, especially for a supported membrane where $p_l$ in Eq. (5.1) can be easily underestimated or measured. When $n$ equals 1, it indicates that surface-

exchange is the rate-limiting step, and further reducing the membrane thickness will not benefit permeation flux anymore, until surface modifications that improve the surface-exchange are used.

## 5.4.2 Pd-Based Membranes for Hydrogen Separation

Tubular and foil membrane units are commercially available, with the Pd membranes usually quite thick. Despite high perm-selectivity to hydrogen, as well as proper permeation fluxes, Pd is very costly, and as a result preparing thinner Pd membranes, which is also beneficial to further increased hydrogen permeation flux, is economically meaningful. When the membrane is becoming thinner, some factors that may not be significant for thick Pd membranes start to raise concerns, because the chance of forming pinholes or defects, either through the membrane fabrication processes or during the membrane operations, can be detrimental to membrane selectivity.

### 5.4.2.1 Chemical Stabilities

For pure palladium, hydrogen embrittlement can occur when exposed to hydrogen at temperatures below 300°C. This is mainly due to the phase transition from an α phase, interstitial hydrogen in solid solution, to a β phase forming palladium hydride, with the hydrogen/palladium ratio increased significantly. The phase transition of this type is accompanied by a volume increase of around 10% [13], leading to the change of internal structures and accumulation of stress, which finally causes mechanical failure of the membrane. The hydrogen embrittlement limits the used of pure palladium membrane to temperatures above 300°C.

Actual used of Pd membrane for hydrogen separation involves the contact with different chemicals, such as CO, $H_2S$, $O_2$, hydrocarbons, and steam. [13, 30]. $H_2S$ is corrosive to Pd and has irreversible poisoning effects on Pd membrane surface, which is detrimental to the membrane permeability. CO can also affect hydrogen permeation through a Pd membrane by occupying adsorption sites on membrane surface at low temperatures, and at high temperatures decomposed into carbon due to the catalytic activity of Pd. Carbon can block pathways for hydrogen transport, and form pinholes when there is oxygen, which is a fatal reason for poor membrane selectivity, especially for ultra-thin Pd membranes. Effects of oxygen can be positive and negative. Air treatment has been found beneficial for Pd-based membranes because it helps to remove impurities on the membrane surface and also roughen the surface, which improves hydrogen adsorption and dissociation (Fig. 5.7). While for ultra-thin membranes, the roughened surface can lead to the formation of open pin holes that ruins perm-selectivity.

### 5.4.2.2 Pd-Based Alloys

Palladium is capable of forming solid solutions with different metals [31], forming Pd-based alloys that have improved chemical stability, as well as better mechanical properties and hydrogen permeability [13, 27]. The most successful alloy is Pd77-Ag23, which is the most used formula in commercially operating units [32]. In addition to a broader operating temperature window, by significantly mitigating hydrogen embrittlement, hydrogen permeability is also much higher than pure palladium, which makes it one of the most investigated alloying materials. Other Pd-based alloys include Pd-Cu, Pd-Au, as well as ternary alloys, with details can be found in other resources [13]. Some Pd-based alloys showed improved chemical stabilities against impurities such as CO and $H_2S$, while at the same time element segregation can occur [13], which changes the actual membrane composition and consequently gradually reduces membrane performance.

## 5.4.3 Formation of Pd-Based Membrane

Self-supported tubular and foil membranes made of Pd are commercially available. They are typically made through metallurgical processes, with good control of material compositions and low costs of manufacture. Membranes of this type usually are quite thick, for example, 20 μm is required for mechanical stability of a tubular geometry [33], with bulk diffusion typically as the rate-limiting step. Apart from relative low permeation, high material costs are another concerning factor, although these membranes can be very durable owing to the membrane thickness.

Reducing the membrane thickness is efficient in lowering material costs, particularly for precious metals like Pd, and increasing hydrogen permeation. Driven by these two factors, more interests have been directed to developing supported membrane, and the two essential factors of fabricating high quality supported Pd-based membranes are membrane support and membrane formation methods.

### 5.4.3.1 The Roles of the Membrane Support

Despite its great importance, membrane support has so far received much less attention when compared with the Pd-based membrane itself. These porous supports can, from different aspects, affect the selection of fabrication process, membrane microstructure, and subsequently the membrane separating performance (selectivity and permeation).

Surface smoothness, which is directly related to the average surface pore size of the porous support, is the factor determining how thin an integrated membrane can be achieved. It has been reported that the thickness of a Pd layer needs to be approximately three times the size of the largest
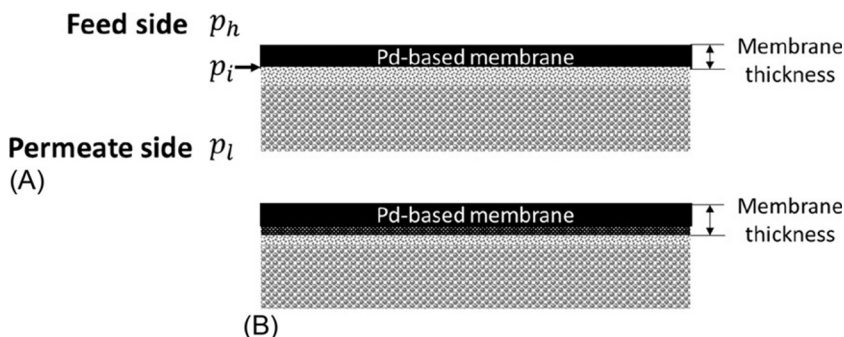
**FIG. 5.8** Schematic presentation of a Pd-based membrane on a porous support, (A) without penetration into support pores and (B) with penetration into the support pores.

pore of the porous support [34]. The largest pore here indicates the one on the surface, for both symmetric and asymmetric support microstructures, because the support surface is the interface between the support and the Pd-based metallic layer. As represented in Fig. 5.8A, the largest surface pore is also the weakest part of the membrane, which will be used under high-pressure differences and temperatures for a prolonged period of time. As thus, a support with a large number of narrowly distributed surface pores of a small size is usually preferred, for a thinner but highly integrated and durable Pd-based membrane.

In addition to providing mechanical strength, another requirement to the support is to generate as little as possible resistance for hydrogen transport. As can also be seen in Fig. 5.8A, hydrogen partial pressures at the feed side ($p_h$) and permeate side ($p_l$) are measurable and are usually used for calculating the hydrogen permeation (Eq. 5.1). This is feasible when the support resistance is negligible ($p_i = p_l$, $p_i$ is the pressure at the interface). If not, the $n$ value in Eq. (5.1) will deviate from the actual value it should be. Porous supports a larger average pore size usually have lower gas permeation resistance. While in addition to requiring a thicker Pd-layer, as discussed above, it is easier for membrane penetration (Fig. 5.8B) to occur during the fabrication process. This further increases the actual membrane thickness and reduces the permeation flux. As a result, porous support of an asymmetric microstructure (Fig. 5.1) is better concerning balancing the effects of a small surface pore size and low support resistance, for forming high-quality Pd-based membranes.

Regarding support materials, vycor glass with pore sizes between 4 and 300 nm was first used but later replaced by ceramic and stainless steel based materials, due to its limited thermal stabilities. Ceramic supports made of alumina, silica, zirconia, and titania and of various configurations have been studied, mainly due to their outstanding thermal and chemical robustness, as well as the preferred asymmetric microstructure either

commercially available or achievable via a phase-inversion assisted process [10]. The primary challenge of using ceramic based support is the thermal expansion behavior very different from the Pd-based metallic layer, especially considering the long-term use of such composite membranes with repeated thermal cycles. Other concerns include complexity regarding assembling and handling the membrane modules, due to the brittleness of ceramic and sealing when configured into an engineering process where metallic pipes are commonly used.

Alternatively, metallic support such as stainless steel is a more favorable choice, because welding can be used when attaching a membrane module to engineering processes. Other advantages of metallic support include thermal expansion behavior similar to Pd-based membranes, mechanical robustness, and relatively economical manufacturing. The primary concerns of such support include relatively big pore size, which requires a thicker membrane as previously discussed, and intermetallic diffusion with the Pd-based membrane, which gradually impairs the membrane performance. As a result, surface modification and an intermediate layer are required to address these problems [13]

### 5.4.3.2 Membrane Formation Methods

Various methods have been developed to fabricate thin and highly integrated Pd-based membranes on porous supports of different configurations, which include physical vapor deposition (PVD), electroless plating (ELP), chemical vapor deposition (CVD), electroplating, spray pyrolysis, and pulsed laser deposition [13, 27]. Among these fabricating methods, PVD and ELP are very commonly used.

PVD allows the formation of a layer of a solid material onto a support by condensing the vaporized form of this material without any chemical reactions involved [13]. This technique is capable of forming nanostructured and ultra-thin films with excellent control of alloy compositions [27], together with little impurities introduced during this process that can affect the membrane microstructure and performance. However, all these rely heavily on expensive and complicated processes, and require a well-conditioned substrate, to avoid possible defect formation.

In contrast, ELP is a more versatile and economical choice, and the support surface does not have to be flat. ELP is an autocatalytic process in which Pd complexes are reduced in situ with simultaneous oxidation of a reducing agent in aqueous solutions. To speed up the film formation, the surface of the porous supports is preferred to be activated by depositing Pd seeds, via an activation and sensitization process. Recipes for specific alloy compositions usually vary from each other, while popular alloys such as Pd-Ag and Pd-Cu can be prepared by this method. The alloys can be achieved by codeposition or forming separate metallic layers followed by intermetallic diffusion under high temperatures. For both

routes, uniformity in composition needs to be carefully controlled. Thickness control over the membrane and the presence of impurities such as tin belong to the disadvantages of ELP, although processes without using tin-containing sensitizer have been developed. Moreover, pore-penetration (Fig. 5.8B) is another disadvantage of this method, because plating solutions can wet the porous support during the fabrication. This increases the actual thickness of the membrane, depending on the microstructure of the porous support, and consequently resulting in possible conflicting results between different research groups.

## 5.5 MICROPOROUS MEMBRANES

In contrast to the dense membranes introduced in Sections 5.3 and 5.4, which rely on a solution-diffusion type mechanism for gas separation, porous membranes consist of open and connected pore network for fluid to pass through, and as thus rely mainly on the dimensions of pores to achieve required separation performance. According to the standard of IUPAC, pore sizes of porous membranes are categorized as macropores (pore diameter $d_p > 50$ nm), mesopores (2 nm $< d_p < 50$ nm) and micropores (0 nm $< d_p < 2$ nm). Macroporous and mesoporous membranes are essential for a wide range of membrane separation processes, such as micro- and ultra-filtrations [35], while their pore size is too big for gas separations, considering the much smaller kinetic diameter of gas molecules. As a result, only microporous membranes will be introduced in this section.

Inorganic microporous membranes are mainly made of three types of materials, such as silica, zeolite, and carbon, prepared by different methods and with the resultant membranes of different microstructures and physical/chemical properties [4, 9, 16, 35–37].

### 5.5.1 Silica Membranes

Silica membranes are generally prepared by a sol-gel method, and considering the mechanical properties of silica itself, supported membranes are always preferred. In most cases, precursor sol with designed compositions and rheology is applied onto a high-quality porous support (Section 5.4.3.1), before being transferred into a continuous gel and subsequently thin and integrated membrane. For achieving an ultra-thin silica microporous membrane, considering the relatively high transport resistance of micropores supports with a mesoporous surface is more favorable [4].

### 5.5.1.1  Sol-Gel Methods

There are three types of well-known sol-gel methods for preparing silica microporous membranes, based on compositions of the sol and the way of forming micropores inside the resultant membrane [4].

*Polymeric silica sol*: the sol of this type is generally prepared by acid-catalyzed hydrolysis and condensation of an alkoxysilane precursor polymer, such as tetraethyloxosilane (TEOS), under controlled conditions, with the help of a mutual solvent, usually a mixture of water and ethanol. The polymers used are preferred to be more or less linear for preparing microporous membranes because the resultant particle size is different from the one using well-branched polymer structure. Proper adjustment of the sol composition and extent of the reaction, as well as other factors such as packing and rearrangement of polymers during gelation, can improve the control over the microstructure and integrity of the resultant membrane, and subsequently the gas separation performance.

*Particulate sol*: silica colloidal sol can be prepared by hydrolysis and condensation of TEOS, assisted by a catalyst, followed by boiling the sol to allow the growth of the particles. This means that, by controlling the synthesis parameters, particle sizes of silica in the sol of this type can be adjusted, and can be further used to control the pore size of the membrane after forming a thin layer on a porous support. For example, particles less than 5 nm in the sol are capable of forming a silica membrane with the pore size of around 1 nm [4]. To prepare a highly integrated membrane via this method, ideal packing of such nanosized particles is needed but always challenging. Moreover, additives are sometimes needed to avoid infiltration of nanoparticles into the porous support, because possible pore-clogging will increase the overall membrane resistance for gas transport.

*Templated sol*: organic templates, such as surfactant, ligand, and polymer, are used to create residual porosity or pore network inside the membrane, after being removed under following heat treatment processes.

### 5.5.1.2  Applying Sol Onto a Porous Support

Depending on the configurations and microstructures of the porous supports, different methods can be used to apply the sol to form a thin and continuous layer. Among these methods, dip-coating and slip-coating, which are quite similar with a slight difference regarding the relative moving part, support or sol, respectively, are very popular. Properties of the sol, such as viscosity and rheology, and the surface microstructure and properties of the support codetermine the parameters, such as contacting time, as well as uniformity and repeatability of the

coated sol. This further affects the thickness and microstructure of the resultant membrane.

Due to the relatively high resistance of micropores, a very thin microporous silica layer is always preferred for good permeation flux. This generates extra challenges regarding the formation of a thin and defect-free membrane. For instance, solid impurities from supports, sol, and air can potentially travel into the coated sol during dip- or slip-coating, leaving pin-holes inside the resultant membranes. Moreover, the following gelation and heat treatment processes involve quite some other factors that can affect the final quality of the membrane. As a result, quality control and repeatability of sol-gel derived silica membrane, in addition to the thermal stabilities, are still of concerns, when considering larger scaled applications of such membranes.

## 5.5.2 Zeolite Membranes

Zeolites represent a vast group of crystalline aluminosilicates materials with micropores inside their diverse structures, which are constructed via various connections of $SiO_4$ or $AlO_4$ in a tetrahedral form. Most zeolites are usually in the form of micron-sized powder prepared via a hydrothermal method. The micropores inside, sometimes called zeolitic pores, can be of a variety of size and structure, which can be controlled by adjusting the $Si/Al$ ratio of the framework, as well as type and quantity of nonframework cations for charge balance. Materials of this type can offer substantial specific surface areas, together with tunable surface properties such as hydrophobicity and hydrophilicity. As a result, zeolites are very useful as a catalyst or adsorbent, in addition to a microporous membrane for gas separation. Further details about zeolites and the latest progress can be found through IZA Structure Commission (http://www.iza-structure.org/).

Hydrothermal method is, so far, the primary way of preparing zeolite membranes, which normally involves heterogeneous nucleation of crystal seeds on the surface of a porous support or deposition of nuclei, followed by the growth of polycrystalline grains under controlled hydrothermal conditions into a continuous layer (Fig. 5.9).

It should be noted here that, different from the zeolitic pores, the second type of pores, which are typically between zeolite grains, can be formed inside the membrane. When the intercrystalline pores of this type are more significant than the corresponding zeolitic pores, they are detrimental to the membrane selectivity, and should be addressed during membrane fabrication.

Regarding preparing a microporous zeolite membrane, in situ hydrothermal method, secondary growth method, and vapor phase transport method have been commonly used.
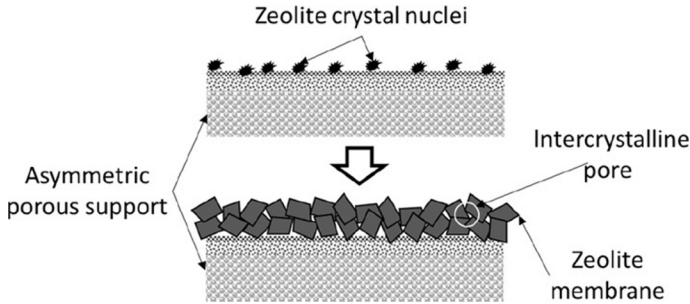
**FIG. 5.9**  Schematic presentation of forming zeolite membranes under hydrothermal conditions. *Redrawn based on Fig. 2 of Salleh WNW, Ismail AF, Carbon membranes for gas separation processes: recent progress and future perspective. J Membr Sci Res 2015;1(1):2–15.*

### 5.5.2.1  Fabrication Methods

#### 5.5.2.1.1  In Situ Hydrothermal Method

An in situ hydrothermal method is prevalent for preparing microporous zeolite membranes. Generally, a porous support is in direct contact with a synthesis solution or gel consisting of sources of silicon and aluminum, sodium, water, and sometimes templates. Under desired hydrothermal conditions, zeolite nuclei start to form at the liquid/solid interface, followed by growth of crystals from these nuclei to form a continuous layer (Fig. 5.9). The composite membrane is then removed from the residual solution or gel, rinsed, dried and if needed calcined to remove templates, before being tested for gas separation. Fabricating parameters of zeolite membranes are, in many cases, very similar to those used for synthesizing zeolite powders, in which the formation of initial nuclei (induction period) usually takes much longer time than the subsequent growth of zeolite grains [4]. To shorten the overall synthesis time, microwave heating can be used. In addition to quicker and more uniform heating, microwave fields can also affect the nucleation and crystal growth.

While due to the wide variety of zeolite compositions and structures, many fabrication conditions for synthesizing powder zeolites do not work for the corresponding membranes, and as thus demanding many try-and-error style attempts. Parameters such as compositions of synthesis solution/gel, pH, temperature, and synthesizing time need to be systematically investigated to obtain uniform and integrated zeolite membranes. Another fabricating parameter that can affect the formation of zeolite membranes is the composition of the support, which can assist heterogeneous nucleation of zeolite crystals in alkaline solutions. In contrast to sol-gel derived silica membranes, support with the surface pores larger than mesopores can be used for zeolite membranes, mainly due to the relatively large grain sizes of zeolites.

### 5.5.2.1.2 Secondary Growth

For an in situ hydrothermal method, induction period can be extended when initial nuclei are formed, which lowers the overall efficiency of the fabrication process, especially for large-scale production. Moreover, the possible time distribution of initial nucleation can cause nonuniformity in the size and distribution of nuclei on a support surface, leading to a less controlled growth of zeolite crystals and consequently forming intercrystalline pores in the resultant membranes (Fig. 5.9), despite stringent synthesizing conditions applied. To overcome these difficulties, secondary growth method has been developed and widely used to improve the quality of zeolite membranes.

The secondary growth method generally consists of two steps, like applying zeolite crystal seeds onto a support surface, and growing a continuous zeolite layer under hydrothermal conditions. Zeolite crystal seeds can be easily applied onto support surface by physical methods such as brushing, or dip-coating zeolite sol containing nanostructured seed particles. Uniformity regarding size and distribution of such seeds can directly determine the growth of zeolite layer in the second step, in which a more homogeneous contact between these seeds and the synthesis solution allows a more uniform growth of zeolite grains that can minimize and seal the intercrystalline pores. As a result, more integrated zeolite membranes can be prepared under conditions much less stringent than the in situ counterpart, such as lower temperatures, shorter time and more dilute synthesis solutions. In some cases, high-quality zeolite membranes can only be prepared via the secondary growth method.

### 5.5.2.1.3 Phase Transport Method

This method consists typically of two steps, applying hydrogel containing silicon, and sodium onto the support, and introducing vaporized solvents toward the dry hydrogel (inside an autoclave) to allow crystallization to occur. Templates can be added to either the hydrogel or solvent, with the latter one being more difficult to utilize the templating material fully. Compared to the in situ hydrothermal method, precursor materials inside hydrogel can be used more efficiently, and zeolite membranes with a higher Si/Al ratio can be achieved [4].

## 5.5.2.2 Modifications of Zeolite Membranes

Each fabrication method above introduced has certain advantages and disadvantages, while for the zeolite membrane prepared, there is always a chance of forming nonzeolitic pores, which includes intercrystalline pores, and even macro- and mesopores. The existence of such defects is harmful to the membrane selectivity, and "short-circuits" the role of zeolitic pores that are designed for separating purpose.

As a result, some processes have been developed to "repair" these defects, by filling nonzeolitic pores with carbon or silica that is converted from the corresponding precursor materials [4, 37]. Such membrane modifications can be efficient regarding promoting the membrane selectivity, by blocking or reducing the size of nonzeolitic pores. However, careful selection of the precursor materials, which should not enter into zeolitic pores, is also important, to avoid a significant decrease in membrane permeation flux.

### 5.5.3 Carbon Membrane

In addition to silica membranes, carbon membrane is another type of amorphous inorganic membranes. Benefit from the great thermal and chemical robustness, as well as high gas permeance and selectivity, carbon membranes are raising increasing interest for various applications, particularly gas separations. Membranes of this type are usually prepared by carbonization or pyrolysis of different types of polymeric precursors [16], which are usually thermosetting polymers [4].

The preparation process consists of two significant steps. The first step is forming a polymeric precursor membrane of required configurations, such as self-supported hollow fiber membranes that can be fabricated via temperature or solvent induced phase inversion process, and polymeric film supported by porous planar or tubular supports, via methods such as dip-coating and spin-coating, etc. In the first step, selection of suitable polymeric material and formation of a uniform membrane/film are the critical factors for consideration. Polymeric materials are the sources of the carbon, which directly determines factors such as pore size and mechanical properties of the resultant carbon membranes. For the self-supported hollow fiber membranes, uniformity of the membrane microstructures is an essential factor, because the resultant carbon membrane usually is of the same geometry and microstructure. For supported membranes, a polymeric film is formed on a porous support made of inorganic materials such as alumina or stainless steel. Proper adhesion between the carbon membrane and the support is essential and challenging [38], and will affect the separating performance and durability of the composite membranes for large-scale applications.

The second step is to convert these polymeric precursors into a carbon membrane at high temperatures and under vacuum or controlled nonoxidative atmospheres. In the second step, operating parameters such as temperature and nonoxidative environment are key factors affecting the microstructure of resultant carbon membranes.

#### 5.5.3.1 Precursor Polymeric Materials

Precursor polymeric materials are the source of carbon, and as thus play a critical role in deciding the final microstructure of the carbon membrane. This is entirely reasonable because two polymers of different

compositions and structures will give different forms of carbon, even if the same pyrolysis conditions were used. To date, a wide variety of polymeric materials have been investigated as the carbon source, which include polyimides, polyfurfuryl alcohol, polyetherimide, phenolic resin, and polyphenylene oxide, etc. [38]. Among these materials, the aromatic polyimide-type polymer is a very promising choice regarding fabricating high-quality carbon membranes, due to advantageous characteristics such as excellent thermal and structural stability, and high glass transition temperature and melting point [39]. Sometimes, the precursor polymeric materials can be modified through cross-linking, polymer-blending, and employing functional materials such as metal-organic-framework (MOF) [38] to obtain carbon membranes with further improved separation performance.

### 5.5.3.2 Converting Conditions

Under controlled conditions, such as temperature and atmosphere, precursor polymeric materials are converted into carbon, during which micropores are formed when gaseous molecules get away from the solid matrix of the precursor membrane. Carbon membranes can have micropores of different sizes [40], which include molecular sieve carbon membranes (MSCM) with small pores (<4 Å) and adsorption selective carbon membranes (ASCM) with larger pores (5–7 Å) [16]. In addition to the nature of the precursor polymeric materials, converting conditions play important role in affecting how densely carbon is packed and pore size distributions, and as thus the separating performance of carbon membranes. In contrast to polymeric membranes, separating performance of carbon membranes can exceed upper bound, while still limited by the trade-off between selectivity and permeability. This means that a more permeable carbon membrane is very likely to provide a lower permselectivity, which is entirely different from dense inorganic membranes previously introduced.

### 5.5.3.3 Membrane Configurations

Carbon hollow fiber membrane is the primary self-supported membrane configuration, due to advantages such as a well-developed technique for fabricating precursor membranes, high packing density due to the small membrane diameter, and good separating performance. However, the brittleness of such membranes is still challenging for engineering applications [38]. Alternatively, supported carbon membranes can be very thin, flexible in membrane configurations (planar and tubular) and mechanically stable. To survive the carbonization or pyrolysis conditions, inorganic porous supports have to be used, which raise another challenge regarding the excellent adhesion between the carbon membrane and the support. Processes such as repeated coating, modification of support surface, adding inorganic particles into polymeric precursor, applying

intermediate buffering layer and using plasma-enhanced chemical vapor deposition (PECVD), etc. [38] have been attempted. Similar to the supported dense membranes previous introduced, further improvement is still needed to address this challenge before suitable engineering applications can be implemented.

## 5.5.4 Gas Transport Through Microporous Membranes

Gas transport through microporous membranes can be complicated, with various theories developed to describe and explain this process. Several factors leading to the complexity of this type, which is very different from the dense inorganic membranes, include:

1. *Interactions between membrane material and gas species*: microporous membranes made of silica, zeolite and carbon are distinct in material properties (e.g., hydrophobicity and hydrophilicity), which interact with various gas species (different in terms of size/kinetic diameter and properties) in different ways, such as adsorption, not only on membrane surface, but also inside membrane pore network (pore wall) when gas molecules travel through.
2. *Actual pore size distribution*: microporous membranes are defined with pore sizes less than 2 nm. While the actual pore size distribution can be wider due to the presence of nonstructural pores, such as intercrystalline pores of zeolite membrane and mesopores in silica and carbon membranes. This allows the gas transport through the membrane to proceed via multiple mechanisms.
3. *Operating conditions*: pressure and temperature can change the gas transport behavior, not only by changing the extent of driving force, but also the interactions between gas species and membrane materials, which can lead to different transport mechanisms under different operating conditions.
4. *Gas mixtures*: interactions between gas molecules in a gas mixture can also intervene the gas transport through microporous membrane, for example, competitive adsorption between gas molecules. It is thus not uncommon to see membrane selectivity based on single gas permeation to be different from gas mixtures.

Standard mechanisms for gas transport through a porous membrane include Knudsen diffusion, surface diffusion, condensation-permeation and molecular sieving. Knudsen diffusion is important when the mean free path of gas molecules is much larger than membrane pore size, and molecular collisions against pore wall are more significant than the one between gas molecules. Surface diffusion occurs when there is a strong affinity between gas species and pore wall at a sufficiently low temperature and high pressure. The per-selectivity is codetermined by the extent of

adsorption and mobility of the adsorbed molecules. Condensation-permeation occurs when a condensable gas forms a liquid phase that filling in the pores. This allows good selectivity because noncondensable gases are blocked from passing through the membrane by this liquid phase. Molecular sieving uses sufficiently small pores to allow smaller molecules to pass through and retain the one larger than membrane pores.

When the operating temperatures are relative low, condensation-permeation can be important for applications involving volatile organic solvents. Surface diffusion/competitive adsorption-diffusion can be the primary transport mechanism for microporous silica, zeolite and carbon membranes. Gas species preferentially adsorbed onto the pore wall reduce the free spaces for nonadsorbing or weakly adsorbing molecules to enter, benefiting the membrane selectivity. Adsorbed molecules transport via surface diffusion. This combined effect leads to membrane selectivity to gas mixtures different from single gas. At elevated temperatures, preferred adsorption is weakened, with more pore space open to nonadsorbing species, leading to increased permeation of nonadsorbing species and changes of membrane selectivity with the operating temperatures.

As previously introduced, the gas transport through a microporous inorganic membrane can be complicated [4, 16, 37], and affected by different factors. In many cases, the transport process can be cogoverned by multiple mechanisms. Despite different theories available, experimental tests on gas separation under different conditions (gas compositions, temperature, pressure, etc.) are still the dominant standard to validate and interpret the actual gas transport through a microporous membrane.

## 5.6  SUMMARY

Inorganic membranes are playing gradually more essential roles in various membrane processes, particularly gas separation that can be further coupled with catalytic reactions to develop membrane reactors. In contrast to polymeric counterparts, inorganic membranes are unique in terms of their outstanding thermal, chemical and mechanical robustness, while less adopted by engineering applications due to factors such as relatively high material costs, complicated membrane fabricating processes, and temperature induced compatibility issues such as high-temperature sealing, although the membrane separating performance can exceed polymeric membranes. To address these issues, a breakthrough in material design and development is critically important, as exampled by the MIEC membranes for oxygen separation. Also, sustainable development of supported membranes can be very beneficial, while in many cases limited by the mismatch in the natures of materials, which also requires further innovations in material design and development.

Despite these challenges for inorganic membranes, fast and significant progress have been achieved in the last several decades, driven by various demands for more energy efficient and environmentally friendly separation processes. In this chapter, essential and fundamental concepts and principles of developing inorganic membranes for gas separations have been outlined, which aims at benefiting the readers who are seeking for appropriate knowledge in this area, before being capable of exploring more professional expertise of this technology.

# References

[1] Scott K. Handbook of industrial membranes. 1st ed. Oxford, UK: Elsevier Advanced Technology; 1995.

[2] Nunes SP, Peinemann K-V. Membrane technology: in the chemical industry. Weinheim, Federal Republic of Germany: Wiley-VCH Verlag GmbH; 2001.

[3] Baker RW. Membrane technology and applications. 2nd ed. West Sussex, England: John Wiley & Sons, Ltd; 2004.

[4] Lin YS, et al. Microporous inorganic membranes. Sep Purif Methods 2002;31(2):229–379.

[5] Baker RW. Future directions of membrane gas separation technology. Ind Eng Chem Res 2002;41(6):1393–411.

[6] Bernardo P, Drioli E, Golemme G. Membrane gas separation: a review/state of the art. Ind Eng Chem Res 2009;48(10):4638–63.

[7] Gas separation membranes market, by type, application and region—growth, future prospects and competitive analysis, 2016–2024. https://www.credenceresearch.com/report/gas-separation-membranes-market.

[8] Pandey P, Chauhan RS. Membranes for gas separation. Prog Polym Sci 2001;26(6): 853–93.

[9] Lin YS. Microporous and dense inorganic membranes: current status and prospective. Sep Purif Technol 2001;25(1-3):39–55.

[10] Li K. Ceramic membranes for separation and reaction. West Sussex, England: John Wiley & Sons Ltd; 2007.

[11] Burggraaf AJ, Cot L. Fundamentals of inorganic membrane science and technology. Membrane science and technology series, 4. The Netherlands: Elsevier Science B.V.; 1996.

[12] Gallucci F, et al. Recent advances on membranes and membrane reactors for hydrogen production. Chem Eng Sci 2013;92:40–66.

[13] Conde JJ, Marono M, Sanchez-Hervas JM. Pd-based membranes for hydrogen separation: review of alloying elements and their influence on membrane properties. Sep Purif Rev 2017;46(2):152–77.

[14] Lu GQ, et al. Inorganic membranes for hydrogen production and purification: a critical review and perspective. J Colloid Interface Sci 2007;314(2):589–603.

[15] Hashim SM, Mohamed AR, Bhatia S. Current status of ceramic-based membranes for oxygen separation from air. Adv Colloid Interface Sci 2010;160(1–2):88–100.

[16] Li H, et al. Inorganic microporous membranes for H-2 and $CO_2$ separation-Review of experimental and modeling progress. Chem Eng Sci 2015;127:401–17.

[17] Javaid A. Membranes for solubility-based gas separation applications. Chem Eng J 2005;112(1-3):219–26.

[18] Sunarso J, et al. Membranes for helium recovery: an overview on the context, materials and future directions. Sep Purif Technol 2017;176:335–83.

[19] Tong Z, Ho WSW. Facilitated transport membranes for $CO_2$ separation and capture. Sep Sci Technol 2017;52(2):156–67.

[20] Norby T, Haugsrud R. Dense ceramic membranes for hydrogen separation. In: Nonporous inorganic membranes. Weinheim: Wiley-VCH Verlag GmbH & Co. KGaA; 2006. p. 1–48.

[21] Sirman J. The evolution of materials and architecture for oxygen transport membranes. In: Nonporous inorganic membranes. Wiley-VCH Verlag GmbH & Co. KGaA; 2006. p. 165–84.

[22] Zhang C, Sunarso J, Liu SM. Designing $CO_2$-resistant oxygen-selective mixed ionic-electronic conducting membranes: guidelines, recent advances, and forward directions. Chem Soc Rev 2017;46(10):2941–3005.

[23] Malzbender J. Mechanical aspects of ceramic membrane materials. Ceram Int 2016; 42(7):7899–911.

[24] Gupta VK, Lin JYS. Ceramic proton conductors. In: Nonporous inorganic membranes. Weinheim: Wiley-VCH Verlag GmbH & Co. KGaA; 2006. p. 49–76.

[25] Iwahara H, et al. Proton conduction in sintered oxides and its application to steam electrolysis for hydrogen production. Solid State Ion 1981;3–4:359–63.

[26] Yajima T, Iwahara H, Uchida H. Protonic and oxide ionic conduction in $BaCeO_3$-based ceramics—effect of partial substitution for Ba in $BaCe_{0.9}O_{3-\alpha}$ with Ca. Solid State Ion 1991;47(1–2):117–24.

[27] Paglieri SN. Palladium membranes. In: Nonporous inorganic membranes. Weinheim: Wiley-VCH Verlag GmbH & Co. KGaA; 2006. p. 77–105.

[28] Plazaola AA, et al. Recent advances in Pd-based membranes for membrane reactors. Molecules 2017;22(1).

[29] Peters TA, et al. High pressure performance of thin Pd–23%Ag/stainless steel composite membranes in water gas shift gas mixtures; influence of dilution, mass transfer and surface effects on the hydrogen flux. J Membr Sci 2008;316(1):119–27.

[30] Gao HY, et al. Chemical stability and its improvement of palladium-based metallic membranes. Ind Eng Chem Res 2004;43(22):6920–30.

[31] Burkhanov BGS, et al. Palladium-based alloy membranes for separation of high purity hydrogen from hydrogen-containing gas mixtures. Platin Met Rev 2011;55(1):3–12.

[32] Young JR. Purity of hydrogen permeating through Pd, Pd–25% Ag, and Ni. Rev Sci Instrum 1963;34(8):891–2.

[33] Paglieri SN, Way JD. Innovations in palladium membrane research. Sep Purif Methods 2002;31(1):1–169.

[34] Mardilovich IP, Engwall E, Ma YH. Dependence of hydrogen flux on the pore size and plating surface topology of asymmetric Pd-porous stainless steel membranes. Desalination 2002;144(1):85–9.

[35] Tsuru T. Nano/subnano-tuning of porous ceramic membranes for molecular separation. J Sol-Gel Sci Technol 2008;46(3):349–61.

[36] Yeo ZY, et al. Synthesis and performance of microporous inorganic membranes for $CO_2$ separation: a review. J Porous Mater 2013;20(6):1457–75.

[37] Dong J, et al. Microporous inorganic membranes for high temperature hydrogen purification. J Appl Phys 2008;104(12).

[38] Salleh WNW, Ismail AF. Carbon membranes for gas separation processes: recent progress and future perspective. J Membr Sci Res 2015;1(1):2–15.

[39] Salleh WNW, et al. Precursor selection and process conditions in the preparation of carbon membrane for gas separation: a review. Sep Purif Rev 2011;40(4):261–311.

[40] Steel KM, Koros WJ. An investigation of the effects of pyrolysis parameters on gas separation properties of carbon materials. Carbon 2005;43(9):1843–56.

# Further Reading

[41] Yun S, Oyama ST. Correlations in palladium membranes for hydrogen separation: a review. J Membr Sci 2011;375(1):28–45.

CHAPTER

# 6

# Pervaporation and Vapor Separation

*Gui Min Shi[a], Dan Hua[a], Tai Shung Chung*

**Department of Chemical and Biomolecular Engineering, National University of Singapore, Singapore, Singapore**

OUTLINE

[a]These authors contributed equally to this work.

## 6.1  INTRODUCTION

Pervaporation and vapor permeation are energy efficient membrane-based separation processes for azeotrope mixtures and close-boiling liquids [1, 2]. The processes can be used for water removal, organic recovery and the separation of organic mixtures. Pervaporation is a process where a liquid feed mixture evaporates at a membrane and permeates through the membrane whereas vapor permeation is the permeation of organic vapors or gases through a membrane. Both processes achieve the separation by selectively permeating a particular component to other feed components.

One of the primary applications for water removal is the dewatering of alcohols in particular ethanol [3, 4]. The water content of bioethanol must not exceed 1% (v/v) [5] to be blended into gasoline. There has been a keen interest in the pharmaceutical industry to purify and recycle solvents because it could lower $CO_2$ emission and result in greener and more sustainable manufacture processes [6]. Besides, this chapter will also focus on pervaporation recovery of organic compounds. The last application is the separation of organic-organic azeotropes or mixtures with close boiling points such as isomers [7].

Despite the high expectation of the membrane-based processes for vapor separation, the actual industrial adoption of the processes is low [1]. This may be attributed to the high initial cost of the membrane-based processes and the lack of robustness of the membranes. The ideal membrane-based separation processes must not only have membranes with high flux and selectivity but also have long-term stability and robustness in various feed mixtures and harsh testing conditions. Depending on the applications, suitable membranes need to be employed. Generally, hydrophilic membranes or molecular sieving membranes are used for water removal whereas hydrophobic membranes are employed for organic recovery and organic-organic separation.

The first commercial dehydration membrane was developed by GFT [8]. It was a composite membrane consisting of poly(vinyl alcohol) (PVA) and polyacrylonitrile (PAN). Although it was the first breakthrough for the industrialization of pervaporation dehydration of organic solvents, the PVA/PAN composite membranes had relatively low separation performance [9]. Since then, polyimides [10], polyamides [11], and

polybenzimidazole (PBI) [12] membranes were developed to improve the thermal and chemical stability of feeds containing acids and acetone. However, polyimides might go through hydrolysis and cause degradation of membranes over time [13]. Also, both the polyimides and PBI membranes required cross-linking modifications to improve their chemical resistance toward polar solvents like acetone [14]. Other chemically resistant membranes made of perfluoro polymers, such as Hyflon [3] and Teflon [15], were also investigated (the materials were invented for other applications, and later for dehydration) to dehydrate alcohols for vapor permeation applications at temperatures as high as 120°C. Teflon AF2400 has higher thermal stability than Hyflon AD60 due to its higher glass transition temperature (240°C vs. 125°C). Besides, significant efforts have been focused on the use of mixed matrix membranes to improve the separation performance of polymeric membranes. In particular, metal organic frameworks (MOFs) [16–18] have been incorporated in various polymeric membranes for solvent dehydration.

Polydimethylsiloxane (PDMS) has been the benchmark membrane material for removing alcohols and other organics from aqueous streams. Efforts were made to find alternative membranes made of other new hydrophobic materials such as poly(1-trimethylsilyl-1-propyne) (PTMSP) [19] polyether block amide (PEBA) [20, 21], polymer with intrinsic microporosity-1 (PIM-1) [22], Teflon [23], PVDF [24], silicalite-1[25], ZSM-5 [26], and MOFs [27]. Among them, the inorganic membranes had a selectivity several times higher than the polymeric membranes. Compared to PDMS, there were no polymeric membranes with a much better selectivity for organic solvents except PTMSP, but the permeability of the latter decreased with time. To enhance the separation performance of PDMS and the other types of membranes, functional particles such as MOFs, carbon nanotubes and silane-grafted silicalite-1 were incorporated in the polymeric matrix to improve their selectivity for alcohols [28–31].

The challenge for organic recovery was to have polymeric membranes with a high selectivity for a wide range of feeds to compete with other separation technologies such as steam stripping, adsorption, and distillation. Usually, the membranes could achieve high selectivity and enrich the organics from their lower concentrations. However, due to the membrane swelling and saturation of hydrophobic sites, it was hard to further enrich the organics from a low concentration to a high concentration because the separation factor is not much higher than the separation factor achieved by the vapor-liquid equilibrium [32, 33]. Therefore, the membrane recovery alone may not achieve the purification objective for the recovery of bioalcohols from fermentation broths because the alcohol concentrations in the feed are about 2–10 wt%.

Lastly, the membrane development for organic-organic separation has been limited because few membrane materials have the specific affinity to

one of the organic compounds and the required solvent stability. Only a few materials such as polyimides [34], polyether ether ketone (PEEK) [35] and MOFs [27, 36] were explored for the separation of aromatic/aliphatic mixtures. In most cases, inorganic fillers like graphene oxide (GO) [37], carbon nanotubes [38] and MOFs [39, 40] were added into the polymeric matrix to enhance the separation performance. So far, the separation of organic-organic mixtures remains one of the least investigated areas for pervaporation membranes [41]. The separation is challenging as each separation requires a particular type of membrane unlike solvent dehydration and organic recovery.

Pervaporation and vapor separation membrane processes are essential additions to the industrial separation processes. Pervaporation/vapor permeation plants using Sulzer's membranes for solvent dehydration was reported to have ∼200 installations worldwide in 2012 [1]. Therefore, we aim to cover the theoretical separation mechanisms, polymeric membrane fabrication, membrane material selection for various types of applications and membrane characterizations in this chapter.

## 6.2  THEORY BACKGROUND

It is essential to understand the fundamentals of pervaporation and vapor permeation processes to select the appropriate membrane materials and develop the suitable membranes for vapor separation applications.

### 6.2.1  Transport Mechanism

The solution-diffusion model is the most widely accepted transport mechanism for pervaporation and vapor permeation processes [42]. The model defines the transport of the permeating components through a membrane consisting of three consecutive steps (Fig. 6.1):
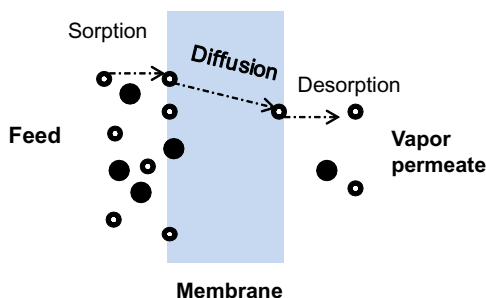


FIG. 6.1  Schematic presentation of the solution-diffusion mechanism.

(i) Sorption of the feed components into the membrane;
(ii) Diffusion of the permeating components through the membrane;
(iii) Desorption of the permeating components to the vapor phase on the downstream of the membrane.

The dominant steps are the sorption and the diffusion of the feed components whereas the desorption step is very fast because vacuum or sweeping gas is applied to remove the diffused components.

The flux of the permeating component $i$, $J_i$, can be expressed by the following equation:

$$J_i = -D_i \frac{dC_i}{dx} \tag{6.1}$$

where $D_i$ and $dC_i/dx$ are the diffusion coefficient and the concentration gradient, respectively, of component $i$ in the membrane. The concentrations of component $i$ at the feed and permeate sides of the membrane are the products of the partial pressure of component $i$ at the two sides ($P_i^f$ and $P_i^P$, respectively) and partition coefficient $S_i$. Therefore, Eq. (6.1) can be integrated as:

$$J_i = \frac{D_i S_i \left( P_{i'}^f - P_i^p \right)}{l} \tag{6.2}$$

where $l$ is the membrane thickness. Expressing the term $D_i S_i$ as permeability ($P_i$), and substituting it into Eq. (6.2), one can obtain Eq. (6.3) as follows:

$$J_i = \frac{P_i \left( P_{i'}^f - P_i^p \right)}{l} \tag{6.3}$$

The transport in pervaporation and vapor permeation processes is determined by two factors: (1) the solubility of a feed component in the membrane and (2) the diffusion rate of the permeant through the membrane. It is worth noting that the two factors are tightly coupled because a higher solubility of the component in a membrane may significantly swell up the membrane and leads to a significantly higher diffusivity for that component [43].

## 6.2.2 Evaluation of Pervaporation and Vapor Separation Membranes

For pervaporation and vapor separation, the reported separation performance in literature is not as standardized as those in gas separation. Hence, a comparison of performance data available in the literature is not so straightforward because the driving force (i.e., the vapor pressure across the membrane) may or may not be included in the calculation of separation performance. Mass flux ($J$ in kg/m$^2$h or g/m$^2$h) and

separation factor ($\beta$) have been widely used as the performance indices for pervaporation and vapor separations, but they are not normalized by the driving force. As a result, the reported separation performance is the performance of the pervaporation process rather than the membrane itself. Generally, the permeate flux $J$ can be calculated using the following equation:

$$J = \frac{Q}{(A \cdot t)} \tag{6.4}$$

where $Q$ is the total mass of the permeate over time $t$, and $A$ is the membrane area. Separation factor can be calculated using the following equation:

$$\beta_{a/b} = \frac{y_a/y_b}{x_a/x_b} \tag{6.5}$$

where $x$, $y$ are the mass fractions of the components in the feed, and the permeate, respectively, and the subscripts refer to the components $a$ and $b$. In some literature, the enrichment factor of a component, the ratio of the permeate concentration to the feed concentration, is also used instead of the separation factor.

To determine the intrinsic permeance (permeability/membrane thickness, see below) and selectivity of a pervaporation membrane, the driving force which is the difference between the partial vapor pressures of the component at the upstream (feed) and downstream (permeate) sides of the membrane should be considered. The partial vapor pressure (fugacity) of component $i$ on the feed side can be calculated based on its mole fraction, $x_i$, in the feed liquid mixture.

$$P_i^f = x_i \gamma_i P_{i'}^{sat} \tag{6.6}$$

where $\gamma_i$ is the activity coefficient and $P_{i'}^{sat}$ is the vapor pressure of component $i$ in the feed. Combining Eqs. (6.3), (6.6) and applying Dalton's law to derive the permeate partial pressure, one may obtain the following basic transport equation for pervaporation:

$$J_i = \frac{P_i \left( x_i \gamma_i P_{i'}^{sat} - y_i P^p \right)}{l} \tag{6.7}$$

where $P_i$ and $y_i$ are the permeability and the mole fraction in the permeate, respectively, of component $i$, $l$ is the membrane thickness, and $P^p$ is the total permeate pressure. However, the term $\frac{P_i}{l}$ known as permeance is often used for asymmetric membranes because of the difficulties to obtain the exact thickness of the selective layer. By rearranging the above equation, the permeance could be rewritten as follows:

$$\frac{P_i}{l} = \frac{J_i}{\left( x_i \gamma_i P_{i'}^{sat} - y_i P^p \right)} \tag{6.8}$$

The selectivity of the membrane for two components, *a* and *b*, is defined as the ratio of their permeability.

$$\alpha_{b/a} = \frac{P_b}{P_a} \tag{6.9}$$

# 6.3 FABRICATION OF PERVAPORATION AND VAPOR SEPARATION MEMBRANES

Based on the membrane structure, membranes for pervaporation/vapor permeation can be either dense or asymmetric with a dense selective layer as illustrated in Fig. 6.2. Dense membranes are normally used in the laboratory to study the properties of membrane materials rather than real industrial applications due to their low permeation fluxes and large transport resistance caused by the large thickness. In contrast, asymmetric membranes possessing a thin dense selective layer and a relatively thick microporous substrate have a much higher flux due to the reduced substructure resistance. Some common fabrication methods for pervaporation/vapor permeation membranes are introduced below.

## 6.3.1 Solution Casting

Solution casting is the most common method for fabricating flat-sheet membranes with different membrane structures, which consists of three steps: (1) the polymer and potential additives are dissolved in a solvent to form a homogeneous polymer solution; (2) the polymer solution is



**Dense membrane**

Homogeneous structure

**Asymmetric membrane**

Wholly integral asymmetric structure made from the same material

Asymmetric structure consisting of layers made from different materials (composite membranes)
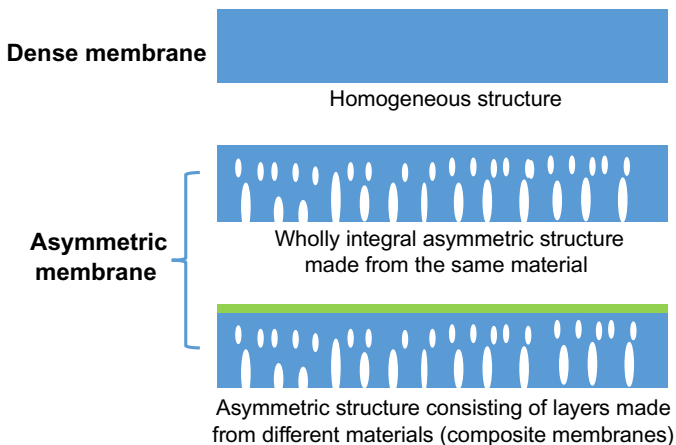
FIG. 6.2  Polymeric membranes classified by the membrane structure.

spread evenly onto a flat support; (3) the solvent in the nascent membrane is removed by evaporation and/or nonsolvent induced phase inversion processes.

Dense membranes are prepared by the slow and complete evaporation of the solvent to form dense homogeneous structures, whereas asymmetric membranes with interconnected cell structures as a support layer are obtained when the solvent removal procedure involves a nonsolvent induced phase inversion process [44]. Besides, the addition of highly volatile solvents into the casting solution followed by evaporation before the phase inversion promotes the formation of a top dense layer for asymmetric membranes. Also, multilayered asymmetric membranes can be prepared by casting several polymer solutions with different compositions simultaneously.

For the case of mixed matrix membranes (MMMs), the inorganic fillers are dispersed into a polymer dope solution with the assistance of sonication and thorough stirring to avoid the agglomeration of the fillers. Subsequently, MMMs are formed by the similar procedures as aforementioned.

## 6.3.2 Hollow Fiber Spinning

As compared with flat sheet membranes, hollow fiber membranes possess superior advantages such as higher surface area, higher packing density, excellent flexibility, self-support property, and ease of fabrication as well as scale-up [45–47]. Fig. 6.3 illustrates a typical hollow fiber spinning process via nonsolvent induced phase inversion method.

During hollow fiber spinning, the predegassed dope solution is extruded simultaneously with the bore fluid in the lumen side of the nascent fiber with specific flow rates. Coagulation at the internal surface of the nascent fiber occurs right away after it emerges from the spinneret. Meanwhile, partial coagulation starts at the outer surface when the
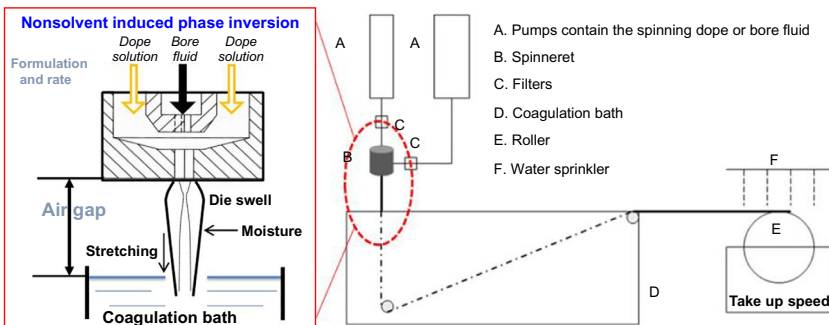


FIG. 6.3    The scheme of a typical hollow fiber spinning process.

nascent fiber travels a certain air-gap distance due to the humidity in the air. Then the fiber enters the coagulation bath, where the whole phase inversion process takes place via the full precipitation of the fiber. Afterward, the hollow fiber is collected by a rolling drum with a controlled take-up speed. During the whole process, the structure and morphology of hollow fiber membranes are influenced by a variety of process parameters, including spinneret design, dope formulation, bore fluid formulation, flow rates of both dope solution and bore fluid, coagulation bath composition, spinning temperature, air gap distance, humidity and take-up speed, etc. The spinning process becomes more complicated when the spinning changes from single layer to dual layer coextrusion. The dual-layer spinning technique has attracted much attention Because it possesses the advantages of cost reduction as well as more freedom in customization of materials and morphology for the selective layer and supports [48, 49]. The conventional single-layer and dual-layer hollow fiber membranes have single-bore geometry. To enhance the mechanical properties, multibore hollow fiber membranes have also been developed for pervaporation by using a specially designed three-bore spinneret with a blossom geometry [50].

## 6.3.3 Typical Methods for Fabricating Composite Membranes

Composite membranes are a type of asymmetric membranes. The composite approach gives more freedom to design and engineer high-performance membranes because they consist of multilayers made from different materials. For example, researchers can choose a small number of expensive materials with excellent separation performance as the ultra-thin selective layer and use cheap materials for the porous support. Therefore, the composite membranes are more cost-effective and have great potential for industrialization.

There are two strategies to fabricate composite membranes. One is to simultaneously fabricate both the top selective layer and porous support in one step by multilayer solution casting or dual-layer hollow fiber spinning as mentioned above. The other is to fabricate the porous membrane substrate first, and then to deposit the dense selective layer on the substrate via coating, interfacial polymerization, in-situ growth or layer by layer method. Some relevant technologies are summarized below.

### 6.3.3.1 Solution Coating

The solution coating technologies are widely used for fabricating composite pervaporation/vapor permeation membranes, including spin coating, dip coating, spray coating and so on [51–53]. The intrusion of the top selective layer into the substrate should be minimized during coating

either by prewetting of the substrate or coating a permeable gutter layer on the substrate first to stop the intrusion [54, 55]. The coating conditions are also critical to achieving a uniform and thin dense selective layer.

### 6.3.3.2 Interfacial Polymerization

As demonstrated in Fig. 6.4, during the interfacial polymerization process, two monomers are dissolved in two immiscible solvents, respectively. Then the polymerization of the two monomers takes place at the interface of the two liquid phases on top of the substrate. Thus, an ultrathin layer is formed. The thin-film composite (TFC) membranes fabricated via interfacial polymerization have drawn attention in recent years for pervaporation due to its excellent separation performance and ease of fabrication [56–62]. The morphology, hydrophilicity, as well as free-volume properties of the formed thin-film selective layer, can be adjusted via using different monomers, varying monomer concentration, changing solvent chemistry, adding surfactants or catalysts, or adjusting surface morphology of the support. Hence, TFC membranes fabricated from this technology are promising because the thickness of the dense selective layer could be controlled in molecular level easily and thus achieve both high flux and separation factor.

### 6.3.3.3 Layer-by-Layer Technology

The layer-by-layer technology is also used to develop composite membranes, in which the selective layer is typically formed by depositing alternating layers of oppositely charged polyelectrolyte materials based on their attractive forces [63, 64]. However, the long-term stability of composite membranes fabricated by this method in aqueous solutions may be an issue. Therefore, some researchers have used other materials via layer-by-layer technology based on covalent bond interaction, which has been proved to possess a stable performance for alcohol dehydration [65].

In summary, several criteria are needed when fabricating composite membranes: (1) Good compatibility between the layer materials is
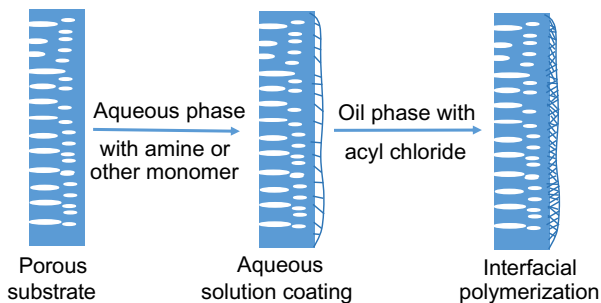


FIG. 6.4   A typical procedure of TFC membranes fabricated via interfacial polymerization.

essential so that there is no delamination between layers; (2) The solvent used to form the top selective layer should not damage the bottom layer; (3) The intrusion of the top layer material into the bottom layer should be minimized in order to decrease the substrate resistance. (4) An ultra-thin selective layer and a porous substrate are desired to achieve high productivity.

### 6.3.4 Physicochemical Modifications

Postmodification is commonly used to improve the separation performance and stability of pervaporation/vapor permeation membranes, including crosslinking, grafting, and thermal annealing. Among them, crosslinking is the most common technique to stabilize membranes and to suppress their swelling caused by direct contact with liquid or vapor-state organic solvents. Besides, grafting of functional groups onto membranes can help to adjust the hydrophilicity or hydrophobicity and thus improve the affinity between the permeating molecules and the membranes. Also, postannealing is a versatile and efficient technique to eliminate defects in the selective layer and improve its separation performance.

## 6.4  PERVAPORATION MEMBRANES

### 6.4.1  Dehydration of Organics

#### 6.4.1.1  Highly Hydrophilic Polymeric Membranes

At the early stage of membrane development for dehydration, highly hydrophilic membranes such as poly(acrylic acid), PVA, sodium alginate and chitosan received much attention due to their excellent solubility selectivity [66–69]. However, they lack mechanical strength and show severe swelling in aqueous solutions. As a result, crosslinking is necessarily employed to stabilize these membranes. In recent years, the development of dehydration membranes has shifted toward the exploration of new chemically and thermally stable materials. Polymers with stiff and rigid chains have been considered to dehydrate aggressive solvents at elevated operating temperatures. Some representative materials will be introduced in detail in the following sections, and Table 6.1 summarizes their separation performance.

#### 6.4.1.2  Polyimide Membranes

Polyimides have emerged as potential alternative materials for the dehydration of alcohols and other organic solvents [10, 12, 67, 71, 90–92]. This is because they have excellent thermal, chemical and

**TABLE 6.1**   Selected Polymeric Membranes for Solvent Dehydration

| Membranes | Configuration | Feed | Temperature (°C) | Flux (g m$^{-2}$ h$^{-1}$) | Normalized flux (g μm m$^{-2}$ h$^{-1}$) | Separation factor (water/ solvent) | Ref. |
|---|---|---|---|---|---|---|---|
| *POLYIMIDE* | | | | | | | |
| HPEI mediated GA modified Torlon | HF | Isopropanol/water (85/15 wt%) | 50 | 1521 | NA | 791 | [70] |
| HPEI mediated BA modified Torlon | HF | Isopropanol/water (85/15 wt%) | 50 | 2285 | NA | 316 | [70] |
| HPEI mediated GA modified Ultem | HF | Isopropanol/water (85/15 wt%) | 50 | 2192 | NA | 202 | [70] |
| TAEA crosslinked P84 | FS | Acetone/water (85/15 wt%) | 50 | 658 | NA | 983 | [71] |
| EDA vapor crosslinked P84 | FS | Acetone/water (85/15 wt%) | 50 | 1800 | NA | 53 | [14] |
| P84 | Dense FS | Isopropanol/water (85/15 wt%) | 60 | 18 | 720 | >5000 | [72] |
| cPIM-1 (10%)/P84 | Dense FS | Isopropanol/water (85/15 wt%) | 60 | 31 | 1240 | >5000 | [72] |
| hPIM-1 (20%)/polyimide (i.e., Matrimid, Torlon, and P84) | Dense FS | Ethanol/water (85/15 wt%) | 60 | 36.9, 17, 38 | 1845, 850, 1900 | 340, 157, 199 | [73] |
| hPIM-1 (20%)/polyimide (i.e., Matrimid, Torlon, and P84) | Dense FS | Isopropanol/water (85/15 wt%) | 60 | 39.5, 24.0, 41.5 | 1975, 1200, 2075 | 780, 719, >5000 | [73] |

| | | | | | | | |
|---|---|---|---|---|---|---|---|
| hPIM-1 (20%)/polyimide (i.e. Matrimid, Torlon, and P84) | Dense FS | *n*-Butanol/water (85/15 wt%) | 60 | 47.8, 19.6, 40.0 | 2390, 980, 2000 | >5000, >5000, >5000 | [73] |
| 6FDA-NDA/DABA (9:1) polyimide | Dense FS | Ethanol/water (85/15 wt%) | 25 | 133.4 | 2668 | 119 | [74] |
| 6FDA-NDA/DABA PI/SPI/ Ultem (3 wt% SPI)—thermal treatment | HF | Ethanol/water (85/15 wt%) | 60 | 2600 | NA | 130 | [75] |
| 6FDA-NDA/DABA PI/SPI/ Ultem (3 wt% SPI) – POSS modification | HF | Ethanol/water (85/15 wt%) | 60 | 2000 | NA | 237 | [75] |
| 6FDA/HAB/DABA poly (benzoxazole-co-imide) | Dense FS | Isopropanol/water (85/15 wt%) | 60 | 90 | 2108 | 2458 | [76] |

**OTHER AROMATIC POLYMERS**

| | | | | | | | |
|---|---|---|---|---|---|---|---|
| PBI | Single-layer HF | Ethylene glycol/ water (50/50 wt%) | 60 | 1147 | NA | 116 | [77] |
| PBI/Ultem | Dual-layer HF | Ethylene glycol/ water (50/50 wt%) | 60 | 232–732 | NA | 303-2288 | [77] |
| Sulfonated PBI | Dense FS | Acetic acid/water (50/50 wt%) | 60 | 207 | 4140 | 5461 | [78] |
| PBI | Dense FS | Isopropanol/water (70/30 wt%) | 70 | 137 | 5480 | 106 | [79] |
| Chitosan-modified PBI | Dense FS | Isopropanol/water (70/30 wt%) | 70 | 250 | 10,000 | 108 | [79] |

**TABLE 6.1** Selected Polymeric Membranes for Solvent Dehydration—cont'd

| Membranes | Configuration | Feed | Temperature (°C) | Flux (g m$^{-2}$ h$^{-1}$) | Normalized flux (g µm m$^{-2}$ h$^{-1}$) | Separation factor (water/ solvent) | Ref. |
|---|---|---|---|---|---|---|---|
| Thermally rearranged PBO | Dense FS | Ethanol/water (90/10 wt%) | 25 | 42 | NA | 56 | [80] |
| Thermally rearranged PBO | Dense FS | Isopropanol/water (90/10 wt%) | 80 | 135 | 3375 | 171 | [80] |
| Thermally rearranged PBO | Dense FS | $n$-Butanol/water (90/10 wt%) | 80 | 58 | 1450 | 441 | [80] |
| Poly[(methylene-bisanthranilamide) 4,4′-diphenyloxidicarboxylic acid] (precursor) | Dense FS | Isopropanol/water (90/10 wt%) | 50 | 60 | 1200 | 140 | [81] |
| Poly(benz-3,1-oxazinone-4) | Dense FS | Isopropanol/water (90/10 wt%) | 50 | 3 | 60 | 9000 | [81] |
| *POLYAMIDE* | | | | | | | |
| TAEA-TMC polyamide/mPAN | FS | Ethanol/water (90/10 wt%) | 25 | 1151 | NA | 1491 | [82] |
| HPEI-2K-TMC polyamide/ Torlon | HF | Isopropanol/water (85/15 wt%) | 50 | 1282 | NA | 624 | [56] |
| (MPD-TMC) polyamide/ceramic with HPEI pretreatment and PDMS coating. | HF | Isopropanol/water (85/15 wt%) | 50 | 2190 | NA | 2800 | [61] |

| HGOTMS grafted HEPI-2K-TMC polyamide/Ultem | HF | Isopropanol/water (85/15 wt%) | 50 | 3121 | NA | 467 | [83] |
|---|---|---|---|---|---|---|---|
| HPEI/MPD-TMC polyamide/ Ultem tri-bore hollow fiber | HF | Isopropanol/water (85/15 wt%) | 50 | 2647 | NA | 261 | [50] |
| MPD-TMC polyamide/modified PVDF | HF | Ethanol/water (85/15 wt%) | 50 | 1288 | NA | 40 | [84] |
| HPEI-TMC polyamide/PES with polydopamine pre- and postcoating | FS | Ethylene glycol/ water (80.8/19.2 wt%) | 38 | 429 | NA | 196 | [85] |
| **PERFLUORO POLYMERS** | | | | | | | |
| Perfluorodimethyldioxole-tetrafluoroethylene (PDD-TFE) copolymer | FS | Hydrogen peroxide/ water (43/57 wt%) | 25 | 61.5 | 6765 | 12 | [86] |
| Perfluoro-2,2-dimethyl-1,1,3-dioxole copolymerized with tetrafluoroethylene | Dense FS | N,N-Dimethylformamide/ water (90/10 wt%) | 50 | 77 | 1925 | 12,500 | [87] |
| Perfluoro-2,2-dimethyl-1,1,3-dioxole copolymerized with tetrafluoroethylene (CMS-3) | Dense FS | N,N-Dimethylacetamide/ water (90/10 wt%) | 50 | 9.1 | 227.5 | 1500 | [87] |
| Perfluoro-2,2-dimethyl-1,1,3-dioxole copolymerized with tetrafluoroethylene | Dense FS | N,N-Dimethylsulfoxide/ water (90/10 wt%) | 50 | 8.1 | 202.5 | 1500 | [87] |
| Hyflon AD/cellulose ester | FS | Ethanol/water (90.2/9.8 wt%) | 75 | 1746 | NA | 409 | [3] |

*Continued*

**TABLE 6.1** Selected Polymeric Membranes for Solvent Dehydration—cont'd

| Membranes | Configuration | Feed | Temperature (°C) | Flux (g m$^{-2}$ h$^{-1}$) | Normalized flux (g μm m$^{-2}$ h$^{-1}$) | Separation factor (water/solvent) | Ref. |
|---|---|---|---|---|---|---|---|
| Hyflon AD60X/PVDF | FS | n-Butanol/water (95/5 wt%) | 20 | 156 | NA | 1564 | [88] |
| Perfluoro-2,2-dimethyl-1,1,3-dioxole copolymerized with tetrafluoroethylene (CMS-3) | Dense FS | Acetone/ethanol/n-butanol/water (27.7/5.3/56.2/10.8 wt%) | 50 | 33 | 825 | 200, 1000, 5200 | [89] |
| Perfluoro-2,2-dimethyl-1,1,3-dioxole copolymerized with tetrafluoroethylene (CMS-3) | Dense FS | Ethylene glycol/water (80.8/19.2 wt%) | 30 | 24.1 | 603 | 2419 | [89] |

*Note*: *HF*, hollow fiber; *FS*, flat sheet; *NA*, not available; *HPEI*, hyperbranched polyethyleneimine; *GA*, glyoxylic acid; *BA*, benzaldehyde; *TAEA*, tris(2-aminoethyl)amine; *EDA*, ethylene diamine; *PIM*, polymers of intrinsic microporosity; *cPIM-1*, carboxylated PIM-1; *hPIM-1*, hydrolyzed PIM-1; *6FDA*, 4,4′-(hexafluoroisopropylidene) diphthalic anhydride; *NDA*, naphthalene diamine; *DABA*, 3,5-diaminobenzoic acid; *HAB*, 3,3′-dihydroxybenzidine diamine; *PI*, polyimide; *SPI*, sulfonated polyimide; *POSS*, polyoctahedral oligomeric silsequioxanes; *PBI*, polybenzimidazole; *PBO*, polybenzoxazole; *mPAN*, modified polyacrylonitrile; *TMC*, trimesoyl chloride; *MPD*, *m*-phenylenediamine; *PDMS*, polydimethylsiloxane; *PVDF*, poly(vinylidene fluoride).
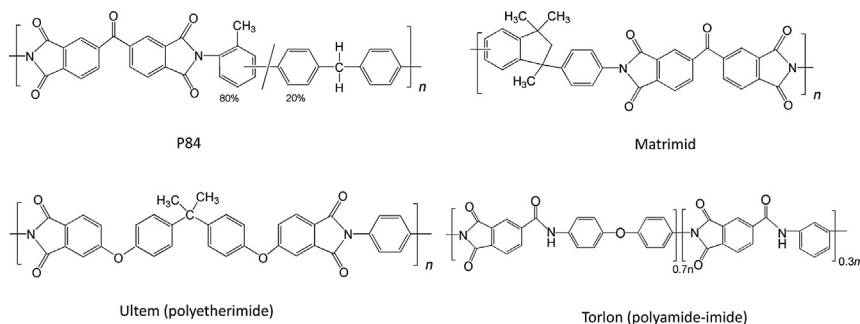
**FIG. 6.5** The chemical structures of commercial polyimides P84, Matrimid, Ultem, and Torlon.

mechanical stabilities, high water selectivity, and less degree of swelling compared with hydrophilic polymers such as polyvinyl alcohol [10, 91, 93]. Because the development of polyimide membranes for pervaporation has been extensively reviewed [10], only the recent ones will be introduced here. Fig. 6.5 shows the chemical structures of four commercially available polyimide materials. They are P84, Matrimid, Ultem, and Torlon. Both their pristine and modified polymers have been studied extensively for pervaporation dehydration. Hua et al. studied Torlon and Ultem hollow fibers and proposed a universal approach consisting of hyperbranched polyethyleneimine (HPEI) pretreatment and aldehyde modification to improve their separation factors and fluxes for the dehydration of isopropanol [70]. To develop the polyimide membrane suitable for the dehydration of acetone (i.e., a harsh organic solvent), Madgindaan et al. used tripodal amine and ethylenediamine to crosslink the P84 asymmetric membranes using liquid immersion and vapor crosslinking methods, respectively [14, 71]. The former resulted in membranes with a high separation factor and a reasonable flux while the latter achieved a high flux and a reasonable separation factor. Besides, polymers of intrinsic microporosity (PIM) and their derivatives such as carboxylated PIM-1, hydrolyzed PIM-1 as well as their blends with P84 have been explored for alcohol dehydration [72, 73]. Results showed that by optimizing the blending ratio, one might obtain both good flux and separation factor simultaneously. It is worth noting that the commercial polyimide materials also serve as excellent substrates when developing composite membranes for pervaporation, which will be mentioned below.

Besides the modifications of commercially available polyimide materials, researchers also designed and synthesized new polyimides for pervaporation membranes based on the reaction between the bifunctional carboxylic acid anhydrides and primary diamines. Le et al. synthesized copoly(1,5-naphthalene/3,5-benzoic acid-2,2′-bis(3,4-dicarboxyphenyl)

6FDA (dianhydride)　　　　HAB (diamine)　　　　DABA (diamine)

Durene (diamine)　　　NDA (diamine)
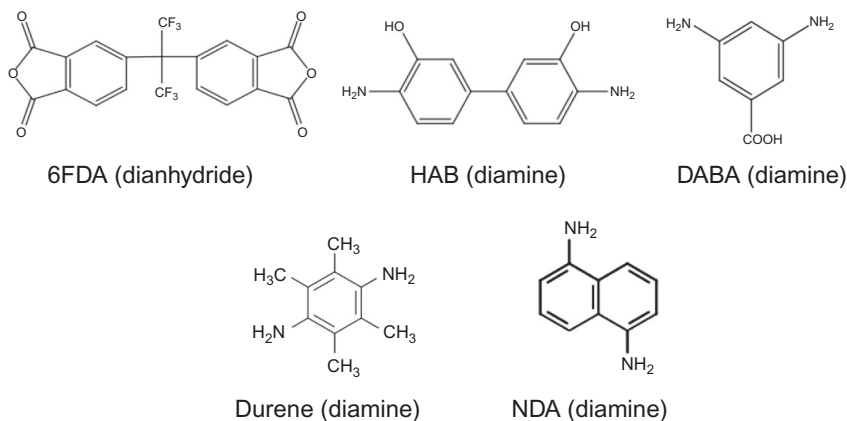
FIG. 6.6　The chemical structures of monomers involved in polyimide synthesis, such as 6FDA (4,4'-(hexafluoroisopropylidene) diphthalic anhydride), HAB (3,3'-dihydroxybenzidine diamine), DABA (3,5-diaminobenzoic acid), durene (2,3,5,6-tetramethyl-1,4-phenylenediamine), NDA (naphthalene diamine).

hexafluoropropanedimide (6FDA-NDA/DABA) and further modified it with various crosslinking methods, including thermal, diamino and diol cross-linking modifications [74]. The developed dense membranes showed good antiswelling properties and separation performance for ethanol dehydration. Later, they further synthesized a sulfonated 6FDA-NDA/DABA polyimide and used it as a water-selective layer in the sulfonated 6FDA-NDA/DABA polyimide/Ultem dual-layer hollow fiber membranes for ethanol dehydration [75]. A surface modification using polyhedral oligosilsesquioxane (POSS) particles was employed to enhance the antiswelling property. Salehian et al. developed pervaporation membranes for isopropanol dehydration via synthesizing a 6FDA-durene-DABA polyimide, adjusting the membrane pore size by cross-linking it with the aid of iron(III) acetylacetonate and post thermal treatment [94]. Xu et al. synthesized a new polyimide precursor by the polycondensation of three monomers; namely, 6FDA, 3,3'-dihydroxybenzidine diamine (HAB) and DABA, followed by a thermal crosslinking to form poly(benzoxazol-co-imide). This material showed impressive results for isopropanol dehydration [76]. Fig. 6.6 depicts the chemical structures of monomers involved in the aforementioned polyimide syntheses.

### 6.4.1.3 Membranes From Other Aromatic Polymers

Other aromatic polymers such as polybenzimidazole (PBI), polybenzoxazole (PBO), and polybenzoxazinone (PBOZ) have also shown great potential in solvent dehydration due to their excellent chemical and
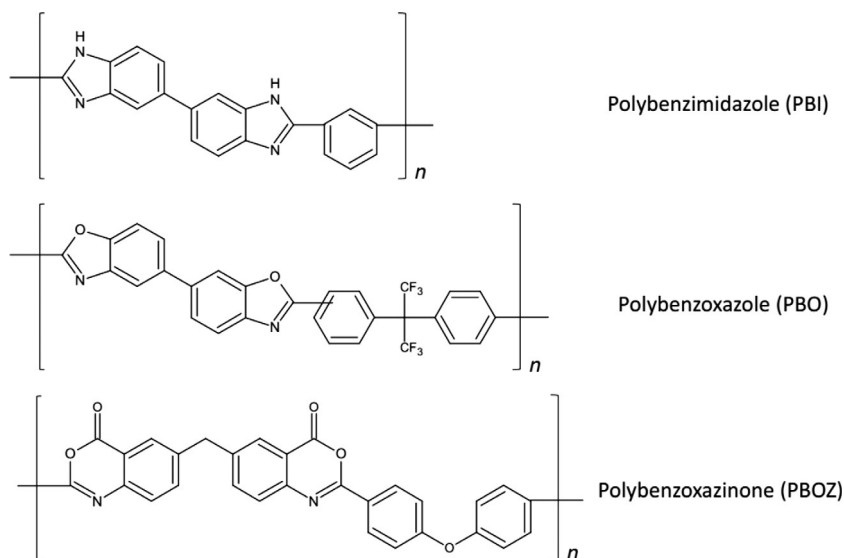
**FIG. 6.7** The chemical structures of PBI, PBO, and PBOZ.

thermal resistance. Fig. 6.7 shows their chemical structures. The PBI-based pervaporation membranes were pioneered by Chung's group. They developed PBI and sulfonated PBI membranes in the forms of flat-sheet and hollow fiber configurations for dehydration of various solvents such as alcohols, glycols, acetone and acetic acid [77, 78, 95]. Besides, Han et al. improved the dehydration performance of PBI membranes by modifying their surfaces with hydrophilic chitosan for isopropanol (IPA) dehydration [79]. In contrast, both PBO and PBOZ membranes were synthesized by the thermal rearrangement process from their respective precursors [76, 80, 81]. Ong et al. and Xu et al. reported that both thermally rearranged PBO and poly(benzoxazole-co-imide) exhibited stable separation performance in IPA dehydration for more than 200 h [76, 80] whereas Pulyalina et al. found that the PBOZ showed effectiveness in dehydration of water-isopropanol mixtures with a high separation factor [81].

### 6.4.1.4 Polyamide Membranes

Polyamides known as nylon are a group of heat-resistant materials with good chemical and mechanical stability. They can be synthesized by step-growth polymerization, such as interfacial polymerization. However, their dense membranes exhibit an extremely low permeability [96]. Therefore, a thin-film polyamide is usually synthesized on top of membrane supports via interfacial polymerization and the resultant membranes are often referred to as thin-film composite (TFC) membranes, as introduced in Section 6.3.3.2 and Fig. 6.4. In recent years, polyamide based

Aqueous phase monomers:



MPD          MPDSA          TAEA          HPEI
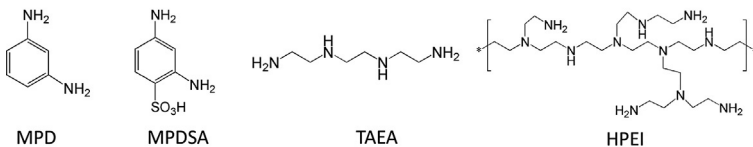
(A)

Organic phase monomers:



NTAC          TMC          TBAC          TDI
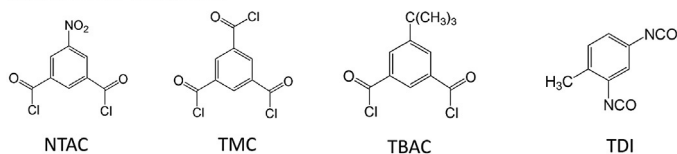
(B)

**FIG. 6.8**    The chemical structures of (A) aqueous phase monomers and (B) organic phase monomers for interfacial polymerization.

TFC membranes have emerged as a great candidate for dehydration of organics via pervaporation. Most of these studies focused on interfacial polymerization as functions of monomer types, substrates, pretreatment and posttreatment conditions [11, 50, 56–58, 61, 62, 82, 84, 85, 97–99]. Some typical monomers in both aqueous and organic phases for interfacial polymerization are shown in Fig. 6.8. A detailed review on recent development of TFC membranes for pervaporation can be found in the literature [2].

### 6.4.1.5 Membranes From Perfluoro Polymers

Amorphous, solvent-processable perfluoro polymers (PFPs) such as Teflon AF, Cytop, and Hyflon AD are another family of promising membrane materials developed in the past 30 years [23, 100–106]. Fig. 6.9 illustrates their chemical structures. Because they have extraordinary thermal and chemical resistance, they are unaffected by most aggressive chemicals including acids, bases, organic solvents, oils and strong oxidizers [107]. PFPs have been explored by several research groups to



Teflon AF (DuPont, USA)          Hyflon AD (Ausimont, Italy)          Cytop (Asahi Glass, Japan)
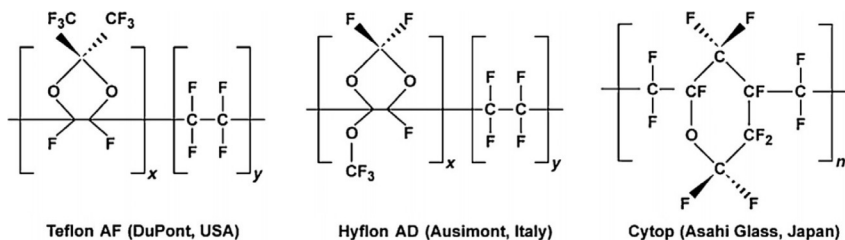
**FIG. 6.9**    The chemical structures and trade names of commercial perfluoro polymers [3]. *Reprinted with permission from American Chemical Society.*

dehydrate solvents including alcohols, acetone, *N,N*-dimethylformamide, *N,N*-dimethylsulfoxide, *N,N*-dimethylacetamide, and hydrogen peroxide [3, 86–89, 108–111]. Despite their intrinsic super-hydrophobicity, the size exclusion mechanism has been considered as the dominant separation mechanism for these amorphous perfluoropolymer membranes in dehydration applications [111].

In summary, these rigid polymeric membranes show outstanding antiswelling properties and excellent selectivity; however, they normally have a low water permeability, which could be overcome by making the selective layer ultra-thin (≤100 nm) or blending them with other polymers or inorganic fillers to enhance the free volume.

### 6.4.1.6 Mixed Matrix Membranes (MMMs)

Most commercialized inorganic membranes are made from zeolites [112–114], silica [115–117], and ceramic [118, 119]. Other inorganic materials such as carbon [120, 121] and graphene oxide [122–127] are still at the stage of research. Normally the commercial inorganic membranes possess a flux several times higher than polymeric membranes and also have a superior selectivity [116, 117, 128]. However, their production costs are more expensive than those of polymeric membranes. Moreover, they also show limitations such as poor stability in harsh feeds and difficulties in scale-up. For example, zeolite membranes cannot withstand acid environments whereas carbon and graphene oxide membranes have difficulties of being scaled up.

Therefore, the concept of MMMs was proposed in the mid-1980s to combine the strengths of both polymeric and inorganic materials in membranes to overcome their limitations [129, 130]. Afterward, various types of inorganic fillers have been incorporated into the polymeric matrix to enhance the dehydration performance of polymeric membranes, including zeolites [131, 132], silicalite [133, 134], metal oxide [135], carbon nanotubes [136], and MOFs [16, 17]. The effects of inorganic fillers on MMMs are various. Some reported a flux enhancement but sacrificed the separation factor, while others observed enhancements in both flux and separation factor. The differences resulted from several aspects, including the interfacial voids between inorganic fillers and the polymeric matrix, the hydrophilic nature of fillers, the pore size and porosity of fillers, and the rigidification of polymer chains by fillers [17, 137, 138]. Normally, larger voids result in a higher permeability but a lower selectivity, while fillers with a right pore size and good compatibility with the polymer matrix lead to better separation performance.

Achieving a homogeneous dispersion of inorganic fillers in the polymer matrix is a big challenge in developing MMMs. The agglomeration of inorganic fillers causes defects in membranes and reduces the selectivity. To improve the filler dispersion and enhance the MMM performance, several methods could be tried: (1) Controlling the filler size to be less than

100 nm [139]; (2) Modifying the fillers with agents that induce strong bonding with the polymer matrix [140]; (3) Coating the fillers with a thin-layer of charged polymer [17, 138]; (4) Using less rigid fillers which contain both organic and inorganic components such as polyhedral oligomeric silsesquioxane [141, 142] and MOFs [16, 143]. Separation performance of MMMs for solvent dehydration has been summarized in recent review papers [2, 40]. Therefore, Table 6.2 only shows some of the most recently developed ones. MOFs particles are emerging as very popular fillers in MMMs due to their highly porous structure, high surface area, and flexibility, which help enhance the free volume of polymeric materials. Not only do they improve permeability, but also some of them enhance the selectivity.

## 6.4.2 Removal of Organics From Aqueous Solutions

Removal of organics from a dilute aqueous solution is a minor application of pervaporation. It includes (1) the removal of a trace amount of VOCs from wastewater for environmental protection [149, 150]; (2) the recovery of valuable organics from aqueous solutions such as natural aroma recovery from the food industries using organophilic pervaporation [151, 152]; and (3) the removal of butanol from acetone-butanol-ethanol fermentation broths that not only reduces the inhibitory effect from butanol but also improve the productivity of ethanol and acetone via a continuous production flow. Contrary to dehydration of organics, the removal of organics from aqueous solutions requires membranes made from organophilic materials which prefer the permeation of organic compounds.

### 6.4.2.1 Hydrophobic Polymeric Membranes

PDMS, commonly known as silicon rubber, is the most widely studied hydrophobic material and often regarded as the benchmark material for the removal of organics. Besides PDMS, other hydrophobic materials have also been studied. They are polyoctylmethyl siloxane (POMS) [153] and polymethylphenylsiloxane (PMPS) [154, 155], PEBA [20, 21, 156–159], fluoropolymers like polyvinylidene fluoride (PVDF) [24, 160–162] and PTFE [161, 162], poly(3-hydroxybutyrate) (PHB) [163], poly(1-trimethylsilyl-1-propyne) (PTMSP) [19, 164], and polymers of intrinsic microporosity (PIMs) [22, 165], etc. Fig. 6.10 depicts their chemical structures. Table 6.3 shows some selected polymeric membranes developed in recent years for organic/organic separation via pervaporationin. Among them, the silicone rubber based membranes are prepared via crosslinking process, their permeation fluxes are usually low. The PEBA membranes can be prepared easily because of no crosslinking reaction; they show a high solvent

TABLE 6.2 Selected MMMs for Solvent Dehydration

| MMM | | Filler loading (wt%) | Configuration | Feed mixture | Temperature (°C) | Total flux (g m$^{-2}$ h$^{-1}$) | Normalized flux (g µm m$^{-2}$ h$^{-1}$) | Separation factor (organic/water) | Ref. |
|---|---|---|---|---|---|---|---|---|---|
| Polymer | Filler | | | | | | | | |
| PBI | ZIF-8 | 33.7 | Dense FS | Isopropanol/water (85/15 wt%) | 60 | 103 | 5150 | 1686 | [16] |
| PVA | H-ZSM5 | 7 | Dense FS | Isopropanol/water (90/10 wt%) | 30 | 144–138 | 7200–6900 | 568–334 | [144] |
| PVA | H-ZSM5 | 7 | Dense FS | Ethanol/water (96/4 wt%) | 30 | 125–118 | 6250–5900 | 349–236 | [144] |
| P84 | SPES primed ZIF-90 | 30 | Dense FS | Isopropanol/water (85/15 wt%) | 60 | 109 | 2398 | 5668 | [17] |
| 6FDA-HAB/DABA polyimide | UIO-66 | 30 | Dense FS | Isopropanol/water (85/15 wt%) | 60 | 190 | 4750 | 1883 | [18] |
| 6FDA-HAB/DABA polyimide | UIO-66 | 30 | Dense FS | n-Butanol/water (85/15 wt%) | 60 | 150 | 4500 | 5661 | [18] |

**TABLE 6.2** Selected MMMs for Solvent Dehydration—cont'd

| MMM | | Filler loading (wt%) | Configuration | Feed mixture | Temperature (°C) | Total flux (g m$^{-2}$ h$^{-1}$) | Normalized flux (g μm m$^{-2}$ h$^{-1}$) | Separation factor (organic/water) | Ref. |
|---|---|---|---|---|---|---|---|---|---|
| Polymer | Filler | | | | | | | | |
| PVA | ZIF-8-NH$_2$ | 7.5 | | Ethanol/water (96/4 wt%) | 50 | 158 | 2370 | 148 | [145] |
| 6FDA polyimide | Ammonia functionalized graphene oxide | 0.5 | Dense FS | Isopropanol/water (85/15 wt%) | 60 | 161.5 | 4038 | >5000 | [146] |
| Chitosan | ZIF-8 | 5 | Dense FS | Isopropanol/water (85/15 wt%) | 30 | 410 | 20,500 | 723 | [147] |
| PVA | Polydopamine coated SO$_3$H-MIL-101-Cr | 30 | Dense FS | Ethylene glycol/water (90/10 wt%) | 30 | 325 | 1300 | 4700 | [148] |

*Note*: *HF*, hollow fiber; *FS*, flat sheet; *PBI*, polybenzimidazole; *ZIF*, zeolitic imidazolate framework; *PVA*, poly(vinyl alcohol); *6FDA*, 4,4′-(hexafluoroisopropylidene) diphthalic anhydride; *HAB*, 3,3′-dihydroxybenzidine diamine; *DABA*, 3,5-diaminobenzoic acid.
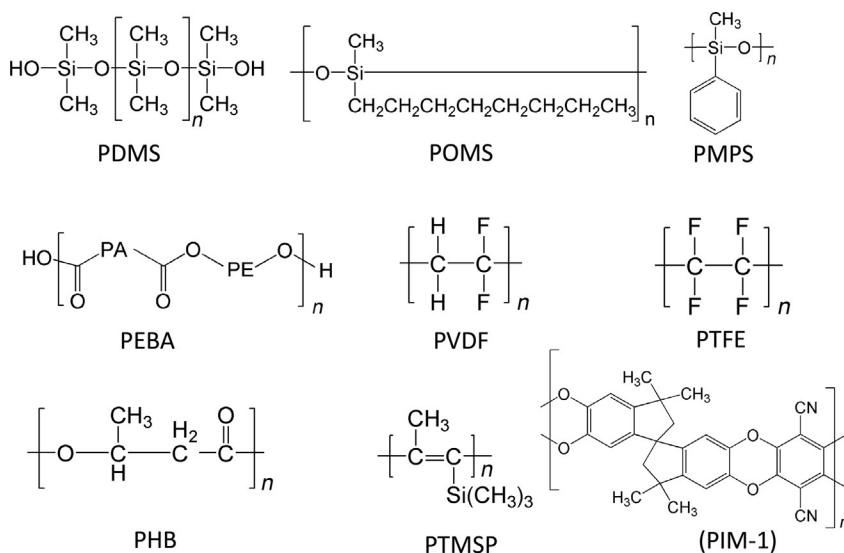
FIG. 6.10  Hydrophobic polymers applied in recovery of organics via pervaporation process: *PDMS*, polydimethylsiloxane; *POMS*, polyoctylmethyl siloxane; *PMPS*, polymethylphenylsiloxane; *PEBA*, polyetherblock-polyamides; *PVDF*, polyvinylidene fluoride; *PTFE*, polytetrafluoroethylene; *PHB*, poly(3-hydroxybutyrate); *PTMSP*, poly(1-trimethylsilyl-1-propyne); *PIM-1*, polymer of intrinsic microporosity-1.

permeability [20, 156]. The fluoropolymer membranes possess very good stability and good permeability [24, 161, 162, 166]. Other hydrophobic polymers such as PTMSP and PIMs also exhibit a high permeability due to their high free volumes [22, 165].

Because the available hydrophobic materials for recovery applications are still limited, substantial researches have been conducted to improve the existing pervaporation membranes by modifying their fabrication processes. Taking PDMS as an example, one may change its viscosity and solution composition as well as substrates properties (i.e., pore size, porosity, etc.) to improve the overall performance of composite membranes. Moreover, researchers have also made efforts to develop new materials for organic recovery. Grimaldi et al. prepared a new class of easy-to-synthesize polymeric membranes comprising hydrophobic brush-like structures as a selective layer by grafting hydrophobic vinyl monomers on light-sensitive poly(ether sulfone) nanofiltration support membranes [167]. Kim et al. synthesized block and random copolymers of norbornene monomers bearing hydroxyhexafluoroisopropyl and *n*-butyl substituents via living vinyl addition polymerization and made them into selective layers of thin film composite membranes for *n*-butanol concentration [168]. Huang and coworks developed polyurethane based interpenetrating polymer network membranes for butanol recovery [169, 170].

**TABLE 6.3**  Selected Polymeric Membranes for Solvent Recovery

| Membranes | Configuration | Organic in aqueous feed | Temperature (°C) | Total flux (g m$^{-2}$ h$^{-1}$) | Normalized flux (g μm m$^{-2}$ h$^{-1}$) | Separation factor (organic/water) | Ref. |
|---|---|---|---|---|---|---|---|
| PMPS | FS | Furfural/water (1/99 wt%) | 80 | 46 | NA | 28 | [154] |
| PEBA | Dense FS | Ethanol/water (5/95 wt%) | 25 | 80 | 1600 | 5 | [20] |
| PVDF | HF | Ethanol/water (5/95 wt%) | 50 | 3500–8800 | NA | 5–8 | [24] |
| PDMS | FS | Acetonitrile/ water (5/95 wt%) | 50 | 4800 | NA | 3 | [161] |
| PVDF | FS | Acetonitrile/ water (5/95 wt%) | 50 | 12,000 | NA | 5 | [161] |
| PTFE | FS | Acetonitrile/ water (5/95 wt%) | 50 | 20,000 | NA | 10 | [161] |
| P(VDF-HFP) | FS | Ethyl acetate/ water (5/95 wt%) | 45 | 433 | NA | 76 | [166] |
| PIM-1 | Dense FS | Ethyl acetate/ water (1/99 mol%) | 30 | 1362.068966 | 39,500 | 189 | [165] |

*Note*: *HF*, hollow fiber; *FS*, flat sheet; *NA*, not available; *PMPS*, polymethylphenylsiloxane; *PEBA*, polyether block amide; *PVDF*, poly(vinylidene fluoride); *PDMS*, polydimethylsiloxane; *PTFE*, polytetrafluoroethylene; *P(VDF-HFP)*, poly(vinylidenefluoride-co-hexafluoropropylene); *PIM*, polymers of intrinsic microporosity.

### 6.4.2.2 MMMs

Because the available polymeric membranes for the removal of organics are limited, and the cost of high-performance inorganic membranes is high [67], fabricating organophilic MMMs is an effective way to enhance the separation performance of hydrophobic polymeric membranes via increasing their free volumes or adsorption capacities of organics. Several types of inorganic particles have been explored as fillers, including hydrophobic zeolites such as ZSM-5 [157] and silicalite-1 with or without modifications [31, 158, 171–173], silica [19, 174], POSS [20], hydrophobic MOFs such as ZIF-7 [29], ZIF-8 [154, 155, 175–178], ZIF-71 [21] and MIL-53 [179], carbon nanotubes [30, 180], as well as graphene [22, 181], etc. Table 6.4 summarizes their MMM performance for organic recovery.

## 6.4.3 Organic/Organic Separation Membranes

The development of pervaporation membranes for organic/organic separation is the most challenging. This may be due to the lack of robust membrane materials as well as the modules that can withstand the long-term exposure to organic solvents. The primary applications in organic-organic separation are summarized in Fig. 6.11. A detailed review regarding the background of this application was provided by Smitha et al. [7]. Recent studies in this application have focused on the separation of mixtures such as aromatic/aliphatic, alcohols/tertiary butyl ethers, and removal of sulfur compounds from gasoline.

### 6.4.3.1 Polymeric Membranes

A series of rubbery and glassy polymeric materials have been explored for the separation of aromatic/aliphatic mixtures. Table 6.5 tabulates some of their performance. Among them, polyimides draw much attention due to their good stability [34, 182–185], followed by rubbery materials such as PEBA and styrene-butadiene rubber, poly(γ-benzyl-l-glutamate) [186–188]. Moreover, several blend membranes also exhibit good separation performance, such as blends of polyimide/polybenzimidazole, ionic liquids/polyurethane, poly(vinyl chloride)/polystyrene, soft segments materials/waterborne polyurethane, carboxymethyl cellulose and sodium alginate [34, 182, 189–192].

On the other hand, polymeric membranes were employed to separate methanol/methyl *tert*-butyl ether (MeOH/MTBE) and ethanol/ethyl *tert*-butyl ether (EtOH/ETBE) mixtures. Billy et al. fabricated membranes for EtOH/ETBE separation by grafting poly(methyl diethylene glycol methacrylate) onto cellulose acetate [193]. Zereshki et al. incorporated cardo (lactone) groups into the backbone of PEEK to reduce its crystallinity and employed the modified PEEK membrane for MeOH/MTBE

**TABLE 6.4** MMMs Developed for the Removal of Organics From Aqueous Solutions

| MMM | | Filler loading (wt%) | Configuration | Organic in aqueous feed | Temperature (°C) | Total flux (g m$^{-2}$ h$^{-1}$) | Separation factor (organic/ water) | Ref. |
|---|---|---|---|---|---|---|---|---|
| Polymer | Filler | | | | | | | |
| PDMS | Trimethylsilanol hydrophobized silica | 3 | FS | Isopropanol/ water (4/96 wt%) | 50 | 405 | 31.7 | [174] |
| | | | | Ethanol/water (4/96 wt%) | | 329 | 26 | |
| PTMSP | Cab-O-Sil TS 530 hydrophobic silica | 25 | FS | Ethanol/water (5/95 wt%) | 50 | 9500 | 18.3 | [19] |
| | | | | n-Butanol water (5/95 wt%) | | 9500 | 104 | |
| PEBA 2533 | POSS (AL0136) | 2 | FS | Ethanol water (5/95 wt%) | 25 | 183.5 | 4.6 | [20] |
| | | | | | 65 | 427 | 5.7 | |
| PEBA 2533 | ZSM-5 zeolite | 5 | FS | n-Butanol/water (2.5/97.5 wt%) | 35 | 392 | 30 | [157] |
| PEBA 2533 | MCM-41 | 2 | FS | n-Butanol/water (2.5/97.5 wt%) | 35 | 500 | 25 | [158] |
| PIM | Amine-functionalized graphene oxide | 0.5 | FS | Ethanol/water (5/95 wt%) | 65 | 2000 | 7 | [22] |
| | | | | n-Butanol/water (5/95 wt%) | | 2000 | 40 | |
| PDMS | Silicalite-1 | 30 | FS | Ethanol/water (4/96 wt%) | 25 | 171 | 15.7 | [171] |
| | | | | | 65 | 811 | 11.6 | |

| PDMS | Hollow silicalite sphere | 30 | FS | Ethanol/water (6/94 wt%) | 40 | 71.6 | 1.3 | [172] |
|---|---|---|---|---|---|---|---|---|
| Vinyl terminated RTV 615 PDMS | Vinyltriethoxysilane-grafted-silicalite-1 | NA | FS | Methanol/water (10.5/89.5 wt%) | 65 | 535 | 10 | [173] |
| Thin film vinyl terminated RTV 615 PDMS/PAN ultrafiltration membrane | Vinyltriethoxysilane-grafted-silicalite-1 | 50 | FS | Ethanol/ fermentation broth containing yeast cells (7.5/92.5 wt%) | 35 | 270 | 17.5 | [31] |
| PMPS | ZIF-7 | 10 | FS | Isobutanol/water (3/97 wt%) | 80 | 8600 | 34.9 | [175] |
|  | ZIF-8 |  |  | Isobutanol/water (1/99 wt%) |  | 6400 | 40.1 |  |
| PMPS | ZIF-8 | 10 | FS | Isobutanol/water (3/97 wt%) | 80 | 4453 | 35.0 | [155] |
|  | Modified ZIF-8 |  |  |  |  | 4453 | 44.7 |  |
| PMPS/ hierarchically ordered stainless-steel-mesh | ZIF-8 | 41.3 | FS | Furfural/water (1/99 wt%) | 80 | 900 | 53.3 | [154] |
| PEBA 2533 | ZIF-71 | 20 | FS | Model fermentation broth: 0.6 wt% acetone, 1.2 wt% butanol, 0.2 wt% ethanol | 37 | 520 | 18.8 (butanol) | [21] |
| PDMS/ polysulfone substrate | ZIF-8 | 50 | FS | n-Butanol/water (5/95 wt%) | 80 | 2800 | 52.8 | [176] |

**TABLE 6.4** MMMs Developed for the Removal of Organics From Aqueous Solutions—cont'd

| MMM | | Filler loading (wt%) | Configuration | Organic in aqueous feed | Temperature (°C) | Total flux (g m$^{-2}$ h$^{-1}$) | Separation factor (organic/water) | Ref. |
|---|---|---|---|---|---|---|---|---|
| Polymer | Filler | | | | | | | |
| PDMS/polysulfone substrate | ZIF-8 | 40 | FS | $n$-Butanol/water (1/99 wt%) | 80 | 4846 | 81.6 | [177] |
| PDMS/polysulfone substrate | MIL-53 | 40 | FS | Ethanol/water (5/95 wt%) | 70 | 5467 | 11.1 | [179] |
| PDMS/PVDF membrane | ZIF-7 | 20 | FS | $n$-Butanol/water (1/99 wt%) | 60 | 1689 | 66 | [29] |
| PEBA-2533 | ZIF-8 | 10 | FS | Phenol/water (0.8/99.2 vol%) | 70 | 1310 | 53 | [178] |
| PDMS | Carbon nanotubes | 10 | FS | $n$-Butanol/water (1.5/98.5 wt%) | 37 | 244 | 32.9 | [30] |
| PDMS | Carbon nanotubes | 10 | FS | Ethanol/water (8/92 wt%) | 60 | 128.7 | 8.2 | [180] |
| PEBA | Graphene | 1.5 | FS | Isopropanol/water (4/96 wt%) | 50 | 248.5 | 10 | [181] |

*Note*: *HF*, hollow fiber; *FS*, flat sheet; *PDMS*, polydimethylsiloxane; *PTMSP*, poly(1-trimethylsilyl-1-propyne); *PEBA*, polyether block amide; *PIM*, polymers of intrinsic microporosity; *PMPS*, polymethylphenylsiloxane; *POSS*, polyhedral oligosilsesquioxane; *PVDF*, poly(vinylidene fluoride); *ZIF*, zeolitic imidazolate framework.

```
┌─────────────────────────────────────────────┐
│        Major categories of organic mixtures   │
└─────────────────────────────────────────────┘
```

| Polar/nonpolar | Aromatic/aliphatic | Aromatic/alicyclic | Isomers |

e.g.

e.g.

e.g.

e.g.

Benzene/*i*-octane
Benzene/*n*-heptane
Toluene/*n*-octane
Toluene/*n*-heptane

Benzene/cyclohexane
Toluene/cyclohexane

Methanol/toluene
Ethanol/benzene
*i*-Propanol/toluene
Methanol/MTBE
Ethanol/ETBE

Isomeric xylenes,
*n/i* Heptane
*n*-Propanol/*i*-propanol
$C_4$–$C_8$ isomers
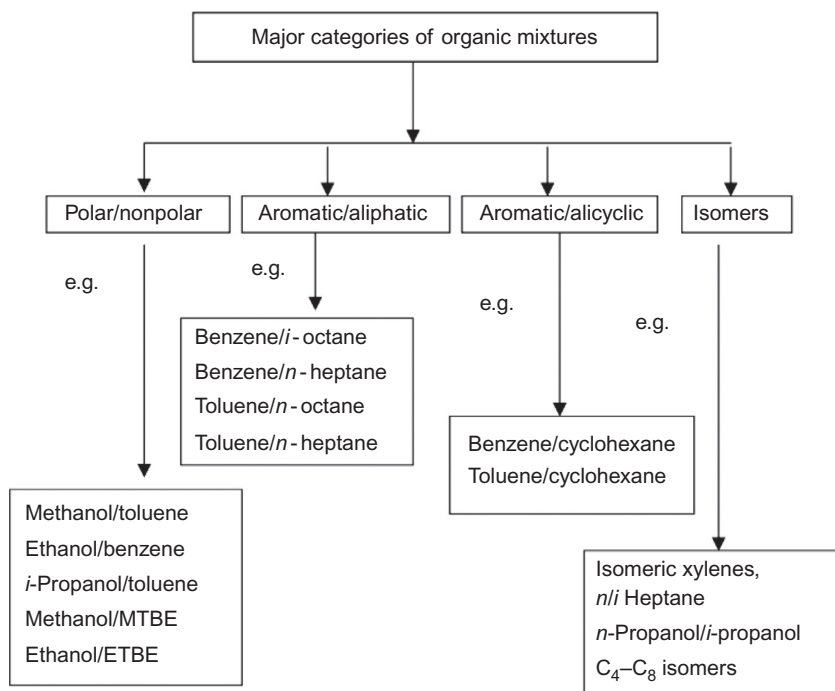
FIG. 6.11   Major applications of pervaporation process in organic-organic separation [7]. *Reprinted with permission from Elsevier.*

separation [35]. Liu's group studied the material consisting of polyary-lethersulfone and cardo (PES-C) for MeOH/MTBE separation [194]. It showed high separation factors but low permeation fluxes. They further blended it with poly(vinyl pyrrolidone) or sulfonating polymer to enhance the flux [195, 196]. Besides, they also developed polyelectrolyte complex membranes based on SPES-C and polyethyleneimine for this application with an enhanced flux [197].

Because the Environmental Protection Agency in the United States would lower the sulfur content in gasoline to a maximum of only 10 ppm in its Tier 3 program beginning in 2017 [198], it has pushed the application of pervaporation for gasoline desulfurization. For example, polyimide membranes and PEBA/PVDF composite membranes were developed for this application [199, 200].

In addition to these three applications, viz., MeOH/MTBE, EtOH/ETBE and gasoline desulfurization, there are also several other organic/organic mixtures to separate. Ong et al. developed PVDF membranes suitable for bioalcohol (ethanol/acetone) separation [201]. Polyamide-6 membranes were explored for separating methanol from methylacetate

**TABLE 6.5** Polymeric Membranes for Organic/Organic Separation via Pervaporation

| Membranes | Configuration | Feed mixture (A/B) | Temperature (°C) | Flux (g m$^{-2}$ h$^{-1}$) | Normalized flux (g μm m$^{-2}$ h$^{-1}$) | Separation factor (A/B) | Ref. |
|---|---|---|---|---|---|---|---|
| **Aromatic/aliphatic separation** | | | | | | | |
| PI/PBI blend | HF | Toluene/isooctane (50/50 wt%) | 60 | 1350 | NA | 200 | [34] |
| Various synthesized polyimides | FS | Toluene/n-heptane (40/60 wt%) | 80 | NA | 17–19,500 | 1.4–8.1 | [182] |
| | | Benzene/n-heptane (40/60 wt%) | | NA | 9180–16,670 | 2.8–6.0 | |
| Sulfur-containing copolyimide | FS | Toluene/n-decane (60/40 wt%) | 110 | NA | 2500 | 11.8 | [183] |
| | | Toluene/n-decane (80/20 wt%) | 110 | NA | 7000 | 9.3 | |
| Aromatic polyimide | FS | Phenanthrene/n-tetradecane | 120 | 745 | 7580 | 2.8 | [184] |
| Styrene-butadiene rubber | FS | Benzene/cyclohexane (10/90 wt%) | 30 | 901 | 117,130 | 5.78 | [186] |
| | | Benzene/cyclohexane (50/50 wt%) | 30 | 1401 | 182,130 | 1.83 | |
| PEBA/ceramic tubular substrates | Tubular | Toluene/n-heptane (50/50 wt%) | 40 | 65 | 195 | 4.3 | [187] |

| Poly(γ-benzyl-L-glutamate)/poly(amide-imide) support | | Toluene/*n*-heptane (3/97 wt%) | 20 | 110 | 200 | 88 | [188] |
|---|---|---|---|---|---|---|---|
| | | Toluene/*n*-heptane (50/50 wt%) | 40 | 280 | 540 | 3.8 | |
| Sodium alginate/sodium carboxymethyl cellulose blend | FS | Benzene/cyclohexane (19.6/80.4 wt%) | 30 | 1540 | 77,000 | 88.7 | [189] |
| [C4mim]BF4/polyurethane | FS | Benzene/cyclohexane (50/50 wt%) | 45 | 20 | NA | 27.5 | [190] |
| [C4mim]PF6/polyurethane | FS | Benzene/cyclohexane (50/50 wt%) | 45 | 12.5 | NA | 34.4 | |
| Poly(vinyl chloride)/polystyrene blend | FS | Benzene/cyclohexane (10/90 wt%) | 30 | 55 | 3740 | 29 | [191] |
| | | Benzene/cyclohexane (50/50 wt%) | 30 | 96 | 6528 | 16 | |

**Alcohol/tert-butyl ether separation**

| Graft copolymer cellulose acetate-*g*-poly(MDEGMA) | | EtOH/ETBE (20/80%) | 50 | 75.1 | 4355.8 | 67 | [193] |
|---|---|---|---|---|---|---|---|

*Continued*

**TABLE 6.5** Polymeric Membranes for Organic/Organic Separation via Pervaporation—cont'd

| Membranes | Configuration | Feed mixture (A/B) | Temperature (°C) | Flux (g m$^{-2}$ h$^{-1}$) | Normalized flux (g μm m$^{-2}$ h$^{-1}$) | Separation factor (A/B) | Ref. |
|---|---|---|---|---|---|---|---|
| Modified poly(ether ether ketone) | FS | MeOH/MTBE (1–87 wt% MeOH) | 30 | NA | 600–4520 | 254–0.8 | [35] |
| PES-C | FS | MeOH/MTBE (5–40 wt% MeOH) | 40 | 27.5–102 | 1210–4520 | 3124–99.6 | [194] |
| PES-C/poly (vinyl pyrrolidone) blend | FS | MeOH/MTBE (15 wt% MeOH) | 40 | 190 | 3980 | 753.6 | [195] |
| SPES-C | FS | MeOH/MTBE (15 wt% MeOH) | 40 | 153 | 4060 | 1300 | [196] |
| (SPES-C)/PEI polyelectrolyte complex membranes | FS | MeOH/MTBE (15 wt% MeOH) | 40 | 194 | 4753 | 1860 | [197] |
| *Removal of sulfur compounds* | | | | | | | |
| PEBAX 2533/PVDF composite | FS | Thiophene/*n*-heptane (1000 ppm thiophene) | 40 | 3800 | 41,800 | 4 | [199] |
| Polyimide 6FDA-BDAF | FS | Thiophene/*n*-heptane (50-900 ppm thiophene) | 50–90 | 7960–37,610 | NA | 3.1 | [200] |

*Note*: *HF*, hollow fiber; *FS*, flat sheet; *NA*, not available; *PI*, polyimide; *PBI*, polybenzimidazole; *PEBA or PEBAX*, polyether-block-amide; *poly(MDEGMA)*, poly(methyl diethylene glycol methacrylate); *PES-C*, polyarylethersulfone with cardo; *SPES-C*, sulfonated polyethersulfone with cardo; *PEI*, polyethyleneimine; *PVDF*, poly(vinylidene fluoride); *6FDA*, 4,4′-(hexafluoroisopro-pylidene) diphthalic anhydride; *BDAF*, *m*-2,2-bis[4-(4-aminophenoxy) phenyl] hexafluoropropane; *MeOH*, methanol; *EtOH*, ethanol; *MTBE*, methyl *tert*-butyl ether; *ETBE*, ethyl *tert*-butyl ether.

mixture [202]. Ethylene chlorotrifluoroethylene, a type of PFP, was developed as pervaporation membranes using thermally induced phase inversion. This material showed higher affinity to polar solvents than nonpolar solvents and thus was applied for ethanol/cyclohexane separation [203]. However, it is difficult to develop a membrane suitable for all organic/organic mixtures Because different materials have different solvent stability and affinity to the organics. For example, Parvez et al. studied eight types of commercially available membranes (PolyAn GmbH, Germany) for acetate-isooctane mixtures, but found only two of them were preferentially permeable to ethyl acetate and chemically stable in the feed [204].

### 6.4.3.2 MMMs

Again, inorganic materials are applied to enhance the separation performance of polymer materials. The inorganic fillers used in MMMs for organic/organic separation included bentonite [189], CNT [38, 205], graphene oxide [37, 206], graphite [187], carbon [207], MOFs [208], and metal organic polyhedra (MOP), etc. [209, 210]. It is worth noting that MOPs are discrete metal-organic molecular assemblies constructed from metal nodes and organic ligands, which are similar to MOFs. However, MOPs are molecule-based porous materials with a strictly uniform molecule size/shape and are soluble in some solvents. Their molecular surfaces are also easy to be functionalized through ligand modifications. These attractive features of MOPs make them perfect fillers to fabricate high-quality hybrid membranes. Therefore, they have been reported to be good fillers to greatly enhance the performance of organic/organic separation in recent years [209, 210]. Their separation performance is summarized in Table 6.6.

## 6.5  VAPOR PERMEATION

Similar to pervaporation, vapor permeation membranes can be used for dehydration of organics, removal of organics from aqueous solutions, and organic/organic separation. Besides, vapor permeation can also be used to remove water or organic vapors from gas streams. Among these applications, vapor permeation has been mainly applied for dehydration as it can be integrated at the downstream of a distillation column. As such, the membranes need to be stable in organic vapor at high temperatures.

Polyimides have emerged as potential membrane materials for vapor permeation due to their excellent thermal, chemical and mechanical stabilities as well as high water selectivity [212–214]. Huang et al. and Hua et al. developed composite membranes by coating a PFP layer on top of a hydrophilic polymer selective layer and a polyimide membrane,

**TABLE 6.6** Separation Performance of MMMs Developed for Solvent/Solvent Separation

| MMM | | Filler loading (wt%) | Configuration | Feed mixture (A/B) | Temperature (°C) | Flux (g m$^{-2}$ h$^{-1}$) | Normalized flux (g μm m$^{-2}$ h$^{-1}$) | Separation factor (A/B) | Ref. |
|---|---|---|---|---|---|---|---|---|---|
| Polymer | Filler | | | | | | | | |
| Sodium alginate/ sodium carboxymethyl cellulose blend | Bentonite | 8 | FS | Benzene/ cyclohexane (19.6/80.4 wt%) | 30 | 713 | 35,650 | 212 | [189] |
| PEBA/ceramic tubular substrates | Graphite | 10 | Tubular | Toluene/ $n$-heptane (50/50 wt%) | 40 | NA | 29 | 10.4 | [187] |
| Chitosan | Ag$^+$ grafted carbon nanotubes | 1.5 | FS | Benzene/ cyclohexane (50/50 wt%) | 20 | 358 | 823 | 7.9 | [38] |
| Polyurethane | Multiwall carbon nanotuges-NH$_2$ | 1 | FS | Benzene/ cyclohexane (50/50 wt%) | 30 | NA | NA | 40 | [205] |
| Poly(vinyl alcohol) | Graphene oxide | 0.1 ppm | FS | Toluene/$n$- heptane (50/50 wt%) | 40 | 27 | NA | 12.9 | [37] |
| Polyimide | Silver-graphene oxide | 15 | FS | Benzene/ cyclohexane (50/50 wt%) | 30 | 1573 | 39,325 | 35 | [206] |
| Poly (vinylchloride) | Activated carbon Maxsorb | 40 | FS | Toluene/heptane (41.2/58.8 wt%) | 54 | 20 | 1800 | 9.1 | [207] |
| | | | | | 74 | 80 | 16,320 | 6.3 | |

| Poly(ether-block-amide) (PEBA)/ceramic tube | Co(HCOO)$_2$ | 4 | Tubular | Toluene/isooctane (10/90 wt%) | 40 | 826 | 2478 | 7.2 | [208] |
|---|---|---|---|---|---|---|---|---|---|
| | | | | Benzene/cyclohexane (10/90 wt%) | | 760 | 2280 | 4.6 | |
| | | | | Toluene/cyclohexane (10/90 wt%) | | 685 | 2055 | 4 | |
| | | | | Toluene/$n$-heptane (10/90 wt%) | | 771 | 2313 | 5.1 | |
| Hyperbranched polymer (Boltorn W3000)/ceramic tube | Metal-organic molecule nanocages Cu$_{24}$(5-tBu-1,3-BDC)$_{24}$(S)$_{24}$ | 4.8 | Tubular | Toluene/$n$-heptane (50/50 wt%) | 40 | 220 | NA | 20 | [209] |
| | | | | Benzene/cyclohexane (50/50 wt%) | | 400 | NA | 15 | |
| Hyperbranched polymer (Boltorn W3000)/ceramic tube | Functionalized metal-organic molecule nanocages MOP-SO$_3$NanHm | 5 | Tubular | Toluene/$n$-heptane (50/50 wt%) | 40 | 528 | 1056 | 8.3 | [210] |
| | | | | Benzene/cyclohexane (50/50 wt%) | | 540 | 1080 | 8.4 | |
| Copolyimide | Glycidyl-POSS | 1 | | Benzothiophene/$n$-dodecane (3/97 wt%) | 100 | 1404 | 40,000 | 2.2 | [211] |
| | | 10 | | | | 1475 | 45,000 | 2.4 | |

*Note*: *HF*, hollow fiber; *FS*, flat sheet; *NA*, not available; *PI*, polyimide; *PEBA*, polyether-block-amide; *MOP*, metal organic polyhedral; *POSS*, polyhedral oligosilsesquioxane.

respectively [15, 110]. They found that the PFP layer served as a protective layer which helped enhance the dehydration selectivity and durability at high temperatures.

## 6.6 USEFUL CHARACTERIZATION METHODS FOR PERVAPORATION AND VAPOR SEPARATION MEMBRANES

There are various methods for characterizing pervaporation and vapor separation membranes. The membrane surface chemistry can be analyzed by Fourier transform infrared spectroscopy (FTIR) and X-ray photoelectron spectroscopy (XPS). The membrane morphology could be studied using optical microscopy, different kinds of scanning electronic microscopy (SEM), and atomic force microscope (AFM). The microstructure could be analyzed using X-ray diffraction (XRD), density measurement and positron annihilation spectroscopy. The membranes affinity to solvents and water could be measured by the contact angle measurement, liquid sorption, and vapor sorption tests. Among them, PAS has emerged as a useful tool for the analysis of the free-volume properties of membranes at the subnanometer scale (0.1–1 nm), which are very important properties for analyzing the diffusion of components inside the membrane [43, 215–217]. Besides, vapor sorption is also a useful tool because it can help to obtain both sorption and diffusion information of vapor separation membranes [16, 17, 43, 218].

## 6.7 CONCLUSIONS AND PERSPECTIVE

In this book chapter, the latest development of pervaporation and vapor separation membranes is comprehensively discussed. The applications, transport mechanism, the preparation and selection of the suitable membranes as well as the characterization techniques are systematically presented. The following can be concluded:

(1) Promising polymeric membranes, e.g., polyimides, polyamide, polybenzimidazole and perfluoro polymer membranes, with high thermal and chemical stability have been developed to dehydrate many aggressive organic solvents.

(2) Hydrophobic polymers such as PVDF, PTFE, and PIMs have been investigated for the removal of organics. Among them, PTFE and PVDF membranes have higher fluxes but equal or lower separation factors for most organics compared to PDMS membranes.

**(3)** Polyimides and perflorinated polymer membranes are promising for aliphatic/aromatic separation and gasoline desulfurization. More research on new membranes is necessary for other organic-organic separation.

**(4)** Many inorganic fillers such as MOFs, zeolites, and carbon nanotubes have been incorporated into polymers to enhance the separation performance of polymeric membranes. Among them, MOFs have been extensively investigated because of their compatibility with polymers, high porosity, various pore sizes and hydrophilicity/hydrophobicity. However, long-term stability of these new membranes is rarely reported.

The development of new materials and novel membranes is essential to push the boundary of separation performance and membrane stability in harsh feed environments. While the researchers continue to develop new pervaporation and vapor separation membranes with higher separation performance and stability, research on long-term stability in harsh feed environments such as high temperatures (100–150°C), corrosive solvents and extreme pH conditions must also be pursued to broaden the boundaries of applications. Also, innovative integration of membrane processes and pilot studies are urgently needed to solve the actual separation issues in the industry as well as to bridge the industrial applications with the research community [3, 219–222]. Only then, pervaporation and vapor separation membrane processes can be effectively employed for versatile industrial applications.

# References

[1] Baker RW. Membrane technology and applications. Chichester: Wiley; 2012.

[2] Ong YK, Shi GM, Le NL, Tang YP, Zuo J, Nunes SP, et al. Recent membrane development for pervaporation processes. Prog Polym Sci 2016;57:1–31.

[3] Huang Y, Baker RW, Wijmans JG. Perfluoro-coated hydrophilic membranes with improved selectivity. Ind Eng Chem Res 2013;52(3):1141–9.

[4] Morigami Y, Kondo M, Abe J, Kita H, Okamoto K. The first large-scale pervaporation plant using tubular-type module with zeolite NaA membrane. Sep Purif Technol 2001;25(1–3):251–60.

[5] Kujawski W. Application of pervaporation and vapor permeation in environmental protection. Pol J Environ Stud 2000;9(1):13–26.

[6] Slater CS, Savelski MJ, Moroz TM, Raymond MJ. Pervaporation as a green drying process for tetrahydrofuran recovery in pharmaceutical synthesis. Green Chem Lett Rev 2012;5(1):55–64.

[7] Smitha B, Suhanya D, Sridhar S, Ramakrishna M. Separation of organic–organic mixtures by pervaporation—a review. J Membr Sci 2004;241(1):1–21.

[8] Sander U, Soukup P. Design and operation of a pervaporation plant for ethanol dehydration. J Membr Sci 1988;36:463–75.

[9] Qiao XY, Chung TS, Guo WF, Matsuura T, Teoh MM. Dehydration of isopropanol and its comparison with dehydration of butanol isomers from thermodynamic and molecular aspects. J Membr Sci 2005;252(1–2):37–49.

[10] Jiang LY, Wang Y, Chung TS, Qiao XY, Lai JY. Polyimides membranes for pervaporation and biofuels separation. Prog Polym Sci 2009;34(11):1135–60.

[11] Zuo J, Lai JY, Chung TS. In-situ synthesis and cross-linking of polyamide thin film composite (TFC) membranes for bioethanol applications. J Membr Sci 2014;458:47–57.

[12] Shi GM, Wang Y, Chung TS. Dual-layer PBI/P84 hollow fibers for pervaporation dehydration of acetone. AIChE J 2012;58(4):1133–45.

[13] Kreiter R, Wolfs DP, Engelen CWR, van Veen HM, Vente JF. High-temperature pervaporation performance of ceramic-supported polyimide membranes in the dehydration of alcohols. J Membr Sci 2008;319(1–2):126–32.

[14] Mangindaan DW, Shi GM, Chung TS. Pervaporation dehydration of acetone using P84 co-polyimide flat sheet membranes modified by vapor phase crosslinking. J Membr Sci 2014;458:76–85.

[15] Hua D, Chung TS, Shi GM, Fang C. Teflon AF2400/Ultem composite hollow fiber membranes for alcohol dehydration by high-temperature vapor permeation. AIChE J 2016; 62(5):1747–57.

[16] Shi GM, Yang T, Chung TS. Polybenzimidazole (PBI)/zeolitic imidazolate frameworks (ZIF-8) mixed matrix membranes for pervaporation dehydration of alcohols. J Membr Sci 2012;415–416:577–86.

[17] Hua D, Ong YK, Wang Y, Yang T, Chung TS. ZIF-90/P84 mixed matrix membranes for pervaporation dehydration of isopropanol. J Membr Sci 2014;453:155–67.

[18] Xu YM, Chung TS. High-performance UiO-66/polyimide mixed matrix membranes for ethanol, isopropanol and n-butanol dehydration via pervaporation. J Membr Sci 2017;531:16–26.

[19] Claes S, Vandezande P, Mullens S, De Sitter K, Peeters R, Van Bael MK. Preparation and benchmarking of thin film supported PTMSP-silica pervaporation membranes. J Membr Sci 2012;389:265–71.

[20] Le NL, Wang Y, Chung TS. Pebax/POSS mixed matrix membranes for ethanol recovery from aqueous solutions via pervaporation. J Membr Sci 2011;379(1–2):174–83.

[21] Liu S, Liu G, Zhao X, Jin W. Hydrophobic-ZIF-71 filled PEBA mixed matrix membranes for recovery of biobutanol via pervaporation. J Membr Sci 2013;446:181–8.

[22] Gorgojo P, Alberto M, Luque-Alled JM, Gao L, Illut M, Vijayaraghavan A, et al. In: Escobar IC, editor. PIM-1/graphene pervaporation membranes for bioalcohol recovery. ECI Symposium Series. USA: University of Arkansas; 2016.

[23] Polyakov A, Bondarenko G, Tokarev A, Yampolskii Y. Intermolecular interactions in target organophilic pervaporation through the films of amorphous Teflon AF2400. J Membr Sci 2006;277(1–2):108–19.

[24] Sukitpaneenit P, Chung TS. Molecular design of the morphology and pore size of PVDF hollow fiber membranes for ethanol–water separation employing the modified pore-flow concept. J Membr Sci 2011;374(1–2):67–82.

[25] Huang J, Meagher MM. Pervaporative recovery of n-butanol from aqueous solutions and ABE fermentation broth using thin-film silicalite-filled silicone composite membranes. J Membr Sci 2001;192(1–2):231–42.

[26] Zhang C, Yang L, Bai Y, Gu J, Sun Y. ZSM-5 filled polyurethaneurea membranes for pervaporation separation isopropyl acetate from aqueous solution. Sep Purif Technol 2012;85:8–16.

[27] Kasik A, Lin YS. Organic solvent pervaporation properties of MOF-5 membranes. Sep Purif Technol 2014;121:38–45.

[28] Naik PV, Wee LH, Meledina M, Turner S, Li Y, Van Tendeloo G, et al. PDMS membranes containing ZIF-coated mesoporous silica spheres for efficient ethanol recovery via pervaporation. J Mater Chem A 2016;4(33):12790–8.

[29] Wang X, Chen J, Fang M, Wang T, Yu L, Li J. ZIF-7/PDMS mixed matrix membranes for pervaporation recovery of butanol from aqueous solution. Sep Purif Technol 2016;163:39–47.

[30] Xue C, Du G-Q, Chen L-J, Ren J-G, Sun J-X, Bai F-W, et al. A carbon nanotube filled polydimethylsiloxane hybrid membrane for enhanced butanol recovery. Sci Rep 2014;4:1–7.

[31] Yi S, Wan Y. Separation performance of novel vinyltriethoxysilane (VTES)-g-silicalite-1/PDMS/PAN thin-film composite membrane in the recovery of bioethanol from fermentation broths by pervaporation. J Membr Sci 2017;524:132–40.

[32] Liu X, Li Y, Liu Y, Zhu G, Liu J, Yang W. Capillary supported ultrathin homogeneous silicalite-poly(dimethylsiloxane) nanocomposite membrane for bio-butanol recovery. J Membr Sci 2011;369(1–2):228–32.

[33] Vane LM. Pervaporation and Vapor Permeation Tutorial: Membrane Processes for the Selective Separation of Liquid and Vapor Mixtures. Separ Sci Technol 2013;48 (3):429–37.

[34] Kung G, Jiang LY, Wang Y, Chung TS. Asymmetric hollow fibers by polyimide and polybenzimidazole blends for toluene/iso-octane separation. J Membr Sci 2010;360 (1–2):303–14.

[35] Zereshki S, Figoli A, Madaeni SS, Simone S, Esmailinezhad M, Drioli E. Pervaporation separation of MeOH/MTBE mixtures with modified PEEK membrane: effect of operating conditions. J Membr Sci 2011;371(1–2):1–9.

[36] Ibrahim A, Lin YS. Pervaporation separation of organic mixtures by MOF-5 membranes. Ind Eng Chem Res 2016;55(31):8652–8.

[37] Wang N, Ji S, Li J, Zhang R, Zhang G. Poly (vinyl alcohol)–graphene oxide nanohybrid "pore-filling" membrane for pervaporation of toluene/n-heptane mixtures. J Membr Sci 2014;455:113–20.

[38] Shen J-n, Chu Y-x, Ruan H-m, Wu L-g, Gao C-j, Van der Bruggen B. Pervaporation of benzene/cyclohexane mixtures through mixed matrix membranes of chitosan and $Ag^+$/carbon nanotubes. J Membr Sci 2014;462:160–9.

[39] Sorribas S, Kudasheva A, Almendro E, Zornoza B, de la Iglesia Ó, Téllez C, et al. Pervaporation and membrane reactor performance of polyimide based mixed matrix membranes containing MOF HKUST-1. Chem Eng Sci 2015;124:37–44.

[40] Jia Z, Wu G. Metal-organic frameworks based mixed matrix membranes for pervaporation. Microporous Mesoporous Mater 2016;235:151–9.

[41] Galiano F, Falbo F, Figoli A, Visakh P, Nazarenko O. Polymeric pervaporation membranes: organic-organic separation. In: Nanostructured Polymer Membranes, Volume 2: Applications; Beverly: Scrivener Publishing; 2016. p. 287.

[42] Wijmans JG, Baker RW. The solution-diffusion model-a review. J Membr Sci 1995;107 (1–2):1–21.

[43] Shi GM, Chen H, Jean YC, Chung TS. Sorption, swelling, and free volume of polybenzimidazole (PBI) and PBI/zeolitic imidazolate framework (ZIF-8) nano-composite membranes for pervaporation. Polymer 2013;54(2):774–83.

[44] Sidney L, Srinivasa S. High flow porous membranes for separating water from saline solutions. US 3133132 A; 1960.

[45] Atsumi S, Liao JC. Metabolic engineering for advanced biofuels production from Escherichia coli. Curr Opin Biotech 2008;19(5):414–9.

[46] Liu G, Yang D, Zhu Y, Ma J, Nie M, Jiang Z. Titanate nanotubes-embedded chitosan nanocomposite membranes with high isopropanol dehydration performance. Chem Eng Sci 2011;66(18):4221–8.

[47] Liu G, Wei W, Jin W. Pervaporation membranes for biobutanol production. ACS Sustain Chem Eng 2014;2(4):546–60.

[48] Peng N, Widjojo N, Sukitpaneenit P, Teoh MM, Lipscomb GG, Chung TS, et al. Evolution of polymeric hollow fibers as sustainable technologies: past, present, and future. Prog Polym Sci 2012;37(10):1401–24.

[49] Ong YK, Chung TS. Pushing the limits of high performance dual-layer hollow fiber fabricated via I2PS process in dehydration of ethanol. AIChE J 2013;59(8):3006–18.

[50] Hua D, Ong YK, Wang P, Chung TS. Thin-film composite tri-bore hollow fiber (TFC TbHF) membranes for isopropanol dehydration by pervaporation. J Membr Sci 2014;471:155–67.

[51] Page CA, Fouda AE, Matsuura T. Pervaporation performance of polyetherimide membranes spin- and dip-coated with polydimethylsiloxane. J Appl Polym Sci 1994;54 (7):975–89.

[52] Yanagishita H, Kitamoto D, Haraya K, Nakane T, Okada T, Matsuda H, et al. Separation performance of polyimide composite membrane prepared by dip coating process. J Membr Sci 2001;188(2):165–72.

[53] Wang R, Shan L, Zhang G, Ji S. Multiple sprayed composite membranes with high flux for alcohol permselective pervaporation. J Membr Sci 2013;432:33–41.

[54] Chung TS, Kafchinski ER, Kohn RS, Foley P, Straff RS. Fabrication of composite hollow fibers for air separation. J Appl Polym Sci 1994;53(5):701–8.

[55] Li P, Chen HZ, Chung TS. The effects of substrate characteristics and pre-wetting agents on PAN–PDMS composite hollow fiber membranes for $CO_2/N_2$ and $O_2/N_2$ separation. J Membr Sci 2013;434:18–25.

[56] Zuo J, Wang Y, Sun SP, Chung TS. Molecular design of thin film composite (TFC) hollow fiber membranes for isopropanol dehydration via pervaporation. J Membr Sci 2012;405–406:123–33.

[57] Zuo J, Wang Y, Chung TS. Novel organic-inorganic thin film composite membranes with separation performance surpassing ceramic membranes for isopropanol dehydration. J Membr Sci 2013;433:60–71.

[58] Zuo J, Chung TS. Design and synthesis of a fluoro-silane amine monomer for novel thin film composite membranes to dehydrate ethanol via pervaporation. J Mater Chem A 2013;1(34):9814.

[59] Huang SH, Wu CH, Lee KR, Lai JY. Polysulfonamide thin-film composite membranes applied to dehydrate isopropanol by pervaporation. Appl Mech Mater 2013;377:222–6.

[60] Tsai HA, Chung LH, Lee KR, Lai JY. The preparation of polyamide/polyacrylonitrile composite hollow fiber membranes for pervaporation. Appl Mech Mater 2013;377:246–9.

[61] Shi GM, Chung TS. Thin film composite membranes on ceramic for pervaporation dehydration of isopropanol. J Membr Sci 2013;448:34–43.

[62] Sukitpaneenit P, Chung TS. Fabrication and use of hollow fiber thin film composite membranes for ethanol dehydration. J Membr Sci 2014;450:124–37.

[63] Krasemann L, Toutianoush A, Tieke B. Self-assembled polyelectrolyte multilayer membranes with highly improved pervaporation separation of ethanol/water mixtures. J Membr Sci 2001;181(2):221–8.

[64] Zhang G, Yan H, Ji S, Liu Z. Self-assembly of polyelectrolyte multilayer pervaporation membranes by a dynamic layer-by-layer technique on a hydrolyzed polyacrylonitrile ultrafiltration membrane. J Membr Sci 2007;292(1–2):1–8.

[65] Zhang G, Dai L, Ji S. Dynamic pressure-driven covalent assembly of inner skin hollow fiber multilayer membrane. AIChE J 2011;57(10):2746–54.

[66] Semenova SI, Ohya H, Soontarapa K. Hydrophilic membranes for pervaporation: an analytical review. Desalination 1997;110(3):251–86.

[67] Chapman PD, Oliveira T, Livingston AG, Li K. Membranes for the dehydration of solvents by pervaporation. J Membr Sci 2008;318(1–2):5–37.

[68] Bolto B, Tran T, Hoang M, Xie Z. Crosslinked poly(vinyl alcohol) membranes. Prog Polym Sci 2009;34(9):969–81.

[69] Bolto B, Hoang M, Xie Z. A review of membrane selection for the dehydration of aqueous ethanol by pervaporation. Chem Eng Process Process Intensif 2011;50(3):227–35.

[70] Hua D, Chung TS. Universal surface modification by aldehydes on polymeric membranes for isopropanol dehydration via pervaporation. J Membr Sci 2015;492:197–208.

[71] Mangindaan DW, Woon NM, Shi GM, Chung TS. P84 polyimide membranes modified by a tripodal amine for enhanced pervaporation dehydration of acetone. Chem Eng Sci 2015;122:14–23.

[72] Salehian P, Yong WF, Chung TS. Development of high performance carboxylated PIM-1/P84 blend membranes for pervaporation dehydration of isopropanol and $CO_2/CH_4$ separation. J Membr Sci 2016;518:110–9.

[73] Yong WF, Salehian P, Zhang L, Chung TS. Effects of hydrolyzed PIM-1 in polyimide-based membranes on C2–C4 alcohols dehydration via pervaporation. J Membr Sci 2017;523:430–8.

[74] Le NL, Wang Y, Chung TS. Synthesis, cross-linking modifications of 6FDA-NDA/DABA polyimide membranes for ethanol dehydration via pervaporation. J Membr Sci 2012;415–416:109–21.

[75] Le NL, Chung TS. High-performance sulfonated polyimide/polyimide/polyhedral oligosilsesquioxane hybrid membranes for ethanol dehydration applications. J Membr Sci 2014;454:62–73.

[76] Xu YM, Le NL, Zuo J, Chung TS. Aromatic polyimide and crosslinked thermally rearranged poly(benzoxazole-co-imide) membranes for isopropanol dehydration via pervaporation. J Membr Sci 2016;499:317–25.

[77] Wang Y, Gruender M, Chung TS. Pervaporation dehydration of ethylene glycol through polybenzimidazole (PBI)-based membranes. 1. Membrane fabrication. J Membr Sci 2010;363(1–2):149–59.

[78] Wang Y, Shung Chung T, Gruender M. Sulfonated polybenzimidazole membranes for pervaporation dehydration of acetic acid. J Membr Sci 2012;415–416:486–95.

[79] Han Y-J, Wang K-H, Lai J-Y, Liu Y-L. Hydrophilic chitosan-modified polybenzoimidazole membranes for pervaporation dehydration of isopropanol aqueous solutions. J Membr Sci 2014;463:17–23.

[80] Ong YK, Wang H, Chung TS. A prospective study on the application of thermally rearranged acetate-containing polyimide membranes in dehydration of biofuels via pervaporation. Chem Eng Sci 2012;79:41–53.

[81] Pulyalina A, Polotskaya G, Goikhman M, Podeshvo I, Kalyuzhnaya L, Chislov M, et al. Study on polybenzoxazinone membrane in pervaporation processes. J Appl Polym Sci 2013;130(6):4024–31.

[82] Huang S-H, Hung W-S, Liaw D-J, Lo C-H, Chao W-C, Hu C-C, et al. Interfacially polymerized thin-film composite polyamide membranes: effects of annealing processes on pervaporative dehydration of aqueous alcohol solutions. Sep Purif Technol 2010;72(1):40–7.

[83] Kujawa J, Cerneaux S, Kujawski W. Highly hydrophobic ceramic membranes applied to the removal of volatile organic compounds in pervaporation. Chem Eng J 2015;260:43–54.

[84] Zhang Y, Le NL, Chung TS, Wang Y. Thin-film composite membranes with modified polyvinylidene fluoride substrate for ethanol dehydration via pervaporation. Chem Eng Sci 2014;118:173–83.

[85] Wu D, Martin J, Du J, Zhang Y, Lawless D, Feng X. Thin film composite membranes comprising of polyamide and polydopamine for dehydration of ethylene glycol by pervaporation. J Membr Sci 2015;493:622–35.

[86] Roy S, Thongsukmak A, Tang J, Sirkar KK. Concentration of aqueous hydrogen peroxide solution by pervaporation. J Membr Sci 2012;389:17–24.

[87] Tang J, Sirkar KK. Perfluoropolymer membrane behaves like a zeolite membrane in dehydration of aprotic solvents. J Membr Sci 2012;421–422:211–6.

[88] Jalal TA, Bettahalli NMS, Le NL, Nunes SP. Hydrophobic Hyflon AD/poly(vinylidene fluoride) membranes for butanol dehydration via pervaporation. Ind Eng Chem Res 2015;54(44):11180–7.

[89] Tang J, Sirkar KK, Majumdar S. Pervaporative dehydration of concentrated aqueous solutions of selected polar organics by a perfluoropolymer membrane. Sep Purif Technol 2017;175:122–9.

[90] Qiao XY, Chung TS. Fundamental characteristics of sorption, swelling, and permeation of P84 co-polyimide membranes for pervaporation dehydration of alcohols. Ind Eng Chem Res 2005;8938–43.

[91] Xu Y, Chen C, Li J. Experimental study on physical properties and pervaporation performances of polyimide membranes. Chem Eng Sci 2007;62(9):2466–73.

[92] Wang Y, Goh SH, Chung TS, Na P. Polyamide-imide/polyetherimide dual-layer hollow fiber membranes for pervaporation dehydration of C1–C4 alcohols. J Membr Sci 2009;326(1):222–33.

[93] Vanherck K, Koeckelberghs G, Vankelecom IFJ. Crosslinking polyimides for membrane applications: a review. Prog Polym Sci 2013;38(6):874–96.

[94] Salehian P, Chua ML, Askari M, Shi GM, Chung TS. In situ regulation of micro-pore to design high performance polyimide membranes for pervaporation dehydration of isopropanol. J Membr Sci 2015;493:299–310.

[95] Wang KY, Chung TS, Rajagopalan R. Dehydration of tetrafluoropropanol (TFP) by pervaporation via novel PBI/BTDA-TDI/MDI co-polyimide (P84) dual-layer hollow fiber membranes. J Membr Sci 2007;287(1):60–6.

[96] Chan W-H, Ng C-F, Lam-Leung S-Y, He X, Cheung O-C. Water–alcohol separation by pervaporation through poly(amide-sulfonamide)s (PASAs) membranes. J Appl Polym Sci 1997;65(6):1113–9.

[97] Kao S-T, Huang S-H, Liaw D-J, Chao W-C, Hu C-C, Li C-L, et al. Interfacially polymerized thin-film composite polyamide membrane: positron annihilation spectroscopic study, characterization and pervaporation performance. Polym J 2010; 42(3):242–8.

[98] Albo J, Wang J, Tsuru T. Application of interfacially polymerized polyamide composite membranes to isopropanol dehydration: effect of membrane pre-treatment and temperature. J Membr Sci 2014;453:384–93.

[99] Huang Y-H, Huang S-H, Chao W-C, Li C-L, Hsieh Y-Y, Hung W-S, et al. A study on the characteristics and pervaporation performance of polyamide thin-film composite membranes with modified polyacrylonitrile as substrate for bioethanol dehydration. Polym Int 2014;63(8):1478–86.

[100] Squire EN. Optical fibers comprising cores clad with amorphous copolymers of perfluoro-2,2-dimethyl-1,3-dioxole. US4530569 A; 1985.

[101] Nakamura M, Kaneko I, Oharu K, Kojima G, Matsuo M, Samejima S, et al. Cyclic polymerization. US 4910276 A; 1990.

[102] Squire EN. Amorphous copolymers of perfluoro-2,2-dimethyl-1,3-dioxole. US4999248 A; 1991.

[103] Colaianna P, Brinati G, Arcella V. Amorphous perfluoropolymers. US 5883177 A; 1999.

[104] Merkel TC, Bondar V, Nagai K, Freeman BD, Yampolskii YP. Gas sorption, diffusion, and permeation in poly(2,2-bis(trifluoromethyl)-4,5-difluoro-1,3-dioxole-co-tetrafluoroethylene). Macromolecules 1999;32(25):8427–40.

[105] Alentiev AY, Shantarovich VP, Merkel TC, Bondar VI, Freeman BD, Yampolskii YP. Gas and vapor sorption, permeation, and diffusion in glassy amorphous Teflon AF1600. Macromolecules 2002;35(25):9513–22.

[106] Polyakov AM, Starannikova LE, Yampolskii YP. Amorphous Teflons AF as organophilic pervaporation materials: transport of individual components. J Membr Sci 2003; 216(1–2):241–56.

[107] Merkel TC, Pinnau I, Prabhakar R, Freeman BD. Gas and vapor transport properties of perfluoropolymers. In: Materials science of membranes for gas and vapor separation. Chichester: John Wiley & Sons Ltd; 2006. p. 251–70.

[108] Huang Y, Baker RW, Aldajani T, Ly J. Dehydration processes using membranes with hydrophobic coating. WO2009029719 A1; 2009.

[109] Campos D, Nemser SM, Lazzeri J. Separations with highly selective fluoropolymer membranes. WO2010080753 A1; 2010.

[110] Huang Y, Ly J, Nguyen D, Baker RW. Ethanol dehydration using hydrophobic and hydrophilic polymer membranes. Ind Eng Chem Res 2010;49(23):12067–73.

[111] Smuleac V, Wu J, Nemser S, Majumdar S, Bhattacharyya D. Novel perfluorinated polymer-based pervaporation membranes for the separation of solvent/water mixtures. J Membr Sci 2010;352(1–2):41–9.

[112] Chen X, Wang J, Yin D, Yang J, Lu J, Zhang Y, et al. High-performance zeolite T membrane for dehydration of organics by a new varying temperature hot-dip coating method. AIChE J 2013;59(3):936–47.

[113] Huang B, Liu Q, Caro J, Huang A. Iso-butanol dehydration by pervaporation using zeolite LTA membranes prepared on 3-aminopropyltriethoxysilane-modified alumina tubes. J Membr Sci 2014;455:200–6.

[114] Shao J, Zhan Z, Li J, Wang Z, Li K, Yan Y. Zeolite NaA membranes supported on alumina hollow fibers: Effect of support resistances on pervaporation performance. J Membr Sci 2014;451:10–7.

[115] Verkerk AW, van Male P, Vorstman MAG, Keurentjes JTF. Description of dehydration performance of amorphous silica pervaporation membranes. J Membr Sci 2001;193(2):227–38.

[116] Gallego-Lizon T, Ho YS, Freitas dos Santos L. Comparative study of commercially available polymeric and microporous silica membranes for the dehydration of IPA/water mixtures by pervaporation/vapour permeation. Desalination 2002;149(1–3):3–8.

[117] Gallego-Lizon T, Edwards E, Lobiundo G, Freitas dos Santos L. Dehydration of water/t-butanol mixtures by pervaporation: comparative study of commercially available polymeric, microporous silica and zeolite membranes. J Membr Sci 2002;197(1–2):309–19.

[118] van Gemert RW, Cuperus FP. Newly developed ceramic membranes for dehydration and separation of organic mixtures by pervaporation. J Membr Sci 1995;105(3):287–91.

[119] Verkerk AW, van Male P, Vorstman MAG, Keurentjes JTF. Properties of high flux ceramic pervaporation membranes for dehydration of alcohol/water mixtures. Sep Purif Technol 2001;22–23:689–95.

[120] Tin PS, Lin HY, Ong RC, Chung TS. Carbon molecular sieve membranes for biofuel separation. Carbon 2011;49(2):369–75.

[121] Yoshimune M, Mizoguchi K, Haraya K. Alcohol dehydration by pervaporation using a carbon hollow fiber membrane derived from sulfonated poly(phenylene oxide). J Membr Sci 2013;425–426:149–55.

[122] Yeh T-M, Wang Z, Mahajan D, Hsiao BS, Chu B. High flux ethanol dehydration using nanofibrous membranes containing graphene oxide barrier layers. J Mater Chem A 2013;1(41):12998–3003.

[123] Hung W-S, An Q-F, De Guzman M, Lin H-Y, Huang S-H, Liu W-R, et al. Pressure-assisted self-assembly technique for fabricating composite membranes consisting of highly ordered selective laminate layers of amphiphilic graphene oxide. Carbon 2014;68:670–7.

[124] Hung W-S, Tsou C-H, De Guzman M, An Q-F, Liu Y-L, Zhang Y-M, et al. Cross-linking with diamine monomers to prepare composite graphene oxide-framework membranes with varying d-spacing. Chem Mater 2014;26(9):2983–90.

[125] Tang YP, Paul DR, Chung TS. Free-standing graphene oxide thin films assembled by a pressurized ultrafiltration method for dehydration of ethanol. J Membr Sci 2014;458:199–208.

[126] Chen X, Liu G, Zhang H, Fan Y. Fabrication of graphene oxide composite membranes and their application for pervaporation dehydration of butanol. Chinese J Chem Eng 2015;23:1102–9.

[127] Hua D, Rai RK, Zhang Y, Chung TS. Aldehyde functionalized graphene oxide frameworks as robust membrane materials for pervaporative alcohol dehydration. Chem Eng Sci 2017;161:341–9.

[128] Van Hoof V, Dotremont C, Buekenhoudt A. Performance of Mitsui NaA type zeolite membranes for the dehydration of organic solvents in comparison with commercial polymeric pervaporation membranes. Sep Purif Technol 2006;48(3):304–9.

[129] Kulprathipanja S, Neuzil RW, Li NN. Separation of fluids by means of mixed matrix membranes. US4740219 A; 1988.

[130] te Hennepe HJC, Bargeman D, Mulder MHV, Smolders CA. Zeolite-filled silicone rubber membranes: Part 1. Membrane preparation and pervaporation results. J Membr Sci 1987;35(1):39–55.

[131] Khosravi T, Mosleh S, Bakhtiari O, Mohammadi T. Mixed matrix membranes of Matrimid 5218 loaded with zeolite 4A for pervaporation separation of water–isopropanol mixtures. Chem Eng Res Des 2012;90(12):2353–63.

[132] Qiao X, Chung TS, Rajagopalan R. Zeolite filled P84 co-polyimide membranes for dehydration of isopropanol through pervaporation process. Chem Eng Sci 2006;61(20):6816–25.

[133] Adoor SG, Prathab B, Manjeshwar LS, Aminabhavi TM. Mixed matrix membranes of sodium alginate and poly(vinyl alcohol) for pervaporation dehydration of isopropanol at different temperatures. Polymer 2007;48(18):5417–30.

[134] Das P, Ray SK, Kuila SB, Samanta HS, Singha NR. Systematic choice of crosslinker and filler for pervaporation membrane: a case study with dehydration of isopropyl alcohol–water mixtures by polyvinyl alcohol membranes. Sep Purif Technol 2011;81(2):159–73.

[135] Jiang LY, Chung TS, Rajagopalan R. Matrimid®/MgO mixed matrix membranes for pervaporation. AIChE J 2007;53(7):1745–57.

[136] Qiu S, Wu L, Shi G, Zhang L, Chen H, Gao C. Preparation and pervaporation property of chitosan membrane with functionalized multiwalled carbon nanotubes. Ind Eng Chem Res 2010;49(22):11667–75.

[137] Zimmerman CM, Singh A, Koros WJ. Tailoring mixed matrix composite membranes for gas separations. J Membr Sci 1997;137(1–2):145–54.

[138] Li Y, Krantz WB, Chung TS. A novel primer to prevent nanoparticle agglomeration in mixed matrix membranes. AIChE J 2007;53(9):2470–5.

[139] Chung TS, Jiang LY, Li Y, Kulprathipanja S. Mixed matrix membranes (MMMs) comprising organic polymers with dispersed inorganic fillers for gas separation. Prog Polym Sci 2007;32(4):483–507.

[140] Vankelecom IFJ, Van den broeck S, Merckx E, Geerts H, Grobet P, Uytterhoeven JB. Silylation to improve incorporation of zeolites in polyimide films. J Phys Chem 1996;100(9):3753–8.

[141] Xu D, Loo LS, Wang K. Pervaporation performance of novel chitosan-POSS hybrid membranes: effects of POSS and operating conditions. J Polym Sci B Polym Phys 2010;48(21):2185–92.

[142] Le NL, Tang YP, Chung TS. The development of high-performance 6FDA-NDA/DABA/POSS/Ultem® dual-layer hollow fibers for ethanol dehydration via pervaporation. J Membr Sci 2013;447:163–76.

[143] Car A, Stropnik C, Peinemann K-V. Hybrid membrane materials with different metal–organic frameworks (MOFs) for gas separation. Desalination 2006;200(1–3):424–6.

[144] Suhas DP, Aminabhavi TM, Raghu AV. Mixed matrix membranes of H-ZSM5-loaded poly(vinyl alcohol) used in pervaporation dehydration of alcohols: Influence of silica/alumina ratio. Polym Eng Sci 2014;54(8):1774–82.

[145] Zhang H, Wang Y. Poly(vinyl alcohol)/ZIF-8-NH$_2$ mixed matrix membranes for ethanol dehydration via pervaporation. AIChE J 2016;62(5):1728–39.

[146] Salehian P, Chung TS. Thermally treated ammonia functionalized graphene oxide/polyimide membranes for pervaporation dehydration of isopropanol. J Membr Sci 2017;528:231–42.

[147] Fazlifard S, Mohammadi T, Bakhtiari O. Chitosan/ZIF-8 mixed-matrix membranes for pervaporation dehydration of isopropanol. Chem Eng Technol 2017;40(4):648–55.

[148] Zhang W, Ying Y, Ma J, Guo X, Huang H, Liu D, et al. Mixed matrix membranes incorporated with polydopamine-coated metal-organic framework for dehydration of ethylene glycol by pervaporation. J Membr Sci 2017;527:8–17.

[149] Hitchens L, Vane LM, Alvarez FR. VOC removal from water and surfactant solutions by pervaporation: a pilot study. Sep Purif Technol 2001;24(1–2):67–84.

[150] Vane LM, Alvarez FR. Full-scale vibrating pervaporation membrane unit: VOC removal from water and surfactant solutions. J Membr Sci 2002;202(1–2):177–93.

[151] Lipnizki F, Olsson J, Trägårdh G. Scale-up of pervaporation for the recovery of natural aroma compounds in the food industry. Part 1: simulation and performance. J Food Eng 2002;54(3):183–95.

[152] Willemsen JHA, Dijkink BH, Togtema A. Organophilic pervaporation for aroma isolation - industrial and commercial prospects. Membr Technol 2004;2004(2):5–10.

[153] Rom A, Friedl A. Investigation of pervaporation performance of POMS membrane during separation of butanol from water and the effect of added acetone and ethanol. Sep Purif Technol 2016;170:40–8.

[154] Liu X, Jin H, Li Y, Bux H, Hu Z, Ban Y, et al. Metal–organic framework ZIF-8 nanocomposite membrane for efficient recovery of furfural via pervaporation and vapor permeation. J Membr Sci 2013;428:498–506.

[155] Liu X, Li Y, Ban Y, Peng Y, Jin H, Bux H, et al. Improvement of hydrothermal stability of zeolitic imidazolate frameworks. Chem Commun 2013;49(80):9140–2.

[156] Yen H-W, Lin S-F, Yang I-K. Use of poly(ether-block-amide) in pervaporation coupling with a fermentor to enhance butanol production in the cultivation of Clostridium acetobutylicum. J Biosci Bioeng 2012;113(3):372–7.

[157] Tan H, Wu Y, Li T. Pervaporation of n-butanol aqueous solution through ZSM-5-PEBA composite membranes. J Appl Polym Sci 2013;129(1):105–12.

[158] Tan H, Wu Y, Zhou Y, Liu Z, Li T. Pervaporative recovery of n-butanol from aqueous solutions with MCM-41 filled PEBA mixed matrix membrane. J Membr Sci 2014;453:302–11.

[159] Li Y, Shen J, Guan K, Liu G, Zhou H, Jin W. PEBA/ceramic hollow fiber composite membrane for high-efficiency recovery of bio-butanol via pervaporation. J Membr Sci 2016;510:338–47.

[160] Sukitpaneenit P, Chung TS, Jiang LY. Modified pore-flow model for pervaporation mass transport in PVDF hollow fiber membranes for ethanol–water separation. J Membr Sci 2010;362(1–2):393–406.

[161] Jadav V, Mukhopadhyay M, Murthy ZVP. Comparative study of separation of acetonitrile from aqueous solutions by pervaporation using different membranes. Separ Sci Technol 2012;47(16):2299–304.

[162] Lende AB, Swati S, Kaur H, Kulkarni PS. Pervaporation of acetone, n-butanol and ethanol from fermentation broth using hydrophobic membranes. In: International Conference Recent Trends in Engineering and Material Science. Volume: Perspectives in Science, Elsevier; 2016. ISBN 978-93-5254-230-7.

[163] Villegas M, C. Vidaurre EF, Gottifredi JC. Sorption and pervaporation of methanol/water mixtures with poly(3-hydroxybutyrate) membranes. Chem Eng Res Des 2015;94:254–65.

[164] Borisov IL, Malakhov AO, Khotimsky VS, Litvinova EG, Finkelshtein ES, Ushakov NV, et al. Novel PTMSP-based membranes containing elastomeric fillers: enhanced 1-butanol/water pervaporation selectivity and permeability. J Membr Sci 2014;466:322–30.

[165] Wu XM, Zhang QG, Soyekwo F, Liu QL, Zhu AM. Pervaporation removal of volatile organic compounds from aqueous solutions using the highly permeable PIM-1 membrane. AIChE J 2016;62(3):842–51.

[166] Dong Y, Wang M, Chen L, Li M. Preparation, characterization of P (VDF-HFP)/[bmim]
      BF 4 ionic liquids hybrid membranes and their pervaporation performance for ethyl
      acetate recovery from water. Desalination 2012;295:53–60.
[167] Grimaldi J, Imbrogno J, Kilduff J, Belfort G. New class of synthetic membranes: orga-
      nophilic pervaporation brushes for organics recovery. Chem Mater 2015;27(11):4142–8.
[168] Kim D-G, Takigawa T, Kashino T, Burtovyy O, Bell A, Register RA. Hydroxyhexafluor-
      oisopropylnorbornene block and random copolymers via vinyl addition polymeriza-
      tion and their application as biobutanol pervaporation membranes. Chem Mater
      2015;27(19):6791–801.
[169] Sun L, Hu M, Feng B, Ma Y, Liao J, Huang C. Polyurethane–fluoropolymer interpene-
      trating polymer network membrane for pervaporation recovery of butanol. Polym Bull
      2016;74(6):2331–47.
[170] Hu M, Gao L, Fu W, Liu X, Huang F, Luo Y, et al. High-performance interpenetrating
      polymer network polyurethane pervaporation membranes for butanol recovery.
      J Chem Technol Biot 2015;90(12):2195–207.
[171] Yadav A, Lind ML, Ma X, Lin YS. Nanocomposite silicalite-1/polydimethylsiloxane
      membranes for pervaporation of ethanol from dilute aqueous solutions. Ind Eng Chem
      Res 2013;52(14):5207–12.
[172] Naik PV, Kerkhofs S, Martens JA, Vankelecom IFJ. PDMS mixed matrix membranes
      containing hollow silicalite sphere for ethanol/water separation by pervaporation.
      J Membr Sci 2016;502:48–56.
[173] Yi S, Wan Y. Volatile organic compounds (VOCs) recovery from aqueous solutions via
      pervaporation with vinyltriethoxysilane-grafted-silicalite-1/polydimethylsiloxane
      mixed matrix membrane. Chem Eng J 2016;313:1639–46.
[174] Shirazi Y, Ghadimi A, Mohammadi T. Recovery of alcohols from water using
      polydimethylsiloxane–silica nanocomposite membranes: characterization and perva-
      poration performance. J Appl Polym Sci 2012;124(4):2871–82.
[175] Liu X-L, Li Y-S, Zhu G-Q, Ban Y-J, Xu L-Y, Yang W-S. An organophilic pervaporation
      membrane derived from metal-organic framework nanoparticles for efficient recovery
      of bio-alcohols. Angew Chem Int Ed 2011;50(45):10636–9.
[176] Fan H, Wang N, Ji S, Yan H, Zhang G. Nanodisperse ZIF-8/PDMS hybrid membranes
      for biobutanol permselective pervaporation. J Mater Chem A 2014;2(48):20947–57.
[177] Fan H, Shi Q, Yan H, Ji S, Dong J, Zhang G. Simultaneous spray self-assembly of highly
      loaded ZIF-8–PDMS nanohybrid membranes exhibiting exceptionally high biobutanol-
      permselective pervaporation. Angew Chem Int Ed 2014;53(22):5578–82.
[178] Ding C, Zhang X, Li C, Hao X, Wang Y, Guan G. ZIF-8 incorporated polyether block
      amide membrane for phenol permselective pervaporation with high efficiency. Sep
      Purif Technol 2016;166:252–61.
[179] Zhang G, Li J, Wang N, Fan H, Zhang R, Ji S. Enhanced flux of polydimethylsiloxane
      membrane for ethanol permselective pervaporation via incorporation of MIL-53 parti-
      cles. J Membr Sci 2015;492:322–30.
[180] Xue C, Wang Z-X, Du G-Q, Fan L-H, Mu Y, Ren J-G, et al. Integration of ethanol
      removal using carbon nanotube (CNT)-mixed membrane and ethanol fermentation
      by self-flocculating yeast for antifouling ethanol recovery. Process Biochem
      2016;51:1140–6.
[181] Najafi M, Mousavi SM, Saljoughi E. Preparation and characterization of poly (ether
      block amide)/graphene membrane for recovery of isopropanol from aqueous solution
      via pervaporation. Polym Compos 2016. https://doi.org/10.1002/pc.24203.
[182] Ribeiro CP, Freeman BD, Kalika DS, Kalakkunnath S. Aromatic polyimide and poly-
      benzoxazole membranes for the fractionation of aromatic/aliphatic hydrocarbons by
      pervaporation. J Membr Sci 2012;390–391:182–93.
[183] Suding MTH, Staudt C. Sulfur-containing copolyimides for the membrane-based sep-
      aration of aromatic/aliphatic mixtures. J Appl Polym Sci 2013;127(6):5065–74.

[184] Roychowdhury S, Mitra D. Separation of phenanthrene/N-tetradecane mixtures (model diesel) via pervaporation using an aromatic polyimide membrane. Polym Eng Sci 2016;57:392–402.

[185] Xu W, Paul DR, Koros WJ. Carboxylic acid containing polyimides for pervaporation separations of toluene/iso-octane mixtures. J Membr Sci 2003;219(1):89–102.

[186] Benguergoura H, Moulay S. Styrene–butadiene rubber membranes for the pervaporative separation of benzene/cyclohexane mixtures. J Appl Polym Sci 2012;123(3): 1455–67.

[187] Wu T, Wang N, Li J, Wang L, Zhang W, Zhang G, et al. Tubular thermal crosslinked-PEBA/ceramic membrane for aromatic/aliphatic pervaporation. J Membr Sci 2015;486:1–9.

[188] Kononova SV, Kremnev RV, Suvorova EI, Baklagina YG, Volchek BZ, Uchytil P, et al. Pervaporation membranes with poly (γ-benzyl-L-glutamate) selective layers for separation of toluene–n-heptane mixtures. J Membr Sci 2015;477:14–24.

[189] Kuila SB, Ray SK. Separation of benzene–cyclohexane mixtures by filled blend membranes of carboxymethyl cellulose and sodium alginate. Sep Purif Technol 2014;123:45–52.

[190] Dong Y, Guo H, Su Z, Wei W, Wu X. Pervaporation separation of benzene/cyclohexane through AAOM-ionic liquids/polyurethane membranes. Chem Eng Process Process Intensif 2015;89:62–9.

[191] Aouak T, Alghamdi AA, Alrashdi AA, Ouladsmane M, Alam MM, AlOthman Z, et al. Miscibility enhancement of poly (vinyl chloride)/polystyrene blend: Application to membrane separation of benzene from benzene/cyclohexane mixture by pervaporation. Separ Sci Technol 2016;51(14):2440–54.

[192] Yao L, Song Y, Ye H, Xi T, Cui P. The effect of the soft segments materials to waterborne polyurethane membranes: Structures and pervaporation of benzene/cyclohexane mixture. In: Chemeca 2016: chemical engineering-regeneration, recovery and reinvention; Melbourne, Australia: Engineers Australia; 2016. p. 859.

[193] Billy M, Costa ARD, Lochon P, Clément R, Dresch M, Jonquières A. Cellulose acetate graft copolymers with nano-structured architectures: application to the purification of bio-fuels by pervaporation. J Membr Sci 2010;348(1–2):389–96.

[194] Han GL, Zhang QG, Zhu AM, Liu QL. Pervaporation separation of methanol/methyl tert-butyl ether mixtures using polyarylethersulfone with cardo membranes. Sep Purif Technol 2013;107:211–8.

[195] Han GL, Gong Y, Zhang QG, Liu QL. Polyarylethersulfone with cardo/poly (vinyl pyrrolidone) blend membrane for pervaporation of methanol/methyl tert-butyl ether mixtures. J Membr Sci 2013;448:55–61.

[196] Han GL, Zhang QG, Liu QL. Separation of methanol/methyl tert-butyl ether using sulfonated polyarylethersulfone with cardo (SPES-C) membranes. J Membr Sci 2013;430:180–7.

[197] Han GL, Gong Y, Zhang QG, Zhu AM, Ye ML, Liu QL. Facile preparation of homogeneous polyelectrolyte complex membranes for separation of methanol/methyl tert-butyl ether mixtures. J Membr Sci 2013;447:246–52.

[198] https://www.epa.gov/gasoline-standards/gasoline-sulfur.

[199] Liu K, Fang C-J, Li Z-Q, Young M. Separation of thiophene/n-heptane mixtures using PEBAX/PVDF-composited membranes via pervaporation. J Membr Sci 2014;451:24–31.

[200] Yang X-d, Ye H, Li Y-t, Li J, Li J-d, Zhao B-q, et al. An asymmetric membrane of polyimide 6FDA-BDAF and its pervaporation desulfurization for n-heptane/thiophene mixtures. J Integr Agric 2015;14(12):2529–37.

[201] Ong YK, Widjojo N, Chung TS. Fundamentals of semi-crystalline poly(vinylidene fluoride) membrane formation and its prospects for biofuel (ethanol and acetone) separation via pervaporation. J Membr Sci 2011;378(1–2):149–62.

[202] Abdallah H, El-Gendi A, El-Zanati E, Matsuura T. Pervaporation of methanol from methylacetate mixture using polyamide-6 membrane. Desalin Water Treat 2013;51 (40–42):7807–14.

[203] Falbo F, Santoro S, Galiano F, Simone S, Davoli M, Drioli E, et al. Organic/organic mixture separation by using novel ECTFE polymeric pervaporation membranes. Polymer 2016;98:110–7.

[204] Parvez AM, Luis P, Ooms T, Vreysen S, Vandezande P, Degrève J, et al. Separation of ethyl acetate–isooctane mixtures by pervaporation and pervaporation-based hybrid methods. Chem Eng J 2012;210:252–62.

[205] Wang T, Shen J-n, Wu L-g, Van der Bruggen B. Improvement in the permeation performance of hybrid membranes by the incorporation of functional multi-walled carbon nanotubes. J Membr Sci 2014;466:338–47.

[206] Dai S-q, Jiang Y-y, Wang T, Wu L-g, Yu X-y, Lin J-z. Enhanced performance of polyimide hybrid membranes for benzene separation by incorporating three-dimensional Ag–graphene oxide. J Colloid Interf Sci 2016;.

[207] Aouinti L, Roizard D, Belbachir M. PVC–activated carbon based matrices: a promising combination for pervaporation membranes useful for aromatic–alkane separations. Sep Purif Technol 2015;147:51–61.

[208] Zhang Y, Wang N, Zhao C, Wang L, Ji S, Li J-R. Co(HCOO)$_2$-based hybrid membranes for the pervaporation separation of aromatic/aliphatic hydrocarbon mixtures. J Membr Sci 2016;520:646–56.

[209] Zhao C, Wang N, Wang L, Huang H, Zhang R, Yang F, et al. Hybrid membranes of metal–organic molecule nanocages for aromatic/aliphatic hydrocarbon separation by pervaporation. Chem Commun 2014;50(90):13921–3.

[210] Zhao C, Wang N, Wang L, Sheng S, Fan H, Yang F, et al. Functionalized metal-organic polyhedra hybrid membranes for aromatic hydrocarbons recovery. AIChE J 2016;62:3706–16.

[211] Konietzny R, Koschine T, Rätzke K, Staudt C. POSS-hybrid membranes for the removal of sulfur aromatics by pervaporation. Sep Purif Technol 2014;123:175–82.

[212] Okamoto K, Tanihara N, Watanabe H, Tanaka K, Kita H, Nakamura A, et al. Vapor permeation and pervaporation separation of water-ethanol mixtures through polyimide membranes. J Membr Sci 1992;68(1–2):53–63.

[213] Tanihara N, Tanaka K, Kita H, Okamoto K-i, Nakamura A, Kusuki Y, et al. Vapor-permeation separation of water-ethanol mixtures by asymmetric polyimide hollow-fiber membrane modules. J Chem Eng Jpn 1992;25(4):388–96.

[214] Cranford RJ, Darmstadt H, Yang J, Roy C. Polyetherimide/polyvinylpyrrolidone vapor permeation membranes. Physical and chemical characterization. J Membr Sci 1999;155(2):231–40.

[215] Jean YC, Mallon PE, Schrader DM. Principles and applications of positron and positronium chemistry. Singapore: World Scientific; 2003.

[216] Hung W-S, An Q-F, Hu C-C, Lee K-R, Jean Y-C, Lai J-Y. Non-destructive means of probing a composite polyamide membrane for characteristic free volume, void, and chemical composition. RSC Adv 2016;6(88):85019–25.

[217] Peng F, Lu L, Sun H, Jiang Z. Analysis of annealing effect on pervaporation properties of PVA-GPTMS hybrid membranes through PALS. J Membr Sci 2006;281(1):600–8.

[218] Blume I, Schwering PJF, Mulder MHV, Smolders CA. Vapour sorption and permeation properties of poly (dimethylsiloxane) films. J Membr Sci 1991;61:85–97.

[219] Bernal MP, Coronas J, Menendez M, Santamaria J. Coupling of reaction and separation at the microscopic level: esterification processes in a H-ZSM-5 membrane reactor. Chem Eng Sci 2002;57(9):1557–62.

[220] Zhu MH, Kumakiri I, Tanaka K, Kita H. Dehydration of acetic acid and esterification product by acid-stable ZSM-5 membrane. Microporous Mesoporous Mater 2013;181:47–53.

[221] Baudot A, Marin M. Improved recovery of an ester flavor compound by pervaporation coupled with a flash condensation. Ind Eng Chem Res 1999;38(11):4458–69.

[222] Zuo J, Hua D, Maricar V, Ong YK, Chung TS. Dehydration of industrial isopropanol (IPA) waste by pervaporation and vapor permeation membranes. J Appl Polym Sci 2017;135:1–7.

# Pervaporation and Hybrid Vacuum Membrane Distillation Technology and Applications

*Fakhir U. Baig*

**Petro Sep Corporation, Mississauga, ON, Canada**

O U T L I N E

# 7.1 INTRODUCTION

Pervaporation (PV) and vacuum membrane distillation (VMD) are similar in many ways and many applications. PV is a process in which organic solvent/water mixture or organic solvent/organic solvent mixtures can be separated by partial vaporization through a non-porous perm-selective membrane. In this process, a liquid feed mixture is in contact with the active nonporous side of the membrane while a vacuum is applied on the other side of the membrane. A phase change of the permeant takes place in the membrane. The permeant diffuses through the membrane and desorbs on the permeate side of the membrane as vapor with the help of a vacuum.

The transport of the permeant through a nonporous permeate-selective membrane is quite complex and the separation is effected at each step of sorption, diffusion, and desorption.

Membrane distillation (MD) is a process suited for applications in which water is the major primary component of the feed solution. In MD vapor is transported through a nonwetted porous hydrophobic membrane, the driving force is the partial pressure difference between both ends of the membrane pore. VMD and organic selective PV look very similar, the major difference being the membranes used in these processes; the porous hydrophobic membrane is used in VMD while the nonporous hydrophobic membrane is used in organic selective PV.

PV has been known to the scientific world since the early 1900s. In 1906, Kahlenberg [1] reported some qualitative observations concerning the selective transport of hydrocarbon-alcohol mixtures through a thin rubber sheet. The term pervaporation was first introduced by Kober [2] in a study published in 1917 in the Journal of the American Chemical Society. In 1949, Schwob [3] demonstrated dehydration of alcohols by using 20-μm thin membrane in his experimental work. In 1961, Binning [4] from American Oil Company, Texas City, United States, carried out several experiments to separate various hydrocarbons by using pervaporation experiments. He made a pilot plant consisting of 10 m$^2$ of membrane area to separate hydrocarbons. However, after several years of work the technology was not commercialized.

PV research has continued in various parts of the world without any significant breakthrough in commercialization. In 1982, G.F.T., a German

company, commercialized PV plant for alcohol dehydration. This plant could produce 1300 L of ethanol per day of 99.2% purity from predistilled ethanol. In 1987, G.F.T. was taken over by a French company Carbone Lorraine. In 1994, Carbone Lorraine sold its pervaporation technology to Sulzer Chemtech. In Japan, during the same period Mitsui, Sasakura Engineering, and Asahi Chemicals made many efforts in R & D to commercialize the pervaporation technology.

In 1999, based on the earlier 20 years of research by the Petro Sep scientists together with the collaboration of Industrial Membrane Research Institute (IMRI) of University of Ottawa, Petro Sep Membrane Technologies Inc. of Oakville, Canada, introduced a new type of PV membranes. In 2012 Petro Sep Group was consolidated into Petro Sep Corporation to continue their efforts in commercialization of their innovative membranes, which had lasted over 25 years. Petro Sep membranes are very robust and chemically resistant and are available in hollow fiber as well as flat sheet configuration. The design is very user-friendly and economical. Petro Sep has already built many pilot scale and full-scale plants for dehydration of solvents. As well, Petro Sep has constructed several complete solvent recycling plants by using AZEO SEP™, VOC SEP™ PV technologies, and AQUA SEP™ VMD technology. Petro Sep continues to serve the industry by their innovative membranes to provide solutions for many complex separation problems.

There are four kinds of PV membranes.

1. Hydrophilic membranes,
2. Hydrophobic membranes,
3. Organophilic membranes, and
4. Hydrophobic semiporous semipermeable membranes.


1. Hydrophilic nonporous, semipermeable membranes can be used to dehydrate organic solvents or organic solvent mixtures. The membranes are made of hydrophilic polymers. These membranes are cross-linked by using various types of cross-linking agents to provide mechanical strength, a better separation factor as well as a higher flux as compared to noncross-linked hydrophilic membranes. The membrane chemistry is designed to attract water molecules to the surface of the membrane. PV takes place in the membrane. Water molecules diffuse through the membrane and evaporate on the permeate side with the help of vacuum. Later, vapors condense in a condenser. Examples of applications for these membranes are numerous. There are many organic solvents which form azeotropes with water. Using these hydrophilic membranes, PV can break the azeotropes in the solvents.

2. Hydrophobic nonporous, semipermeable membranes can be used to extract organic solvents or volatile organic compounds (VOCs) from the water. The membranes are made of hydrophobic cross-linked polymers. The membrane chemistry is designed to attract VOC molecules to the surface of the membrane. PV takes place in the membrane. VOCs diffuse through the membrane and evaporate on the permeate side with the help of vacuum. These VOCs later condense in a condenser. Examples of these membrane applications include extraction of numerous types of VOC's from water, extraction of aromatics from water, ketones from water, esters from water and many more.

3. Organophilic nonporous, semipermeable membranes can be used to extract organic solvents from organic solvents. The membranes are designed to attract certain organic molecules to the membrane surface. The membranes can reject other types of organic molecules. The molecules travel toward the surface, diffuse through the membrane, and evaporate on the permeate side with the help of a vacuum. These organics later condense in a condenser. An example is the extraction of VOC's from glycols. Another example is the separation of aromatics from aliphatics, and many more.

4. Hydrophobic semiporous and semipermeable membranes can be used to extract organic solvents or volatile organic compounds (VOCs) from the water. The membranes are made of hydrophobic cross-linked polymers. The membrane chemistry is designed to attract VOC molecules to the surface of the membrane. PV takes place in one part of the membrane, while VMD takes place in the other part of the membrane. VOCs diffuse through the membrane and evaporate on the permeate side with the help of vacuum. These VOCs later condense in a condenser. Examples of these membrane applications include extraction of numerous types of VOCs from water, extraction of aromatics from water, ketones from water, esters from water and many more.

## 7.2 VACUUM MEMBRANE DISTILLATION AND HYBRID PERVAPORATION MEMBRANES

Among various MD configurations, VMD is least used next to sweeping gas membrane distillation (SGMD). It has been considered until now that MD would remain in the laboratory development stage, although the concept has been known for more than 40 years [5], which is however no longer true. Petro Sep's breakthrough in research in 2004 and the continued work that followed enabled successful commercialization of VMD in 2012. Petro Sep's innovative design of heat recovery system together with

its hollow fiber configuration made the treatment of the reject from RO seawater desalination plants one of the most economical processes. AQUA SEP™ is a VMD process which makes use of the heat formed within the system, without requiring the supply of heat from external sources.

## 7.3  AZEO-SEP™, VOC-SEP™, AND AQUA-SEP™: PRODUCTS OF PETRO SEP

AZEO SEP™ is based on hydrophilic membranes which can break the Azeotropes. It works on the principle of PV.

VOC SEP™ is based on hydrophobic membranes that can extract any volatile organic solvents from the water. It works on the principle of PV.

AQUA SEP™ is based on hydrophobic membranes for many different applications. It works on the principles of VMD.

VOC SEP™/AQUA SEP™ HYBRID MEMBRANE is a hybrid hydrophobic membrane. The membrane operates on the principle of PV and VMD. This membrane is used in a VOC SEP™ system. The membrane can reduce the concentration of VOCs in water from 10,000 ppm to less than 50 ppm.

One of the significant challenges that industries are facing today is the complex separation problems arising due to the azeotrope formation in the various processes in the chemical industry. Until 1999 membrane companies did not have a complete solution for such problems. However, after the breakthrough of Petro Sep Membrane Research Inc., a subsidiary of Petro Sep Membrane Technologies Inc., it became possible to provide the complete solution for the industries facing complex separation problems. In particular, Petro Sep Corporation was successful in introducing in 2012 a new hybrid membrane VOC SEP™/AQUA SEP™, in which PV and VMD are combined.

The two categories of major significant complex separations involve organic mixtures of acidic as well as basic essential nature forming azeotropes with water. It has been proven that mixtures of organics having pH less than 1 can be dehydrated as well as fractioned by the hybrid AZEO SEP™/AQUA SEP™ membrane. Organic mixtures having pH greater than 9 can also be dehydrated as well as separated.

In the past, it was impossible to dehydrate amines and nitrates by using membrane technology. Various companies have tried to dehydrate amines by a membrane; however, none of them were successful. One of the major primary reasons was the failure of membranes. Similarly, in the resin industry it was impossible to recover the reactants from the wastewater. The only way to treat such wastewater was incineration particularly when the organic loading was very high. AZEO SEP™ pervaporation system has given a solution by proving that these reactants

can be recovered and recycled. This process not only resolves the wastewater problem but also can provide significant cost savings for the chemical industry by recovering a large significant amount of organic solvents from the wastewater.

It is quite common in the chemical process industry to use various kinds of salts to dehydrate complex mixtures of solvents in azeotropic distillation. These salts can cause many serious problems in the process such as rusting in the piping system. The disposal of toxic wastewater is a colossal issue for the chemical industry. AZEO SEP™/AQUA SEP™ hybrid system can eliminate the use of salt and can break down the azeotropes for further use in the process.

In the semiconductor industry, a large significant amount of organic solvents is used in various washing processes. If the concentration of organic solvents is high in the wastewater, it cannot be treated by biological methods, advanced oxidation, membrane bioreactor, or any other methods. The only method available is incineration. Worldwide incineration regulations are becoming more stringent, and it is difficult for the industries to meet the regulation. The AZEO SEP/AQUA SEP hybrid system enables the complete recycle of the valuable solvents and can resolve the wastewater problems. The solvents can be purified to the level up to 99.90% and can be reused. Thus, the system allows the industry to reduce consumption of valuable solvents.

Some of the plants constructed by Petro Sep are shown below with the process flow sheet.

## 7.4 SOLVENT RECOVERY AND WASTEWATER TREATMENT

As already mentioned solvents should be recovered and reused in many industries. Such industries include the pharmaceutical industry, specialty chemical, printing and paint industry, cosmetic industry, and petrochemical industry. The solvents form azeotropes with water, which makes dehydration very difficult. VOC SEP™ PV membranes have demonstrated that even complex solvent mixtures can be dehydrated to a very high level of purity. Fig. 7.1 shows the flow sheet of the solvent recovery process.

Feed water enters through a TFE (thin film evaporator) unit which is connected to the solvent recovery column. TFE removes the suspended solids in the feed and acts as a pre-heater for the solvent recovery column. The top of the solvent recovery column collects all the solvents vapors and transfer it to a solvent recovery condenser. Solvents are then transferred to a solvent collection tank. The bottom of the solvent recovery column collects all the water with the traces of solvents. This water is then transferred
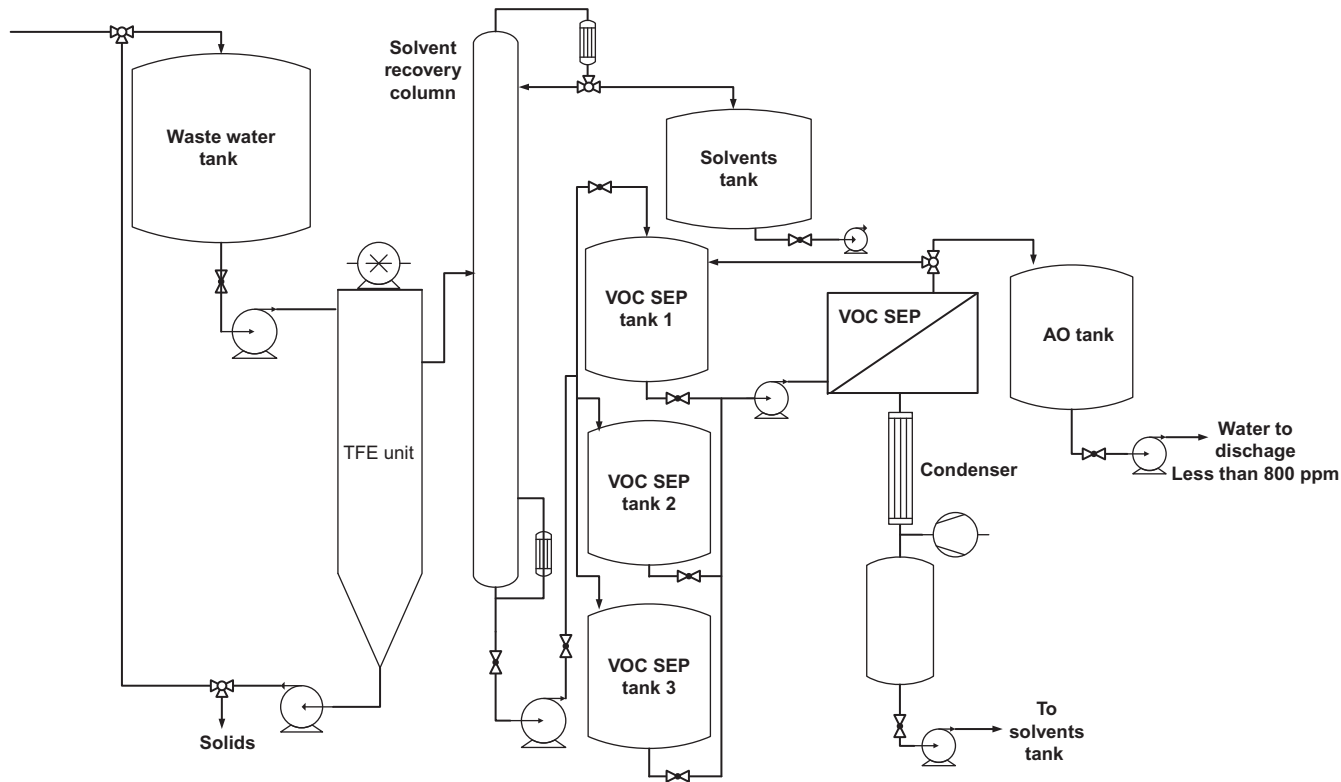
**FIG. 7.1** 15,000 L per day capacity VOC SEP™ hybrid pervaporation plant for water purification and solvent recovery.

to a feed tank of VOC SEP™ to purify the water further. The solvent collected from the VOC SEP™ goes back to the solvent recovery tank to improve the yield of solvents. A carbon bed further polishes the water, and if needed, it goes to an advanced oxidation (AO) tank for peroxide dozing. AO is a safeguard for the process to make sure the discharge water will always remain below 800 ppm. A vacuum pump maintains the vacuum around 100–150 Torr (see Fig. 7.1).

## 7.5  RECOVERY OF NITRATES, SOLVENTS, AND WATER FROM WASTEWATER OF GOLD AND SILVER PLATING INDUSTRY BY USING HYBRID VOC SEP™/ AQUA SEP™ HYBRID MEMBRANE AND DISTILLATION

Gold and silver plating industry is facing challenges in their wastewater management. According to the new regulations it is not allowed to discharge wastewater without treatment, which will cause a significant surcharge. A hybrid system produced by Petro Sep has demonstrated that wastewater, containing nitrates, which include but not limited to ammonium nitrate and silver nitrate, solvents, and water, from any of plating industries can be treated. The valuable components of the wastewater can be recycled and reused.

The water from the wastewater tank first enters the Aqua Sep™ module where nitrates are separated from solvents and water. Then the permeate from Aqua Sep™ goes into VOC Sep™, where solvents are collected in the permeate. The solvents further go to the distillation column and condense on the top of the column. The solvents then go back to the plating unit to be reused in the process. The deionized water comes out from the bottom of the distillation column and then goes back to the first stage of the process.

All the energy to heat the feed is recovered by the condensers from the blower with the help of Aqua Sep™ and VOC Sep™ vacuum pump, this makes the process very economical and self-sufficient. A vacuum pump provides vacuum required for pervaporation as well as for the removal of non-condensable. Feed enters at 70°C and exists from the modules at 30°C. A vacuum pump maintains the vacuum at 100 Torr.

A feed pump maintains the turbulent flow in the modules to avoid concentration polarization. Thus, the membrane can maintain a high selectivity with a high flux. Some of the nitrates crystalize at the bottom of the feed tank. To avoid carry-over of the nitrates, the feed draw takes place from the side of the feed tanks instead of the bottom of the feed tank.

Fig. 7.2 shown the picture of the pilot plant of this process constructed by Petro Sep.

**FIG. 7.2** Vacuum system of 100,000 L per day capacity AQUA SEP™, VOC SEP™ hybrid pervaporation and membrane distillation plant for nitrates, solvents and water purification.

## 7.6 RECOVERY OF MEG, SOLVENTS, SALTS, AND WATER BY USING HYBRID AZEO SEP™, VOC SEP™ SYSTEM

PET (polyethylene terephthalate) recycling by using chemicals to dissolve PET is a relatively new process which faces a challenge in the treatment of a bi-products stream consisting of mono ethylene glycol (MEG), mixed solvents, salts, and water. The membrane technology can overcome this challenge. A simple process flow diagram of the process is shown in Fig. 7.3. This technology is applicable not only for PET recycling but also in any industries where similar byproducts are produced.

The by-products stream is first fed to the feed tank on a continuous basis. From the feed tank, it enters a custom designed TFE. In TFE (thin film evaporator) evaporate all the liquid components leaving behind salts and some MEG. Depending on the type of the solvents, an entertainer is necessary to be added in TFE.

In the solvent recovery column that follows TFE, MEG with trace water goes to the bottom while the solvents and water with a trace amount of MEG go to the top of the column.

The solvents and water from the top of the column go to VOC SEP™ where solvents and water are separated as the permeate and the retentate, respectively. Then, solvents go to the solvent tank, and water goes to (AO) tank.

From the bottom of the solvent recovery column, MEG with trace water go to AZEO SEP™ to dehydrate and purify MEG.
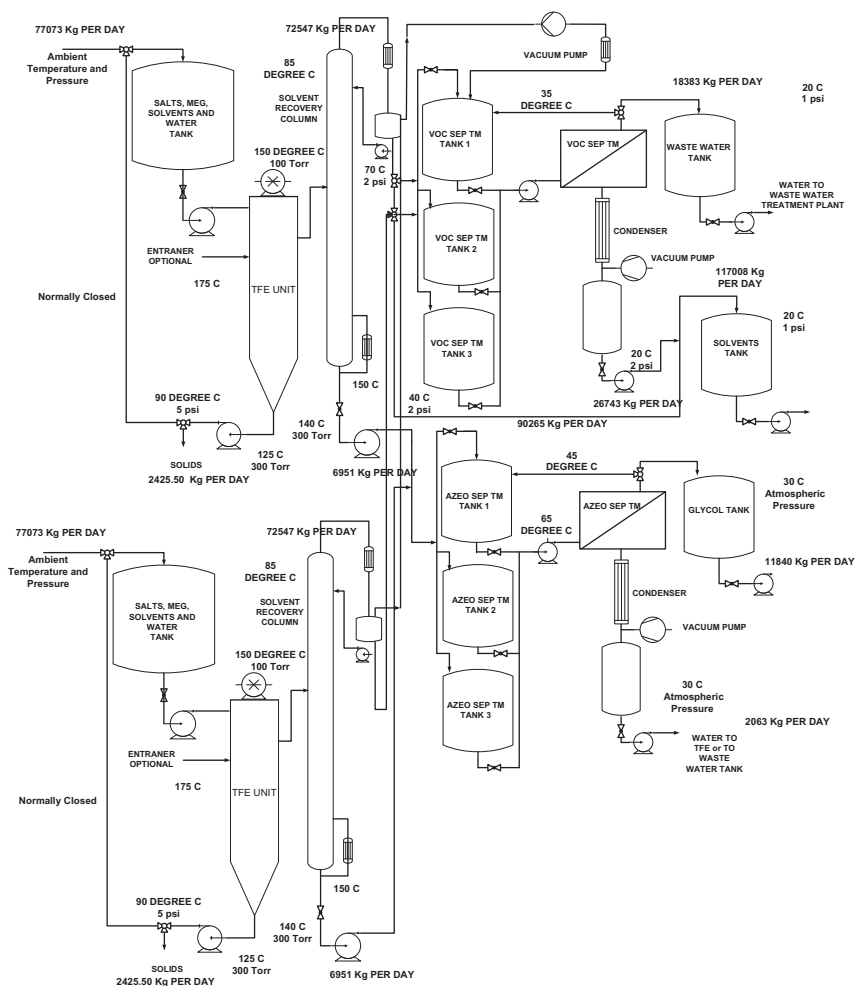
**FIG. 7.3**    154,146 L per day capacity VOC SEP™, AZEO SEP™ hybrid pervaporation plant for MEG, solvent recovery and water purification.

The products of this process are thus, MEG, mixed solvents, water, and salts.

## 7.7  PRODUCTION OF SUGAR FROM MSW BY AQUA SEP™, VOC SEP™ AND AZEO SEP™ SYSTEMS

Extraction of sugar from MSW (municipality solid waste) can be done by biomass hydrolysis. After extraction of sugars, the sugar solution becomes very lean due to the presence of 90% water. To make it economically viable, it is necessary to dehydrate the sugar solution inexpensively. Any evaporation technique will be costly to evaporate such a significant

amount of water. Aqua Sep™ is an ideal process to dehydrate sugar solution at 60°C while maintaining the required temperature by the self-generation of the heat. During the dehydration process, some of the sugar is fermented due to the presence of natural bacteria. Hence, this process produces ethanol as a by-product. The picture of the pilot plant constructed by Petro Sep is shown in Figs. 7.4 and 7.5.



**FIG. 7.4** 25,000 L per day capacity AQUA SEP™ hybrid membrane distillation plant for sugar extraction and purification from MSW.



**FIG. 7.5** 25,000 L per day capacity AQUA SEP™ hybrid membrane distillation plant for sugar extraction and purification from MSW.

## 7.8 PRODUCTION OF L-QUEBRACHITOL BY USING AQUA SEP™ AND VOC SEP™ HYBRID SYSTEM

In this process, feed consists of wastewater from a natural rubber industry. An optically active polyol, L-Quebrachitol, is contained in the wastewater together with other impurities such as VOCs.

The wastewater is first pretreated by centrifuge, followed by a series of filter press, MF, and UF/NF before entering Aqua Sep™. Two tanks are attached before each filtration step to enable the continuous operation. While one tank is in operation, the other is either in the discharge or in the filling stage. Proteins collected as the retentate of MF and UF/NF are sent to a drying system.

Then permeate from the UF/NF SEP™ then goes to the Aqua Sep™, via a feed tank, operated at the vacuum of 100–150 Torr. Water collected as vapor on the permeate side of the Aqua Sep™ goes to the heat exchanger via a blower at which the vapor is compressed in the compression ratio of 1.5–2.0. The retentate of Aqua Sep™ in which L-Quebrachitol is concentrated also goes to the heat exchanger to recover the heat from the water vapor. Isopropyl alcohol (IPA) is then added to the Aqua Sep™ retentate tank to recover and purify the targeted product L-Quebrachitol by crystallization.

The L-Quebrachitol/IPA mixture with remaining water is then transferred to TFE dryer to collect L-Quebrachitol crystals at the bottom. IPA and remaining water are separated by the following solvent recovery column where IPA evaporates and condenses at the top of the column. The IPA goes to the IPA tank, which makes almost 90% IPA recovery for reuse. The 10% IPA in water goes to VOC SEP™ from the bottom of the column to recover IPA. Retentate water of VOC SEP™ needs to be polished by AO before discharge (Fig. 7.6).

## 7.9 RECOVERY OF WATER IN MINING WASTEWATER TREATMENT BY USING AQUA SEP™

The mining industry uses a significant amount of water for the extraction of minerals. After the extraction of minerals, water becomes contaminated with chemicals and becomes toxic. This toxic water is exceptionally harmful to the environment. The current practice is based on the creation of tailing ponds. This is just a temporary solution to hold toxic water but not the complete solution to the problem. In some cases, the toxic water is diluted by using more water from Aquafer before being discharged to small streams called tailings. Both the above practices are disastrous for

**FIG. 7.6** 25,000 L per day capacity AQUA SEP™ hybrid membrane distillation plant for L-Quebrachitol and proteins production.

the environment. A new process has been developed by Petro Sep to treat the toxic wastewater in the mining industry.

As shown in Fig. 7.7, wastewater enters into the Aqua Sep™ feed tanks after the pre-treatment by UF. Aqua Sep™ feed pump circulates the toxic brine water through the Aqua Sep™ membrane modules. The permeate water vapor goes to the heat exchanger via blower at a compression ratio of 1.5–2.0. The heat is transferred to the retente of the Aqua Sep™ for further concentration of the toxic brine. The condensed water is clean enough to be discharged. The vacuum pump maintains the vacuum around 100–150 Torr and removes the noncondensable.

As the time passes the brine becomes concentrated in the concentrated salt tank. When the salt concentration reaches near the solubility limit, the concentrated brine is transferred to the TFE dryer to dry the salts. Remaining moisture also condenses at the top of TFE. The water from TFE

**FIG. 7.7** 5000 L per hour capacity AQUA SEP™ ZLD brine treatment plant.

condenser also goes back to the finished water tank. That makes almost 100% water recovery. Recovered water TDS remains below 10 ppm.

## 7.10  AZEO SEP™ USED IN A MEMBRANE REACTOR

In the resin manufacturing industry, 30% of the reactants remain unreacted and lost in the wastewater, because, like esterification, the reaction slows down due to the formation of water which inhibits the reaction. Hence, it takes a long time to complete the reaction, especially in the batch process. Combining AZEO SEP™ with the conventional reactor, removes water and thus reduces the inhibition, leading to the enhancement of reaction rate and yield. As well, the problem of wastewater discharge is solved. An enormous cost saving by the reactant recovery is also expected. The field test has demonstrated that AZEO SEP™ PV membrane is long lasting and robust in such a harsh environment.

PV membranes can be made in flat sheet or hollow fiber configuration. Until now, flat sheet membranes in plate-and-frame modules were the only ones available, and even those were used for very few PV applications, mainly for ethanol dehydration. Spiral wound and hollow fiber modules have been considered a failure due to the instability of the membrane as well as lack of compatibility of epoxy and glue in the module construction.

Recent developments in Petro Sep™ have changed the current situation of PV. For the first time in the PV history, AZEO SEP™ solvent-resistant membranes are now available in plate and frame (flat sheet) as well as hollow fiber configuration. Significant work has been done on solvent resistant epoxy and module design to use hollow fiber pervaporation membrane configuration.

The following Figs. 7.8–7.11 show the pictures of the pilot plants constructed by Petro Sep for various applications.

## 7.11  CONCLUSION

Since pervaporation (PV) was discovered as a phenomenon in the early twentieth century and proposed as one of membrane separation processes in the 1960s, there have been remarkable efforts worldwide to develop PV membrane technology. Similarly, the research on membrane distillation (MD) has a history of over 50 years.

PV was considered to become a powerful tool to separate azeotropic mixtures, by which many problems encountered by the chemical industry could be resolved. For this reason, millions of dollars have been invested to commercialize PV and MD technologies. However, there was no great

**FIG. 7.8**    20,000 L per day capacity AZEO SEP™ pervaporation plant for dehydration of solvents.



**FIG. 7.9**    40,000 L per day capacity AZEO SEP™ pervaporation plant for solvent dehydration.
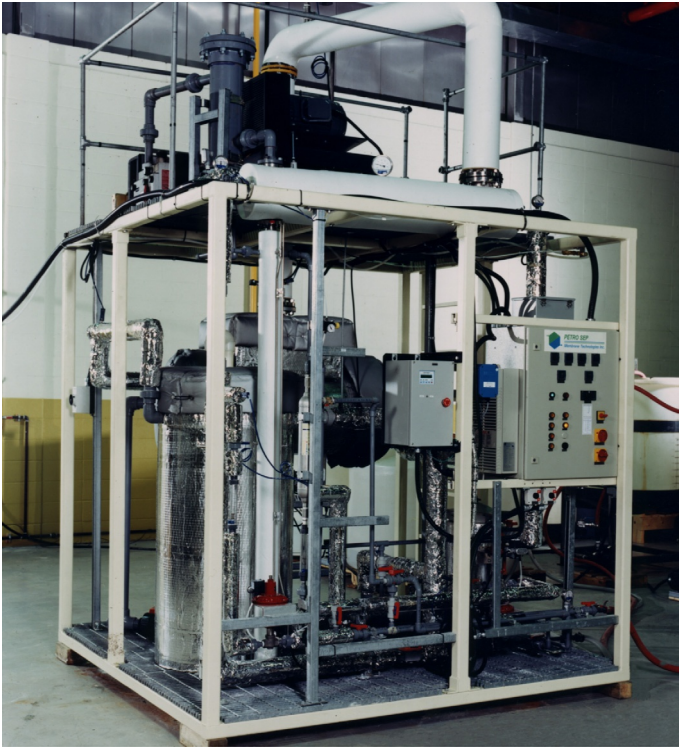
**FIG. 7.10** 10,000 L capacity per day pervaporation AQUA SEP™ to concentrate brine, based on hollow fiber membranes.



**FIG. 7.11** VOC SEP™/AQUA SEP™ HYBRID hollow fiber plant to treat 100,000 L water/day.

success in processing azeotropic solvents, with only one exception of alcohol dehydration in alcohols industry. Particularly, no one could treat a complex mixture of solvents, salts, and water. Thus, PV and MD were not thought to be economically viable, and the research started to decline since the end of the 1990s.

Over the last 20 years, R & D of PV and MD have been revitalized, demonstrating that PV technology could indeed become the solution for the separation of complex azeotropic mixtures. Especially, hybrid PV/MD systems provided the solution for the treatment of mixtures which consist of solvents, salts, and water. Another interesting technological development is the use of the hollow fiber module, which has long been considered impractical due to the lack of solvent resistant membrane as well as epoxy resin for module sealing. It was proven recently by the field test, for the first time in the history of PV and MD, that the hollow fiber module can be useful in breaking azeotropic mixtures and dehydrating many solvents even at an operating temperature of 120$^{\circ}$C, providing an excellent economical option. Another notable development in recent years is the fabrication of a hybrid membrane in which PV and MD functions are combined. It was found that the hybrid membrane increases the flux significantly without sacrificing selectivity.

Thus, the recent R & D activities at Petro Sep have opened new doors that lead to the solutions of many complex separation problems.

## References

[1] Kahlenberg L. On the nature of the process of osmosis and osmotic pressure with observations concerning dialysis. J Phys Chem 1906;10:141.

[2] Kober PA. Pervaporation, perstillation and percrystallization. J Am Chem Soc 1917;39:944–50.

[3] Schwob Y. Sur L'hemipereabilite a l'eau, des membrane de cellulose regeneree. Toulouse, France, 23 MAI, 1949.

[4] Binning RC, Lee RJ, Jenning JF, Martin EC. Separation of liquid mixture by permeation. Ind Eng Chem 1961;53:45–50.

[5] Khayet M. Membrane distillation, advance membrane technology and applications. New York: John Wiley & Sons, Inc; 2008.

C H A P T E R

# 8

# An Overview of Membrane Distillation

*Zhong Sheng Tai, Mohd Haiqal Abd Aziz, Mohd Hafiz Dzarfan Othman, Ahmad Fauzi Ismail, Mukhlis A. Rahman, Juhana Jaafar*

**Advanced Membrane Technology Research Centre (AMTEC), Faculty of Chemical and Energy Engineering, Universiti Teknologi Malaysia, Skudai, Malaysia**

O U T L I N E

# 8.1  INTRODUCTION

Freshwater scarcity has been one of the major challenges in this modern era. Global climate change, flourishing agricultural and industrial development, rapid global population expansion as well as aggravating water pollution have played significant roles in making the situation worse. It has been estimated that more than one billion people face difficulties to access to clean, fresh water [1]. Desalination is deemed as one of the most promising methods to enhance the fresh water capacity in order to cater the immense water needs. Through desalination, seawater and brackish water can be converted to fresh water by removing the dissolved solutes. Currently, reverse osmosis (RO) accounts for about 65% of the total desalination erections in the world because of its capabilities to produce high purity water [2]. However, this technology requires high operating pressure which makes it very susceptible to membrane fouling which then affects the freshwater productivity and quality [3, 4]. Thermal desalination is another significant key desalination technology and widely used in many of the desalination plants in the Middle East [3, 5]. This technology is energy intensive and commonly fueled by fossil fuels, which is not sustainable due to the high carbon emission and the threat of fossil fuel reserves depletion [6, 7]. Therefore, the development of desalination technology with consistent fresh water productivity and quality as well as sustainable energy is needed for fresh water production.

Membrane distillation (MD) is an arising desalination technology and can be a replacement for conventional desalination processes. It is a hybrid of thermal and membrane processes that separates the volatile solutes from the supply solution through a microporous hydrophobic membrane at fairly high temperatures. MD has several promising characteristics such as (i) lower operating temperatures than the thermal desalination technologies as the supply solution does not require to be heated to its boiling point for the distillation to occur, (ii) lower operating pressure compared to RO, (iii) theoretically 100% nonvolatile solute rejection, and (iv) the process performance is not affected by the salinity of the supply solution [8–11]. Despite the significant energy consumption, the integration of MD with the renewable energy such as solar and geothermal energy, as well as low-temperature industrial waste stream makes it particularly attractive in reducing the operating cost [12–14]. Moreover, the lower operating pressure condition allows the use of membranes with larger pore size and lower requirements for membrane mechanical properties compared to RO, thus making MD to be cost effective [9, 15].

The membranes with hydrophobic properties and larger pore size also reduce the susceptibility of MD to fouling [8, 9].

MD was first filed for patent by Bodell on 3rd June 1963 [16] and the first paper on MD was issued 4 years later by Findley in 1967 [17]. However, MD did not garner much interest at that time somewhat due to lower production was observed compared to the RO technology [18]. MD started to receive attention in the early of 1980s with the patent filings [19, 20] and the discoveries of the membranes and modules with better characteristics [21, 22]. The slow progress in the commercialization of MD technology has always been associated to the lack of membranes with appropriate characteristics for the MD applications, energy consuming process, high possibility of membrane wetting, low flux, as well as the limited module design [9, 18, 23]. However, with the growing efforts in realizing MD as a useful separation technology which could be seen from the significant increase in number of MD publications during the last decade or so, this process has been gaining the popularity with the availability of membranes with better characteristics as well as the feasibility to integrate with the alternative energy sources [23]. To date, the applications of MD have further been explored and expanded to various separation processes other than desalination such as removal of heavy metals, recovery of valuable materials, clarification of juices, which will be further discussed in the section later.

## 8.2  FUNDAMENTALS OF MD

### 8.2.1  Fundamental Principles of MD

In MD, the supply solution and permeate product are separated by a hydrophobic membrane. During the process, the supply solution with a high concentration of solutes is vaporized through heating whereas the permeate product is kept at lower temperatures. The difference in the temperatures between both sides of the membrane leads to the formation of vapor pressure difference. This induces the transport of vapor from one side of the membrane to the other through the membrane pores. The hydrophobic properties of the membrane only allow the transfer of vapor and completely refrains the flow of liquid from entering the pores. Therefore, the unwanted dissolved solutes which are in liquid phase are blocked and retained at the supply side. Finally, the vapor collected at the other side of the membrane is then condensed as a pure liquid product. The overall principle of MD is illustrated in Fig. 8.1.

As mentioned earlier, the hydrophobic membranes only allow the passage of vapors, which consequently leads to the accumulation of the nonvolatile solutes at the membrane surface facing the supply side. Eventually, the concentration of the nonvolatile solute at the membrane
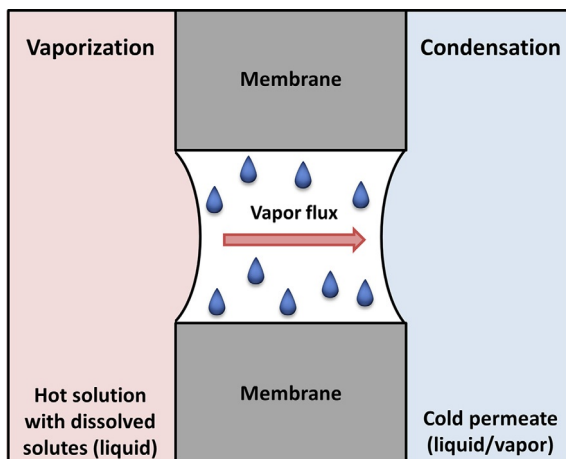
FIG. 8.1    Schematic representation of the fundamental principles of MD.

surface surpasses that of the bulk supply and leads to concentration polarization. The formation of concentration polarization layer at the supply side suppresses the transport of the vapor, leading to the reduction of the transmembrane flux [18, 24, 25]. The mass transfer resistance exerted by the concentration polarization layer at the supply side can be determined using concentration polarization coefficient (CPC) as shown in Eq. (8.1).

$$CPC = \frac{C_{fm}}{C_{fb}} \tag{8.1}$$

where $C_{fm}$ and $C_{fb}$ represent the solutes concentration at the membrane surface facing the supply side and bulk supply, respectively. It is also noteworthy to mention that the same phenomenon also occurs at the membrane surface facing the permeate side due to the decrease in solute concentration as a result from the condensation of vapor on the permeate side (Fig. 8.2) [24, 25].

The mass transfer through the membrane pores is related to dusty gas model as illustrated in Fig. 8.3. The vapor transport through the pores is mainly controlled by three mass transfer mechanisms which are Knudsen and molecular diffusions, as well as Poisseuille flow (viscous flow) relying on the membrane pore size, the existence of trapped air in the pores as well as the mean free path of the vapor molecules [9, 26–28]. This is due to the mass transfer resistance exerted by the collisions of vapor molecules with the pore wall (Knudsen resistance), collisions among the vapor molecules and/or with the air molecules trapped in the pores (molecular resistance), and transfer of momentum through the pores (viscous flow) [9]. It is worthwhile to point out that the surface diffusion mechanism is assumed to be negligible because of the small surface area of the membrane matrix where the diffusion occurs compared to the membrane pore area.
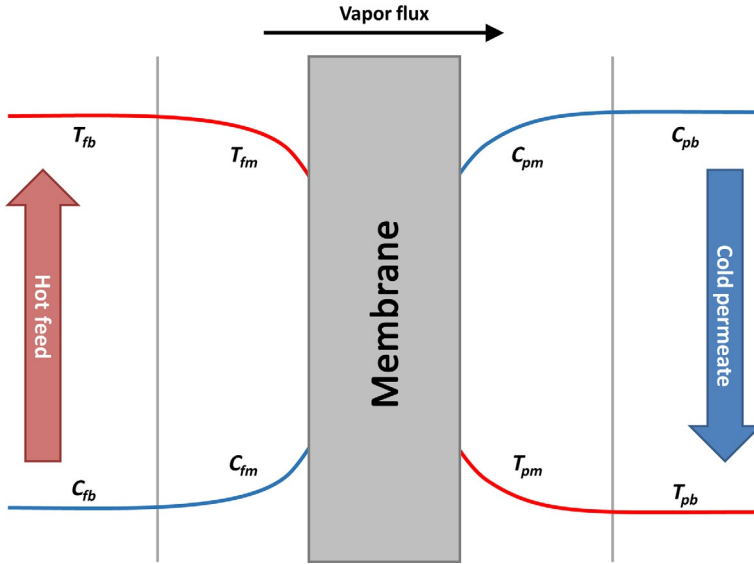
FIG. 8.2 Schematic illustration of the concentration and thermal polarizations in MD, where $C_{fm}$ and $C_{fb}$ are the solutes concentration at the membrane surface facing the permeate side, and bulk permeate, respectively, $T_{fm}$, $T_{pm}$, $T_{fb}$, and $T_{pb}$ are the membrane surface temperatures and bulk temperatures at the supply and permeate sides, respectively.
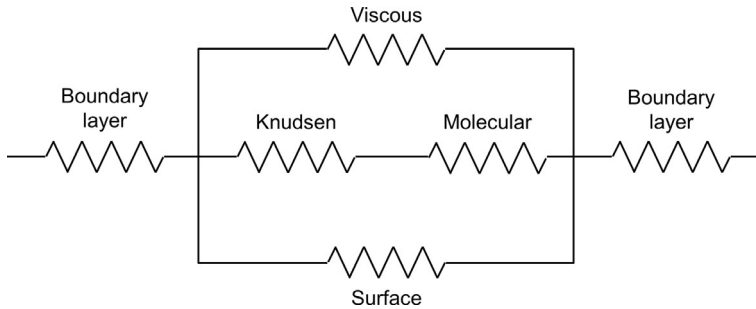


FIG. 8.3 Mass transfer resistances based on the dusty gas model.

Not to mention, the effect of the resistance at the membrane boundary layers toward the mass transfer are also generally insignificant.

Interestingly, the heat transfer happens concurrently with the mass transfer in MD. In general, the heat flows from the hotter to the colder temperature regions, and the rate of heat transfer is directly proportional to the extent of temperature difference. In this thermally driven process, a significant amount of heat energy is supplied to vaporize the liquid at the membrane surface facing the supply side. This creates a heat transfer boundary layer at that membrane surface which imposes resistance to the heat transfer due to the lower temperature gradient at the

liquid/membrane interfaces, giving rise to the adverse effects on the driving force for the mass transfer. This phenomenon is known as temperature polarization. The same effect also occurs at the membrane facing the permeate side which has the higher temperature than that of the bulk permeate (Fig. 8.2). The temperature polarization coefficient (TPC), which is the ratio of the transmembrane temperature to the bulk temperature difference, can be determined using Eq. (8.2).

$$\text{TPC} = \frac{T_{fm} - T_{fb}}{T_{pm} - T_{pb}} \tag{8.2}$$

where $T_{fm}$, $T_{pm}$, $T_{fb}$, and $T_{pb}$ are the membrane surface temperatures and bulk temperatures at the supply and permeate sides, respectively.

The heat transfers across the membrane occur through two different modes, namely latent heat of vaporization and conduction [29]. The portion of heat transferred by conduction through the membrane matrix and the pore occupied with gas is considered as heat loss. It is crucial to minimize the convective heat loss to lower the effects of temperature polarization and improve the MD process efficiency [18]. This could be achieved by applying the thin membranes with low thermal conductivity. Besides that, the presence of gases such as air and vapor with much lower thermal conductivity than that of the membrane material could contribute to lowering the conductive heat loss [9, 26]. Therefore, the membranes with high porosity could play their parts in enhancing the thermal efficiency of the MD process. More information on mass and heat transfers of the MD process can be found elsewhere [18, 23, 26, 27, 29].

## 8.2.2 MD Configurations

MD is commonly categorized into four necessary arrangements namely direct contact membrane distillation (DCMD), air gap membrane distillation (AGMD), sweeping gas membrane distillation (SGMD) and vacuum membrane distillation (VMD). The supply solutions of all these configurations are in direct contact with one side of the membrane. The differences between all these four configurations are the types of medium in contact with the membrane at the permeate side and how the condensation of vapor occurs [25]. The four basic MD configurations are as illustrated in Fig. 8.4.

### 8.2.2.1 Direct Contact Membrane Distillation (DCMD)

In DCMD, the hot supply and cold permeate are in direct contact with both sides of the hydrophobic membranes. It is the simplest and most commonly studied MD configuration because it does not involve additional equipment such as a condenser. DCMD has high permeate flux due to the direct contact of the membrane with supply and permeate, which minimizes the mass transfer resistance [30]. However, the continuous contact between the hot supply, membrane, and permeate promotes
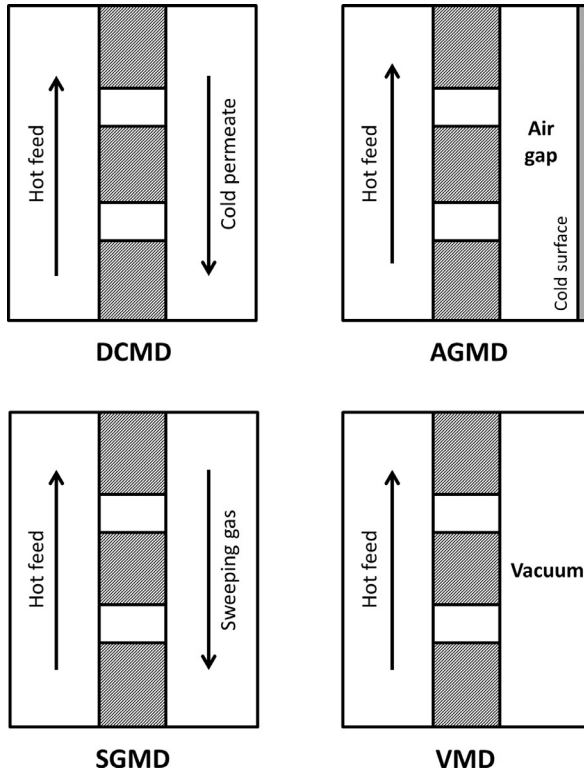
**FIG. 8.4**   The basic MD configurations.

the conductive heat losses and contributes to the highest thermal polarization among all the configurations [23]. This configuration is widely studied for desalination, concentration of fruit juices, or acid manufacturing [31–36].

### 8.2.2.2  *Air Gap Membrane Distillation (AGMD)*

In AGMD, stagnant air is introduced to separate the membrane from the cold condensation surface. The presence of this isolating air layer imposes a greater resistance to the mass transfer and consequently results in lower transmembrane flux than that of DCMD [29]. Despite that, this air layer possesses low thermal conductivity which contributes to enhancing the thermal resistance of the membrane, thus leading to lower conductive heat loss through the membrane. This configuration can be used in all the applications similar to those of DCMD. Besides that, it is also suitable to be used to remove the volatile substances like alcohols from the aqueous solution. These volatile substances have lower surface tension and/or smaller contact angles with the membrane, thus could lead to membrane wetting [37]. Because the permeate does not come in direct contact with

the membrane, AGMD has no issue with the membrane wetting at the permeate side and less tendency to fouling [23, 29, 37].

### 8.2.2.3 *Sweeping Gas Membrane Distillation (SGMD)*

Inert gas is incorporated in SGMD to carry the permeate vapor out of the membrane module where the subsequent condensation process takes place. Just like AGMD, the gas barrier in this configuration contributes to lowering the conductive heat loss. Different from AGMD, the gas in SGMD is continuously moving which in turn improves the mass transfer coefficient substantially, resulting in higher flux compared to AGMD. Moreover, this configuration can also be applied for the removal of volatile substances from the aqueous solution as it is not susceptible to wetting at the permeate side of the membrane. Despite all the advantages mentioned, this configuration requires a gas source in which the transportation of gas is costly [18]. The installation of a condenser with large capacity also increases the capital and operating costs because a significant amount of sweep gas is used [9]. Therefore, SGMD is less economically competitive, and this could be the main reason that it has not received much attention compared to DCMD [18, 29]. Not to mention, the involvement of additional equipment increases the complexity of the configuration and hinders the heat recovery [23, 29].

### 8.2.2.4 *Vacuum Membrane Distillation (VMD)*

VMD gives the highest permeate flux compared to other types of basic MD configurations. This is due to the reason that this configuration allows higher partial pressure gradient [30, 38, 39]. In VMD, a vacuum is applied at the permeate side to maintain the driving force, and the condensation occurs outside of the membrane module because the applied vacuum pressure is lower than the equilibrium vapor pressure [25]. This configuration has very low thermal polarization and negligible heat conductive loss [9, 23]. However, VMD has several disadvantages such as more susceptible to membrane wetting and fouling compared to other MD configurations [23, 30]. In addition, the heat recovery of VMD is also complicated due to the complexity of the configuration [30].

## 8.3 MEMBRANES FOR MD

## 8.3.1 Materials of Membranes

The development of membrane for MD process began with the use of silicone coated glass fibers and nylon which had demonstrated unsatisfactory wetting resistance [17, 40]. Since then, a number of hydrophobic membranes have been introduced for MD process including both polymeric

and ceramic membranes. Polymeric membranes have received much attention compared to ceramic membranes due to their intrinsic hydrophobic properties, ease of fabrication and cheaper cost. Currently, polytetrafluoroethylene (PTFE), polyvinylidenefluoride (PVDF) and polypropylene (PP) are among the most commonly used polymeric membranes for the MD applications. PTFE is the most suitable material for MD membrane fabrication as it has the highest hydrophobicity character with the surface energy of around $9–20 \times 10^{-3}$ N/m and a thermal conductivity of $\sim 0.25$ W/m K [29, 40, 41]. It also possesses outstanding thermal stability and resistance toward chemicals. Nonetheless, this polymeric material is difficult to process because it is practically not soluble in any regular solvents [23, 25, 40]. Therefore, despite of the outstanding properties of PTFE membrane, PVDF membrane is the most studied membrane due to its easy processability [23]. It has a surface energy of $30.3 \times 10^{-3}$ N/m and a thermal conductivity of $\sim 0.19$ W/m K [29, 41]. PVDF has high solubility in regular solvents such as dimethylformamide (DMF), N-methyl-2-pyrrolidone (NMP), triethylphosphate (TEP) and dimethylacetamide (DMAC). Thus, it is generally fabricated through phase inversion methods [25, 40]. PP membrane exhibits high crystallinity and excellent solvent resistant properties. This membrane has a surface energy of $30.0 \times 10^{-3}$ and a thermal conductivity of $\sim 0.17$ W/m K [29, 41]. PP membrane has the advantages in terms of material and manufacturing costs, but its symmetric structure and moderate thermal stability at higher operating temperatures could affect its MD performance [40].

Ceramic membranes are the arising MD membranes due to their excellent intrinsic properties regarding thermal, chemical, and mechanical stabilities [42, 43]. Ceramic membranes are hydrophilic, and thus surface modifications are needed to acquire hydrophobicity for the MD process. The first paper on the application of ceramic in MD was published in 2004 by Larbot and his research partners [44]. They modified the surface of zirconia and alumina membranes with 1H, 1H, 2H, 2H-perfluorodecyltriethoxysilane which successfully enhanced their contact angles up to 145 degrees. The membranes were used for desalination and achieved the salt rejections of close to 100%. To date, some studies have been conducted to investigate and enhance the ceramic membranes (alumina, zirconia, silicon nitride, titania, and β-sialon) for the MD applications [43, 45–47]. Ceramic membranes have a high thermal conductivity which leads to significant conductive heat loss through the membrane during MD operations [28]. Besides that, ceramic membranes are often more expensive than polymeric membranes due to the expensive ceramic materials and complicated fabrication processes [42, 48]. Recently, there has been an increasing effort in fabricating ceramic membranes using low-cost materials such as natural clays and wastes, which makes this kind of membranes to be much more exciting and exhibits the potential to be applied in the MD process [49–51].

Recently, carbon nanotubes (CNTs) have been gaining some attention in the MD applications. CNTs have several unique advantages including high hydrophobicity, porosity and surface area, antifouling as well as offering good thermal and mechanical stabilities, which can significantly benefit the physical and chemical properties of the membranes for the MD applications [52]. CNTs have been used in various forms such as stand-alone membranes [53–56] or nanofiller reinforcements in nanofiber membranes [57–59]. Dumée and his research group [53] developed the self-supported CNTs bucky paper membranes through vacuum filtration technique, in which the CNTs were only held together by the van der Waals forces. The membranes possessed high hydrophobic properties with a contact angle of 113 degrees and high porosity of 90%. A high salt rejection of 99% was achieved for the DCMD, indicating its excellent potential for the MD applications. However, CNTs bucky paper membranes possessed several disadvantages such as the delamination issues due to aging, as well as the relatively high thermal conductivity of $\sim$2.7 kW/m$^2$ h. To address these issues, the same research group conducted the chemical modifications on the CNTs via (i) UV/ozone treatment to produce hydroxyl groups which were then replaced with alkoxylsilane based groups [54], and (ii) coating with a thin layer of PTFE [55]. The hydrophobicity of the membranes was significantly enhanced and consequently contributed to the improvement in permeate flux. The stability of the modified membranes was also increased which then improved the membrane lifespan. However, the development of CNTs membranes is still at the beginning phase and full of challenges which might hinder their future development. The effective CNTs production methods and costs, as well as potential human and environmental risks, should be explored and accessed critically to ensure the development to their full potential [60].

## 8.3.2 Optimal Membrane Characteristics

### 8.3.2.1 Liquid Entry Pressure (LEP)

Membrane pore wetting is a crucial issue for MD applications as it affects the permeate quality and productivity. Liquid entry pressure (LEP) is defined as the minimum pressure required to force the liquid to penetrate into the hydrophobic membrane pores. Pore wetting can be prevented if the transmembrane pressure of the aqueous solution is lower than the LEP of the membrane. It is recommended that the MD membranes should have a minimum LEP value of 2.5 bar to ensure an effective performance under fluctuating operating conditions in the real plant operations [28, 61]. LEP of the membranes relies strongly on the hydrophobicity and maximum pore size of the membranes. A high LEP value can be obtained by using the membrane materials with excellent intrinsic

hydrophobic properties and small maximum pore size or modify the membrane surface using the materials with low surface energy and large contact angle. The LEP value can be determined using the Laplace-Young equation from Eq. (8.3) [62, 63].

$$\text{LEP} = \Delta P_{entry} = \frac{-2B\gamma_l \cos\theta}{r_{max}} \qquad (8.3)$$

where $\Delta P_{entry}$ is the entry pressure difference, $B$ is the geometric pore coefficient depending on the geometry of the membrane pores ($B = 1$ for cylindrical pores), $\gamma_l$ is the surface tension of liquid (N m$^{-1}$), $\theta$ is the contact angle (degrees), and $r_{max}$ is the maximum membrane pore size (m).

### 8.3.2.2 *Mean Pore Size and Pore Size Distribution*

The membranes used in MD system generally have the pore sizes in the range of 100 nm to 1 μm [18]. The mean pore size has the significant effect on the membrane permeability. The permeability of the membrane increases with the larger mean pore size, thus allowing higher transmembrane flux. However, the LEP value decreases at larger mean pore size which increases the possibility of membrane wetting. Therefore, the optimum pore size should be determined without compromising the permeability and LEP of the membrane [26, 27].

The membranes employed in the MD applications do not have uniform pore size. Instead, they exhibit a pore size distribution. It is important to keep the pore size distribution narrow because it would affect the uniformity of the mass transfer mechanisms [26, 27, 64]. In general, several mass transfer mechanisms (Knudsen diffusion, molecular diffusion, and/or Poisseuille flow) coincide in MD as mentioned in the earlier part because of the pore size distribution and MD operating conditions [18].

### 8.3.2.3 *Porosity and Tortuosity*

Membrane porosity refers to the void volume fraction of the membrane open to MD vapor flux. It is always recommended that the porosity of the membrane should be as high as possible to enhance the permeate flux and reduce the heat loss through conduction. According to El-Bourawi et al. [18], the membranes employed in MD applications exhibit the porosity in the range of 30%–85%. However, the membranes with high porosity exhibit a significant weakness in term of mechanical strength and tend to crack or compress under mild pressure [41]. Therefore, the mechanical strength should also be taken into account when enhancing the porosity of the membranes. The porosity of the membrane can be calculated by the Smolder-Franken equation (Eq. 8.4) [65, 66]:

$$\varepsilon = 1 - \frac{\rho_m}{\rho_{pol}} \tag{8.4}$$

where $\varepsilon$ is the porosity whereas $\rho_m$ and $\rho_{pol}$ are the densities of the membrane and polymeric material, respectively.

Membrane tortuosity refers to the deviation of the pore structure from the straight cylindrical pores normal to the membrane surface. Generally, the membrane pores are not straight but full of twists and turns. The diffusing vapor molecules must pass along the tortuous paths to reach the other side of the membrane, which leads to lower flux. Thus, the membrane tortuosity should be as small as possible to ensure higher flux. According to Srisurichan et al. [67], the tortuosity factor can be successfully derived from the correlation proposed by Mackile and Meares [68] as shown in Eq. (8.5).

$$\tau = \frac{(2 - \varepsilon)^2}{\varepsilon} \tag{8.5}$$

where $\tau$ is the tortuosity factor. It is worth to mention that a tortuosity value of 2 is frequently assumed to predict the transmembrane flux in the MD studies [27].

### 8.3.2.4 Membrane Thickness

Membrane thickness is inversely proportional to the permeate flux in the MD applications. The membrane should be as thin as possible to acquire higher permeate flux. However, the thermal resistance becomes lower with the decrease in membrane thickness. Therefore, for a single-layered membrane, the membrane thickness should be optimized to obtain high permeate flux and low conductive heat loss. A theoretical study by Lagana and his coworkers [69] estimated that the optimum membrane thickness lied in the range of 30–60 μm by considering the thermal conductivity of the commercial MD membranes. In the case of multilayered composite membranes with hydrophobic and hydrophilic layers, the hydrophobic layer should be kept as thin as possible [26, 27]. It is worth pointing out that the membrane thickness has negligible effects on the AGMD performance because the mass transfer resistance in this configuration is provided predominantly by the air gap [18].

### 8.3.2.5 Thermal Conductivity

Membrane thermal conductivity is another vital issue in MD. The high thermal conductivity of the membrane contributes to the degree of conductive heat loss through the membrane. The polymeric membranes commonly used in MD (e.g., PTFE, PVDF, and PP) usually have the thermal conductivity of higher than 0.2 W/m K [10]. Ceramic membranes have high thermal conductivity and could cause sizeable conductive heat loss and a decrease in permeate flux. Hendren et al. [70] reported that the

commercial alumina anodisc membranes have high thermal conductivity of 18 W/m K. A later study by Wang and his colleagues [43] has discovered a β-sialon ceramic membrane with lower thermal conductivity of <2 W/m K. Therefore, it is crucial to discover and use the membrane material with low thermal conductivity in order to improve the permeate flux. Besides that, the membranes with high porosities exhibit lower thermal conductivity due to the larger amount of entrapped gases (such as air and water vapor) in the membrane pores. Moreover, the use of porous hydrophobic/hydrophilic composite membranes could also be a suitable approach to enhance the MD membrane performance. The hydrophobic layer is responsible for the mass transport and should be as thin as possible, whereas the hydrophilic layer helps to enhance the conductive heat transfer resistance [10, 26, 27]. However, it must always be remembered that the hydrophilic layer should not have the thickness that could pose an adverse effect on the mass transfer in the membrane [26, 27].

## 8.4 HYDROPHOBIZATION OF MEMBRANES FOR MD

### 8.4.1 Hydrophobicity

Hydrophobicity is the critical requirement for MD process. This is inspired by the biosurface of lotus leaf that has excellent water repellency and self-cleaning properties. In MD, the hydrophobic membrane repels the supply solution to maintain the membrane pores dry. Generally, the wettability of a membrane can be quantified by contact angle ($\theta_{CA}$). The membrane is often characterized as hydrophobic when $\theta_{CA} > 90$ degrees or otherwise, it is regarded as hydrophilic ($\theta_{CA} < 90$ degrees). The membrane can be categorized as super-repellant and super-antiwetting (superhydrophobic) if $\theta_{CA} > 150$ degrees [71, 72]. In general, the membranes can acquire superhydrophobic properties via surface roughening of specific low surface energy materials, chemical modification via grafting using low surface energy materials or the combination of both surface roughening and chemical modification [71–73].

The fascinating phenomena of the hydrophobic surface were described by Thomas Young >200 years ago [72]. According to Young's equation (Eq. 8.6), the contact angle of a liquid droplet spreading on the surface is defined by the mechanical equilibrium of the droplet under the three interfacial forces [74].

$$\cos\theta_{CA} = \frac{\gamma_{SL} - \gamma_{SV}}{\gamma_{LV}} \tag{8.6}$$

where $\gamma_{SL}$, $\gamma_{SV}$, and $\gamma_{LV}$ are the solid-liquid, solid-vapor, and liquid-vapor interfacial forces, respectively.

Young's equation assumes ideal surfaces (Fig. 8.5A) that are homogeneous, smooth, and do not change their characteristics despite external
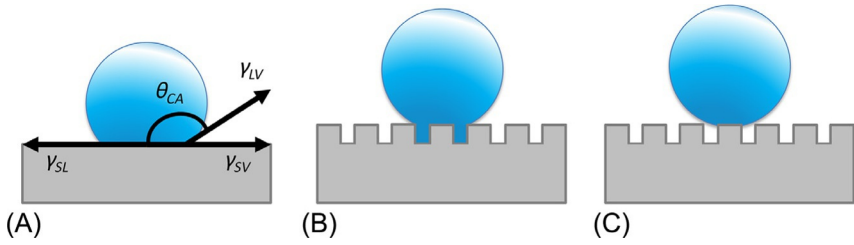
FIG. 8.5 Schematic representations of a liquid droplet spreading on a smooth surface according to Young's model (A), as well as rough surfaces based on Wenzel (B) and Cassie-Baxter (C) regimes.

interactions or forces [75]. Realizing there is no such ideal surface in the real world, two different models have been developed, particularly Wenzel and Cassie-Baxter regimes. Both of these regimes consider the surface roughness in their improved sets of equations.

In the Wenzel regime [76], the liquid droplet spreads across the rough surface without entrapped air underneath (Fig. 8.5B). Surface ratio (R) is introduced and defined as the ratio of the actual surface area to the apparent surface. The actual surface area is always greater than the apparent surface because of the surface roughness. The surface roughness in this regime can promote the wettability or nonwettability depending on the intrinsic properties of the surface. The true contact angle of the surface is described as follows (Eq. 8.7):

$$\cos\theta_{CA} = R\left(\frac{\gamma_{SL} - \gamma_{SV}}{\gamma_{LV}}\right) \tag{8.7}$$

The wetting phenomenon for the rough surface with small protrusions that are filled with air can be described with the Cassie-Baxter regime [77] (Fig. 8.5C). This phenomenon is necessary to create low adhesion hydrophobic surfaces that limit the contact of liquid droplet with the surface. Therefore, the liquid droplet can be easily rolled off from the surface. This regime is described in the following equation (Eq. 8.8).

$$\cos\theta_{CA} = -1 + \Phi_S\left(1 + \frac{\gamma_{SL} - \gamma_{SV}}{\gamma_{LV}}\right) \tag{8.8}$$

where $\Phi_S$ is the fraction of the surface that is in contact with the liquid droplet.

## 8.4.2 Hydrophobic Polymeric Membranes

Several efforts have been made to enhance the hydrophobicity of the polymeric materials by combining the polymeric materials especially PVDF with fluoropolymers. Fluoropolymers have low surface tension

due to the low polarity and strong electronegativity of the fluorine atom, as well as the strong C—F bond (485 kJ mol$^{-1}$) [78]. Thus, they have been an excellent choice for hydrophobicity enhancement. The copolymers such as poly(vinylidene fluoride-co-hexafluoropropylene) (PVDF-HFP) [58, 79], poly(vinylidene fluoride-co-tetrafluroethylene) (PVDF-TFE) [80] and poly(vinylidene fluoride-co-chlorotrifluoroethylene) (PVDF-CTFE) [81] possess better hydrophobicity and are used in membrane fabrication for the MD applications. For instance, the incorporation of hexafluoropropylene (HFP) in PVDF increases the amount of fluoride content and thus enhances the hydrophobicity of the copolymer [78, 82].

Apart from the employment of copolymer with high hydrophobicity, the hydrophobicity of the polymeric membrane can also be enhanced through the surface modification. There are three major surface modification techniques, namely hydrophobic polymeric coating, plasma treatment and incorporation of fluorinated surface modifying macromolecules (SMM). Several polymeric materials have been studied for hydrophobic membrane surface coatings such as silicon rubber [83], styrene-butadiene [84] and perfluoropolyether [85]. Jin et al. [83] modified the poly(phthalazinone ether sulfone ketone) (PPESK) hollow fiber composite membranes with a silicone rubber coating, and a contact angle of 128 degrees was obtained. The membrane was applied in VMD and achieved a high salt rejection of 99%. However, pore blockage occurred due to the gelation of the silicon rubber resulted from the prolonged heating, and this had affected the permeate flux adversely [83, 86]. Yang and his coworkers [85] modified the PVDF membrane surface with perfluoropolyether. The modified PVDF possessed a contact angle of 115 degrees and LEP value of 3.9 bar. The permeate flux remained stable over 1 month of DCMD testing, and 100% of salt rejection was obtained. Therefore, the selection of coating material is essential as the membrane properties could be affected either positively or negatively, which in turn would affect the membrane performance in the MD applications [86].

In plasma treatment, the monomer molecules are ionized to form free and active radicals, ions, electrons and molecules which would then adsorbed, condensed and polymerized on the membrane surfaces. Cross-linking or chemical bonding occurs between the electrons, ions and deposited molecules, resulting in the formation of the dense hydrophobic coating layer that imparts enhanced hydrophobicity to the membrane surfaces [86]. The process of plasma treatment is simple, and it does not alter the membrane matrix [87]. Besides that, the hydrophobic layer possesses an excellent adhesive ability to the membrane surface resulting in a dense and robust coating layer. The disadvantages of this treatment include the involvement of expensive equipment as well as the extra cares on the handling of the toxic monomer gases [86]. Several examples of the polymeric membranes surface modification through

plasma treatment for the MD application purposes include the tetrafluor-omethane (CF$_4$) plasma modification of hydrophilic polyethersulfone (PES) membrane [88], vacuum plasma coating on poly(ethylene tere-phthalate) (PET) membrane using perfluorohexane and hexafluoroben-zene [89] and octafluorocyclobutane plasma treatment on cellulose nitrate membrane [90].

The incorporation of fluorinated surface modifying macromolecules (SMM) in the phase inversion process is another facile method to produce a polymeric membrane with high hydrophobicity. SMM is an oligomeric fluoropolymer synthesized by polyurethane chemistry, and the polyure-thane chain is ended with two low polarity fluorinated groups [27, 86]. The membrane incorporated with SMM exhibits excellent hydrophobicity due to the formation of a thin hydrophobic layer on the membrane surface resulting from the migration of SMM to the membrane surface during the solvent exchange process in the phase inversion [91]. The incorporation of SMM for the preparation of composite hollow fiber membranes for MD has been widely studied. For instance, Khayet and his colleagues [92] pre-pared composite hydrophobic/hydrophilic porous membranes for DCMD by incorporating SMM with polyetherimide (PEI). It was found that SMM modified PEI membranes possessed higher contact angles (up to 97.7 degrees) and LEP values (>3.41 bar) than the unmodified PEI. Despite their lower pore size and porosities, the SMM modified PEI membranes exhibited the permeability of the same order of magni-tude to that of the commercial PTFE membranes. The literature of the incorporation of SMM in the preparation of other composite hydropho-bic/hydrophilic membranes for the MD applications can be found else-where [93, 94].

## 8.4.3 Hydrophobic Ceramic Membranes

The surface modification using low surface energy materials has been widely known to be effective for the preparation of the hydrophobic ceramic membranes [95]. There are several types of modifying agents used in the grafting process such as organosilanes, alcohols and lipid solutions [86, 96]. The alcohols and lipid solutions are not suitable to be used in MD applications because of their low thermal and chemical stabilities, as well as the limitation of oil used [97, 98]. Organosilane is a silane that contains at least one carbon-silicon bond structure. Fluoroalkylsilanes (FAS), which is a type of organosilane, have been commonly used as the ceramic mem-brane surface modifiers due to their ease of handling. The presence of hydrophobic groups such as CF$_2$-CF$_2$, CF$_2$-CF$_3$, Si-C, C-C, and C-O pro-vide FAS with lower surface tension and hydrophobic effects [99]. In gen-eral, hydrophobic ceramic membranes can be prepared through three

organosilane grafting techniques, particularly immersion, chemical vapor deposition (CVD) and sol-gel methods.

Organosilane grafting via immersion is the most widely used method due to its simple procedure and short treatment time [86]. In this method, the organosilane is first hydrolyzed in the solvents in which the active silanols are formed. The active silanols are then reacted with the hydroxyl groups present on the surface of the ceramic membrane, imparting hydrophobic character on the membrane surface. Organosilane with two or three silanol species can further adjoin with the adjacent molecules through the Si—O—Si bond, and a hydrophobic complex is formed [100]. Besides, the vertical polymerization occurs beyond the intermolecular reaction for hydrophobic monolayer to form grafted polysilozane as illustrated in Fig. 8.6. The polymerization reaction of organosilane on membrane surface was reported by Lu and his coworkers [101]. The authors observed the formation of a needle-like structure on the surface of the membrane and the size of the structure became larger after being grafted for four times as a result of polymerization. The needle-like structure enhanced the surface hydrophobicity but at the same time, introducing greater mass transfer resistance and consequently affected the water flux. The effectiveness of organosilane immersion grafting in providing hydrophobicity to the ceramic membranes is directly affected by the types of functional groups in the organosilane structure, hydrophobic tail
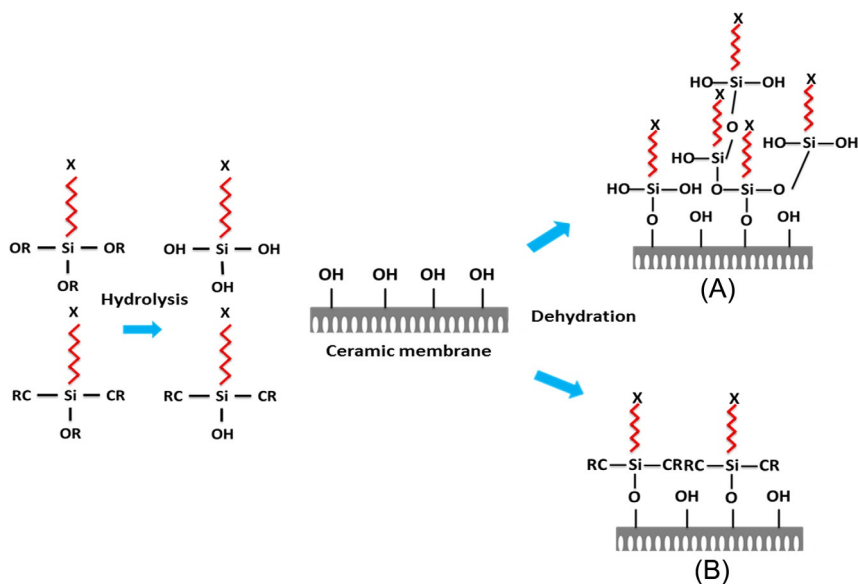


FIG. 8.6  Reaction of organosilane molecules on the membrane surface: (A) vertical polymerization and (B) single silanol species (—Si—OH).

length, grafting duration, amount of hydroxyl group on the surface of the ceramic membrane, membrane surface roughness and grafting multiplicity [95, 96].

CVD is an alternative ceramic membrane grafting technique which involves the chemical reactions of reactive vapor with the membrane surface at the elevated temperatures. In CVD, the organosilane is heated at its boiling points, and the reactive vapor forms chemical bonding with the hydroxyl groups on the ceramic membrane surface to form a hydrophobic coating. The formation of covalent bonding between the hydroxyl groups on the membrane surface with the organosilane vapor is similar to that of immersion grafting [86]. CVD has several advantages over the solution-based coating such as the use of small amount of solvent, as well as shorter treatment process compared to a solvent-based coating which requires drying process. However, this process is energy consuming and requires extra safety precautions in handling the toxic organosilane vapor. Currently, the application of CVD grafting in the ceramic membrane is insufficient probably due to the requirements of the processing vessel as well as the limitation of the organosilane compounds with low boiling points.

In sol-gel method, the ceramic membrane is dip-coated in the sol-gel containing organosilane. This is finally followed by the pyrolysis of the coated ceramic membrane at high temperature to remove the sol. De Vos et al. [102] prepared the hydrophobic silica membrane through dip coating the membrane with a sol containing methyltriethoxysilane followed by the calcination of the membrane at 400°C. It was found that the membrane acquired ten times higher hydrophobicity compared to the virgin silica membrane. Wang and his colleagues [103] reported the fabrication of hydrophobic β-sialon ceramic membranes by coating with polydimethylsiloxane (PDMS) layer though poly-condensation reaction. The membranes demonstrated high hydrophobicity with the contact angle of up to 140 degrees. An increasing in contact angle values with the elevated pyrolysis temperature from 200 to 600°C was reported. However, the hydrophobicity decreased after the pyrolysis temperature was raised to 700°C and the membrane became hydrophilic at 800°C. This was due to the reason that the polymer film was burnt off at a high temperature causing the membrane to lose its hydrophobicity. The membrane obtained successfully showed excellent MD performance with the salt rejection of >99%.

## 8.4.4 Applications of Nanotechnology in Hydrophobic Membranes for MD

Research interest has been devoted to mimicking the natural superhydrophobic surface through the employment of multireentrance structure on the membrane surface and low surface tension materials. The

functionalization of nanoparticles such as $SiO_2$, $TiO_2$, carbon nanotubes (CNTs), and graphene has garnered significant attention for the manufacturing of the hydrophobic membranes. This functionalization technique contributes to generating hierarchical structure on the membrane surfaces which imparts self-cleaning or hydrophobic properties to the membrane. An overview of hydrophobic membrane surfaces with macro/nanocomposite will be discussed in this section.

### 8.4.4.1 *Applications in Polymeric Membranes*

A material surface is deemed as amphiphobic if it possesses repellency toward water as well as other low surface tension oils. The material can acquire amphiphobic properties through the combination of the macro/nanosurface roughness with the low surface energy materials. Recently, PVDF membranes with amphiphobic properties have been developed through the functionalization with $SiO_2$ and $TiO_2$ nanoparticles and fluorosilanized with low surface energy organosilanes [104, 105]. The resultant exhibited antifouling and antiwetting properties against kerosene, humic acid and glycerol. Meng et al. [106] reported that the hierarchical structure of $TiO_2$-coated PVDF membrane enhanced the overall surface roughness of the low surface energy 1H, 1H, 2H, 2H-perfluorododecyltrichlorosilane layer, thus further enhancing the hydrophobicity. This behavior is in accordance with the Wenzel's regime which has stated that the surface roughness can promote the hydrophilicity and hydrophobicity of the surfaces depending on their chemical properties [72]. Razmjou and his research group [105] found that the multilevel roughness $TiO_2$-coated membrane demonstrated better antifouling performance compared to the virgin membrane. The $TiO_2$-coated membrane obtained high flux recovery after chemical cleaning and maintained its super-repellency toward humic acid.

The omniphobicity of the membrane can also be improved with the higher level of reentrant structures and lower surface energy. Membrane omniphobicity is defined as the ability of the membrane to repel water and liquids with low surface tension like oils, ethanol. Boo and coworkers [107] introduced the secondary reentrant structures through the spherical $SiO_2$ nanoparticles coating on the FAS-functionalized glass cylindrical fibers. The secondary reentrant structures introduced an air gap between the liquid and membrane surface which allowed the liquid with low surface tension to achieve a metastable Cassie-Baxter state (refer to Fig. 8.7), thus enhancing the antiwetting properties. The authors also found that the membrane functionalized with longer FAS chain and coated with $SiO_2$ nanoparticles demonstrated steady flux and salt rejection in DCMD for treating the saline solution (1 M) containing the sodium dodecyl sulfate (SDS) concentration of up to 0.2 mM. This was attributed to the multilevel reentrant structure and lower surface energy of the FAS with a longer
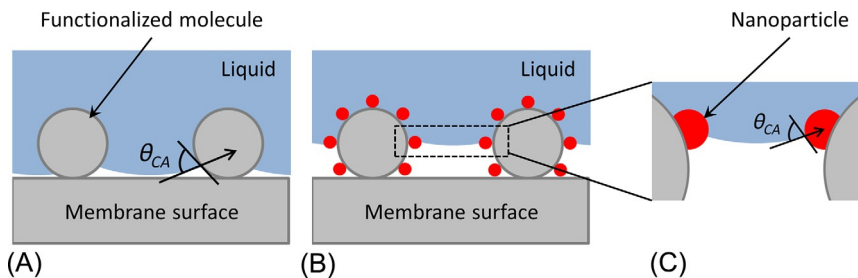
**FIG. 8.7** Schematic illustration of the putative air-liquid interface on the membranes with single reentrant (A) and secondary reentrant structures achieved by the introduction of nanoparticles (B and C).

chain. A similar outcome on the reentrant structures in providing omniphobic properties to the membrane surfaces was also described by Li et al. [108]. The omniphobic membrane coated with $SiO_2$ nanoparticles showed steady DCMD performance with more consistent flux and salt rejection during the treatment of saline water containing SDS in comparison with those of commercial hydrophobic PTFE membrane. All of these works demonstrated that the surface modification through the functionalization of low surface energy materials together with nanoparticles coating can be an effective way to sustain a robust MD operation and exhibits great potential to be applied in various separation applications especially those involves low surface tension supply solutions.

### 8.4.4.2 Applications in Ceramic Membranes

Surface modification using low surface energy material, in particular, organosilane, has been widely employed to prepare hydrophobic ceramic membranes. However, the modification of the surface architecture of the ceramic membrane to acquire super-hydrophobicity for the MD process has not been extensively investigated. Recently, Huang et al. [109] introduced a superamphiphobic silica-based fibrous membrane by creating nanoscale surface roughness with the $SiO_2$ nanoparticles. The membrane was fabricated using coaxial electrospinning with a blend of polyvinyl alcohol (PVA)/silica as the substrate and PVA/silica nanoparticles as the surface modifier to prepare membrane with nanoscale surface roughness. Later, the membrane was calcined at 800°C to remove the PVA and lastly followed by the fluorination with 1H,1H,2H,2H-perfluorodecyltriethoxysilane. The overall process is as illustrated in Fig. 8.8. The second scale reentrant structure provided this membrane with amphiphobic properties with high deionized water and oil contact angles of 154 and 149 degrees, respectively. Interestingly, the membrane demonstrated outstanding and consistent DCMD flux and a salt rejection of 100% even with
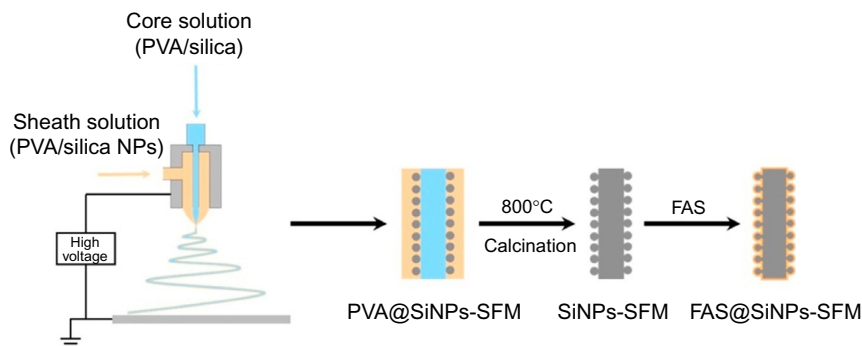
FIG. 8.8   Schematics of the preparation of the fluorinated silica-based fibrous membrane coated with SiO$_2$ nanoparticles (FAS@SiNPs-SFM). *Modified from Fig. 1. of Huang Y-X, Wang Z, Hou D, Lin S. Coaxially electrospun super-amphiphobic silica-based membrane for anti-surfactant-wetting membrane distillation. J Membr Sci 2017;531:122–8 with permission. License # 4285691225631.*

the increase in SDS concentration of up to 0.4 mM. These findings have proven the effectiveness of hierarchical surface roughness in improving the antiwetting properties of the ceramic membrane.

### 8.4.4.3  Hydrophobic Carbon-Based Materials

As mentioned in the earlier part, CNTs have several outstanding characteristics which give them an excellent potential for the MD applications. CNTs can be incorporated in polymeric nanofiber membranes to enhance their hydrophobicity. A study done by Tijing and coworkers [57] demonstrated that the incorporation of CNTs in the nanofiber membranes contributed to the bead formation that provided the micro/nanomembrane surface roughness and consequently improved the hydrophobicity of the membranes. However, the modified membrane exhibited lower LEP values compared to that of the commercial PVDF membrane and this was mainly due to their larger pore size. Moreover, the tensile strength of the membrane was also found to be stronger after the addition of 5 wt% of CNTs compared to the commercial PVDF membrane and pristine nanofiber membrane. Besides that, the membrane modifications with CNTs have also been reported for their effectiveness in boosting the vapor permeability by altering the vapor-membrane interactions. The incorporation CNT in nanofiber membranes enhances the antiwetting properties of the membrane pores and promotes the mass transfer [110]. The enhanced hydrophobicity of the membrane pores endowed by CNTs causes the pore walls and vapor molecules to have higher repulsive energy. The increment in the repulsion of the vapor molecules to the pore wall enhances the Knudsen and molecular diffusions. In addition, viscous flow can also
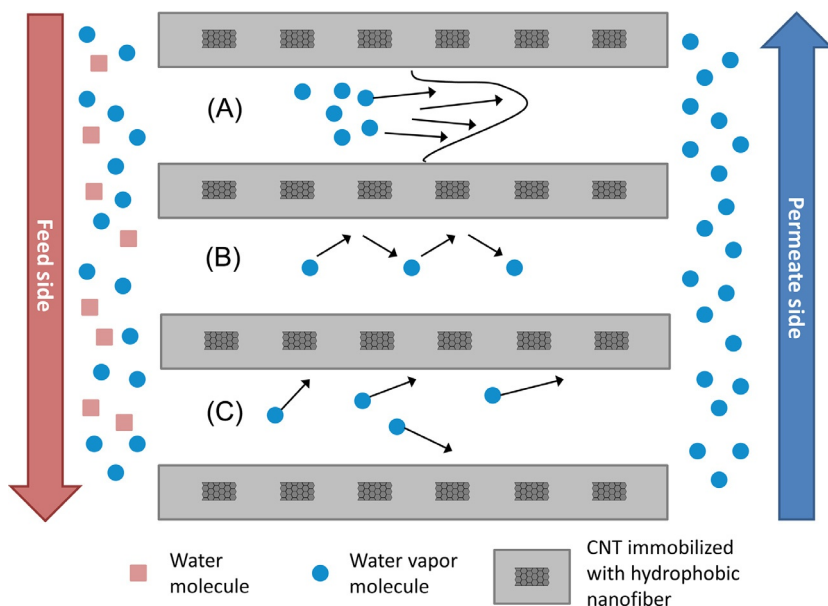
**FIG. 8.9** Effects of CNTs on three different mass transfer mechanisms across the nanofiber membranes: (A) viscous flow, (B) Knudsen, and (C) molecular diffusions. *Adapted from Fig. 5. of Lee J-G, Lee E-J, Jeong S, Guo J, An AK, Guo H, et al. Theoretical modeling and experimental validation of transport and separation properties of carbon nanotube electrospun membrane distillation. J Membr Sci 2017;526:395–408 with permission. License # 4286230738497.*

be improved as a result from the reduction in the nonslip condition zone in membrane pores due to the enhanced repulsion force. The effects of CNTs on the mass transfer mechanisms across the membrane are illustrated in Fig. 8.9. To sum up, the mass transfer in the CNT-incorporated nanofiber membranes can be enhanced due to less molecule collision and shorter wall collision distance. The movement of vapor across the pores like a magnetic levitation train could also reduce the chances of pore wetting [111].

Graphene nanomaterial has also been used in MD membranes due to its hydrophobic properties, resistivity to fouling as well as high thermal and mechanical stability [59, 112]. Woo et al. [59] reported that the incorporation of graphene contributed in modifying the surface architecture of the electrospun PVDF-HFP membrane. The multilevel membrane surface roughness provided the membrane with higher hydrophobicity and consequently the antiwetting properties. The graphene incorporated nanofiber membrane successfully achieved higher flux than that of the commercial PVDF membrane due to the large available surface area and pore volume, higher hydrophobicity, and high thermal conductivity.

## 8.5 APPLICATIONS OF MD

### 8.5.1 Desalination

MD was designed initially as an alternative to RO and thermal processes for desalination purposes. Currently, the majority of the MD desalination applications are still limited in the laboratory or small pilot scales studies. Song and his research group [113] set up a small pilot plant for DCMD desalination which operated on a daily basis for 3 months. City water with different salt contents (0%, 3.5%, 6%, or 10%) and seawater were used as the hot brine for the plant. The plant managed to achieve the highest distillate production rate of 141 L/h and did not show significant flux reduction in treating seawater with salt concentrations of 19.5%. Recently, the performance of DCMD and AGMD desalination modules in laboratory and pilot scales was compared by Eykens et al. [114]. It was found that AGMD exhibited the flux of 1.2 times higher compared to that of DCMD in pilot scale. The results were in contrast with the laboratory outcomes, which demonstrated that DCMD had four times higher flux than AGMD. The difference between the outcomes of laboratory and pilot scales was attributed to the different scale setup conditions.

Recently, many efforts have been made to commercialize this technology for the real desalination applications. Some MD specialized organizations have set up a number of MD pilot plants for desalination. For instance, Memstill tested their AGMD modules in three desalination pilot plants located in Singapore and Netherland before commercialization. An economic evaluation revealed that Memstill system could reduce the desalination costs to $0.50/m$^3$ or lower depending on the types of heat sources used [115, 116]. Besides, the pilot plants equipped with vacuum multieffect membrane distillation (V-MEMD) designed by Memsys has also been installed in several countries like Singapore, Australia, and India [41]. In 2014, Aquaver successfully commissioned the first commercial MD desalination plant in the world in the Maldives. This desalination plant utilizes the waste heat produced by a local power plant to produce clean drinking water with the capacity of up to $p$ to 10,000 L/day [117].

### 8.5.2 Removal of Heavy Metals

The presence of heavy metal in water has been a significant challenge in this modern world. A variety of heavy metals removal techniques has been developed, including ion exchange, adsorption, chemical coagulation-precipitation and membrane process. However, these processes have their own disadvantages. For instance, ion exchange is not feasible to treat supply waters with high salinity. The disposal of adsorbent media, use of chemicals during regeneration and cleaning, as well as the

loss of absorbing capacity over time, are the primary concerns for the adsorption method. Meanwhile, chemical coagulation-precipitation process is not ecological friendly due to the disposal of sludge. Not to mention, the pressure-driven membrane process like RO and nanofiltration are also not sufficient to treat supply stream with a high concentration of metals. MD has been applied successfully in treating water containing heavy metals such as arsenic and lead, thus can be an alternative for the abovementioned techniques. Arsenic can be removed from the water through pressure-driven membrane separation. However, a preoxidation step is often required to convert As(III) to As(V) for higher rejection in negatively charged membranes [118, 119]. This preoxidation step can be avoided with the use of MD as high arsenic rejection could be obtained irrespective of its forms. It was proven by a study conducted by Qu et al. [118] showing the high removal efficiencies of over 99.95% for both As(III) and As(V) using DCMD. Attia and research partners [120] reported that the flux of AGMD was not significantly affected by the heavy metal concentration. The authors employed the PVDF nanofibrous membranes coated with $Al_2O_3$ nanoparticles to treat solution containing lead (Pb) and a high Pb rejection of 99.36% was achieved.

## 8.5.3 Recovery of Valuable Materials

MD could also be a compelling alternative to other treatment methods like the traditional distillation process, air stripping, bioreactors, anaerobic/aerobic biological treatment and advanced oxidation process to recover valuable materials [121]. The unique properties of MD that operate based on vapor pressure and volatility make it an attractive way to concentrate these materials either in the supply stream or permeate stream. Some research has been conducted on the recovery of valuable materials such as alcohol, sugar, fruit juices, mineral acids and many more [40]. For instance, pure glycerol can be obtained by dewatering process through SGMD mode [122]. Interestingly, the process was able to give a high level of solute rejection of >99%. Besides that, the production of ethanol from whey through the bioreactor coupled with DCMD (MDBR) achieved an efficiency of two times higher than the stand-alone bioreactor [123]. MD has also demonstrated its capability in concentrating clarified fruit juice in the food industry. A study has shown an increase in the concentration of orange juice from 9.5 to 65 °Brix through two-steps DCMD process without significant deterioration in juice quality [124]. It was also found that MD can be a promising alternative to the conventional thermal evaporation technique for the concentration of tomato juice. The well-preserved color and reduction of the formations of furan and hydroxymethylfurfural could make MD an attractive option for the tomato juice concentration process [125].

## 8.6 CONCLUSIONS

MD is perceived as an emerging separation technology with several remarkable and outstanding advantages compared to other separation processes concerning mild operating conditions, high product quality as well as the feasibility to treat supply solutions of different salinity and couple with low-grade energy sources. This technology has been known for more than 50 years and widely studied for various applications especially in desalination. However, the commercialization progress of MD technology is still slow because it is still not fully developed at the industrial scale. The challenges such as low availability of membranes with suitable characteristics for MD applications, high possibility of membrane wetting and limitations of commercially available MD modules, are the main obstacles that must be overcome with to promote this technology for the real applications.

MD technology has always been labeled with its low flux performance due to the lack of membranes with excellent characteristics. This chapter has discussed the membranes materials and the optimal membrane characteristics for the MD process. Polymeric membranes are the most widely used membranes for MD applications due to their intrinsic hydrophobic properties, ease of fabrication and low cost. Besides that, ceramic and CNTs membranes have also been gaining interest recently for MD applications owing to their unique properties and advantages. The developments of these two types of membranes for the MD process are still at the early stages, and numerous challenges are still yet to be overcome to allow them to perform up to their full potential in the MD applications. In overall, more works need to be done to optimize the membrane characteristics with the aims to enhance the MD performance as well as the process stabilities and lifespan.

Membrane wetting is another critical issue that affects the MD performance. It can be resolved by improving the hydrophobicity of the membranes. Different approaches have been conducted to improve the membrane hydrophobicity such as the use of membrane materials with excellent intrinsic hydrophobic properties and/or functionalization with low surface energy materials. However, in the real-life applications, the supply solutions do not only contain water but might also contain some other low surface tension liquids such as alcohols and oils. This would limit the performance of the MD process, and consequently, the products quality would be adversely affected. Thus, the membranes should be equipped with amphiphobic or omniphobic properties to prevent the membrane wetting from occurring. This can be achieved by increasing the membrane surface roughness as well as imparting higher membrane hydrophobicity. Recently, several efforts have been made to acquire the amphiphobic or omniphobic properties for the MD membranes through

the applications of nanotechnology. The membranes obtained successfully demonstrated outstanding antiwetting properties. Future work will also have to be done to apply these membranes in pilot-scale research and access the long-term stabilities of the membrane performance.

# References

[1] Eckardt NA, Cominelli E, Galbiati M, Tonelli C. The future of science: food and water for life. Plant Cell 2009;21(2):368–72.

[2] Pankratz TIDA. Desalination yearbook 2014–2015. Topsfield, MA: IDA; 2014.

[3] Greenlee LF, Lawler DF, Freeman BD, Marrot B, Moulin P. Reverse osmosis desalination: water sources, technology, and today's challenges. Water Res 2009;43(9):2317–48.

[4] Jiang S, Li Y, Ladewig BP. A review of reverse osmosis membrane fouling and control strategies. Sci Total Environ 2017;595:567–83.

[5] Fritzmann C, Löwenberg J, Wintgens T, Melin T. State-of-the-art of reverse osmosis desalination. Desalination 2007;216:1):1–76.

[6] Kalogirou SA. Seawater desalination using renewable energy sources. Prog Energy Combust Sci 2005;31(3):242–81.

[7] Gude VG, Nirmalakhandan N, Deng S. Desalination using solar energy: towards sustainability. Energy 2011;36(1):78–85.

[8] Ashoor BB, Mansour S, Giwa A, Dufour V, Hasan SW. Principles and applications of direct contact membrane distillation (DCMD): a comprehensive review. Desalination 2016;398:222–46.

[9] Alkhudhiri A, Darwish N, Hilal N. Membrane distillation: a comprehensive review. Desalination 2012;287:2–18.

[10] Al-Obaidani S, Curcio E, Macedonio F, Di Profio G, Al-Hinai H, Drioli E. Potential of membrane distillation in seawater desalination: thermal efficiency, sensitivity study, and cost estimation. J Membr Sci 2008;323(1):85–98.

[11] Banat FA, Al-Shannag M. Recovery of dilute acetone–butanol–ethanol (ABE) solvents from aqueous solutions via membrane distillation. Bioprocess Eng 2000;23(6):643–9.

[12] Blanco Gálvez J, García-Rodríguez L, Martín-Mateos I. Seawater desalination by an innovative solar-powered membrane distillation system: the MEDESOL project. Desalination 2009;246(1):567–76.

[13] Sarbatly R, Chiam C-K. Evaluation of geothermal energy in desalination by vacuum membrane distillation. Appl Energy 2013;112:737–46.

[14] Lokare OR, Tavakkoli S, Rodriguez G, Khanna V, Vidic RD. Integrating membrane distillation with waste heat from natural gas compressor stations for produced water treatment in Pennsylvania. Desalination 2017;413:144–53.

[15] Tijing LD, Woo YC, Choi J-S, Lee S, Kim S-H, Shon HK. Fouling and its control in membrane distillation—a review. J Membr Sci 2015;475:215–44.

[16] Bodell BR. Silicone rubber vapor diffusion in saline water distillation. United States patent 285,032; 1963.

[17] Findley ME. Vaporization through porous membranes. Ind Eng Chem Process Des Dev 1967;6(2):226–30.

[18] El-Bourawi MS, Ding Z, Ma R, Khayet M. A framework for better understanding membrane distillation separation process. J Membr Sci 2006;285(1):4–29.

[19] Cheng DY, Wiersma SJ, International Power Technology Inc. Apparatus and method for thermal membrane distillation. United States patent US4419187A; 1983.

[20] Cheng DY, Wiersma SJ, International Power Technology Inc. Composite membrane for a membrane distillation system. United States patent US4419242A; 1983.

[21] Gore DW, editor. Gore-tex membrane distillation. Proceedings of the 10th annual convention of the Water Supply Improvement Assoc., Honolulu, USA, July 25–29; 1982.

[22] Andersson SI, Kjellander N, Rodesjö B. Design and field tests of a new membrane distillation desalination process. Desalination 1985;56:345–54.

[23] Drioli E, Ali A, Macedonio F. Membrane distillation: recent developments and perspectives. Desalination 2015;356:56–84.

[24] Ravindra Babu B, Rastogi NK, Raghavarao KSMS. Concentration and temperature polarization effects during osmotic membrane distillation. J Membr Sci 2008;322(1):146–53.

[25] Onsekizoglu P. Membrane distillation: principle, advances, limitations and future prospects in food industry. In: Zereshki S, editor. Distillation-advances from modeling to applications. Croatia: InTech; 2012.

[26] Khayet M. Membranes and theoretical modeling of membrane distillation: a review. Adv Colloid Interf Sci 2011;164(1):56–88.

[27] Khayet M, Matsuura T. Membrane distillation: principles and applications. Great Britain: Elsevier; 2011.

[28] Eykens L, De Sitter K, Dotremont C, Pinoy L, Van der Bruggen B. Membrane synthesis for membrane distillation: a review. Sep Purif Technol 2017;182:36–51.

[29] González D, Amigo J, Suárez F. Membrane distillation: perspectives for sustainable and improved desalination. Renew Sust Energ Rev 2017;80:238–59.

[30] Abu-Zeid MAE-R, Zhang Y, Dong H, Zhang L, Chen H-L, Hou L. A comprehensive review of vacuum membrane distillation technique. Desalination 2015;356:1–14.

[31] Hsu ST, Cheng KT, Chiou JS. Seawater desalination by direct contact membrane distillation. Desalination 2002;143(3):279–87.

[32] Cath TY, Adams VD, Childress AE. Experimental study of desalination using direct contact membrane distillation: a new approach to flux enhancement. J Membr Sci 2004;228(1):5–16.

[33] Khalifa A, Ahmad H, Antar M, Laoui T, Khayet M. Experimental and theoretical investigations on water desalination using direct contact membrane distillation. Desalination 2017;404:22–34.

[34] Alves VD, Coelhoso IM. Orange juice concentration by osmotic evaporation and membrane distillation: a comparative study. J Food Eng 2006;74(1):125–33.

[35] Gunko S, Verbych S, Bryk M, Hilal N. Concentration of apple juice using direct contact membrane distillation. Desalination 2006;190(1):117–24.

[36] Feng X, Jiang LY, Song Y. Titanium white sulfuric acid concentration by direct contact membrane distillation. Chem Eng J 2016;285:101–11.

[37] Meindersma GW, Guijt CM, de Haan AB. Desalination and water recycling by air gap membrane distillation. Desalination 2006;187(1):291–301.

[38] Mericq J-P, Laborie S, Cabassud C. Vacuum membrane distillation for an integrated seawater desalination process. Desalin Water Treat 2009;9(1):287–96.

[39] Banat FA, Simandl J. Membrane distillation for dilute ethanol: separation from aqueous streams. J Membr Sci 1999;163(2):333–48.

[40] Wang P, Chung T-S. Recent advances in membrane distillation processes: membrane development, configuration design and application exploring. J Membr Sci 2015;474:39–56.

[41] Camacho L, Dumée L, Zhang J, Li J-d, Duke M, Gomez J, et al. Advances in membrane distillation for water desalination and purification applications. Water 2013;5(1):94.

[42] Li K. Ceramic membranes for separation and reaction. Great Britain: John Wiley & Sons Ltd; 2007.

[43] Wang J-W, Li L, Zhang J-W, Xu X, Chen C-S. β-Sialon ceramic hollow fiber membranes with high strength and low thermal conductivity for membrane distillation. J Eur Ceram Soc 2016;36(1):59–65.

[44] Larbot A, Gazagnes L, Krajewski S, Bukowska M, Wojciech K. Water desalination using ceramic membrane distillation. Desalination 2004;168:367–72.

[45] Gazagnes L, Cerneaux S, Persin M, Prouzet E, Larbot A. Desalination of sodium chloride solutions and seawater with hydrophobic ceramic membranes. Desalination 2007;217(1):260–6.

[46] Zhang J-W, Fang H, Wang J-W, Hao L-Y, Xu X, Chen C-S. Preparation and characterization of silicon nitride hollow fiber membranes for seawater desalination. J Membr Sci 2014;450:197–206.

[47] Fan Y, Chen S, Zhao H, Liu Y. Distillation membrane constructed by $TiO_2$ nanofiber followed by fluorination for excellent water desalination performance. Desalination 2017;405:51–8.

[48] Gitis V, Rothenberg G. Ceramic membranes: new opportunities and practical applications. Germany: Wiley-VCH Verlag GmbH & Co. KGaA; 2016.

[49] Hubadillah SK, Othman MHD, Matsuura T, Ismail AF, Rahman MA, Harun Z, et al. Fabrications and applications of low cost ceramic membrane from kaolin: a comprehensive review. Ceram Int 2018;44(5):4538–60.

[50] Khemakhem S, Amar RB. Modification of Tunisian clay membrane surface by silane grafting: application for desalination with air gap membrane distillation process. Colloids Surf A: Physicochem Eng Asp 2011;387(1):79–85.

[51] Dong Y, Liu X, Ma Q, Meng G. Preparation of cordierite-based porous ceramic microfiltration membranes using waste fly ash as the main raw materials. J Membr Sci 2006;285(1):173–81.

[52] Ashraf A, Salih H, Nam S, Dastgheib SA. Robust carbon nanotube membranes directly grown on Hastelloy substrates and their potential application for membrane distillation. Carbon 2016;106:243–51.

[53] Dumée LF, Sears K, Schütz J, Finn N, Huynh C, Hawkins S, et al. Characterization and evaluation of carbon nanotube Bucky-paper membranes for direct contact membrane distillation. J Membr Sci 2010;351(1):36–43.

[54] Dumée L, Germain V, Sears K, Schütz J, Finn N, Duke M, et al. Enhanced durability and hydrophobicity of carbon nanotube Bucky paper membranes in membrane distillation. J Membr Sci 2011;376(1):241–6.

[55] Dumée L, Campbell JL, Sears K, Schütz J, Finn N, Duke M, et al. The impact of hydrophobic coating on the performance of carbon nanotube Bucky-paper membranes in membrane distillation. Desalination 2011;283:64–7.

[56] Gethard K, Sae-Khow O, Mitra S. Water desalination using carbon-nanotube-enhanced membrane distillation. ACS Appl Mater Interfaces 2011;3(2):110–4.

[57] Tijing LD, Woo YC, Shim W-G, He T, Choi J-S, Kim S-H, et al. Superhydrophobic nanofiber membrane containing carbon nanotubes for high-performance direct contact membrane distillation. J Membr Sci 2016;502:158–70.

[58] An X, Liu Z, Hu Y. Amphiphobic surface modification of electrospun nanofibrous membranes for anti-wetting performance in membrane distillation. Desalination 2018;432:23–31.

[59] Woo YC, Tijing LD, Shim W-G, Choi J-S, Kim S-H, He T, et al. Water desalination using graphene-enhanced electrospun nanofiber membrane via air gap membrane distillation. J Membr Sci 2016;520:99–110.

[60] Goh PS, Ismail AF, Ng BC. Carbon nanotubes for desalination: performance evaluation and current hurdles. Desalination 2013;308:2–14.

[61] Schneider K, Hölz W, Wollbeck R, Ripperger S. Membranes and modules for transmembrane distillation. J Membr Sci 1988;39(1):25–42.

[62] Lawson KW, Lloyd DR. Membrane distillation. J Membr Sci 1997;124(1):1–25.

[63] Franken ACM, Nolten JAM, Mulder MHV, Bargeman D, Smolders CA. Wetting criteria for the applicability of membrane distillation. J Membr Sci 1987;33(3):315–28.

[64] Susanto H. Towards practical implementations of membrane distillation. Chem Eng Process Process Intensif 2011;50(2):139–50.

[65] Smolders K, Franken ACM. Terminology for membrane distillation. Desalination 1989;72(3):249–62.

[66] Khayet M, Matsuura T. Preparation and characterization of Polyvinylidene fluoride membranes for membrane distillation. Ind Eng Chem Res 2001;40(24):5710–8.

[67] Srisurichan S, Jiraratananon R, Fane AG. Mass transfer mechanisms and transport resistances in direct contact membrane distillation process. J Membr Sci 2006;277(1):186–94.

[68] Mackie JS, Meares P. The diffusion of electrolytes in a cation-exchange resin membrane I. Theoretical. Proc R Soc London, Ser A 1955;232(1191):498–509.

[69] Laganà F, Barbieri G, Drioli E. Direct contact membrane distillation: modelling and concentration experiments. J Membr Sci 2000;166(1):1–11.

[70] Hendren ZD, Brant J, Wiesner MR. Surface modification of nanostructured ceramic membranes for direct contact membrane distillation. J Membr Sci 2009;331:1):1–10.

[71] Ma M, Hill RM. Superhydrophobic surfaces. Curr Opin Colloid Interface Sci 2006;11(4):193–202.

[72] Chu Z, Seeger S. Superamphiphobic surfaces. Chem Soc Rev 2014;43(8):2784–98.

[73] Han KD, Leo CP, Chai SP. Fabrication and characterization of superhydrophobic surface by using water vapor impingement method. Appl Surf Sci 2012;258(18):6739–44.

[74] Yuan Y, Lee TR. Contact angle and wetting properties. In: Bracco G, Holst B, editors. Surface science techniques. springer series in surface sciences, vol. 51. Berlin and Heidelberg: Springer-Verlag Berlin Heidelberg; 2013. p. 3–34.

[75] Genzer J, Efimenko K. Recent developments in superhydrophobic surfaces and their relevance to marine fouling: a review. Biofouling 2006;22(5–6):339–60.

[76] Wenzel RN. Resistance of solid surfaces to wetting by water. Ind Eng Chem 1936;28(8):988–94.

[77] Cassie ABD, Baxter S. Wettability of porous surfaces. Trans Faraday Soc 1944;40:546–51.

[78] Cui Z, Drioli E, Lee YM. Recent progress in fluoropolymers for membranes. Prog Polym Sci 2014;39(1):164–98.

[79] Lalia BS, Guillen-Burrieza E, Arafat HA, Hashaikeh R. Fabrication and characterization of polyvinylidenefluoride-co-hexafluoropropylene (PVDF-HFP) electrospun membranes for direct contact membrane distillation. J Membr Sci 2013;428:104–15.

[80] Feng C, Shi B, Li G, Wu Y. Preparation and properties of microporous membrane from poly(vinylidene fluoride-co-tetrafluoroethylene) (F2.4) for membrane distillation. J Membr Sci 2004;237(1):15–24.

[81] Zheng L, Wu Z, Wei Y, Zhang Y, Yuan Y, Wang J. Preparation of PVDF-CTFE hydrophobic membranes for MD application: effect of LiCl-based mixed additives. J Membr Sci 2016;506:71–85.

[82] Shi L, Wang R, Cao Y, Feng C, Liang DT, Tay JH. Fabrication of poly(vinylidene fluoride-co-hexafluropropylene) (PVDF-HFP) asymmetric microporous hollow fiber membranes. J Membr Sci 2007;305(1):215–25.

[83] Jin Z, Yang DL, Zhang SH, Jian XG. Hydrophobic modification of poly(phthalazinone ether sulfone ketone) hollow fiber membrane for vacuum membrane distillation. J Membr Sci 2008;310(1):20–7.

[84] Jung J, Shin Y, Choi Y-J, Sohn J, Lee S, An K. Hydrophobic surface modification of membrane distillation (MD) membranes using water-repelling polymer based on urethane rubber. Desalin Water Treat 2016;57(22):10031–41.

[85] Yang X, Wang R, Shi L, Fane AG, Debowski M. Performance improvement of PVDF hollow fiber-based membrane distillation process. J Membr Sci 2011;369(1):437–47.

[86] Ahmad NA, Leo CP, Ahmad AL, Ramli WKW. Membranes with great hydrophobicity: a review on preparation and characterization. Sep Purif Rev 2015;44(2):109–34.

[87] Yasuda H, Gazicki M. Biomedical applications of plasma polymerization and plasma treatment of polymer surfaces. Biomaterials 1982;3(2):68–77.

[88] Wei X, Zhao B, Li X-M, Wang Z, He B-Q, He T, et al. CF4 plasma surface modification of asymmetric hydrophilic polyethersulfone membranes for direct contact membrane distillation. J Membr Sci 2012;407-408:164–75.

[89] Gancarz I, Bryjak M, Kujawski J, Wolska J, Kujawa J, Kujawski W. Plasma deposited fluorinated films on porous membranes. Mater Chem Phys 2015;151:233–42.

[90] Kong Y, Lin X, Wu Y, Chen J, Xu J. Plasma polymerization of octafluorocyclobutane and hydrophobic microporous composite membranes for membrane distillation. J Appl Polym Sci 1992;46(2):191–9.

[91] Khayet M, Matsuura T. Application of surface modifying macromolecules for the preparation of membranes for membrane distillation. Desalination 2003;158(1):51–6.

[92] Khayet M, Mengual JI, Matsuura T. Porous hydrophobic/hydrophilic composite membranes: application in desalination using direct contact membrane distillation. J Membr Sci 2005;252(1):101–13.

[93] Qtaishat M, Khayet M, Matsuura T. Novel porous composite hydrophobic/hydrophilic polysulfone membranes for desalination by direct contact membrane distillation. J Membr Sci 2009;341(1):139–48.

[94] Essalhi M, Khayet M. Surface segregation of fluorinated modifying macromolecule for hydrophobic/hydrophilic membrane preparation and application in air gap and direct contact membrane distillation. J Membr Sci 2012;417-418:163–73.

[95] Kujawski W, Kujawa J, Wierzbowska E, Cerneaux S, Bryjak M, Kujawski J. Influence of hydrophobization conditions and ceramic membranes pore size on their properties in vacuum membrane distillation of water–organic solvent mixtures. J Membr Sci 2016;499:442–51.

[96] Koonaphapdeelert S, Li K. Preparation and characterization of hydrophobic ceramic hollow fibre membrane. J Membr Sci 2007;291(1):70–6.

[97] Romero J, Draga H, Belleville MP, Sanchez J, Combe-James C, Dornier M, et al. New hydrophobic membranes for contactor processes—applications to isothermal concentration of solutions. Desalination 2006;193(1):280–5.

[98] Dafinov A, Garcia-Valls R, Font J. Modification of ceramic membranes by alcohol adsorption. J Membr Sci 2002;196(1):69–77.

[99] Sugimura H, Hozumi A, Kameyama T, Takai O. Organosilane self-assembled monolayers formed at the vapour/solid interface. Surf Interface Anal 2002;34(1):550–4.

[100] Fadeev AY, McCarthy TJ. Self-assembly is not the only reaction possible between alkyltrichlorosilanes and surfaces: monomolecular and oligomeric covalently attached layers of dichloro- and trichloroalkylsilanes on silicon. Langmuir 2000;16(18):7268–74.

[101] Lu J, Yu Y, Zhou J, Song L, Hu X, Larbot A. FAS grafted superhydrophobic ceramic membrane. Appl Surf Sci 2009;255(22):9092–9.

[102] de Vos RM, Maier WF, Verweij H. Hydrophobic silica membranes for gas separation. J Membr Sci 1999;158(1):277–88.

[103] Wang J-W, Li X-Z, Fan M, Gu J-Q, Hao L-Y, Xu X, et al. Porous β-sialon planar membrane with a robust polymer-derived hydrophobic ceramic surface. J Membr Sci 2017;535:63–9.

[104] Lu X, Peng Y, Ge L, Lin R, Zhu Z, Liu S. Amphiphobic PVDF composite membranes for anti-fouling direct contact membrane distillation. J Membr Sci 2016;505:61–9.

[105] Razmjou A, Arifin E, Dong G, Mansouri J, Chen V. Superhydrophobic modification of $TiO_2$ nanocomposite PVDF membranes for applications in membrane distillation. J Membr Sci 2012;415-416:850–63.

[106] Meng S, Mansouri J, Ye Y, Chen V. Effect of templating agents on the properties and membrane distillation performance of $TiO_2$-coated PVDF membranes. J Membr Sci 2014;450:48–59.

[107] Boo C, Lee J, Elimelech M. Engineering surface energy and nanostructure of microporous films for expanded membrane distillation applications. Environ Sci Technol 2016;50(15):8112–9.

[108] Lin S, Nejati S, Boo C, Hu Y, Osuji CO, Elimelech M. Omniphobic membrane for robust membrane distillation. Environ Sci Technol Lett 2014;1(11):443–7.

[109] Huang Y-X, Wang Z, Hou D, Lin S. Coaxially electrospun super-amphiphobic silica-based membrane for anti-surfactant-wetting membrane distillation. J Membr Sci 2017;531:122–8.

[110] Lee J-G, Lee E-J, Jeong S, Guo J, An AK, Guo H, et al. Theoretical modeling and experimental validation of transport and separation properties of carbon nanotube electrospun membrane distillation. J Membr Sci 2017;526:395–408.

[111] An AK, Lee E-J, Guo J, Jeong S, Lee J-G, Ghaffour N. Enhanced vapor transport in membrane distillation via functionalized carbon nanotubes anchored into electrospun nanofibres. Sci Rep 2017;7.

[112] Homaeigohar S, Elbahri M. Graphene membranes for water desalination. NPG Asia Mater 2017;9.

[113] Song L, Ma Z, Liao X, Kosaraju PB, Irish JR, Sirkar KK. Pilot plant studies of novel membranes and devices for direct contact membrane distillation-based desalination. J Membr Sci 2008;323(2):257–70.

[114] Eykens L, Hitsov I, De Sitter K, Dotremont C, Pinoy L, Van der Bruggen B. Direct contact and air gap membrane distillation: differences and similarities between lab and pilot scale. Desalination 2017;422:91–100.

[115] Hanemaaijer JH, van Medevoort J, Jansen AE, Dotremont C, van Sonsbeek E, Yuan T, et al. Memstill membrane distillation—a future desalination technology. Desalination 2006;199(1):175–6.

[116] Jansen AE, Assink JW, Hanemaaijer JH, van Medevoort J, van Sonsbeek E. Development and pilot testing of full-scale membrane distillation modules for deployment of waste heat. Desalination 2013;323:55–65.

[117] Dutch Water Sector. Aquaver commissions world's first desalination plant based on membrane distillation on Gulhi Island, Maldives. Available from: https://www.dutchwatersector.com/news-events/news/9417-aquaver-commissions-world-s-first-desalination-plant-based-on-membrane.html; 2014.

[118] Qu D, Wang J, Hou D, Luan Z, Fan B, Zhao C. Experimental study of arsenic removal by direct contact membrane distillation. J Hazard Mater 2009;163(2):874–9.

[119] Dao TD, Laborie S, Cabassud C. Direct as(III) removal from brackish groundwater by vacuum membrane distillation: effect of organic matter and salts on membrane fouling. Sep Purif Technol 2016;157:35–44.

[120] Attia H, Alexander S, Wright CJ, Hilal N. Superhydrophobic electrospun membrane for heavy metals removal by air gap membrane distillation (AGMD). Desalination 2017;420:318–29.

[121] Kujawa J, Cerneaux S, Kujawski W. Removal of hazardous volatile organic compounds from water by vacuum pervaporation with hydrophobic ceramic membranes. J Membr Sci 2015;474:11–9.

[122] Shirazi MMA, Kargari A, Tabatabaei M, Ismail AF, Matsuura T. Concentration of glycerol from dilute glycerol wastewater using sweeping gas membrane distillation. Chem Eng Process Process Intensif 2014;78:58–66.

[123] Tomaszewska M, Białończyk L. Ethanol production from whey in a bioreactor coupled with direct contact membrane distillation. Catal Today 2016;268:156–63.

[124] Quist-Jensen CA, Macedonio F, Conidi C, Cassano A, Aljlil S, Alharbi OA, et al. Direct contact membrane distillation for the concentration of clarified orange juice. J Food Eng 2016;187:37–43.

[125] Savaş Bahçeci K, Gül Akıllıoğlu H, Gökmen V. Osmotic and membrane distillation for the concentration of tomato juice: effects on quality and safety characteristics. Innovative Food Sci Emerg Technol 2015;31:131–8.

CHAPTER

# 9

# Hemodialysis Membrane for Blood Purification Process

*Ahmad Fauzi Ismail, Muhammad Nidzhom Zainol Abidin, Sumarni Mansur, Muhamad Zulhilmi Zailani, Noresah Said, Yanuardi Raharjo, Sarina Mat Rosid, Mohd Hafiz Dzarfan Othman, Pei Sean Goh, Hasrinah Hasbullah*

**Advanced Membrane Technology Research Centre (AMTEC), Faculty of Chemical and Energy Engineering, Universiti Teknologi Malaysia, Skudai, Malaysia**

OUTLINE

## 9.1 INTRODUCTION

Hemodialysis is a process of purifying the blood of a person whose kidneys are not working normally, using thousands of membrane fibers, fitted into a single membrane module commonly known as hemodialyzer. Membrane technology keeps developing until it has been successfully used for hemodialysis treatment for patients who suffer from acute renal disease and end-stage renal failure (ESRF). ESRF is a disease state in which long-term kidney failure has caused drastic reduction of glomerular filtration rate to below than 5 mL/min [1]. As a result of kidney failure, metabolites originated from body metabolic reactions will increase progressively, where the retention of a large number of molecules is called uremic syndrome [2]. These uremic toxins can be classified in three groups based on their physiochemical properties that influence their dialytic removal. The classification is made based on the molecular weight (MW) or in the ability to bind to proteins like albumin. Uremic toxins with MW below 500 Da are classified as small water-soluble molecules, while molecules with MW from 500 Da to approximately 15,000 Da are called middle molecules. Independently of the MW, if a uremic toxin is capable of binding to a protein, it belongs to the category of protein bound.

In general, the main component of hemodialysis machine is dialyzer, where semipermeable membranes are arranged in the middle, serves as membrane contactor to form separate adjacent paths for blood and dialysate (Fig. 9.1). It filters waste products (i.e., urea, creatinine, $\beta_2$-microglobulin), removes excess water and balances electrolytes such as sodium, potassium, and bicarbonate. Hemodialysis involves the movement of water containing solutes across semipermeable membranes by diffusion and ultrafiltration (UF). Diffusion and UF are the two fundamental processes involved in continuous renal replacement therapy.

Diffusion can be referred as the movement of solutes from high solute concentration to lower solute concentration [3]. Dialysate runs countercurrent to blood flowing on the other side of a membrane to maximize solutes concentration gradient for efficient diffusion. Small molecules such as urea will move smoothly along the concentration gradient into the dialysate fluid. Diffusive clearance of a solute usually depends on its MW, electrical charge, the blood-dialysis fluid concentration gradient, blood and dialysis flow rates and on membrane characteristics, such as the diffusion coefficient. Ideally, solute removal is directly proportional to the dialysate flow rate [4]. Meanwhile, UF is a process whereby solute is carried by a fluid across a semipermeable membrane as the result of a pressure gradient. This represents what happens in the healthy human kidney. The rate of UF depends on the membrane porosity and the hydrostatic blood pressure, which depends upon blood flow. This process is very effective for the removal of fluid along with middle-sized molecules, which are believed to cause uremia.
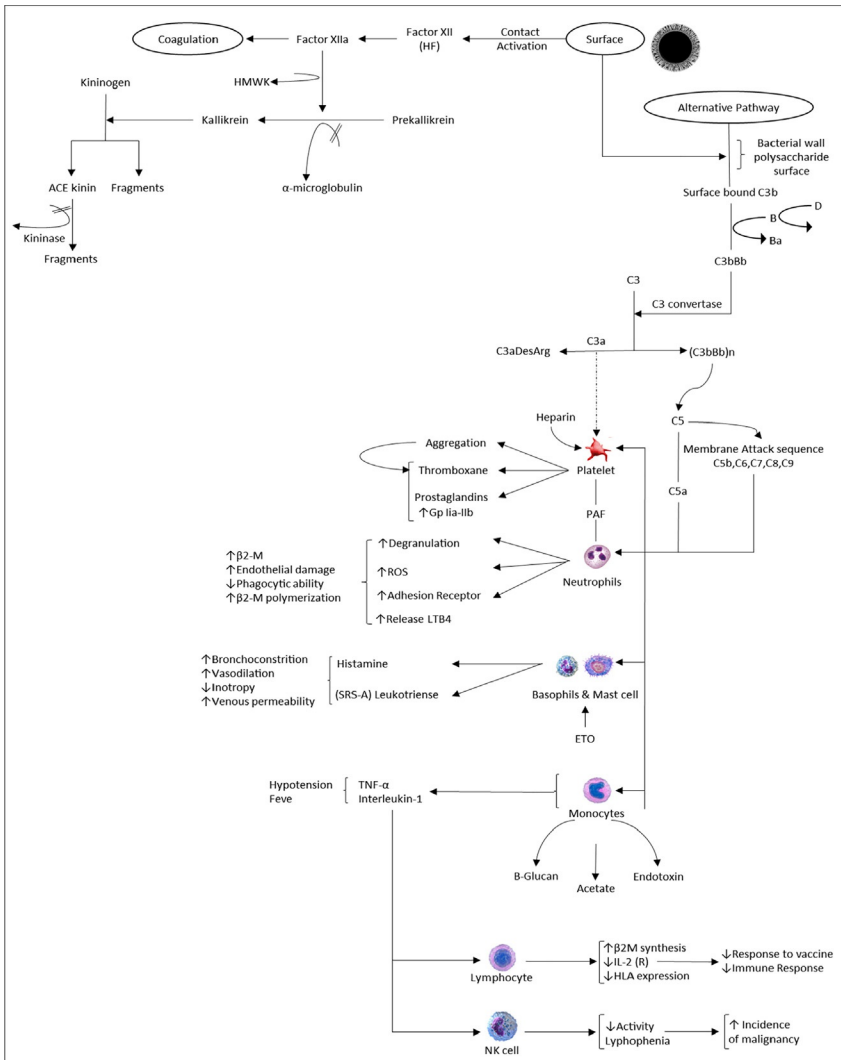
**FIG. 9.1**    Blood-membrane interaction [35].

Hemodialysis membrane is a type of low pressure-driven membrane which separates molecules by size-exclusion. The hemodialysis membrane performance is determined by the membrane's solute clearance and UF characteristics [5]. Solute clearance represents the membrane's efficiency while UF characteristics will determine whether the membrane is low flux or high flux. Hemodialysis membranes are classified based on their chemical nature and morphology. Due to the bioincompatibility issues of cellulose-based membranes, synthetic polymeric membranes have been prevalently used and commercialized. Regarding morphology,

asymmetric structure of the membrane is gaining much attention over symmetric membrane due to its superior separation performance.

## 9.2  PROPERTIES OF HEMODIALYSIS MEMBRANE

### 9.2.1  Selection Factors

The hemodialyzer is made up of thousands of hollow fiber polymeric membranes (approximately 10,000 hollow fibers) that are bundled together into a module [6]. This module acts as a support structure that houses the hollow fiber membrane, enabling the dialysis process between the patient's blood and the dialysate [6]. The fabrication technique, properties of the fabricated membranes, clearance of the uremic toxins, and performance in ultrafiltration (fluid removal) and dialysis are related. For example, electrospinning technique produced high specific surface areas that are suitable for gas separation and oil-water separation application [7]. Thus, it is important to identify the principle used during hemodialysis procedure and the morphology of the membrane that are suitable for dialysis process prior to choosing the membrane fabrication technique [8]. During hemodialysis procedure, the movement of molecule fluid and solute from blood to dialysate and vice versa involve a combination of three system which are dialysis, ultrafiltration and convection [4]. Uremic toxins such as urea and creatinine range from size 10,000–55,000 Da needs to be excreted out from the blood. While, proteins such as albumin (66,000 Da) need to be retained. The penetration of urea, toxin and waste substances can be estimated based on the formula of 1 kDA of substance is equilibrium to 0.2 μm. The sieving coefficient of a dialysis membrane is determined by its pore size. Thus, the membrane pore size need to be in the range 1–10 or 10–100 nm for the filtration and retention occur efficiently [9]. Based on the mean pore size, membrane for hemodialysis can be categorized as either nanofiltration or ultrafiltration membranes. The physical structure or morphology of a fabricated membrane is a major concern in determining the efficiency of a dialysis membrane. Different type of membranes morphology will give a different result in term of its permeability and clearance efficiency. Two types of the most common hollow fiber membrane morphology for dialysis membrane are homogenous and asymmetry hollow fiber membrane [10].

An asymmetric membrane consists of a dense thin layer on the inner surface of the membrane called "skin layer" and the density of the membrane gradually decreasing in the radial direction. The skin layer represents the selective layer of the membrane and water molecules. While the thick layer on top of the skin layer is known as "support layer." This layer has a minimal function in solute resistance and water transport.

However, it provides enough mechanical strength for the membrane structure. A typical inner diameter for synthetic dialysis membranes is ranged between 180 and 220 μm and a wall thickness range between 20 and 50 μm. While the skin layer of the membrane is range between 0.1 and 1.0 μm thick and support layer range from 100 to 200 μm thick. The membranes are fabricated through phase inversion technique where an integral structure with skin and support layer made from a single material is produced in a single process to produce an asymmetric membrane [11].

A homogeneous membrane is a dense membrane where its entire thickness contributes to the transport resistance for solutes and water. The permeability of a homogenous membrane is rather low as compared to an asymmetric membrane. Most of the cellulosic membrane and some of the synthetic polymeric membrane such as EVAL, PMMA, and AN-69 are homogenous. For homogeneous membrane, its entire dense membrane involved in the separation process during hemodialysis. This can cause middle-molecule adsorption at the membrane surface, consequently lead to the adverse effect of complement system activation.

### 9.2.2  Pore Size

A hemodialysis membrane should closely resemble with the glomerulus in real kidney especially for filtration process in clearance of low and middle protein molecular weight uremic toxins like urea, creatinine, and $\beta_2$-microglobulin. Consequent to that matter, pore size is one of the essential properties to achieve an excellent solute transfer. Pore size can be described as the mean size of the pores on the surface of a membrane. Moreover, it also refers to the particle size that the membrane can reject, as well as the characterization of the membrane itself.

There are three types of pores of membrane: cylindrical, sponge and blind pores. Cylinder shaped pores usually pass through in an entire membrane and have lower surface area compared to spongy pores. Meanwhile, the pores of sponge have randomly shaped of cavities and channels, across the membrane. This type of pores has a large surface area and mostly charged in the trapping of particles [12]. However, the pores are less uniform because of their number of configurations inside the membrane. According to Kosutic and Kunst [13], both cylindrical and spongy pores in membrane practically are not uniformly shaped. Lastly, blind pores are the pores which do not go through up to the top layer of the membrane. Consequently, no permeation has been penetrated into these pores and it only exists as bubbles within the surface membrane. In the characterization of a membrane, the presence of blind pores will indicate the ability of the medium to penetrate the membrane.

There are four types of central membranes, namely microfiltration (MF), ultrafiltration (UF), nanofiltration (NF) and also reverse osmosis

(RO) that have a size ranging from 1000 to 0.0001 μm [14, 15]. Microfiltration mostly has a pore size of 0.1–5 μm and is the largest of pore size compared to other three. Its size of pores is large enough to filter blood cells, flour, bacteria, and many other fine powders in solution. Besides that, this type of filtration can operate under low pressures and low energy. On the other hand, ultrafiltration has a pore size range from 0.1 to 0.01 μm. It rejects particles such as silica, viruses, endotoxins, proteins, plastics and smog/fumes such as ZnO. Due to the decrease in pore size, the osmotic pressure required is higher than that of MF.

Nanofiltration has a pore size range of 0.001–0.01 μm and can filter particles, including sugars, synthetic matrices, and some salts, however, it cannot remove the aqueous salts and metal ions. Meanwhile, a pore size of reverse osmosis is in the range of 0.0001–0.001 μm. It is mostly used in industry for a large scale in separation material such as for desalination and water purification, as it filters out everything except for water molecules. From the size of the pores indicate that this type of membrane is solely capable of filtering salts and metal ions from the water. As the size of pores, RO membrane is quite small. Therefore a large amount of osmotic pressure is needed to force the filtration [13]. The different type of filtration processes has been summarized as shown in Table 9.1.

TABLE 9.1   Different Type of Filtration Processes by Pore Size Ranges and Their Application

| | Microfiltration (MF) | Ultrafiltration (UF) | Nanofiltration (NF) | Reverse osmosis (RO) |
|---|---|---|---|---|
| Size of pore | 0.1–5 μm | 0.1–0.01 μm | 0.001–0.01 μm | 0.0001–0.001 μm |
| Operating pressure | 0.5–5 bar | 1–10 bar | 7–30 bar | 20–100 bar |
| Types of materials removed | Bacteria, blood cells, flour, talc, etc. | Silica, viruses, endotoxins, proteins, plastics, smog/fumes | Some salts, synthetic dyes, sugars, starch, pesticides, detergents | Salts, metal ions, sugars, amino acids |
| Applications | Water purification, sterilization | Separation of molecular mixtures, artificial kidney | Desalination, food processing, separation of molecular mixture, water treatment | Sea and brackish water desalination |

For hemodialysis membrane, it involves the diffusion of the solutes through a semipermeable membrane by ultrafiltration process. Moreover, in an extracorporeal circuit, the movement of the dialysate is in the opposite direction with the blood flow. Therefore, the removal of the fluid is affected by changing the hydrostatic pressure in the dialysate compartment, which causes the free water and some solutes to dissolve through the membrane along the created pressure gradient.

Dialyzer membranes have been categorized into two types based on their different pore sizes. The flux, on the other hand, is interpreted as the ability of the membrane to filter the plasma. Therefore, the dialyzer that has small pore sizes are referred as low-flux meanwhile the one with large pore sizes are referred as high-flux [9]. According to Klaus and Suzana [16], a flow rate of less than 10 mL/h/mmHg is considered to be a low-flux dialyzer while a dialyzer with a flow rate of more than 20 mL/h/mmHg is considered to be a high-flux dialyzer. Mostly in low-flux dialyzers, the large molecules like $\beta_2$-microglobulin are challenging to be removed. Consequent to that matter, the trend has been shifted to use high-flux dialyzers instead of low-flux dialyzers by improving the dialysis solution and membrane itself using nanotechnology method.

## 9.2.3 Porosity

Pore density or also known as porosity is one of the factors that determine the dialyzer membrane diffusive transport. Porosity is determined by measuring the void spaces in a material, which is the fraction of void volume over the total volume is between 0 and 1, or in percentage between 0% and 100% [17]. The porosity ($\phi$) is determined by dividing the volume of void space ($V_V$) over the total volume of the material ($V_T$) as in Eq. (9.1):

$$\phi = Vv/V_T \qquad (9.1)$$

According to Mike and Yunhong [17], the value of porosity will be changed if some of the modification in the process such as hydrothermal alteration, deformation and producing secondary or fracture porosity has been made. This is supported by Manger (1963) that stated the total porosity could be varied based on density used, and the method of absorptions for different fluids or gases. The porosity value can be determined using various ways such as Mercury intrusion porosimetry, gas bubble pressure method, and gas expansion method.

Mercury intrusion porosimetry is used to measure the pressure that is required to expel a nonwetting liquid (mercury) through pores in the material. In this method, high pressure is required to force the viscous mercury to go through the small pores which could disturb the flexibility of nanofiber membranes. Mostly, liquid extrusion porosimetry is the suitable method for testing of nanofiber membranes however it only measures

the total pore volume instead of the diameter of the pores in the throat [18]. All instruments will assume that the shape of the pores is in cylindrical and determined by using Young-Laplace equation that has been modified:

$$\Delta P = \sigma \times \cos\theta \times (1/r_1 + 1/r_2) = 2 \times \sigma \times \cos\theta / r_{pore} \qquad (9.2)$$

This equation relates to the difference of pressure over the curved mercury interface as described in $r_1$ and $r_2$ to the pore size by using the value of surface tension of mercury ($\sigma$) and the contact angle between mercury and the solid. However, the assumption of pore shape is in a cylinder can give great differences between reality and analysis as the real shape of pores that form is quite different. On the other hand, one of the limitations of this method is that mercury porosimetry does not measure the internal pore size, but rather determines the largest connection (pore or throat channel) from surface of the sample to this pore. Thus, mercury porosimetry results always show a smaller pore size comparable to the results of the image analysis method. In fact, it cannot be used to analyze closed pores because mercury has no way to enter this pore. Besides that, the amount of mercury in filling the smallest pore size usually is restricted based on the maximum pressure achieved by the instrument.

Gas bubble pressure is a method introduced by Bechhold in 1908 [19]. In this method, the pressure ($P$) is required to blow through the capillary that filled with a liquid that is inversely proportional to the radius of the capillary ($r$). The size of pores can be calculated by using the Cantor equation as below:

$$P = 2 - \gamma/r \cdot \cos\theta \qquad (9.3)$$

The bubble point is the measure of the radius of the largest pore as soon as the gas passed first. The advantages of this method are a simple procedure, nondestructive and helpful in integrity test. Vice versa, it also has a disadvantage as this method does not provide information for pore size distribution in the membrane, and as for gas permeation, it requires high air-water surface tension to go through small pores which can cause membrane compression instead.

In gas expansion method, it used Boyle-Marriote gas law. This method most widely used to determine porosity. The test usually carried out at the constant temperature. A valve connects two chambers with known volumes. The sample is placed in the chamber $V_1$ with the pressure $P_1$. Meanwhile, second chamber $V_2$ initiated at pressure $P_0$ is connected to the first one by opening the valve between them, thus permitting the gas to expand isothermally. From Boyle-Marriote law, if the final pressure is $P_2$:

$$P_1(V_1 - V_s)/Z(P_1) + P_0 \times V_2/Z(P_0) = P_2(V_1 + V_2 - V_s)/Z(P_2) \qquad (9.4)$$

$V_2$ is for grain volume, and helium gas has been used as it an approximately ideal gas (assume $Z = 1$) at low pressure.

## 9.2.4 Pore Size Distribution

The other of membrane properties is pore size distribution (PSD) that are important for determining the efficiency of filtration process in hemodialysis treatment. According to Supriyo and Keith [20], the pore size distribution (PSD) is interpreted as the statistical distribution of the radius of the largest sphere that can be fitted inside a pore at a given point. Besides that, it also describes the range of pore sizes that exist in a membrane with more precision about particle sizes that preserve by the membrane itself. On the other hand, the filtration flux is directly related to pore size and pore distribution. This is supported by Khayet and Matsuura [21] that stated by observing the mean pore; it can reflect the solute transport technique used in the membrane.

There are a few of methods used to measure the pore size distribution like gas adsorption method, permoporometry, and thermoporometry [21]. In the gas adsorption method, pore size distribution can be determined by observing the adsorption and desorption of gas nitrogen through the pores based on the process of adsorption and condensation of a capillary. This method is applied if the membrane has pore sizes in the range of 17–100 Å [22]. Meanwhile, the permoporometry method is used if the pore sizes are in the range of 20–300 Å. This method is applied when the vapor pressure on a liquid surface depends on the curvature of the surface. The vapor pressure will rise from 0 to 1 to fill all the pores. On the other hand, thermoporometry is referred as a calorimetric study of the liquid capillary that goes through condensation process by saturation of porous material. This method is used if the pore sizes are in the range of 15–1500 Å, and especially for materials that are compressed without structural change [23].

## 9.2.5 Contact Angle

According to Tylkowski et al. [19], the contact angle is an analysis to characterize the membrane hydrophilic/hydrophobic behavior. Moreover, it also can be used to investigate the effect of chemical modification that has been made like cross-linking between the other materials [24] or by addition of hydrophilic or hydrophobic solvent as a supporter into polymeric materials to find optimal flux without sacrificing selectivity [25]. According to Feng et al. [26], contact angle also refers to the roughness and thickness of the outer parameter produced membrane. This is an essential key element to further understanding of other techniques like permporometry, which are associated with the thickness of the sorption layer [27].

Hydrophobicity or hydrophilicity of solids is significant in many processes like wetting, flotation, improved oil recovery, purification

technology, super hydrophobicity, fluid spreading, plants protection, and others. These words are used to explain the affinity of solids to water extending on their surface [19]. Contact angle ($\theta$) also is a measurement for unequal molecular interactions which involved at least two materials in contact known as wettability. If $\theta < 90$ degrees, it means that the membrane is hydrophilic. This is determined based on the solid that is partially moistened with a liquid such as water. Meanwhile, if $\theta > 90$ degrees, it means that the surface is not wetted and is known as a hydrophobic membrane. However, if the water contact angle is above 140 degrees, it is known as superhydrophobic. This type of membrane can be obtained through an appropriate modification such as roughening, micro patterning, machining, or etching [19].

## 9.2.6 Biocompatibility of Hemodialysis Membrane

### 9.2.6.1 Definition of Membrane Biocompatibility

Biocompatibility is required for material that has surface that comes into contact with the biological system [28]. Initially, the Dictionary of Biomaterials defines biocompatibility as "the ability of a material to perform with an appropriate response in a specific application" [29, 30]. Lately, biocompatibility is defined as "the biological performance of a certain material in a specific application and its acceptance/suitability for such application if both host and material responses are optimal" [31]. Besides, in blood purification applications like hemodialysis, biocompatibility is defined as "a concept to stipulate safety of blood purification therapy by an index based on interaction in the body arising from blood purification therapy itself" [32].

Membrane biocompatibility is considering one of the significant aspects to be a concern for the hemodialysis membrane. The demand properties of material biocompatibility depend on its applications of the end-product. For hemodialysis, properties such as blood compatible or hemocompatible are necessary for the material involved in the process related to the reduced coagulation, platelet adhesion, protein adsorption, and hemolysis [31]. During the hemodialysis process, numerous biological responses arise when blood expose to the extracorporeal circuit that includes exposure to membrane materials, removal of solute, exposure to dialysate components, or contamination in which the membrane area was the foremost part expose [28, 33]. Blood-membrane contact during hemodialysis creates a series reaction of the biological event (Fig. 9.1), which will lead to an adverse effect on the membrane performance and also patient health. Bioincompatibility may affect the incidence of infection, malignancy, cardiopulmonary disease, and malnutrition as well as induce novel disease processes [34].

### 9.2.6.2  *Protein Adsorption*

Protein adsorption can be defined as "adsorption which is adhesion or sticking of protein(s) on one of the surfaces." Proteins are commonly serum proteins, enzymes, antibodies, and foreign antigens; sometimes genes included even though they are not proteins in fact [36]. During hemodialysis, the deposition of protein layers happens instantaneously after blood contact with the foreign surface of the membrane [37]. Once deposited, protein initiates all subsequent body biological event in blood, which cause coagulation and complement activation and also initiates blood cell activation and attach on membrane surfaces [37, 38]. Adsorbed plasma proteins, such as factor XII, fibrinogen, vitronectin, high-molecular-weight kininogen (HMWK), von Willebrand factor and others provide a significant criterion for their thrombogenicity. The adsorption of these plasma proteins to membrane surfaces leads to a receptor-mediated (GPIIb/IIIa) adhesion and activation of platelets, and as a result to aggregation, and in an advanced stage, to thromboembolic processes [39].

Beside affect membrane biocompatibility, irreversible protein deposition on membrane surface also cause a progressive decline in flux and a change of membrane selectivity that known as membrane fouling [38]. Several factors such as membrane surface chemistry as well as protein size, shape, charge and isoelectric point causing protein adsorption. It is necessary for biocompatible membranes must not have surface nucleophils, yet should have small surface charge and a well scattered hydrophilic and hydrophobic areas [31].

### 9.2.6.3  *Contact Activation of Coagulation*

Clotting happens by the contact of plasma with membrane surface that produces adsorbing interface. This leading opinions by Johlin's works in 1929 show activation of the plasma-coagulation cascade is apparently catalyzed by contact of specific blood factors with surfaces and does not necessarily require adsorption of these factors [40]. Upon blood contacting with hemodialysis membrane, plasma-coagulation cascade was activated through contact activation which also termed an intrinsic pathway of coagulation [41].

The intrinsic pathway being initiated by contact activation of high molecular weight kininogen (HMWK), prekallikrein and Factor XII and generally, these fragments need interaction with negatively charged membrane surfaces for zymogen activation in-vitro. Factor XII is stimulated by adsorption, FXIIa transforms prekallikrein into kallikrein and with HMWK as a cofactor initiates Factor XI to Factor FXIa. Factor XIa activates Factor IX to Factor IXa. After a process of reactions involving (among others) the intrinsic tenase complex (Factor IXa and Factor VIIIa), prothrombin is changed into thrombin. At last, thrombin converts

the soluble fibrinogen into insoluble fibrin, which is then stabilized by FXIIIa to form stable clots [42].

### 9.2.6.4 Complement Activation

The membrane biocompatibility usually been determined based on the severity of the complement activated [43] as the complement is components of the inflammatory response induced by the membrane [42]. Hemodialysis membrane activate complement system through alterative pathway [44]. The adsorption of C3b on membrane surface by covalently bonded of C3b to hydroxyl (OH—) or amine (—R—NH$_2$) groups on the membrane surface with the carbonyl group in the C3b thioester binding site [42]. It subsequently activates C3 convertase which cleaves to form C3a and C3b. The C3a later facilitates the formation of C5 convertase that later cleaves to form C5a and C5b. C5b induced the formation of membrane attack complex (MAC), which cause pathogen cell to lyse and triggered further cells activation [45]. C3a and C5a are biologically active agents that capable to cause high vascular smooth muscle contraction and induce anaphylaxis in some animal models, therefore the name "anaphylatoxins" given [35]. Complement C3a anaphylatoxin activates platelets, enhancing their aggregation and activation [45, 46]. Also, complement C5a anaphylatoxin caused thrombosis, through activation of tissue factor (TF) in peripheral blood neutrophils that trigger in-vivo blood coagulation process [47].

### 9.2.6.5 Platelets Activation and Adhesion

Platelets in nature involved in early hemostatic response when any vascular injury happens [41]. During hemodialysis a rapid plasma protein adsorption especially fibrinogen and exposure toward membrane surface could lead activation of platelet, platelets adhesion and aggregation on the membrane surface to form a thrombus on the hemodialyzer membrane's surface (Fig. 9.2) [33, 48]. Coagulation pathways activate platelets through the release of thrombin from prothrombin conversion, while the anaphylatoxin C3a complement induces platelet activation and aggregation [43, 45]. The thrombocytopenia is also a well-known complication of hemodialysis treatment. It was found that thrombocytopenic incidences occurring with hemodialysis were associated with complement activation (C3a) in addition to activation of platelets themselves [49] by the membrane.

### 9.2.6.6 Hemolysis

Hemolysis or degradation or the red blood cell (erythrocytes) caused by shear stresses that occur when blood was flowing along the membrane surface however it rarely happens during hemodialysis process. The hemolysis also can be caused by activation of the complement system followed by formation of the membrane attack complex (MAC) (Fig. 9.3) [43].
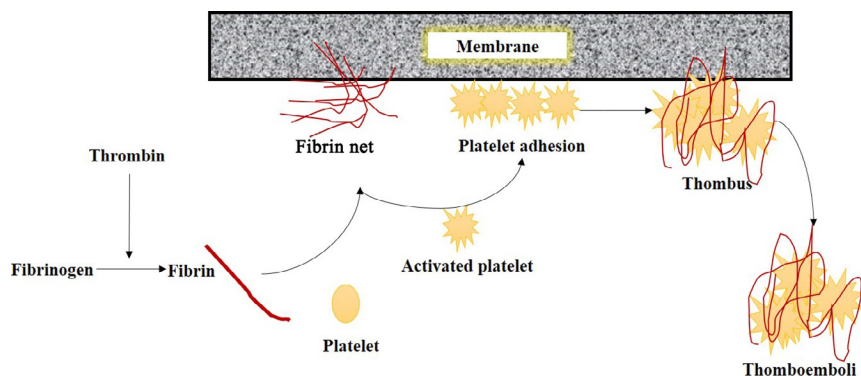
**FIG. 9.2**   Formation of thrombus following the adhesion of fibrin and platelets on the membrane surface from Ref. [50].
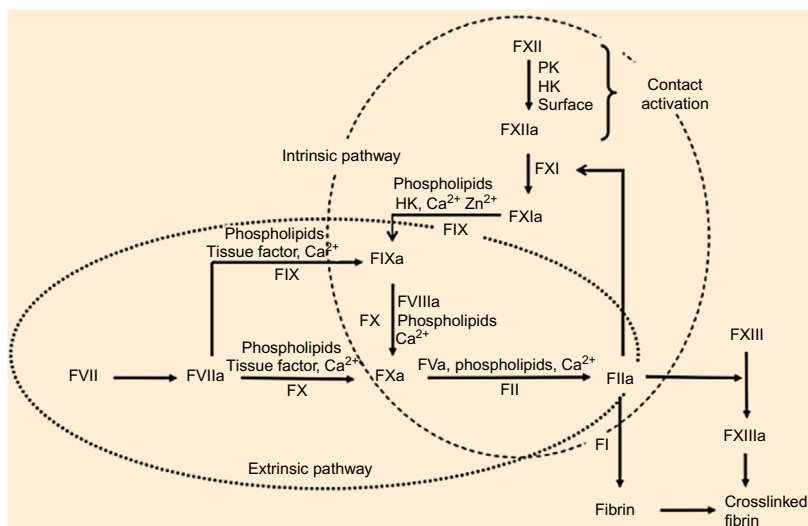


**FIG. 9.3**   Plasma coagulation cascade. Both extrinsic and intrinsic pathway of activation converges enzyme complexes converting factor X to Xa. Factor Xa is part of the prothrombinase complex, which activates prothrombin to thrombin. Thrombin is the enzyme converting soluble fibrinogen to insoluble fibrin mesh. *Courtesy from Vogler EA, Siedlecki CA. Contact activation of blood-plasma coagulation. Biomaterials 2009;30:1857–69. https://doi.org/10.1016/j.biomaterials.2008.12.041. Copyright © 2009 by Elsevier. All right reserved. License no.: 4185681069094.*

### 9.2.6.7 Leukocyte

Leukocytes activation and adhesion is mediated by complement components system. The activation of complement system via alternative pathway particularly C3a and C5a significantly activate leukocytes causing leukopenia in the first 10–15 min of dialysis [10].

Poor biocompatibility membrane such as cuprophan initiate release vast amount of reactive oxygen species (ROS) by neutrophils that activated by hemodialysis membrane [10, 43] and also cause neutropenia [51]. Chronic complication of the ROS release causing anemia, amyloidosis, accelerated atherosclerosis, and malnutrition [52]. The previous study had reported that various membranes were causing platelets-leukocytes aggregation due to shear stress, contact activation, or agonist activation. This coaggregates cells could cause atherosclerotic plaques, and a severe clinical situation in which platelet-neutrophil interactions have been implicated is in the pathophysiology of septic shock and multiple organ system failure [51].

## 9.3  THE MEMBRANE USED IN HEMODIALYSIS

Hemodialysis membranes, in general, are made up of polymer. A polymer is dissolved in a conventional organic solvent, or sometimes acid depending on its solubility. The polymer solution, or commonly denoted as the dope solution can contain either entirely organic compound or exists as a mixture of organic and inorganic compounds. This dope solution will then be shaped into a membrane via phase inversion. There is a wide range of membranes that can be used to develop a hemodialysis membrane. In brief, hemodialysis membranes can be classified based on two main criteria: (i) chemical natures of the primary polymer and (ii) the types of modification the membranes undergo.

### 9.3.1  Chemical Natures of Polymer

At the early stage of the development, there were three types of hemodialysis membrane, namely cellulosic, modified cellulosic, and synthetic membranes (Ruthven, 1997). This classification was made based on the chemical natures of the polymer used.

#### 9.3.1.1  Cellulosic Membrane

Cellulose membranes were used at the earlier development of hemodialyzer. They are fabricated from cellobiose which is ubiquitous as a saccharide. These membranes are symmetric concerning morphology, indicating a substantially uniform resistance to mass transfer over the entire wall thickness. Besides, these membranes are characterized by the low mean size of a pore and pronounced hydrophilicity [53, 54]. The long duration of popularity was due to their particular suitability for a diffusion-based procedure. The hydrogel structure allows the combination of low wall thickness and high porosity to be attained. This

permits satisfactory transport rate within the diffusive membrane, which results in efficient removal of small water-soluble uremic toxins like urea and creatinine. In early years, cellulosic membranes such as cuprophan are popularly used due to their abundance in nature and having excellent transport properties to remove wastes from the blood.

However, it was found that the membrane is clinically undesirable and carries many shortcomings regarding biocompatibility [5]. The cellulose surface tends to activate complement pathway once it comes into contact with blood. The presence of high free hydroxyl group density in cellobiose has aroused the activation of the alternative complement pathway. In addition to their low biocompatibility, the incapability of cellulosic membranes to extend their MW range for solutes removal contributes to the decreased in the membranes popularity [54]. For the removal of $\beta_2$-microglobulin, cellulose derived membrane is impermeable to $\beta_2$-microglobulin due to its dense symmetrical structure which does not permit the natural diffusion or convection of proteins through the membrane. Moreover, the demand for cellulosic membranes declined over the past decades with the progress in other material in the same area.

### 9.3.1.2 Modified Cellulosic Membrane

The evolution of hemodialysis membranes continues to counter the bioincompatibility issues faced by cellulosic membranes [55]. Some modifications were made onto the cellulose surface. There are two types of modified cellulosic membranes depending on the molecules that are replacing the hydroxyl groups, namely cellulose acetate membranes and hemophan membranes [54].

Similar to an unmodified cellulosic membrane, these membranes own a symmetric structure with low wall thickness (6–15 μm). In contrast, these membranes have larger mean pore size compared to the unmodified cellulosic membrane (22 μm). This resulted in more substantial porosity, higher water permeability, and middle molecule clearance. However, the weak hydraulic permeability and low MWCO near 2000 Da still limit the development of cellulose-based material [56]. Modified cellulosic membranes were first used for hemodialysis in 1980s. The modified cellulose membranes still could not provide excellent separation.

### 9.3.1.3 Synthetic Membrane

In the early 1970s, the utilization of cellulosic membranes in hemodialysis treatment has revolutionized to synthetic membranes. Since that, many synthetic polymers such as polysulfone (PSf), polyethersulfone (PES), poly(methyl methacrylate) (PMMA), polyacrylonitrile (PAN) and polyvinylidenefluoride (PVDF) have been employed in the fabrication of hemodialysis membranes [54]. While both modified and unmodified

cellulosic membrane is prepared from a naturally existing polymer, a synthetic membrane is made from thermoplastic polymer [53].

Synthetic membranes possess larger mean pore size and thicker wall structure. These features offer high UF rate at relatively low transmembrane pressure. Synthetic membranes are preferable due to their better performance and great stability over a more prolonged period. The transition toward the use of synthetic polymer for hemodialysis has triggered much effort to discover the suitability of each well-known polymer. There were abundant studies conducted to study the suitability of different synthetic polymers to be used in hemodialysis as well as their effects on hemodialysis performance.

For hemodialysis treatment, the membrane should be hydrophilic to permit water part of the blood (plasma) to pass through the membrane. Besides, the selection of materials for hemodialysis membrane must also consider the capacity to remove targeted molecules. For example, the change of $\beta_2$-microglobulin level in blood plasma may not merely be a result of transmembrane transport. In fact, the protein adsorption to the membrane may also play a role in the observed changes [57]. It was reported that PAN, PSf and PMMA membrane could be used for the removal of $\beta_2$-microglobulin [58]. Other than removing the $\beta_2$-microglobulin by size exclusion, PMMA membrane tends to adsorb $\beta_2$-microglobulin.

To tackle the problem of inefficient removal of $\beta_2$-microglobulin, the membranes must be able to filter both small and middle molecular weight molecules. In the case of PES membrane, the removal of large molecules was due to its asymmetric structure and the high ultrafiltration capacity, as the result of its surface hydrophilicity and larger pore size [59]. Table 9.2 presents the different types of polymer generally used for hemodialysis treatment.

### 9.3.1.4 Copolymers

Historically, polymer composites, blends, and copolymers have been developed to combine component properties, or to optimize the cost and properties relationship. A homopolymer is called for polymers prepared by one monomer, copolymer by two monomers, and terpolymer by three or more monomers. The purposes of developing of copolymer and terpolymer are to improve the characteristics of the polymer properties to suit the membrane requirements according to the applications.

In the copolymers of Fig. 9.4A and B represent the other and statistical copolymer chains. The number of monomers composer will affect the properties of materials which is formed. The monomers usually present in one phase and the property of the copolymer composed is approximate of the average properties for the monomers composers. Meanwhile, if the copolymers composed by domains of each monomer (Block and Graft in Fig. 9.4C and D respectively), the property of the copolymer composed

**TABLE 9.2**  Different Types of Synthetic Polymer Used for Hemodialysis

| Polymer | Advantages | Disadvantages | References |
|---------|-----------|---------------|------------|
| PMMA | • Good solute permeability<br>• Less cytokine production<br>• Adsorbs and removes factor D which triggers alternative pathway complement activation | • Has lower sieving coefficient for β-2-microglobulin | [32, 60] |
| PAN or AN69 | • Improve the blood compatibility<br>• Reduce anaphylatoxin formation | • A negatively charged surface can activate dialyzer reactions | [53, 61] |
| PSf and PES | • High thermal stability<br>• Wide pH tolerance<br>• Good chemical resistance<br>• Flexibility in fabrication<br>• High mechanical strength | • Hydrophobic<br>• Oxidative stress | [62, 63] |
| PVDF | • Thermally stable<br>• High mechanical strength | • Hydrophobic<br>• Low chemical resistance | [64] |
| Polyamide | • Wide pH tolerance<br>• High thermal stability<br>• High mechanical properties | • Hydrophobic<br>• Low chemical resistance<br>• Complement activation | [64, 65] |
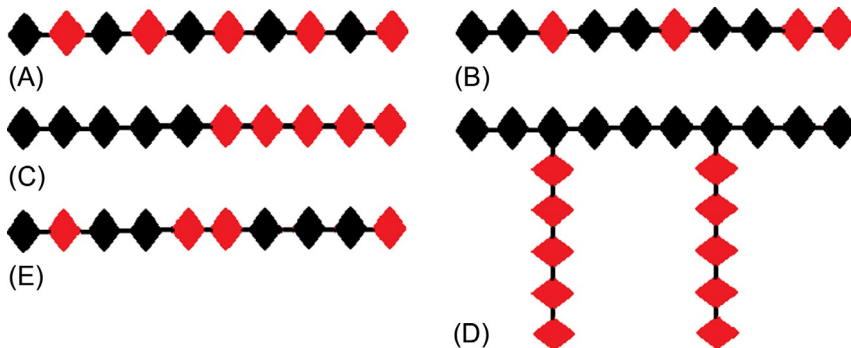


**FIG. 9.4**  Types of copolymers. Alternate; statistical; block; graft; gradient respectively from A to E [67].

is a combination between two monomers and formed a homopolymer. Fig. 9.4E showed the gradient copolymers. In this copolymer, the properties of a copolymer composed are dependent upon the number of constituent monomers [66].

Current extensive efforts to improve hemodialysis membranes are focusing on removal of β-microglobulin and improving blood compatibility. To support these goals, the polymers used as hemodialysis membranes can be modified by copolymerization technique. Some materials have been developed to produce the hemodialysis membranes. These materials are ethylene-vinyl alcohol copolymer (EVAL), poly(lactic acid)-block-poly(2-hydroxyethyl methacrylate) (PLA-PHEMA), polysulfone-graft-poly(lactic acid) (PSf-g-PLA) [68].

The other copolymers materials very worth to be applied into hemodialysis application include: poly(L-lactic-co-ε-caprolactone)-sericin (PLCL-SC) copolymer membranes using Wharton's jelly mesenchymal stem cells; copolymer by blending an amphiphilic triblock copolymer of poly(vinyl pyrrolidone)-b-poly(methyl methacrylate)-b-poly(vinyl pyrrolidone) [69]; and also copolymer between polyether urethane, polypropylene oxide, and a polyether polyester [70]. These materials, produced from the copolymerization process are the candidates to become hemodialysis membrane, with regards to their biocompatibility aspects. The other purpose of a copolymer is to enhance the antifouling performance of hemodialysis membrane.

## 9.3.2 Modification of Hemodialysis Membranes

When dealing with hemodialysis membranes of any origin, there are a few parameters need to be considered to enhance their biocompatibility as well as to reduce membrane fouling. One of the parameters is hydrophilicity/hydrophobicity configuration of membrane surface, which is closely related to the membrane materials. Bioincompatibility between membrane polymer and a blood sample will cause rapid adsorption of protein onto the membrane surface due to the hydrophobicity of polymeric-based membrane, and eventually, platelets coagulation will occur on the surface of the membrane. On the other side, membrane fouling happens due to adsorption of nonpolar solutes and hydrophobic bacteria. This would shorten the life expectancy of the membrane and subsequently increase the cost.

Hence, modification of conventional hydrophobic hemodialysis membranes, such as PES and PSf membranes to increase the antifouling property, biocompatibility and other specific functions become a more promising strategy to improve the hemodialysis performance. The modifications allow the alteration of desired hydrophobicity and hydrophilicity balance by adding the hydrophilic material specifically in the membrane pores, where they have a positive effect on flux and fouling reduction. Proper control of modification also endows particular functionality to the biocompatible membranes. Two approaches have been

commonly attempted to modify a hemodialysis membrane: (a) blending of additive or filler during dope solution preparation and (b) surface coating of the prepared membrane. The membrane undergoing either one of these approaches would be later known as a composite membrane.

### 9.3.2.1 Blending

Due to its simplicity, blending is the most widely used method to modify hemodialysis membranes. An organic compound which shares the similar polarity with solvent and same chemical properties to the primary polymer would blend perfectly in the membrane matrix. In contrast, the inorganic compound is somewhat challenging to be blended in its raw state. It has to be modified to ensure its compatibility with the polymer and distribution across the membrane matrix.

#### 9.3.2.1.1 Addition of Hydrophilic Polymer

Hydrophobic membranes are easily modified by blending with hydrophilic polymers such as PVP [71, 72] and PEG [73]. PVP is highly polar, nonionic, amphiphilic, and physiologically inert. The water-soluble polymer is accessible in various MW either in powder or liquid form. To improve the biocompatibility and hydrophilicity of PES, PVP is commonly used as the hydrophilic additives [74]. PVP helps in reducing membrane fouling by inhibiting the protein adsorption on the membrane surface and plays a crucial role in pore formation. The positive influence of PVP on the membrane hydrophilicity allows the increase in the antifouling property and blood compatibility [71].

The extent of PVP's influence toward hydrophobic membrane was further investigated by the preparation of a copolymer of poly(vinyl pyrrolidone-co-methyl methacrylate-co-acrylic acid) via one-pot reaction to being blended with PES [75]. The results suggested that the modified PES membrane showed better cytocompatibility based on the cell morphology and low hemolysis ratios.

#### 9.3.2.1.2 Addition of Biomaterials

Biomaterials are being used as membrane additives to improve the biological interactions between blood and membrane surface. Sometimes, a relatively more biocompatible polymer than that of the primary polymer is added to reduce the body antiinflammatory response. The addition of sulfonated polyether ether ketone into PES membrane, for example, has enhanced the membrane hemocompatibility as a result of emerging repulsive forces between negative charges on the membrane surface and blood components [76]. On the other hand, the blending of polyurethane (PU) with PES has led to the enhanced antifouling and antithrombotic properties as compared to neat PES membrane [77].

Many efforts have been made to produce biomimicking materials which later being added into hemodialysis membranes. The molecular structures of anticoagulants like heparin and citric acid (citrate), which can be used to disrupt the coagulation cascade and prevent clotting, or antioxidants like vitamin E are utilized as a template to synthesize these biomimicking materials. In a study by [78], a substantial increase in the blood coagulation time was reported when the PES membrane, blended with poly(1,8-octanediol citrate) (POC) was incubated in blood plasma. The enhanced antithrombotic property of the membrane was supported by the reduced concentration of calcium ions detected in the plasma after the incubation with the membrane. The citrate groups in the POC act as chelating agent and bind to the calcium in the blood. By reducing the amount of calcium, there will be no regulation of the binding, and the blood coagulation cascade cannot begin [79]. The similar outcomes happened when citric acid-grafted PU was incorporated in PES membrane by blending [80]. The blended membranes have better blood compatibility in which the adsorption of protein was lowered, thus restraining platelet adhesion and prolonged blood clotting time. In another work, a heparin-mimicking PU was synthesized for the modification of PES membrane for the same reason [81].

The activation of a cellular element as well as an inflammatory response during hemodialysis process would most likely result in an increased reactive oxygen species. Hence, a composite PSf membrane which consists of Vitamin E TPGS was made. The presence of TPGS in the membrane matrix improved the membrane biocompatibility by suppressing the number of reactive oxygen species. Regarding separation, the membrane displayed pure water flux and urea clearance of about two orders of magnitude better than commercial hemodialysis membranes.

### 9.3.2.1.3 Addition of Sorbent

Adsorption becomes another method besides diffusion that has been successfully investigated by researchers notably to eliminate uremic toxins (middle molecular weight and protein bound). Research by Davankov et al. [82] stated that a combination of the strength of dialysis membranes with the adsorption power of high surface area sorbents could be very beneficial for the blood purification especially when dealing with small protein-bound toxins. Inspired by the concept of an adsorptive membrane, attempts were made to combine membrane filtration and adsorption columns two separate steps [83]. By the combined actions of diffusion and adsorption, the removal of low MW particles is more efficient due to the increasing adsorption capacity of the membrane.

Since that, the efforts have been shifted to the development of mixed matrix membranes (MMMs), in which inorganic fillers or sorbents are incorporated in the polymer matrix [84]. The research by Tijink et al.

[85, 86] established a novel approach to blood cleaning focusing on the improvement of adsorption capacity of a membrane. They fabricated MMMs combining diffusion and adsorption in one step. Adsorption particle was incorporated into the mixture of PES and PVP in $N$-methyl-2-pyrrolidone. Dual layer MMMs were fabricated in which a particle free membrane layer was formed on top of an MMM layer containing activated carbon. The results showed a better creatinine clearance from blood compared to conventional method.

Other sorbents used in hemodialysis membrane include hydroxyapatite (HAP) and zeolites. HAP has good adsorption to protein and usually used in the medical field due to its biocompatibility and bioactivity [87]. Zeolites, on the other hand, are microporous, aluminosilicate minerals commonly used as commercial adsorbents and catalyst. Wernert et al. [88] have successfully tried the zeolites in the development of hemodialysis membrane [88]. The membrane can eliminate about 67% creatinine and 29% $p$-cresol. It was also proven that zeolite could be used and added to the hemodialysis membrane to clear middle molecule toxins [89].

### 9.3.2.1.4 Addition of Inorganic Nanoparticles

In recent events, the focus has been placed on tackling membrane fouling which has resulted in flux declination. One of the membrane surface modification techniques is through the nanoparticles incorporation [90] to form nanocomposite membranes, which is becoming an emerging trend in membrane technology. Nanoparticles are particles between 1 and 100 nm in size. The different unique properties of nanoparticles especially the large surface area are the main reasons for their employment. There are two types of commonly used nanoparticles, that is, (i) carbon nanoparticles such as carbon nanotubes (CNTs) and graphene and (ii) metal oxide nanoparticles like titanium dioxide and iron oxide nanoparticles. It was found that the combined actions of embedded nanoparticles and the membrane can improve the durability of polymeric membranes toward chemical degradation, fouling and thermal instability as well as heighten the performance of the resultant membrane [91, 92]. For instance, titanium and silver-based nanoparticles have antibacterial and antiviral properties which can reduce biofouling of membrane.

Among the membrane applications, hemodialysis is an application that might experience a very precautionary transition from commercial polymeric membranes to the utilization of this nanocomposite membrane. Previously, insufficient numbers of studies have been reported on the development of hemodialysis membranes incorporated with nanofillers. The study by Zare-Zardini et al. [93] for example only focused on the hazardous effects of silver nanoparticles and arginine-treated carbon nanotubes (CNTs) on blood cells during hemodialysis.

For the past 3 years, there have been a growing number of studies on hemodialysis nanocomposite membrane, but are mostly limited to CNTs as the nanofillers [94–97].

The first attempt was made by Irfan et al. [94] using acid-treated multiwalled carbon nanotubes (MWCNTs), resulting in the improved clearance of uremic toxins. Nie et al. [95] later produced the PES nanocomposite membrane incorporated with the heparin-mimicking polymer brush grafted CNTs, with the primary focus to improve the biocompatibility of the membrane. The membrane exhibited antifouling ability in ultrafiltration, excellent blood and cell compatibility and efficient toxic molecules removal ratio [95]. The versatility of CNTs as fillers for hemodialysis membrane is further supported by the research conducted by Abidin et al. [96, 97]. A safe and high-performance PES/MWCNTs nanocomposite membrane was fabricated by first growing hyperbranched poly(citric acid) on the MWCNTs surface. The PES/MWCNTs nanocomposite membrane showed both improved biocompatibility and antifouling performance. Newest, there has been a claim where iron oxide nanoparticles show a promising quality for hemodialysis when embedded in PSf membrane [98].

### 9.3.2.2 Surface Coating

Surface coating was seldom performed for the development of hemodialysis membrane. A membrane with a layer coated on it is impractical for extended usage, not until recently when various methods have been introduced to ensure the coating layer becomes intact with the supporting layer. The development of long-term complications in hemodialysis patients, such as anemia, has motivated a study by Bargnoux et al. [99] to minimize oxidative stress which is a strong pathogenic cofactor for such complications. As a solution, vitamin E was coated on a PSf membrane to improve red blood cell antioxidant activity when in contact with the membrane surface. This effort has resulted in a preventive effect on oxidative stress.

Later, Gao et al. [56] have prepared a heparin-immobilized PLA membrane for hemodialysis. Heparin adhered to the PLA membrane surface via the strong adhesion of polydopamine, previously coated on the membrane surface. The hemocompatibility of the membrane was significantly improved after the surface heparinization, based on the suppressed platelet adhesion, extended plasma recalcification time and decreased hemolysis ratio. Performance-wise, 79% of urea and 18% of lysozyme were successfully removed, and over 90% of BSA was retained. In another work by Mahlicli and Altinkaya [100], alpha lipoic acid was immobilized onto PSf membrane, intended to suppress oxidative stress induced by hemodialysis process. In addition to reducing oxidative stress, the coating of alpha lipoic acid also prolongs blood coagulation time.

Besides biomimicking materials, hydrophilic polymers themselves are also known for their good biocompatibility. However, hydrophilic membranes such as polyvinyl alcohol (PVA) membrane have a tendency to
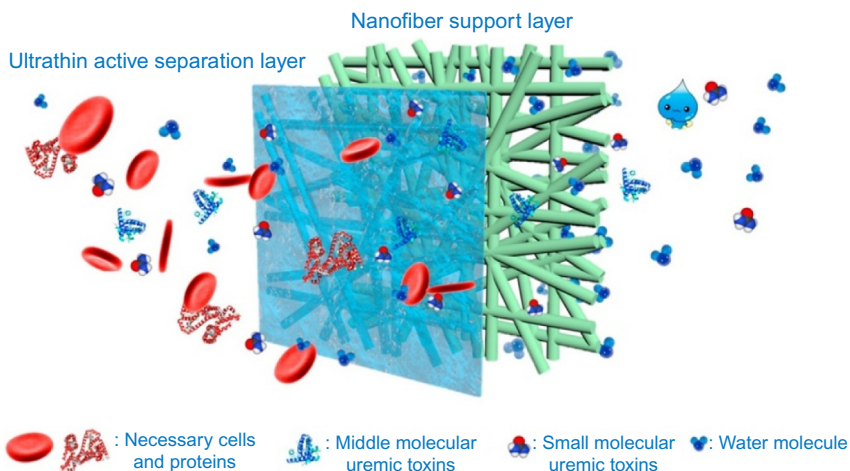
**FIG. 9.5** Schematic of a two-tier composite structure with an ultrathin active separation layer and a scaffold-like nanofiber supporting layer. *Courtesy of Yu X, Shen L, Zhu Y, Li X, Yang Y, Wang X, et al. High performance thin-film nanofibrous composite hemodialysis membranes with efficient middle-molecule uremic toxin removal. J Memb Sci 2017;523:173–84. https://doi.org/10.1016/j.memsci.2016.09.057. Copyright © 2010 by Journal of Membrane Science. All right reserved. License no.: 4185720821444.*

swell in water, which results in a loss of mechanical strength and often a reduction of rejections that can be attained [101]. To make use of its useful properties, the ingenious way is to coat the hydrophilic polymer on top of the robust hydrophobic support, facing the blood. Yu et al. [102] have successfully produced a thin film nanofibrous composite membrane which consists of a two-tier composite structure, namely an ultrathin hydrophilic active layer of chemically cross-linked PVA and an electrospun PAN nanofibrous supporting layer (Fig. 9.5). The membrane exhibited excellent permeability and selectivity due to its unique structure. It also possessed good mechanical strength and comparable hemocompatibility. Most importantly, the membrane was able to remove 45.8% of middle molecular weight toxins, which is the best so far [102].

# 9.4  PREPARATION OF HEMODIALYSIS MEMBRANE

## 9.4.1  Nonsolvent Induced Phase Separation (NIPS)

Phase inversion is a technique involved in the demixing process whereby the homogenously prepare dope solution is transformed from a liquid to a solid state in a controlled manner. The phase inversion technique can be categorized into several techniques which include immersion precipitation or known as nonsolvent induced phase separation (NIPS),

thermally induced phase separation (TIPS), evaporation-induced phase separation, and vapor-induced phase inversion (VIPS). This topic will focus more in NIPS as it is one of the most common methods in the fabrication of hemodialysis hollow fiber membrane. This fabrication technique is suitable for producing ultrafiltration (UF) membrane where the average pore size of the fabricated membrane is in the range of 0.001–0.1 μm [8]. In NIPS process, the dope solution is immersed in a nonsolvent coagulation bath. Here, demixing and precipitation occur due to the solvent and nonsolvent exchange. Many factors are needed to control and manipulated prior, during and after the NIPS spinning process.

### 9.4.1.1 Preparation of Dope Solution

Polymer pellet is dried for few hours to remove moisture content before dope solution preparation. Next, the polymer is dissolved in a suitable solvent such as *N*-methyl-2-pyrrolidone (NMP), dimethylformamide (DMF), dimethylacetamide (DMAc), and dimethylsulfoxide (DMSO) to form a polymer solution or known as a dope solution. The solvent selection can be related to Hansen solubility parameter, thermodynamic behavior and the mutual affinity (miscibility) of the solvent toward the polymer used. Theoretically, the higher the miscibility between the solvent and nonsolvent will cause instantaneous demixing which leads to a more porous membrane. If the miscibility between solvent and nonsolvent is low, there is high possibility an asymmetric membrane with a dense, nonporous top layer is obtained [103]. Both polysulfone (PSf) and polyethersulfone (PES) are the most common polymer used to make hemodialysis membrane by phase inversion process. Both polymers have been used in several medical field application including microbiology fluid applications, life science, tissue culture, media sterilization, clinical, and general filtration. This is due to their excellent physical and chemical properties which include high thermal stability, excellent hydrolytic stability, and excellent mechanical strength. NMP, DMF, and DMAc are the most common solvents used for both PSf and PES. The PSf and PES membrane generally are simple to be prepared by immersing the dope solution into the nonsolvent coagulation bath, such as water [103].

### 9.4.1.2 Spinning Parameters

The morphology of the fabricated membrane is highly influence by the criteria of the spinning parameter used during the fabrication process. Few factors need to be manipulated to achieve the desired membrane, whether a dense, symmetric or asymmetric hollow fiber membrane. Some of the factors that need to be determined are listed in Table 9.3.

**TABLE 9.3**  NIPS Spinning Parameter

| Parameter | Descriptions | Reference(s) |
|---|---|---|
| Polymer solution | Polymer or dope solution is prepared by mixing polymer with solvent or sometimes nonsolvent. The viscosity of the polymer solution need to be measured prior the spinning process occur to predict the morphology of the fabricated fiber. If the polymer concentration of the dope solution is low, the viscosity of the dope solution is diluted. This will cause the outer layer membrane to become porous due to fast phase inversion process. When dope solution viscosity is high, the outer layer membrane become dense. This is because the viscous solution will hinder the movement of the pore former and solvent during the phase inversion and increase the density of the membrane. | [9] |
| Bore fluid | Bore fluid or bore liquid is the fluid that helps in the formation of the hollow fiber lumen. Distilled water is the most common bore fluid that is used for the fiber formation. However, some researcher manipulates the morphology of the skin layer based on the percentage of the solvent used in the bore fluid. | [104] |
| Nozzle/ spinneret dimension | A hollow fiber membrane spinneret is a device used to extrude polymer solution to form fibers. It is used to mold the shape of the fiber. The size is varied based on the desired hollow fiber dimension size. For hemodialysis application, the smallest dimension size is used to ensure the size of the fabricated hollow fiber is less than 200 µm. | [6] |
| Dope extrusion rate | Dope extrusion rate (DER) is defined as the total dope solution (mL) extrude from dope reservoir per minute. It usually counts as mL/min or in RPM. | [11] |
| Bore fluid extrusion rate | Bore fluid flow rate (BFFR) is defined as the total bore fluid (mL) flow out per minute. It usually counts as mL/min. | [11] |
| Air gap distance | The air gap distance is measured from the end of the nozzle to the surface of the water. The air gap distance is where dry phase inversion happens, whereby the dope solution will start to solidify when it is introduced to the atmosphere. When The distance apply during the fabrication of the membrane also will influenced the size and morphology of the membrane. When the dope solution extruded out from the spinneret, gravitational force or additional stretching during | [11] |

*Continued*

TABLE 9.3    NIPS Spinning Parameter—cont'd

| Parameter | Descriptions | Reference(s) |
|---|---|---|
| | the take-up of the fibers will cause elongational stresses in the air gap region which helps stretching the fiber. If the air gap distance higher, the elongational stresses increases, thus producing smaller diameter of fiber. | |
| Coagulation bath | Water is the most common coagulation bath used not only due to its lower cost but to fully precipitate and stabilize the nascent membrane structure. After being extruded out from the spinneret, low strength coagulant in the coagulation bath may result in a porous outer surface, while a high strength bore fluid may produce a tight inner skin. | [9] |

## 9.5  FUTURE PROSPECT

As a conclusion, membrane technology is yet to show its full eminence in blood purification process despite the outstanding quality and prospect. From an observational standpoint, the membrane performance matters the most after the safety of the membrane is fulfilled. Thus, the focus has now been shifted on how to improve a membrane's capacity to remove middle molecular and protein-bound toxins. In an attempt to mimic glomerular removal of middle molecules, the effort is made to increase pore size while sharpening the molecular weight cut off of high flux membranes. The truth is this concept might not be practiced in the real treatment due to the high possibility of facing the risk of losing essential proteins from blood via convection.

Hence, the alternative and probably safer way to be done is by shifting the approach from convection to adsorption. High flux membrane based on enhanced adsorption, could be widely used in clinical situations. The combination of the strength of dialysis membranes with the adsorption power of high surface area sorbents can be very beneficial for the blood purification efficacy [85]. The membrane, however, must have minimum protein adsorption and high adsorption capacity to a wide range of toxins especially middle molecular and protein-bound toxins.

Another use of adsorptive membrane should be expected in future when scientists and researchers have started to develop portable hemodialysis device to mimic the natural kidney and its functions to continually cleansing the toxins in the blood. A dialysate regenerating technology would be needed to clean the spent dialysate, before recycling the dialysate back into the hemodialyzer. An adsorptive membrane would be a

perfect candidate to replace the current dialysate regenerating technology using sorbent. The membrane, however, must have a high adsorption capacity of small and middle molecules.

## References

[1] Kalra S, McBryde CW, Lawrence T. Intracapsular hip fractures in end-stage renal failure. Injury 2006;37:175–84. https://doi.org/10.1016/j.injury.2005.11.006.

[2] Vanholder R, De Smet R, Glorieux G, Argilés A, Baurmeister U, Brunet P, et al. Review on uremic toxins: classification, concentration, and interindividual variability. Kidney Int 2003;63:1934–43. https://doi.org/10.1046/j.1523-1755.2003.00924.x.

[3] Yamashita AC, Sakurai K. Dialysis membranes—physicochemical structures and features. Update Hemodial 2015; https://doi.org/10.5772/59430.

[4] Vilar E, Farrington K. Haemodialysis. Medicine (Baltimore) 2011;39:429–33. https://doi.org/10.1016/j.mpmed.2011.04.004.

[5] Ahmad S. Manual of clinical dialysis. 1–245. https://doi.org/10.1007/978-0-387-09651-3.

[6] Sakai K. Dialysis membranes for blood purification. Front Med Biol Eng 2000;10:117–29. https://doi.org/10.1163/15685570052061973.

[7] Ahmed FE, Lalia BS, Hashaikeh R. A review on electrospinning for membrane fabrication: challenges and applications. Desalination 2015;356:15–30. https://doi.org/10.1016/j.desal.2014.09.033.

[8] Lalia BS, Kochkodan V, Hashaikeh R, Hilal N. A review on membrane fabrication: structure, properties and performance relationship. Desalination 2013;326:77–95. https://doi.org/10.1016/j.desal.2013.06.016.

[9] Yang Q, Chung TS, Santoso YE. Tailoring pore size and pore size distribution of kidney dialysis hollow fiber membranes via dual-bath coagulation approach. J Membr Sci 2007;290:153–63. https://doi.org/10.1016/j.memsci.2006.12.036.

[10] Krieter DH, Hackl A, Rodriguez A, Chenine L, Moragues HL, Lemke HD, et al. Protein-bound uraemic toxin removal in haemodialysis and post-dilution haemodiafiltration. Nephrol Dial Transplant 2010;25:212–8. https://doi.org/10.1093/ndt/gfp437.

[11] Mansur S, Othman MHD, Ismail AF, Sheikh Abdul Kadir SH, Kamal F, Goh PS, et al. Investigation on the effect of spinning conditions on the properties of hollow fiber membrane for hemodialysis application. J Appl Polym Sci 2016;133:1–10. https://doi.org/10.1002/app.43633.

[12] Deng L, Guo W, Ngo HH, Zhang J, Liang S, Xia S, et al. A comparison study on membrane fouling in a sponge-submerged membrane bioreactor and a conventional membrane bioreactor. Bioresour Technol 2014;165:69–74. https://doi.org/10.1016/j.biortech.2014.02.111.

[13] Košutić K, Kunst B. RO and NF membrane fouling and cleaning and pore size distribution variations. Desalination 2002;150:113–20. https://doi.org/10.1016/S0011-9164(02)00936-0.

[14] Sakai K. Determination of pore size and pore size distribution: 2. Dialysis membrane. J Membr Sci 1994;96:91–130. https://doi.org/10.1016/0376-7388(94)00126-X.

[15] Yoon S-H. Membrane bioreactor processes: principles and applications; 2015. https://doi.org/10.2175/106143013X13698672321940.

[16] Peinemann KV, Nunes SP. Membranes for the life sciences. Membr Life Sci 2010;1. https://doi.org/10.1002/9783527631360.

[17] Lawrence M, Jiang Y. Bio-aggregates based building materials. vol. 23; 2017. https://doi.org/10.1007/978-94-024-1031-0.

[18] Li D, Frey MW, Joo YL. Characterization of nanofibrous membranes with capillary flow porometry. J Membr Sci 2006;286:104–14. https://doi.org/10.1016/j.memsci.2006.09.020.

[19] Tylkowski B, Tsibranska I. Overview of main techniques used for membrane characterization. J Chem Technol Metall 2015;50:3–12.

[20] Bhattacharya S, Gubbins KE. Fast method for computing pore size distributions of model materials. Langmuir 2006;22:7726–31. https://doi.org/10.1021/la052651k.

[21] Khayet M, Matsuura T. Determination of surface and bulk pore sizes of flat-sheet and hollow-fiber membranes by atomic force microscopy, gas permeation and solute transport methods. Desalination 2003;158:57–64. https://doi.org/10.1016/S0011-9164(03)00433-8.

[22] Miyata T, Endo A, Ohmori T, Akiya T, Nakaiwa M. Evaluation of pore size distribution in boundary region of micropore and mesopore using gas adsorption method. J Colloid Interface Sci 2003;262:116–25. https://doi.org/10.1016/S0021-9797(02)00254-0.

[23] Zhao C, Zhou X, Yue Y. Determination of pore size and pore size distribution on the surface of hollow-fiber filtration membranes: a review of methods. Desalination 2000;129:107–23. https://doi.org/10.1016/S0011-9164(00)00054-0.

[24] Valtcheva IB, Kumbharkar SC, Kim JF, Bhole Y, Livingston AG. Beyond polyimide: crosslinked polybenzimidazole membranes for organic solvent nanofiltration (OSN) in harsh environments. J Membr Sci 2014;457:62–72. https://doi.org/10.1016/j.memsci.2013.12.069.

[25] Fukumoto T, Yoshioka T, Nagasawa H, Kanezashi M, Tsuru T. Development and gas permeation properties of microporous amorphous $TiO_2$-$ZrO_2$-organic composite membranes using chelating ligands. J Membr Sci 2014;461:96–105. https://doi.org/10.1016/j.memsci.2014.02.031.

[26] Feng CY, Khulbe KC, Matsuura T, Ismail AF. Recent progresses in polymeric hollow fiber membrane preparation, characterization and applications. Sep Purif Technol 2013;111:43–71. https://doi.org/10.1016/j.seppur.2013.03.017.

[27] Tung KL, Chang KS, Wu TT, Lin NJ, Lee KR, Lai JY. Recent advances in the characterization of membrane morphology. Curr Opin Chem Eng 2014;4:121–7. https://doi.org/10.1016/j.coche.2014.03.002.

[28] Chen H, Yuan L, Song W, Wu Z, Li D. Biocompatible polymer materials: role of protein-surface interactions. Prog Polym Sci 2008;33:1059–87. https://doi.org/10.1016/j.progpolymsci.2008.07.006.

[29] Williams DF. On the mechanisms of biocompatibility. Biomaterials 2008;29:2941–53. https://doi.org/10.1016/j.biomaterials.2008.04.023.

[30] Hoenich NA. Update on the biocompatibility of hemodialysis membranes. Hong Kong J Nephrol 2004;6:74–8. https://doi.org/10.1016/S1561-5413(09)60162-9.

[31] Stamatialis DF, Papenburg BJ, Gironés M, Saiful S, Bettahalli SNM, Schmitmeier S, et al. Medical applications of membranes: drug delivery, artificial organs and tissue engineering. J Membr Sci 2008;308:1–34. https://doi.org/10.1016/j.memsci.2007.09.059.

[32] Abe T, Kato K, Fujioka T, Akizawa T. The blood compatibilies of blood purification membranes and other materials developed in Japan. Int J Biomater 2011; https://doi.org/10.1155/2011/375390.

[33] Kokubo K, Kurihara Y, Kobayashi K, Tsukao H, Kobayashi H. Evaluation of the biocompatibility of dialysis membranes. Blood Purif 2015;40:293–7. https://doi.org/10.1159/000441576.

[34] Lazarus JM, Owen WF. Role of bioincompatibility in dialysis morbidity and mortality. Am J Kidney Dis 1994;24:1019–32. https://doi.org/10.1016/S0272-6386(12)81077-8.

[35] Hakim RM. Clinical implications of hemodialysis membrane biocompatibility. Kidney Int 1993;44:484–94.

[36] Kim J. Protein adsorption on polymer particles. J Biomed Mater Res 2002;21:4373–81. https://doi.org/10.1002/jbm.820210202.

[37] Pieroni L, Levi Mortera S, Greco V, Sirolli V, Ronci M, Felaco P, et al. Biocompatibility assessment of haemodialysis membrane materials by proteomic investigations. Mol BioSyst 2015;11:1633–43. https://doi.org/10.1039/C5MB00058K.

[38] Sun S, Yue Y, Huang X, Meng D. Protein adsorption on blood-contact membranes. J Membr Sci 2003;222:3–18. https://doi.org/10.1016/S0376-7388(03)00313-2.

[39] Weber N, Wendel HP, Ziemer G. Hemocompatibility of heparin-coated surfaces and the role of selective plasma protein adsorption. Biomaterials 2002;23:429–39. https://doi.org/10.1016/S0142-9612(01)00122-3.

[40] Vogler EA, Siedlecki CA. Contact activation of blood-plasma coagulation. Biomaterials 2009;30:1857–69. https://doi.org/10.1016/j.biomaterials.2008.12.041.

[41] Fischer KG. Essentials of anticoagulation in hemodialysis. Hemodial Int 2007;11:178–89. https://doi.org/10.1111/j.1542-4758.2007.00166.x.

[42] Gorbet MB, Sefton MV. Biomaterial-associated thrombosis: roles of coagulation factors, complement, platelets and leukocytes. Biomaterials 2004;25:5681–703. https://doi.org/10.1016/j.biomaterials.2004.01.023.

[43] Azar AT. Modeling and control of dialysis systems. vol. 53. Berlin Heidelberg: Springer-Verlag; 2013. https://doi.org/10.1017/CBO9781107415324.004.

[44] Cheung AK. Biocompatibility of hemodialysis membranes. J Am Soc Nephrol 1990;I:150–61.

[45] Markiewski MM, Nilsson B, Ekdahl KN, Mollnes TE, Lambris JD. Complement and coagulation: strangers or partners in crime? Trends Immunol 2007;28:184–92. https://doi.org/10.1016/j.it.2007.02.006.

[46] Nilsson B, Ekdahl KN, Mollnes TE, Lambris JD. The role of complement in biomaterial-induced inflammation. Mol Immunol 2007;44:82–94. https://doi.org/10.1016/j.molimm.2006.06.020.

[47] Kourtzelis I, Markiewski MM, Doumas M, Rafail S, Kambas K, Mitroulis I, et al. Complement anaphylatoxin C5a contributes to hemodialysis-associated thrombosis. Blood 2010;116:631–9. https://doi.org/10.1182/blood-2010-01-264051.

[48] Koh LB, Rodriguez I, Venkatraman SS. The effect of topography of polymer surfaces on platelet adhesion. Biomaterials 2010;31:1533–45. https://doi.org/10.1016/j.biomaterials.2009.11.022.

[49] Muir KB, Packer CD. Thrombocytopenia in the setting of hemodialysis using biocompatible membranes. Case Rep Med 2012;2012:1–4. https://doi.org/10.1155/2012/358024.

[50] Sefton MV, Gemmell CH, Gorbet MB. What really is blood compatibility? J Biomater Sci Polym Ed 2000;11:1165–82. https://doi.org/10.1163/156856200744255.

[51] Gawaz MP, Mujais SK, Schmidt B, Blumenstein M, Gurland HJ. Platelet-leukocyte aggregates during hemodialysis: effect of membrane type. Artif Organs 1999;23:29–36. https://doi.org/10.1046/j.1525-1594.1999.06289.x.

[52] Morena M, Delbosc S, Dupuy A-M, Canaud B, Cristol J-P. Overproduction of reactive oxygen species in end-stage renal disease patients: a potential component of hemodialysis-associated inflammation. Hemodial Int 2005;9:37–46. https://doi.org/10.1111/j.1492-7535.2005.01116.x.

[53] Gautham A, Muhammed MJ, Manavalan M, Najeeb MA. Hemodialysis membranes: past, present and future trends. Int Res J Pharm 2013;4:16–9. https://doi.org/10.7897/2230-8407.04505.

[54] Clark WR, Gao D. Properties of membranes used for hemodialysis therapy. Semin Dial 2002;15:191–5. https://doi.org/10.1046/j.1525-139X.2002.00019.x.

[55] Chanard J, Lavaud S, Randoux C, Rieu P. New insights in dialysis membrane biocompatibility: relevance of adsorption properties and heparin binding. Nephrol Dial Transplant 2003;18:252–7. https://doi.org/10.1093/ndt/18.2.252.

[56] Gao A, Liu F, Xue L. Preparation and evaluation of heparin-immobilized poly (lactic acid) (PLA) membrane for hemodialysis. J Membr Sci 2014;452:390–9. https://doi.org/10.1016/j.memsci.2013.10.016.

[57] Hoenich N, Katopodis K. Clinical characterization of a new polymeric membrane for use in renal replacement therapy. Biomaterials 2002;23:3853–8.

[58] Moachon N, Boullanger C, Fraud S, Vial E, Thomas M, Quash G. Influence of the charge of low molecular weight proteins on their efficacy of filtration and/or adsorption on dialysis membranes with different intrinsic properties. Biomaterials 2002;23:651–8. https://doi.org/10.1016/S0142-9612(01)00151-X.

[59] Su B, Sun S, Zhao C. Polyethersulfone hollow fiber membranes for hemodialysis, Croatia: InTech; 2011.

[60] Aucella F, Vigilante M, Gesuete A. Review: the effect of polymethylmethacrylate dialysis membranes on uraemic pruritus. NDT Plus 2010;3:10–3. https://doi.org/10.1093/ndtplus/sfq031.

[61] Liu T-Y, Lin W-C, Huang L-Y, Chen S-Y, Yang M-C. Hemocompatibility and anaphylatoxin formation of protein-immobilizing polyacrylonitrile hemodialysis membrane. Biomaterials 2005;26:1437–44. https://doi.org/10.1016/j.biomaterials.2004.04.039.

[62] Barzin J, Madaeni SS, Mirzadeh H, Mehrabzadeh M. Effect of preparation conditions on morphology and performance of hemodialysis membranes prepared from polyether sulphone and polyvinylpyrrolidone. Iran Polym J 2005;14:353–60.

[63] Bowry SK, Gatti E, Vienken J. Contribution of polysulfone membranes to the success of convective dialysis therapies. In: High-performance membrane dialyzers, vol. 173; 2011. p. 110–8. https://doi.org/10.1002/9783805598132.ch14.

[64] Judd S, Judd C. The MBR book (second edition): principles and applications of membrane bioreactors for water and wastewater treatment; 2011. https://doi.org/10.1016/B978-0-08-096682-3.10007-1.

[65] Sastri VR. Plastics in medical devices; 2010. https://doi.org/10.1016/B978-0-8155-2027-6.10009-1.

[66] Jasso-Gastinel CF. 8-Gradients in homopolymers, blends, and copolymers. Modif Polym Prop 2017;185–210. https://doi.org/10.1016/B978-0-323-44353-1.00008-7.

[67] Jasso-Gastinel CF, Kenny JM. Modification of polymer properties. New York: Elsevier; 2016.

[68] Yu X, Liu F, Wang L, Xiong Z, Wang Y. Robust poly(lactic acid) membranes improved by polysulfone-g-poly(lactic acid) copolymers for hemodialysis. RSC Adv 2015;5:78306–14. https://doi.org/10.1039/C5RA15816H.

[69] Ran F, Nie S, Zhao W, Li J, Su B, Sun S, et al. Acta biomaterialia biocompatibility of modified polyethersulfone membranes by blending an amphiphilic triblock co-polymer of poly (vinyl pyrrolidone)-b-poly (methyl methacrylate)-b-poly (vinyl pyrrolidone). Acta Biomater 2011;7:3370–81. https://doi.org/10.1016/j.actbio.2011.05.026.

[70] Grote JJ. Biocompatibility of a polyether urethane, polypropylene oxide, and a polyether polyester copolymer. A qualitative and quantitative study of three alloplastic tympanic membrane materials in the rat middle ear. J Biomed Mater Res 1990;24:489–515.

[71] Wang H, Yu T, Zhao C, Du Q. Improvement of hydrophilicity and blood compatibility on polyethersulfone membrane by adding polyvinylpyrrolidone. Fibers Polym 2009;10:1–5.

[72] Su BH, Fu P, Li Q, Tao Y, Li Z, Zao HS, et al. Evaluation of polyethersulfone highflux hemodialysis membrane in vitro and in vivo. J Mater Sci Mater Med 2008;19:745–51. https://doi.org/10.1007/s10856-007-3006-9.

[73] Wang YQ, Wang T, Su YL, Peng FB, Wu H, Jiang ZY. Protein-adsorption-resistance and permeation property of polyethersulfone and soybean phosphatidylcholine blend ultrafiltration membranes. J Membr Sci 2006;270:108–14. https://doi.org/10.1016/j.memsci.2005.06.044.

[74] Barzin J, Feng C, Khulbe KC, Matsuura T, Madaeni SS, Mirzadeh H. Characterization of polyethersulfone hemodialysis membrane by ultrafiltration and atomic force microscopy. J Membr Sci 2004;237:77–85. https://doi.org/10.1016/j.memsci.2004.02.029.

[75] Li J, Nie S, Wang L, Sun S, Ran F, Zhao C. One-pot synthesized poly(vinyl pyrrolidone-co-methyl methacrylate-co-acrylic acid) blended with poly(ether sulfone) to prepare blood-compatible membranes. J Appl Polym Sci 2013;130:4284–98. https://doi.org/10.1002/app.39463.

[76] Salimi E, Ghaee A, Ismail AF. Improving blood compatibility of polyethersulfone hollow fiber membranes via blending with sulfonated polyether ether ketone. Macromol Mater Eng 2016;301:1084–95. https://doi.org/10.1002/mame.201600108.

[77] Yin Z, Cheng C, Qin H, Nie C, He C, Zhao C. Hemocompatible polyethersulfone/polyurethane composite membrane for high-performance antifouling and antithrombotic dialyzer. J Biomed Mater Res B: Appl Biomater 2014;103:97–105. https://doi.org/10.1002/jbm.b.33177.

[78] Zailani MZ, Ismail AF, Kadir SHSA, Othman MHD, Goh PS, Hasbullah H, et al. Hemocompatiblilty evaluation polyethersulfone membranes of blend. J Biomed Mater Res A 2017;105:1510–20. https://doi.org/10.1002/jbm.a.35986.

[79] Halkier T. Mechanisms in blood coagulation, fibrinolysis and the complement system. Cambridge: Cambridge University Press; 2008.

[80] Li L, Cheng C, Xiang T, Tang M, Zhao W, Sun S, et al. Modification of polyethersulfone hemodialysis membrane by blending citric acid grafted polyurethane and its anticoagulant activity. J Membr Sci 2012;405–406:261–74. https://doi.org/10.1016/j.memsci.2012.03.015.

[81] Ma L, Su B, Cheng C, Yin Z, Qin H, Zhao J, et al. Toward highly blood compatible hemodialysis membranes via blending with heparin-mimicking polyurethane: study in vitro and in vivo. J Membr Sci 2014;470:90–101. https://doi.org/10.1016/j.memsci.2014.07.030.

[82] Davankov VA, Pavlova LA, Tsyurupa MP, Tur DR. Novel polymeric solid-phase extraction material for complex biological matrices. Portable and disposable artificial kidney. J Chromatogr B: Biomed Appl 1997;689:117–22. https://doi.org/10.1016/S0378-4347(96)00307-6.

[83] Davenport A, Gura V, Ronco C, Beizai M, Ezon C, Rambod E. A wearable haemodialysis device for patients with end-stage renal failure: a pilot study. Lancet 2007;370:2005–10. https://doi.org/10.1016/S0140-6736(07)61864-9.

[84] Albrecht W, Weigel T, Groth T, Hilke R, Paul D. Formation of porous bilayer hollow fibre membranes. Macromol Symp 2002;188:131–42. https://doi.org/10.1002/1521-3900(200211)188:1<131::AID-MASY131>3.0.CO;2-8.

[85] Tijink MSL, Wester M, Sun J, Saris A, Bolhuis-Versteeg LAM, Saiful S, et al. A novel approach for blood purification: mixed-matrix membranes combining diffusion and adsorption in one step. Acta Biomater 2012;8:2279–87. https://doi.org/10.1016/j.actbio.2012.03.008.

[86] Tijink MSL, Wester M, Glorieux G, Gerritsen KGF, Sun J, Swart PC, et al. Mixed matrix hollow fiber membranes for removal of protein-bound toxins from human plasma. Biomaterials 2013;34:7819–28. https://doi.org/10.1016/j.biomaterials.2013.07.008.

[87] Sun J, Wu L. Polyether sulfone/hydroxyapatite mixed matrix membranes for protein purification. Appl Surf Sci 2014;308:155–60. https://doi.org/10.1016/j.apsusc.2014.04.123.

[88] Wernert V, Scha O, Ghobarkar H, Denoyel R. Adsorption properties of zeolites for artificial kidney applications. Micropor Mesopor Mater 2005;83:101–13. https://doi.org/10.1016/j.micromeso.2005.03.018.

[89] Lu L, Yeow JTW. An adsorption study of indoxyl sulfate by zeolites and polyethersulfone–zeolite composite membranes. Mater Des 2017;120:328–35. https://doi.org/10.1016/j.matdes.2017.01.094.

[90] Yu S, Zuo X, Bao R, Xu X, Wang J, Xu J. Effect of SiO2 nanoparticle addition on the characteristics of a new organic-inorganic hybrid membrane. Polymer (Guildf) 2009;50:553–9. https://doi.org/10.1016/j.polymer.2008.11.012.

[91] Souza VC, Quadri MGN. Organic-inorganic hybrid membranes in separation processes: a 10-year review. Braz J Chem Eng 2013;30:683–700. https://doi.org/10.1590/S0104-66322013000400001.

[92] Cao X, Ma J, Shi X, Ren Z. Effect of $TiO_2$ nanoparticle size on the performance of PVDF membrane. Appl Surf Sci 2006;253:2003–10. https://doi.org/10.1016/j.apsusc.2006.03.090.

[93] Amiri A, Chew BT, Razmjou A. In vitro and in vivo study of hazardous effects of Ag nanoparticles and Arginine-treated multi walled carbon nanotubes on blood cells: application in hemodialysis membranes: application in hemodialysis membranes. J Biomed Mater Res A 2015;103:1–31. https://doi.org/10.1002/jbm.a.35425.

[94] Irfan M, Idris A, Yusof NM, Khairuddin NFM, Akhmal H. Surface modification and performance enhancement of nano-hybrid f-MWCNT/PVP90/PES hemodialysis membranes. J Membr Sci 2014;467:73–84. https://doi.org/10.1016/j.memsci.2014.05.001.

[95] Nie C, Ma L, Xia Y, He C, Deng J, Wang L, et al. Novel heparin-mimicking polymer brush grafted carbon nanotube/PES composite membranes for safe and efficient blood purification. J Membr Sci 2015;475:455–68. https://doi.org/10.1016/j.memsci.2014.11.005.

[96] Abidin MNZ, Goh PS, Ismail AF, Othman MHD, Hasbullah H, Said N, et al. Antifouling polyethersulfone hemodialysis membranes incorporated with poly (citric acid) polymerized multi-walled carbon nanotubes. Mater Sci Eng C 2016;68:540–50. https://doi.org/10.1016/j.msec.2016.06.039.

[97] Abidin MNZ, Goh PS, Ismail AF, Othman MHD, Hasbullah H, Said N, et al. Development of biocompatible and safe polyethersulfone hemodialysis membrane incorporated with functionalized multi-walled carbon nanotubes. Mater Sci Eng C 2017;77:572–82. https://doi.org/10.1016/j.msec.2017.03.273.

[98] Said N, Hasbullah H, Ismail AF, Othman MHD, Goh PS, Zainol Abidin MN, et al. Enhanced hydrophilic polysulfone hollow fiber membranes with addition of iron oxide nanoparticles. Polym Int 2017;66:1424–9. https://doi.org/10.1002/pi.5401.

[99] Bargnoux AS, Cristol JP, Jaussent I, Chalabi L, Bories P, Dion JJ, et al. Vitamin E-coated polysulfone membrane improved red blood cell antioxidant status in hemodialysis patients. J Nephrol 2013;26:556–63. https://doi.org/10.5301/jn.5000195.

[100] Mahlicli FY, Altinkaya SA. Immobilization of alpha lipoic acid onto polysulfone membranes to suppress hemodialysis induced oxidative stress. J Membr Sci 2014;449:27–37. https://doi.org/10.1016/j.memsci.2013.07.061.

[101] Zhao C, Xue J, Ran F, Sun S. Modification of polyethersulfone membranes-a review of methods. Prog Mater Sci 2013;58:76–150. https://doi.org/10.1016/j.pmatsci.2012.07.002.

[102] Yu X, Shen L, Zhu Y, Li X, Yang Y, Wang X, et al. High performance thin-film nanofibrous composite hemodialysis membranes with efficient middle-molecule uremic toxin removal. J Membr Sci 2017;523:173–84. https://doi.org/10.1016/j.memsci.2016.09.057.

[103] Guillen GR, Pan Y, Li M, Hoek EMV. Preparation and characterization of membranes formed by nonsolvent induced phase separation: a review. Ind Eng Chem Res 2011;50:3798–817. https://doi.org/10.1021/ie101928r.

[104] Zhang Q, Lu X, Liu J, Zhao L. Preparation and preliminary dialysis performance research of polyvinylidene fluoride hollow fiber membranes. Membranes (Basel, Switz) 2015;5:120–35. https://doi.org/10.3390/membranes5010120.

# Forward Osmosis for Desalination Application

*Nur Zhatul Shima Yahaya\*, Mohamad Zahir Mohd Pauzi\*, Nizar Mu'ammar Mahpoz\*, Mukhlis A. Rahman\*, Khairul Hamimah Abas[†], Ahmad Fauzi Ismail\*, Mohd Hafiz Dzarfan Othman\*, Juhana Jaafar\**

**\*Advanced Membrane Technology Research Centre (AMTEC), Faculty of Chemical and Energy Engineering, Universiti Teknologi Malaysia, Skudai, Malaysia[†]Faculty of Electrical Engineering, Universiti Teknologi Malaysia, Skudai, Malaysia**

## 10.1 DEFINITION AND CONCEPT

Forward osmosis (FO) is an emerging osmotically driven membrane process (ODMPs) for water separation and purification. To date, it has been regarded as a promising separation process due to its low energy consumption. The concept of FO itself is solely based on the natural osmosis process in which water will flow spontaneously from a dilute region (feed) to a highly concentrated region (draw). This process is trying to achieve a balance concentration in both regions. The osmotic pressure is relatively higher in the draw compared to the feed. Therefore, the movement of water flow is conceptually being induced by the difference in the osmotic pressure between these two regions [1]. Also, a highly selective membrane will be placed in between the feed and the draw solution to complete the separation process as it only allows water to pass through it and retaining the unwanted solutes.

Seawater desalination is one of the membrane applications that had increasingly gained attention nowadays. This is because conversion of abundant seawater into freshwater will provide water sustainability in the long term. Reverse osmosis (RO) which currently being employed in this application process faced an obstacle to consuming too much energy as RO operated based on a pressure-driven mechanism. In this process, water from a highly concentrated solution is forced to move to a diluted solution across the membrane with the assistance of hydraulic pressure. When the solute is too concentrated, for example the seawater, the amount of pressure applied needs to be higher. Hence, as an alternative to this process, FO is introduced as the problem solver because its process mechanism is the opposite of RO and only utilizes the natural-build osmotic pressure. Also, it is reported that FO is less susceptible to membrane fouling and reversible by membrane backwashing. Thus, FO is regarded as a greener and economically efficient alternative for water separation application. A schematic diagram of FO and RO process is shown in Fig. 10.1. The difference in the water flow leads to different products, pure water and dilute draw solution in RO and FO, respectively.

For the production of potable water from FO process especially for desalination, the pure water should be recovered from the dilutive draw solution. Typically, there are several methods available for this recovery including pressure-driven membrane separation (reverse osmosis/nanofiltration), membrane distillation and standard distillation. However, it needs to be noted that in other applications such as concentration of juice or dilution of fertilizer where the desired end product is not pure, the recovery step is unnecessary [3]. The following Fig. 10.2 illustrates the full process of FO desalination. All steps shown are contributed to the majority of energy involved in the FO itself.
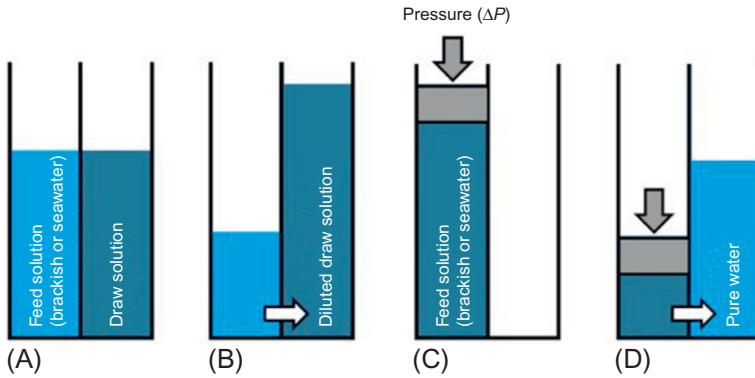
FIG. 10.1 Comparison of flow of water in FO (A and B) and RO (C and D). *Data from Qasim M, Darwish NA, Sarp S, Hilal N. Water desalination by forward (direct) osmosisphenomenon: a comprehensive review. Desalination 2015;374:47–69.*
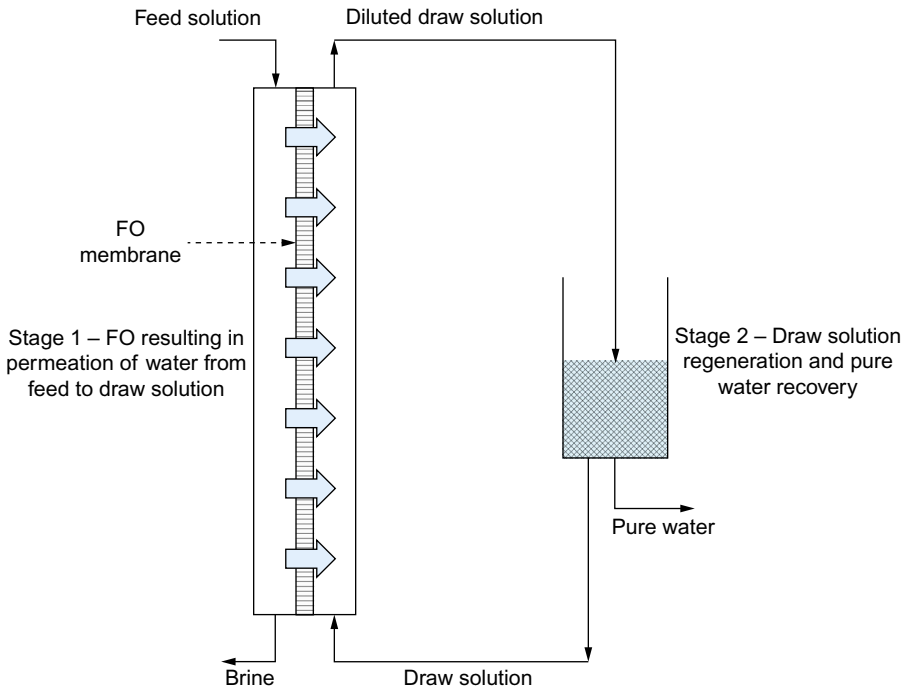


FIG. 10.2 Schematic diagram of fresh water production by FO desalination. *Data from Qasim M, Darwish NA, Sarp S, Hilal N. Water desalination by forward (direct) osmosisphenomenon: a comprehensive review. Desalination 2015;374:47–69.*

## 10.2  MOST RECOGNIZED FO MEMBRANE

Among the recognized FO membrane, thin-film composite (TFC) appear to be the most fabricated and studied so far. It was first developed in the 1980s and currently is receiving interest to be used as desalination membranes because it possesses high intrinsic water permeability and great stability regardless of any pH values [4]. Although the name is emphasized as a thin-film, this membrane configurations are not only restricted to a flat sheet figure but also can be found in the shape of a hollow fiber [5]. Structure of this membrane consists of thin polyamide (PA) layer that incorporated on a porous support [6]. This thin layer is usually fabricated using interfacial polymerization (IP) method and act as the active layer that controls the rejection and permeation behavior. Another concerning factor of this membrane fabrication is the selection of the membrane support. This step is crucial as it determines the membrane mechanical strength when operated under continuous vibration and backwashing process. Typically, inorganic, nanofiber, and organic-inorganic materials will be incorporated with polymeric material to form membrane supports [7,8]. Common examples of polymer used for this applications are polysulfone (PSF), polyethersulfone (PES), polyacrylonitrile (PAN), and polyetherimide (PEI) [5,6,9,10]. These unique composite structures which combined two or more different materials enable the membrane to optimize FO performance separately. Typical structure of these supports can be seen in Fig. 10.3. In addition, along with the development of membrane technology, there are several modifications made on the TFC membrane to further improve its properties as mentioned by Zirehpour et al. [11]. Current approach in the modifications mainly focus on its thin-film and substrate structures which results in development of the new kinds of TFC membrane called thin-film nanocomposites (TFN) and porous matrix membrane (PMM). TFN was fabricated when the selective layer (thin-film) was incorporated with nanoparticles such as zeolite and silica [4,12–14], as shown in Fig. 10.4. Meanwhile, PMM was developed when additives or pore filler such as hybrid inorganic-organic compound namely metal-organic framework (MOF) was added into the substrate dope solution to improve the membrane structure and performances [10,15]. Both membranes developed have their own characteristics that suited with filtration of different kind of solutes using FO process.

## 10.3  FO MEMBRANE DESALINATION PERFORMANCE EVALUATIONS

Although there are variations in the FO membrane developed, all of them undergo the same performance evaluations. Water flux and reverse solute flux are the most common test done on the FO membrane. Following
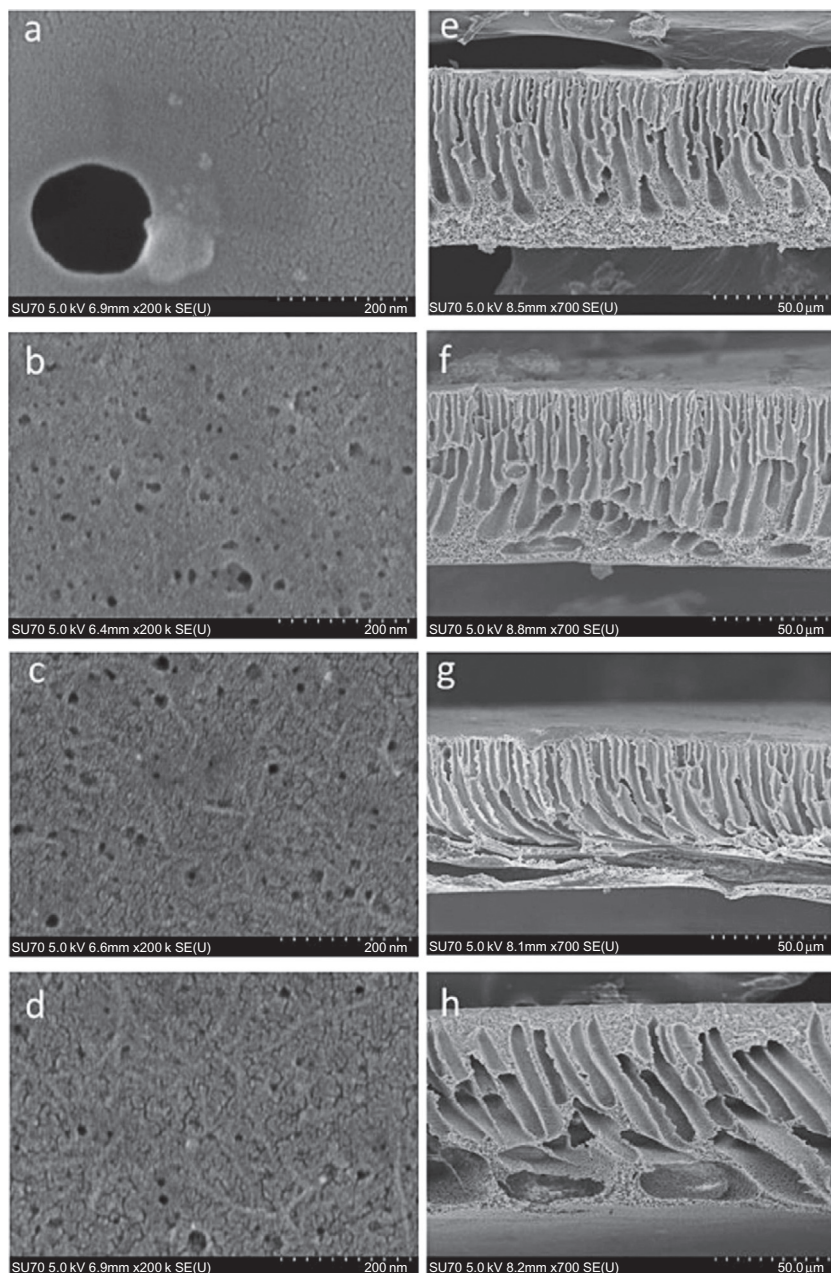
**FIG. 10.3**    FESEM images of the top surface *(left)* and the cross section *(right)* of (A and E) TFC substrate *(control)*, (B and F) substrate 0.33 imogolite nanotubes (INTs), (C and G) substrate 0.66 INTs and (D and H) substrate 1.0 INTs. *Data from Pan Y, Zhao Q, Gu L, Wu Q. Thin film nanocomposite membranes based on imologitenanotubes blended substrates for forward osmosis desalination. Desalination 2017;421(April):160–8.*
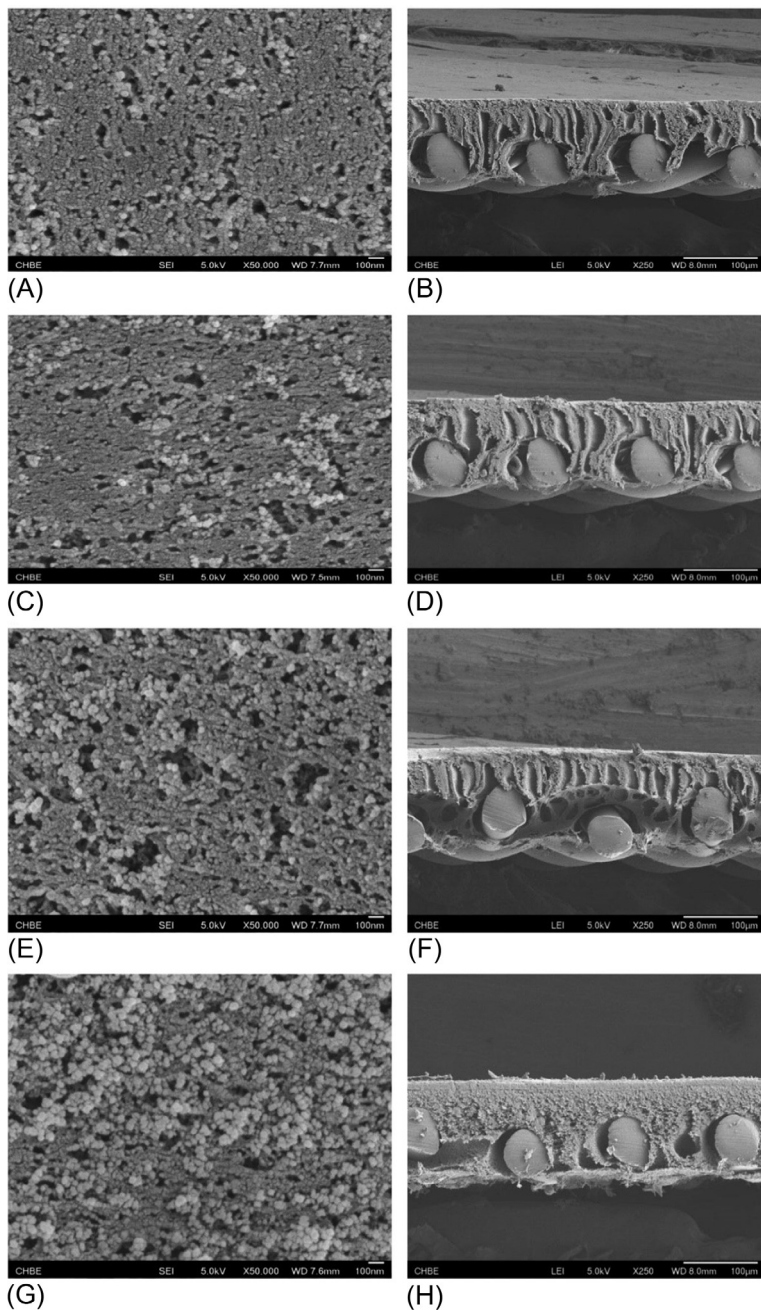
**FIG. 10.4** FESEM images of layered silica-polysulfone mixed matrix membrane (A–H) with increasing loading ratio of silica but decreasing loading ratio of PSf. *Data from Liu X, Yong H. Fabrication of layered silica–polysulfone mixed matrix substrate membrane for enhancing performance of thin-film composite forward osmosis membrane.J Membr Sci 2015;481:148–63.*

the osmosis concept, the water flux is the permeate water that passes through the membrane from a low concentration solution (feed) to a high concentration solution (draw). Meanwhile, reverse solute flux is defined as the permeate salt that transfers from the draw to the feed. Both performances are mainly determined using a laboratory-scale cross-flow filtration unit. Regular equations used to calculate the water flux and reverse solute flux in the FO process are shown as the following:

$$J_w = \frac{\Delta m / \rho}{A_m \times \Delta t} \tag{10.1}$$

$$J_s = \frac{\Delta(C_t \cdot V_t)}{\Delta t \times A_m} \tag{10.2}$$

in which $J_w$ is the water flux, $J_s$ is the reverse solute flux, $\Delta m$ is the weight change of feed solution, $\rho$ is the density of feed solution, $A_m$ is the effective area of the membrane and $\Delta t$ is the measuring time. Also, $C_t$ and $V_t$ are the salt concentration and volume of feed solution mainly based on the time interval [16,17]. Conductivity measurement is used in the determination of the salt concentration.

Another performance evaluation for the FO membrane is the solute rejection. Solute rejection ($R_s$) determined how much solute can be retained in the draw solution instead of passing through the membrane layer. Usually, this test is conducted using the cross-flow reverse osmosis (RO) filtration setup to get the accurate results. Coefficients for water permeability ($A$) and water permeability ($B$) also being calculated based on the RO test. As an important parameter that indicates FO membrane selectivity, small solute permeability/water permeability ($B/A$) ratio is desired and describe a better selectivity in the FO system. Besides that, $J_s/J_w$ ratio which is recognized as the specific solute flux also indicates the membrane selectivity and productivity. The lower the specific solute flux ratio, the higher the productivity of the membrane performances [11,18–20]. The following equations demonstrate how the $R_s$, $A$ and $B$ coefficients are being determined:

$$R_s = \frac{c_f - c_p}{c_f} \times 100\% \tag{10.3}$$

$$J_v = \frac{\Delta V}{\Delta t \times A_m} \tag{10.4}$$

$$A = \frac{J_v}{\Delta P} \tag{10.5}$$

$$\frac{1 - R_s}{R_s} = \frac{B}{A(\Delta P - \Delta \pi)} \tag{10.6}$$

$C_f$ is the concentration of salt in the feed and $C_p$ is the concentration of salt in the permeate solution. Meanwhile, $J_v$ is the pure water flux, $\Delta V$ is the permeate volume, $\Delta t$ is the time needed to obtain $\Delta V$, $\Delta P$ is the operating pressure and $\Delta \pi$ is the osmotic pressure difference across the membrane [16,21].

Even with the most recent fabricated FO membranes, common problems related to FO process still could not be solved completely. In an experimental study done by Fang et al. in which the original FO membrane was accompanied with double skin (RO-like layer and NF-like layer) still could not prevent the reverse solute flux from happening during the FO process although it did improve the water flux performance [22]. Besides that, some studies indeed increased its water flux performance to a better level but at the same time, the reverse solute flux also increased rapidly [5,11,15]. Therefore, it remains a challenge to fabricate the FO membrane with incredible water flux and high salt rejection as well as none occurrence of reverse solute flux. The following table summarized the water flux, reverse solute flux and salt rejection of the previously developed FO membrane.

## 10.4 FACTORS THAT AFFECTING FO PERFORMANCE

### 10.4.1 Internal Concentration Polarization

Internal concentration polarization (ICP) is one of the factors that hinder the performance of FO membrane. It occurs within the membrane support layer that reduced the driving force (osmotic pressure) which substantially lowering the water flux and increase the reverse solute flux. ICP can cause water flux reduction as high as 80% which can significantly contribute to the worst membrane performance [23]. Besides that, it is much difficult to alleviate ICP rather than ECP as ECP can be solved by increasing the flow velocity or introducing turbulence flow due to support layer being relatively thicker [2]. With no specific solution to completely remove the ICP, it can be concluded that the effect from ICP is much severe. Also, there are two types of ICP, namely concentrative and dilutive ICP which depends on the forward osmosis mode orientation.

Concentrative ICP most likely happened in the active layer facing draw solution (AL-facing DS) configuration which is also known as the PRO mode. ICP affecting the osmotic pressure difference between draw and feed solution by changing the concentration of solution inside support layer. In concentrative ICP, concentration of feed inside the support layer is relatively higher than the bulk feed solution, thus reducing osmotic pressure difference to draw solution. Similar process occurs for dilutive ICP in which the difference in osmotic pressure is caused by the diluted

| Year | Type of membrane | Configuration | Materials | FO performance | | | Feed solution, FS | Draw solution, DS | Ref |
|------|------------------|---------------|-----------|------|------|------|-------------------|-------------------|-----|
| | | | | Mode | $J_w$ (L/m$^2$ h) | $J_s$ (g/m$^2$ h) | | | |
| 2017 | TFN | Flat sheet | PES substrate, MOF incorporated polyamide layer (silver, 1,3,5-benzene tricarboxylic acid) | AL-FS | 46.0 | $5.84 \times 10^3$ | Deionized water | 2 M NaCl | [11] |
| | | | | AL-DS | 82.0 | N/A | | | |
| 2016 | Mixed matrix membrane | Flat sheet | Cellulosic acetate/ triacetate, CTA (polymer), copper-based MOF (Cu-BTC) | AL-FS | 45.0 | $6.60 \times 10^3$ | Deionized water | 2 M NaCl | [15] |
| | | | | AL-DS | 63.0 | N/A | | | |
| 2016 | TFC | Hollow fiber | Polyetherimide (PEI) substrate, LiCl, aquaporin polyamide layer | AL-FS | 49.1 | 5.0 | Deionized water | 1 M NaCl | [6] |
| | | | | AL-DS | 90.0 | 10.0 | | | |
| 2015 | Thin-film porous matrix membrane | Flat sheet | Polyacrylonitrile (PAN) substrate, MOF, thin selective layer (PAH & PSS) | AL-FS | 43.0 | N/A | Deionized water | 0.5 MgCl$_2$ | [10] |
| | | | | AL-DS | 110 | N/A | | | |
| 2015 | Thin-film matrix membrane | Flat sheet | Polysulfone (PSf) substrate, nanosized silica, polyamide layer | AL-FS | 31.0 | 7.4 | Deionized water | 1 M NaCl | [7] |
| | | | | AL-DS | 60.5 | 16.0 | | | |
| 2013 | TFN | Flat sheet | Polysulfone (PSf) substrate, polyvinyl pyrrolidone (PVP), functionalized multiwall carbon nanotubes (F-MWCNT) | AL-FS | 35.0 | 2.5 | 10 mM NaCl | 2 M NaCl | [13] |
| | | | | AL-DS | 75.0 | 4.8 | | | |

draw solution inside support layer. Thus, the development of FO membrane with reduce thickness of support layer and low structural parameter is necessary to overcome this ICP obstacle. Also, optimizing selection of draw solutions is equally important to mitigate the detrimental effect of ICP.

## 10.4.2 External Concentration Polarization

Concentration polarization (CP) occurs due to the equality effect that occurs between flux, rejection and diffusion, and the event lowers the flux and membrane selectivity. Usually, ICP occurs in the process of FO but for external concentration polarization (ECP), the condition can be found in the dense surface of active layer [1]. ECP also have the mode of concentrative ECP and dilutive ECP based on where feed solution is channeled out. When feed solution is faced on the active layer surface, the effect of concentrative ECP can be seen as the solute started to build up on the surface of the active layer. Simultaneously, when draw solution is placed on the permeate side of the membrane, the concentrated draw is diluted by permeate that passes through the membrane barrier. This event is termed as dilutive ECP. Both dilutive and concentrative ECP can lead to the reduction of effective osmotic pressure. Theoretically, the adverse effect of ECP can be reduced by increasing the flow velocity to create high turbulence effect at the membrane surface or by manipulating the water flux [23]. However, the ability to lessen the effect of ECP using water flux manipulation might be limited due to low water flux produced in FO.

## 10.4.3 Structural Parameter

In the development of most FO membranes, the structural parameter (S) is one of the critical factors that can affect FO membrane performance. As stated by Lee et al. in their research, this value is closely related to the membrane intrinsic properties such as pore structure, membrane wettability, membrane thickness and tortuosity of the FO substrate [10]. Generally, the relation of these properties is shown as the following.

$$S = \frac{\text{thickness} \times \text{tortuosity}}{\text{porosity}} \tag{10.7}$$

Based on this equation, it can be concluded that when the porosity of a membrane is smaller, the S value will be bigger and results to a more severe ICP which in return lowering the membrane performance. Hence, through this simple relation, determination of S value would indicate the FO membrane structure contribution quantitatively on the ICP [15,24].

Also, the existing approach had adopted a fitted parameter mass transfer model to calculate the $S$ value.

There are two different equations for available FO modes which are active layer facing feed solution (AL-FS) and active layer facing draw solution (AL-DS/PRO) [21,25]. The first equation demonstrates the $S$ parameter for AL-FS mode and the later one is the AL-DS mode.

$$S = \frac{D}{J_w} \ln \frac{B + A\pi_D}{B + J_w + A\pi_F} \tag{10.8}$$

$$S = \frac{D}{J_w} \ln \frac{B - J_w + A\pi_D}{B + A\pi_F} \tag{10.9}$$

In these models, $D$ is the solute diffusion coefficient, $\pi_D$ and $\pi_F$ are osmotic pressures of draw solution and feed solution, $J_w$ is the water flux while $A$ and $B$ are water permeability and solute permeability coefficients. Measurements of $A$ and $B$ which related to the active layer parameters are obtained from the reverse osmosis (RO) mode experiments which apply a trans-membrane hydraulic pressure. It is then followed by the osmotic driving force experiment to determine the support layer structural parameter [24]. Although these models had been used extensively, some questions had been raised for its accuracy in determining the S value because parameters A and B are slightly different under pressure in RO and FO mode. Tiraferri et al. also stated that in RO mode, solute concentration in contact with membrane selective layer is much lower when compared to the FO [24,25]. Inconsistency with these values raises the need to build another alternative equations to calculate S value with only a single experiment (FO mode).

One of the alternative models had been developed by Bui et al. to calculate the $S$ value accurately because it can describe the flux behavior of the membrane used [26]. Their proposed mathematical model includes the ECP effects which considered in-series resistances for solute transport based on the intrinsic properties, boundary layers at membrane surfaces and also within the support layer. By employing this model, Li et al. derived their structural parameter calculations as the following [6]:

$$S = \frac{D_D}{J_v} \ln \frac{BA\pi_{D,b}}{J_v + (B + A\pi_{F,b}) \exp\left(\frac{J_v}{k_F}\right)} - \frac{D_D}{k_D} \tag{10.10}$$

where $D_D$ is the solute diffusivity in the draw solution, $A$ is intrinsic water permeability coefficient, $\pi$ is the osmotic pressure while $k_D$ and $k_F$ are the mass transfer coefficients in the draw and feed, respectively. The following relation demonstrates how the mass transfer coefficient, $k$ was obtained.

$$k = \frac{S_h \cdot D_D}{d_h} \tag{10.11}$$

where $d_h$ is the hydraulic diameter and $S_h$ is the Sherwood number. If the fluids in both channels have laminar flow, $S_h$ could be determined by.

$$S_h = 1.85 R_e^{\frac{1}{3}} S_c^{\frac{1}{3}} \left(\frac{d_h}{L}\right)^{1/3} \tag{10.12}$$

where $R_e$ is the Reynolds number, $Sc$ is the Schmidt number and $L$ is the channel characteristic length. Meanwhile, substrate tortuosity, $\tau$ is calculated by structural parameter, $S$, and membrane porosity, $\varepsilon$, over thickness, $l$ with the following equation.

$$\tau = \frac{S \cdot E}{l} \tag{10.13}$$

However, it needs to be noted that the $S$ and $\tau$ values are only comparable to others when testing conditions and characterizations approach used are similar [6].

## 10.5  MITIGATION METHODS TO REDUCE ICP

### 10.5.1  Membrane Fabrication Methods

Membrane fabrication is a process/method conducted to produce a membrane. The fabrication method is the frontier of any membrane processes, as membrane production will influence the membrane performance. Certain membrane disadvantages cannot be fully avoided but it can be arguably minimized through the membrane fabrication stage. Selections of membrane materials whether it is organic (polymer), inorganic, or composite are reliant in membrane fabrication process as the choice depend on the nature of the operating process conditions and feed streams. Basically, in membrane fabrication, polymeric materials are chosen for its wide availability, ease of processing and relatively inexpensive. However, polymeric materials are prone to chemical and physical damage [27,28]. On the contrary, inorganic membrane seems to have higher robust attribute as it can operate in extreme processing temperatures and pressures [29,30]. It also has great resiliency in withstanding chemical attack and backwashing can be implied toward inorganic membrane without any physical damages. Although it has greater stability compared to the polymeric membrane, the price is inevitably expensive and the knowledge on inorganic membrane in terms of fabrication and operation are still at their early stage. Inorganic membranes usually produced from ceramic materials such as alumina, titanium and zirconium in their fabrication process. Composite membrane is actually a combination of organic and inorganic materials. This membrane is said to have better mechanical properties and possesses higher robustness in coping with high pressure

and have high malleability in module construction. Examples of composite membrane are titanium oxide particles and carbon nanotubes (CNT's).

Apart from membrane fabrication, membrane configuration is also important to ensure that it can be a good selective barrier. Configuration of a membrane is defined as the shape of a membrane when it was fabricated whether it is in flat sheet, spiral, hollow fiber or tubular shape. Every single configuration has its own benefits and advantages and they are fabricated according to their specific applications. Flat-sheet membrane is usually presented in planar configuration, having a flat surface and usually square or rectangular in shape. On conventional purpose, this membrane is stacked into several layers of collated membrane and it is mounted on a rigid frame. Fabrication methods that are usually used to produce this kind of membrane configuration are phase inversion by solvent casting, interfacial polymerization, layer-by-layer deposition and stretching [31]. Other form of configuration that utilized flat-sheet membrane is spiral wound configuration. The difference between flat-sheet and spiral wound configuration is stacking mechanism and the form factor. This kind of membrane consists of collective tube that is wrapped with several stacks of flat-sheet membrane around it [32]. Spiral wound configuration can increase the membrane surface area per unit volume compared to flat-sheet panel. In industries, spiral wound configuration is used in the system that considers pressure drop and not in crosscurrent flow system as it can maximize separation [33]. Meanwhile, hollow fiber configuration is a bit different compared to others as the shape starts to differ forming cylindrical-like shape. The internal and external diameter of hollow fiber membranes usually ranging from $>25\,\mu m$ and $< 1\,mm$ respectively [34]. Currently, development of hollow fiber membrane configuration seems to be increasing as this configuration possesses superior mass-transfer properties. Physical properties of the membrane also remarkable as it has better surface area per unit volume, good mechanical properties, ease of fabrication process, high packing density and the structure of the hollow fiber is self-supporting [35]. In membrane fabrication process, phase inversion, wet-spinning and electrospinning are used to produce hollow fiber configuration [31].

Membrane fabrication consists of several techniques where it implies in making forward osmosis membrane. The techniques that will be mentioned in this subchapter are interfacial polymerization, layer-by-layer deposition and integration of inorganic filler, which can reduce the ICP, ECP and S parameter.

### 10.5.1.1 Interfacial Polymerization

Interfacial polymerization (IP) is a renowned technique in membrane fabrication process as this technique can produce an extremely thin layer of porous supporting structures [31,36]. It is a type of step-growth

polymerization where polymerization process occurs at an interface between one monomer contained in aqueous solution and another monomer inside organic solvent. The commercial membrane used for RO and FO process usually adopted this fabrication method as it is simple and can produce thin-film composite (TFC). The advantage of IP membrane is it can gradually decrease the effect of ICP, which can deliberately increase the performance of FO process in term of water flux and salt rejection. The world's first IP technique was conducted by Cadotte et al., and it dramatically improved the membrane performance in RO application [37]. The study used microporous polysulfone as a support and it is soaked inside polymeric amine aqueous solution. Then the process is completed by immersing the preimpregnated membrane inside the solution containing di-isocyanate in hexane. The finished membrane of TFC polyurea membrane is capable of high salt rejection and high-water flux compared to cellulose acetate membrane at that time [38].

The advantage of IP fabrication method has led to many successful developments of TFC membranes as much work has been done on fabricating IP membrane [39]. Various parameters were studied based on IP fabrication such as solvent type, monomer concentration and posttreatment conditions [40–42]. All these parameters contributed to different structural morphology and composition of the IP layer produced on the support. Usually, most RO and NF membrane produced by IP fabrication have polyamide (PA) layer due to its porosity, high durability, and strength. Compatibility between IP layer and support is also important as low compatibility can lead to pinhole and delamination of the IP layer [36]. IP fabrications on polymeric support have no problem regarding material compatibility but on the inorganic membrane such as ceramic support, the tendency of IP delamination is high. The only problem with polymer support is it has low resiliency and subjected to physical and chemical damage. Recently, there is an effort on fabricating IP layer on top of inorganic membrane support. Maaskant et al. successfully produced thin polyamide layer on top of α-alumina hollow fiber membrane [36]. They stated that to produced IP layer on an inorganic membrane, the ceramic support must have ample amount of hydroxyl group for covalent attachment in preventing delamination and controlled drying steps are crucial to avoid diminishment of liquid on the outer surface of ceramic support. In addition, IP fabrication on ceramic membrane also opens up new path for IP chemistry, as ceramic possesses superior thermal and chemical stability. IP film such as polyimide needs thermal treatment to complete imidization step during fabrication [43].

### 10.5.1.2 Layer-by-Layer Deposition

Layer-by-layer (LbL) deposition is another type of membrane fabrication method in producing thin layer film. The formation of the thin film is

carried out by deposition of charge materials (cationic and anionic) on the membrane support. LbL fabrication method can be accomplished by several ways such as electromagnetism, immersion, spinning, spraying or fluidic. In membrane fabrication, different polyelectrolytes are used to form multiple stacks of deposition on the surface of membrane support. The deposition of polyelectrolyte materials must consist of polyanion and polycation to ensure the charges attracted to each other. LbL deposition is said to be one of the famous membrane fabrication methods as it is natural to be conducted, adjustable surface morphology and specific controllable thickness can be obtained using this method [44,45]. On top of that, LbL assembled layers contain dense charge inside the internal structure enables it to repel charges of heavy metal ions [46]. LbL method is suitable for FO process as the fabrication of the membrane is extremely thin and highly dense. The effect of ICP will be lowered due to the production of an ultrathin layer and dense structure of the membrane will enhanced the reduction of reverse solute across the layer.

A remarkable amount of studies had been conducted on LbL fabrication process for FO application. One of it was a study on the removal performances of heavy metal ions with the assemble LbL FO membrane by Liu et al. [46]. They used polyethylimide (PEI) and sodium alginate (SA) as bilayer on the polymeric support (PVDF). The study found that the LbL membrane with three layers deposition exceeds 99.31% of heavy metal ions rejection and most of it was achieved on AL-FS mode. Another study conducted by Salehi et al. produced a forward osmosis membrane fabricated via LbL method that combined chitosan (CS) with graphene oxide (GO) [47]. The membrane was tested for antifouling properties and its water permeable performance. Their study found that by the incorporation of CS/GO on the surface of TFC support, the water flux was in the range of two to four orders of magnitude higher than bare TFC membrane. The CS/GO incorporated membrane possessed better antifouling properties when compared to the bare TFC membrane when 200-ppm sodium alginate was used in the feed solution. Kwon et al. also produced FO membrane but the assembly used molecular LbL in fabrication process [48]. The fabrication process of polyamide was controlled up to the molecular level in which the cycle number of mLbL was precisely controlled to optimize the FO membrane. Based on their finding, ten cycles of mLbL (mLbL-10) achieved the best FO performance regarding permeability and selectivity. The mLbL-10 produced 3.5 times higher water flux, 60% lower reverse solute flux and 85% lower specific salt flux compared to the commercial membrane (cellulose triacetate HTI membrane).

### 10.5.1.3 Incorporation of Inorganic Filler

Incorporation of inorganic filler inside an FO membrane has become a new trend in research studies as the incorporation of foreign materials

might increase the performance of the FO process. The addition of inorganic filler in membrane fabrication can also boost the mechanical properties as well as increase stability of the membrane depends on the inorganic filler used [49,50]. Moreover, incorporation of inorganic filler also helps in reducing the ICP effect, which may raise the FO performance [50]. Recently, there was a study conducted on the effect of inorganic filler on the FO process. Graphene oxide was employed as a polyelectrolyte that being deposited on both sides of the polymer support [50]. The experimental study achieved remarkable results of ICP reduction because both sides of the membrane were able to conduct the separation process. Another study also did proving that double-skin coating of inorganic filler on a membrane support can achieve higher order-of-magnitude in water flux compared to commercial FO membranes. Inorganic fillers that usually embedded inside FO membrane are GO, CNT, zeolite, and zeolitic imidazolate framework (ZIF).

Jin et al. fabricated polyamide-crosslinked graphene oxide (PA-GO) membrane used for FO process [50]. PA-GO fabrication method indeed shows that the use of more hydrophilic and porous support of FO membrane will potentially reduce the effect of ICP in FO. Their fabricated membrane was tested using three different kinds of draw solutions (trisodium citrate, $Na_2SO_4$, $MgCl_2$) and water flux achieved was the highest on trisodium citrate. Sirinupong et al. also studied the synthesis and characterization processes of $TiO_2$/GO nanocomposite incorporated inside polysulfone support for FO process [51]. Based on the characterization results, surface hydrophilicity and roughness shows an increment after nanomaterials were incorporated into the membrane. These improved characteristics lead to a higher water flux value with minimum reverse solute flux value. Meanwhile, Ma et al. had another approach in enhancing forwarding osmosis performance [49]. They produced zeolite-polyamide thin film nanocomposite (TFN) membrane for forward osmosis application. TFN membrane was incorporated on the surface of polysulfone support. The addition of inorganic nanocomposite does enhance the water permeability due to the porous nature possess by zeolite. However, the further increment in zeolite loading was observed to reduce the water permeability, as too much loading would produce a thicker polyamide layer. The best loading for the membrane to perform holistically is at 0.1 wt/v % where it shows 80% improvement in water permeability compared to the bare TFC membrane.

## 10.5.2 Forward Osmosis Mode Orientations

Developing FO membrane with high efficiency is crucial upon reduction of the ICP [52]. FO membrane usually have two different sides of layer namely, support layer and active layer. When conducting FO process, the usage of lower feed solution (FS) and higher draw solution (DS)

concentration is a must in creating the osmotic pressure difference. The mode of FO orientations can also be changed by only changing the side of FS or DS whether in the support layer or the active layer side. Placement of FS and DS on the active layer of a membrane will create significant differences in terms of ICP formation. As shown in Fig. 10.5, there are two modes of forward osmosis operation; active layer facing draw solution (AL-DS) and active layer facing feed solution (AL-FS). In AL-DS, higher concentration of DS will face toward the acting layer (AL). This orientation enables the salts from the DS to penetrate through the AL and move toward the support layer [1,52]. Continuous transfer of this salt will accumulate higher concentration of salt content in the support layer region compared to the salt content in the FS. The term used for this condition is called concentrative ICP [32]. On the contrary, when the active layer is facing feed solution just like in Fig. 10.5B, the water from FS is permeated toward the support layer and the salt concentration inside the support layer is diluted. This condition is termed as dilutive ICP [32]. Based on this mode, the effective osmotic pressure is also lowered due to the difference in both original concentration of FS and DS. Reduction in effective osmotic pressure in AL-FS due to ICP is far greater than the AL-DS side and eventually reducing the FO performance. However, in real application of FO process, the AL-FS mode is used more often than
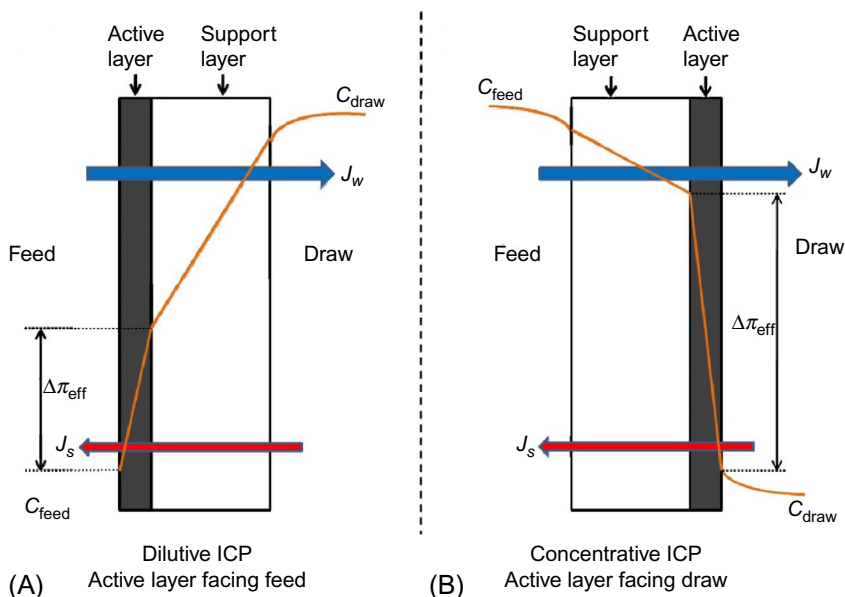


**FIG. 10.5**  Internal concentration polarization that occurs in FO membrane. $\Delta\pi_{eff}$, effective osmotic pressure, $J_w$, water flux, $J_s$, solute flux. *Data from Klaysom C, Cath TY, Depuydt T, Vankelecom IFJ. Forward and pressure retarded osmosis: potential solutions for global challenges in energy and water supply. Chem Soc Rev 2013;42:6959–89.*

the AL-DS mode due to higher obtained flux from the process and usually film pollutant is added inside the FS. For that reason, AL-DS and AL-FS are termed as pressure retarded osmosis (PRO) and FO mode respectively.

## 10.5.3 Selection of Draw Solution

Draw solution is one of the important aspects of the FO process as it provides relatively high osmotic pressure difference with the feed solution to drive the process. Selection of a good draw solution enables FO to produces high water flux, minimal reverse solute diffusion and reduces energy consumption during draw solution regeneration [53,54]. The regeneration process is necessary for the production of fresh water and it contributes most of the energy associated with the FO. By cost-effective draw regeneration method that takes advantages of draw solute properties, the energy consumptions of the process can be reduced further.

### 10.5.3.1 Characteristics of Draw Solution

The solutes should have some characteristics before being utilized as draw solution. First and most important characteristics have high osmotic pressure. It is important for the draw solution to have higher osmotic pressure than the feed solution to induce the osmosis process. The osmotic pressure of the solution can be calculated using an equation proposed by Van't Hoff [54]:

$$\pi = n\left(\frac{c}{M}\right)RT \tag{10.14}$$

$\Pi$ is the osmotic pressure (atm), $n$ is the number of moles, $c$ is the solute concentration (g/L), $M$ is the solute molecular weight (g/mol). $R$ is a gas constant (L atm mol$^-$ K$^-$), and $T$ is the absolute temperature $(K)$. From Eq. (10.14), the osmotic pressure of draw solution is inversely proportional to the molecular weight of a solute. Therefore, draw solute with a low molecular weight is preferable for draw solution as they provide much higher osmotic pressure compared to the solute with high molecular weight although in the same concentration. Also, this helps improve the cost efficiency of FO process, especially during draw solution replenishment process as higher molecular weight compounds have a larger size which can be separated easily by low energy methods such as low-pressure membrane separation.

Moreover, low molecular weight solute is also desirable due to its high diffusivity characteristic. Draw solution with high diffusivity will be diffused easily into the support layer of the membrane and minimizing the effect of ICP [53]. However, regardless of its advantages, low molecular weight draw solutes cannot surpass a major drawback in most FO membrane which contributes to high reverse solute flux. Reverse solute flux is

known as undesirable movement because it can contaminate the feed and cause an osmotic pressure reduction due to the loss of solute. Another characteristics that should be considered in the selection of draw solution are easy replenishment and recovery. Draw solution recovery must employed methods that can minimize energy expenditure, simple and easy to carry out. Last but not least, draw solution that should be selected needs to be toxic-free. Even though the FO performance will not be affected by the draw solution toxicity, it is important to ensure that the final product is safe for delivery and will not harm the environment.

### 10.5.3.2 Classification of Draw Solutions

Draw solutions can be classified into several categories, including inorganic, organic, and other novel draw solutes. In the FO process, the mostly used draw solution is based on an inorganic salts. This type of draw solution in general have high osmotic pressure and widely available at cheaper price which makes them as a feasible draw solute from economical point of view. Achilli et al. have studied and compared 14 different inorganic solutes as a draw solution to optimize the FO process [55]. From the membrane performance standpoint, potassium bicarbonate ($KHCO_3$), sodium bicarbonate ($NaHCO_3$), magnesium chloride ($MgCl_2$), magnesium sulphite ($MgSO_4$) and calcium chloride ($CaCl_2$) draw solutes are the promising candidates for draw solution in FO as they greatly attract high water flux and perform low reverse solute flux. Regardless of the five candidates, $MgCl_2$ is suggested to be the best draw solution for water separation process because it is unlikely to cause scaling on the membrane which can degrade membrane performance over time.

Previous researchers, Kim et al. also had compared four inorganic draw solutions to find the most suitable draw solution based on the economic and environmental perspective [56]. They reported that sodium sulphide ($Na_2SO_4$) draw solution was proved to be the most suitable for hybrid FO and nanofiltration (NF) system. This was due to its relatively inexpensive solute cost, low solute loss and small draw solution replenishment cost as it required minimal energy consumption. In conclusion, their study demonstrates the importance of suitable inorganics draw solution regarding energy and cost efficiency of the FO process during the water recovery and the draw solution regeneration.

Organic compounds such as ethanol, glucose and sucrose had been tested as the draw solute for FO. Like the inorganic draw solution, these organic solutes also possess high osmotic pressure due to their higher solute concentration. Typically, most organic compounds have sizable molecular weight, and their structure consists of bigger size molecules. This property allowed the draw solution to have a reduction in the reverse solute flux during FO process and it can be successfully regenerated via low-pressure ultrafiltration (UF) or NF. Furthermore, Long et al. have

reported a series of gluconate salts as novel draw solution [57]. Based on the results of the experimental studies, potassium gluconate was closely comparable to NaCl performance regarding its water flux and having a much lower solute leakage. The possibility of this feature was achieved through its high osmotic pressure and low viscosity properties. Also, recovery of this organic draw solution had been tested using NF which in return shown an excellent solute rejection of about 91% under the operating pressure of 3.5 bar. Energy consumption for replenishment of organic solution should be substantially lower than the inorganic counterpart.

Recently, another promising draw solution based on hydrophilic magnetic nanoparticles (MNPs) was synthesized. MNPs acquire amazing properties such as high surface area to volume ratios, big particles size, soluble in water and low toxicity [53,54]. One of the interesting advantages of MNPs over the other draw solutes is its superparamagnetic properties. It enables recovery of draw solute using magnetic fields and resulting in an energy efficient FO. Similar to others, MNPs also capable of producing high osmotic pressure. Ge et al. have reported that poly(ethylene glycol)diacid [PEG-$(COOH)_2$ 250] MNPs can exhibit tremendous osmotic pressure as high as 73 atm which is larger than the common seawater osmotic pressure of about 22 atm [58]. Typically, MNPs osmotic pressure is greatly induced by the size of their nanoparticles. The larger the size of nanoparticles size, the higher osmotic pressure will be produced. Therefore, by possessing such properties, MNPs draw solution emerged as a promising candidate for seawater desalination using the FO process.

## 10.6 CONCLUSION

In conclusion, the most recognized FO membrane so far was the TFC membrane. Although different FO membranes have undergone the same performance tests, the results obtained still varied according to various factors. However, by going through several mitigation methods offered, the readers could sort the best way to fabricate a better FO membrane soon.

### Acknowledgments

# References

[1] Lutchmiah K, Verliefde ARD, Roest K, Rietveld LC. Forward osmosis for application in wastewater treatment: a review. Water Res 2014;58:179–97.

[2] Qasim M, Darwish NA, Sarp S, Hilal N. Water desalination by forward (direct) osmosis phenomenon: a comprehensive review. Desalination 2015;374:47–69.

[3] James D, Ali W, Wahab A, Hilal N. Osmotic potential: an overview of draw solutes for forward osmosis. Desalination 2017;434:100–20.

[4] Dong H, Zhao L, Zhang L, Chen H, Gao C, Ho WSW. High-flux reverse osmosis membranes incorporated with NaY zeolite nanoparticles for brackish water desalination. J Membr Sci 2015;476:373–83.

[5] Sukitpaneenit P, Chung T. High performance thin-film composite forward osmosis hollow fiber membranes with macrovoid-free and highly porous structure for sustainable water production. Environ Sci Technol 2012;46(13):7358–65.

[6] Li X, Heng C, Wang R, Widjajanti W, Torres J. Fabrication of a robust high-performance FO membrane by optimizing substrate structure and incorporating aquaporin into selective layer. J Membr Sci 2017;525(October 2016):257–68.

[7] Liu X, Yong H. Fabrication of layered silica–polysulfone mixed matrix substrate membrane for enhancing performance of thin-film composite forward osmosis membrane. J Membr Sci 2015;481:148–63.

[8] You S, Tang C, Yu C, Wang X, Zhang J, Han J, et al. Forward osmosis with a novel thin-film inorganic membrane. Environ Sci Technol 2013;47(15):8733–42.

[9] Phillip WA, Schiffman JD, Elimelech M. High performance thin-film composite forward osmosis membrane. Environ Sci Technol 2010;44(10):3812–8.

[10] Lee J-Y, She Q, Huo F, Tang CY. Metal-organic framework–based porous matrix membranes for improving mass transfer in forward osmosis membranes. J Membr Sci 2015;492:392–9.

[11] Zirehpour A, Rahimpour A, Ulbricht M. Nano-sized metal organic framework to improve the structural properties and desalination performance of thin film composite forward osmosis membrane. J Membr Sci 2017;531(October 2016):59–67.

[12] Jeong B, Hoek EMV, Yan Y, Subramani A, Huang X, Hurwitz G, et al. Interfacial polymerization of thin film nanocomposites: a new concept for reverse osmosis membranes. J Membr Sci 2007;294:1–7.

[13] Amini M, Jahanshahi M, Rahimpour A. Synthesis of novel thin film nanocomposite (TFN) forward osmosis membranes using functionalized multi-walled carbon nanotubes. J Membr Sci 2013;435:233–41.

[14] Jadav GL, Singh PS. Synthesis of novel silica-polyamide nanocomposite membrane with enhanced properties. J Membr Sci 2009;328:257–67.

[15] Zirehpour A, Rahimpour A, Khoshhal S, Firouzjaei MD, Ghoreyshi AA. The impact of MOF feasibility to improve the desalination performance and antifouling properties of FO membranes. RSC Adv 2016;6(74):70174–85.

[16] Pan Y, Zhao Q, Gu L, Wu Q. Thin film nanocomposite membranes based on imologite nanotubes blended substrates for forward osmosis desalination. Desalination 2017;421(April):160–8.

[17] Wu X, Field RW, Jie J, Zhang K. Polyvinylpyrrolidone modified graphene oxide as a modifier for thin film composite forward osmosis membranes. J Membr Sci 2017;540:251–60.

[18] Phillip WA, Yong JUIS, Elimelech M. Reverse draw solute permeation in forward osmosis: modeling and experiments. Environ Sci Technol 2010;44(13):5170–6.

[19] Cath TY. Solute coupled diffusion in osmotically driven membrane processes. Environ Sci Technol 2009;43(17):6769–75.

[20] She Q, Jin X, Tang CY. Osmotic power production from salinity gradient resource by pressure retarded osmosis: effects of operating conditions and reverse solute diffusion. J Membr Sci 2012;401–402:262–73.

[21] Emadzadeh D, Lau WJ, Ismail AF. Synthesis of thin film nanocomposite forward osmosis membrane with enhancement in water flux without sacrificing salt rejection. Desalination 2013;330:90–9.

[22] Fang W, Liu C, Shi L, Wang R. Composite forward osmosis hollow fiber membranes: integration of RO- and NF-like selective layers for enhanced organic fouling resistance. J Membr Sci 2015;492:147–55.

[23] Cath TY, Childress AE, Elimelech M. Forward osmosis: principles, applications and recent developments. J Membr Sci 2006;281:70–87.

[24] Tiraferri A, Yip NY, Straub AP, Castrillon SR. A method for the simultaneous determination of transport and structural parameters of forward osmosis membranes. J Membr Sci 2013;444:523–38.

[25] Manickam SS, Mccutcheon JR. Model thin film composite membranes for forward osmosis: demonstrating the inaccuracy of existing structural parameter models. J Membr Sci 2015;483:70–4.

[26] Bui N, Arena JT, Mccutcheon JR. Proper accounting of mass transfer resistances in forward osmosis: improving the accuracy of model predictions of structural parameter. J Membr Sci 2015;492:289–302.

[27] Baker RW. Membrane technology and applications. Chichester, UK: John Wiley & Sons, Ltd; 2004. p.301–54.

[28] Chen P, Ma X, Zhong Z, Zhang F, Xing W, Fan Y. Performance of ceramic nanofiltration membrane for desalination of dye solutions containing NaCl and $Na_2SO_4$. Desalination 2017;404:102–11.

[29] Wang N, Liu T, Shen H, Ji S, Li JR, Zhang R. Ceramic tubular MOF hybrid membrane fabricated through in situ layer-by-layer self-assembly for nanofiltration. AIChE J 2016 Feb;62(2):538–46.

[30] Yin N, Wang K, Wang L, Li Z. Amino-functionalized MOFs combining ceramic membrane ultrafiltration for Pb (II) removal. Chem Eng J 2016;306:619–28.

[31] Lalia BS, Kochkodan V, Hashaikeh R, Hilal N. A review on membrane fabrication: structure, properties and performance relationship. Desalination 2013;77–95.

[32] Baker RW. Membrane technology and applications. 3rd ed. 73. United Kingdom: John Wiley and Sons Ltd; 2012. p.5.

[33] Wiley D, Weihs GF. In: Drioli E, Giorno L, editors. Encyclopedia of membranes. Berlin, Heidelberg: Springer Berlin Heidelberg; 2016. p. 1–3.

[34] Moch I. Membranes, hollow-fiber. In: Kirk-Othmer encyclopedia of chemical technology. 4. Hoboken, NJ, USA: John Wiley & Sons, Inc; 2000. p. 1–31.

[35] Deng K, Liu Z, Luo F, Xie R, He X, Jiang M, et al. Controllable fabrication of polyethersulfone hollow fiber membranes with a facile double co-axial microfluidic device. J Membr Sci 2017 Mar;526(September 2016):9–17.

[36] Maaskant E, de Wit P, Benes NE. Direct interfacial polymerization onto thin ceramic hollow fibers. J Membr Sci 2018;550:296–301.

[37] Cadotte JE, Petersen RJ, Larson RE, Erickson EE. A new thin-film composite seawater reverse osmosis membrane. Desalination 1980;32(C):25–31.

[38] Cadotte J, Forester R, Kim M, Petersen R, Stocker T. Nanofiltration membranes broaden the use of membrane separation technology. Desalination 1988;70(1–3):77–88.

[39] Lau WJ, Ismail AF, Misdan N, Kassim MAA. Recent progress in thin film composite membrane: a review. Desalination 2012;287:190–9.

[40] Petersen RJ. Composite reverse osmosis and nanofiltration membranes. J Membr Sci 1993;83:81–150.

[41] Juhn I, Greenberg AR, Khare VP. Synthesis and characterization of interfacially polymerized polyamide thin films. Desalination 2006;191(August 2005):279–90.

[42] Ghosh AK, Jeong B, Huang X, Hoek EMV. Impacts of reaction and curing conditions on polyamide composite reverse osmosis membrane properties. J Membr Sci 2008;311:34–45.

[43] Raaijmakers MJT, Kappert EJ, Nijmeijer A, Benes NE. Thermal imidization kinetics of ultrathin films of hybrid poly(POSS- imide)s. Macromolecules 2015;48(9):3031–9.

[44] Liu C, Fang W, Chou S, Shi L, Fane AG, Wang R. Fabrication of layer-by-layer assembled FO hollow fi ber membranes and their performances using low concentration draw solutions. Desalination 2013;308:147–53.

[45] Duong PHH, Zuo J, Chung T. Highly crosslinked layer-by-layer polyelectrolyte FO membranes: understanding effects of salt concentration and deposition time on FO performance. J Membr Sci 2013;427:411–21.

[46] Liu C, Lei X, Wang L, Jia J, Liang X, Zhao X, et al. Investigation on the removal performances of heavy metal ions with the layer-by-layer assembled forward osmosis membranes. Chem Eng J 2017;327:60–70.

[47] Salehi H, Rastgar M, Shakeri A. Anti-fouling and high water permeable forward osmosis membrane fabricated via layer by layer assembly of chitosan/graphene oxide. Appl Surf Sci 2017;413:99–108.

[48] Kwon SB, Lee JS, Kwon SJ, Yun ST, Lee S, Lee JH. Molecular layer-by-layer assembled forward osmosis membranes. J Membr Sci 2015;488:111–20.

[49] Ma N, Wei J, Liao R, Tang CY. Zeolite-polyamide thin film nanocomposite membranes: towards enhanced performance for forward osmosis. J Membr Sci 2012;405–406:149–57.

[50] Jin L, Wang Z, Zheng S, Mi B. Polyamide-crosslinked graphene oxide membrane for forward osmosis. J Membr Sci 2018;545(February 2017):11–8.

[51] Sirinupong T, Youravong W, Tirawat D, Lau WJ, Lai GS, Ismail AF. Synthesis and characterization of thin film composite membranes made of PSF-TiO$_2$/GO nanocomposite substrate for forward osmosis applications. Arab J Chem 2017;.

[52] Uragami T. Science and technology of separation membranes. New York: Wiley; 2017, p. 385–412.

[53] Klaysom C, Cath TY, Depuydt T, Vankelecom IFJ. Forward and pressure retarded osmosis: potential solutions for global challenges in energy and water supply. Chem Soc Rev 2013;42:6959–89.

[54] Chekli L, Phuntsho S, Shon HK, Vigneswaran S, Chanan A. A review of draw solutes in forward osmosis process and their use in modern applications. Desalin Water Treat 2012;43(February 2012):167–84.

[55] Achilli A, Cath TY, Childress AE. Selection of inorganic-based draw solutions for forward osmosis applications. J Membr Sci 2010;364(1–2):233–41.

[56] Eun J, Phuntsho S, Chekli L, Yong J, Kyong H. Environmental and economic assessment of hybrid FO-RO/NF system with selected inorganic draw solutes for the treatment of mine impaired water. Desalination 2018;429(November 2017):96–104.

[57] Long Q, Qi G, Wang Y. Evaluation of renewable gluconate salts as draw solutes in forward osmosis process. ACS Sustain Chem Eng 2015;4:85–93.

[58] Ge Q, Su J, Chung T, Amy G. Hydrophilic superparamagnetic nanoparticles: synthesis, characterization and performance in forward osmosis processes. Ind Eng Chem Res 2011;50(1):382–8.

CHAPTER

# 11

# Pressure-Retarded Osmosis

*Norzeti Hanani Mohd Ripin, Pei Sean Goh, Woei Jye Lau, Ahmad Fauzi Ismail, Be Cheer Ng*

**Advanced Membrane Technology Research Centre (AMTEC), Faculty of Chemical and Energy Engineering, Universiti Teknologi Malaysia, Skudai, Malaysia**

OUTLINE

## 11.1 INTRODUCTION

Currently, one of the most critical worldwide problems is the fast-growing demand for electrical power [1]. According to Han et al. the global energy consumption will increase by 56% in 2040, and the total

energy usage will rise to 240 kTWh [1]. It has been stated that the reserve of fossil fuels is depleting and the emissions of acidic greenhouse gases have changed the global climate. Due to the depleting resources, adverse environmental impacts and hiking price of fossil fuels, communities all over the world are trying to reduce their fossil fuel consumptions. One of the alternatives to reduce the usage of fossil fuel is through the development of renewable resources and the technologies for power generation. To date, the most commonly explored renewable energy sources such as solar, wind, hydro and geothermal. Besides that, the energy harvesting based on the salinity gradient has also been investigated.

Pressure-retarded osmosis (PRO) is known to be an emerging technology to capture energy from mixing fresh water with saltwater [2]. Recently, PRO has been widely studied because it is one of the promising technologies which can overcome the problem of water deficiency, the demand of power generation as well as the increase of the cost of fossil fuel [3,4]. The concept of osmotic power that is based on salinity gradient was proposed in 1954 by R. E Pattle. Since then, the concept has been applied by Sidney Loeb for power generation [5]. As shown in Fig. 11.1, PRO systems can be divided into classes based on their configuration which is open loop and closed loop. The open loop system introduces solar driven processes in which renewable energy is generated when freshwater is mixed with saltwater [6]. On the other hand, a closed-loop PRO-thermal plant uses heat waste for power generation. In this design, waste-heat produced from power generation plants or other industrial processes is used for draw solution regeneration. The mixed solution from the PRO unit is further divided in the evaporator into two flows, such as the feed solution and draw solution. One of the most significant advantages of this design is no discharge of brine waste, but the set up is very limited to the availability of waste-heat source.

Statkraft from Norway has commissioned the first PRO prototype to harvest energy from salinity gradient. The pilot-scale plant was operated by SINTEF Energy Research to generate electricity of 10 kW through the salinity gradient energy harvesting process based on the $1 \, W/m^2$ membrane's energy density [3,4]. The researchers have predicted that the osmotic potentials derived from the salinity gradient represent an energy potential of 2000 TWh across the globe, which corresponds to about 1% of the world energy consumption [7]. Despite the first illustration of energy generation using osmotic power, the capacity of Statkraft plant is too small for practical usage, and the project has been terminated due to the low economic viability of this technology to justify more funding for this research.

Generally, PRO can be addressed as the inverse process of reverse osmosis (RO). Unlike RO which requires hydraulic pressure to counter the osmotic pressure to allow the permeate of feed seawater to produce fresh water, PRO relies on the osmotic pressure of seawater to produce
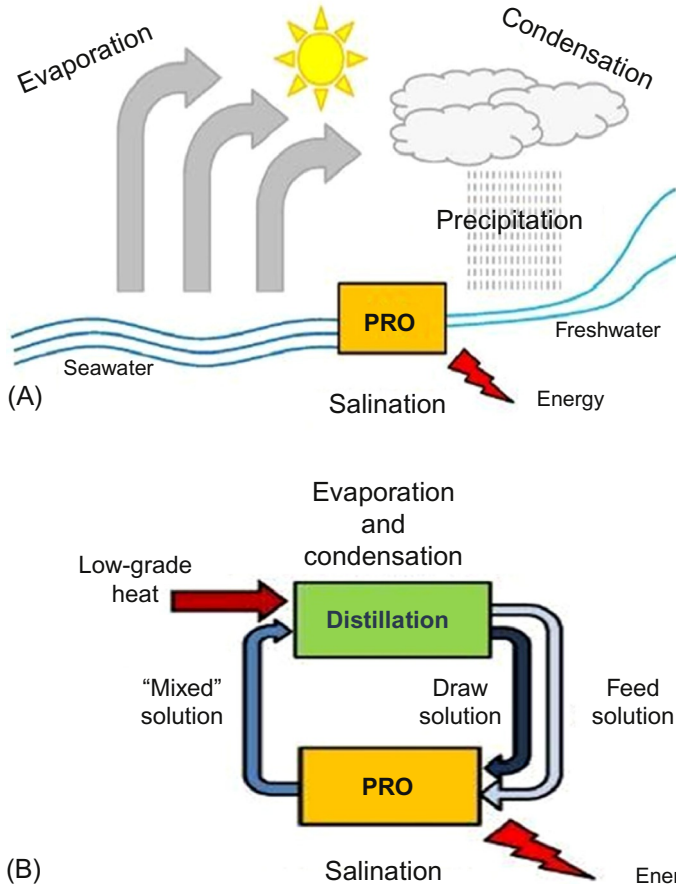
FIG. 11.1 (A) Schematic diagram of an open loop water salination cycle by using PRO to recover solar energy and (B) the closed loop PRO system where it is created to convert low-grade heat into mechanical work [6].

desalinated water while producing energy. In PRO, a low salinity solution permeate, which is usually water, passes through a membrane into the pressurized solution with high salinity. During this process, power is generated through the depressurization of the permeate through a hydro turbine [7]. In a typical filtration system, the membrane is said to be operated with the PRO mode when the draw solution is in contact with the active layer and the feed solution is in contact with the support layer [3]. On the other hand, the FO mode is operated when the draw solution faces the support layer and the feed solution faces the active layer. PRO operating mode typically demonstrates greater water flux compared to that of FO operating mode. However, higher membrane fouling tendency is typically

observed in the PRO operating mode [3,4]. Due to the high osmotic pressure, availability, and cost-free, seawater is a good draw solution candidate [3]. The researcher estimated that when 1 m$^3$ of river water flows into sea water, the highest energy which can be generated is 0.8 kWh. But this also depends on the salinity level of the seawater. However, after considering pretreatment as well as usage the installations of pumps in the PRO process, the net energy is around 0.2 kWh/m$^3$ [3,4]. Owing to the concentration of NaCl which varies from 3.0 to 4.0 wt%, subjected to the source locations, the osmotic pressure of seawater falls typically between 25 and 33 bar at 25°C [9]. It is also found that, the RO retentate collected from SWRO plants which usually has salt concentration ranging from 6.0 to 7.0 wt% could possess higher osmotic pressures of 50–59 bar [9]. Based on this observation, PRO has been addressed as a promising method to recycle and reuse RO brine when a hybrid system of RO-PRO is considered to minimize the discharge of this brine into seawater. In this the hybrid system, RO brine concentrate is recycled as a draw solution [1].

PRO process has been actively explored since 1973 due to the advancement made in the development of membrane technologies. Commonly, the membrane has been identified as one of the essential components to determine the PRO performance. Due to some similar aspects with RO, the initial development of PRO membranes and membrane modules was focused on the application of conventional RO membranes. PRO performance greatly depends on the volume, salinity and the cleanliness of the feed water supply. As membranes are the essential part to ensure the practicability of PRO for energy generation, membrane characteristics have been well concerned and carefully modified to meet the requirement and optimize the osmotic power. The primary stumbling block for the progress of PRO technology is the availability of membranes with desired properties such as high mechanical strength as well as promising separation performance regarding water flux and salt rejection. Additionally, as membrane generally shows the tendency to be attached with various form of foulants which present in the water supply, the quality of the feed water is known to be influential to the membrane performance.

This chapter discusses the PRO performance and the development of the membranes for simultaneous power generation and desalination. In the first section, the basic principles and the theories of PRO for osmotic power generation are focused. The next section discusses the development of PRO membranes which covers the commercial asymmetric cellulose acetate (CA) membranes, thin film composite (TFC) membrane and thin film nanocomposite (TFN) membrane for PRO application. The fouling issues related to PRO membrane are then presented in the next section. Finally, the concluding remarks and brief future outlook of the development of PRO technologies are a highlight.

## 11.2 THEORIES AND BASIC PRO PRINCIPLES

There are three types of osmosis processes which are already well developed, namely RO, forward osmosis (FO) and PRO. The osmosis phenomenon explains the spontaneous water transport which takes place through a semipermeable membrane where the feed stream of higher chemical potential flows into another stream with lower chemical potential [1]. Draw solution refers to the stream with lower chemical potential meanwhile the stream with higher potential is addressed as the feed solution. During the process, the membrane only allows the passage of water but hinder the transport of the solutes. Along the osmosis process, the permeate water will dilute the draw solution speedily while the feed solution is concentrated. The process continuously runs until equilibrium of the chemical potential across the membrane is achieved. In this case, osmotic pressure ($\pi$) refers to the hydrostatic pressure which acts to hinder the transport of solvent across the membrane when it is applied to the draw solution. It can be calculated via van't Hoff equation.

$$\pi = icRT \tag{11.1}$$

where $i$ is van't Hoff factor, $c$ is molar concentration ($mol^{-1} L^{-1}$), $R$ is universal gas constant ($8.31441\ J\ mol^{-1}\ K^{-1}$), and $T$ is absolute temperature ($K$).

As illustrated in Fig. 11.2, all the osmosis process involves a semipermeable membrane. The FO process involves the transportation of water spontaneously across the membrane driven by the osmotic pressure gradient ($\Delta\pi$) between the two solutions. When the side with higher salinity is applied with hydrostatic pressure, the permeation of water is hindered once the $\Delta P$ is equal to $\Delta\pi$. However, the flow of the water will continue to take place into the salty water when $\Delta P$ is between 0 and $\Delta\pi$ because the value of $\Delta\pi$ is higher than $\Delta P$ [1]. Thus, this phenomenon is denominated as PRO where the net driving force for water transport is reduced to $\Delta\pi - \Delta P$ while the RO process occurred when water permeation is taken place is the reverse direction. This process takes place when the transmembrane pressure $\Delta P$ is greater than $\Delta\pi$ and water is forced to pass through the membrane from the high salinity side into the fresh water. RO process tremendously used for seawater desalination. Based on the osmotic principle, PRO is able to produce energy while for RO energy must be provided and no additional energy is needed for FO [1].

In Fig. 11.3, a schematic diagram of a typical PRO osmotic power process is presented. At first, the feeds need to be pretreated through a few types of filtrations to ensure all the impurities are discarded and to reduce the membrane fouling as well. Then, the treated salty water is first pumped through a pressure exchange and then channeled into the high-pressure chamber. In the chamber, the salty water is treated with
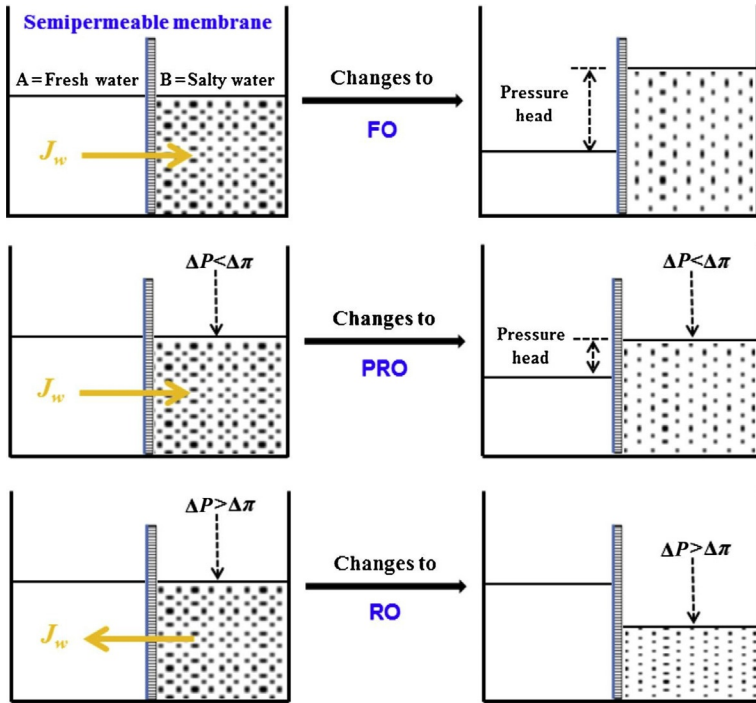
**FIG. 11.2** Schematic diagrams of the osmotic processes [1].
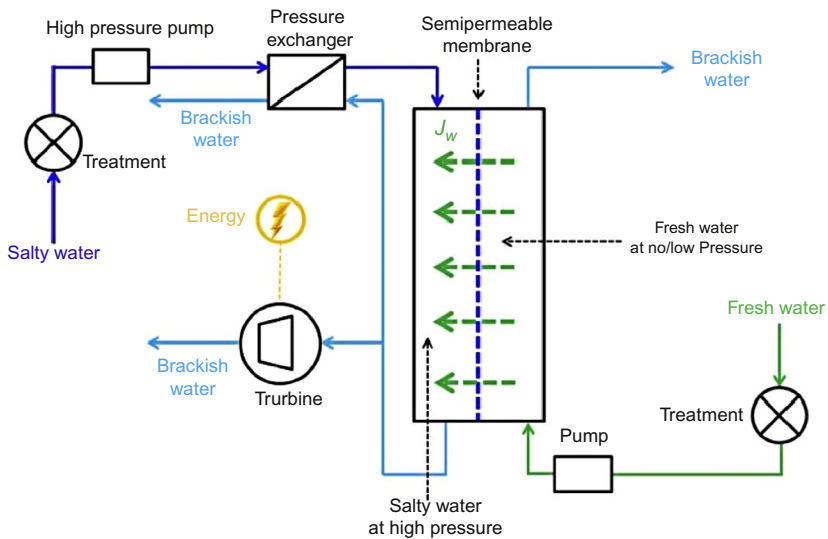


**FIG. 11.3** Schematic diagram which demonstrates the continuous and steady-state flow of a typical PRO osmotic power plant [1].

high hydraulic pressure (Ps). Meanwhile, in another chamber, pretreated fresh water is supplied, but it differs from the high-pressure chamber because this one is none or low hydraulic pressure (Pf) located on the opposite side of the PRO membrane. The fresh water flows against porous membrane support layer while the salty water faces the other part of the membrane which is the active layer. Water transports spontaneous through the membrane due to the existence of the driving force across the membrane. They flow from the fresh water to the salty water at a flow rate of ΔV (Eq. 11.2) [1].

$$\Delta V = J_w \times A_m \tag{11.2}$$

where $Am$ is the membrane area, and $Jw$ is the water permeation flux.

When the water permeates across the membrane, in the high-pressure compartment, there is an increase in pressure. Apart from that, from the low-pressure compartment, the high salinity solution is expanded with the incoming volume ($\Delta V$) hence resulted in the formation of brackish water due to the dilution of the saline water [1]. That brackish water, which is with lower salinity, is then separated into two flows. One stream is used to operate a hydro-turbine to generate electricity while another stream is delivered to the energy recovery device (ERD) such as pressure exchanger. The pressure exerted by the brackish water is recovered by the ERD to the feed saline water. Based on this working principle, a cost-effective PRO system can be realized with the presence of effective ERD to reduce the loss of energy. Otherwise, the turbine energy generated will not meet the targeted amount to pretreat, pump and pressurize the feed waters. Hence, optimization is a crucial factor to improve the actual power output of PRO plant together to (i) optimize module design, (ii) give advance membrane performance, and (iii) enhance the salinity gradient between the water streams [1].

Usually, for PRO applications, the membrane performance is analyzed regarding power density $W$ (Eq. 11.3); the power output per unit membrane area (W/m$^2$). It is imperative to have a high $W$ PRO membrane because it will determine the amount needed for membrane area and the size of a PRO plant for a given capacity of energy production. According to mathematics theory, the product of the trans-membrane hydraulic pressure $\Delta P$ (bar) and the water permeation flux $J_w$ (ms$^{-1}$) across the membrane will determine the value of $W$.

$$W = J_W \Delta P \tag{11.3}$$

The general equation to estimate the PRO membrane water flux, $J_w$ is:

$$J_w = A_w(\Delta \pi - \Delta P) \tag{11.4}$$

where $A_w$ is the intrinsic water permeability coefficient of the membrane (ms$^{-1}$ bar$^{-1}$), $\Delta P$ is the differential feed pressure across the membrane (bar), and $\Delta \pi$ is the osmotic pressure difference between the two solutions (bar).

By substituting (11.4) into (11.3), the ideal power output will be:

$$W = A_w(\Delta\pi - \Delta P)\,\Delta P \tag{11.5}$$

When the hydraulic pressure is equal to the half value of the osmotic pressure gradient ($\Delta P = \Delta\pi/2$) across the PRO membrane, the power density is expected to achieve a maximum theoretical value, $W_{max}$. Eq. (11.5) can be rearranged to calculate $W_{max}$:

$$W_{max} = A_w\frac{\Delta\pi^2}{4} \tag{11.6}$$

Thus, the $W_{max}$ in a PRO system is directly proportional to the membrane water permeability $A$, and the square of the osmotic pressure difference. It is recommended to conduct the PRO process at a pressure close to $\Delta\pi/2$ in return, the maximal power output could be produced. Han et al. [1] stated that the desired operating pressure is approximately 13.0–13.5 bar. This condition can be achieved when river water and saline water are mixed together. However, it should be noted that in the practical PRO processes, the actual osmotic pressure gradient across the membrane is normally smaller than the osmotic pressure difference between the fresh water and saline water. This phenomenon is due to the occurrence of concentration polarization and reverse salt flux which eventually lead to the decline of water flux compared to the figure obtained using Eq. (11.4). Basically, when an asymmetric PRO membrane is considered, the available types of concentration polarizations are first external concentration polarization (ECP) and second one is internal concentration polarization (ICP) [1,3]. Fig. 11.4 demonstrates an asymmetric composite membrane with the active layer facing the draw solution, that is, in PRO mode. $C_s$ and $C_f$ are the salt concentrations of the bulk salt water and fresh water solutions respectively while $C_1$ is the salt concentration at the interference
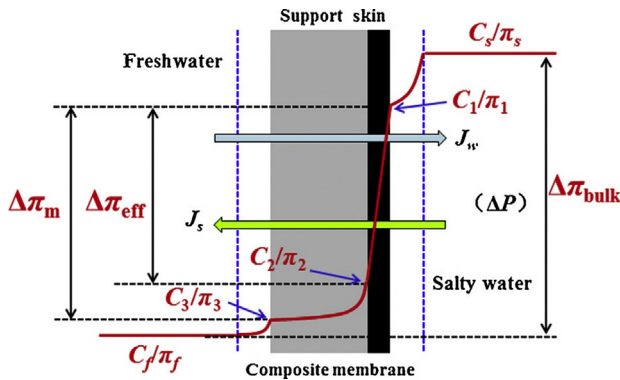


FIG. 11.4　The illustration of the salt concentration and osmotic pressure profiles across an asymmetric PRO thin film composite membranes [1].

between the salty water and the membrane selective layer. The incoming water flux ($J_w$) from the fresh water has the dilution effects. It causes $C_1$ to be smaller than $C_s$ and this resulting in the dilution phenomenon which known as diluted ECP. Likewise, the salt concentration $C_3$ in which situated at the interface of the fresh and the membrane is higher than $C_f$ due to the consumed water and reversed diffused salt ($J_s$). All these will lead to the concentrated ECP phenomenon. With the increasing membrane thickness, the negative impacts of the concentrative ECP can be ignored. It is known that ICP always impart more detrimental effects on the decline in water flux and power density whereas ECP mostly takes place when draw solution with higher concentrations is used. Significantly, it is not easy to reduce the ICP by simply speeding up the feed flow rate and introducing turbulence flow through the membrane surface as ICP is a phenomenon that happens within the porous structures of the polymeric substrate. Previous findings have proved that ICP normally subjected to the morphology of support layer, characteristic of solute as well as the flux of water permeation [1,3,8]. Eq. (11.7) can define the solute resistivity $K$ (s m$^{-1}$) within the polymeric support layer to characterize the ICP effects.

$$K = \frac{S}{D_s} \tag{11.7}$$

where $D_s$ is the solute diffusion coefficient in the membrane substrate (m$^2$ s$^{-1}$) and $S$ is the structural parameter ($m$) that is a function of several membrane parameters:

$$S = \frac{t\tau}{\varepsilon} \tag{11.8}$$

where $t$ is the thickness of the support layer ($m$), $\tau$ is the tortuosity of the support layer, $\varepsilon$ is the porosity of the support layer.

## 11.3 MEMBRANES FOR PRESSURE RETARDED OSMOSIS

As mentioned earlier, $n$ order to obtain the power density that is commercially attractive, a reliable PRO membrane should demonstrate the desired features that are demonstrated by RO and FO membranes. Over the past several years, significant progress has been made in PRO technology via modeling and high-performance membrane design. For the preparation of PRO membranes, two approaches of membrane preparation have generally been developed, such as phase inversion and interfacial polymerization (IP). Broadly, phase inversion is a process that involves the nonsolvent-solvent exchange to form the membrane whereas IP

involves the formation of the skin layer of composite membrane in a conventional TFC membrane through the reaction of two monomers.

## 11.4  CELLULOSE ACETATE MEMBRANE

In membrane preparation, different polymeric materials have been used for the application of water, CA is considered as the typical membrane materials used owing to its good characteristic, promising flux, low cost, long lifetime, less clean requirement and minimal fouling membrane due to its high hydrophilicity [10]. Thin film of CA which has a water permeation rate less than $0.01 \ L/m^2$ h is the first RO membrane with effective salt retention of 98% [11]. CA-based membranes have been commonly used for PRO process. CA-based membranes are known to demonstrate several desired characteristics like enhanced hydrophilicity to promote water flux and reduce the membrane fouling tendency, mechanical robustness and relatively high tolerance toward chlorine attack [3]. However, CA membrane is also known to show low tolerance toward pH change. CA membranes have been commercialized by Hydration Technology Innovations (HTI) in flat sheet and spiral wound modules configuration. However, the cost of production is not favorable for practical commercial applications [3]. The thickness of these CA membrane is approximately 50 μm thick and they are made to tolerate up to 2 ppm of chlorine and pH in the range of 3–8. Table 11.1 simplifies the PRO power generation performance of cellulose tri-acetate (CTA) membrane manufactured by HTI [12]. As mentioned earlier, higher water flux can be attained when the membrane is operated in PRO mode compared to that in the FO mode. The development of more severe ICP in the FO mode decrease the flux and lower power density is observed. On the other hand, by lifting up the hydraulic pressure of draw solution, the output power can be enhanced [13]. Therefore, it is a must to ensure the robustness of the PRO membrane when subjected to increase hydraulic pressure to avoid membrane damages. It is because the deformation made from high pressure could eventually lead to detrimental reverse salt flux and significantly lowered the power density as well as promote the membrane fouling [12,14].

In general, the increase of feed solution salinity has resulted in ICP phenomenon and lower the net driving pressure passing through the membrane. It can be observed that the power density reduced from $5.1 \ W/m^2$ to $4 \ W/m^2$ with the increasing feed salinity by 0.25% using 6% NaCl as draw solution. On the other hand, it was noticed that at a hydraulic pressure of 13 bar, the power density was enhanced from $3.8 \ W/m^2$ to $6.7 \ W/m^2$ when the concentration of draw solution was increased from 6% NaCl to 12% NaCl [3,4]. Saito et al. [15] investigated

**TABLE 11.1** Performance of HTI CTA Membrane for Power Generation in PRO Process

| Feed solution | Draw solution | Power density (W/m$^2$) | Hydraulic pressure (bar) | References |
|---|---|---|---|---|
| 3% NaCl | 6% NaCl | 0.73 | 9.3 | [3] |
| 3% NaCl | 6% NaCl | 2.1 | 12.6 | [3] |
| 3% NaCl | 12% NaCl | 3.2 | 12.6 | [3] |
| 0.06% NaCl | 6% NaCl | 3.8 | 13 | [34] |
| 0.06% NaCl | 12% NaCl | 6.7 | 13 | [34] |
| Deionized water | Seawater | 2.7 | 9.7 | [4] |
| Deionized water | 6% NaCl | 5.1 | 9.7 | [4] |
| 0.25% NaCl | 6% NaCl | 4 | 9.7 | [4] |
| 0.25% NaCl | Seawater | 2.4 | 9.7 | [4] |
| 0.5% NaCl | Seawater | 2.2 | 9.7 | [4] |
| 0.5% NaCl | 6% NaCl | 4 | 9.7 | [4] |

the performance of a CTA hollow fiber membrane manufactured by Toyobo, Japan for power generation in PRO process. The salinity gradient was created between concentrated brine from an SWRO system and feed water from treated sewage. The power density of 7.7 W/m$^2$ was achieved in the prototype PRO plant at 25 bar [15]. However, severe fouling was observed due to the small lumen size of the CTA hollow fiber membrane. To address the fouling issues, it was recommended to control the feed and draw solution quality through pretreatment. Fu et al. [16] also investigated the performance of a dual-layer hollow fiber membrane fabricated via dry-jet wet phase inversion which made up of polybenzimidazole selective outer layer, and polyacrylonitrile inner substrate layer process. The power density of 5.1 W/m$^2$ was harvested at 15 bar when 1 M NaCl and 10 mM NaCl were used as the draw solution and feed, respectively [16].

## 11.5  THIN FILM COMPOSITE MEMBRANE

Besides CTA membrane in flat sheet or hollow fiber configurations, TFC membranes are also attempted for power generation via PRO process. TFC membranes consist of asymmetric porous support at the bottom and a thin selective skin layer at the in which functioning as to provides

the mechanical strength and performs the separation respectively. Owing to its unique structure, TFC membranes possess several advantages such as higher water permeability, durable and greater ability to withstand a wide range of feed pH. However, TFC membranes also exhibit some limitations such as poor tolerance toward oxidants and chlorine chemicals. In the typical fabrication process, PRO TFC membranes are fabricated similarly to that of RO TFC membrane. In brief, the fabrication involves the preparation of a porous support substrate through phase inversion and followed by the formation of PA salt selective layer which is prepared through IP methods [3,17]. During the IP, two reactive monomers which are dissolved in two phases of solvents (organic and aqueous) are allowed to react on the highly porous polymeric support. The IP process allows the formation of a highly crosslinked and ultrathin salt-selective PA layer which dictates the salt rejection performance of the resultant membrane [8]. Due to the high salt-rejection ability and high chemical resistance, PA-TFC membranes are known to be one of the most promising materials for PRO. At present, most of the TFC-PRO flat sheet and hollow fiber membranes are produced by IP of m-phenylenediamine (MPD) and trimesoyl chloride (TMC) [8]. Li et al. [18] prepared TFC-PRO flat-sheet membranes with PA selective layer of different free volumes. Methanol posttreatment was performed to swell up the PA chains. The study revealed that a moderate increase in PA free volume was helpful to enhance the water permeability despite a negligible decrease in salt rejection. This modification approach is beneficial to improve the water flux, hence the power density. Nevertheless, at very high PA free volume, both power density and membrane selectivity were undesirably deteriorated due to the reverse salt flux and ICP effects. Han et al. [19] fabricated a TFC flat sheet membrane for PRO by forming the PA selective layer atop of customized Matrimid membrane support which characterized with full sponge-like structure. The structure allowed the membrane to demonstrate greater mechanical strength hence able to withstand a hydraulic pressure up to 15 bar. Additionally, the PA layer was posttreated with hypochlorite and methanol to enhance the transporting properties. As a result, the modified TFC membrane exhibited an enhanced water permeability. However, a trade-off was observed where the salt rejection was sacrificed [19].

In another study, Zhang et al. [14] fabricated TFC flat sheet membranes on polyacrylonitrile (PAN) supports. It was reported that the post ethanol treatment could positively affect the mechanical strength, pore structure and hydrophilicity of the supporting layer as well as the formation of the PA layer. The PA selective layer can be strengthened by the ethanol treatment to enhance both water flux and withstand hydraulic pressure up to 10 bar, and about 2.6 W/m$^2$ power density was obtained. The study

done by Han et al. [19] reported about the posttreatment using NaOCl. The modification made on the substrate allowed the formation of thinner PA layer without affecting its structural stabilities under the high-pressure PRO process. The primary factor for the high compressive resistance to withstand a hydraulic pressure of 15 bar is the high toughness support. Because the structural parameter was reduced, the power density of 7–12 W/m$^2$ at different feed and water salinity can be produced. It has been reported that the stronger polar aprotic solvents like *N,N*-dimethylformamide (DMF) were used to posttreat the PA layer [18]. This study concluded that the existence of more free volume and voids in the selective layer had facilitated higher water flux in which the highest power density of 18.09 W/m$^2$ was harvested at 22 bar.

## 11.6 THIN FILM NANOCOMPOSITE

TFN membrane is a new type of composite membranes prepared via IP process. The term "TFN membrane" was used by Hoek and his co-workers in their pioneering research work published in early 2007 [17]. Generally, to fabricate a TFC membrane with desired performance, a wide range of nanosized materials such as zeolite and carbon nanotubes (CNT) have been explored. They own exceptional structural properties and surface functionalities regarding enhanced hydrophilicity, antimicrobial functionality, water flux and osmotic power and mechanical property. Hence, by incorporating these nanomaterials in TFC membrane, a high performance of TFN membrane could be fabricated [9]. Verification has been done experimentally and theoretically that CNTs can provide a fast water transport. Thus, CNTs have been proposed as one of the potential nanomaterials which able to improve the water flux in TFC membrane [20].

Tian et al. [21] have designed a novel tiered polyetherimide (PEI) nanofibrous support for the fabrication of PRO composite membrane. PEI was reinforced with functionalized carbon nanotubes (fCNTs) to improve the mechanical property in order to withstand the high-pressure PRO process without imparting the ICP effect to the membrane [21]. The results showed that CNTs can act as a strong reinforcing agents to remarkably strengthen the PEI polymeric nanofibers. It was also found that the water permeability coefficient of the TFN membranes was 10 times higher than the commercial HTI-CTA membrane. The result obtained when using 1.0 M NaCl and DI water as draw solution and feed solution respectively, the peak power density was up to 17.3 W/m$^2$ at 16.9 bar hydraulic pressure. Other than exhibiting advantages such as the improved water

permeability and separation performance, higher mechanical strength and thermal resistance, the TFN is also endowed with anti-fouling properties through the incorporation of nanomaterials which show anti-microbial features. One of these examples is silver nanoparticles (AgNPs) which is found to be effective against various aquatic microorganism [22]. They destroy the microorganisms via direct interaction with cell membranes. In the study performed by Liu et al. [22], PAN was selected as a support material due to its excellent chemical stability and excellent chemical tunability. Hydrolysis was carried out to alter the chemical structure of PAN support in order to improve to adhesion between the PA layer and the support interface. AgNPs with different weight concentrations were physically mixed into the membrane through the simple blending during dope formulation followed by the typical phase inversion technique to fabricate the polymeric membrane substrates [22]. The membrane selective layer of nanocomposite osmotic membranes was formed with layer by layer (LbL) assembly method [22]. Fig. 11.5 illustrates the proposed schematic (cross-section) of the silver nanocomposite osmotic membrane. The result obtained showed that the introduction of AgNPs has improved the hydrophilicity of the PAN substrates and render anti-fouling properties to the PRO membranes. The TFN incorporated with 0.02 wt% AgNPs demonstrated approximately 25% enhancement water permeability when tested in PRO Apart from that, due to the excellent anti-bacterial properties displayed by the AgNPs against Gram-positive *B. subtili*s and Gram-negative *E. coli*, it was observed that less biofilms were formed on the surface of the TFN and the flux decline can be minimized. The water flux was enhanced by 88.2% and the biofilm decreased from $95.9 \pm 3.2\%$ to $69.2 \pm 5.3\%$ [20].

Son et al. [2] synthesized a TFN membrane by using CNT-embedded-polyethersulfone (PES) as a support layer and PA as an active layer. When the membranes were tested using 0.5 M NaCl solution at the draw side, and DI water at the feed side, the water flux and maximum power density



Feed solution
Membrane support layer
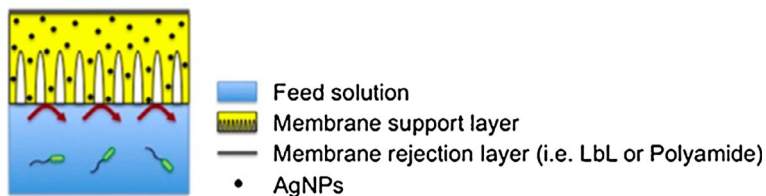Membrane rejection layer (i.e. LbL or Polyamide)
AgNPs

FIG. 11.5    Proposed schematics (cross-section) of the silver nanocomposite osmotic membrane [22].

of the developed TFN membrane was found to be improved by 87% and 110% compared to TFC membranes, respectively [23]. The presence of CNTs and the surface modification through chemical etching has promoted the increase of water flux attributed to the enhanced porosity and the hydrophilicity of the support layer. Fig. 11.6A illustrates that the formation of the voids at the surrounding of CNT has increased the porosity, volume and diameter meanwhile the carboxylic and carbonyl groups which were found on the CNT surface has improved the hydrophilicity of the membrane. However, this study discovered a relatively low power density which is in the range of 0.5–1.6 W/m$^2$ as shown in Fig. 11.6B hence revealed that the osmotic power density resulted in this
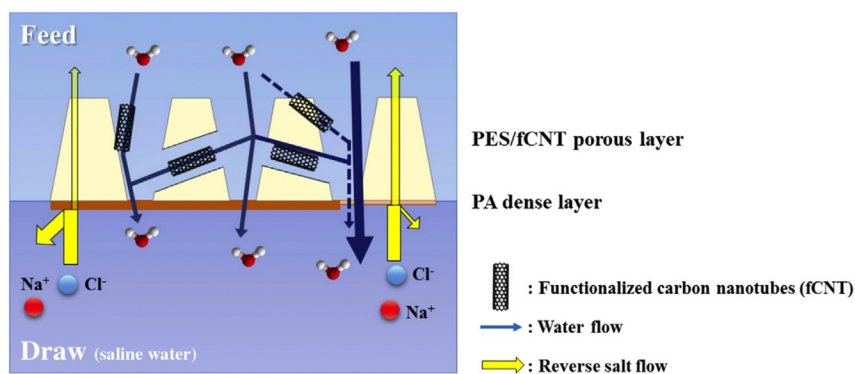


(A)
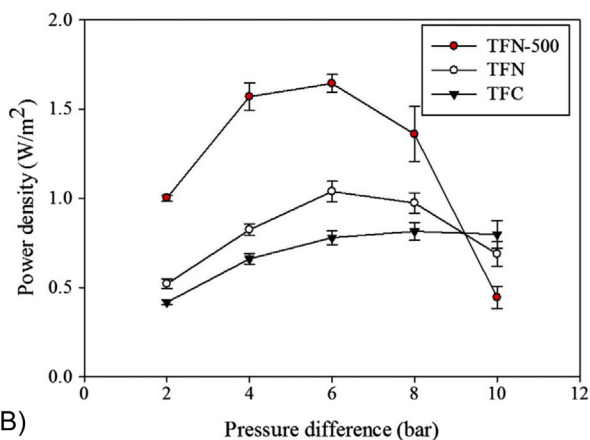


(B)

FIG. 11.6 (A) A schematic illustration of the roles of CNTs in increasing the porosity and hydrophilicity of the TFN membranes. (B) The power density tested in the study [2].

study still do not reach the commercial expectation. Nevertheless, it has been evidenced that CNT embedded within the support layer has several benefits compared to TFN membrane with CNT incorporated in the active layer [23,24]. The CNT can be stabilized within the polymer matrix with less agglomeration owing to the interactions between the sulfonic groups of the polymeric backbones and the carboxylic groups present on the CNT through hydrogen bonding. The active layer properties of the membrane remained intact, hence allowed the optimized water flux and power density. It is also found that the incorporation of CNTs at the support layer requires conventional phase inversion technique and less complicated steps, hence can be easily scaled up [23,24].

## 11.7  FOULING IN PRO

Membrane fouling is an important factor that restricts the PRO performance, especially when a long-term operation commercial-scale plant is taken into consideration [25]. As well agreed, fouling in RO can negatively affect the quality of permeate water, membrane lifespan and the required expenses of maintenance. Although the fouling issue in PRO is recognized to be less severe than that in those pressure-driven processes due to the lower applied hydraulic pressure, the negative impacts resulted from fouling should be carefully considered for their applications. Due to the orientation of the PRO membrane (i.e., active layer facing the draw solution and support layer facing the feed solution, foulants found in the feed solution are expected to deposit within the support layer. As such, an ideal PRO membrane should also be designed by considering the phenomenon of membrane fouling, as it significantly affects the osmotic power production for practical applications [26].

Practically, many types of feed solutions low salinity can be used in PRO processes. These include wastewater effluent, river water, and brackish water [27]. Hence organic foulants are found everywhere in those feed solutions thus can give severe fouling problems and affect the PRO performance. It may lead to PRO performance decay including power density and water flux. So, it is essential to focus on the development of effective PRO fouling control strategies [12]. Wan and Chung [27] observed up to 80% deterioration of PRO performance when the feed solution was changed from the deionized water a wastewater retentate. This incident was due to the severe fouling on the porous membrane substrate. She et al. revealed that, in an osmotically driven membrane process, besides feed solution composition, organic fouling is also significantly affected by the draw solution composition [12]. In fact, the mechanism of reverse solute diffusion also has a significant influence on the organic fouling. It has also been demonstrated that the solutes reversely diffusing from draw

solution into feed solution have potential to interact with the foulants in the feed solution [12,26]. Because that kind of diffusion also occurs in PRO process, the mechanism is likely applicable for PRO fouling.

Up to the present, some studies have been performed to provide useful information on the PRO fouling mechanisms [12,13,19,25,28,29]. Organic fouling behavior in PRO has been studied based on different operating conditions like hydraulic pressure, types, and concentration of draw solutions, types of foulant as well as the pH [12,19]. The fouling PRO due to the deposition of natural organic matter (NOM) found in the feed water has been investigated using CTA and TFC membranes [13,25]. She et al. have systematically investigated the impact of organic fouling on PRO power density based on abovementioned operating conditions [12]. The findings showed that severe alginate fouling occurred when a large number of divalent cations such as $Ca^{2+}$ and/or $Mg^{2+}$ present in the draw solution. This further indicated that the organic fouling is strongly influenced by the ions present in the draw solute as well as their rate of diffusion into the feed solution and their ability to interact with feed foulant. High reverse solute diffusion and initial water flux tend to increase the draw solution concentration and speed up the PRO fouling. On the other hand, they also concluded that, with the increasing applied pressure, the PRO fouling is dictated by the competing results of reduced initial water flux level and elevated reverse solute diffusion. As such, the increase of applied hydraulic pressure was observed to reduce the alginate fouling for NaCl draw solution but worsened the fouling for $CaCl_2$ draw solution due to the competing effects [12].

A recent study conducted by Kim et al. [30] demonstrated that cake layer buildup at the membrane surface is the main contributor the colloidal fouling. The fouling was further worsened with the diffusing salt from the draw solution as the retained salt could increase the salt accumulation on the membrane hence drastically affected the driving force in the PRO system. As a result, substantial flux decline was observed due to the high resistance of the void-less cake layer. Based on the established mitigation strategy, it was found that the adjustment of feed solution pH was the most effective approach to reduce the colloidal fouling, as a result of the particle stabilization at lower pH [30].

## 11.8  PRO HYBRID SYSTEM

The hybrid of PRO with other well-established desalination technologies such as FO and RO has been addressed as an attractive approach to reduce the cost of seawater desalination as well as to alleviate the environmental impact resulted from the direct brine disposal. Even though the hybrid system normally requires more membrane area, the energy

consumption, hence the total desalinated water cost can be significantly reduced. This target can be achieved by diluting seawater or using RO concentrate as feed water in the PRO process. Therefore, compared to the single PRO system, the RO-PRO system is operated with a higher concentration of draw solution. Another significant advantage of this hybrid system is that the draw solution, which is the concentrated brine from RO, has been pretreated in the RO system. This indicates that the brine contains relatively fewer foulants. This is advantageous as it could eliminate the additional energy needed for the pretreatment of single PRO system [31]. Sidney Loeb has proposed the most straightforward RO-PRO hybrid system. In this hybrid system, RO brine concentrate was used as the PRO feed solution. Sidney's work has demonstrated that the coupling the RO-PRO process holds excellent potential for simultaneous desalination and power generation [31].

The modeling of RO-PRO hybrid has been performed by Prante et al. [32]. In their studies, the specific energy consumption (SEC) of the RO-PRO hybrid system was modeled based on the thermodynamic restriction of RO condition using CTA membranes. The findings showed that about 40% reduction is SEC compared to the conventional RO seawater desalination could be achieved. The sensitivity analysis revealed the effects of membrane characteristics on the specific energy production of the PRO process in which the SEC was estimated to be 1.0 kW h per $m^3$ of RO permeate at 50% RO recovery with a maximum power density of around 10 $W/m^2$. The hybrid of RO-PRO has also been proposed in the Japanese's Mega-ton project [33]. This plant has applied PRO as the energy recovery system of seawater RO in which the concentrated RO brine and fresh water collected from the regional water treatment facility were used as the draw and feed solution, respectively. Throughout the 1 year of operation using 10-in. CTA hollow fiber membrane modules, the maximum membrane power density of 13.5 $W/m^2$ has been reported. Based on the operating conditions of Mega-ton PRO prototype, the researchers have estimated the potential market of PRO as 1–2 GW with 10% of energy saving of the RO plants.

## 11.9  CONCLUSION AND FUTURE PROSPECTIVE

PRO is known to be feasible in term of application for power generation. This technology has been acknowledged as one of the most commonly known salinity gradient energy approaches that based on membrane technology. Basically, the major components of the PRO power plant are PRO membrane module and hydroturbine system which is used to convert the hydraulic energy to electricity [11,12]. The present research progress of osmotic power is proliferating. However, energy harvesting using osmotic power still remains challenging for commercial viability.

Membrane characteristics have been recognized as one of the most crucial element that dictates the performance of PRO. Somehow, PRO membrane structure has similarity with RO membrane however PRO membrane's porous support layer is thinner than the conventional RO membrane. In addition, the mechanical strength should be improved to withstand the high hydraulic pressure applied on the draw solution side. Currently, significant advances have been made to heighten the performance of PRO membranes. Advanced techniques such as layer by layer deposition and electrospinning have also provided viable routes to further enhance the desired properties of the PRO membranes. Another critical development in PRO membrane is most probably the interplay between nanomaterial sciences and membrane technology to introduce different unique and exceptional functionalities to further heighten the membrane performance.

Some of the membrane-related issues are their susceptibility to ICP and fouling. At present, the most promising commercially available membranes for PRO are those produced for FO desalination. However, the low power density is still a significant hindrance to be overcome. Technical and economic feasibility is also a significant concern in developing PRO for energy harvesting. Issue has been raised regarding the parasitic process energy requirements of PRO system, which can be related to the water conveyance and prefiltration. A study has been done in investigating a lower bound cost scenario for power generation with PRO to evaluate its economic viability. The study is all about the future economic viability of PRO by pushing the limits of PRO membrane technology in their models. Firstly, two potential methods of reducing the LCOE: harnessing economies of scale and improving membrane performance were identified. The minimum levelized cost of electricity (LCOE min) is reduced by 42% as the net power production is increased from 2 to 75 MW [34]. It was found that by decreasing the structural parameter, results in a more significant decrease in LCOE min than increasing the membrane permeability. With these unique analyses, it conclusively demonstrated that PRO has potential to be economically viable only if extremely high draw salinity is used (at least above 18%). Therefore, it was suggested that future PRO research be focused on challenges associated with implementing highly saline draw solutions [34]. Also, based on the experiences of Statkraft, the generation of 5 W/m$^2$ osmotic power is required to economical break-even in order to be positioned in the same commercial competitiveness as conventional RO membranes. Despite the promising findings reported using lab-scaled membranes, which can reach up to 10 W/m$^2$, the main challenges to be looked into are the availability of high performance and affordable bulk PRO membrane in the marketplace.

In conclusion, despite the great number of studies on the potential of PRO in desalination and energy harvesting, more research is still needed

to provide further insights into the potential and issues of this technology. Membrane design and optimization of operating conditions are some keys to the successful implementation of PRO in commercial scale. It is believed that, with the advancement made in the near future, perhaps in the next 10 years, PRO will represent a membrane technology that shows great promise to address the global challenges in water and energy supply.

## Acknowledgment

## References

[1] Han G, Zhang S, Li X, Chung TS. Progress in pressure retarded osmosis (PRO) membranesfor osmotic power generation. Prog Polym Sci 2015;51:1–27.

[2] Son M, Park H, Liu L, Choi H, Kim JH, Choi H. Thin-film nanocomposite membrane with CNT positioning in support layer for energy harvesting from saline water. Chem Eng J 2016;84:68–77.

[3] Altaee A, Sharif A. Pressure retarded osmosis: advancement in the process applications for power generation and desalination. Desalination 2015;356:31–46.

[4] Altaee A, Zaragoza G, Sharif A. Pressure retarded osmosis for power generation and seawater desalination: performance analysis. Desalination 2014;344:108–15.

[5] Sarp S, Li Z, Saththasivam J. Pressure Retarded Osmosis (PRO): past experiences, current developments, and prospects. Desalination 2016;389:2–14.

[6] Achilli A, Childress AE. Pressure retarded osmosis: from the vision of Sidney Loeb to the first prototype installation-review. Desalination 2010;261:205–11.

[7] Helfer F, Lamckert C. The power of salinity gradients: an Australian example. Renew Sust Energ Rev 2015;50:1–16.

[8] Nagy E, Dudas J, Hegedus I. Improvement of the energy generation by pressure retarded osmosis. Energy 2016;116:1323–33.

[9] Ghanbari M, Emadzadeh D, Lau WJ, Lai SO, Matsuura T, Ismail AF. Synthesis and characterization of novel thin film nanocomposite (TFN) membranes embedded with halloysite nanotubes (HNTs) for water desalination. Desalination 2015;358:33–41.

[10] Nezam El-Din LA, El-Gendi A, Ismail N, Abed KA, Ahmed AI. Evaluation of cellulose acetate membrane with carbon nanotubes additives. J Ind Eng Chem 2015;26:259–64.

[11] Badawi NE, Ramadan AR, Esawi AMK, El-Morsi M. Novel carbon nanotube-cellulose acetate nanocomposite membranes for water filtration applications. Desalination 2014;344:79–85.

[12] She Q, Willis Wong YK, Zhao S, Tang CY. Organic fouling in pressure retarded osmosis: experiments, mechanism, and implications. J Membr Sci 2013;428:181–9.

[13] She Q, Hou D, Liu J, Tan KH, Tang CY. Effect of feed spacer induced membrane deformation on the performance of pressure retarded osmosis (PRO): implications for PRO process operation. J Membr Sci 2013;445:170–82.

[14] Zhang M, Hou D, She Q, Tang CY. Gypsum scalling in pressure retarded osmosis: experiments, mechanisms, and implications. Water Res 2014;48:387–95.

[15] Saito K, Irie M, Zaitsy S, Sakai H, Hayashi H, Tanioka A. Power generation with salinity gradient by pressure retarded osmosis using concentrated brine from SWRO system and treated sewage as pure water. Desalin Water Treat 2012;41:114–21.

[16] Fu FJ, Sun SP, Zhang S, Chung TS. Pressure retarded osmosis dual-layer hollow fiber membranes developed by co-casting method and ammonium persulfate (APS) treatment. J Membr Sci 2014;469:488–98.

[17] Ismail AF, Padaki M, Hilal N, Matsuura T, Lau WJ. Thin film composite membrane—recent development and future potential. Desalination 2015;356:140–8.

[18] Li X, Chung TS. Effects of free volume in thin-film composite membranes on osmotic power generation. AIChE J 2013;59:4749–61.

[19] Han G, Zhang S, Li X, Chung TS. High performance thin film composite pressure retarded osmosis (PRO) membranes for renewable salinity-gradient energy generation. J Membr Sci 2013;440:108–21.

[20] Yip NY, Elimelech M. Influence of natural organic matter fouling and osmotic backwash on pressure retarded osmosis energy production from natural salinity gradients. Environ Sci Technol 2013;50:12607–16.

[21] Tian M, Wong R, Goh K, Fane AG. Synthesis and characterization of high- performance novel thin film nanocomposite PRO membranes with tiered nanofiber support reinforced by functionalized carbon nanotubes. J Membr Sci 2015;486:151–60.

[22] Liu X, Fu LX, Li JY, Cao B, Tang CY. Fabrication and characterization of nanocomposite pressure retarded osmosis (PRO) membranes with excellent anti-biofouling property and enhanced water permeability. Desalination 2016;389:137–48.

[23] Kim DI, Kim J, Hong S. Changing membrane orientation in pressure retarded osmosis for sustainable power generation with low fouling. Desalination 2016;389:197–206.

[24] Wong KC, Goh PS. Gas separation of thin film nanocomposite membranes incorporated with polymethyl methacrylate grafted multi-walled carbon nanotubes. Int Biodeterior Biodegrad 2015;389:339–45.

[25] Kim J, Lee J, Kim SH, Kim JH. Impact of hydraulic pressure and pH on organic fouling in pressure retarded osmosis (PRO). Desalin Water Treat 2015;57:10121–8.

[26] Emadzadeh D, Lau WJ, Matsuura T, Hilal N, Ismail AF. The potential of thin film nanocomposite membrane in reducing organic fouling in forward osmosis process. Desalination 2014;348:82–8.

[27] Cheng ZL, Chung TS. Mass transport of various membrane configurations in pressure retarded osmosis (PRO). J Membr Sci 2017;537:160–76.

[28] Tiraferri A, Yip NY, Philip WA, Schiffman JD, Elimelech M. Relating performance of thin-film composite forward osmosis membranes to support layer formation and structure. J Membr Sci 2011;367:340–52.

[29] Das R, Ali ME, Hamid SBA, Ramakrishna S, Zaman ZC. Carbon nanotube membranes for water purification: a bright future in water desalination. Desalination 2014;336:97–109.

[30] Kim J, Park MJ, Park M, Kim SH, Kim JH. Influence of colloidal fouling on pressure retarded osmosis. Desalination 2016;389:207–14.

[31] Skilhagen SE. Osmotic power—a new, renewable energy source. Desalin Water Treat 2010;15:271–8.

[32] Jeri L, Prante JA. RO-PRO desalination: an integrated low-energy approach to seawater desalination. Appl Energy 2014;120:104–14.

[33] Sakai H, Ueyama T, Irie M, Matsuyama K, Tanioka A, Saito K, Kumano A. Energy recovery by PRO in sea water desalination plant. Desalination 2016;389:52–7.

[34] Chung HW, Banchik LD, Swaminathan J, Lienhard JH. On the present and future economic viability of stand-alone pressure-retarded osmosis. Desalination 2017;408:133–44.

## Further Reading

[35] Sivertsen E, Holt T, Thelin W, Brekke G. Modelling mass transport in hollow fiber membranes used for pressure retarded osmosis. J Membr Sci 2012;417-418:69–79.

# Adsorptive Membranes for Heavy Metals Removal From Water

*Mohd Ridhwan Adam, Siti Khadijah Hubadillah, Mohamad Izrin Mohamad Esham, Mohd Hafiz Dzarfan Othman, Mukhlis A. Rahman, Ahmad Fauzi Ismail, Juhana Jaafar*

**Advanced Membrane Technology Research Centre (AMTEC), Faculty of Chemical and Energy Engineering, Universiti Teknologi Malaysia, Skudai, Malaysia**

O U T L I N E

## 12.1 INTRODUCTION

"Water is life's mater and matrix, mother and medium. There is no life without water" is a well-known quote given by Albert Szent-Györgi, who was a Hungarian biochemist and won the Nobel Prize in Physiology or Medicine in 1937 [1]. Nowadays, the most significant problem that the world is facing today is that of water pollution which causing grave and irreparable damage to the earth. Heavy metal in anionic or cationic forms is one of the dangerous contaminants that can be found in water resulting from manufacturing and mining processes. Some of them are lead (Pb), chromium (Cr), arsenic (As), mercury (Hg) and nickel (Ni). These heavy metals can be found in the water by natural or anthropogenic sources. For instance, these heavy metals are toxic and poisonous even at low concentration, thus, can threaten human beings and animals.

Lead is heavy metal that can cause severe damage to nervous system, kidney, reproductive system and brain [2]. According to Ajitha et al., lead enters the water sources (drinking or wastewater) from various industrial activities such as metal plating, printing and pigment, and finishing, ammunition, battery manufacturing, ceramic and glass industries, soldering material, iron and steel manufacturing [3]. Meanwhile, Goyer and Chisolon stated that contamination of this lead heavy metal in drinking water occurs due to the corrosion and leaching of lead pipes and Pb/Sn solder joints associated with copper services lines used in household plumbing [4]. Recently, a review has been done on an update on childhood lead poisoning [5]. Surprisingly, it was reported in 2012, the Centers for Disease Control & Prevention (CDC) lowered the reference value of blood level (BLL) to 5 µg/L due to 3.6 million American homes with at least one child have significant lead paint hazards. In 2014, nationally U.S. Poison Control Centers (PCC) received 2, 241 calls on possible lead exposure. This is according to Weidenhamer and Yost, toys were sometimes painted with lead-based paint, and some plastic toys have lead added as a softener [6, 7]. It should be mentioned that a child who ingested lead charm was reported died of lead poisoning in 2006 [8].

Chromium exists in two oxidation states which are Cr (III) and Cr (VI), due to the environmental condition [9]. Cr (III) is a bio-element, but Cr (VI) is more toxic than Cr (III) [10]. Chromium exists in the environment by natural input such as volcanic eruptions and geological weathering. Whilst, anthropogenic activities such as the burning of fossil fuels, plastic manufacturing, electroplating of metals and tannery industries are the main reason for chromium poisoning toward human being [11]. Table 12.1 summarizes the use of chromium in various industries. Cr (VI) can cause various health issues by entering into an alimentary tract of the living organism via either breathing in dust, fumes or mist or skin contact with solutions can create more significant health risks. In this regard, health issues such as cancer in respiratory track, irritation in the

**TABLE 12.1**  Use of Chromium in Various Industries [12]

| Industry | Application |
|---|---|
| Metallurgical industry (90%) | Ferrous alloys (steel, cast iron) |
| | Nonferrous alloys (Ni, Al, Cu) |
| Refractory and foundry (5%) | Fiberglass furnace, cement kiln |
| | Mag-chrome refractories |
| | Glass tank regenerator |
| Chemicals (5%) | Chrome plating |
| | Metal finishing |
| | Tanning |
| | Corrosion control |

upper respiratory tract, injury in the nasal septum and inflammation in the nose. Also, Cr (VI) also causes skin problem. Table 12.2 lists the health hazard caused by Cr (VI) and way of exposure.

Arsenic is known as "King of poison" and labeled as the 20th most common element in the Earth's crust [13]. Arsenic contamination in water especially drinking water sources has become a series environmental and health concern because of its toxicity on human beings and other living organisms. According to Almberg et al., arsenic has been classified as Group 1 carcinogen to human as it is linked to some cancers [14]. Like chromium, arsenic also exists primarily as an inorganic form in water which is arsenite [As (III)] and arsenate [As (V)]. Compared with As (V), As (III) is 60 times more toxic to human and has higher mobility in the environment. Similar to the way of other heavy metal exposure, arsenic enters water through anthropogenic activities such as gold mining, nonferrous smelting, petroleum refining and the use of pesticides. Some developing countries, such as India and Bangladesh use groundwater sources. Due to this arsenic toxicity, these countries have been reported to have the highest arsenic contamination problem. Table 12.2 lists other heavy metals that contaminated in water, a way of exposure, its effect on human and environment and drinking water standards.

## 12.2  A CONVENTIONAL TECHNIQUE FOR HEAVY METALS REMOVAL

Over the last few decades, conventional treatment methods such as ion-exchange, coagulation-flocculation, adsorption and membrane technology have been widely used for the heavy metal removal to fulfill the strict environmental regulations. The conventional methods are discussed in the following subsections.

**TABLE 12.2**    List of Other Heavy Metal Found in Drinking Water Sources

| Heavy metals | Way of exposure | Effects | Drinking water standards | Ref |
|---|---|---|---|---|
| Nickel [Ni(II)] | • The manufacturing process of stainless steel, super alloys, metallic alloys, electroplating, and batteries | • Lung and kidney problems<br>• Gastrointestinal distress<br>• Headache<br>• Skin dermatitis | • Environmental Protection Agency (0.1 mg/L)<br>• European Community (0.1 mg/L)<br>• Regulation of water quality-India (0.1 mg/L)<br>• Malaysian standard (0.02 mg/L) | [15] |
| Copper [Cu(II)] | • Industrial activities: galvanizing, petroleum refining, metal finishing, paint, and pigments production, coal mining, smelting, and electroplating | • Long term exposure: damage to kidney, liver, pancreas, and brain<br>• Hemostasis, hypotension, melena. Coma, jaundice, gastrointestinal disease | • Environmental Protection Agency (1.0 mg/L)<br>• European Community (3.0 mg/L)<br>• Regulation of water quality-India (0.01 mg/L)<br>• Malaysian standard (1.0 mg/L) | [16–18] |
| Zinc [Zn(II)] | • Travel through the food chain via bioaccumulation<br>• Galvanizing industries | • Stomach cramps<br>• Skin irritation<br>• Vomiting<br>• Nausea<br>• Anemia | • Environmental Protection Agency (5.0 mg/L)<br>• European Community (5.0 mg/L)<br>• Regulation of water quality-India (0.1 mg/L)<br>• Malaysian standard (3.0 mg/L) | [19] |
| Cadmium [Cd (II)] | • Metal industries<br>• Pigment industries<br>• Plastic manufacturing<br>• Polymer production<br>• Electroplating<br>• Nickel-cadmium batteries<br>• Photography company | • Renal disorder<br>• Osteomalacia<br>• Cancer<br>• Anemia<br>• Bronchitis<br>• Nephrotoxicity | • Environmental Protection Agency (0.005 mg/L)<br>• European Community (0.2 mg/L)<br>• Regulation of water quality-India (0.1 mg/L)<br>• Malaysian standard (0.003 mg/L) | [20] |

**TABLE 12.2**  List of Other Heavy Metal Found in Drinking Water Sources—cont'd

| Heavy metals | Way of exposure | Effects | Drinking water standards | Ref |
|---|---|---|---|---|
| Mercury (Hg) | • Atmospheric deposition<br>• Erosion<br>• Urban discharges<br>• Agricultural materials<br>• Mining<br>• Combustion and industrial discharges | • Poisonous<br>• Causes mutagenic effect<br>• Disturb the cholesterol | • Environmental Protection Agency (0.002 mg/L)<br>• European Community (0.001 mg/L)<br>• Regulation of water quality-India (0.004 mg/L)<br>• Malaysian standard (0.001 mg/L) | [21] |
| Chromium (Cr (VI) | • Air (breathing)<br>• Water (drinking and eating)<br>• Dermal (skin penetration) | • Respiratory tract cancer, lung cancer, tuberculosis, nasal irritation, nasal ulcer, cough and cold<br>• Alimentary tract cancer, stomach cancer, bronchospasm, pneumonia, diarrhea | • Malaysian standard (0.05 mg/L) | [12] |

## 12.2.1  Ion Exchange

Ion exchange is a reversible chemical process that allows heavy metals that have similarly charged with ion exchange resin to attach each other [22]. These heave metals include mercury, arsenic, zinc and so on. During this process, the resins exchange hydrogen ions (H+) for the positively charged ions (such as $Ni^{2+}$ and $Cu^{2+}$) and hydroxyl ions (OH−) for negatively charged sulfates, chromates, and chlorides, as illustrated in Fig. 12.1. Because the quantity of H+ and OH– ions is balanced, as a result, clean water is obtained after the treatment.

The key to an ion-exchange process is the type of resin used and heavy metal that aimed to be removed. A study by Mendow et al. showed a novel process for nitrate reduction in water using bimetallic Pd—Cu catalyst supported on ion exchange resin [23]. The catalyst was supported on commercially macroporous ion-exchange resin, using a solution of $PdCl_2$ (8571 mg/L) dissolved in 0.01 M NaCl and 0.01 M HCl. Fig. 12.2 illustrates the mechanism for the Pd—Cu catalyst via an ion-exchange process. As a result, the newly developed resin showed excellent results with possible
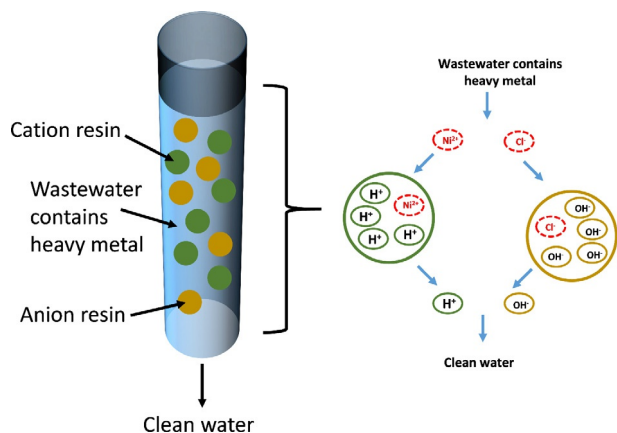
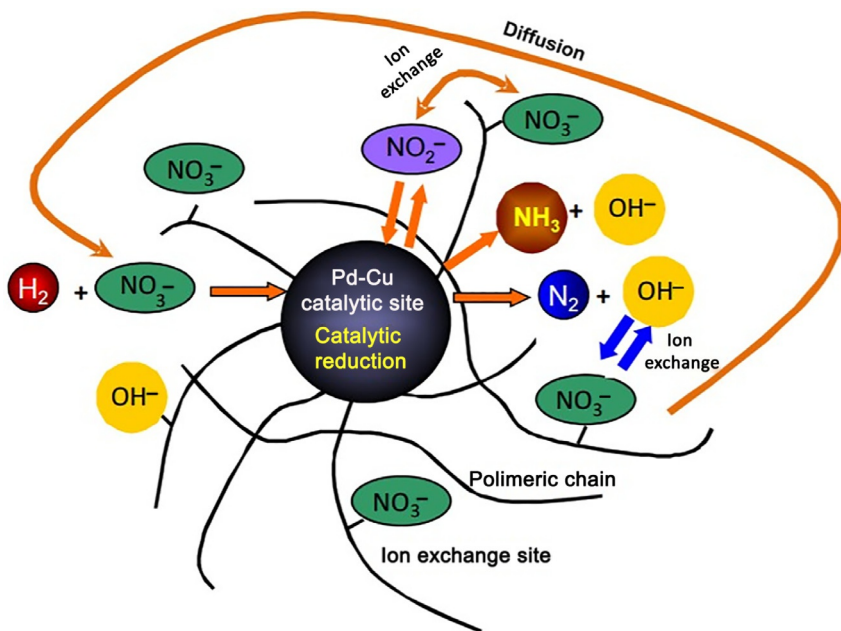**FIG. 12.1**    Mechanism of an ion-exchange process for heavy metal removal.



**FIG. 12.2**    Mechanism for Pd—Cu catalyst on resin during ion-exchange process. *Reproduced with permission from Fig. 1 of Mendow G, Sánchez A, Grosso C, Querini CA. A novel process for nitrate reduction in water using bimetallic Pd-Cu catalysts supported on ion exchange resin. J Environ Chem Eng 2017;5(2):1404–14. License # 4274480797460.*

to eliminate 100% of the nitrates with a final ammonium concentration below 0.5 mg/L and achieved the permissible limit. Another recent study by Lee et al. introduced a new type of ion exchange material to remove arsenic from water [24]. The ion exchanger fiber is relatively developed

material for ion exchanger and has several advantages over conventional ion exchange resins. As a result, As (V) removal efficiency of 98.5% at 60 min was obtained with a capacity of 53 mg/g. Unfortunately, ion exchange was pH dependent, for example, arsenic in this study was efficiently removed at pH 3.04.

## 12.2.2 Coagulation-Flocculation

Coagulation and flocculation are well-known technologies within the wastewater. Indeed, these technologies are essential processes in various disciplines, especially wastewater treatment. It should be noted that coagulation and flocculation can be used as a preliminary or intermediate process during wastewater treatment. For example, they have been used for potable water treatment which clarified using coagulating agents and been practiced for years. They are two different processes but always being used at the same time for wastewater treatment.

Firstly, coagulation with a coagulant such as almonds, alum, and beads. Pioneering work on this technologies, as early as 2000 BCE, was conducted by the Egyptians, who used almonds smeared around vessels to clarify river water. Despite almonds, alum has also been used as coagulant by the Romans in around 77 CE. Interestingly, in 1757, coagulation with alum as coagulant has been practiced in municipal water treatment in England [25]. During the process, coagulants with charges opposite to those of the wastewater are added to neutralize the negative charges on nonsettlable solids. This includes clay and color-producing organic substances. Once the charge is neutralized, the small suspended particles are capable of sticking together.

Secondly, flocculation, where it is a process that involves gentle mixing stage, increases the particle size from submicroscopic microfloc to visible suspended particles. During the process, the particles called microflocs, tend to collision each other. Thus, produce pinflocs through bonding and increase their size. A gradual increase in size is then observed as they continue to bond with inorganic and organic polymers. These particles are then called as macroflocs. Once floc has reached its optimum size and strength, water is ready for sedimentation. Fig. 12.3 shows the complete mechanism of treated water involving coagulation and flocculation.

Coagulation and flocculation process is an essential method in several wastewater treatment operations. Usually, this process was applied before separation through membrane technology, which will be discussed in Section 12.2.4. Untreated wastewater generally contains high levels of organic material, numerous pathogenic microorganisms, nutrients, toxic compounds as well as heavy metals [26]. These wastewaters entail environmental and health hazards and, consequently, must immediately be conveyed away from its generation sources and treated appropriately
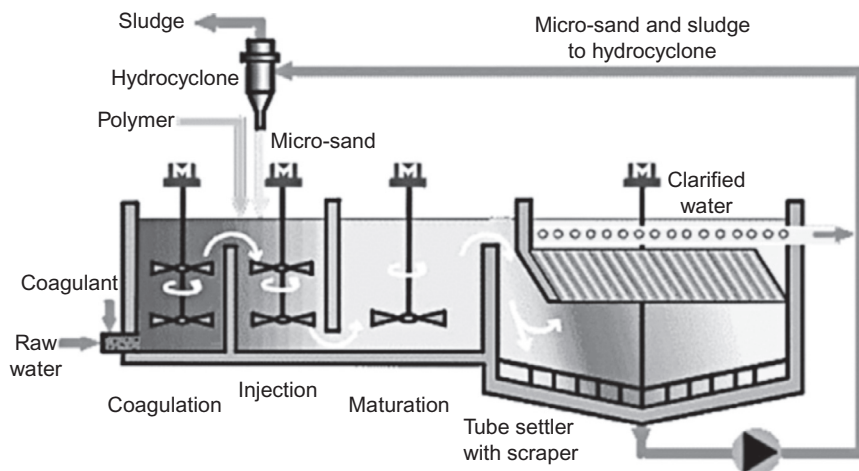
**FIG. 12.3**    Mechanism of coagulation and flocculation in water treatment. *Based on Fig. 1 of Desjardins C, Koudjonou B, Desjardins R. Laboratory study of ballasted flocculation. Water Res 2002;36(3):744–54. License # 4292940918650.*

before final disposal. Ismail et al. investigated these combined process for treatment of municipal wastewater [27]. Alum [$Al_2 (SO_4)_3$], ferrous sulphate [$Fe(SO_4)$], ferric sulphate [$Fe (SO_4)_3$] and lime [$Ca(OH)_2$] were used as coagulants due to their relatively low price. It was found that alum with a quantity of 60 mg/l was the optimum coagulant to treat the municipal wastewater and remove contaminants, especially heavy metals. A recent study by Choumane et al. investigated valorization of a bioflocculant and hydroxyapatites as coagulation and flocculation adjuvants in wastewater treatment of the steppe in the wilaya of Saida (Algeria) [28]. The coagulation and flocculation jar tests of wastewater revealed that ferric chloride, containing a mass of 0.3 g hydroxyapatite is the most effective adjuvant in clarifying the wastewater, with turbidity equal to 98.16%.

## 12.2.3  Adsorption

Adsorption evolved as the most effective techniques for heavy metals removal because the adsorption process offers flexibility in design and operation [29]. Nowadays, there are various forms of adsorbent have been developed such as nanoparticles [30] and beads [31]. Nevertheless, various materials were used as adsorbents such as surfactants [32], synthetic activated carbon [33,34], industrial by-products and wastes [35,36], ferrous material [37,38], iron-based soil amendment [39], and mineral products [40]. More recently, graphene oxide (GO) and its composites have attracted widespread attention as novel adsorbents for the adsorption of various heavy metal contaminants. Peng et al. have made a review of heavy metal ions adsorption from water by graphene oxide (GO) and

its composites [41]. In the review, GO, and its composites are extensively explored as advanced adsorbent materials for the removal of heavy metal ions from water due to their high efficiency, fast kinetics, and strong affinity to various metal ions.

A study by Zhang et al. showed adsorption of lead and mercury from aqueous solution using magnetic $CoFe_2O_4$-reduced graphene oxide [42]. In the work, modified Hummers' method was applied in synthesizing of GO with collaboration through oxidation of graphite powder. Then, a desired amount of GO was first mixed in water by ultrasonication for $CoFe_2O_4$-rGO synthesis. Vigorous stirring was continued for these mixtures. After that, half of NaOH was added to the mixture drop by drop to adjust the solution to pH 12. Interestingly, the as-synthesized solid products were separated by a magnet, washed thoroughly with water and absolute ethanol to remove any impurities, and then dried in a vacuum oven. Fig. 12.4 shows the properties of newly developed $CoFe_2O_4$-rGO.

Another recent study by Su et al. on arsenic removal using iron oxide-graphene oxide nanocomposite adsorbents has been successfully conducted [43]. Fig. 12.5 shows the TEM and high-resolution TEM images of GO, $FeO_x$-GO-36, $FeO_x$-GO-80, and the iron oxide control sample. In
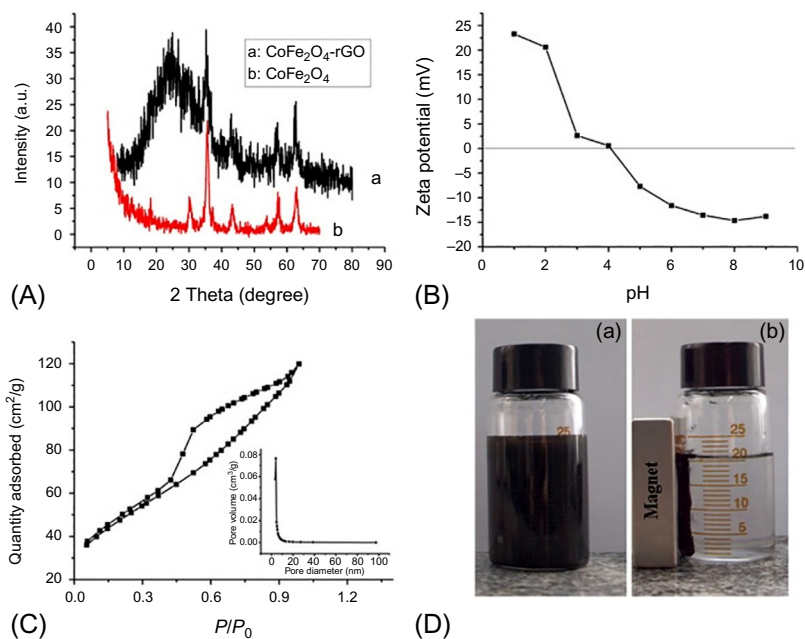


**FIG. 12.4** Properties of newly developed $CoFe_2O_4$-rGO; (A) XRD analysis, (B) zeta potential, (C) BET analysis, and (D) the recovery procedure of $CoFe_2O_4$-rGO. *Data from Fig. 1 of Zhang Y, Yan L, Xu W, Guo X, Cui L, Gao L, et al. Adsorption of Pb(II) and Hg(II) from aqueous solution using magnetic $CoFe_2O_4$-reduced graphene oxide. J Mol Liq 2014;191:177–182. License # 4274481022212.*
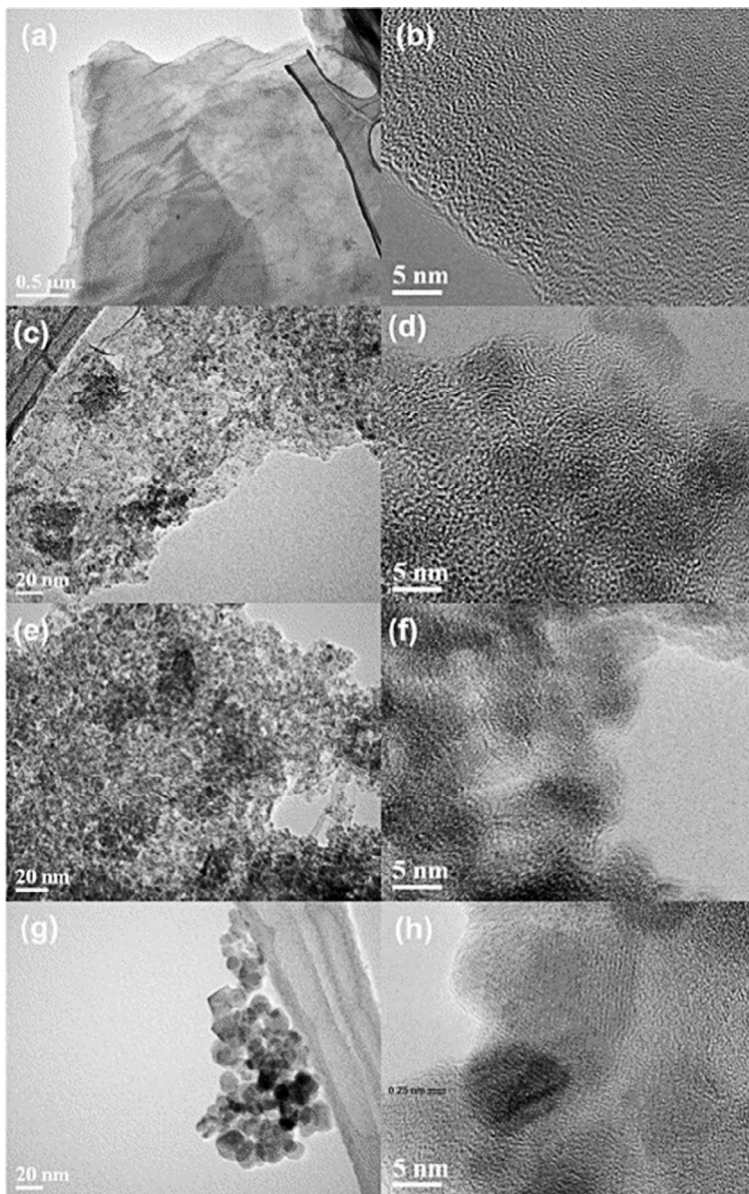
**FIG. 12.5**    TEM and high-resolution TEM images of, (A and B) GO, (C and D) FeO$_x$-GO-36, (E and F) FeO$_x$-GO-80, and (G and H) iron oxide control sample. *Based on Fig. 2 of Su H, Ye Z, Hmidi N. High-performance iron oxide–graphene oxide nanocomposite adsorbents for arsenic removal. Colloids Surf A Physicochem Eng Asp 2017;522:161–72. License # 4274481165441.*

the study, iron oxide-graphene oxide nanocomposite adsorbents show an excellent performance toward adsorption of heavy arsenic metals. It is noteworthy that enhancement of arsenic adsorption capacities is found with the increase of iron oxide content due to the increase in surface area and the generation of more accessible active sites. Overall, the excellent performance shows high $q_{max}$ values of 147 and 113 mg/g for As (III) and As (V), respectively. These values are reported to be the recently highest among all literature reported. Unfortunately, no further study on separation of GO from treated water has been discussed. Accordingly, many studies have been found on a combination of adsorption and membrane separation technologies, which will be discussed in Section 12.3.

## 12.2.4 Membrane Separation Technology

Membrane separation technology, known as worldwide technology has been proven to be a practical and environmental approach to treat wastewater [44]. Earlier investigations toward these technologies were developed from animals such as bladders of pigs, cattle or fish, and sausage casings made of animal gut [45]. However, this investigation fails to pursue further development due to a nonreproducible product. In 1907, Behold introduced nitro cellulose membranes with a graded pore size [46] and the invention has been improved by others. Impressively, by the early 1930s, microporous collodion membranes were ready and commercially available in the market. During the next 30 years, this early microfiltration membrane technology has expanded to other polymers, notably cellulose acetate which is fabricated using phase inversion technique by Loeb and Saurian. [47] This development has made it possible to produce membrane in asymmetric structure. Nowadays, the membrane from various polymeric materials has been widely commercialized worldwide. According to some sources [48], the demand of pure water flux has driven the market for cross-flow membrane equipment and membranes worldwide to increase from \$6.8 billion in 2005 to \$9 billion in 2008. In term of geometry, hollow fiber membrane has received much attention due to its highest surface area (surface area to volume up to 9000 $m^2\,m^{-3}$). This kind of membrane can be produced via phase inversion process.

There are two types of membranes; polymeric membrane and inorganic membrane, as illustrated in Fig. 12.6. In term of pore sizes, there are four types of membrane which are microfiltration (0.05–1.0 μm), ultrafiltration (0.005–0.5 μm), nanofiltration (0.0005–0.01 μm), and reverse osmosis (0.0001–0.001 μm). Accordingly, heavy metals ions were tiny and sometimes they are soluble, such as arsenic, in which it is necessary to reverse the osmosis membrane's size to treat the water. Additionally, the water treated through the RO process may not contained precious minerals such
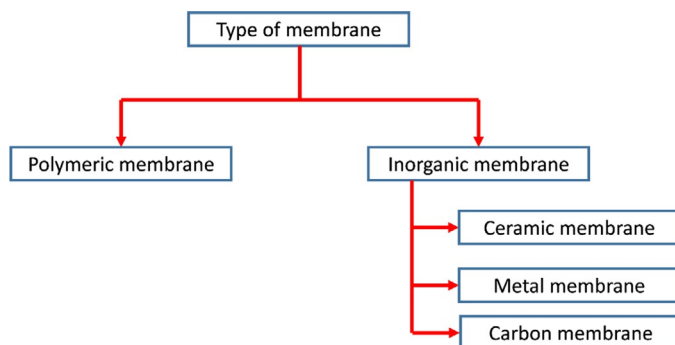
FIG. 12.6 Type of membrane separation.

as calcium and magnesium in which concerned by a human being through drinking water [45]. The hybrid or specifically known as adsorptive membrane that produced by the combination of adsorption and membrane separation processes have been received attention, and discussed in detail in Section 12.3.

## 12.3 HYBRID ADSORPTIVE POLYMERIC MEMBRANES FOR HEAVY METALS REMOVAL

Recently, adsorptive membranes, which combine the advantages of membrane technology and adsorption process, have become as an effective way in removing the heavy metals ions in the aqueous solutions. These membranes' surfaces contain reactive functional groups which include $-NH_2$, $-SO_3H$, and $-COOH$ groups, which used ion exchange or surface complexation mechanism to attract the metal ions. When heavy metal ions are in contact with the membrane surface, it can be removed from aqueous solutions even though the membrane's pore sizes are much more significant than the metal ion dimensions. Compared to the conventional filtration membrane, the advantages of adsorptive membranes are great heavy metal ions retaining performance, plus the lower consumption of energy advantage and also produce better in permeate flux. Also, the membranes process function also can be widening from simple filtration to improved filtration which includes the adsorption.

The elimination of the metal ions using adsorptive membranes also dominance over the adsorptive beads, even though the mechanism of both methods are similar. The adsorptive membranes separation rate are quicker to that of the beads due to the removed heavy metal ions can be transported by convective flow to both internal and external binding sites, rather than slow diffusions to the either internal or external binding sites that is normally occurred in beads systems.

## 12.3.1 Polymeric Membranes

Despite the fact these adsorptive membranes have become a promising solution for the metal ions removal, commercialize feasible adsorptive membranes are very narrowed to inactive polymers, for instance, PVDF, PSF, nylon, polyethylene, and polypropylene (PP). The deficiency of them is an absence of the reactive functional groups. Therefore, surface modification is required to prepare the inert polymer adsorptive membrane, for instance, radiation-induced graft copolymerization method. These methods have often been used for introducing the reactive monomers like acrylic acrylonitrile, acid, acrylamide, and those containing the epoxy-group, such as glycidyl methacrylate, divinylbenzene, onto the surface of the prepared adsorptive membrane. The other example of the methods includes attachment of various dyes chemical to hydrophilic polymer membranes for instance poly (2-hydroxyethyl methacrylate), polyvinyl-butyral, polyvinyalcohol, cellulose and cellulose acetate membrane.

It should be mentioned here that polymeric membranes have gone through the adsorptive membrane modification to gain great adsorption capacity for metal ions, the prepared membranes regularly disintegrated as a result of the severe chemical also a physical treatment for surface modification, or the functional chemicals used to modify the membrane surface are not cost-effective for daily application for metal ions elimination. Another drawback in term of modification of surface which is difficulty in retaining the pore sizes of the membranes as a result of a drastic reduction of membrane performance in permeate flux.

### 12.3.1.1 Natural Polymer

In these past years, some development for removal of heavy metal ions were more focused on using chitosan in fabricating the adsorptive membrane. Chitosan is an abundant natural bio-polymer which obtain a large value of functional group called amine [49]. The chitosan's excellent performance in removing the metal ions in solution has been associated with the potential of the amine functional group which formed surface complexes with many metal ions in aqueous solutions [50]. Chitosan has been found as high-binding-capacity materials [51], usually >1 mM metal/g chitosan, for many heavy ions such as Cu, Hg, Cd, and Pb, and the capacities also have been reported to be even greater than polyaminostyrene, the constituent of expensive ion-exchange-resin.

Nonetheless, almost all past researchers limit the usage of chitosan in the shape of flakes, gel beads, and powder which were very challenging to be applied to practical application and the kinetic adsorption is slow. Because of this, some considerable research interested on preparing high-pack-density chitosan membrane in the form of flat membrane or in the form of hollow fiber membrane for the adsorptive plus separation

purpose which include the removal of the metal ions, but there is limitation in the scope of fabricating the membrane using chitosan due to lack of chemical and mechanical resistance. Insufficient mechanical strength is the most important concern for the usage of pure chitosan as the adsorptive membrane. Some attempts were conducted to overcome this drawback by Premakshi et al. [52]. Applying the chitosan as thin film composites by utilizing proper support, is a straightforward way to enhance the mechanical problem of chitosan flat sheet membrane. Also, to achieve improvement in mechanical resistance, embedding compatible nanobiomaterials has been reported by Karim et al. [15].

The usage of chitosan has been improved and usually been used with the other materials as its supports in the flat membranes to produce composite membranes [53], but there some drawbacks in the method of coating either nonuniform/incomplete coated chitosan on the support membrane or problem with the nonstick coated chitosan. Previously, mixing other polymers with chitosan showed a promising way to counter shortcoming of chitosan, because of the advantages of the method in term of the interaction of chemicals, also improve the usage of chitosan via enhancement of chemical stability and mechanical resistance.

The initial progress has been started by Liu and Bai, fabricated the chitosan adsorptive hollow fiber membrane combined with other polymers, without any extra modification of the surface of the base membranes [54]. In their works, the chitosan hollow fiber membrane enhanced by the blending with cellulose acetate (CA) which produce high porous adsorptive membrane. The prepared membrane was analyzed for the removal of copper (II) metal ions.

The adsorption results showed that the prepared membranes obtained fast rate of adsorption, high capacity of adsorption and short adsorption equilibrium times for copper (II) ions, also run adequately on low concentration of copper (II) ions in reducing the residual level in the solution until as low as 0.1–0.6 mg/L. XPS analysis proved that the copper (II) ions adsorption on the prepared membranes was mostly associated to the surface complexes formed with the nitrogen atoms of chitosan in the membranes; thus the membranes become more adsorptive to copper (II) ions because the presence of chitosan in the prepared hollow fiber membranes is high. The results also proved that copper (II) ions adsorbed on the prepared membranes could be adequately desorbed in an EDTA solution up to 99% of desorption efficiency. The prepared membranes also had the advantage of almost reusable without any defect on the adsorption capacity for copper (II) ions (Figs. 12.7 and 12.8).

Kumar, Isloor, and Ismail were successfully fabricated and analyzed the chitosan adsorptive membranes with another derivative polymer which is polysulfone (PS) [53]. To attain the UF adsorptive membrane, the phase-inversion method was applied, and the scope was focused on
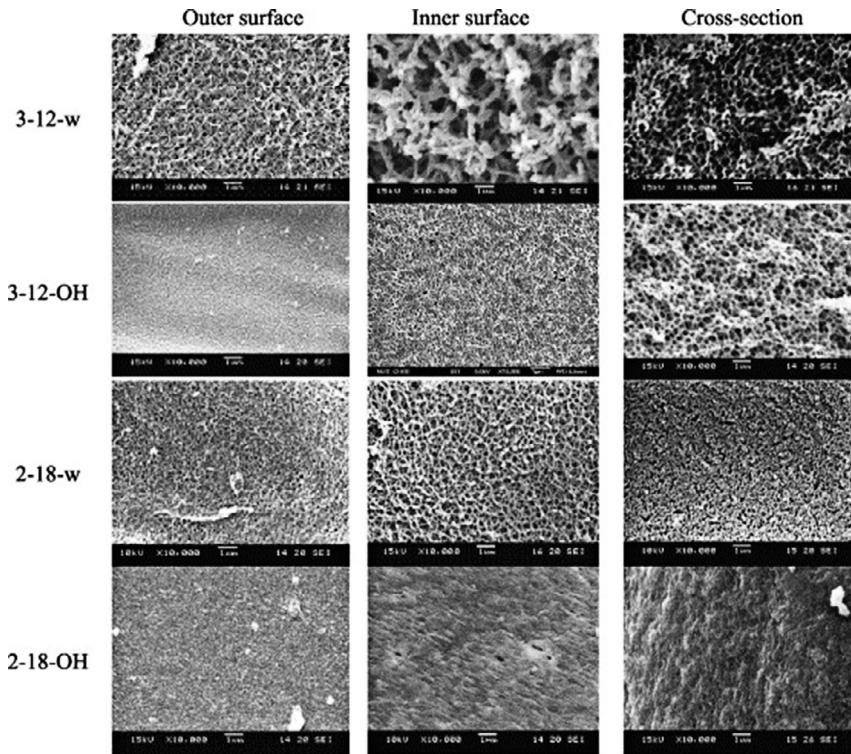
FIG. 12.7   SEM images of the four prepared CS/CA membranes. *Data from Fig. 1 of Liu C, Bai R. Adsorptive removal of copper ions with highly porous chitosan/cellulose acetate blend hollow fiber membranes. J Membr Sci 2006;284(1):313–22. License # 4284030232905.*

removing Cd(II), Cu(II) and Ni(II) metal ions. The increment in the content of chitosan in the prepared PS/CS membrane has eventually increased the rejection of the metal ions.

Next, another study by Kanagaraj et al., in the blended chitosan membrane application for the elimination of the bio-molecules and metal ions. PEI and NPHCs were used in the preparing of the blend solution then after the dried of the casting; it was immersed in the water coagulation bath. Results showed the reduction in the size of the membrane pores, and there is an increment in hydrophilicity. The permeate flux also increased via the rising of NPHCs content. Also, the prepared membranes showed an excellent performance in removal of metal ions for trivalent ions. The results could be explained by the increment of ions charge density and great formation constant of polymer-ion complexes. Other than that, enhanced hydrophilicity as a result of an optimize recovery of flux ratio of 88.6% for the prepared blend membrane with the NPHCs equal to 2 wt%. [55].
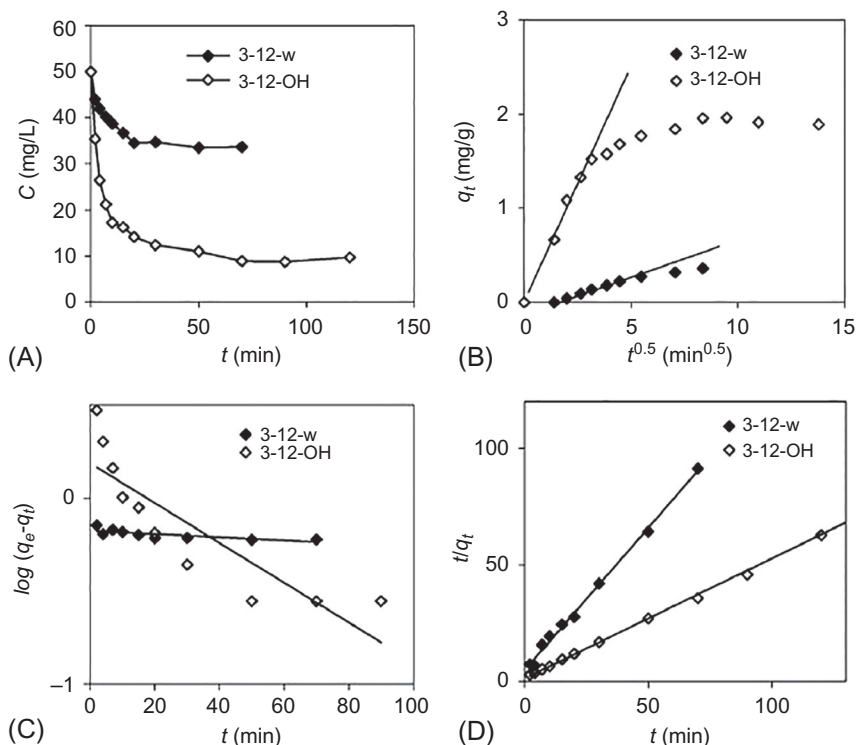
**FIG. 12.8**   Adsorption kinetics of the copper (II) ions of two prepared CS/CA membranes: (A) the results showed the change of the copper ion concentration ($C$, mg/L) in the bulk solution with adsorption time ($t$, min), (B) the fitting of diffusion- or transport-controlled kinetic model, (C) the fitting of the pseudo-first-order kinetic model, (D) the fitting of the pseudo-second-order kinetic model. *Data reproduced from Fig. 1 of Liu C, Bai R. Adsorptive removal of copper ions with highly porous chitosan/cellulose acetate blend hollow fiber membranes. J Membr Sci 2006;284(1):313–22. License # 4284030232905.*

The other study by Han, Liu and Bai on blended chitosan membrane started with the ready up of nanoparticles of chitosan followed by fusing them into the polymer matrix. The usage of a surfactant (SDS) inside chitosan aqueous solution, it will form the chitosan/SDS nanoparticles and were dissolved in an organic nonacidic solvent (NMP). Dissolving CA polymer in the aforementioned suspension prepared a dope solution to be solidified in water during phase inversion. Huge contain chitosan hollow fiber membrane was obtained complete with immense copper (II) ions adsorption efficiency [56].

### 12.3.1.2 Synthetic Polymer

Polyacrylonitrile (PAN) is one of the most abundant synthetic polymer used in UF and MF membranes fabrication due to its cost-effective, excellent solvent stability and excellent mechanical resistance. This polymer

was not readily obtained but its need to be synthesized by some methods. The nitrile (—CN) groups of PAN are easily modified via hydrolysis and a [3 + 2] cycloaddition reaction at an elevated temperature for adsorption of heavy metal ions. Kumar et al. were successfully manufactured an adsorptive ultrafiltration membrane from synthesized polyvinyltetrazole-*co*-polyacrylonitrile (PVT-*co*-PAN) by nonsolvent induced phase separation (NIPS). Also, the study has also shown that the production of adsorptive ultrafiltration membranes from the comprised of polymers is such a possible process [56]. In this study, the authors have manufactured the membranes by synthesizing polyvinyltetrazole-*co*-polyacrylonitrile (PVT-*co*-PAN) by nonsolvent induced phase separation (NIPS) technique. It was shown that the PVT portions have contributed to the alteration of pore size, charge as well as hydrophilicity behavior of the membranes. Upon the presence of PVT, the membrane became more hydrophilic and more negatively charged. On top of it, PVT was served as the primary binding sites for the adsorption of Cu (II) ions from the aqueous solution. This study also suggested that the membrane adsorptive properties were highly selective for the adsorption of Cu (II) ions over Pb (II) ions under the similar experimental conditions. The regeneration of the treated membrane was effectively done by using 0.25 mM ethylenediaminetetraacetic acid (EDTA) solution and could be reused for further heavy metal removal (Fig. 12.9).

The results showed that the membranes charge, hydrophilic behavior, and the pore size were altered by PVT segments. In the presence of PVT segments, the membranes become great in hydrophilicity; also the negative charges are dominance in the membranes. The PVT segments served as the major binding sites for the adsorption of copper (II) ions. In continuous UF and static condition, the maximal adsorption of copper (II) ions was obtained at pH equal to 5. Freundlich Isotherm model showed a great adsorption capacity result which was 44.3 mg/g.
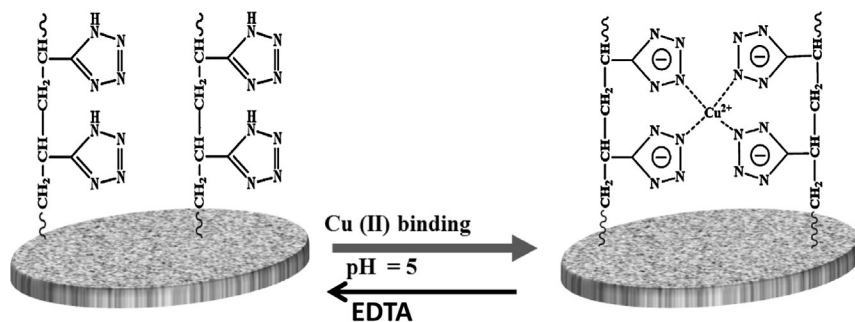


**FIG. 12.9**    Schematic presentation for the adsorption of Cu (II) ions by the PVT-co-PAN membranes from aqueous solution at pH 5 and the regeneration step using EDTA chelation. *Based on Fig. 4 of Kumar M, Shevate R, Hilke R, Peinemann K-V. Novel adsorptive ultrafiltration membranes derived from polyvinyltetrazole-co-polyacrylonitrile for Cu(II) ions removal. Chem Eng J 2016;301:306–14. License # 4284030512153.*

Polyethylene terephthalate (PET) are semicrystalline thermoplastic polymers that can be used in the form of different products such as a bottle, fiber, molded parts, and films. Adsorptive membranes using PET was prepared for the application of removing chromium Cr(VI) from contaminated water [57]. Due to good mechanical properties and ease of processing, PET can be considered as proper material for membrane support production. Furthermore, PET is an inert and hydrophobic polymer, which can accommodate adsorption of chitosan onto its surface effectively after applying an activation process. Different activation procedures can be used to provide binding sites for chitosan onto PET surfaces such as coating the surface with a chemical reagent containing a hydrophilic polymer, irradiation grafting and low-temperature oxygen plasma [58]. The membrane support was prepared by electrospinning of PET bottle waste in the form of nanofibers. Then, the surface of nanofibrous PET was activated by cold plasma followed by functionalizing with chitosan.

Experimental tests showed that the adsorption affinity of the prepared PET nanofibers was improved significantly by using plasma treatment and functionalization with chitosan. The membrane produced under optimum conditions had a maximum adsorption capacity of 5.54 mg/50 mg at initial water pH of 4. Reusability study revealed that the adsorption effectiveness of the prepared membranes could be maintained up to 93.7% of the fresh membrane after five adsorption/desorption cycles (Fig. 12.10).
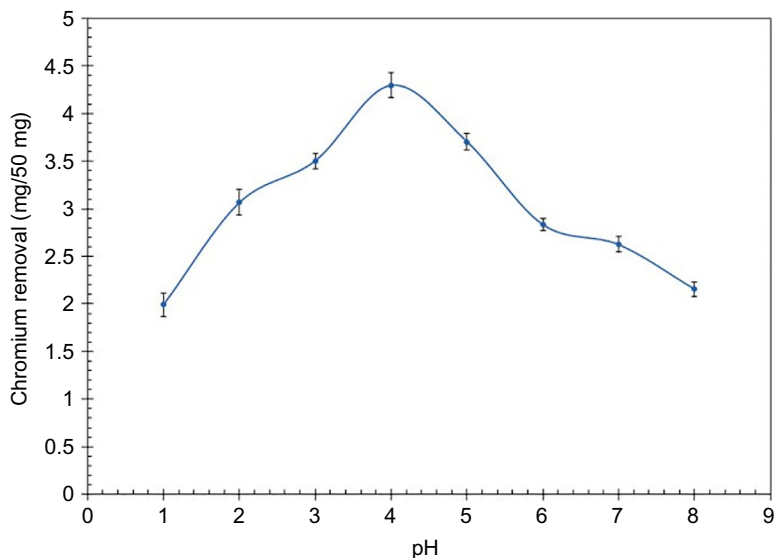


FIG. 12.10    The effect of pH on chromium removal. *Reproduced with permission from Fig. 9 of Khorram M, Mousavi A, Mehranbod N. Chromium removal using adsorptive membranes composed of electrospun plasma-treated functionalized polyethylene terephthalate (PET) with chitosan. J Environ Chem Eng 2017;5(3):2366–77. License # 4284030815890.*

Riaz et al. had successfully synthesized the prepolymer and chain-extended polyurethane with cellulose acetate into blended membranes for the removal of chromium (VI). Cellulose acetate is one of the most commonly used filtration membranes. It has a hydrophilic nature and possesses good fouling resistance; it is cost effective and chlorine resistant with fair biocompatibility. Some of its drawbacks are low mechanical, chemical and thermal strength [59]. To overcome these problems, we have introduced a unique polymer, polyurethane (PU) that is acclaimed to have outstanding mechanical, chemical and thermal attributes [60]. Polyurethane is a heterogeneous matrix composed of an alternating array of soft and hard segments. Soft segments are flexible and usually water soluble such as polyether polyols, and hard segments are rigid, generally containing aromatic or aliphatic diisocyanates allied with diamine or polyols, which are nonsoluble in water. The objective of the research is to synthesize a cost-effective and sustainable synthetic membrane that is used for chromium (VI) ion removal from industrial effluents.

This research involves the synthesis, characterization, and application of polyurethane-cellulose acetate blend membranes. Contact angle measurements and water content values proved that the addition of cellulose acetate had lowered the hydrophilicity of the modified membranes. Because the pure polyurethane membrane is more hydrophilic than pure cellulose acetate. SEM micrographs showed that blend membranes have spongy structures, partially filled up with dense cellulose acetate. Moreover, there are numerous pores on the surface of blend membranes that favors the rate of water flux. The applicability of modified membranes was tested for Ultrafiltration, one of the promising separation techniques by using the aqueous solution of potassium dichromate. The PU-CA1 membrane was subjected to the various chromium ion concentrations at varying pH and pressure. The economy of the process was achieved at pH 3 and 0.4 MPa for all the chromium ion concentrations [61]. These characteristics of PU-CA1 blend membrane prove it an innovative choice for effluent treatment in the textile industry (Fig. 12.11).

## 12.3.2 Mixed Matrix Membranes

Over the years, the development of membrane technology has bloomed glowingly whereby the production of mixed matrix membrane (MMM) has been introduced. The combination of membrane separation technique to that of superior adsorption properties of adsorbent (ordinarily inorganic materials) has eventually turned out in the production of this hybrid membrane. The pioneer work on the fabrication of the MMM has been explored by Ladhe et al. in 2009 [62]. The primary purpose of this study was to capture the silver ions using the MMM of silica and polysulfone and cellulose acetate. In this study, the silica particles have been
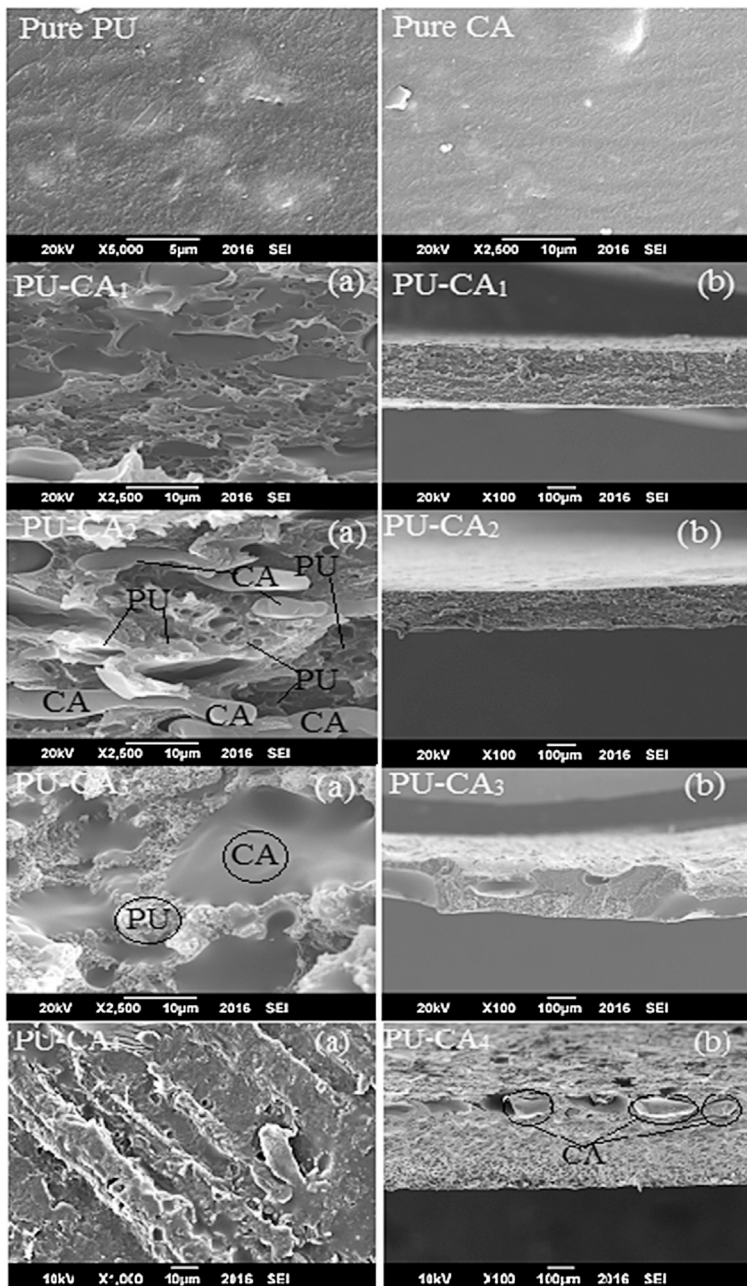
**FIG. 12.11**  SEM images of pure PU, pure CA, and PU-CA blend membranes recorded at the magnification of 2500–5000 for (A) top surface; and (B) 100 for cross sectional. *Data obtained and reproduced with permission from Fig. 5 of Riaz T, Ahmad A, Saleemi S, Adrees M, Jamshed F, Hai AM, et al. Synthesis and characterization of polyurethane-cellulose acetate blend membrane for chromium (VI) removal. Carbohydr Polym 2016;153:582–91. License # 4284030955213.*
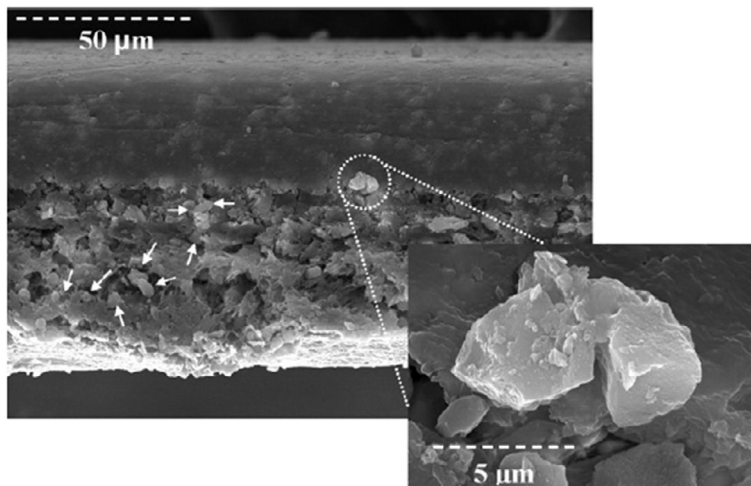
**FIG. 12.12** The silica particles in membrane matrix uniform distribution along the poly-sulfone flat sheet membrane. *Data from Fig. 3 of Ladhe AR, Frailie P, Hua D, Darsillo M, Bhat-tacharyya D. Thiol-functionalized silica–mixed matrix membranes for silver capture from aqueous solutions: experimental results and modeling. J Membr Sci 2009;326(2):460–71. License # 4284031088901.*

thiol-functionalized with 3-mercaptopropyltrimethoxy silane (MPTMS) to enhance the capture process of the silver ions. The authors have also remarked that the successful attempt of their study showed the promising platform for the usage of MMM in the process of heavy metal capture (Fig. 12.12).

For the case of heavy metals removal from wastewater, the treatment via adsorption using inorganic material impregnated on the polymer membrane has been studied by Yilmaz Yurekli in 2016 [63]. In this work, the author has removed the lead and nickel cations for water by using zeolite nanoparticle. This nanoparticle was impregnated onto polysulfone (PSf) membrane prior to the treatment process. The synthesized nanoparticle using the mean of conventional hydrothermal was possessed a great sorption capacity toward the adsorbed heavy metals. The hydraulic permeability of the membranes was improved by mere alteration of the fabrication conditions namely evaporation period of the casting film as well as the zeolite loading. This study also revealed that the hybrid membrane could be effectively used for dynamic removal of lead and nickel ions from water, especially when their concentrations and the operating pressure are low (Fig. 12.13).

The removal of contaminants such as heavy metals through the adsorption process is usually contributed to the ability of the adsorbent to bind with the adsorbate. Compounds that composed of active functional
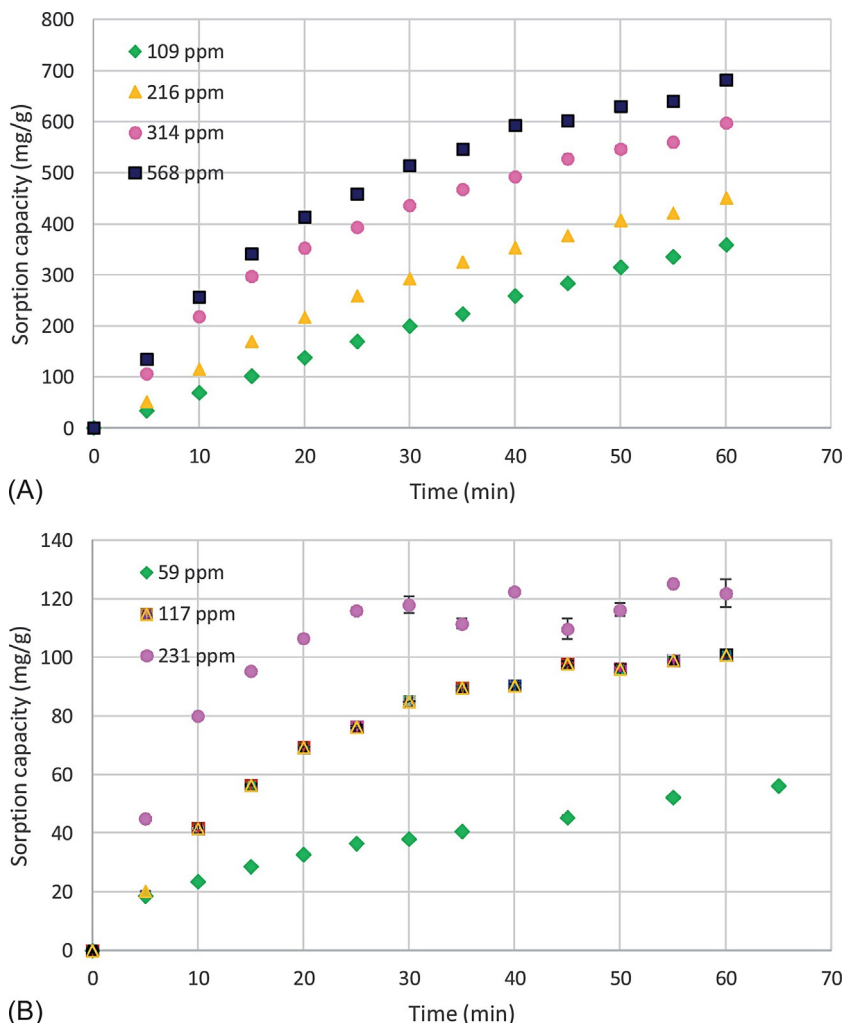
(A)



(B)

FIG. 12.13    Sorption kinetics of (A) $Pb^{2+}$ and (B) $Ni^{2+}$ ions during filtration of metal solution through PSf10-0 membrane. *Data reproduced with permission from Fig. 13 of Yurekli Y. Removal of heavy metals in wastewater by using zeolite nano-particles impregnated polysulfone membranes. J Hazard Mater 2016;309:53–64. License # 4284031265597.*

groups such as phenolic, carboxyl, lactone, and hydroxyl have been effective for heavy metal adsorption [64–66]. The binding process could be attributed to the bond formation between the adsorbate to that of the adsorbent. Sometimes, the ion-exchange mechanisms may take place during the adsorption. The adsorbent possesses typically the active sites compose with free electrons or has an electrical charge to which the electrostatic interaction of the adsorbent and adsorbed species has taken

place. Above all of these characteristics, an adsorbent material, which is usually inorganic, should have owned smaller size of the particle to which in turn offers more substantial surface area and thus increases the active sites distribution to which eventually boosted the adsorption process (Fig. 12.14).

The preparation of hybrid membrane comprising the mixing of the inorganic materials (acts typically as adsorbent) to that of polymer membrane can be varied. A study by Zhang et al. showed two types of membrane preparation methods namely the immersion of the pretreated polyvinylideneflouride (PVDF) films in the zinc oxide (ZnO) suspension (method A) and blended the ZnO nanoparticles with PVDF solution prior the casting films process (method B) [67]. The immersion method somehow required the help of surfactants as the pretreatment of the PVDF films. The results obtained have indicated that the executions of the membranes namely hydrophilicity, contact angles, antifouling ability and water permeability revealed a proportional improvement with the increment in ZnO dosage. This could be attributed to the incorporation of ZnO
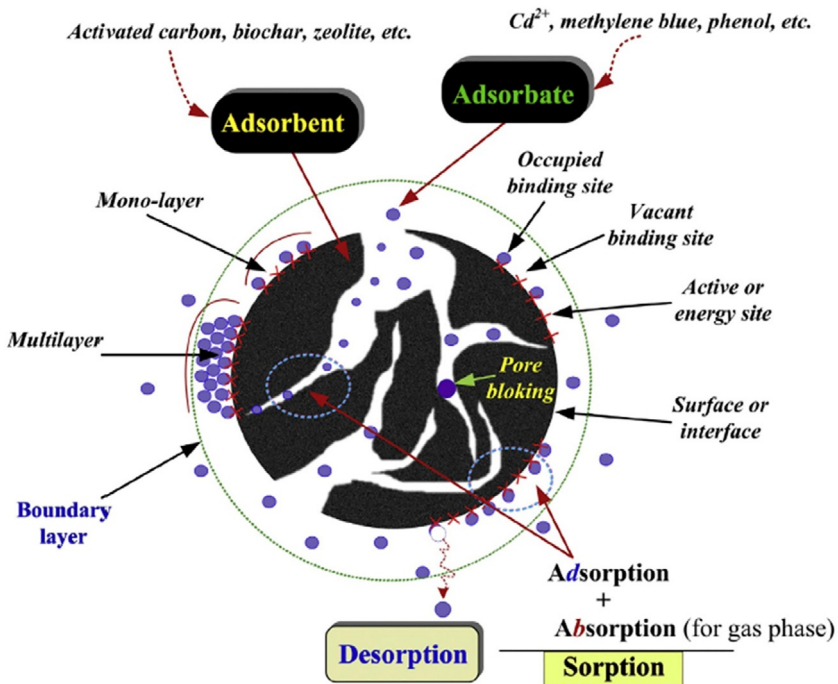


**FIG. 12.14** Some basic terms used in adsorption studies. *Based on Fig. 1 of Tran HN, You S-J, Hosseini-Bandegharaei A, Chao H-P. Mistakes and inconsistencies regarding adsorption of contaminants from aqueous solutions: a critical review. Water Res 2017;120:88–116. License # 4284031392721.*
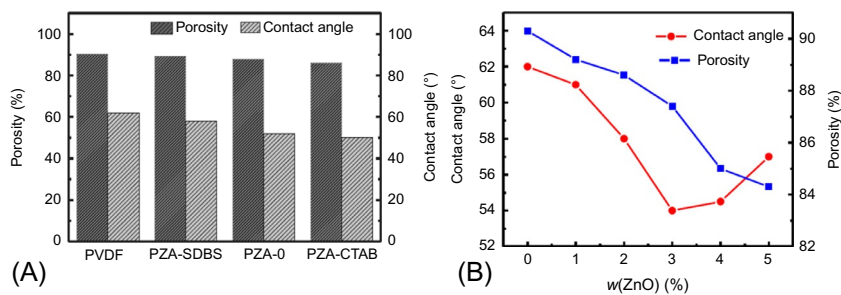
**FIG. 12.15**   Porosity and contact angle of PVDF/ZnO MMMs fabricated by (A) immersion and (B) blending techniques. *Courtesy from a graphical abstract of Zhang X, Wang Y, Liu Y, Xu J, Han Y, Xu X. Preparation, performances of PVDF/ZnO hybrid membranes and their applications in the removal of copper ions. Appl Surf Sci 2014;316:333–40. License # 4284040058517.*

nanoparticles onto the surface of the membrane. On the contrary, the blending method has driven to the more entrapment of nano-ZnO into the pores of PVDF. This technique also showed that the hybrid membrane possessed relatively even structure and the better hydrophilicity of the membrane surface. Amazingly, this PVDF/ZnO MMM possessed a better adsorption capability toward $Cu^{2+}$ ions and the maximum adsorption capacity obtained was more than nine times better to that of original PVDF films (Fig. 12.15).

The progress of MMM has come to a new edge when a study by Zhang et al. in 2011 has developed a multifunctional membrane for the chromatic warning and boosted the removal of cadmium ions via adsorption approach [68]. In this study, a multifunctional membrane for visual warning detection and enhancement in the adsorptive removal of $Cd^{2+}$ ions in aqueous solution was prepared by immobilized an optical indicator ligand for the $Cd^{2+}$ ions detection onto a porous chitosan/cellulose acetate blend base membrane. The ligands namely as 5,10,15,20-tetrakis (1-methyl-4-pyridinio) porphyrin tetra (p-toluenesulfonate) was polymer brushes grafted onto the membrane surface by the mean of surface-initiated atom transfer radical polymerization (ATRP) method. The produced membrane was proficient of exhibiting distinctive color changes in response to the presence of $Cd^{2+}$ ions in aqueous solution. The experimental results indicated significant findings as the membrane can display an instant color change from yellow to green in the presence of $Cd^{2+}$ ions only within 2 min of contact time. Also, the concentration of the cadmium ions is relatively low (5 mg/L), and this membrane also showed a good selectivity toward $Cd^{2+}$ ions when other cationic species namely $K^+$, $Ca^{2+}$, $Na^+$ and $Mg^{2+}$ presented in the solutions (Fig. 12.16).

In these past years, polyvinylidene fluoride (PVDF) also has become a great interest in the preparation of the adsorptive membranes [69]. Zheng et al. selected PVDF for the fabrication of the adsorptive membrane for the
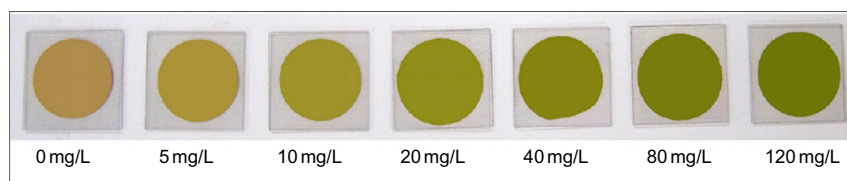
FIG. 12.16   Color changes of the multifunctional membrane responding to $Cd^{2+}$ ions with different initial concentrations. *Data adapted from Fig. 5 of Zhang L, Zhao Y-H, Bai R. Development of a multifunctional membrane for chromatic warning and enhanced adsorptive removal of heavy metal ions: application to cadmium. J Membr Sci 2011;379(1):69–79. License # 4284040336825.*

removal of arsenic. In this study, a PVDF/zirconia blend flat sheet membrane was prepared and possessed a capability in adsorbing the arsenate and eliminating other contaminants such as microorganisms. The introduction of zirconia has eventually enhanced the porosity and hydrophilicity of the membrane, which eventually led to a substantial improvement in the water flux of the membrane [70]. The batch adsorption experiments have revealed that the membrane was effectively removed arsenate for a wide range of optimal pH ranging from 3 to 8. The adsorption equilibrium was obtained within 25 h with the maximum adsorption capacity was 21.5 mg/g. This achievement was comparable to that of most of the available adsorbent. Also, the presence of co-anions such as fluoride has not significantly affected the adsorption. It worth be mentioning that the membrane obtained was efficient for the elimination of arsenate and bacteria (*Escherichia coli*) under continuous filtration. Additionally, the saturated membrane occupied by arsenate could be easily regenerated using an alkaline solution and subsequently be reused. Finally, the results obtained from FTIR and XPS studies could be possibly proposed a potential interaction mechanism between the membrane and arsenate ions (Fig. 12.17).

As for the polymer matrix, polysulfone (PSf) has been widely used in the fabrication of the polymeric membranes due to its promising properties which are low in cost, high mechanical strength, thermal and chemical stabilities, resistance over the wide range of pH, also processability and variety of active functional groups. Most of the study on the PSf materials have combined PSf with other nanomaterials or ceramic materials to improve the properties of the membranes. Shokri et al. have decided to further the discussion on the capability of adsorptive removal contaminants from water by using PSf/organoclay membranes.

In comparison with just pure PSf membrane, the prepared PSf/organoclay membranes exhibited higher pure water flux, surface hydrophilicity and roughness and better mechanical strength [71]. XRD analysis revealed that the organoclays were completely exfoliated when the organoclay
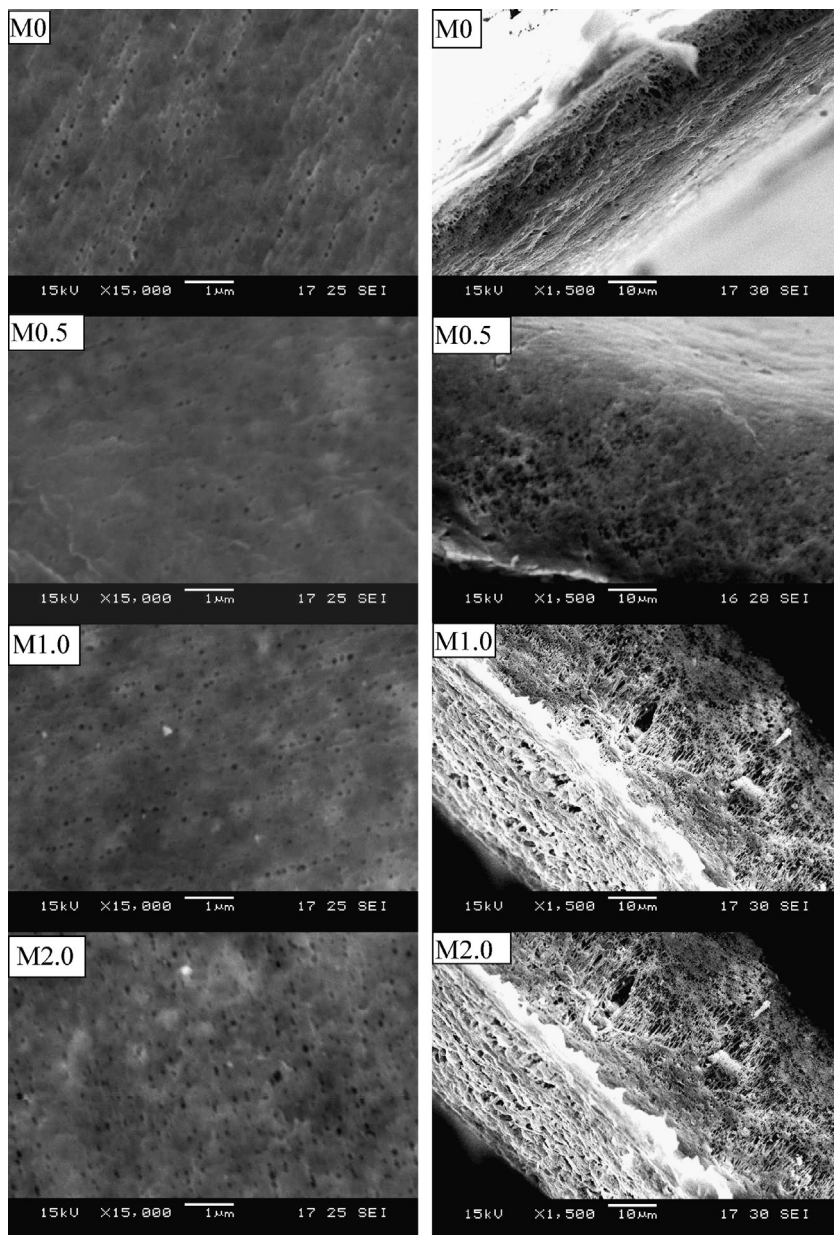
**FIG. 12.17**    SEM images of the top surface *(left)* and cross-section *(right)* of PVDF adsorptive membranes. *Reproduced with permission from Fig. 2 of Zheng Y-M, Zou S-W, Nanayakkara KGN, Matsuura T, Chen JP. Adsorptive removal of arsenic from aqueous solution by a PVDF/zirconia blend flat sheet membrane. J Membr Sci 2011;374(1):1–11. License # 4284040502373.*

content increased from 0 to 1.5 wt%. However, a further increase in organoclay content resulted in the formation of intercalated structure.

Arsenic removal analyses confirmed that the differences in the morphology of the dispersed organoclay could lead to significant variations in the performance of nanocomposite organoclay/PSf membrane. In this regard, the nanocomposite membrane containing 2.0 wt% of organoclay, the highest adsorption capacity was obtained in batch adsorption. It is due to the higher content of dispersed inorganic adsorbents. In dynamic adsorption evaluation of prepared membranes, however, the sample with lower organoclay content but fully exfoliated adsorbents (1.5 wt%) provides better performance than the sample with higher organoclay content and higher adsorption capacity (2.0 wt%). The difference in performance was attributed to the existence of completely separated layers of fully exfoliated organoclays which provide a higher level of accessibility for As (V) adsorption in short contact process. Prepared membranes showed promising re-usability for multiple cycles and fruitful applicability in arsenic removal from real surface water samples.

Gohari et al. in 2013 have also applied PSf in the fabrication of the adsorptive membrane combined with the Fe—Mn binary oxide (FMBO). The results showed the prepared membrane properties had been improved in the present of FBMO in term of membrane mean surface roughness; also the pore size also has been decreased while the pore number has been increased [72]. The significant increase in water flux as the FMBO loading is increased most likely due to the combined effects of the decreased contact angle, increased number of pores and greater surface roughness upon incorporation of hydrophilic FMBO particles. The best performing membranes prepared from the mixture of FMBO/ PES in the ratio of 1.5:1 has exhibited the high pure water flux as of 94.6 L/m$^2$ h at a relatively low operating pressure of 1 bar. This membrane possessed a maximum As (III) uptake capacity of 73.5 mg/g. The continuous UF experiment has revealed that the PES/FMBO MMM can be possibly employed for efficient elimination of As (III) from polluted groundwater by generating a permeate that containing As (III) at the concentration of <10 μg/L. The membrane adsorption capacity of as high as 87.5% of could be regenerated using NaOCl and NaOH solution, thus indicating the reusability and practicability of the membrane for As (III) removal (Figs. 12.18 and 12.19).

Gohari et al. also prepared PSf in the ultrafiltration (UF) mixed membrane combined with hydrous manganese oxide (HMO) for the removal of Pb(II) [73]. The results have shown that although the membrane pore size was tended to be decreased upon the increment in the HMO:PES ratio, the membrane water flux was not significantly affected. Apart from the increment in the membrane flux, the increased in the HMO content has increased the porosity and surface roughness and reduced the contact
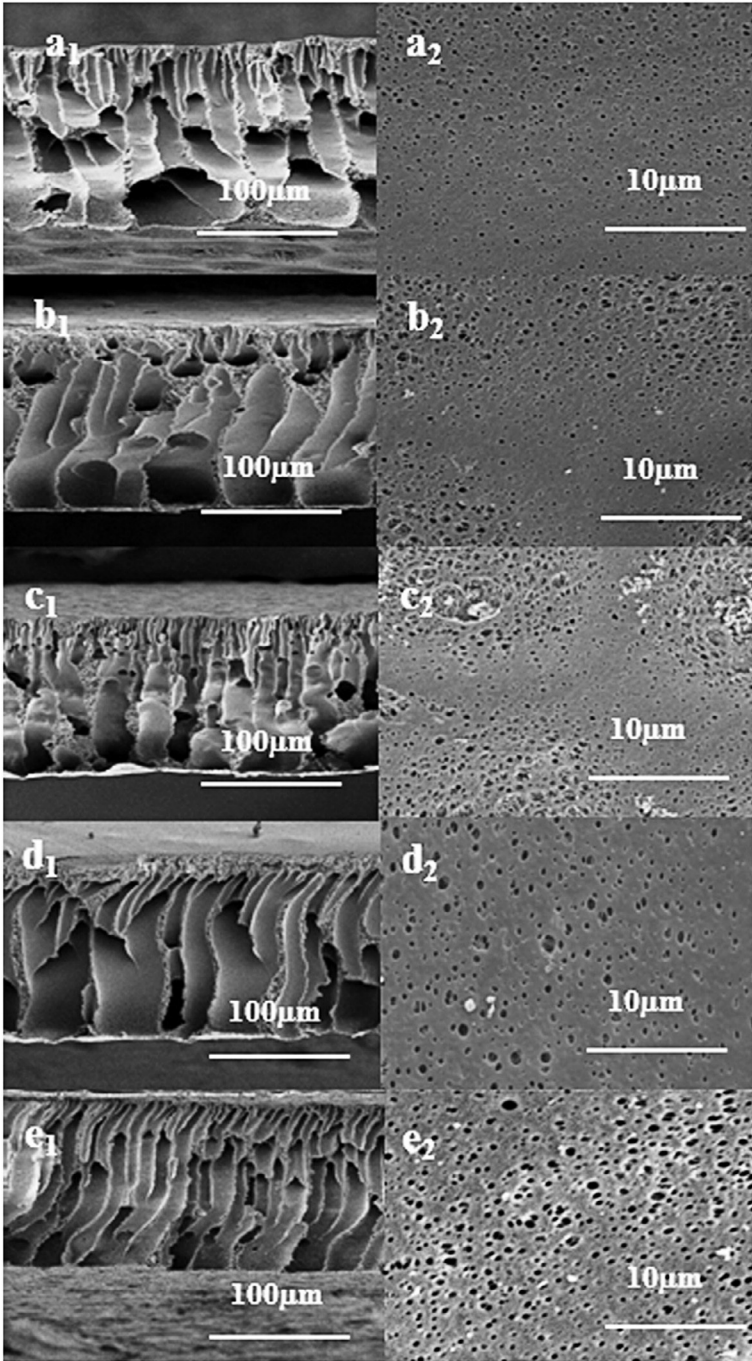
**FIG. 12.18** FE-SEM images of cross-section [1] and top surface [2] of prepared membranes, (A) neat PSf, (B) PSf/C-30B/0.5, (C) PSf/C-30B/1.0, (D) PSf/C-30B/1.5, and (E) PSf/C-30B/2.0. *Data obtained from Fig. 1 of Shokri E, Yegani R, Pourabbas B, Kazemian N. Preparation and characterization of polysulfone/organoclay adsorptive nanocomposite membrane for arsenic removal from contaminated water. Appl Clay Sci 2016;132:611–20. License # 4284040734181.*
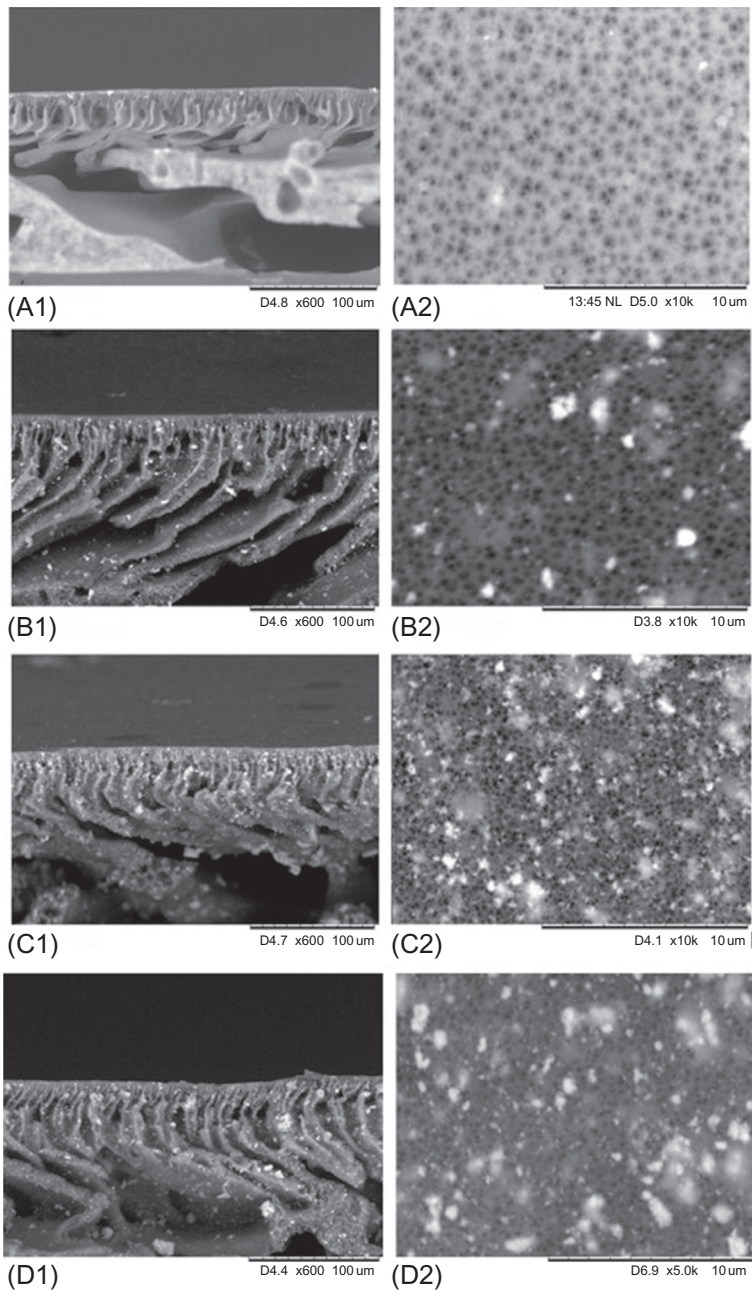
**FIG. 12.19**  SEM photographs of the cross-section (numbered as 1) and the top surface (numbered as 2) of membranes prepared from different FMBO/PES ratios (A) M0, (B) M0.5, (C) M1.0, and (D) M1.5 membrane. *From Fig. 4 of Jamshidi Gohari R, Lau WJ, Matsuura T, Ismail AF. Fabrication and characterization of novel PES/Fe–Mn binary oxide UF mixed matrix membrane for adsorptive removal of As(III) from contaminated water solution. Sep Purif Technol 2103;118:64–72. License # 4284040839403.*

angle value (more hydrophilic). Of all the membranes studied, it was found that the MMM prepared with the highest HMO:PES content ratio possessed the highest uptake capacity of Pb (II) ions (204.1 mg/g), and this value is equivalent to most of the promising composite adsorbents reported in the literature. Furthermore, the continuous UF experiments have shown that the PES/HMO MMM can be possibly effectively used for the elimination of the Pb (II) ions by producing high quality permeate containing <15 µg/L of Pb (II) in water. IIn addition, the simple desorption process of the Pb (II)-adsorbed MMM using HCl solution; it was reported that 97.5% of the original adsorption capacity of the membrane was able to be recovered. This has ensured that the reusability of the membrane for the further uptake of Pb (II) ions.

Another nanocomposite membranes were prepared by incorporating functionalized graphene oxide (GO) nanoparticles using polyaniline (PANI) into the PES matrix membrane [74]. GO nanoparticles were synthesized by Ghaemi et al. using modified Hummer's method. Among the aforementioned nanoparticles, it was found that GO nanoparticles are more adaptable in practical studies due to their chemical structures which contain various oxygenated functionalities including epoxy on the basal plane, hydroxy, carboxylic acid and carbonyl at the edges [75]. Furthermore, GO nanoparticles could be efficiently adsorbed the heavy metal ions and forming the metal complex through the lone electron pair sharing on the oxygen.

Additionally, it was found that the idea of aniline polymerization onto the GO nanoparticles was efficiently improving the membrane performance in removing the heavy metal ions in comparison to that of neat PES membrane. The decreasing in the concentration from 50 to 5 mg/Lby the increment in the feed solution pH from 3.5 to 6.0 has contributed to a higher removal. The optimum experimental conditions: 0.25 wt% of nanoparticles, feed concentration of 5 mg/L and feed pH of 6.0 have eventually resulted in the highest performance of 98%. Overall, the introduction of special functional groups onto the nanocomposite membrane over the polymer modification of the nanoparticles may be considered as a valuable method to attain a more anticipated performance in the elimination of heavy metal ions from water. The outcomes obtained from adsorption experiments showed that the produced membrane in this study offered a high adsorption capacity of 202 mg/g. Also, the adsorption pseudo-first-order kinetic model and Langmuir isotherm model, as well as the reusability tests, have strengthened that the produced membrane could be possibly used for several times in the elimination of lead ions containing in the solution before missing its capability (Fig. 12.20).

The addition of inorganic additives into membrane aimed the enhancement of the membrane selectivity toward the targeted species, reducing the fouling effect and improving the hydrophilicity properties of the
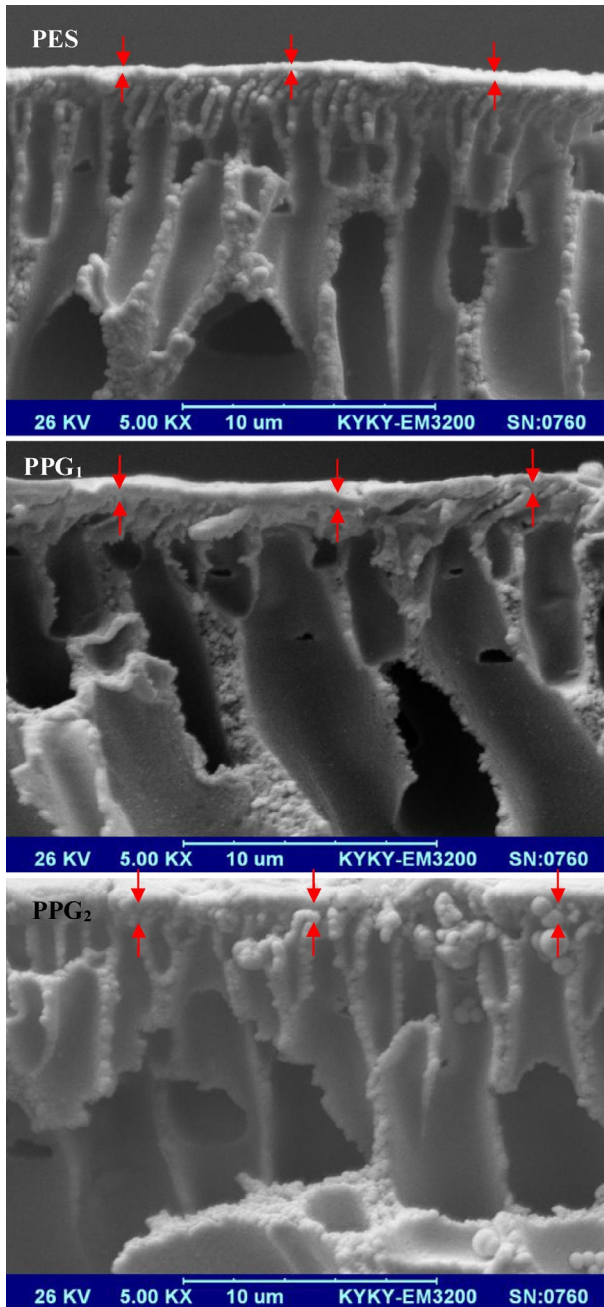
**FIG. 12.20**  SEM micrograph of the cross-section images of prepared membranes. *Based on Fig. 4 of Ghaemi N, Zereshki S, Heidari S. Removal of lead ions from water using PES–based nanocomposite membrane incorporated with polyaniline modified GO nanoparticles: performance optimization by central composite design. Process Saf Environ Prot 2017;111:475-90. License # 4284040975273.*

membrane [76]. However, the limitation of these additives impregnation onto the membrane have are the cost related to the material selection as well as the complexity of the manufacturing. Therefore, there was a study on the impregnation of inexpensive inorganic additives onto the polymeric matrix [77]. In this study, the iron ore slime (IOS) was chemically treated and impregnated in polysulfone (PSf) hollow fiber membrane for the treatment of arsenic contaminated water. The inexpensive IOS was obtained from the wastes of the steel industries was chemically treated to enhance the uptake capacity of this additive toward the targeted heavy metal (Fig. 12.21).

The presence of this additive has also decreased the porosity from 75% to 46%, permeability from $6 \times 10^{-10}$ m/s Pa to $2.6 \times 10^{-10}$ m/s Pa as well as the molecular weight cut off of the membrane to 45 kDa. This somehow has improved the hydrophilicity (contact angle values reduction from 75 to 63 degrees) and increased the surface roughness of the membrane to which in turn, enhanced the arsenic uptake capacity of the membrane. The regeneration of the exhausted membrane has also studied for up to three cycles with breakthrough time for arsenic removal was reduced from 28 h to 22 h and 14 h after second and third cycle, respectively. The fabricated MMM was also able to remove microorganisms and iron simultaneously from real life feed solution below their World Health Organization (WHO) approved permissible level.

As been mentioned earlier, the adsorption of adsorbate species is mainly dominated by the presence of certain functional groups in the adsorbent structure that possessed affinity to bind to that of adsorbed species. A study by Beppu et al. in 2004 has revealed that the uptake of Cu (II) ions was further enhanced upon the functionalization of histidine to the porous chitosan membranes [78]. This study has shown that the impregnation of the chelating groups (histidine) can amplify the uptake capacity of the chitosan membranes. Additionally, the assimilation of the porous membrane with histidine has positively synergized the adsorption capacity of Cu (II) ions. However, this improvement cannot be perceived for the membranes with lower porosities. It was observed that the maximum adsorption uptake capacity for the Cu (II) ion was 2.5 mmol metal/g pristine chitosan membrane. At this stage, there was no influence of membrane porosity observed. Nevertheless, upon the immobilization of the histidine onto the chitosan membrane, the porosity of the chitosan membrane was shown to be an influence that molds the maximum adsorption capacity, with the adsorption capacity values ranging from 2.0 to 3.0 mmol metal/g chitosan membranes. The results indicated that the immobilization of histidine on porous chitosan membranes portrays the synergy with porosity in the ability to complex the Cu (II). This synergism can be either negative or positive and highly liable on the initial porosity of the membrane (Fig. 12.22).
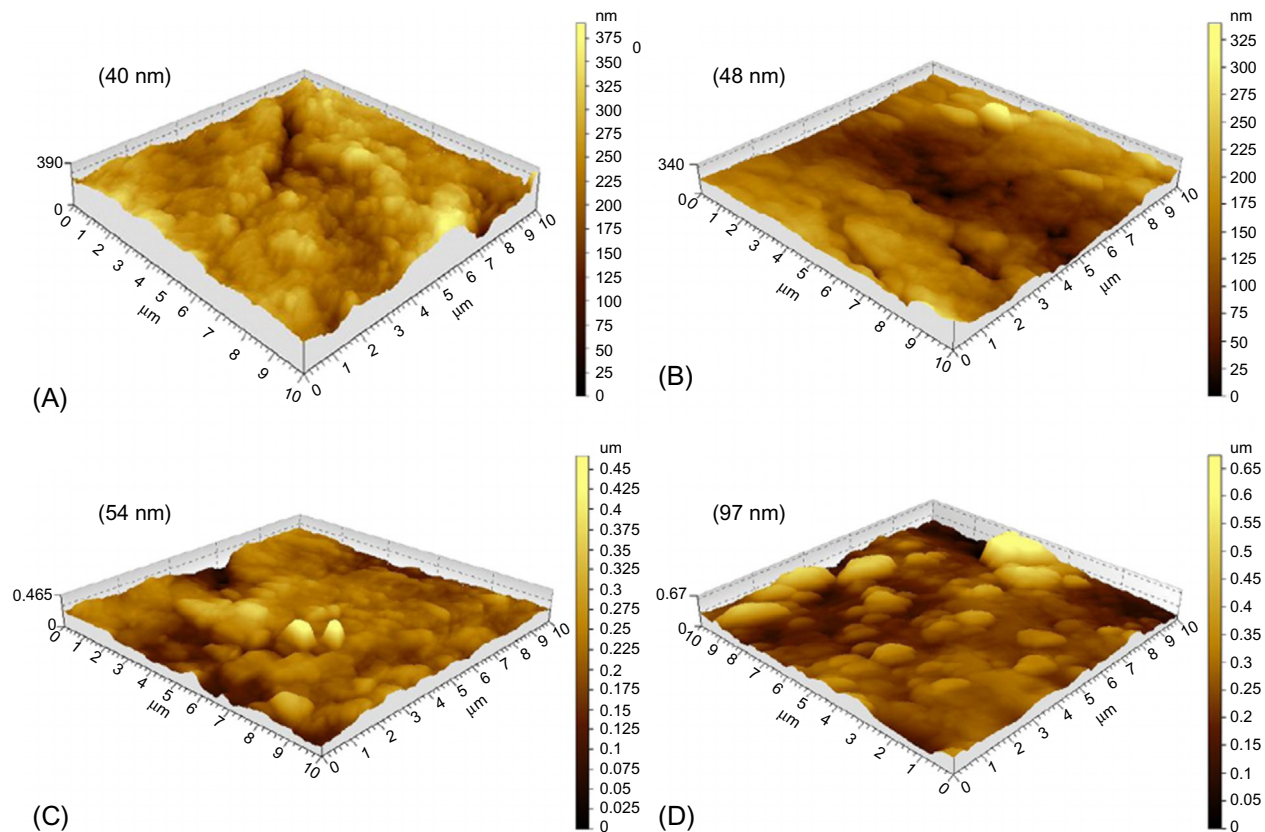
**FIG. 12.21** Atomic force microscopic (AFM) images and surface roughness of mixed matrix hollow fiber membranes with different IOS content of (A) 0 wt%, (B) 4.5 wt%, (C) 6.5 wt% and (D) 10 wt%. *Data from Fig. 2 of Chatterjee S, De S. Adsorptive removal of arsenic from groundwater using chemically treated iron ore slime incorporated mixed matrix hollow fiber membrane. Sep Purif Technol 2017;179:357–68. License # 4284041088564.*
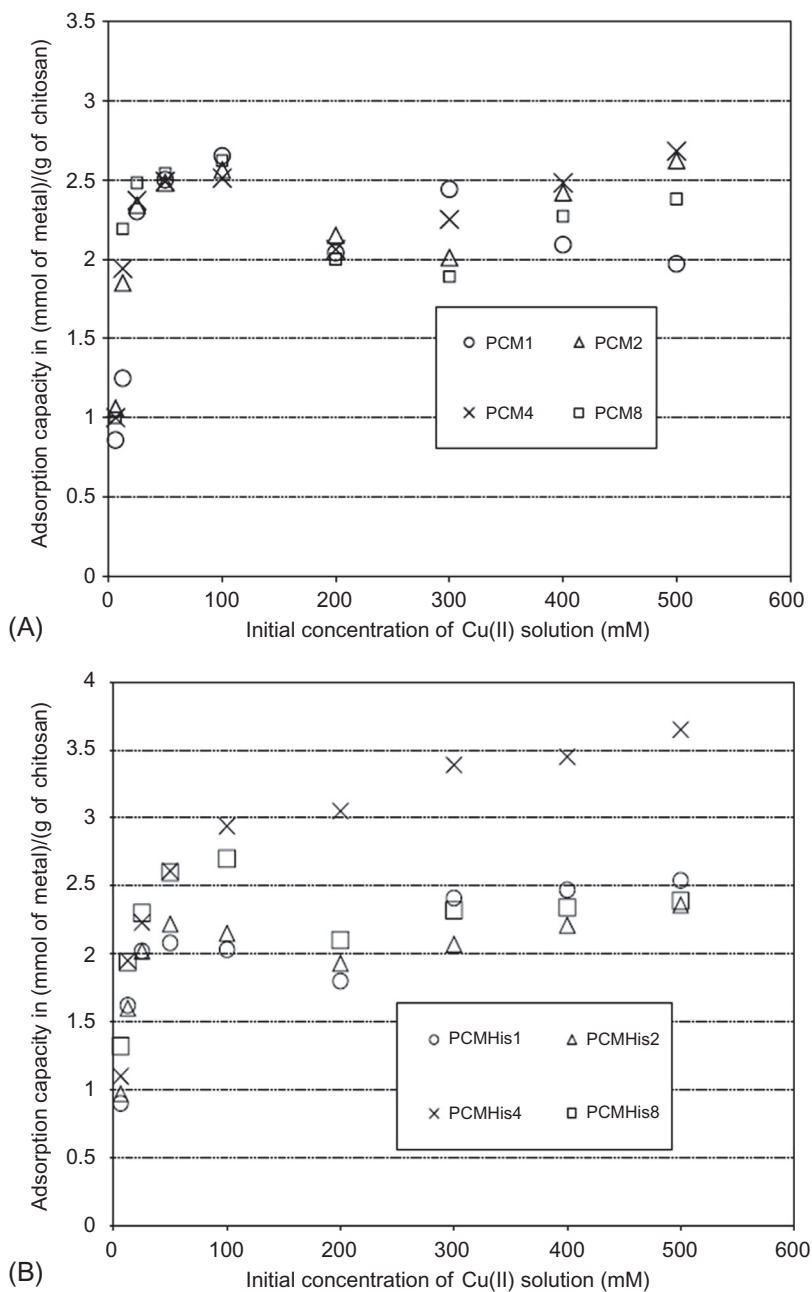
(A)



(B)

**FIG. 12.22** Adsorption capacity of Cu (II) ions by (A) pristine chitosan membrane and (B) chitosan membrane immobilized with histidine. *Note:* PCM4 and PCMHis4 were the most porous chitosan membrane. *Data obtained from Figs. 7 and 8 of Beppu MM, Arruda EJ, Vieira RS, Santos NN. Adsorption of Cu(II) on porous chitosan membranes functionalized with histidine. J Membr Sci 2004;240(1):227–35. License # 4284041266940.*

TABLE 12.3   Mixed Matrix Membranes for Various Water Treatment Applications

| Type of membrane | Type of additive | Application | Ref. |
|---|---|---|---|
| Polyethersulfone (PES) | Acrylonitrile butadiene styrene (ABS), Chitosan | Mercury and sodium ions removal | [79] |
| Chitosan (CS) | Alginate (AG) | Glyphosate herbicide removal | [80] |
| Chitosan (CS) | Hydroxyapatite (Hap) | Lead, cobalt and nickel removal | [81] |
| Polyamide (PA) | Titanium dioxide ($TiO_2$) | Magnesium sulfate ($MgSO_4$) removal | [82] |
| Poly (imide siloxane) copolymer | Carbon nanotube | Gas separation | [83] |
| Poly (vinyl alcohol) (PVA) | N-[3-(trimethoxysilyl) propyl] ethylene damine (TMSPEDA) | Strontium ions removal | [84] |
| Polyethersulfone (PES) | Monodisperse Stöber silica | Humic acid and methylene blue removal | [85] |

Apart from the removal of heavy metals from the aqueous solution, MMMs have other applications too. Of all the findings, the fabrication of MMMs was aimed for the enhancement of the adsorption capacity of the adsorbed species. Table 12.3 summarizes some studies on MMM comprises of its constituents and applications in the various field of analyses.

## 12.4  CONCLUDING REMARKS AND PERSPECTIVES

In summary, the adsorptive membranes have a wide range of applications especially in the treatment of water. The progress in the fabrication of the adsorptive membranes has come to a newly extended edge as the MMMs were developed from the single polymer membranes. The adsorptive removal of contaminants contained in water has also technologically advanced upon the introduction of the adsorptive membrane, over the conventional suspension adsorption process. The single step of contaminants removal has now been achieved instead of multistep of pollutant removal treatment that previously executed. Nevertheless, the hybridization of adsorbent additives and/or the functionalization of pristine membranes have eventually combining the superior adsorptive properties of the adsorbent to that of separation behavior of the membrane.

The fabrication of the adsorptive membranes previously produced was mainly dominated in the form of flat sheet configuration. This form of membrane somehow has some limitation in term of efficiency as the surface area offered are rather low. Thus, the configuration of hollow fiber should now be more focused as it offers a larger surface area for the optimum adsorption process. On the other hand, the hollow fiber configuration is more suitable and applicable for the development of the membrane separation systems, namely membrane contactor and membrane distillation systems. These systems are known to be highly efficient and effective, reliable, and capable of producing clean water, even for drinking purposes.

Aside from polymeric typed membranes discussed throughout this chapter, there shall be another type of material normally fabricated to the membrane. Ceramic materials which are typically hydrophilic owned some functional groups that possess adsorptive behavior toward contaminants especially charged metal ions. Also, the fabricated membrane of ceramic materials revealed superior physical properties, specifically the durability toward the extreme conditions such as high pressure and temperature and harsh condition of highly acidic and alkaline environment. This notable behavior of ceramic membranes has a high potential to be developed as adsorptive membrane systems that are dealing with such environments. The less-reported study on the development of adsorptive ceramic membrane perhaps indicating the bright perspective of the expansion of ceramic membranes aim for the adsorption of heavy metals and other contaminants existed in aqueous solution.

## Acknowledgment

## References

[1] Armon R, Cheruti U. Environmental aspects of zoonotic diseases. London, UK: IWA Publishing; 2012.

[2] Naiya TK, Bhattacharya AK, Mandal S, Das SK. The sorption of lead(II) ions on rice husk ash. J Hazard Mater 2009;163(2–3):1254–64.

[3] Ajitha P, Vijayalakshmi K, Saranya M, Gomathi T, Rani K, Sudha PN, et al. Removal of toxic heavy metal lead (II) using chitosan oligosaccharide-graft-maleic anhydride/polyvinyl alcohol/silk fibroin composite. Int J Biol Macromol 2017;104:1469–82.

[4] Goyer RA, Chisolon IJ. Lead. In: Metallic contamination and human health. New York/London: Academic Press; 1972.

[5] Hauptman M, Bruccoleri R, Woolf AD. An update on childhood lead poisoning. Clin Pediatr Emerg Med 2017;18:181–92.

[6] Weidenhamer JD, Clement ML. Widespread lead contamination of imported low-cost jewelry in the US. Chemosphere 2007;67(5):961–5.

[7] Yost JL, Weidenhamer JD. Lead contamination of inexpensive plastic jewelry. Sci Total Environ 2008;393(2):348–50.

[8] Centers for Disease Control and Prevention. Death of a child after ingestion of a metallic charm – Minnesota. MMWR Morb Mortal Wkly Rep 2006;55(12):340–1.

[9] Gupta VK, Pathania D, Sharma S, Singh P. Preparation of bio-based porous carbon by microwave assisted phosphoric acid activation and its use for adsorption of Cr(VI). J Colloid Interface Sci 2013;401(1):125–32.

[10] Georgieva VG, Tavlieva MP, Genieva SD, Vlaev LT. Adsorption kinetics of Cr(VI) ions from aqueous solutions onto black rice husk ash. J Mol Liq 2015;208:219–26.

[11] Mohan D, Singh KP, Singh VK. Trivalent chromium removal from wastewater using low cost activated carbon derived from agricultural waste material and activated carbon fabric cloth. J Hazard Mater 2006;135(1):280–95.

[12] Biswas P, Karn AK, Balasubramanian P, Kale PG. Biosensor for detection of dissolved chromium in potable water: a review. Biosens Bioelectron 2017;94:589–604.

[13] Parascandola J. King of poisons: a history of arsenic. Washington, DC: Potomac Books Incorporated; 2012.

[14] Almberg KS, Turyk ME, Jones RM, Rankin K, Freels S, Graber JM, et al. Arsenic in drinking water and adverse birth outcomes in Ohio. Environ Res 2017;157:52–9.

[15] Maleki S, Karimi-Jashni A. Effect of ball milling process on the structure of local clay and its adsorption performance for Ni(II) removal. Appl Clay Sci 2017;137:213–24.

[16] Wang X, Wang Z, Chen H, Wu Z. Removal of Cu(II) ions from contaminated waters using a conducting microfiltration membrane. J Hazard Mater 2017;339:182–90.

[17] Arun S, Manikandan NA, Pakshirajan K, Pugazhenthi G, Syiem MB. Cu(II) removal by Nostoc muscorum and its effect on biomass growth and nitrate uptake: a photobioreactor study. Int Biodeterior Biodegrad 2017;119:111–7.

[18] Jalilzadeh M, Şenel S. Removal of Cu(II) ions from water by ion-imprinted magnetic and non-magnetic cryogels: a comparison of their selective Cu(II) removal performances. J Water Process Eng 2016;13:143–52.

[19] Wang H, Yuan X, Wu Y, Huang H, Zeng G, Liu Y, et al. Adsorption characteristics and behaviors of graphene oxide for Zn(II) removal from aqueous solution. Appl Surf Sci 2013;279:432–40.

[20] Bhanjana G, Dilbaghi N, Singhal NK, Kim K-H, Kumar S. Copper oxide nanoblades as novel adsorbent material for cadmium removal. Ceram Int 2017;43(8):6075–81.

[21] Zhang H, Zhao K, Gao Y, Tian Y, Liang P. Inhibitory effects of water vapor on elemental mercury removal performance over cerium-oxide-modified semi-coke. Chem Eng J 2017;324:279–86.

[22] Wachinski AM. Ion exchange treatment for water. Denver, CO: American Water Works Association; 2006.

[23] Mendow G, Sánchez A, Grosso C, Querini CA. A novel process for nitrate reduction in water using bimetallic Pd-Cu catalysts supported on ion exchange resin. J Environ Chem Eng 2017;5(2):1404–14.

[24] Lee C-G, Alvarez PJJ, Nam A, Park S-J, Do T, Choi U-S, et al. Arsenic(V) removal using an amine-doped acrylic ion exchange fiber: kinetic, equilibrium, and regeneration studies. J Hazard Mater 2017;325:223–9.

[25] Bratby J. Coagulation and flocculation in water and wastewater treatment. London: IWA Publishing; 2016.

[26] Rincón GJ, La Motta EJ. Simultaneous removal of oil and grease, and heavy metals from artificial bilge water using electro-coagulation/flotation. J Environ Manag 2014;144:42–50.

[27] Ismail IM, Fawzy AS, Abdel-Monem NM, Mahmoud MH, El-Halwany MA. Combined coagulation flocculation pre treatment unit for municipal wastewater. J Adv Res 2012;3(4):331–6.

[28] Choumane FZ, Benguella B, Maachou B, Saadi N. Valorisation of a bioflocculant and hydroxyapatites as coagulation-flocculation adjuvants in wastewater treatment of the steppe in the wilaya of Saida (Algeria). Ecol Eng 2017;107:152–9.

[29] Hubadillah SK, Othman MHD, Harun Z, Ismail AF, Rahman MA, Jaafar J. A novel green ceramic hollow fiber membrane (CHFM) derived from rice husk ash as combined adsorbent-separator for efficient heavy metals removal. Ceram Int 2017;43(5): 4716–20.

[30] Lata S, Samadder SR. Removal of arsenic from water using nano adsorbents and challenges: a review. J Environ Manag 2016;166:387–406.

[31] Shen C, Wang Y, Xu J, Luo G. Chitosan supported on porous glass beads as a new green adsorbent for heavy metal recovery. Chem Eng J 2013;229:217–24.

[32] Wang Z, Xu S, Acosta E. Heat of adsorption of surfactants and its role on nanoparticle stabilization. J Chem Thermodyn 2015;91:256–66.

[33] Aguayo-Villarreal IA, Bonilla-Petriciolet A, Muñiz-Valencia R. Preparation of activated carbons from pecan nutshell and their application in the antagonistic adsorption of heavy metal ions. J Mol Liq 2017;230:686–95.

[34] Pap S, Šolević Knudsen T, Radonić J, Maletić S, Igić SM, Turk Sekulić M. Utilization of fruit processing industry waste as green activated carbon for the treatment of heavy metals and chlorophenols contaminated water. J Clean Prod 2017;162:958–72.

[35] Banerjee S, Chattopadhyaya MC. Adsorption characteristics for the removal of a toxic dye, tartrazine from aqueous solutions by a low cost agricultural by-product. Arab J Chem 2017;10:S1629–38.

[36] Pode R. Potential applications of rice husk ash waste from rice husk biomass power plant. Renew Sust Energ Rev 2016;53:1468–85.

[37] Sun Y, Lv D, Zhou J, Zhou X, Lou Z, Baig SA, et al. Adsorption of mercury (II) from aqueous solutions using FeS and pyrite: a comparative study. Chemosphere 2017;185:452–61.

[38] Du X, Han Q, Li J, Li H. The behavior of phosphate adsorption and its reactions on the surfaces of Fe–Mn oxide adsorbent. J Taiwan Inst Chem Eng 2017;76:167–75.

[39] Ali I, Al-Othman ZA, Alwarthan A. Molecular uptake of Congo red dye from water on iron composite nano particles. J Mol Liq 2016;224:171–6.

[40] Randall SR, Sherman DM, Ragnarsdottir KV, Collins CR. The mechanism of cadmium surface complexation on iron oxyhydroxide minerals. Geochim Cosmochim Acta 1999;63(19):2971–87.

[41] Peng W, Li H, Liu Y, Song S. A review on heavy metal ions adsorption from water by graphene oxide and its composites. J Mol Liq 2017;230:496–504.

[42] Zhang Y, Yan L, Xu W, Guo X, Cui L, Gao L, et al. Adsorption of Pb(II) and Hg(II) from aqueous solution using magnetic $CoFe_2O_4$-reduced graphene oxide. J Mol Liq 2014;191:177–82.

[43] Su H, Ye Z, Hmidi N. High-performance iron oxide–graphene oxide nanocomposite adsorbents for arsenic removal. Colloids Surf A Physicochem Eng Asp 2017;522:161–72.

[44] Basile A, Cassano A, Rastogi NK. Advances in membrane technologies for water treatment: materials, processes and applications. Cambridge, United Kingdom: Elsevier Science; 2015.

[45] Baker RW. Membrane technology and applications. Oxford, UK: Wiley; 2012.

[46] Bechhold H. Kolloidstudien mit der Filtrationsmethode. Z Physik Chem 1907;60:257–318.

[47] Loeb S, Sourirajan S. Sea water demineralization by means of an osmotic membrane. Saline water conversion-II. Advances in chemistry. Am Chem Soc 1963;38:117–32.

[48] Strathmann H. Membrane separation processes. J Membr Sci 1981;9(1–2):121–89.

[49] Wan M-W, Kan C-C, Rogel BD, Dalida MLP. Adsorption of copper (II) and lead (II) ions from aqueous solution on chitosan-coated sand. Carbohydr Polym 2010;80(3):891–9.

[50] Guibal E. Interactions of metal ions with chitosan-based sorbents: a review. Sep Purif Technol 2004;38(1):43–74.

[51] Liu C, Bai R. Preparation of chitosan/cellulose acetate blend hollow fibers for adsorptive performance. J Membr Sci 2005;267(1):68–77.

[52] Premakshi HG, Ramesh K, Kariduraganavar MY. Modification of crosslinked chitosan membrane using NaY zeolite for pervaporation separation of water–isopropanol mixtures. Chem Eng Res Des 2015;94:32–43.

[53] Salehi E, Daraei P, Arabi Shamsabadi A. A review on chitosan-based adsorptive membranes. Carbohydr Polym 2016;152:419–32.

[54] Liu C, Bai R. Adsorptive removal of copper ions with highly porous chitosan/cellulose acetate blend hollow fiber membranes. J Membr Sci 2006;284(1):313–22.

[55] Kanagaraj P, Nagendran A, Rana D, Matsuura T, Neelakandan S, Karthikkumar T, et al. Influence of N-phthaloyl chitosan on poly (ether imide) ultrafiltration membranes and its application in biomolecules and toxic heavy metal ion separation and their antifouling properties. Appl Surf Sci 2015;329:165–73.

[56] Kumar M, Shevate R, Hilke R, Peinemann K-V. Novel adsorptive ultrafiltration membranes derived from polyvinyltetrazole-co-polyacrylonitrile for Cu(II) ions removal. Chem Eng J 2016;301:306–14.

[57] Khorram M, Mousavi A, Mehranbod N. Chromium removal using adsorptive membranes composed of electrospun plasma-treated functionalized polyethylene terephthalate (PET) with chitosan. J Environ Chem Eng 2017;5(3):2366–77.

[58] Lv J, Zhou Q, Zhi T, Gao D, Wang C. Environmentally friendly surface modification of polyethylene terephthalate (PET) fabric by low-temperature oxygen plasma and carboxymethyl chitosan. J Clean Prod 2016;118:187–96.

[59] Sivakumar M, Malaisamy R, Sajitha CJ, Mohan D, Mohan V, Rangarajan R. Ultrafiltration application of cellulose acetate–polyurethane blend membranes. Eur Polym J 1999;35(9):1647–51.

[60] Howard GT. Biodegradation of polyurethane: a review. Int Biodeterior Biodegrad 2002;49(4):245–52.

[61] Riaz T, Ahmad A, Saleemi S, Adrees M, Jamshed F, Hai AM, et al. Synthesis and characterization of polyurethane-cellulose acetate blend membrane for chromium (VI) removal. Carbohydr Polym 2016;153:582–91.

[62] Ladhe AR, Frailie P, Hua D, Darsillo M, Bhattacharyya D. Thiol-functionalized silica–mixed matrix membranes for silver capture from aqueous solutions: experimental results and modeling. J Membr Sci 2009;326(2):460–71.

[63] Yurekli Y. Removal of heavy metals in wastewater by using zeolite nano-particles impregnated polysulfone membranes. J Hazard Mater 2016;309:53–64.

[64] Georgin J, Dotto GL, Mazutti MA, Foletto EL. Preparation of activated carbon from peanut shell by conventional pyrolysis and microwave irradiation-pyrolysis to remove organic dyes from aqueous solutions. J Environ Chem Eng 2016;4(1):266–75.

[65] Huang Y, Li S, Chen J, Zhang X, Chen Y. Adsorption of Pb(II) on mesoporous activated carbons fabricated from water hyacinth using $H_3PO_4$ activation: adsorption capacity, kinetic and isotherm studies. Appl Surf Sci 2014;293:160–8.

[66] Lemraski EG, Sharafinia S. Kinetics, equilibrium and thermodynamics studies of Pb2+ adsorption onto new activated carbon prepared from Persian mesquite grain. J Mol Liq 2016;219:482–92.

[67] Zhang X, Wang Y, Liu Y, Xu J, Han Y, Xu X. Preparation, performances of PVDF/ZnO hybrid membranes and their applications in the removal of copper ions. Appl Surf Sci 2014;316:333–40.

[68] Zhang L, Zhao Y-H, Bai R. Development of a multifunctional membrane for chromatic warning and enhanced adsorptive removal of heavy metal ions: application to cadmium. J Membr Sci 2011;379(1):69–79.

[69] Jiang X, Ding J, Kumar A. Polyurethane–poly(vinylidene fluoride) (PU–PVDF) thin film composite membranes for gas separation. J Membr Sci 2008;323(2):371–8.

[70] Zheng Y-M, Zou S-W, Nanayakkara KGN, Matsuura T, Chen JP. Adsorptive removal of arsenic from aqueous solution by a PVDF/zirconia blend flat sheet membrane. J Membr Sci 2011;374(1):1–11.

[71] Shokri E, Yegani R, Pourabbas B, Kazemian N. Preparation and characterization of polysulfone/organoclay adsorptive nanocomposite membrane for arsenic removal from contaminated water. Appl Clay Sci 2016;132:611–20.

[72] Jamshidi Gohari R, Lau WJ, Matsuura T, Ismail AF. Fabrication and characterization of novel PES/Fe–Mn binary oxide UF mixed matrix membrane for adsorptive removal of As(III) from contaminated water solution. Sep Purif Technol 2013;118:64–72.

[73] Jamshidi Gohari R, Lau WJ, Matsuura T, Halakoo E, Ismail AF. Adsorptive removal of Pb(II) from aqueous solution by novel PES/HMO ultrafiltration mixed matrix membrane. Sep Purif Technol 2013;120:59–68.

[74] Ghaemi N, Zereshki S, Heidari S. Removal of lead ions from water using PES–based nanocomposite membrane incorporated with polyaniline modified GO nanoparticles: performance optimization by central composite design. Process Saf Environ Prot 2017;111:475–90.

[75] Cui L, Wang Y, Gao L, Hu L, Yan L, Wei Q, et al. EDTA functionalized magnetic graphene oxide for removal of Pb(II), Hg(II) and Cu(II) in water treatment: adsorption mechanism and separation property. Chem Eng J 2015;281:1–10.

[76] Chatterjee S, De S. Adsorptive removal of fluoride by activated alumina doped cellulose acetate phthalate (CAP) mixed matrix membrane. Sep Purif Technol 2014;125:223–38.

[77] Chatterjee S, De S. Adsorptive removal of arsenic from groundwater using chemically treated iron ore slime incorporated mixed matrix hollow fiber membrane. Sep Purif Technol 2017;179:357–68.

[78] Beppu MM, Arruda EJ, Vieira RS, Santos NN. Adsorption of Cu(II) on porous chitosan membranes functionalized with histidine. J Membr Sci 2004;240(1):227–35.

[79] Boricha AG, Murthy ZVP. Acrylonitrile butadiene styrene/chitosan blend membranes: preparation, characterization and performance for the separation of heavy metals. J Membr Sci 2009;339(1):239–49.

[80] Carneiro RTA, Taketa TB, Gomes Neto RJ, Oliveira JL, Campos EVR, de Moraes MA, et al. Removal of glyphosate herbicide from water using biopolymer membranes. J Environ Manag 2015;151:353–60.

[81] Aliabadi M, Irani M, Ismaeili J, Najafzadeh S. Design and evaluation of chitosan/hydroxyapatite composite nanofiber membrane for the removal of heavy metal ions from aqueous solution. J Taiwan Inst Chem Eng 2014;45(2):518–26.

[82] Lee HS, Im SJ, Kim JH, Kim HJ, Kim JP, Min BR. Polyamide thin-film nanofiltration membranes containing TiO$_2$ nanoparticles. Desalination 2008;219(1):48–56.

[83] Kim S, Pechar TW, Marand E. Poly(imide siloxane) and carbon nanotube mixed matrix membranes for gas separation. Desalination 2006;192(1):330–9.

[84] Chu Z, Liu J, Han C. Removal of strontium ions from aqueous solution using hybrid membranes: kinetics and thermodynamics. Chin J Chem Eng 2015;23(10):1620–6.

[85] Lin J, Ye W, Zhong K, Shen J, Jullok N, Sotto A, et al. Enhancement of polyethersulfone (PES) membrane doped by monodisperse Stöber silica for water treatment. Chem Eng Process Process Intensif 2016;107:194–205.

## Further Reading

[86] Desjardins C, Koudjonou B, Desjardins R. Laboratory study of ballasted flocculation. Water Res 2002;36(3):744–54.

[87] Tran HN, You S-J, Hosseini-Bandegharaei A, Chao H-P. Mistakes and inconsistencies regarding adsorption of contaminants from aqueous solutions: a critical review. Water Res 2017;120:88–116.

C H A P T E R

# 13

# Hybrid Processes: Membrane Bioreactor

*Abdul Wahab Mohammad, Yeit Haan Teow, Woon Chan Chong, Kah Chun Ho*

**Centre for Sustainable Process Technology (CESPRO), Faculty of Engineering and Built Environment, Universiti Kebangsaan Malaysia, Selangor, Malaysia**

O U T L I N E

**401**

# 13.1  INTRODUCTION

Membrane bioreactor (MBR) has become an established hybrid or integrated membrane processes for various applications, especially for industrial and municipal wastewater treatments. The MBR market itself was estimated to have a market value of about USD$363 million in 2010 and is increasing as the need for clean water increases [1].

MBR was first introduced in the late 1960s. The first idea was to combine the operation of activated sludge bioreactor with a crossflow membrane filtration loop. Later in 1989, Yamamoto et al. [2] proposed the breakthrough idea of submerging the membranes within the bioreactor. Previous to that MBRs generally consisted of external membrane module (sidestream MBR) that required high transmembrane pressure to maintain permeate flow. With submerged MBRs, the energy requirement is much lower, and the system becomes more cost-effective.

This chapter will discuss the MBR in more detail focusing on membrane material selection, membrane fabrication, membrane characterization, separation mechanism, and applications. In the first part, various types of materials that have been used for membranes in MBR are discussed. The second part looks at the types of membrane fabrication that have been used which include nonsolvent induced phase separation (NIPS), and melt spinning cold stretching (MSCS), track-etched, and electrospinning. Subsequently, various methods of characterization are explained. Next, the chapter looks at the separation mechanism that covers the biological process as well as the membrane process. Finally, the last part will discuss some of the applications of MBRs in various sectors. More detail coverages on MBRs in recent years have been widely available in a major handbook [1] as well as a few excellent reviews covering many aspects of MBRs [3–6].

## 13.2 MEMBRANE MATERIALS SELECTION

The membrane materials selection for MBR application shall fulfill a few criteria to be practically used in the system. The membrane shall possess high resistance to chemical attack, mechanically durable and has some resistance toward thermal attack. The typical range of wastewater pH in MBR is between pH 4 and pH 10. However, during chemical enhanced backwash (CEB) using acidic and basic chemicals such as citric acid, hydrochloric acid, sodium hydroxide or sodium hypochlorite, the pH could be in the range from pH 1 to pH 12 [1]. Therefore, the membrane materials used for MBR application shall be able to tolerate a harsh environment with hazardous and corrosive waste. Membranes with high abrasive resistance would be able to withstand certain pressure, high shear forces from aeration and could last for at least 5 years of lifespan. In addition to the above criteria, the price of the raw materials shall be low or medium to be economically feasible for commercialization and installed in large-scale wastewater treatment plants.

The two primary materials used to produce membranes for MBR are ceramic and polymer. Fig. 13.1 shows the molecular structure of the most commonly used polymeric materials in MBR. Although ceramic membranes are more robust regarding chemical and thermal stability with lower fouling, their application in MBR industry remains limited. This is due to the higher production cost of a ceramic membrane, which makes the large-scale application economically unfeasible. On the other hand, membrane derived from polymeric materials are flexible and could vary widely in their characteristics according to the preparation conditions such as the concentration of polymer, blending speed, temperature, and nonsolvent selection. Among the polymeric membranes, polyvinylidene difluoride (PVDF) material is highly preferable and makes up half of the market share. This is followed by polyethersulfone (PES), derivatives of polyethylene (PE) and polypropylene (PP). The first commercial membranes were made from cellulose acetate (CA), and polysulfone (PS) materials [7] and their application in MBR is limited compared to the above-mentioned materials. The cross-sectional morphology of ceramic and polymeric membranes are shown in Fig. 13.2. Generally,
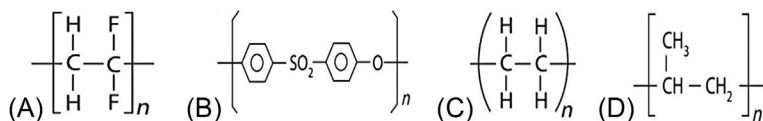


**FIG. 13.1**  Molecular structure of the most commonly used polymeric membranes in MBR (A) PVDF, (B) PES, (C) PE, and (D) PP [7]. *Reprinted from Principles of membrane bioreactors for wastewater treatment, Park H, Chang I, Lee K. membranes, modules, and cassettes, p. 83. Copyright (2015), with permission from Taylor and Francis.*

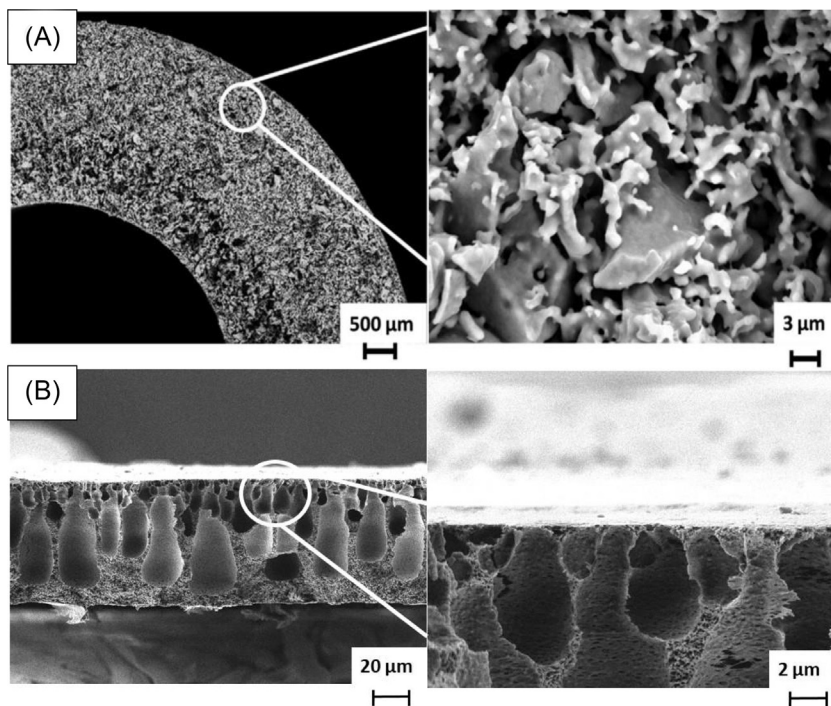**FIG. 13.2** Cross sectional structure of (A) ceramic [8] and (B) polymeric membranes [8a]. *Reprinted from Ceramics International, vol. 43, Hubadillah SK, Othman MHD, Harun Z, Ismail AF, Rahman MA, Jaafar J. A novel green ceramic hollow fiber membrane (CHFM) derived from rice husk ash as combined adsorbent-separator for efficient heavy metals removal, p. 4718. Copyright (2017), with permission from Elsevier.*

ceramic membrane consists mainly sponge-like structure with flaky substances. Polymeric membrane (i.e., PVDF) meanwhile exhibits an abundance of finger-like features with a thin layer skin on the top.

Table 13.1 shows the membrane materials used for some large MBR plants in various countries. Polymeric membranes are commonly used in large-scale municipal wastewater plants. On the other hand, ceramic membranes are preferred for operation in a harsh environment where high temperature, pressure or severe fouling in high strength wastewater are expected. It is worth mentioning that PVDF hollow fiber membranes used in Nordkanal water treatment plant have been operating in its tip-top condition for 13 years without significant replacement of the membranes. This proved that continuous research and optimization study on the plant operation is paramount in maintaining the membrane performance and eventually reduce the overall operational cost.

Modules such as spiral wound, tubular, flat sheet, and hollow fiber have been widely available in the market. A spiral wound is mainly used

**TABLE 13.1**    Membrane Materials Used in Some MBR Plants

| Plant | Capacity | Material | Commissioning year | Type of water |
|---|---|---|---|---|
| Henriksdal WWTP, Stockholm, Sweden | 536–864 MLD Submerged | PVDF 0.04 μm, hollow fiber GEWPT, ZeeWeed 500 | 2019–26 | Municipal wastewater |
| Brussels Sud WWTP, Brussels, Belgium | 66–120 MLD Submerged | PVDF 0.04 μm, hollow fiber GEWPT, Zeeweed 500 D | 2018 | Municipal wastewater |
| Canton Water Reclamation Facility, Canton, USA | 159–333 MLD Submerged | Chlorinated PE 0.4 μm, flat sheet Kubota, SMU | 2017 | Municipal wastewater |
| Shaybah Oil Field WWTP, Saudi Aramco, Saudi Arabia | 750 m³/d Submerged | Chlorinated PE 0.4 μm, flat sheet Kubota, SMU | 2016 | Municipal wastewater |
| Carré de Reunion WWTP, Versailles region, France | 42–144 MLD Submerged | PVDF 0.04 μm, hollow fiber Koch Membrane System, PURON MBR | 2015 | Municipal wastewater |
| Jurong Water Reclamation, Singapore | 4550 m³/d Submerged | Ceramic (α alumina) 0.1 μm, Flat sheet Meidensha | 2014 | Industrial used water |
| Arla Factory WWTP, Vimmerby, Sweden | 400–450 m³/d Sidestream | Ceramic 0.2 μm, disc & tubular Grundfos, Biobooster | 2012 | Dairy wastewater |
| Jing Xi WWTP, Guangzhou, China | 100,000 m³/d Submerged | PVDF Hollow fiber Memstar | 2010 | Municipal wastewater |
| Hutthurm WWTP, Germany | 20,000 PE Submerged | PES 0.038 μm, Flat sheet HUBER, VRM30/544 | 2008 | Municipal wastewater |
| Nordkanal WWTP, Kaarst, Germany | 45 MLD 47,700 m³/d Submerged | PVDF 0.04 μm, hollow fiber GEWPT, Zeeweed 500 | 2003 | Municipal wastewater |

in reverse osmosis or nanofiltration. Tubular has low packing density (smaller surface area) and is only applicable for side-stream application in small-scale MBR plant. Meanwhile, flat sheet and hollow fiber are the most commonly used configurations in submerged MBR system.

## 13.2.1 Ceramic Membrane

Materials that are used to produce ceramic membranes include alumina ($Al_2O_3$), zirconia ($ZrO_2$), glass ($SiO_2$), titania ($TiO_2$) and silicon carbide (SiC). Among these materials, $Al_2O_3$ is the most commonly used ceramic membrane for MBR application. Ceramic membrane is very robust and reliable. It can be used in high acidity and alkalinity conditions (pH 0–14) and able to withstand high pressure (up to 10 bar) and temperature in the separation process where polymeric membrane could not perform [9]. In MBR application, a ceramic membrane is generally used in filtering industrial wastewater which is labeled as challenging wastewater. Besides high manufacturing cost, another main drawback of a ceramic membrane is its brittleness; hence it has to be handled with extra care.

## 13.2.2 PVDF Membrane

PVDF is a semicrystalline polymer and relatively hydrophobic compared with other polymers. As the precipitation during phase inversion occurs slowly, very uniform pore size distribution was formed on the membrane [8]. PVDF membrane possesses distinctive resistance toward a wide range of chemicals, except strong alkalinity chemicals, esters, and ketones. Prolong exposure to high concentration of sodium hypochlorite (NaOCl) during backwash cleaning would lead to membrane aging. Moreover, the membrane's hydraulic performance, chemical and mechanical structure could be altered [10]. Hence, cleaning with a strong concentration of sodium hydroxide (NaOH) and NaOCl shall be minimized to prevent degradation of the polymer. However, PVDF has excellent resistance toward chlorine. Besides, PVDF membrane has better thermal resistance compared to PES membrane [11].

## 13.2.3 PES Membrane

PES is the second widely used membrane material in MBR. In a study by Liu et al. [11], it possesses higher melting point and thermal stability than the other polymeric membranes by only 1% mass loss in air happened at 400°C. Besides, PES is more hydrophilic compared to PVDF due to its molecular structure which facilitates hydrogen bonding with water molecules. Therefore, higher volume of permeate could be attained

using PES membrane [12]. Also, PES is less tolerant to chlorine but more resistance to NaOCl. Although PES has higher mechanical strength than PVDF membrane, it is more rigid due to little elongation ability [13]. A membrane with high flexibility is important in the MBR application as continuous aeration with high shear force could break the membranes. Therefore, additives are commonly incorporated to increase the flexibility of the membrane in the submerged system.

### 13.2.4 Polyolefin Membrane

The most common polyolefin membrane used in the MBR system is polyethylene (PE) and polypropylene (PP). PE is made by polymerization of olefin ethylene while PP is produced from olefin propylene. These membranes are mainly made as MF membrane with a pore size larger than 0.1 μm. The main advantages of these membranes are lower production cost due to cheaper raw material price. PE membrane was the earliest membrane material used in the MBR system. As the membrane is very hydrophobic (more hydrophobic than PVDF), its blending capacity with additives is limited. It usually undergoes posttreatment to become hydrophilic. Currently, chlorinated PE flat sheet membrane was manufactured by Kubota and applied in some MBR plants (Table 13.1). Although polyolefin membrane has high tolerance to chemicals, its tolerance toward chlorine was lower compared to PVDF membrane.

The characteristics of each membrane were summarized in Table 13.2. Each membrane material has its advantages and disadvantages. Polymeric membranes are typically selected for municipal wastewater treatment in large scale due to its flexibility, lower production cost, and simplicity of manufacturing process. Although most polymer materials have high thermal resistance, operating temperature of 5–40°C are recommended for a commercial polymeric membrane. Meanwhile, ceramic membranes are highly advantageous over polymeric membranes regarding high temperature, pressure, fouling, and chemical resistance. Membrane modification has been conducted to improve their properties to obtain high quality of membranes. Besides, continuous research on process optimization, maintenance of membranes, training of operators shall be implemented to achieve a sustainable system in wastewater treatment plants.

## 13.3 MEMBRANE FABRICATION

Because most of the full-scale MBR plants apply polymeric membranes as they can be manufactured at a relatively low cost, hence this section focuses on membrane fabrication method for the polymeric membrane.

**TABLE 13.2**    Advantages and Disadvantages of Various Membrane Materials

| Material | Characteristics |
|---|---|
| Ceramic | • Brittle<br>• Excellent thermal resistance<br>• Excellent chemical resistance<br>• Very expensive<br>• MF and UF membranes |
| PVDF | • Medium strength with high elongation (flexible)<br>• Medium thermal resistance<br>• High chemical tolerant to chlorine and most oxidants<br>• Medium tolerant to high alkalinity solution especially NaOCl<br>• Highly commercialized, price in the medium range<br>• Hydrophobic, could be modified by hydrophilic additives<br>• MF and UF membranes |
| PES | • High strength but more rigid (less flexible)<br>• High thermal resistance<br>• High chemical tolerant to NaOCl<br>• Medium chemical tolerant to chlorine<br>• Highly commercialized, price in the medium range<br>• Hydrophobic, could be modified by hydrophilic additives<br>• MF and UF membranes |
| PE and PP | • Low strength<br>• Low thermal resistance<br>• Low chemical tolerant to chlorine<br>• Lowest manufacturing cost<br>• Very hydrophobic, difficult to be modified via blending method<br>• Mainly MF membranes |

Generally, MBR membrane fabrication methods can be categorized into NIPS, and MSCS, track-etched, and electrospinning.

## 13.3.1 Membrane Fabrication Methods

### 13.3.1.1 NIPS

Among them, NIPS is the most commonly used and mature method owing to its simplicity and flexibility in preparing a great variety of membranes. As depicted in Fig. 13.3, the polymer is dissolved in a solvent to form a polymer solution and subsequently cast onto suitable support followed by immersion in a nonsolvent bath (coagulation bath) to induce liquid-solid and/or liquid-liquid phase separation. During this process, the solvent and nonsolvent exchange paths where the transfers occur from the polymer solution to the coagulation bath vice versa. The space that is occupied by solvent originally becomes the pores when the membrane solidified. Finger-like voids are generally preferred due to lower
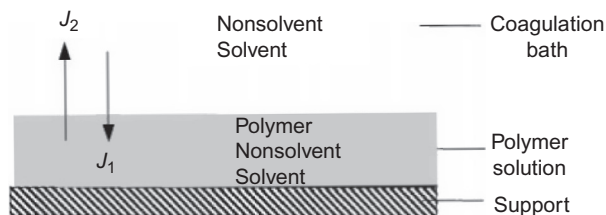
FIG. 13.3 Schematic illustration of a polymer casting film-bath interface. $J_1$ is the nonsolvent flux, and $J_2$ is the solvent flux [14]. *Reprinted from Encyclopedia of Separation Science, Mulder M. Membrane preparation: phase inversion membranes, p. 3341. Copyright (2000), with permission from Elsevier.*

membrane resistance thus high membrane permeability. Few parameters can affect the structure of the membrane including the composition of polymer casting solution, amount of solvent, the composition of coagulation bath, the temperature of coagulation bath, exposure time, the thickness of casting solution, and type of membrane support. For instance, Zinadini et al. [15] had prepared PES membrane in different concentrations of 13, 15, and 17 wt% of polymer for MBR application in dairy wastewater. Based on their results, it was shown that increasing polymer concentration resulted in a denser and thicker skin layer, leading to higher membrane pressure resistance and improved separation capability. Besides, the finger-like structure becomes narrow as the polymer concentration increases as shown in Fig. 13.4.

### 13.3.1.2 MSCS

In comparison to NIPS, MSCS process does not require any organic solvents that may result in solvent waste and environmental damage. MSCS is mainly used for thermoplastic polymers such as PTFE, polypropylene (PP) and polyethylene (PE) which is difficult to dissolve in common solvent [16]. During MSCS process, melted polymer is spun and undergoes a cold-stretching step where a mechanical force is applied uniaxially and biaxially to form a microporous membrane as visualized in Fig. 13.5 [14]. In this process, the membrane properties and pore structure are greatly influenced by the polymer's properties (crystallinity, melting point, tensile strength, etc.) and MSCS processing condition. The primary advantage of this method is solvent-less and compatible with the low-cost polymer. For MBR application, Li et al. [18] have fabricated PP hollow fiber microporous membrane with a porosity of $45.9 \pm 3.1\%$ and average pore diameter of $0.11 \pm 0.04$ µm via MSCS method. They then combined 100 bundles of hollow fibers to develop a U-shaped hollow fiber membrane in MBR filled with synthetic wastewater and seed activated sludge.
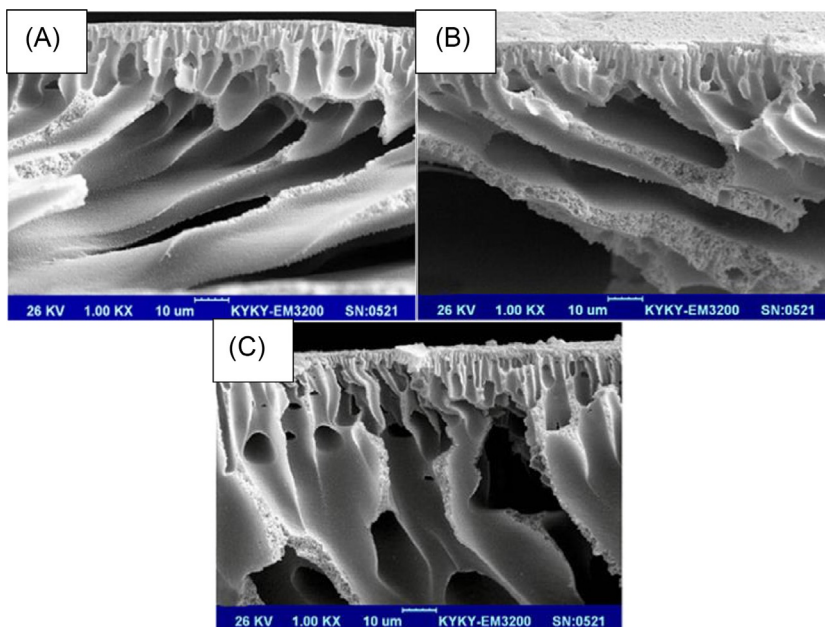
FIG. 13.4    Cross-section SEM images of (A) 13 wt%, (B) 15 wt%, and (C) 17 wt% PES membrane [15a,16]. *Reprinted from Journal of Water Process Engineering, vol. 7, Zinadini S, Vatanpour V, Zinatizadeh AA, Rahimi M, Rahimi Z, Kian M. Preparation and characterization of antifouling graphene oxide/polyethersulfone ultrafiltration membrane: application in MBR for dairy wastewater treatment, p. 286. Copyright (2015), with permission from Elsevier.*
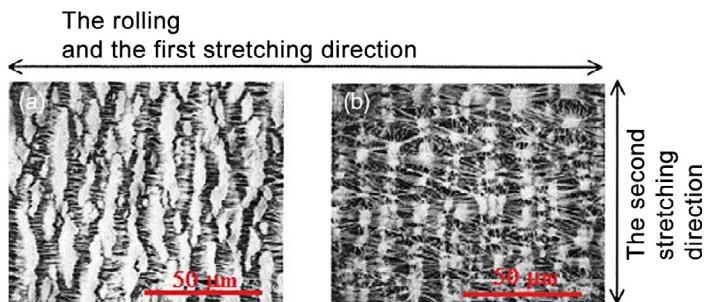


FIG. 13.5    Surface morphology of PTFE membrane fabricated by MSCS method during (A) uniaxially stretching and (B) biaxially stretching [20]. *Reprinted from Journal of Membrane Science, vol. 149, Kurumada KI, Kitamura T, Fukumoto N, Oshima M, Tanigaki M, Kanazawa SI. Structure generation in PTFE porous membranes induced by the uniaxial and biaxial stretching operations, p. 53. Copyright (1998), with permission from Elsevier.*

However, there are limited studies in MBR application using membrane fabricated by this method due to difficulty in controlling membrane pore size. Besides, this method does not provide an effective dispersion of the filler in the membrane matrix that can be achieved by NIPS method.

### 13.3.1.3 Track-Etching

Track-etching method offers more advantages over NIPS and MSCS due to their uniform cylindrical pores and narrow pore size distribution. As shown in Fig. 13.6, the track-etched membrane can be formed when a thin raw polymer film is exposed to charged particles or high energy ions at an accelerator to produce tracks along their trajectories. Then, this film is immersed in etch bath that etches the polymer where nucleation occurs to form pores. The number of membrane pores will be determined by the exposure time of the film to radiation while the pore diameter is determined by the etch time [20]. Polycarbonate or PE film is usually used as the polymer material and NaOH as the etching solution. Choi et al. [21] had compared the performance of tracked-etched polycarbonate (PCTE) and phase-inversed polytetrafluoroethylene (PTFE) in MBR for municipal wastewater treatment. Their results evidenced that PCTE had the lowest increment in the filtration resistance owing to its smoother surface as shown in Fig. 13.7. However, the conventional production of track-etching method is too costly for large-scale production; hence, there is much research that focuses on developing a new production method that can significantly reduce investment production costs.
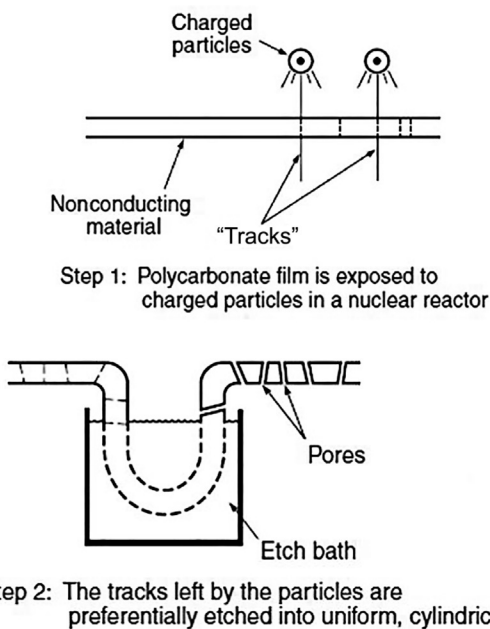


FIG. 13.6 Schematic illustration of the two-step process to fabricate track-etched membrane [19]. *Reprinted from John Wiley & Sons, Ltd., vol. 23, Baker RW, Baker WR. Membrane technology and applications, p. 94. Copyright (2012), with permission from John Wiley & Sons, Ltd.*
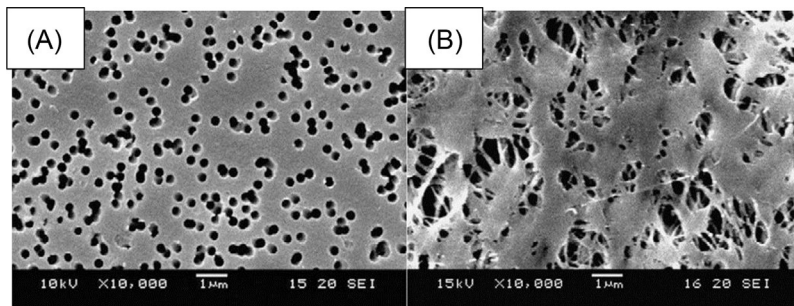
**FIG. 13.7** SEM images of (A) track-etched PCTE and (B) phase-inversed PTFE membrane [22]. *Reprinted from Separation and Purification Technology, vol. 65, Choi J-H, Park S-K, Ng H-Y. Membrane fouling in a submerged membrane bioreactor using track-etched and phase-inversed porous membranes, p. 185. Copyright (2009), with permission from Elsevier.*

### 13.3.1.4 Electrospinning

Electrospinning is a relatively novel technique to fabricate membrane in MBR. In this process, a high DC voltage is applied between negatively charged polymer solution or melt and a metallic collector as shown in Fig. 13.8. Subsequently, fine polymer fiber is discharged from the nozzle and form randomly oriented fibrous on the metal collector. Length and diameter, as well as the morphology of fiber, can be tuned by solution viscosity, applied electric potential, and the polymer solution feed rate. Whereas, porosity, pore size distribution, hydrophobicity, and surface morphology of membrane can be manipulated by the fiber diameter and its morphology [17]. For MBR application, Bilad et al. [19] had
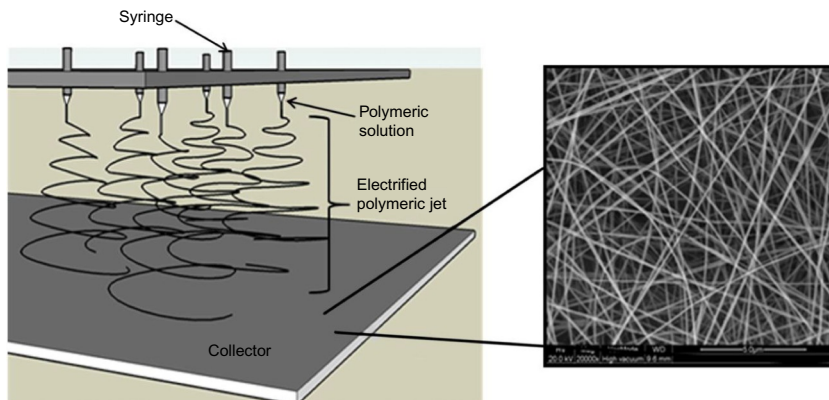


**FIG. 13.8** Schematic showing electrospinning of polymer cast solution and nanofiber membrane (inset) [23]. *Reprinted from Desalination, vol. 257, Daels N, De Vrieze S, Decostere B, Dejans P, Dumoulin A, De Clerck K, et al. The use of electrospun flat sheet nanofibre membranes in MBR applications, p. 171. Copyright (2010), with permission from Elsevier.*

prepared electrospun nanofiber membrane from polyamide polymers, and their result showed that the performance of the novel membrane is comparable to the commercial PVDF and PE membranes at short and long term. Compared to NIPS fabrication method, electrospinning produces a membrane that has a higher hydrophobic surface, high porosity, interconnected open pore structure, high surface-to-mass (or volume) ratio, highly ordered polymer chains, and a more controllable structure which is ideal for membrane distillation (MD) process [22,22a]. Nonetheless, further development in cost reduction and fabrication on a large-scale is still needed to expand the electrospinning application.

## 13.3.2 Membrane Modification Methods

To alleviate membrane fouling in MBR, numerous studies have been conducted to modify the membrane characteristics via blending modification and surface modification which usually performed during or after membrane fabrication. Generally, the purpose of membrane modification is to reduce or prevent the adhesion of foulants on the membrane surface and inner pore that leads to higher MBR operation cost, intensive energy demand, and reduced lifespan of the membrane.

### 13.3.2.1 Blending Modification

For blending strategy, the method usually involves the incorporation of a variety of hydrophilic filler into the membrane matrix targeting to improve the membrane antifouling properties. Nanoparticles are generally used as filler due to their large surface area to volume ratio. Thus, relatively minor amount is needed for sufficient modification efficiency. Blending modification has been widely studied as one-step membrane fabrication due to the convenient operation and mild conditions. Besides, the modified membrane can combine fundamental properties of additives for excellent separation performance, enhanced thermal and chemical resistance for harsh wastewater environments. Fig. 13.9 has shown that blending modification by alumina ($Al_2O_3$), graphene oxide (GO), iron oxide ($Fe_3O_4$), multiwalled carbon nanotubes (MWCNTs), nanodiamond, titanium oxide ($TiO_2$) and zirconium dioxide ($ZrO_2$) can significantly improve the hydrophilicity property and reduce membrane fouling. Fig. 13.10 depicts the schematic diagram to prepare GO blended polysulfone (PSF) membrane by NIPS membrane. According to studies conducted by Zhao et al. [25], modified PVDF blended with 3 wt% GO exhibited sustained permeability, lower cleaning frequency, and three-times longer filtration time than neat PVDF membrane due to improved surface hydrophilicity and antifouling properties [25a].
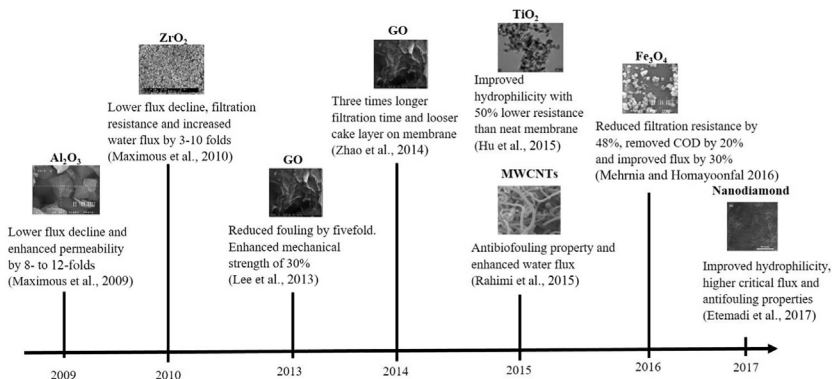
**FIG. 13.9**    Chronology of membrane blending method for MBR application.
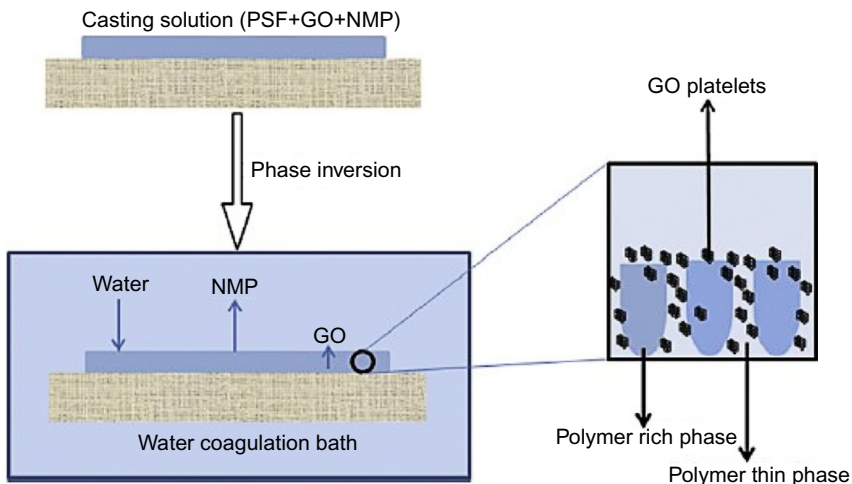


**FIG. 13.10**    Preparation of GO blended PSf membrane by NIPS method [24]. *Reprinted from Desalination, vol. 313, Ganesh BM, Isloor AM, Ismail AF. Enhanced hydrophilicity and salt rejection study of graphene oxide-polysulfone mixed matrix membrane, p. 204. Copyright (2013), with permission from Elsevier.*

Besides direct blending of the nanoparticles, research started to pay attention to surface functionalization to reduce the aggregation of nanoparticles and improve membrane performance. Etemadi et al. [26] prepared CA membrane by blending amino-functionalized nanodiamond (ND-NH$_2$), and polyethylene glycol grafted ND (ND-PEG) for MBR in treating pharmaceutical wastewater. Their results showed that modified membrane at low concentration functionalized ND of 0.5 wt% demonstrated high hydrophilicity and excellent antibiofouling properties. However, the maximum modification efficiency obtained by blending method

is usually limited due to the nanoparticles tend to trapped in the membrane bulk material. Hence, surface modification method is performed to tune only the membrane surface where the adsorption of microbial products such as extracellular polymeric substances (EPS) usually occurs.

### 13.3.2.2  Surface Modification

As shown in Table 13.3, for surface medication method, usual approaches are physical coating or adsorption, chemical reactions on the membrane surface, plasma treatment, and grafting. The membrane surface modification aims to introduce hydrophilic groups on the membrane surface to minimize undesired interactions with the foulants.

Physical coating or adsorption is usually performed by direct filtering of hydrophilic materials over the membrane surface by pressure. Significant improvement of the hydrophilicity and antifouling properties of the

**TABLE 13.3**  Membrane Surface Modification Method for MBR Application

| Reference | MBR application | Method | Procedure |
|---|---|---|---|
| [27] | Synthetic wastewater treatment | Physical coating/ adsorption | Dipping PSF membrane into 1% $TiO_2$ suspension and pressurized at 4 bar |
| [23] | Synthetic wastewater treatment | Chemical reactions on a membrane surface | Modified terylene membrane was prepared by dip-coating and cross-linking with glutaraldehyde to immobilize polyrotaxanes, $TiO_2$, and PVA |
| [28] | Synthetic wastewater treatment | | Coating chitosan on nonwoven fabric by cross-linking agent glutaraldehyde |
| [24] | Synthetic wastewater treatment | | A membrane was dipped into $TiO_2$ sol-gel and $TiO_2$ nanoparticles were bonded on membrane surface by chemical coprecipitation-peptization |
| [29] | Synthetic wastewater treatment | | Diatomite coated nonwoven fiber was cross-linked in PVA solution |
| [30] | Yeast solution | | Polymerization of polyaniline doped with phytic acid on graphene deposited filter cloth |
| [31] | Synthetic wastewater treatment | | Surface-tailored silica nanoparticles were tethered to poly(methacrylic acid)-grafted PVDF membrane |

*Continued*

**TABLE 13.3**    Membrane Surface Modification Method for MBR Application—cont'd

| Reference | MBR application | Method | Procedure |
|---|---|---|---|
| [32–34] | Synthetic wastewater treatment | Plasma treatment | PP hollow fiber microporous membrane was surface-modified by argon, air, $N_2$, $CO_2$, $NH_3$ plasma treatment |
| [35] | Synthetic wastewater treatment | Grafting | PVDF membrane was coated with amphiphilic graft copolymer PVDF-*graft*-poly(oxyethylene) methacrylate |
| [18] | Synthetic wastewater treatment | | Surface modification of the PP hollow fiber microporous membrane by sequential photoinduced graft polymerization of acrylic acid and acrylamide |
| [36] | Synthetic wastewater treatment | | PP hollow fiber microporous membrane was surface-modified by photoinduced graft polymerization of acrylamide |
| [37] | Synthetic wastewater treatment | | PP hollow fiber microporous membrane was surface-modified by photoinduced graft polymerization of 2-aminoethyl methacrylate |
| [38] | Synthetic wastewater treatment | | Radiation-induced graft polymerization was used to modify PVDF membrane with glycidyl methacrylate and sodium sulfite using radiation-induced graft polymerization |

coated membrane was observed. However, the nanoparticles were also found easily detached from the membrane surface because of the weak adsorption between hydrophilic nanoparticles and the hydrophobic membrane surface. Therefore, chemical reactions are initiated to introduce various functional groups that act as an anchor site for chemical bonding with nanoparticles. For instance, Su et al. [24] had prepared $TiO_2$ modified membrane by dipping neat membrane into $TiO_2$ sol for chemical coprecipitation-peptization. Their results showed that most $TiO_2$ particles were still firmly coated on the surface of the membrane even after vigorous ultrasonic washing as shown in Fig. 13.11. The parameters that affect the morphology of the modified membrane are the composition of filler, use of a cross-linking agent, reaction time, and homogeneity of filler suspension.

Plasma treatment is another method to generate active groups on membrane surface at the presence of gas. Typically, most plasma treatments were conducted at frequencies of 2–50 Hz and an inert gas such as helium and argon is injected to initiate plasma condition [20]. For example, Liang
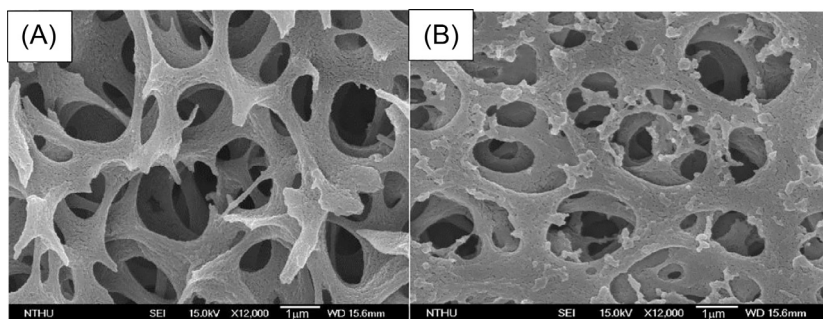
FIG. 13.11    SEM images of (A) neat cellulose acetate membrane and (B) surface modified membrane by TiO$_2$ [33]. *Reprinted from Journal of Environmental Engineering-Asce, vol. 138, Su YC, Huang CP, Pan JR, Hsieh WP, Chu MC. Fouling mitigation by TiO$_2$ composite membrane in membrane bioreactors, p. 348. Copyright (2012), with permission from Elsevier.*

et al. [39] excited the PVDF membrane surface with argon plasma at pressure 0.037 kPa, power of 18 W, and frequency of 8–12 MHz, and then exposed to air to facilitate the formation of peroxides and hydroperoxides on the membrane surface as shown in Fig. 13.12. The degree of surface modification by plasma treatment can be governed by several factors including a gas composition in the discharge, composition of the treated sample, and the process parameters. For MBR application, Yu et al. [41] had performed PP hollow fiber membrane surface modification by argon plasma treatment, and their results showed that flux recovery and flux ratio was improved by 20% and 143%, respectively. Nonetheless, the chemical reaction of the plasma treatment is rather complex where the susceptibility of polymer to plasma treatment is unpredictable. Therefore, the detail surface chemistry of the modified surface remains unknown; hence it is currently difficult to extend plasma treatment from existing laboratory to the large-scale application. Besides, the mechanical strength of the modified membrane deteriorated drastically after plasma treatment thus unsuitable for long-hour operation.
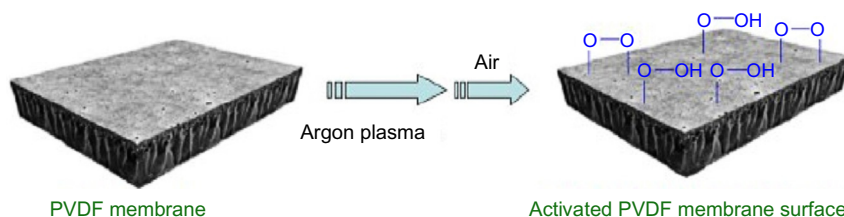


FIG. 13.12    Schematic diagram for argon plasma treatment of PVDF membrane [40]. *Reprinted from ACS Applied Materials and Interfaces, vol. 5, Liang S, Kang Y, Tiraferri A, Giannelis EP, Huang X, Elimelech M. Highly hydrophilic polyvinylidene fluoride (PVDF) ultrafiltration membranes via postfabrication grafting of surface-tailored silica nanoparticles, p. 6695. Copyright (2013), with permission from American Chemical Society.*

Apart from the method mentioned above, grafting is an alternative solution for membrane surface modification and usually initiated by UV photo-irradiation, plasma, and high energy irradiation as well as "living" controlled polymerization. In contrast to plasma treatment, grafting is adhesion of hydrophilic modifiers after the polymer chains are activated. UV photo-irradiation is more commonly used because this method is relatively simple, energy-efficient, and cost-effective. For instance, Yu et al. [36] had prepared PP hollow fiber microporous membrane by photoinduced graft polymerization of acrylamide as shown in Fig. 13.13. The hollow fiber was dipped in acrylamide solution and then exposed to UV
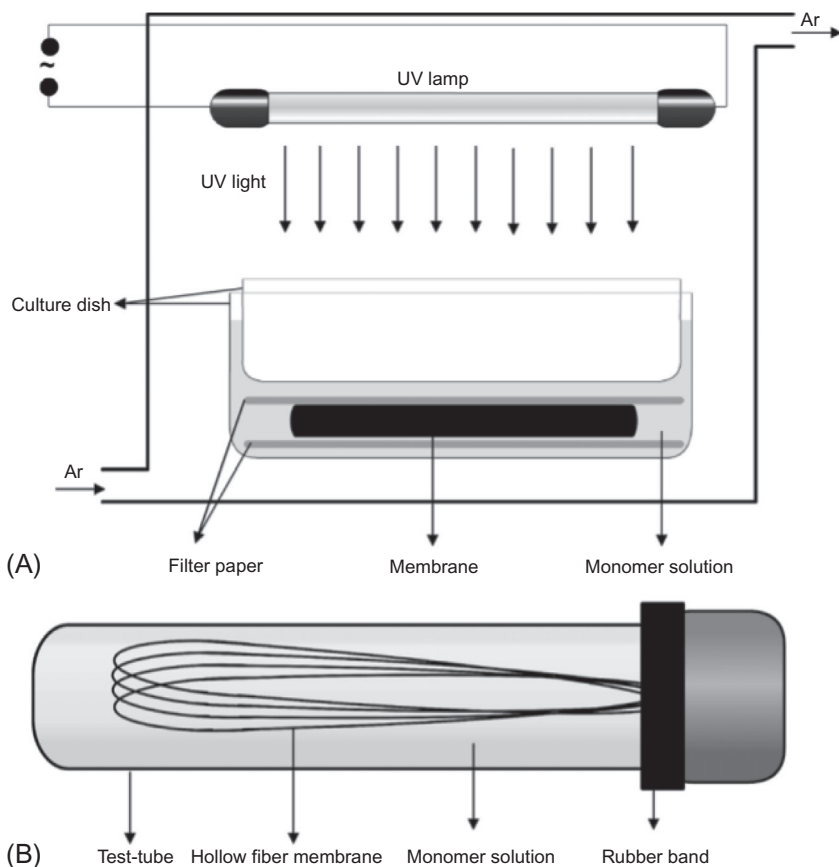


**FIG. 13.13**    Schematic diagram of UV photoinduced graft polymerization [42]. *Reprinted from Separation and Purification Technology, vol. 53, Yu HY, Xu ZK, Lei H, Hu MX, Yang Q. Photoinduced graft polymerization of acrylamide on polypropylene microporous membranes for the improvement of antifouling characteristics in a submerged membrane-bioreactor, p. 120. Copyright (2007), with permission from Elsevier.*

irradiation where the surface radicals were generated and anchored to the monomers. For MBR application, Yu et al. [42] compared the performance modified membrane fabricated by plasma treatment and photoinduced graft polymerization, and their results showed that surface-grafted membrane has higher flux ratio compared to the plasma-treated membrane. This is probably because grafted membrane possesses higher negative surface charge owing to attachment of amino acids on membrane surface thus prevent accumulation of foulants due to charge repulsion effects. However, suitable grafting time, monomer concentration, grafting density and chain length, should be studied to avoid surface pore blockage and lost membrane permeability.

All in all, there are many methods to fabricate membrane and to improve membrane performance for steady and long MBR process. Selection of membrane fabrication should depend on the compatibility of polymer used, the stability of filler, cost of membrane fabrication, type of membrane operation, propensity on the large-scale fabrication that produce the desired membrane properties.

## 13.4  MEMBRANE CHARACTERIZATION

Membranes are commonly characterized by its chemical and physical characteristics. Physical parameters included membrane pore size, porosity and surface morphology. Meanwhile, chemical parameters involve membrane hydrophilicity and surface charge. The significance of these parameters in MBR will be discussed in this section.

### 13.4.1  Membrane Pore Size and Porosity

The pore size of membranes used in MBR process varies, ranges from microfiltration of 0.1–0.4 μm to ultrafiltration range of 0.02–0.1 μm. Meanwhile, the permeation flux of membranes in MBR plants ranges typically from 10 to 80 $L/m^2 h$. Numerous studies have been performed to investigate the effect of membrane pore size and porosity on the performance of various membranes regarding rejections and fouling behavior. Interestingly, conflicting trends were observed between a wide range of membrane pore size and their hydraulic performance in MBR process.

Jin et al. [43] tested four ceramic membranes (80–300 nm) in MBR using domestic wastewater. Initially, the 80-nm membrane was able to reject more organics due to smaller pore size. However, the discrepancy of organics removal efficiency among the membranes became insignificant when running in extended period. The cake layer developed on membrane surface in long-term had provided perm-selectivity to the filtration

process on all the membranes regardless of the pore size. In fouling study, as expected, the 300-nm membrane experienced the lowest initial TMP while the 80 nm membrane had the highest initial TMP. However, eventually, the 300-nm membrane reached TMP of 30 kPa on day 72 which was 79 days earlier than the 80 nm membrane in the first fouling cycle. This could be explained that membrane with dense structure (smaller pore size) retained a wide range of foulants on the membrane surface, forming a fouling layer with higher resistance which is mostly reversible. Sheer force could easily remove this fouling layer from the aeration. However, Miyoshi et al. [44] found that membrane fouling propensity was not affected by pore size, but membrane materials. Three membrane materials, cellulose acetate butyrate (CAB), polyvinyl butyral (PVB) and PVDF with various pore size were examined. Results revealed that using PVDF membranes, the degree of fouling was in the following order: 0.02 μm > 0.25 μm > 0.4 μm. In contrast, the fouling development of CAB was in the descending order of 0.2 μm > 0.05 μm > 0.04 μm. For PVB membranes, no correlation or trend was observed with corresponding to the pore size. Therefore, the fouling propensity of membranes with their pore size is significantly affected by the membrane materials. The similar trend was observed in a study done by Bilad et al. [40], where PVDF membrane with a smaller pore size (PVDF-15, 16 nm) exhibited earlier fouling than more porous membrane (PVDF-9, 62 nm) [40a]. However, PVDF-15 reached TMP of 25 kPa at day 6, while PVDF-9 only achieved TMP of 20 kPa at day 10. Although having lower fouling rate, PVDF-9 prone to suffer more irreversible fouling due to pore blocking where small organic and inorganic compounds easily enter the pores and attached strongly to the substrate. In a nutshell, no consistent general trends noted on the effect of pore size on membrane performance as previously reported [1].

### 13.4.2 Membrane Roughness

Membrane roughness is an important physical parameter which greatly affects the fouling propensity of the membrane. The surface morphology of membranes can be captured, and their roughness can be measured by means of atomic force microscope (AFM). In molecular scale, the surface of the membrane is not smooth, but consists of an abundance of "peaks" and "valleys." Higher peaks or lower valleys would form a rough surface and vice versa. Fig. 13.14 illustrates the interaction of various foulants (solutes, small particles, and large particles) with membranes. Solutes such as soluble microbial products (SMP) and EPS in a chain-like structure are flexible and easily fit into the gaps between the peaks (valleys). On the other hand, large particles would not be able to deposit or fit into the gaps.
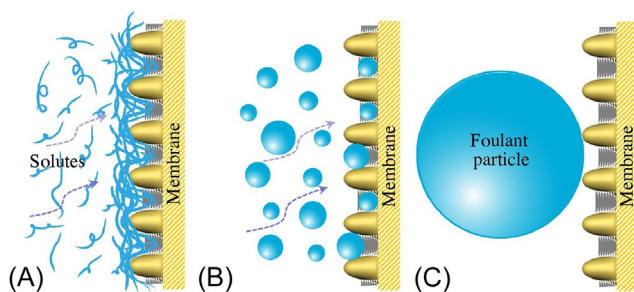
**FIG. 13.14** Schematics of the interaction scenarios: (A) associated with solutes, (B) associated with small size foulant particles, and (C) associated with large size foulant particles [45]. *Reprinted from Bioresource Technology, vol. 175, Zhang M, Liao B, Zhou X, He Y, Hong H, Lin H, Chen J. Effects of hydrophilicity/hydrophobicity of membrane on membrane fouling in a submerged membrane bioreactor, p. 64. Copyright (2015), with permission from Elsevier.*

As membrane morphology has a significant impact on membrane performance, various modifications have been employed to alter the membrane surface. Among the efforts are coating membranes with $TiO_2$ nanoparticles [46] and blending with inorganic nanomaterials such as Zeolitic Imidazolate Frameworks [47] and GO nanocomposites [25].

It has been observed that typically membranes with rough surface provide a higher surface area for the adsorption of foulants and results in greater fouling propensity [15, 48]. Woo et al. [49] investigated the impact of membrane surface roughness on both permeability and fouling of two PVDF membranes with similar properties such as pore size, materials and contact angle (73.46°). A membrane with a smoother surface (PVDF-B2, 47.013 nm as RMS) showed greater permeation flux as well as normalized flux compared with rough membrane surface (PVDF-B1, 166.433 nm as RMS). Initially, PVDF-B1 membrane showed higher permeation flux due to its slightly larger pore size (10.4 nm bigger than PVDF-B2 membrane of 227.3 nm). However, humic acid as foulant model was prone to deposited on the uneven membrane surface of the PVDF-B1 membrane and blocked most of the pores as shown in Fig. 13.15. As a consequence, PVDF-B1 membrane exhibited lower permeability and normalized permeation flux along the 120 min filtration.

However, the previous study by Hashino et al. [51] noticed that membrane with a higher projection on the outer surface experienced better antifouling ability and recovery after backwash. By observing foulants deposition behavior via SEM, most foulants accumulated in the valleys but hardly be found on the top of the projection. Later, Zhao et al. [45] found that the impact of surface roughness on fouling is complicated. It was easier for foulants to adhere on rough membrane surface as the attractive interaction energy between foulants and membrane decreased with membrane roughness. As a consequence, energy barrier was lower for
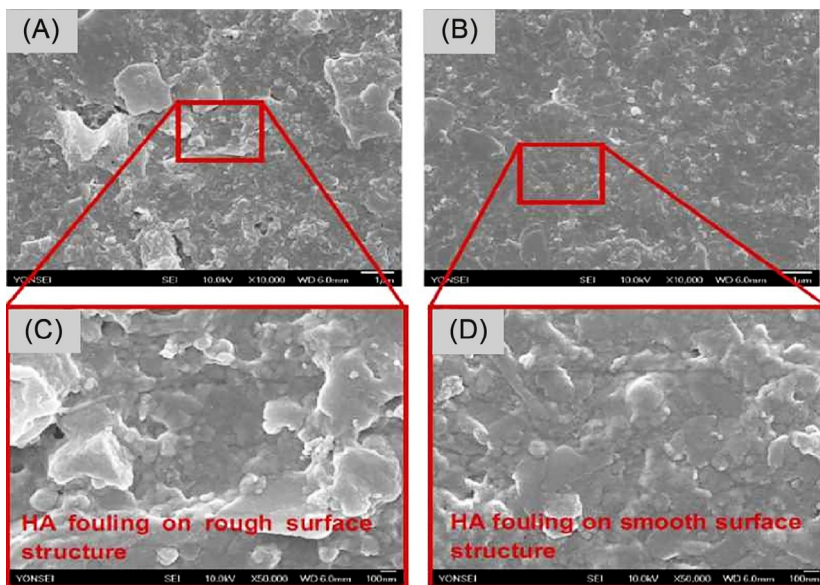
FIG. 13.15    Fouling behavior on membrane surfaces observed using FESEM: (A) fouled rough B1 and (B) fouled smooth B2 (magnified at 10,000×), (C) fouled rough B1 and (D) fouled smooth B2 (magnified at 50,000×) membrane surfaces [50]. *Reprinted from Separation and Purification Technology, vol. 146, Woo SH, Park J, Min BR. Relationship between permeate flux and surface roughness of membranes with similar water contact angle values, p. 187–191. Copyright (2015), with permission from Elsevier.*

foulants to overcome and attach on the membrane surface. Yet, the foulants were easier to detach from rough membrane surface under disturb condition (aeration). Therefore, it was suggested that rough membrane surface is more beneficial in fouling mitigation in MBR process.

## 13.4.3 Membrane Hydrophilicity

Membrane contact angle is the measurement of membrane's hydrophilicity. The degree of hydrophilicity can be determined with the sessile-drop method, by measuring the angle between a water droplet and membrane surface using contact angle meter. Smaller contact angle implies greater hydrophilicity of membranes due to the attraction of water molecules toward the membrane by forming a hydrogen bond with the membrane materials. Therefore, hydrophilic membranes always show higher permeability compared with hydrophobic membranes [25, 52].

Natural organic matters (NOMs) contain in wastewater consist of mainly proteins and carbohydrates with both hydrophobic and hydrophilic properties [53]. Although hydrophilic organic matters had been

known to contribute to membrane irreversible fouling, the majority of the NOMs are hydrophobic. These hydrophobic foulants exhibit strong adhesive potential with hydrophobic membranes, eventually forming cake layer on the membrane surface. Therefore, usually, membranes were modified to become hydrophilic as water boundary would form on the membrane surface, minimize the contact and adsorption of foulants and eventually enhances membrane's antifouling ability [50, 54].

Some studies have been conducted to examine the impact of membrane hydrophilicity toward fouling. In a study done by Miyoshi et al. [44], no correlation of fouling propensity with membrane hydrophilicity was noticed in MBR. The hydrophobicity of membranes was in descending order of PVDF > PVB > CAB. However, the time required for the membranes to reach the targeted TMP was in the descending order of PVB > PVDF > CAB. This suggested that hydrophilicity not be the dominant factor in determining fouling propensity of membranes. Matar et al. [55] found that with same pore size, hydrophobic membranes (polyoxadiazole (POX) and polytriazole (PTA)) achieved higher TMP values than hydrophilic membranes (sulfonated polytriazole (SPTA) and sulfonated polysulfone (SPSU)). This was due to adsorption of foulants which were hydrophobic predominant on the hydrophobic membrane surface. The accumulation of foulants (mainly proteins in the beginning) on SPSU (the most hydrophilic membrane) in early days was the lowest. Nonetheless, in longer filtration, the quantity of humic substances was higher for PTA and SPTA membranes than POX and SPSU membranes. This indicated that membranes lost their hydrophilicity or hydrophobicity characteristic when the fouling layer developed and covered the membranes exposing an area in the extended filtration period.

Membrane hydrophilicity property always relates to pore size, surface charge, morphology and membrane materials. For example, the addition of hydrophilic agents such as amino ($NH_2$), carboxyl (COOH) and sulfonic acid ($SO_3H$) groups enhanced the hydrophilicity of PTFE membranes, at the same time increased membrane pore size as well as surface charge [56]. Although membrane hydrophilicity often correlated directly with membrane permeability [57], though it is difficult to assess its relationship with fouling propensity accurately.

## 13.4.4 Surface Charge

Membrane surface charge is one of the most critical parameters in governing membrane performance. The surface charge or surface potential can be measured with streaming potential, sedimentation potential and electrophoresis techniques [58]. Organic matters in MBR wastewater consist mainly of the negative charge of proteins and polysaccharides as

foulants. It is well established that particles with the opposite electrostatic charge would attract each other while those with the same electrostatic charge would repel. Foulants with high negative zeta potential tended to form higher cake porosity, cake compressibility, and specific cake resistance and hence resulted in lower fouling potential. Besides, it was noticed that effect of foulants zeta potential significantly outweighed the cake porosity in response to specific resistance in a study by Lorenzen et al. [59].

Specific energy barrier should be overcome for a foulant to adhere on the membrane surface. By using XDLVO approach, interaction energy between a foulant and different membrane surface charge (Fig. 13.16) could be identified by setting constant values for membrane roughness, foulant radius, foulant zeta potential and solution pH. A membrane with higher negative surface charge (Fig. 13.16B) exhibited higher energy barrier, indicated the usefulness of negative surface charge in fouling mitigation [60].

Numerous modification techniques have been applied to increase the negative surface charge of membranes such as in situ cross-linked polymerization using acrylic acid and vinyltriethoxysilane [61], blending with graphene oxide [54] and employed plasma polymerization with maleic anhydride and vinylimidazole [62]. These studies showed that the modified membranes with the smoother surface not only less susceptible to fouling, also showed great improvement of foulant rejection.

Hydrophilic particles have a higher tendency for entering the inner structures of the pores and cause irreversible fouling in hydrophilic membranes. Meanwhile, hydrophobic particles tend to form a dense cake layer on membrane surface [63]. In algal-MBR, although the algal organic matter (AOM) contained a high amount of hydrophilic substances, the
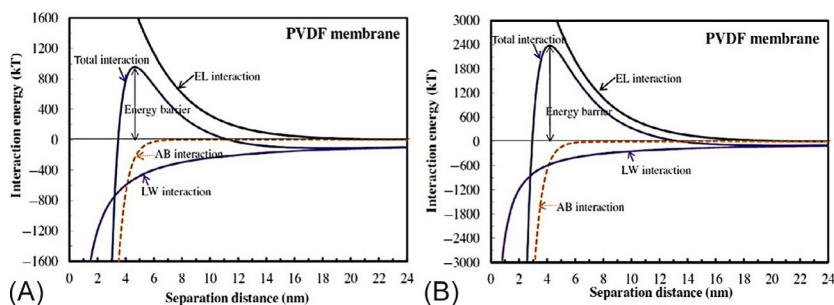


**FIG. 13.16** Profiles of interaction energies between a foulant particle and the smooth surface of PVDF membranes for membrane zeta potential of (A) −17.4 mV and (B) −31.0 mV (AB: Lewis acid-base, EL: electrostatic double layer, LW: Lifshitz-van der Waals) [45]. *Reprinted from Bioresource Technology, vol. 175, Zhang M, Liao B, Zhou X, He Y, Hong H, Lin H, Chen J. Effects of hydrophilicity/hydrophobicity of membrane on membrane fouling in a submerged membrane bioreactor, p. 65. Copyright (2015), with permission from Elsevier.*

**TABLE 13.4**  Characteristics of Various Modified PVDF Membranes [65]

| Parameter | Pristine PVDF | PVDF-TEPA | PVDF-lysine | PVDF-PSS | PVDF-PEG |
|---|---|---|---|---|---|
| Surface charge at pH 7 (mV) | −40 | +40 | −8 | −52 | −45 |
| Surface contact angle (°) | 132 | 25 | 114 | 121 | 92 |

electrostatic interaction between negatively charged membrane and AOM had significantly reduced the fouling behavior [64]. Some studies reported that surface charge was dominant in controlling membrane fouling behavior than membrane hydrophilicity [60, 65]. Breite et al. [65] modified the surface potential of PVDF membranes as well as foulant (PS beads) as presented in Table 13.4 to investigate their electrostatic interaction on membrane fouling. In this study, PVDF-PEG and PVDF-PSS membranes exhibited great fouling resistance with anionic PS beads while experienced severe fouling with pristine PVDF, PVDF-TEPA, and PVDF-lysine membranes. By using cationic PS beads, no fouling was observed on PVDF-TEPA membrane, but strong and instantaneous fouling was noticed on others membranes. On the other hand, uncharged PS beads caused pore blocking and decreased permeation flux in PVDF-TEPA, PVDF-lysine, and pristine PVDF membranes, but showed great fouling resistance on PVDF-PSS and PVDF-PEG membranes. A PVDF-lysine membrane with nearly zero charges experienced fouling by all PS beads. These results indicated electrostatic repulsive interaction was dominant on surfaces of same charges while electrostatic attractive interaction was the driving force on surfaces of opposite charges. It is worth noting that PVDF-TEPA membrane with a contact angle of 25° had high adsorption of anionic and uncharged PS beads but high resistance toward cationic PS beads. This implied the driving force of fouling was electrostatic interaction, which was capable of overcoming high membrane hydrophilicity. Instead, the hydrophobic interaction was dominant for highly hydrophobic membrane as pristine PVDF membrane was fouled by all PS beads.

A comprehensive investigation of membrane pore size, surface charge, hydrophilicity and morphology of different membrane materials would be useful in optimizing the membrane design. Besides the membrane properties, the effect of feed wastewater characteristics such as particle size distribution, zeta potential, and biological compounds would also affect the performance of the membranes. Also, consistent cleaning would be feasible to restore the hydrophilicity and surface charge of the membranes by removing the fouling layer.

## 13.5  SEPARATION MECHANISM

This section will discuss biological and membrane process which is the primary separation mechanism in MBR process.

### 13.5.1  Biological Process

In the biological treatment of MBR, organic carbon and nutrients in the wastewater are digested by a diversity of microbes such as prokaryotes (bacteria), eukaryotes (protozoa, nematodes, rotifer), and viruses through biodegradation. The removal of organic compounds can be determined regarding biochemical or chemical oxygen demand (BOD or COD, respectively). In general, the biological process can be divided into an aerobic and anaerobic process. Aerobic digestion is a process where the organic compound is broken down in the presence of oxygen to produce carbon dioxide and water. Whereas, anaerobic digestion is an organic compound degradation in the absence of oxygen to produce biogas typically methane and carbon dioxide. The removal efficiency of the biological treatment would mainly depend on the operating conditions such as mixed liquor suspended solids (MLSS), organic loading rate (OLR), hydraulic retention time (HRT), solid retention time (SRT), temperature, pH, and aeration.

To measure the microorganism concentration in the activated sludge system, MLSS was typically used. By increasing MLSS, the removal efficiency will increase; however, higher MLSS will increase the sludge viscosity thus result in mass transfer limitation for both the oxygen and organic compound where higher aeration is needed. Values varying from 10 to 15 g MLSS/L are the typical values for MLSS concentration in MBR. OLR refers to the influent COD concentration typically range from 1.1–1.6 kg/COD/$m^3$.day. It was discovered that MLSS raised with increasing OLR, an increase in the OLR provides bacterial growth leading to higher MLSS concentration. OLR is one of the important design factors in MBR system as it combines the effect of hydraulic loading and organic concentration. Findings of Chan et al. [66] stated that the COD removal efficiency is a function of the OLR. However, beyond maximum organic loading of OLR, the removal efficiency of COD and BOD showed falling trend because of the increase in organic loading in the influent that would cause substrate inhibition to the native biomass growth and its metabolic activities. Therefore, it is important to determine the maximum achievable OLR to improve the biological degradation and prevent process breakdown due to overloading.

Another essential operating condition is HRT which is the retention time for effluent to pass through the reactor which ranges from 4 h to several days for MBR process. As shown in Fig. 13.17, Vijayaraghavan et al. [68] studies showed that as the HRT increased, the COD removal efficiency also
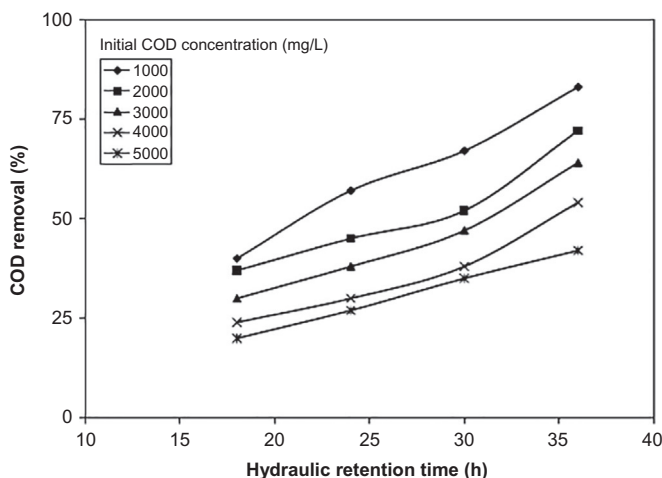
FIG. 13.17 COD removal efficiency at different HRTs [67]. *Reprinted from Journal of Environmental Management, vol. 82, Vijayaraghavan K, Ahmad D, Ezani Bin Abdul Aziz M. Aerobic treatment of palm oil mill, p. 28. Copyright (2007), with permission from Elsevier.*

increased. The possible reason for the decrease in COD could be due to the degradation of organic matter by longer contact time with the microorganism in the MBR. Apart from HRT, SRT probably is the most significant factor in determining biological degradation efficiency. In contrast to conventional activated sludge system, MBR allows complete control of SRT independently from HRT. High SRT increases the sludge concentration, and therefore the pollutant degradation would also increase. This allows the growth of slow-growing microorganisms to remove pollutants contained in the wastewater. In some cases, to regulate a large amount of biomass, MBR is operated with no discharged of sludge at an infinite SRT. However, high SRT will lead to the high viscosity of biomass and high fouling rates of membrane process.

Generally, the temperature is a significant factor to control the growth of a microorganism in MBR. Drews et al. [69] studied the impact of temperature on the rejection of SMP in MBR. As shown in Fig. 13.18, lower temperature at 10°C caused an increase in sludge concentration which was reversible when the temperature was increased. This is probably because of the reduction of the active bacteria when the temperature was lowered, suggesting a limited oxygen transfer, partly due to reduced viscosity of mixed liquor at a lower temperature. Therefore, proper control of temperature range is crucial to ensure the survival of bacteria especially effluent from industries that might experience temperature fluctuation. Another factor that affects the growth of the microorganism is pH, such as acidity or alkalinity of the environment. During biological degradation, pH might vary due to the activity of the bacteria. pH value increases by ammonia accumulation during degradation of proteins, while the
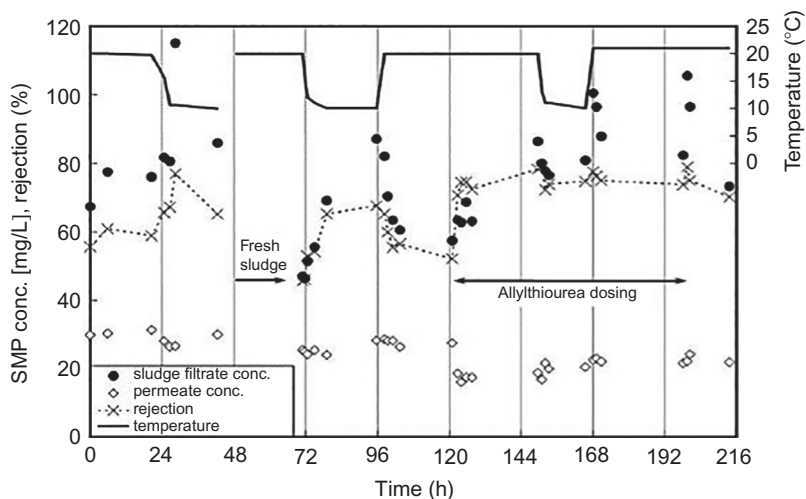
**FIG. 13.18**    Effect of temperature changes on SMP concentration [70]. *Reprinted from Water Research, vol. 41, Drews A, Mante J, Iversen V, Vocks M, Lesjean B, Kraume M. Impact of ambient conditions on SMP elimination and rejection in MBRs, p. 3855. Copyright (2007), with permission from Elsevier.*

accumulation of volatile fatty acid decreases the pH value which should greatly depend on the source of influent. For instance, Vijayaraghavan et al. [68] investigated the effect of pH on the biohydrogen production from palm oil mill effluent (POME). It was shown that pH value of 5 was optimum as the metabolic reaction of the hydrogen generating bacterial species occurs at the slightly acidic condition.

Last but not least, aeration plays a significant role in MBR. Aeration not only supplies dissolved oxygen for bacteria activity (aerobic) but also creates shear stress around the membrane to reduce adhesion of foulant on a membrane surface. However, it should be noted that increasing aeration intensity beyond a critical value had virtually no effect on MBR efficiency. For MBR application, Wicaksana et al. [71] studied the fiber movement induced by mechanical and bubbling on membrane fouling rate in MBR. Their results showed that bubble-induced shear and fiber movement were able to reduce fouling rate up to 10-fold due to the presence of uniform fine bubbles and higher cross-flow velocities around the membrane.

## 13.5.2 Membrane Process

Apart of biological process, membranes also play an essential role in MBR process and determine the technological and economic efficiency. In general, a membrane can be categorized into the pressure-driven

process, and extractive/diffusive process depends on their separation mechanism. The former membrane processes apply external pressure to force feed through a semipermeable material that allows some physical or chemical components to permeate through it while retaining others that rejected by it. Whereas, the latter membrane processes including forward osmosis (FO) and MD will be discussed shortly. Typically, membrane applied for pressure-driven separation in MBR can be distinguished on the basis of average pore diameter: 90–10 μm for microfiltration (MF), 2–100 nm for ultrafiltration (UF), 0.5–9 nm for nanofiltration (NF), and 0.2–5 nm for reverse osmosis (RO) as shown in Fig. 13.19. However, RO membrane is less studied for MBR application hence not covered in this section. Table 13.5 shows different membrane fabrication technique and type of polymer used to prepare polymeric membrane. The details of the fabrication method have been covered in Section 13.3 and critically reviewed by Lalia et al. [17].

Most MBR process uses MF and UF membranes as MBR are commonly emerged as secondary treatment technology before posttreatment by a
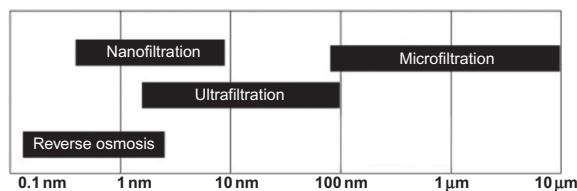


**FIG. 13.19**   Average pore diameter of the pressure-drive membrane [25]. *Reprinted from Desalination, vol. 326, Lalia BS, Kochkodan V, Hashaikeh R, Hilal N. A review on membrane fabrication: structure, properties and performance relationship, p. 78. Copyright (2013), with permission from Elsevier.*

**TABLE 13.5**   Summary of Membrane Fabrication Technique and Type of Polymer Used for Membrane Process

| Membrane process | Polymer | Fabrication technique |
|---|---|---|
| MF | PVDF, PTFE, PP, PE, PES | Phase inversion, stretching, track-etching |
| UF | PAN, PES, PS, PES | Phase inversion, solution wet-spinning |
| NF | Polyamides, polysulfones, polyols, polyphenols | Interfacial polymerization, layer-by-layer deposition, phase inversion, interfacial polymerization |
| FO | Cellulose acetate, thin-film composite (TFC) | Phase inversion, electrospinning |
| MD | PTFE, PVDF | Phase inversion, stretching, electrospinning |

Membrane cross-section
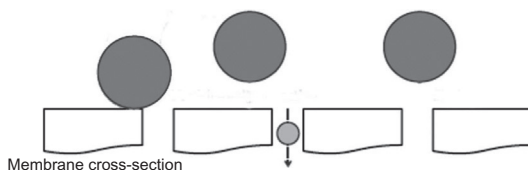
FIG. 13.20   Separation mechanism based on size based exclusion [7]. *Reprinted from Principles of Membrane Bioreactors for Wastewater Treatment, Park H, Chang I, Lee K. Membranes, modules, and cassettes, p. 76. Copyright (2015), with permission from Taylor and Francis.*

membrane with a smaller pore size such as NF or RO membrane. For MF and UF, the separation mechanism is greatly based on steric mechanism or size based exclusion (sieving). This type of mechanism implies that bigger molecule will be restricted by the membrane while smaller molecule will pass through the membrane freely as shown in Fig. 13.20. Hence, the separation efficiency greatly depends on the quality of the wastewater to be treated. In treating high strength wastewater with shock loading of matter, MF and UF membranes are preferable due to prolonging the membrane usage and cost factors. Sometimes, with the formation of fouling layer on the membrane surface, it also acts as a secondary active layer which would improve the sieving efficiency. Jin et al. [43] had compared the fouling characteristics using different pore-sized ceramic membrane (80, 100, 200, and 300 nm) in MBR. Surprisingly, a ceramic membrane with the smallest pore size of 80 nm (R80) was found to foul the slowest whereas the ceramic membrane with the largest pore size of 300 nm (R300) fouled the fastest. This could be due to the surface roughness of R80 is six times lower compared to R300. Rougher membrane surface will contribute to higher organic adsorption hence leads to severe membrane fouling.

NF membranes are typically used in drinking water production, wastewater reclamation, and pretreatment for desalination. In contrast to UF and MF membranes, NF can reject smaller size molecules such as trace organic molecules and ions in water treatment. For NF membrane, mono- and di-valent ions have typical rejections of 30%–80% and 70%–95%, respectively. It is important to highlight that NF is not only relying on size based exclusion but also Donnan and dielectric effects which had been critically reviewed by Mohammad et al. [72]. Donnan or electrical exclusion is an electrostatic effect which responsible for the rejection of ionic components by the membrane surface; diffusion of anion through the negatively-charged membrane is slower than cation diffusion or vice versa. As shown in Fig. 13.21, the dielectric exclusion provides an additional mechanism of ions exclusion which occurs when the solvent is confined in nanopores. For MBR application, Choi et al. [74] had compared the sludge characteristics and microbial community diversity between the NF and MF membranes in treating the municipal wastewater. Due
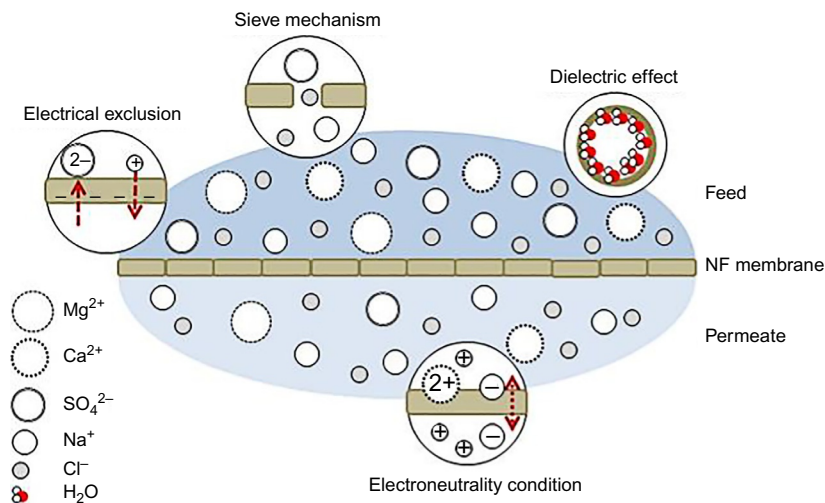
**FIG. 13.21** Separation mechanism based on size exclusion, Donnan and dielectric effect [73]. *Reprinted from Separation and Purification Technology, vol. 171, Nicolini JV, Borges CP, Ferraz HC. Selective rejection of ions and correlation with surface properties of nanofiltration membranes. Copyright (2016), with permission from Elsevier.*

to the smaller pore size of NF membrane, a higher number of organic molecules were retained in the retentate which resulted in higher dissolved organic carbon (DOC), total phosphorus (TP) and salts than those by MF membrane [74a]. However, the higher concentration of organic molecules did not significantly affect the microbial diversity. Their studies indicated great potential of NF membrane coupled with biological degradation in MBR process to produce high quality of effluent.

Compared to a pressure-driven membrane, FO membrane is considered to be more energy efficient because it does not need external hydraulic pressure. FO process is an osmotically-driven separation which utilizes the osmotic pressure difference between a concentrated draw solution (DS) and a dilute feed solution (FS) to move water molecules from the FS to the DS; then the DS requires further treatment for reuse application as shown in Fig. 13.22 [67]. As reported by Chen et al. [70], despite excellent contaminant removal demonstrated by FO membrane, reverse transport of salt from DS enhanced the accumulation of SMPs which contributed to a significant decline of membrane flux. Their result also supported by Zhang et al. [77] where biofilm and inorganic scaling were formed on the FO membrane. Later, Wang et al. [78] reported MF coupled with FO membrane in MBR for synthetic domestic wastewater treatment. Their results evidenced that MF membrane effectively reduced salt accumulation in the bioreactor thus enable the MBR to attain a long-run continuous operation. Nonetheless, there are still issues for the large-scale
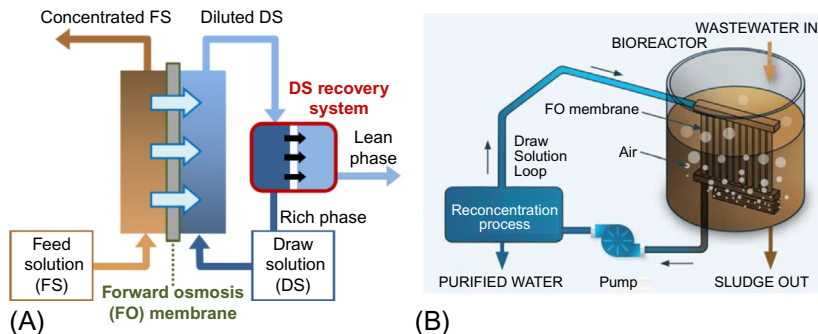
**FIG. 13.22** Schematic illustration of (A) FO process with DS recovery [75] and (B) FO membrane for MBR wastewater treatment [76]. *(A) Reprinted from Advanced Powder Technology, vol. 27, Mino Y, Ogawa D, Matsuyama H. Functional magnetic particles providing osmotic pressure as reusable draw solutes in forward osmosis membrane process, p. 9. Copyright (2016), with permission from Elsevier. (B) Reprinted from Desalination, vol. 239, Achilli A, Marchand EA. The forward osmosis membrane bioreactor: A low fouling alternative to MBR processes, p. 12. Copyright (2009), with permission from Elsevier.*

application of FO. This has been hindered mainly due to the lack of ideal membrane properties namely low support layer resistance of water transport, high water permeability, minimum reverse solute permeability, excellent mechanical properties, and a wide range of pH tolerance [79,79a,79b].

Lastly, MD is a thermal-driven membrane separation where only vapor molecules are allowed to pass through a porous hydrophobic membrane. As shown in Fig. 13.23A, with the temperature difference being the driving force, condensation takes place on the cooler side of the membrane leading to a pressure difference between the warm and cool surfaces [73]. Compared to the pressure-driven membrane, MD has the potential to generate high-quality drinking water using low-grade heat sources such as waste heat from industrial processes and solar energy. Phattaranawil et al. [82] first studied membrane distillation bioreactor (MDBR) which integrates a wastewater bioreactor with MD process as depicted in Fig. 13.23B. Their results showed that the MDBR produced high-quality effluent with very low TOC and negligible salts which are comparable to combined MBR and RO process. Later, Goh et al. [83] had performed tech-economic analysis that affirmed the electrical requirement by MDBR is 0.9 kWh/m$^3$ which is lower than combined MBR-RO process (1–1.3 kWh/m$^3$). Besides, the greenhouse gas emission from the MDBR system is lower than the combined MBR-RO process where hot wastewater and waste heat is captured [83a].

Nevertheless, MD process is still in the early phase and not fully implemented in the industry mainly due to lack of suitable membrane. Hence, Khayeet [84] had outlined following membrane requirements for an effective MD process:
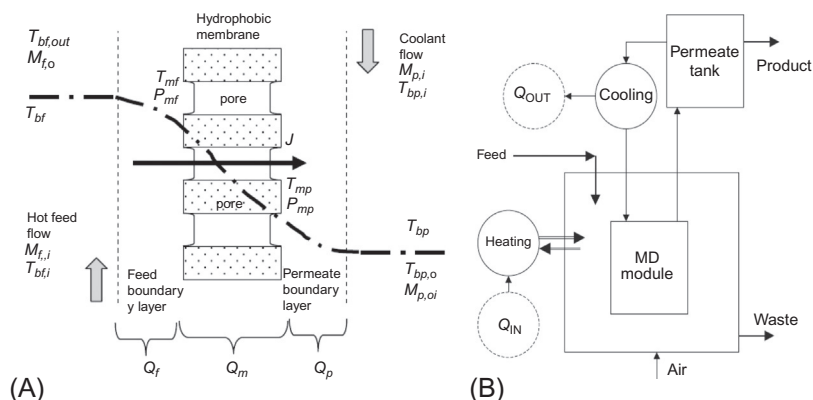
**FIG. 13.23** Illustration of (A) Heat, mass and pressure transfer across MD membrane [80] and (B) MDBR setup [81]. *(A) Reprinted from Desalination, vol. 284, Adnan S, Hoang M, Wang H, Xie Z. Commercial PTFE membranes for membrane distillation application: effect of microstructure and support material, p. 298. Copyright (2012), with permission from Elsevier. (B) Reprinted from Desalination, vol. 223, Phattaranawik J, Fane AG, Pasquier ACS, Bing W. A novel membrane bioreactor based on membrane distillation, p. 10. Copyright (2008), with permission from Elsevier.*

1. At least one of the membrane layers should be hydrophobic.
2. Pore size range from several nanometers to a few micrometers with a narrow distribution and high liquid entry pressure (LEP).
3. Small tortuosity factor (a measure of the deviation of the pore structure from straight cylindrical pores normal to the surface).
4. High porosity to provide a large area for evaporation.
5. Optimum membrane thickness to maximum mass transport and minimum heat loss.
6. Low thermal conductivity to reduce heat loss.
7. High fouling resistance.
8. Long-term thermal stability (up to $100°C$).
9. Excellent chemical resistance to various environment.
10. Allow stable and long life performance.

# 13.6 APPLICATIONS

## 13.6.1 Municipal Wastewater

Monclús et al. [85] operated a pilot plant MBR with University of Cape Town (UCT) configuration (Fig. 13.24) in treating raw municipal wastewater, mainly focusing on the biological nutrient removal. The UCT configuration is a typical single-sludge system, in which the sludge is recycled to the anoxic tank, and the mixed liquor is continuously returned from the
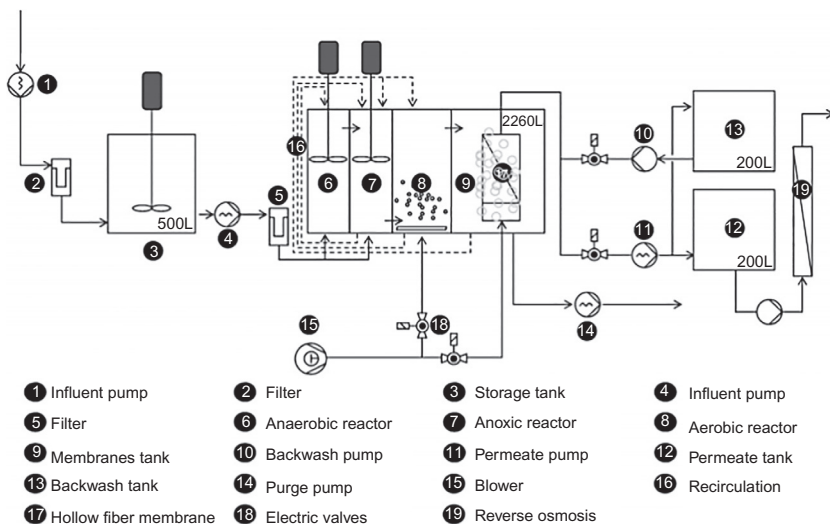
**FIG. 13.24** Scheme of the MBR pilot plant showing the different compartments, flow directions, and main instruments and equipment [86]. *Reprinted from Desalination, vol. 250, Monclús H, Sipma J, Ferrero G, Comas J, Rodriguez-Roda I. Optimization of biological nutrient removal in a pilot plant UCT-MBR treating municipal wastewater during start-up., p. 593. Copyright (2010), with permission from Elsevier.*

anoxic reactor to the anaerobic compartment. Experiment data showed that the system was able to obtain high nutrient removal efficiency even during the start-up. >94% COD removal, 89%–93% N removal, and 80%–92% P removal have been achieved at the end of the stage. As a continuous from this study, Monclús et al. [87] optimized the simultaneous removal of C, N, and P from the system through the determination of setpoint values for internal recycle with the use of an optimization spreadsheet based on ASM2d model.

Some research outcomes found that temperature would influence the performance of biological treatment in conventional activated sludge processes [75]. Same goes for MBR where the temperature not only affect the bioconversion rate but also influence the microbial community, membrane fouling rate, and sludge morphology [76]. Thus, Gurung et al. [88] assessed the performance of a submerged pilot-scale MBR in treating real municipal wastewater during the winter season at Finland. An accelerated membrane fouling was observed when the sludge temperature inside the MBR unit was below 10°C while maintaining aeration intensity below the normal value. The substantial decrease in membrane permeability was about 75%, leading to frequent membrane cleaning. However, the pathogens and emerging micropollutants removal competency of MBR was not affected. The average log reductions of 1.82, 3.02, and

1.94 log units were achieved for norovirus GI, norovirus GII, and adenoviruses, respectively. Removal of Escherichia coli and enterococci was >5.6 log units. Among the four trace organic compounds, the average removal efficiency of bisoprolol, diclofenac, and bisphenol A were 65%, 38%, and >97%, respectively. However, carbamazepine (CBZZ) was not efficiently removed (−89% to 28%). Regarding trace metals, an average removal of >80% was achieved for Cd, Pb, and V. For the rest of the metals, the removal capacity was in the range of 30%–60%.

## 13.6.2 Leachate

Landfill leachate (LFL) contains a high concentration of ammonia, heavy metals, and recalcitrant organic matters, and low concentration of phosphorus [81]. This is the reason why it is considered the most challenging wastewater. The use of MBR for leachate treatment has increased to comprise almost the half of new landfill leachate treatment processes (LFLTPs), increasing its share to 8% of total LFLTPs worldwide [3]. Zolfaghari et al. [81] utilized synthetic LFL to study the feasibility of submerged membrane bioreactor (SMBR) for the treatment of LFL by eliminating all interfering factors and providing realistic view on the behavior of highly hydrophobic organic matters and metals in MBR with the presence of humic acid (HA) as a representative of recalcitrant organic matter. The results revealed that SMBR in this study has high nitrification, BOD, phosphorous, and heavy metal removal except for molybdenum, arsenic, manganese, and nickel, owing to strong interaction with negative charge sludge. Whereas, the irreversible strong bound of HA and di-2-ethyl hexyl phthalate (DEHP), a highly hydrophobic contaminant in LFL has dramatically decreased the MBR biodegradability, therefore decreased its removal efficiency. The result of biodegradation showed that the presence of 100 mg/L of HA decreased the biodegradation rate from 37 to 7.9 µg DEHP/g VS/day.

In Chiemchaisri et al. [89] study, a two-stage MBR utilizing incline tube in first stage anoxic reactor for biomass separation from re-circulated sludge followed by an aerobic reactor with a submerged hollow-fiber membrane for solid-liquid separation had been developed and successfully applied for solid waste leachate treatment. However, there have been few studies that reported on the removal efficiency of emerging contaminants by microbial sludge operated in long-term and the analysis of emerging contaminant removal kinetics. Owing to this, Boonnorat et al. [80] have investigated the long-term fate of emerging contaminants in MBR system and determined their maximum removal capacity under long-term operation (500 days) without sludge withdraw. Their findings showed that the emerging contaminants were effectively removed in MBR with the removal of 99.5%, 99.0%, 99.5%, 97.9%, 96.8%, and 95.7% for

Bisphenol A (BPA), 2,6-di-tert-butylphenol (2,6-DTBP), 2,6-di-tert-4-methyl-butylphenol (BHT), ethyl phthalate (DEP), butyl phthalate (DBP), and DEHP compounds, respectively. Based on that previous study, Boonnorat et al. [90] had extended their research work to investigate the kinetic of phenolic and phthalic acid esters (PAEs) biodegradation in MBR in treating municipal LFL. Laboratory-scale MBR was fed with the mixture of fresh and stabilized LFL containing carbon to nitrogen (C/N) ratio of 10, 6, 3 and operated under different SRT of 90, 15, and 5 days. It was found that the optimum operation of MBR occurred at C/N ratio of 6 and SRT of 90 days for the treatment with highest biodegradation rate for phenolic and PAEs where the first order biodegradation rate constant ($k$) obtained was 0.059–0.092/h.

Brown et al. [86] were the first to treat compost leachate using MBR. The COD of the effluent was successfully reduced by >99%. A high reduction was also observed for ammonia, caffeine, and many other metals. On the other hand, recent studies showed that the addition of granular activated carbon (GAC) into mixed liquid was effective in alleviating membrane fouling. Yu et al. [91] had inspired Wang et al. [92] to combined GAC with MBR process for LFL treatment. A pilot-scale anoxic/aerobic granular active carbon assisted membrane bioreactors (A/O-GAC-MBR) integrated with nanofiltration (NF)–reverse osmosis (RO) (Fig. 13.25) was used by Wang et al. [92] for old leachate treatment. Results demonstrated that the addition of GAC had enhanced the bioflocculation and settability of flocs in addition to improving the removal efficiency of hazardous organic pollutants and heavy metals to meet the re-utilization requirement. This has led to considerable reduction in membrane fouling and subsequently the operational cost.

## 13.6.3 Dye and Textile

Due to its high color, heavy toxicity, and nonbiodegradable characteristics, the treatment of dye wastewater has been one of the most challenging even at very low concentration [94, 95]. MBR has been shown to be one of the most promising biological technologies in water treatment and thus has great potential for stable and efficient degradation of textile wastewater [96]. Friha et al. [97] studied the performance of pilot-scale aerobic submerged MBR for the treatment of raw textile wastewater under different MBR operational parameters. Extremely high treatment efficiency was achieved by MBR where COD, $BOD_5$, and SS were successfully reduced up to 100%, 98%, and 96%, respectively. On top of that, the cytotoxicity caused by raw textile wastewater was significantly reduced by 53% at HRT of 2 days. Hence, MBR was considered as a highly effective raw textile wastewater treatment method from both physic-chemical and toxicological point of views.
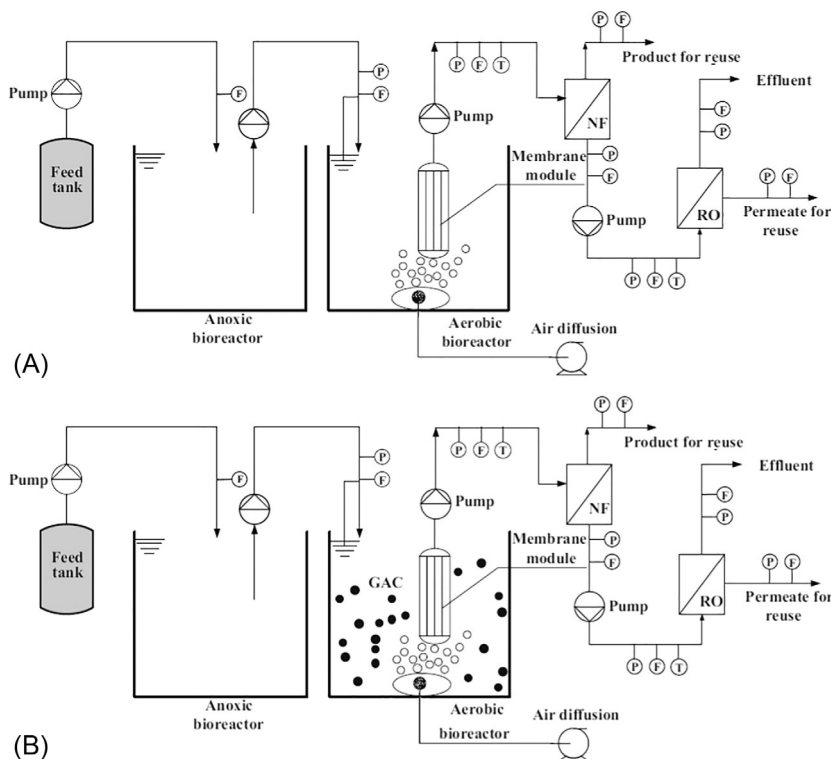
**FIG. 13.25** Schematic diagram of A/O-MBR combined with NF/RO process [93]. *Reprinted from Desalination, vol. 349, Wang G, Fan Z, Wu D, Qin L, Zhang G, Gao C, et al. Anoxic/aerobic granular active carbon assisted MBR integrated with nanofiltration and reverse osmosis for advanced treatment of municipal landfill leachate, p. 138. Copyright (2014), with permission from Elsevier.*

Rondon et al. [98] investigated the performance of an enhanced membrane bioreactor (eMBR) comprising of two anoxic bioreactors followed by an aerobic MBR, a UV disinfection unit, and a GAC filter to treat remazol blue (BR) dye as synthetic textile effluent over a period of 100 days. The system was able to remove 95% of BR, 99.1% of COD, 97% of nitrogen, and 65.1% of phosphorus. Despite the efficiency of MBR for textile wastewater treatment, membrane fouling is still a significant problem limiting its application [99]. Therefore, Qin et al. [100] have developed another type of eMBR with internal micro-electrolysis (IE) as pretreatment (Fig. 13.26) for textile wastewater treatment. A hybrid MBR (HMBR) with iron ions fed and an iron controlled MBR (CMBR) were operated in parallel for 30 days. The results demonstrated that IE pretreatment had successfully alleviated the membrane fouling in MBR system, mainly due to the improvement of settleability and compactibility of flocs, as well as the
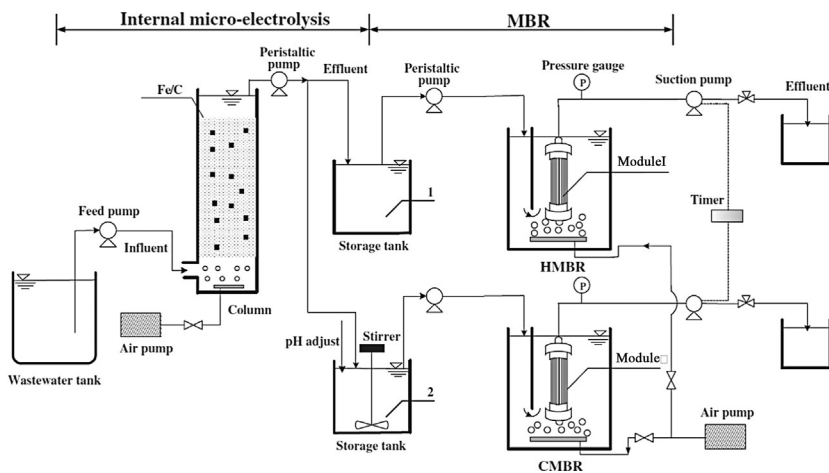
FIG. 13.26   Schematic diagram of experimental process [100]. *Reprinted from Chemical Engineering Journal, vol. 210. Qin L, Zhang G, Meng Q, Xu L, Lv B. Enhanced MBR by internal micro-electrolysis for degradation of anthraquinone dye wastewater, p. 578. Copyright (2012), with permission from Elsevier.*

increase in the particle size. The reduction of color, COD, and $NH_3$-N were achieved >90% for both MBR systems.

In Deveci et al. [101] study, a novel integrated process of fungal membrane bioreactor (FMBR) and semiconductor photocatalytic membrane bioreactor (PMBR) (Fig. 13.27) has been shown to be able to treat industrial textile washing bath wastewater. It was found that photocatalytic process achieved faster color degradation than COD reduction. Whereas, fungal biodegradation process performed in the other way. The integrated FMBR-PMR system had shown the best performance compared to the two single systems, where the color and COD removal was as high as 93% and 99%, respectively, suggesting it to be an optional treatment process for textile washing bath wastewater treatment.

## 13.6.4 Petrochemical

Several investigations have been carried out to study the treatment of petrochemical wastewater using MBR [93, 103]. In Fallah et al. [104] study, MBR was utilized for the removal of styrene from synthetic petrochemical industrial wastewater; Lebrero et al. [105] applied MBR for the treatment of methylmercaptan, toluene, alpha-pinene and hexane at trace level concentrations. High removal efficiency was recorded by MBR system. Whereas, Deveci et al. [93] were the first to investigate the technical feasibility of MBR as a practical approach for the treatment of ethylene oxide/ethylene glycol (EO/EG) and olefin units. An average wastewater treatment efficiency of 97.5% was accomplished for the optimum HRT of
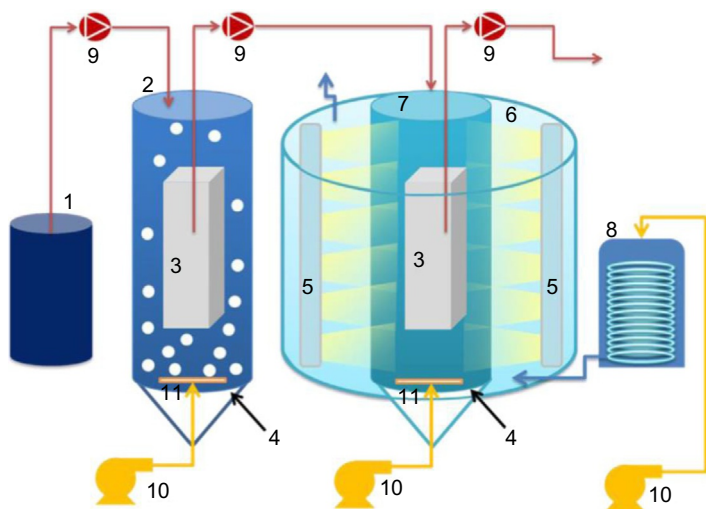
**FIG. 13.27** The experimental setup of the sequential photocatalytic membrane reactor (PMR) and fungal membrane bioreactor (FMBR) integrated process 1. Stock wastewater, 2. Pyrex glass reactor (FMBR), 3. Membrane module, 4. Fritz filter, 5. UVA lamps, 6. Lid for keeping the light in, 7. Pyrex glass reactor (PMR), 8. Ice vessel, 9. Peristaltic pump, 10, 11. Air blower [102]. *Reprinted from Biochemical Engineering Journal, vol. 105, Deveci EÜ, Dizge N, Yatmaz HC, Aytepe Y. Integrated process of fungal membrane bioreactor and photocatalytic membrane reactor for the treatment of industrial textile wastewater, p. 422. Copyright (2016), with permission from Elsevier.*

13.5 h and MLSS concentration of 8 g/L. The results indicated that MBR is a promising technology for the treatment of high fluctuating toxic components in petrochemical wastewater.

Wang et al. [106] have developed a novel energy-saving anaerobic hybrid membrane bioreactor (AnHMBR) with mesh filter, which takes advantage of AnMBR and fixed-bed biofilm reactor, for low-strength 2-chlorophenol (2-CP)-contained wastewater treatment. High COD and 2-CP removals were achieved, and the percent of removal for each parameter was $82.3\% \pm 5.7\%$ and $92.6\% \pm 10.4\%$, respectively. The energy demand for AnHMBR was primarily contributed by the feed pump, which was estimated to be $0.0045–0.0063$ kWh/m$^3$, relatively low compared to the energy consumption reported by other researchers to mitigate membrane fouling.

### 13.6.5 Food and Beverage

Galacto-oligosaccharides (GOS) have gained increasing interest as an ingredient in several functional foods [107]. Córdova et al. [108] assessed the performance of a crossflow UF-MBR as a continuous process strategy to improve the synthesis of GOS, using high lactose concentration, as well

as examining the operational stability of the system during several hours of operation. The operational variables of UF-MBR had greatly affected the flux and enzyme productivity for GOS synthesis process. The operating condition at 4.38 bar TMP, 7.35 m/s crossflow velocity, and at 53.1°C was optimal for simultaneous flux and specific enzyme productivity.

The dairy industry is one of the most polluting sectors among food industry [102, 109]. It is characterized by high BOD, COD, suspended solids, fats and oils, and nutrients content [110, 111]. Fraga et al. [112] had evaluated the performance of a pilot-scale MBR in treating dairy wastewater to investigate the potential for water reuse. The MBR was placed at two different locations: (i) receiving the wastewater from the industrial process after passing through a grease removal pond (high load stream) and (ii) receiving the wastewater after passing through the grease removal pond and an anaerobic pond (low load stream). The MBR was effective in removing organic matter with COD, BOD, and $NH_4$-N removal efficiency of 94.2%, 98.1%, and 99.6%, respectively, regardless the type of influent wastewater to the MBR. The treated effluent complied with most of the drinking water standards in Uruguay except its pathogen content, TDS, and sodium concentration. On the other hand, Buntner et al. [113] combined up-flow anaerobic sludge blanket (UASB) and MBR system (Fig. 13.28) for the treatment of dairy wastewater. The proposed system proved to be highly efficient in the treatment of wastewater with high tolerance to loading changes and temperature fluctuations, where the average total and soluble COD removal were above 95% and average methane production of 73%.

Sheldon and Erdogan [115] evaluated the performance of multistage expanded granular sludge bed (EGSB)/MBR system for the treatment of soft drink industry wastewater (SDIW). The EGSB anaerobic pretreatment for the SDIW showed the excellent and efficient removal of organic constituents and biogas production without adding external carbon sources and nutrients. The integrated EGSB/MBR treatment had achieved up to 95% COD removal, rendering the treated water safe for discharge. Conversely, Bolzonella et al. [116] ran a full-scale MBR to treat 110 $m^3$/day of sparkling white wine-making effluent with organic loading up to 1600 kg COD/day at north-east Italy. The results showed that MBR was able to handle high organic loading effluent obtained during the harvest period, producing permeate with good quality and relatively small amount of wasted sludge. The average COD removal efficiency was around 95% while the corresponding sludge yield was only 0.1 kg MLVSS/kg COD removed.

## 13.6.6 Pharmaceutical

Pharmaceutically active compounds (PhACs) have been detected in sewerage treatment plant (STP) effluents as well as in surface water, groundwater, and even drinking water all over the world [114, 117–122].
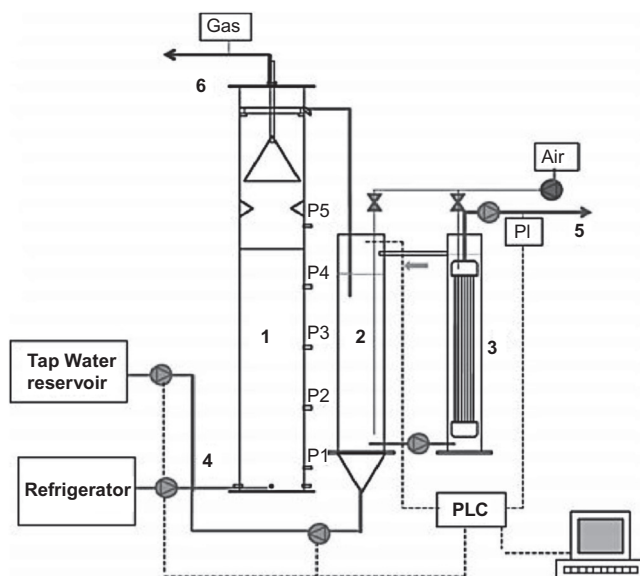
FIG. 13.28 Schematic diagram of combined UASB and MBR system. 1. UASB chamber, 2. Biofilm aerobic chamber, 3. Membrane chamber, 4. Feeding and recirculation, 5. Permeate (backwashing), and 6. Biogas outlet [114]. *Reprinted from Chemical Engineering Journal, vol. 230, Buntner D, Sánchez A, Garrido JM. Feasibility of combined UASB and MBR system in dairy wastewater treatment at ambient temperatures, p. 476. Copyright (2013), with permission from Elsevier.*

The frequent occurrence of PhAcs in the aquatic environment as well as in treated drinking water has raised public concern due to their potential impact on environmental and public health. These include the occurrence of aquatic toxicity, increased resistance of pathogenic bacteria, genotoxicity, and endocrine disruption [123–125]. Tambosi et al. [126] evaluated the treatment of wastewater containing six pharmaceuticals of high consumption worldwide, three NSAIDs (acetaminophen, ketoprofen, and naproxen) and three antibiotics (roxithromycin, sulfamethoxazole, and trimethoprim) in two MBR pilot plants with submerged membranes, operated at SRT of 15 days (MBR-15) and 30 days (MBR-30) over a period of 4 weeks. The results showed that MBR-30 presented higher removal efficiency than MBR-15 for all studied compounds. The NSAIDs were removed at higher efficiency while antibiotics exhibited persistence to microbial attack and were removed at a lesser extent in both MBRs. On the other hand, Siera et al. [127] operated MBR for the removal of cytostatic drug (cyclophosphamide), an anticancer drug which had received little attention from the public [128, 129]. The removal efficiency of 60% was observed despite some variation in the influent. This removal was higher than reported in most of the studies in the literature.

Prasertkulsak et al. [130] investigated the removal efficiency of pilot-scale MBR for the treatment of pharmaceutical compounds in hospital wastewater at short HRT of 3 h. In that study, 11 pharmaceutical compounds in actual hospital wastewater were investigated for their removal in MBR, including diclofenac (DCF), sulfamethoxazole (SMX), trimethoprim (TMP), CBZ, tramadol (TMD), naproxen (NPX), propanolol (PPL), ibuprofen (IBP), 17b-Estradiol (E2), triclosan (TCS), and gemfibrozil (GFZ). The results revealed that majority of pharmaceutical compounds in hospital wastewater could be effectively removed in MBR operated at short HRT of 3 h. However, as demonstrated by the results in Prasertkulsak et al. [130] study, the removal mechanism among the studied compounds were different where the removal of SMX, TMP, CBZ, TMD, NPX, PPL, E2, and TCS were mainly due to adsorption, while the removal of DCF, IBP, and GFZ were mainly through biodegradation.

7-Aminocephalosporanic acid (7-ACA) is a very crucial intermediate for synthesizing cephalosporin antibiotics, widely used antibiotics all over the international markets [131]. Chemical lysis method for the production of 7-ACA causes serious water pollution problems attributed to a significant amount of toxic organic compounds discharged together with washing wastewater during the production process [131, 132]. However, 7-ACA is extremely difficult to be treated by conventional separation and purification methods [132]. Owing to this, Chen et al. [133] have set up three novel multi-sparger multistage airlift membrane bioreactors (Ms$^2$ALBRs) (Fig. 13.29) in parallel for treating synthetic high-strength 7-ACA pharmaceutical wastewater. During the 200-day operating time, all three Ms$^2$ALBRs showed good performance with average COD removal efficiency of 94.96%, 96.05%, and 93.9%. Whereas, the average 7-ACA removal efficiency was 66.44%, 59.04%, and 59.60%, respectively. The optimal operating conditions for Ms$^2$ALBRs were 10 h HRT, 15–35°C operating temperature, and at pH 7–9.

It has been reported that pharmaceutical wastewater generally contains high salinity which could affect the biological processes in MBR as the high salinity could cause unbalance osmotic stress across the cell wall that leads to plasmolysis as water is lost from microbial cells through osmosis [135, 136]. Therefore, biological treatment of saline wastewater usually results in low activity of cells in the presence of high salt content (>2%) [137]. Ng et al. [138] were the first to study the coastal sediment microorganism coupled with a membrane, named as salt marsh sediment membrane bioreactor (SMSMBR) and bio-entrapped membrane bioreactor (BEMR) for the treatment of high salinity pharmaceutical wastewater over 6 months. The results demonstrated that the conventional biomass in BEMR was not able to tolerate the hypersaline condition, resulting in TCOD removal efficiency of only 4.2%–68.0% compared to SMSMBR which had achieved 74.7%–90.9% of TCOD removal efficiency as the microorganisms in SMSMBR seeded from coastal shore were able to degrade the complex and recalcitrant organic matter in the presence of salt.
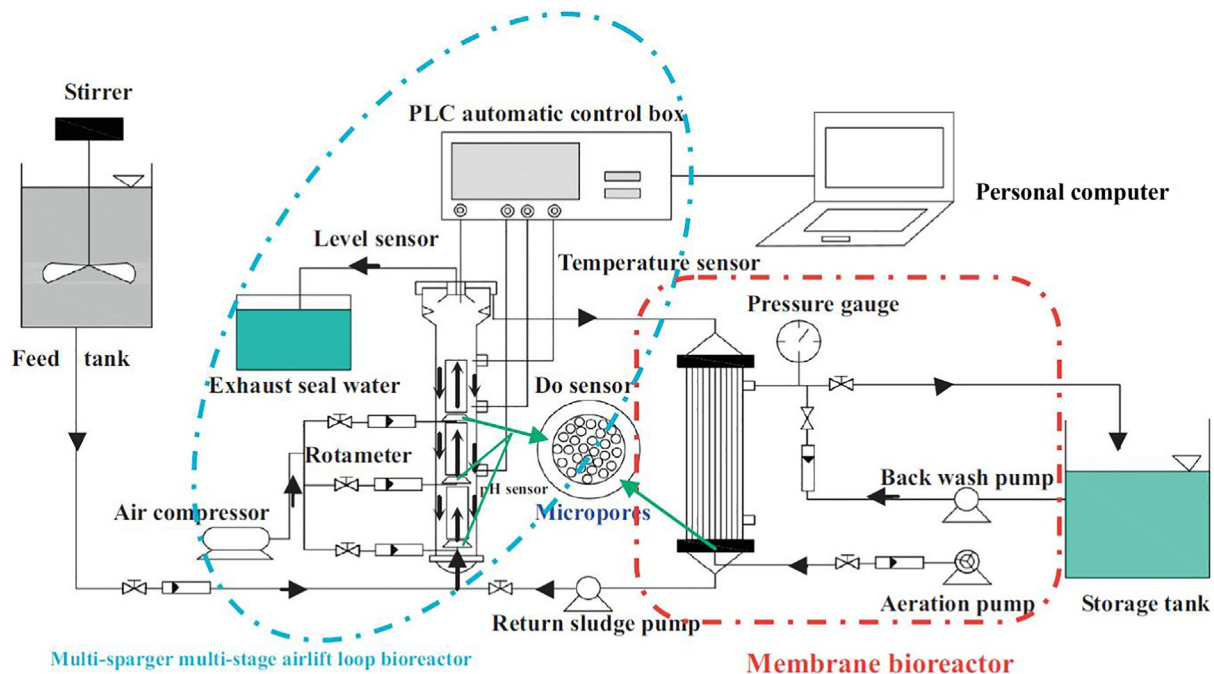
**FIG. 13.29** Schematic diagram of novel multisparger multistage airlift loop MBR [134]. *Reprinted from Bioresource Technology, vol. 167, Chen Z Bo, He Z Wei, Tang C Cong, Hu D Xue, Cui Y Bo, Wang A Jie, et al. Performance and model of a novel multi-sparger multi-stage airlift loop membrane bioreactor to treat high-strength 7-ACA pharmaceutical wastewater: effect of hydraulic retention time, temperature and pH, p. 243. Copyright (2014), with permission from Elsevier.*

García-Gómez et al. [139] demonstrated a combined system of MBR with electrochemical oxidation for the removal of CBZ. An integrated system of MBR with electrochemical oxidation was effective for COD, TOC, and CBZ removal. Although CBZ was not highly biodegradable (20% of removal after 120 days of operation), it did not inhibit the biomass activity, evidenced by the high extent of COD removal in MBR system. With the support of EO system, CBZ was almost entirely degraded (99.99% of removal). Conversely, Wang et al. [140] developed a double membrane pilot system comprising MBR and NF membrane for the treatment of antibiotic production wastewater over a three-month period at a pharmaceutical company in Wuxi, China. The system combining MBR and NF was shown to be useful for the treatment of antibiotic production wastewater by recycling the NF concentrate into MBR, afforded higher water yield of 92% ± 5.6%. The permeate water quality obtained from pilot-scale MBR-NF system was excellent and could be reused for industrial applications.

There have been few studies dealing with the treatment of pharmaceutical wastewater in an anaerobic membrane bioreactor (AnMBR), particularly in pilot plant treating real wastewater or in full-scale operation. Svojitka et al. [141] study focused on the performance of AnMBR pilot plant, which was fed by real wastewater originating from pharmaceutical and chemical production. The results depicted that pharmaceutical industrial wastewater alone showed good anaerobic degradability in AnMBR. However, low feed concentration and variation in feed composition had decreased the treatment efficiency. Constant and high removal efficiency (COD removal up to 97%) was achieved when methanol (up to 25 g/L as COD) was added into the influent and variation of its feed composition was limited.

## 13.6.7 Others

Sun et al. [142] developed an integrated biofilm-MBR system (Fig. 13.30) for shipboard wastewater treatment, including grey water, black water, and bilge water for the reuse of all wastewater streams onboard the ships. Both dead-end side-stream and recycle side-stream configurations of the biofilm-MBR system were investigated. Good membrane permeate quality with low oil concentration (<5 mg/L) was achieved in each process configuration for various feed water compositions. However, the inclusion of bilge water resulted in higher membrane fouling rate in dead-end side-stream configuration when applying with high membrane recovery (93%). Recycle side-stream configuration which recycling the membrane concentrate into the biofilm reactor had improved the membrane performance and permeate quality attributed to the enhancement of bio-flocculation and biodegradation of oil compounds and biomass aggregates, resulting in a more sustainable treatment scheme.
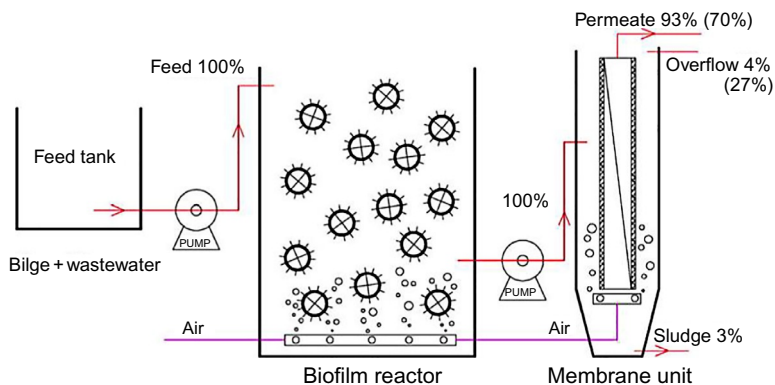
**FIG. 13.30** Dead-end side-stream configuration of biofilm-MBR, membrane filtration unit recovery: 93% or 70% [142]. *Reprinted from Desalination, vol. 250, Sun C, Leiknes T, Weitzenböck J, Thorstensen B. Development of a biofilm-MBR for shipboard wastewater treatment: the effect of process configuration, p. 746. Copyright (2010), with permission from Elsevier.*

In another study, Umaiyakunjaram and Shanmugam [134] dealt with the treatment of high suspended solids raw tannery wastewater using flat sheet submerged anaerobic membrane bioreactor (SAMBR). The SAMBR was acclimatized with mixed hypersaline anaerobic seed sludge for biogas generation. Results showed that the SAMBR treatment of raw tannery wastewater achieved 90% COD removal with biogas yield of 0.161 L biogas produced/g COD$_{removed}$, and ammonia generation of 1181 mg/L. The high removal of COD and the high biogas yield confirmed the feasibility of SAMBR for treating raw tannery wastewater with high suspended solids, eliminating the need of expensive chemical treatment (primary clariflocculator), aerobic biological treatment, and secondary clarifiers [134].

Bamboo industry wastewater (BIWW) is characterized by high COD and NH$_4^+$-N concentration with low pH value [143, 144]. In Xia et al. [145] study, a control system of AnMBRs and an AnMBR system with BC (bamboo charcoal) added (B-AnMBR) were established and operated for 150 days to treat BIWW. During the steady-phase period, COD removal efficiencies of 94.5% ± 2.9% and 89.1% ± 3.1% were achieved by the B-AnMBR and AnMBR, respectively. Whereas, the B-AnMBR achieving methane yield of 0.25 L CH$_4$/g COD in the steady state, while the AnMBR achieved an average value of 0.13 L CH$_4$/g COD. The addition of BC in AnMBR system enriched the amount of biomass and improved its performance in treating BIWW to obtain higher COD removal efficiency and methane yield. At the same time, BC prolonged the operation time by decreasing the concentrations of SMPs content by approximately 62.73 mg/L and reducing pore blockage and cake layer resistance, thereby mitigating membrane fouling. Table 13.6 summarized the application of MBRs in various industries.

**TABLE 13.6** Application of MBR in Different Industries

| Industry area | System | Membrane type | Operating conditions | Performance | Reference |
|---|---|---|---|---|---|
| Municipal | SMBR | Polymer | COD $= 459 \pm 191$ mg/L<br>BOD$_5$ $= 293 \pm 79.1$ mg/L<br>TKN $= 50.6 \pm 20.5$ mg/L<br>NH$_4^+$ $= 29.1 \pm 10.2$ mg/L<br>NO$_x^-$ $= 0.3 \pm 0.3$ mg/L<br>PO$_4^{3-}$ $= 3.63 \pm 1.3$ mg/L<br>C/N/P ratio $= 100/11/0.8$<br>Membrane pore size $= 0.1$ μm<br>Membrane surface area $= 12.5$ m$^2$<br>DO flow rate $= 1.5$ mg/L<br>Working volume $= 2.26$ m$^3$ | Rejection $\geq$94% COD, 89–93% N, 80%–92% P | [85] |
| | SMBR | Polymer | TSS $= 126.9 \pm 19.6$ mg/L<br>COD $= 265.6 \pm 53.1$ mg/L<br>NH$_4$-$N$ $= 45.9 \pm 9.2$ mg/L<br>TP $= 4.7 \pm 0.8$ mg/L<br>CBZ $= 0.63 \pm 0.2$ mg/L<br>BIS $= 0.43 \pm 0.2$ mg/L<br>DCF $= 1.84 \pm 0.4$ mg/L<br>BPA $= 0.95 \pm 0.2$ mg/L<br>Zn $= 75.86 \pm 17.5$ μg/L<br>Ni $= 14.93 \pm 3.9$ μg/L<br>Co $= 6.66 \pm 2.3$ μg/L<br>Cu $= 6.19 \pm 3.5$ μg/L<br>V $= 2.73 \pm 1.0$ μg/L<br>Cr $= 1.64 \pm 0.7$ μg/L<br>As $= 0.68 \pm 0.2$ μg/L<br>Pb $= 0.65 \pm 0.3$ μg/L<br>Cd $= 0.1 \pm 0.1$ μg/L<br>Membrane pore size $= 0.4$ μm<br>Membrane surface area $= 16$ m$^2$<br>Permeate flux $= 7.80$ L/m$^2$ h | TSS $\leq 1$ mg/L<br>COD $= 18.7 \pm 2.9$ mg/L<br>NH$_4$-$N \leq 0.02$<br>TP $= 0.43 \pm 0.1$ mg/L<br>CBZ $= 0.77 \pm 0.1$ mg/L<br>BIS $= 0.14 \pm 0.1$ mg/L<br>DCF $= 1.12 \pm 0.4$ mg/L<br>BPA $\leq 0.05$ mg/L<br>Zn $= 31.43 \pm 14.3$ μg/L<br>Ni $= 9.75 \pm 1.8$ μg/L<br>Co $= 2.6 \pm 1.4$ μg/L<br>Cu $= 3.87 \pm 2.0$ μg/L<br>V $= 0.35 \pm 0.1$ μg/L<br>Cr $= 0.81 \pm 0.2$ μg/L<br>As $= 0.34 \pm 0.1$ μg/L<br>Pb $= 0.11 \pm 0.1$ μg/L<br>Cd $= 0.01 \pm 0.0$ μg/L | [88] |

| | | | | | |
|---|---|---|---|---|---|
| | | | MLSS = 5300–9800 mg/L<br>Aeration intensity = 0.4–0.6/m$^3$ m$^2$ h<br>pH = 6.6–7.3<br>Operating temperature = 7–10°C<br>Operating duration = 120 days<br>HRT = 35 h<br>SRT = 25–30 days<br>Working volume = 3 m$^3$ | | |
| Leachate | SMBR | Polymer | COD = 2200 mg/L<br>DEHP = 450 µg/L<br>N-NH$_4^+$ = 250 mg/L<br>P-PO$_4^{3+}$ = 11 mg/L<br>Total alkalinity = 2370 mg/L<br>C/N/P ratio = 200/22.7/1<br>Membrane pore size = 0.04 µm<br>Membrane surface area = 0.047 m$^2$<br>DO = 2 mg/L<br>pH = 7.5 ± 0.2<br>HRT = 9 h<br>Operating temperature = 17.5 ± 1°C | Rejection ≥95% BOD, 60% DEHP | [81] |
| | Two-stage MBR | | BPA = 479 ± 227 µg/L<br>2,6-DTBP = 319 ± 146 µg/L<br>BHT = 410 ± 115 µg/L<br>DEP = 394 ± 238 µg/L<br>DBP = 597 ± 316 µg/L<br>DEHP = 284 ± 153 µg/L<br>Membrane pore size = 0.4 µm<br>Membrane surface area = 9 m$^2$<br>Permeate flor rate = 2 m$^3$/day<br>DO level = 4–5 mg/L<br>MLSS = 7–9 g/L | • Anoxic<br>  BPA = 298 ± 109 µg/L<br>  2,6-DTBP = 211 ± 87 µg/L<br>  BHT = 279 ± 113 µg/L<br>  DEP = 286 ± 178 µg/L<br>  DBP = 448 ± 215 µg/L<br>  DEHP = 247 ± 96 µg/L<br><br>• MBR<br>  BPA = 2 ± 5 µg/L | [80] |

TABLE 13.6    Application of MBR in Different Industries—cont'd

| Industry area | System | Membrane type | Operating conditions | Performance | Reference |
|---|---|---|---|---|---|
| | | | HRT $= 1$ day<br>*Re*-circulation rate $= 100\%$<br>Working volume $= 1\ m^3$<br>Operating duration $= 500$ days | 2,6-DTBP $= 3 \pm 10\ \mu g/L$<br>BHT $= 2 \pm 9\ \mu g/L$<br>DEP $= 8 \pm 23\ \mu g/L$<br>DBP $= 19 \pm 15\ \mu g/L$<br>DEHP $= 12 \pm 8\ \mu g/L$ | |
| | SMBR | PVDF | BOD $= 3260\ mg/L$<br>COD $= 6740\ mg/L$<br>$NH_3$-$N = 170\ mg/L$<br>TKN $= 410\ mg/L$<br>TP $= 50\ mg/L$<br>Membrane pore size $= 0.4\ \mu m$<br>Membrane surface area $= 0.07\ m^2$<br>C/N ratio $= 6$<br>SRT $= 90$ days<br>MLSS $= 7\ g/L$<br>DO $= 5\ mg/L$<br>pH $= 7.5$<br>HRT $= 24$ h<br>Working volume $= 9\ L$ | Rejection $= 90\%$–$99\%$ | [90] |
| | SMBR | Polymer | Caffeine $= 1330\ mg/L$<br>Aluminum $= 39{,}800\ mg/L$<br>Antimony $\leq 100\ mg/L$<br>Arsenic $= 634\ mg/L$<br>Barium $= 1190\ mg/L$<br>Beryllium $\leq 100\ mg/L$<br>Bismuth $\leq 100\ mg/L$<br>Boron $= 4890\ mg/L$<br>Cadmium $= 20.0\ mg/L$<br>Chromium $= 401\ mg/L$<br>Cobalt $= 220\ mg/L$ | • Percent of reduction<br>Caffeine $= 99.95\%$<br>Aluminum $= 99.93\%$<br>Arsenic $= 97.00\%$<br>Barium $= 98.99\%$<br>Boron $= 82.74\%$<br>Chromium $= 98.75\%$<br>Cobalt $= 97.27\%$<br>Iron $= 99.87\%$<br>Lead $= 99.90\%$<br>Manganese $= 99.95\%$ | [86] |

| | | Copper = 113 mg/L<br>Iron = 297,000 mg/L<br>Lead = 811.0 mg/L<br>Manganese = 51,000 mg/L<br>Molybdenum = 147 mg/L<br>Nickel = 589 mg/L<br>Selenium ≤ 100 mg/L<br>Silver ≤ 25 mg/L<br>Strontium = 27,100 mg/L<br>Thallium ≤ 5 mg/L<br>Tin ≤ 100 mg/L<br>Titanium = 1370 mg/L<br>Uranium ≤ 5 mg/L<br>Vanadium = 136 mg/L<br>Zinc = 13,500 mg/L<br>Influent flow rate = 0.83 Ml/MIN<br>Membrane pore size = 20–30 nm<br>Membrane surface area = 1.10 m$^2$<br>Air flow rate = 1100 L/h<br>SRT = 10–20 days<br>pH = 5.10<br>Operating temperature = 25 ± 1°C<br>Working volume = 114 L | Molybdenum = 93.20%<br>Nickel = 88.79%<br>Strontium = 89.19%<br>Titanium = 99.49%<br>Vanadium = 98.53%<br>Zinc = 99.50% | |
| A/O-GAC-MBR | PVDF | BOD = 450 mg/L<br>COD = 3134. 88 mg/L<br>$NH_3$-$N$ = 434.76 mg/L<br>Conductivity = 7150 μS/cm<br>Na = 10.32–15.84 mg/L<br>K = 50.30–69.70 mg/L<br>Mg = 2.58–3.93 mg/L<br>Fe = 0.028–0.048 mg/L | • MBR<br>  COD = 597.7 mg/L<br>  $NH_3$-$N$ = 33 mg/L<br>  Conductivity = 4510 μS/cm<br>  Cd = 0.047 mg/L<br>  Pb = 0.12 mg/L<br>  Cr = 0.17 mg/L | [92] |

*Continued*

TABLE 13.6    Application of MBR in Different Industries—cont'd

| Industry area | System | Membrane type | Operating conditions | Performance | Reference |
|---|---|---|---|---|---|
| | | | Cu = 0.09–0.16 mg/L<br>Cd = 0.12–0.20 mg/L<br>Pb = 0.09–0.16 mg/L<br>Cr = 0.12–0.20 mg/L<br>Membrane pore size = 0.2 μm<br>Membrane surface area = 0.25 m$^2$<br>Flux = 6.25 L/m$^2$ h<br>DO = 2–4 mg/L<br>MLSS = 4–5 g/L<br>SRT = 40 days<br>HRT = 2 days<br>pH = 7.85<br>Operating temperature = 25°C<br>Working volume = 50 L | • NFCOD = 276.25 mg/L<br>  $NH_3$-$N$ = 26.55 mg/L<br>  Conductivity = 3740 μS/cm<br>  Cd = ND<br>  Pb = ND<br>  Cr = ND<br><br>• ROCOD = 12.39 mg/L<br>  $NH_3$-$N$ = 2.6 mg/L<br>  Conductivity = 134.22 μS/cm<br>  Cd = ND<br>  Pb = ND<br>  Cr = ND | |
| Dye and Textile | SMBR | Polymer | EC = 5.12–13.22 Ms./cm<br>COD = 187.1–2220 mg/L<br>$BOD_5$ = 300–1375 mg/L<br>TOC = 439–898 mg/L<br>TSS = 0.21–1.21 g/L<br>VSS = 0.01–0.71 g/L<br>Calcium = 1.34–11.9 mg/L<br>Potassium = 1.13–110.8 mg/L<br>Sodium = 100.4–226.0 mg/L<br>Magnesium = 8.39–40.39 mg/L<br>Copper = 0.000–0.003 mg/L<br>Zinc = 0.012–0.179 mg/L<br>Nickel = 0.000–0.027 mg/L | Rejection = 100% color, 98% COD, 96% $BOD_5$, 100% SS | [97] |

| | | Cadmium = 0.000–0.008 mg/L<br>Ph = 10.95–12.60<br>MWCO = 150 kDa<br>Membrane surface area = 0.39 m$^2$<br>TMP = 70–350 mbar<br>MLSS = 5.22 g/L<br>Aeration rate = 1–2 m$^3$/h<br>Operating temperature = 24–29°C<br>Working volume = 60 L<br>Operating duration = 7 months | | |
|---|---|---|---|---|
| eMBR | PVDF | COD = 7.78 ± 70 mg/L<br>True color = 1.19 ± 0.16 Abs<br>NH$_3$-$N$ = 28.3 ± 2.2 mg/L<br>TN = 35.1 ± 4 mg/L<br>Glucose = 400 mg/L<br>Sodium acetate anhydrous = 400 mg/L<br>NH$_4$Cl = 100 mg/L<br>KH$_2$PO$_4$ = 25 mg/L<br>KNO$_3$ = 50 mg/L<br>CaCl$_2$·2H$_2$O = 10 mg/L<br>MgCl$_2$·6H$_2$O = 10 mg/L<br>BR = 200 mg/L<br>IE column diameter = 11 cm<br>IE column length = 100 cm<br>Recation time = 30 min<br>Membrane pore size = 0.05 μm<br>Membrane surface area = 0.25 m$^2$<br>Permeate flux = 4.5 L/m$^2$ h<br>MLSS = 4000–5000 mg/L<br>Air flow rate = 0.3 L/min<br>pH = 5.9–6.8<br>Operating temeprature = 5–15°C<br>SRT = 30 days | • IE<br>  COD = 41.8%<br>  True color = 95.7%<br>  NH$_3$-$N$ = 24.7%<br>  TN = 25.1%<br><br>• HMBR<br>  COD = 93.2%<br>  True color = 97.7%<br>  NH$_3$-$N$ = 95.8%<br>  TN = 92.9%<br><br>• CMBR<br>  COD = 93.5%<br>  True color = 98.7%<br>  NH$_3$-$N$ = 97.6%<br>  TN = 67.5% | [100] |

*Continued*

TABLE 13.6    Application of MBR in Different Industries—cont'd

| Industry area | System | Membrane type | Operating conditions | Performance | Reference |
|---|---|---|---|---|---|
| | eMBR | PES | HRT = 20 h<br>Working volume = 18 L<br><br>BR = 50–100 mg/L<br>COD = 2334 mg/L<br>Ammonium acetate = 200 mg/L<br>Sodium hydrogen carbonate = 750 mg/L<br>Ammonium chloride = 30 mg/L<br>Potassium dihydrogen phosphate = 30 mg/L<br>Potassium hydrogen phosphate = 60 mg/L<br>Magnesium sulphate = 50 mg/L<br>Calcium chloride = 30 mg/L<br>Sodium chloride = 30 mg/L<br>Membrane pore size = 0.1 μm<br>Membrane surface area = 0.032 m$^2$<br>Flux = 6.5 L/m$^2$ h<br>DO = 5 mg/L<br>UV wavelength = 254 nm<br>UV dosage = 6.602 Wsec/cm$^2$<br>GAC column height = 27 cm<br>GAC internal diameter = 7 cm<br>GAC column volume = 270 cm$^3$<br>GAC column flow rate = 0.56 L/s<br>Working volume = 8 L<br>Operating duration = 100 days | Rejection = 95% BR, 99.1% COD, 97% nitrogen, 65.1% phosphorus | [98] |

| | | | | | |
|---|---|---|---|---|---|
| | FMBR-PMR | PES | Total COD = 1125 ± 70 mg/L<br>Soluble COD = 800 ± 100 mg/L<br>SS = 35 ± 2 mg/L<br>Conductivity = 2660 ± 16 μS/cm<br>Color = Very dark violet<br>Membrane pore size = 0.05 μm<br>Membrane surface area = 30 cm$^2$<br>Air flow rate = 100 mL/min<br>UV intensity = 3.5 mW/cm$^2$<br>Operating temperature = 25 ± 1°C<br>pH = 8.7 ± 0.5<br>HRT = 15 h<br>PMR woking volume = 900 mL<br>FMBR working volume = 500 mL | Rejection = 93% COD, 99% color | [101] |
| Petrochemical | SMBR | PES | COD = 1730 mg/L<br>BOD = 1266 mg/L<br>Monoethylene glycole = 452 mg/L<br>Acetaldehyde = 220 mg/L<br>Formaldehyde ≤ 1.0 mg/L<br>Membrane pore size = 0.04 μm<br>Membrane surface area = 10 m$^2$<br>Residence time = 1 day<br>MLSS = 8 g/L<br>HRT = 13.5 h<br>Working volume = 2.5 m$^3$ | COD = 155 mg/L<br>BOD = 21 mg/L<br>Monoethylene glycole ≤ 10 mg/L<br>Acetaldehyde = 3.3 mg/L<br>Formaldehyde ≤ 1.0 mg/L | [93] |
| | AnHMBR | | COD = 39.5–85.3 mg/L<br>2-CP = 0.6–2.7 mg/L<br>Mesh filter pore size = 0.7 μm<br>Mesh filter filtration area = 0.022 m$^2$ | Rejection = 82.3 ± 5.7% COD, 92.6 ± 10.4%<br>2-CP | [106] |

TABLE 13.6 Application of MBR in Different Industries—cont'd

| Industry area | System | Membrane type | Operating conditions | Performance | Reference |
|---|---|---|---|---|---|
| | | | Operating temperature $= 25°C$<br>Working volume of GAC column $= 0.78$ L | | |
| Food and Beverage | UF-MBR | Ceramic | Lactose $= 48.30 \pm 1.05\%$ *w*/w<br>GOS $= 27.44 \pm 0.65\%$ w/w<br>Glucose $= 17.48 \pm 0.44\%$ w/w<br>Galactose $= 6.79 \pm 0.52\%$ w/w<br>MWCO $= 50$ kDa<br>Membrane surface area $= 0.0047$ m$^2$<br>pH $= 4.78 \pm 0.20$<br>Working volume $= 2.5$ L<br>Operating duration $= 240$ min | • Optimum operating conditions<br>Transmembrane pressure $= 4.38$ bar<br>Crossflow velocity $= 7.35$ m/s<br>Temperature $= 53.1°C$ | [108] |
| | SMBR | Polymer | • Low load stream<br>COD $= 142$–795 mg/L<br>BOD$_5$ $= 46$–231 mg/L<br>TP $= 92.2$–22 mg/L<br>NH$_4$-N $= 33$–80 mg/L<br>TN $= 71$–135 mg/L<br>TSS $= 30$–186 mg/L<br><br>• High load stream<br>COD $= 965$–2142 mg/L<br>BOD$_5$ $= 683$–1293 mg/L<br>TP $= 9.9$–15 mg/L<br>NH$_4$-N $= 23$–57 mg/L<br>TN $= 74$–127 mg/L<br>TSS $= 238$–344 mg/L | • Low load stream<br>COD $= 8$–108 mg/L<br>BOD$_5$ $= 2$–5 mg/L<br>TP $= 3.2$–12 mg/L<br>NH$_4$-N $= 0.1$–0.4 mg/L<br>TN $= 17$–91 mg/L<br>TSS $\leq 15$ mg/L<br><br>• High load stream<br>COD $= 26$–47 mg/L<br>BOD$_5$ $= 2$–3 mg/L<br>TP $= 0.4$–5 mg/L<br>NH$_4$-N $= 0.1$–0.4 mg/L | [112] |

| | | | | |
|---|---|---|---|---|
| | | Membrane pore size $= 0.04$ μm<br>Membrane surface area $= 6.6$ m$^2$<br>Permeate flux $= 7.3$ L/m$^2$ h<br>Air flow rate $= 205$ L/min<br>SRT $=$ infinite<br>HRT $= 25.5$ h<br>Operating temperature $= 25$–$32$°C | TN $= 5$–$6$ mg/L<br>TSS $\leq 15$ mg/L | |
| UASB-MBR | PVDF | COD $= 1000$–$2000$ mg/L<br>NaHCO$_3$ $= 200$ mg/L<br>FeCl$_3$·6H$_2$O $= 1.5$ mg/L<br>H$_3$BO$_3$ $= 0.15$ m/L<br>CuSO$_4$·5H$_2$O $= 0.03$ mg/L<br>Kl $= 0.03$ mg/L<br>ZnSO$_4$·7H$_2$O $= 0.12$ mg/L<br>CoCl$_2$·6H$_2$O $= 0.15$ mg/L<br>MnCl$_2$·4H$_2$O $= 0.12$ mg/L<br>UASB storage volume $= 120$ L<br>Aerobic chamber working volume $= 36$ L<br>Membrane pore size $= 0.04$ μm<br>Membrane surface area $= 0.9$ m$^2$<br>Membrane filtration working<br>volume $= 20$ L<br>Operating duration $= 292$ days | Total and soluble COD removal $= 95\%$<br>Methane production $= 73\%$ | [113] |
| EGSB/MBR | Ceramic | • ESGB<br>  Material $=$ PVC<br>  Internal diameter $= 104$ mm<br>  Height $= 2070$ mm<br>  TSS $= 1182$ mg/L<br>  VSS $= 24.5\%$<br>  Operating temperature $= 35$–$37$°C<br>  Working volume $= 24$ L<br>  Operating duration $= 135$ days | • ESGB<br>  EC $= 4057$ μS/cm<br>  TDS $= 2725$ mg/L<br>  COD$_t$ $= 2245$ mg/L<br>  COD$_s$ $= 2051$ mg/L<br>  Turbidity $= 50.7$ NTU<br>  TSS $= 99$ mg/L<br>  Fructose $= 189$ mg/L<br>  Sucrose $= 631$ mg/L | [115] |

TABLE 13.6   Application of MBR in Different Industries—cont'd

| Industry area | System | Membrane type | Operating conditions | Performance | Reference |
|---|---|---|---|---|---|
| | | | • MBR<br>  TSS = 1064 mg/L<br>  VSS = 15%<br>  Membrane pore size = 0.2 and 0.4 μm<br>  Membrane surface area = 0.058 m$^2$ | • MBR<br>  EC = 4129 μS/cm<br>  TDS = 2753 mg/L<br>  COD$_t$ = 253.5 mg/L<br>  COD$_s$ = 185.5 mg/L<br>  Turbidity = 79.1 NTU<br>  TSS = 211 mg/L<br>  Fructose = 25 mg/L<br>  Sucrose = 70.9 mg/L | |
| | SMBR | Polymer | COD = 4728 ± 2807 mg/L<br>SCOD = 3898 ± 2639 mg/L<br>RBCOD = 3591 ± 2581 mg/L<br>TSS = 320 ± 125 mg/L<br>TN = 60 ± 21 mg N/L<br>TKN = 22 ± 9 mg N/L<br>N-NO$_3$ = 38 ± 19 mg N/L<br>TP = 35 ± 16 mg P/L<br>Ethanol = 275 ± 5 mg/L<br>Glucose = 21 ± 16 mg/L<br>Fructose = 48 ± 40 mg/L<br>Sucrose = 4 ± 7 mg/L<br>MBR capacity = 325 m$^3$<br>Air flow rate = 500–1220 m$^3$/h<br>Membrane pore size = 0.4 μm<br>Operating duration = 2 years | Rejection = 95% COD | [116] |
| Pharmaceuticals | SMBR | PES | Membrane surface area = 1.43 m$^2$<br>Membrane pore size = 0.04 μm<br>Operating duration = 4 weeks<br><br>• MBR-15<br>  SRT = 15 days<br>  Sludge concentration = 12 g/L | • MBR-15<br>  Rejection = 100% Acetaminophen, 98% Ketoprofen, 86% Naproxen, 57% Roxithromycin, 55% Sulfamethoxazole, 86% Trimethoprim | [126] |

| SMBR | | | |
|---|---|---|---|

| | | HRT = 9 h<br>Working volume = 260 L<br><br>• MBR-30<br>SRT = 30 days<br>Sludge concentration = 12 g/L<br>HRT = 13 h<br>Working volume = 240 L | • MBR-30<br>Rejection = 100% Acetaminophen, 100% Ketoprofen, 89% Naproxen, 81% Roxithromycin, 64% Sulfamethoxazole, 94% Trimethoprim | |
|---|---|---|---|
| SMBR | Ceramic | COD = 1750 mg/L<br>TN = 125 mg/L<br>TP = 25 mg/L<br>Cyclophosphamide = 5 µg/L<br>Membrane surface area = 0.0055 m$^2$<br>Membrane pore size = 0.2 µm<br>Permeate flow rate = 13.3 L/day<br>HRT = 36 h<br>SRT = 20 days<br>DO level = 0–4.5 mg/L<br>Operating temperature = 25–32°C<br>pH = 7–8<br>Working volume = 20 L | Rejection = 98% ± 1% COD, 94% ± 5% TN, 60% Cyclophosphamide | [127] |
| SMBR | PVDF | DCF = 3.81 µg/L<br>SMX = 27.62 µg/L<br>TMP = 32.40 µg/L<br>CBZ = 7.50 µg/L<br>TMD = 102.33 µg/L<br>NPX = 51.76 µg/L<br>PPL = 5.45 µg/L<br>IBP = 36.50 µg/L<br>E2 = 128.19 µg/L<br>TCS = 40.31 µg/L<br>GFZ = 50.82 µg/L<br>Membrane pore size = 0.4 µm<br>Membrane surface area = 18.0 m$^2$ | • Day 0–42<br>Rejection = −50.1% DCF, 78.5% SMX, 80.1% TMP, −94.5% CBZ, 14.4% TMD, 82.3% NPX, −57.8% PPL, 100% IBP, 100% E2, 100% TCS, 45.8% GFZ<br><br>• Day 43–76<br>Rejection = −270.2% DCF, −43.9% SMX, 24.6% TMP, −6.8% CBZ, −79.4% TMD, 23.6% NPX, 34.2% PPL, 100% IBP, 100% E2, 100% TCS, −84.6% GFZ | [130] |

TABLE 13.6 Application of MBR in Different Industries—cont'd

| Industry area | System | Membrane type | Operating conditions | Performance | Reference |
|---|---|---|---|---|---|
| | | | Permeate flux = 14 L/m$^2$ h<br>Total flow rate = 500 L/h<br>Air flowrate = 340 L/min<br>HRT = 3 h<br>pH = 6.7 ± 0.2<br>Working volume = 1.3 m$^3$ | | |
| | Ms$^2$ALBRs | PVDF | 7-ACA concentration = 100 mg/L<br>Membrane surface area = 0.22 m$^2$<br>Membrane pore size = 0.22 µm<br>MWCO = 15,000 D<br>DO supply = 2 ± 0.2 mg/L<br>SRT = 30 days<br>HRT = 4–10<br>Operating temperature = 10–45°C<br>pH = 4–11<br>Working volume = 4.0 L<br>Operating duration = 200 days | Rejection = 94.96% COD, 66.44% 7-ACA | [133] |
| | BEMR | Ceramic | TCOD = 17,143 ± 1873 mg/L<br>TOC = 7238 ± 1623 mg/L<br>TDS = 26,664 ± 4594 mg/L<br>NH$_3$-$N$ = 68.3 ± 8.7 mg/L<br>Chlorides = 19,960 ± 3391 mg/L<br>Fluoride = 104 ± 37 mg/L<br>Sulfates = 126 ± 33 mg/L<br>Phosphate = 138 ± 29 mg/L<br>Sodium = 9825 ± 1749 mg/L<br>Potassium = 3837 ± 780 mg/L<br>Calcium = 56 ± 26 mg/L | • HRT = 120 hTCOD = 5743 ± 488 mg/L<br>TOC = 3243 ± 450 mg/L<br>TDS = 24,367 ± 3253 mg/L<br>NH$_3$-$N$ = 187.6 ± 34.6 mg/L<br>Chlorides = 15,345 ± 2141 mg/L<br>Fluoride = 28 ± 11 mg/L<br>Sulfates = 87 ± 21 mg/L<br>Phosphate = 123 ± 38 mg/L<br>Sodium = 7277 ± 883 mg/L<br>Potassium = 2551 ± 447 mg/L | [138] |

| | | | | |
|---|---|---|---|---|
| | | Membrane pore size = 300 nm<br>Membrane surface area = 0.08 m$^2$<br>Permeate flux = 1.04–2.08 L/m$^2$ h<br>Carrier diameter = 2.5 cm<br>Pack ratio = 16.7%<br>Void volume = 2 L<br>SRT = 200 days<br>Attached biomass = 11,000 mg/L<br>MLSS = 3040–5380 mg/L<br>Organic loading rate = 3.1–8.2 kg COD/m$^3$ day<br>Operating temperature = 27.0 ± 1.0°C<br>pH = 7.02<br>Working volume = 10 L | Calcium = 30 ± 16 mg/L<br><br>• HRT = 60 hTCOD = 7399 ± 733 mg/L<br>TOC = 3574 ± 919 mg/L<br>TDS = 24,919 ± 4419 mg/L<br>NH$_3$-N = 218.5 ± 31.5 mg/L<br>Chlorides = 14,359 ± 3744 mg/L<br>Fluoride = 20 ± 17 mg/L<br>Sulfates = 183 ± 91 mg/L<br>Phosphate = 174 ± 69 mg/L<br>Sodium = 7583 ± 1639<br>Potassium = 2921 ± 821 mg/L<br>Calcium = 55 ± 13 mg/L | |
| SMSMBR | Ceramic | TCOD = 17,143 ± 1873 mg/L<br>TOC = 7238 ± 1623 mg/L<br>TDS = 26,664 ± 4594 mg/L<br>NH$_3$-N = 68.3 ± 8.7 mg/L<br>Chlorides = 19,960 ± 3391 mg/L<br>Fluoride = 104 ± 37 mg/L<br>Sulfates = 126 ± 33 mg/L<br>Phosphate = 138 ± 29 mg/L<br>Sodium = 9825 ± 1749 mg/L<br>Potassium = 3837 ± 780 mg/L<br>Calcium = 56 ± 26 mg/L<br>Membrane pore size = 300 nm<br>Membrane surface area = 0.08 m$^2$<br>Permeate flux = 1.04–2.08 L/m$^2$ h<br>SRT = 200 days<br>MLSS = 3040–5380 mg/L<br>Organic loading rate = 3.1–8.2 kg COD/m$^3$ day | • HRT = 120 hTCOD = 1803 ± 203 mg/L<br>TOC = 923 ± 218 mg/L<br>TDS = 27,225 ± 1983 mg/L<br>NH$_3$-N = 213.4 ± 51.1 mg/L<br>Chlorides = 18,899 ± 4032 mg/L<br>Fluoride = 21 ± 5 mg/L<br>Sulfates = 140 ± 67 mg/L<br>Phosphate = 138 ± 15 mg/L<br>Sodium = 7928 ± 1717 mg/L<br>Potassium = 2820 ± 484 mg/L<br>Calcium = 24 ± 7 mg/L<br><br>• HRT = 60 hTCOD = 3193 ± 412 mg/L<br>TOC = 1277 ± 421 mg/L<br>TDS = 26,325 ± 3413 mg/L<br>NH$_3$-N = 253.0 ± 47.4 mg/L<br>Chlorides = 17,068 ± 1578 mg/L<br>Fluoride = 26 ± 23 mg/L | [138] |

TABLE 13.6    Application of MBR in Different Industries—cont'd

| Industry area | System | Membrane type | Operating conditions | Performance | Reference |
|---|---|---|---|---|---|
| | | | Operating temperature $= 27.0 \pm 1.0°C$<br>pH $= 7.02$<br>Working volume $= 10$ L | Sulfates $= 128 \pm 50$ mg/L<br>Phosphate $= 105 \pm 34$ mg/L<br>Sodium $= 8480 \pm 823$ mg/L<br>Potassium $= 3081 \pm 421$ mg/L<br>Calcium $= 51 \pm 5$ mg/L | |
| | MBR-Electrochemical oxidation | Polymer | CBZ $= 22.45 \pm 0.84$ µg/L<br>COD $= 402.7 \pm 4.8$ mg $O_2$/L<br>TOC $= 295.33 \pm 4.16$ mg/L<br>$NH_4^+$-$N = 68.56 \pm 3.42$ mg/L<br>$PO_4^-$-$P = 20.42 \pm 2.02$ mg/L<br>Membrane pore diameter $= 0.04$ µm<br>Membrane surface area $= 0.047$ m$^2$<br>Mixing speed $= 400$ rpm<br>Operating temperature $= 20 \pm 2°C$<br>pH $= 7.0 \pm 1.0$<br>HRT $= 10$ h<br>Working volume $= 6$ L | • MBR<br>  CBZ $= 20.12 \pm 0.77$ µg/L<br>  COD $= 11.14 \pm 1.54$ mg $O_2$/L<br>  TOC $= 4.93 \pm 0.94$ mg/L<br>  $NH_4^+$-$N = 13.05 \pm 1.96$ mg/L<br>  $PO_4^-$-$P = 14.38 \pm 2.63$ mg/L<br><br>• Electrochemical oxidation<br>  CBZ $\leq 0.06$ µg/L<br>  COD $= 7.76 \pm 0.67$ mg $O_2$/L<br>  TOC $= 4.67 \pm 0.18$ mg/L<br>  $NH_4^+$-$N = 8.78 \pm 1.01$ mg/L<br>  $PO_4^-$-$P = 14.21 \pm 2.09$ mg/L | [139] |
| | MBR-NF | PVDF | Spiramycin $= 1.99$–$2.79$ mg/L<br>New spiramycin $= 0.98$–$1.35$ mg/L<br><br>• MBR<br>  Membrane pore size $= 0.1$ µm<br>  Membrane surface area $= 34 \times 0.25$ m$^2$<br>  pH $= 7.09 \pm 0.4$<br>  HRT $= 30$–$36$ h<br>  Working volume $= 1.5$ m$^3$<br><br>• NF<br>  Membrane surface area $= 5.2$ m$^2$<br>  TMP $= 5.0$ bar<br>  Cross-flow rate $= 2.0$ m3/h | Water yield $= 92\% \pm 5.6\%$<br><br>• MBR<br>  Rejection $= 51\%$–$55\%$<br><br>• NF<br>  Rejection $= 95\%$ | [140] |

| | | | | | |
|---|---|---|---|---|---|
| | AnMBR | Ceramic | COD = 0.55–10.6 g/L<br>Membrane surface area = 0.25 m$^2$<br>Flux = 8.4 L/m$^2$ h<br>SRT = 120 days and 450 days<br>Operating temperature = 35–37°C<br>pH = 7.0–7.5<br>Working volume = 50 L | • Phase 1<br>Rejection = 44%–94%<br><br>• Phase 2<br>Rejection = 89%–93%<br><br>• Phase 3<br>Rejection = 91%–97% | [141] |
| Shipboard | Integrated biofilm-MBR | Ceramic | Oil concentration = 0 mg/L<br>Flux = 13.5 LMH<br>HRT = 4 h<br>Configuration = dead-end | • Recovery 70%<br>Rejection = 42.03% TSS, 39.23% TCOD, 48.54% FCOD<br><br>• Recovery 93%<br>Rejection = 47.83% TSS, 35.41% TCOD, 31.07% FCOD | [142] |
| Leather | SAMBR | PVDF | TSS = 8590–12,930 mg/L<br>VSS = 5930–9480 mg/L<br>COD = 11,224–12,898 mg/L<br>Alkalinity = 940–1746 mg/L<br>VFA = 1252–1648 mg/L<br>Membrane pore size = 0.4 µm<br>MWCO = 30 kDa<br>Membrane area = 0.25 m$^2$<br>Slurry mixing rate = 18 L/min<br>Biogas re-circulating flow rate = 0.4 L/min<br>HRT = 40 h<br>Operating duration = 2 months | • SAMBR<br>TSS = 6640–18,390 mg/L<br>VSS = 5420–11,420 mg/L<br>COD = 9087–16,793 mg/L<br>Alkalinity = 923–2967 mg/L<br>VFA = 197–6197 mg/L<br><br>• Effluent<br>TSS = 2450–4140 mg/L<br>VSS = 23–520 mg/L<br>COD = 1257–8039 mg/L<br>Alkalinity = 507–2635 mg/L<br>VFA = 158–3956 mg/L | [134] |
| Bamboo | AnMBR | PVDF | Membrane pore size = 0.02 µm<br>Membrane area = 0.07 m$^2$<br>Recirculating flow ratio = 10<br>Particle size of BC = 0.5 mm<br>HRT = 3 days | • B-AnMBR<br>Rejection = 94.5% ± 2.9% COD<br><br>• AnMBR<br>Rejection = 89.1% ± 3.1% COD | [145] |

# 13.7  CONCLUSION

MBR has increasingly found applications in various sectors due to the need of having a compact treatment system. Membranes made from various materials have been used to improve the MBR processes and these membranes were produced using various fabrication techniques including NIPS, and MSCS, track-etched, and electrospinning. These membranes were normally characterized to find the suitable pore size and porosity, surface roughness, hydrophilicity and surface charge which are very important to get the best performance from the membranes. These advances have helped to push MBRs to have applications for wastewater treatment in many sectors including those for municipal, leachate, dye and textile, petrochemical, food and beverage, and pharmaceutical industries. As more researches are carried out, MBRs will be one of the most competitive technologies for wastewater treatment and other applications.

# References

[1]   Judd S. The MBR book: principles and applications of membrane bioreactors for water and wastewater treatment. 2nd ed. Oxford: Elsevier; 2011.

[2]   Yamamoto K, Hiasa M, Mahmood T, Matsuo T. Direct solid-liquid separation using hollow fiber membrane in an activated sludge aeration tank. Water Sci Technol 1989;21:43–54.

[3]   Ahmed FN, Lan CQ. Treatment of landfill leachate using membrane bioreactors: a review. Desalination 2012;287:41–54.

[4]   Besha AT, Gebreyohannes AY, Tufa RA, Bekele DN, Curcio E, Giorno L. Removal of emerging micropollutants by activated sludge process and membrane bioreactors and the effects of micropollutants on membrane fouling: a review. J Environ Chem Eng 2017;5:2395–414.

[5]   Jegatheesan V, Kumar B, Chen J, Navaratna D. Bioresource technology treatment of textile wastewater with membrane bioreactor: a critical review. Bioresour Technol 2016;204:202–12.

[6]   Krzeminski P, Leverette L, Malamis S, Katsou E. Membrane bioreactors—a review on recent developments in energy reduction, fouling control, novel configurations, LCA and market prospects. J Memb Sci 2016;527:207–27.

[7]   Ren J, Wang R. Preparation of polymeric membrane. In: Wang LK, Chen PJ, Hung YT, Shammas NK, editors. Membr desalin technol. vol. 13. Totowa, NJ: Humana Press; 2011. p. 47–100.

[8]   Park H, Chang I, Lee K. Principles of membrane bioreactors for wastewater treatment. Boca Raton: Taylor & Francis; 2015.

[8a]  Hubadillah SK, Othman MHD, Harun Z, Ismail AF, Rahman MA, Jaafar J. A novel green ceramic hollow fiber membrane (CHFM) derived from rice husk ash as combined adsorbent-separator for efficient heavy metals removal. Ceram Int 2017;43:4716–20.

[9]   Tijana M, Predrag V, Goran V, Branka B. Investigations of hydrodynamics permeability ceramic membranes for microfiltration. J Agric Sci 2006;51:151–64.

[10] Puspitasari V, Granville A, Le-Clech P, Chen V. Cleaning and ageing effect of sodium hypochlorite on polyvinylidene fluoride (PVDF) membrane. Sep Purif Technol 2010;72:301–8.

[11] Liu F, Hashim NA, Liu Y, Abed MRM, Li K. Progress in the production and modification of PVDF membranes. J Memb Sci 2011;375:1–27.

[12] Fan G, Su Z, Lin R, Lin X, Xu R, Chen W. Influence of membrane materials and operational modes on the performance of ultrafiltration modules for drinking water treatment. Int J Polym Sci 2016;2016:1–8.

[13] Pearce G. Introduction to membranes—membrane selection. Filtr Sep 2007;44:35–7.

[14] Kim JJ, Jang TS, Kwon YD, Kim UY, Kim SS. Structural study of microporous polypropylene hollow fiber membranes made by the melt-spinning and cold-stretching method. J Memb Sci 1994;93:209–15.

[15] Zinadini S, Vatanpour V, Zinatizadeh AA, Rahimi M, Rahimi Z, Kian M. Preparation and characterization of antifouling graphene oxide/polyethersulfone ultrafiltration membrane: application in MBR for dairy wastewater treatment. J Water Process Eng 2015;7:280–94.

[15a] Mulder M. Membrane preparation: phase inversion membranes. In: Wilson I, Poole C, Cooke M, editors. Encyclopedia of Separation Science. 1st ed. Elsevier; 2000. p. 3331–46. https://doi.org/10.1016/B0-12-226770-2/05271-6.

[16] Hu XY, Chen YB, Liang HX, Xiao CF. Preparation of polyurethane/poly(vinylidene fluoride) blend hollow fibre membrane using melt spinning and stretching. Mater Sci Technol 2011;27:661–5.

[17] Lalia BS, Kochkodan V, Hashaikeh R, Hilal N. A review on membrane fabrication: structure, properties and performance relationship. Desalination 2013;326:77–95.

[18] Li W, Zhou J, Gu JS, Yu HY. Fouling control in a submerged membrane-bioreactor by the membrane surface modification. J Appl Polym Sci 2010;115:2302–9.

[19] Bilad MR, Westbroek P, Vankelecom IFJ. Assessment and optimization of electrospun nanofiber-membranes in a membrane bioreactor (MBR). J Memb Sci 2011;380:181–91.

[20] Baker RW, Baker WR. Membr technol and applications. vol. vol. 23. John Wiley & Sons, Ltd; 2012. https://doi.org/10.1016/S0376-7388(00)83139-7.

[21] Choi J-H, Park S-K, Ng H-Y. Membrane fouling in a submerged membrane bioreactor using track-etched and phase-inversed porous membranes. Sep Purif Technol 2009;65:184–92.

[22] Liao Y, Wang R, Tian M, Qiu C, Fane AG. Fabrication of polyvinylidene fluoride (PVDF) nanofiber membranes by electro-spinning for direct contact membrane distillation. J Memb Sci 2013;425–426:30–9.

[22a] Daels N, De Vrieze S, Decostere B, Dejans P, Dumoulin A, De Clerck K, et al. The use of electrospun flat sheet nanofibre membranes in MBR applications. Desalination 2010;257:170–6.

[23] Liu L, Xiao L, Yang F. Terylene membrane modification with polyrotaxanes, $TiO_2$ and polyvinyl alcohol for better antifouling and adsorption property. J Memb Sci 2009;333:110–7.

[24] Su YC, Huang CP, Pan JR, Hsieh WP, Chu MC. Fouling mitigation by $TiO_2$ composite membrane in membrane bioreactors. J Environ Eng 2012;138:344–50.

[25] Zhao C, Xu X, Chen J, Wang G, Yang F. Highly effective antifouling performance of PVDF/graphene oxide composite membrane in membrane bioreactor (MBR) system. Desalination 2014;340:59–66.

[25a] Ganesh BM, Isloor AM, Ismail AF. Enhanced hydrophilicity and salt rejection study of graphene oxide-polysulfone mixed matrix membrane. Desalination 2013;313:199–207.

[26] Etemadi H, Yegani R, Seyfollahi M. The effect of amino functionalized and polyethylene glycol grafted nanodiamond on anti-biofouling properties of cellulose acetate membrane in membrane bioreactor systems. Sep Purif Technol 2017;177:350–62.

[27] Bae TH, Tak TM. Effect of $TiO_2$ nanoparticles on fouling mitigation of ultrafiltration membranes for activated sludge filtration. J Memb Sci 2005;249:1–8.

[28] Wang C, Yang F, Meng F, Zhang H, Xue Y, Fu G. High flux and antifouling filtration membrane based on non-woven fabric with chitosan coating for membrane bioreactors. Bioresour Technol 2010;101:5469–74.

[29] He Y, Zhang W, Rao P, Jin P. Diatomite- and polyvinyl alcohol-modified nonwoven fabric in membrane bioreactor for wastewater reclamation. Desalin Water Treat 2016;57:2952–8.

[30] Li N, Liu L, Yang F. Highly conductive graphene/PANi-phytic acid modified cathodic filter membrane and its antifouling property in EMBR in neutral conditions. Desalination 2014;338:10–6.

[31] Liang S, Qi G, Xiao K, Sun J, Giannelis EP, Huang X, et al. Organic fouling behavior of superhydrophilic polyvinylidene fluoride (PVDF) ultrafiltration membranes functionalized with surface-tailored nanoparticles: implications for organic fouling in membrane bioreactors. J Memb Sci 2014;463:94–101.

[32] Yu HY, Hu MX, Xu ZK, Wang JL, Wang SY. Surface modification of polypropylene microporous membranes to improve their antifouling property in MBR: $NH_3$ plasma treatment. Sep Purif Technol 2005;45:8–15.

[33] Yu HY, Xie YJ, Hu MX, Wang JL, Wang SY, Xu ZK. Surface modification of polypropylene microporous membrane to improve its antifouling property in MBR: $CO_2$ plasma treatment. J Memb Sci 2005;254:219–27.

[34] Yu HY, Liu LQ, Tang ZQ, Yan MG, Gu JS, Wei XW. Surface modification of polypropylene microporous membrane to improve its antifouling characteristics in an SMBR: air plasma treatment. J Memb Sci 2008;311:216–24.

[35] Asatekin A, Menniti A, Kang S, Elimelech M, Morgenroth E, Mayes AM. Antifouling nanofiltration membranes for membrane bioreactors from self-assembling graft copolymers. J Memb Sci 2006;285:81–9.

[36] Yu HY, Xu ZK, Lei H, Hu MX, Yang Q. Photoinduced graft polymerization of acrylamide on polypropylene microporous membranes for the improvement of antifouling characteristics in a submerged membrane-bioreactor. Sep Purif Technol 2007;53:119–25.

[37] Yu HY, He JM, Liu LQ, He XC, Gu JS, Wei XW. Photoinduced graft polymerization to improve antifouling characteristics of an SMBR. J Memb Sci 2007;302:235–42.

[38] Shin IH, Hong S, Lim SJ, Son Y-S, Kim T-H. Surface modification of PVDF membrane by radiation-induced graft polymerization for novel membrane bioreactor. J Ind Eng Chem 2017;46:103–10.

[39] Liang S, Kang Y, Tiraferri A, Giannelis EP, Huang X, Elimelech M. Highly hydrophilic polyvinylidene fluoride (PVDF) ultrafiltration membranes via postfabrication grafting of surface-tailored silica nanoparticles. ACS Appl Mater Interfaces 2013;5:6694–703.

[40] Bilad, M.R., Druyts, J. and Vankelecom IFJ. Role of surface pores on fouling of polyvinylidene fluoride membranes in submerged membrane bioreactors. In: Proc 2017 IOP Conf Ser: Mater Sci Eng: 180, 012272, 2017.

[40a] Zhang M, Liao B, Zhou X, He Y, Hong H, Lin H, et al. Effects of hydrophilicity/hydrophobicity of membrane on membrane fouling in a submerged membrane bioreactor. Bioresour Technol 2015;175:59–67.

[41] Yu HY, Tang ZQ, Huang L, Cheng G, Li W, Zhou J, et al. Surface modification of polypropylene macroporous membrane to improve its antifouling characteristics in a submerged membrane-bioreactor: Ar plasma treatment. Membr Water Treat 2010;1:83–92.

[42] Yu HY, Liu LQ, Tang ZQ, Yan MG, Gu JS, Wei XW. Mitigated membrane fouling in an SMBR by surface modification. J Memb Sci 2008;310:409–17.

[43] Jin L, Ong SL, Ng HY. Comparison of fouling characteristics in different pore-sized submerged ceramic membrane bioreactors. Water Res 2010;44:5907–18.

[44] Miyoshi T, Yuasa K, Ishigami T, Rajabzadeh S, Kamio E, Ohmukai Y, et al. Effect of membrane polymeric materials on relationship between surface pore size and membrane fouling in membrane bioreactors. Appl Surf Sci 2015;330:351–7.

[45] Zhao L, Shen L, He Y, Hong H, Lin H. Influence of membrane surface roughness on interfacial interactions with sludge flocs in a submerged membrane bioreactor. J Colloid Interface Sci 2015;446:84–90.

[46] Teow YH, Ahmad AL, Lim JK, Ooi BS. Preparation and characterization of PVDF/TiO$_2$ mixed matrix membrane via in situ colloidal precipitation method. Desalination 2012;295:61–9.

[47] Low ZX, Razmjou A, Wang K, Gray S, Duke M, Wang H. Effect of addition of two-dimensional ZIF-L nanoflakes on the properties of polyethersulfone ultrafiltration membrane. J Memb Sci 2014;460:9–17.

[48] Kochkodan V, Johnson DJ, Hilal N. Polymeric membranes: surface modification for minimizing (bio) colloidal fouling. Adv Colloid Interf Sci 2014;206:116–40.

[49] Woo SH, Park J, Min BR. Relationship between permeate flux and surface roughness of membranes with similar water contact angle values. Sep Purif Technol 2015;146:187–91.

[50] Hong J, He Y. Polyvinylidene fluoride ultrafiltration membrane blended with nano-ZnO particle for photo-catalysis self-cleaning. Desalination 2014;332:67–75.

[51] Hashino M, Katagiri T, Kubota N, Ohmukai Y, Maruyama T, Matsuyama H. Effect of surface roughness of hollow fiber membranes with gear-shaped structure on membrane fouling by sodium alginate. J Memb Sci 2011;366:389–97.

[52] Mahmoudi E, Ng LY, Ba-Abbad MM, Mohammad AW. Novel nanohybrid polysulfone membrane embedded with silver nanoparticles on graphene oxide nanoplates. Chem Eng J 2015;277:1–10.

[53] Yamamura H, Okimoto K, Kimura K, Watanabe Y. Hydrophilic fraction of natural organic matter causing irreversible fouling of microfiltration and ultrafiltration membranes. Water Res 2014;54:123–36.

[54] Lee J, Chae H-R, Won YJ, Lee K, Lee C-H, Lee HH, et al. Graphene oxide nanoplatelets composite membrane with hydrophilic and antifouling properties for wastewater treatment. J Memb Sci 2013;448:223–30.

[55] Matar G, Gonzalez-Gil G, Maab H, Nunes S, Le-Clech P, Vrouwenvelder J, et al. Temporal changes in extracellular polymeric substances on hydrophobic and hydrophilic membrane surfaces in a submerged membrane bioreactor. Water Res 2016;95:27–38.

[56] Wang F, Zhu H, Zhang H, Tang H, Chen J, Guo Y. Effect of surface hydrophilic modification on the wettability, surface charge property and separation performance of PTFE membrane. J Water Process Eng 2015;8:11–8.

[57] Chung YT, Ba-Abbad MM, Mohammad AW, Benamor A. Functionalization of zinc oxide (ZnO) nanoparticles and its effects on polysulfone-ZnO membranes. Desalin Water Treat 2015;57:1–11.

[58] Kissa E. Dispersions: characterization, testing, and measurement. vol. 84. CRC Press; 1999.

[59] Lorenzen S, Keiding K, Christensen ML. The effect of particle surface charge density on filter cake properties during dead-end filtration. Chem Eng Sci 2017;163:155–66.

[60] Zhang M, Liao B, Zhou X, He Y, Hong H, Lin H, et al. Effects of hydrophilicity/hydrophobicity of membrane on membrane fouling in a submerged membrane bioreactor. Bioresour Technol 2015;175:59–67.

[61] Zhu L, Song H, Zhang D, Wang G, Zeng Z, Xue Q. Negatively charged polysulfone membranes with hydrophilicity and antifouling properties based on in situ cross-linked polymerization. J Colloid Interface Sci 2017;498:136–43.

[62] Reis R, Duke M, Merenda A, Winther-Jensen B, Puskar L, Tobin MJ, et al. Customizing the surface charge of thin-film composite membranes by surface plasma thin film polymerization. J Memb Sci 2017;537:1–10.

[63] Zhang X, Devanadera MCE, Roddick FA, Fan L, Dalida MLP. Impact of algal organic matter released from Microcystis aeruginosa and Chlorella sp. on the fouling of a ceramic microfiltration membrane. Water Res 2016;103:391–400.

[64] Marbelia L, Mulier M, Vandamme D, Muylaert K, Szymczyk A, Vankelecom IFJ. Polyacrylonitrile membranes for microalgae filtration: influence of porosity, surface charge and microalgae species on membrane fouling. Algal Res 2016;19:128–37.

[65] Breite D, Went M, Prager A, Schulze A. Tailoring membrane surface charges: a novel study on electrostatic interactions during membrane fouling. Polymers (Basel) 2015;7:2017–30.

[66] Chan YJ, Chong MF, Law CL. Biological treatment of anaerobically digested palm oil mill effluent (POME) using a lab-scale sequencing batch reactor (SBR). J Environ Manag 2010;91:1738–46.

[67] Charcosset C. Preparation of emulsions and particles by membrane emulsification for the food processing industry. J Food Eng 2009;92:241–9.

[68] Vijayaraghavan K, Ahmad D, Ezani Bin Abdul Aziz M. Aerobic treatment of palm oil mill effluent. J Environ Manag 2007;82:24–31.

[69] Drews A, Mante J, Iversen V, Vocks M, Lesjean B, Kraume M. Impact of ambient conditions on SMP elimination and rejection in MBRs. Water Res 2007;41:3850–8.

[70] Chen L, Gu Y, Cao C, Zhang J, Ng JW, Tang C. Performance of a submerged anaerobic membrane bioreactor with forward osmosis membrane for low-strength wastewater treatment. Water Res 2014;50:114–23.

[71] Wicaksana F, Fane AG, Chen V. Fibre movement induced by bubbling using submerged hollow fibre membranes. J Memb Sci 2006;271:186–95.

[72] Mohammad AW, Teow YH, Ang WL, Chung YT, Oatley-Radcliffe DL, Hilal N. Nanofiltration membranes review: recent advances and future prospects. State-of-the-Art Rev Desalin 2015;356:226–54.

[73] Bolto B, Tran T, Hoang M. Membrane distillation—a low energy desalting technique? Water 2007;34:59–62.

[74] Choi JH, Lee SH, Fukushi K, Yamamoto K. Comparison of sludge characteristics and PCR-DGGE based microbial diversity of nanofiltration and microfiltration membrane bioreactors. Chemosphere 2007;67:1543–50.

[74a] Nicolini JV, Borges CP, Ferraz HC. Selective rejection of ions and correlation with surface properties of nanofiltration membranes. Sep Purif Technol 2016;171:238–47.

[75] Arévalo J, Ruiz LM, Pérez J, Gómez MA. Effect of temperature on membrane bioreactor performance working with high hydraulic and sludge retention time. Biochem Eng J 2014;88:42–9.

[76] Zhang C, Wang G, Hu Z. Changes in wastewater treatment performance and activated sludge properties of a membrane bioreactor at low temperature operation. Environ Sci Process Impacts 2014;16:2199–207.

[77] Zhang J, Loong WLC, Chou S, Tang C, Wang R, Fane AG. Membrane biofouling and scaling in forward osmosis membrane bioreactor. J Memb Sci 2012;403–404:8–14.

[78] Wang X, Wang C, Tang CY, Hu T, Li X, Ren Y. Development of a novel anaerobic membrane bioreactor simultaneously integrating microfiltration and forward osmosis membranes for low-strength wastewater treatment. J Memb Sci 2017;527:1–7.

[79] Sirinupong T, Youravong W, Tirawat D, Lau WJ, Lai GS, Ismail AF. Synthesis and characterization of thin film composite membranes made of PSF-TiO$_2$/GO nanocomposite substrate for forward osmosis applications. Arab J Chem 2017;541:510–8.

[79a] Mino Y, Ogawa D, Matsuyama H. Functional magnetic particles providing osmotic pressure as reusable draw solutes in forward osmosis membrane process. Adv Powder Technol 2016;27:2136–44.

[79b] Achilli A, Marchand EA. The forward osmosis membrane bioreactor : A low fouling alternative to MBR processes. Desalination 2009;242:215–27.

[80] Boonnorat J, Chiemchaisri C, Chiemchaisri W, Yamamoto K. Removals of phenolic compounds and phthalic acid esters in landfill leachate by microbial sludge of two-stage membrane bioreactor. J Hazard Mater 2014;277:93–101.

[81] Zolfaghari M, Droguia P, Brar SK, Buelna G, Dube R. Effect of bioavailability on the fate of hydrophobic organic compounds and metal in treatment of young landfill leachate by membrane bioreactor. Chemosphere 2016;161:390–9.

[82] Phattaranawik J, Fane AG, Pasquier ACS, Bing W. A novel membrane bioreactor based on membrane distillation. Desalination 2008;223:386–95.

[83] Goh S, Zhang J, Liu Y, Fane AG. Membrane distillation bioreactor (MDBR)—a lower green-house-gas (GHG) option for industrial wastewater reclamation. Chemosphere 2015;140:129–42.

[83a] Adnan S, Hoang M, Wang H, Xie Z. Commercial PTFE membranes for membrane distillation application: Effect of microstructure and support material. Desalination 2012;284:297–308.

[84] Khayet M. Membranes and theoretical modeling of membrane distillation: a review. Adv Colloid Interf Sci 2011;164:56–88.

[85] Monclús H, Sipma J, Ferrero G, Comas J, Rodriguez-Roda I. Optimization of biological nutrient removal in a pilot plant UCT-MBR treating municipal wastewater during start-up. Desalination 2010;250:592–7.

[86] Brown K, Ghoshdastidar AJ, Hanmore J, Frazee J, Tong AZ. Membrane bioreactor technology: a novel approach to the treatment of compost leachate. Waste Manag 2013;33:2188–94.

[87] Monclus H, Sipma J, Ferrero G, Rodriguez-Roda I, Comas J. Biological nutrient removal in an MBR treating municipal wastewater with special focus on biological phosphorus removal. Bioresour Technol 2010;101:3984–91.

[88] Gurung K, Ncibi MC, Sillanpää M. Assessing membrane fouling and the performance of pilot-scale membrane bioreactor (MBR) to treat real municipal wastewater during winter season in Nordic regions. Sci Total Environ 2017;579:1289–97.

[89] Chiemchaisri C, Chiemchaisri W, Nindee P, Chang CY, Yamamoto K. Treatment performance and microbial characteristics in two-stage membrane bioreactor applied to partially stabilized leachate. Water Sci Technol 2011;64:1064–72.

[90] Boonnorat J, Chiemchaisri C, Chiemchaisri W, Yamamoto K. Kinetics of phenolic and phthalic acid esters biodegradation in membrane bioreactor (MBR) treating municipal landfill leachate. Chemosphere 2016;150:639–49.

[91] Yu J, He C, Liu X, Wu J, Hu Y, Zhang Y. Removal of perfluorinated compounds by membrane bioreactor with powdered activated carbon (PAC): adsorption onto sludge and PAC. Desalination 2014;334:23–8.

[92] Wang G, Fan Z, Wu D, Qin L, Zhang G, Gao C, et al. Anoxic/aerobic granular active carbon assisted MBR integrated with nanofiltration and reverse osmosis for advanced treatment of municipal landfill leachate. Desalination 2014;349:136–44.

[93] Bayat M, Mehrnia MR, Hosseinzadeh M, Sheikh-Sofla R. Petrochemical wastewater treatment and reuse by MBR: a pilot study for ethylene oxide/ethylene glycol and olefin units. J Ind Eng Chem 2015;25:265–71.

[94] Li WH, Yue QY, Gao BY, Ma ZH, Li YJ, Zhao HX. Preparation and utilization of sludge-based activated carbon for the adsorption of dyes from aqueous solutions. Chem Eng J 2011;171:320–7.

[95] Xu X, Gao BY, Yue QY, Zhong QQ, Li Q. Preparation of new types of anion exchange resins from agricultural by-products and their utilization in the removal of various toxic anions from solutions. Chem Eng J 2011;167:104–11.

[96] Ravindran V, Tsai HH, Williams MD, Pirbazari M. Hybrid membrane bioreactor technology for small water treatment utilities: process evaluation and primordial considerations. J Memb Sci 2009;344:39–54.

[97]   Friha I, Bradai M, Johnson D, Hilal N, Loukil S, Ben Amor F, et al. Treatment of textile wastewater by submerged membrane bioreactor: in vitro bioassays for the assessment of stress response elicited by raw and reclaimed wastewater. J Environ Manag 2015;160:184–92.

[98]   Rondon H, El-Cheikh W, Boluarte IAR, Chang CY, Bagshaw S, Farago L, et al. Application of enhanced membrane bioreactor (eMBR) to treat dye wastewater. Bioresour Technol 2015;183:78–85.

[99]   Psoch C, Schiewer S. Anti-fouling application of air sparging and backflushing for MBR. J Memb Sci 2006;283:273–80.

[100]  Qin L, Zhang G, Meng Q, Xu L, Lv B. Enhanced MBR by internal micro-electrolysis for degradation of anthraquinone dye wastewater. Chem Eng J 2012;210:575–84.

[101]  Deveci EÜ, Dizge N, Yatmaz HC, Aytepe Y. Integrated process of fungal membrane bioreactor and photocatalytic membrane reactor for the treatment of industrial textile wastewater. Biochem Eng J 2016;105:420–7.

[102]  Andrade L, Motta G, Amaral M. Treatment of dairy wastewater with a membrane bioreactor. Brazilian J Chem Eng 2013;30:759–70.

[103]  Sadeghi F, Mehrnia MR, Nabizadeh R, Sarrafzadeh MH. Treatment of synthetic olefin plant wastewater at various salt concentrations in a membrane bioreactor. Clean Soil Air Water 2012;40:416–21.

[104]  Fallah N, Bonakdarpour B, Nasernejad B, Alavi Moghadam MR. Long-term operation of submerged membrane bioreactor (MBR) for the treatment of synthetic wastewater containing styrene as volatile organic compound (VOC): effect of hydraulic retention time (HRT). J Hazard Mater 2010;178:718–24.

[105]  Lebrero R, Gondim AC, Perez R, Garcia-Encina PA, Munoz R. Comparative assessment of a biofilter, a biotrickling filter and a hollow fiber membrane bioreactor for odor treatment in wastewater treatment plants. Water Res 2014;49:339–50.

[106]  Wang YK, Pan XR, Sheng GP, Li WW, Shi BJ, Yu HQ. Development of an energy-saving anaerobic hybrid membrane bioreactors for 2-chlorophenol-contained wastewater treatment. Chemosphere 2015;140:79–84.

[107]  Michelon M, Manera AP, Carvalho AL, Maugeri Filho F. Concentration and purification of galacto-oligosaccharides using nanofiltration membranes. Int J Food Sci Technol 2014;49:1953–61.

[108]  Córdova A, Astudillo C, Vera C, Guerrero C, Illanes A. Performance of an ultra-filtration membrane bioreactor (UF-MBR) as a processing strategy for the synthesis of galacto-oligosaccharides at high substrate concentrations. J Biotechnol 2016;223:26–35.

[109]  Andrade LH, Mendes FDS, Espindola JC, Amaral MCS. Nanofiltration as tertiary treatment for the reuse of dairy wastewater treated by membrane bioreactor. Sep Purif Technol 2014;126:21–9.

[110]  Farizoglu B, Uzuner S. The investigation of dairy industry wastewater treatment in a biological high performance membrane system. Biochem Eng J 2011;57:46–54.

[111]  Praneeth K, Moulik S, Vadthya P, Bhargava SK, Tardio J, Sridhar S. Performance assessment and hydrodynamic analysis of a submerged membrane bioreactor for treating dairy industrial effluent. J Hazard Mater 2014;274:300–13.

[112]  Fraga FA, García HA, Hooijmans CM, Míguez D, Brdjanovic D. Evaluation of a membrane bioreactor on dairy wastewater treatment and reuse in Uruguay. Int Biodeterior Biodegradat 2017;119:552–64.

[113]  Buntner D, Sánchez A, Garrido JM. Feasibility of combined UASB and MBR system in dairy wastewater treatment at ambient temperatures. Chem Eng J 2013;230:475–81.

[114]  Santos JL, Aparicio I, Alonso E. Occurrence and risk assessment of pharmaceutically active compounds in wastewater treatment plants. A case study: Seville city (Spain). Environ Int 2007;33:596–601.

[115] Sheldon MS, Erdogan IG. Multi-stage EGSB/MBR treatment of soft drink industry wastewater. Chem Eng J 2016;285:368–77.

[116] Bolzonella D, Fatone F, Pavan P, Cecchi F. Application of a membrane bioreactor for winery wastewater treatment. Water Sci Technol 2010;62:2754–9.

[117] Brown KD, Kulis J, Thomson B, Chapman TH, Mawhinney DB. Occurrence of antibiotics in hospital, residential, and dairy effluent, municipal wastewater, and the Rio Grande in New Mexico. Sci Total Environ 2006;366:772–83.

[118] Castiglioni S, Fanelli R, Calamari D, Bagnati R, Zuccato E. Methodological approaches for studying pharmaceuticals in the environment by comparing predicted and measured concentrations in River Po, Italy. Regul Toxicol Pharmacol 2004;39:25–32.

[119] Favier M, Sena RF, Jose HJ, Bieling U, Schroder HF. In: Liquid chromatography-tandem mass spectrometry for the screening of pharmaceuticals and metabolites in various water bodies. Int Conf sustain Sanit "food water Secur Lat am, Florianópolis, Santa Catarina, Brazil. Paper presented at the Ecosan-Fortaleza, conference, Fortaleza, Ceará, Brazil; 2007.

[120] Fent K, Weston AA, Caminada D. Ecotoxicology of human pharmaceuticals. Aquat Toxicol 2006;76:122–59.

[121] Gulkowska A, Leung HW, So MK, Taniyasu S, Yamashita N, Yeung LWY, et al. Removal of antibiotics from wastewater by sewage treatment facilities in Hong Kong and Shenzhen, China. Water Res 2008;42:395–403.

[122] Miao X, Bishay F, Chen M, Metcalfe CD. Occurrence of antimicrobials in the final effluents of wastewater treatment plants in Canada. Environ Sci Technol 2004;38: 3533–41.

[123] Halling-Sørensen B, Nors Nielsen S, Lanzky PF, Ingerslev F, Holten Lützhøft HC, Jørgensen SE. Occurrence, fate and effects of pharmaceutical substances in the environment—a review. Chemo 1998;36:357–93.

[124] Kummerer K. Resistance in the environment. J Antimicrob Chemother 2004;54: 311–20.

[125] Sumpter JP. Xenoendocrine disrupters—environmental impacts. Toxicol Lett 1998;102:337–42.

[126] Tambosi JL, de Sena RF, Favier M, Gebhardt W, José HJ, Schröder HF, Moreira Rd. FPM. Removal of pharmaceutical compounds in membrane bioreactors (MBR) applying submerged membranes. Desalination 2010;261:148–56.

[127] Seira J, Sablayrolles C, Montrejaud-Vignoles M, Albasi C, Joannis-Cassan C. Elimination of an anticancer drug (cyclophosphamide) by a membrane bioreactor: comprehensive study of mechanisms. Biochem Eng J 2016;114:155–63.

[128] Verlicchi P, Al Aukidy M, Zambello E. What have we learned from worldwide experiences on the management and treatment of hospital effluent? An overview and a discussion on perspectives. Sci Total Environ 2015;514:467–91.

[129] Zhang J, Chang VWC, Giannis A, Wang J. Removal of cytostatic drugs from aquatic environment: a review. Sci Total Environ 2013;445–446:281–98.

[130] Prasertkulsak S, Chiemchaisri C, Chiemchaisri W, Itonaga T, Yamamoto K. Removals of pharmaceutical compounds from hospital wastewater in membrane bioreactor operated under short hydraulic retention time. Chemosphere 2016;150:624–31.

[131] Zhao BH. Enzymatic production of 7-aminocephalosporanic acid. Doctoral, Zhejiang Univ China; 2007.

[132] Jiang B, Wang L, Lin Y, Sun P. Study about cleaner production potentials of 7-ACA. Environ Sci Manag 2011;36:184–6.

[133] Bo CZ, Wei HZ, Cong TC, Xue HD, bo CY, Jie WA, et al. Performance and model of a novel multi-sparger multi-stage airlift loop membrane bioreactor to treat high-strength 7-ACA pharmaceutical wastewater: effect of hydraulic retention time, temperature and pH. Bioresour Technol 2014;167:241–50.

[134] Umaiyakunjaram R, Shanmugam P. Study on submerged anaerobic membrane biore-actor (SAMBR) treating high suspended solids raw tannery wastewater for biogas pro-duction. Bioresour Technol 2016;216:785–92.

[135] Ng KK, Shi X, Tang MKY, Ng HY. A novel application of anaerobic bio-entrapped membrane reactor for the treatment of chemical synthesis-based pharmaceutical wastewater. Sep Purif Technol 2014;132:634–43.

[136] Shi X, Lefebvre O, Ng KK, Ng HY. Sequential anaerobic-aerobic treatment of pharma-ceutical wastewater with high salinity. Bioresour Technol 2014;153:79–86.

[137] Jang D, Hwang Y, Shin H, Lee W. Effects of salinity on the characteristics of biomass and membrane fouling in membrane bioreactors. Bioresour Technol 2013;141:50–6.

[138] Ng KK, Shi X, Yao Y, Ng HY. Bio-entrapped membrane reactor and salt marsh sedi-ment membrane bioreactor for the treatment of pharmaceutical wastewater: treatment performance and microbial communities. Bioresour Technol 2014;171:265–73.

[139] García-Gómez C, Drogui P, Seyhi B, Gortáres-Moroyoqui P, Buelna G, Estrada-Alvgarado MI, Álvarez LH. Combined membrane bioreactor and electrochemical oxi-dation using Ti/PbO$_2$ anode for the removal of carbamazepine. J Taiwan Inst Chem Eng 2016;64:211–9.

[140] Wang J, Li K, Wei Y, Cheng Y, Wei D, Li M. Performance and fate of organics in a pilot MBR-NF for treating antibiotic production wastewater with recycling NF concentrate. Chemosphere 2015;121:92–100.

[141] Svojitka J, Dvořák L, Studer M, Straub JO, Frömelt H, Wintgens T. Performance of an anaerobic membrane bioreactor for pharmaceutical wastewater treatment. Bioresour Technol 2017;229:180–9.

[142] Sun C, Leiknes T, Weitzenböck J, Thorstensen B. Development of a biofilm-MBR for shipboard wastewater treatment: the effect of process configuration. Desalination 2010;250:745–50.

[143] DongLei W, Wei W, ShaoJun C, ZhiZhong Y, GuangMing T, Baig SA, et al. Advanced bamboo industry wastewater treatment through nanofiltration membrane technology. Desalin Water Treat 2013;51:3454–62.

[144] Wu DL, Wang W, Guo QW, Shen YH. Combined Fenton-SBR process for bamboo industry wastewater treatment. Chem Eng J 2013;214:278–84.

[145] Xia T, Gao X, Wang C, Xu X, Zhu L. An enhanced anaerobic membrane bioreactor treat-ing bamboo industry wastewater by bamboo charcoal addition: performance and microbial community analysis. Bioresour Technol 2016;220:1–7.